PROCEEDINGS

VETERINARY PATHOLOGY SERVICE
WEDNESDAY SLIDE CONFERENCE
2013-2014

JOINT PATHOLOGY CENTER
SILVER SPRING, MD 20910
2014

ML2014

JOINT PATHOLOGY CENTER
VETERINARY PATHOLOGY SERVICE

WEDNESDAY SLIDE CONFERENCE
2013-2014

100 Cases

JOINT PATHOLOGY CENTER
SILVER SPRING, MD 20910
2013

ML2014

PREFACE

The Veterinary Pathology Service of the Joint Pathology Center (JPC), formerly known as the Armed Forces Institute of Pathology, has conducted a weekly slide conference during the resident training year since 12 November 1953. This ever-changing educational endeavor has evolved into the annual Wednesday Slide Conference program in which cases are presented on 25 Wednesdays throughout the academic year and distributed to 135 contributing military and civilian institutions from around the world. Many of these institutions provide structured veterinary pathology resident training programs. During the course of the training year, histopathology slides, digital images, and histories from selected cases are distributed to the participating institutions and to the JPC Veterinary Pathology Service. Following the conferences, the case diagnoses, comments, and reference listings are posted online to all participants.

This study set has been assembled in an effort to make Wednesday Slide Conference materials available to a wider circle of interested pathologists and scientists, and to further the education of veterinary pathologists and residents-in-training. The number of histopathology slides that can be reproduced from smaller lesions requires us to limit the number of participating institutions.

For their participation and permission to use their cases in this study set, we wish to thank each institution, and especially the individuals who prepared and submitted the selected cases.

A special note of appreciation is extended to the reviewers who helped edit and review this year's individual case summaries:

A final note of thanks goes to the moderators, who unselfishly gave of their time and expertise to help make each conference both enjoyable and educational.

Gross images and photomicrographs were submitted by contributing institutions where indicated. Additional photomicrographs were taken by

Joint Pathology Center
WEDNESDAY SLIDE CONFERENCE 2013-2014
Table of Contents

WSC 2013-2014 Table of Contents

WSC 2013-2014 Table of Contents

Joint Pathology Center
Veterinary Pathology Services

WEDNESDAY SLIDE CONFERENCE 2013-2014

Conference 1

11 September 2013

CASE I: 12-236 (JPC 4032712).

Signalment: 3-year-old male Labrador Retriever cross dog, (*Canis familiaris*).

History: The dog presented to the referring veterinarian with a one-day history of inappetance, unusual behavior, ataxia, falling 1 over, vocalizing, incontinence, and apparent pain in the hips and back. The dog was hospitalized with rapid progression of clinical signs including rigidity of all four limbs, profuse salivation, opisthotonos, and nystagmus. Pentobarbital was administered. The dog later became unresponsive to sound and touch, and was found dead in the cage the next morning. A necropsy was performed by the referring veterinarian. Gross lesions were not observed.

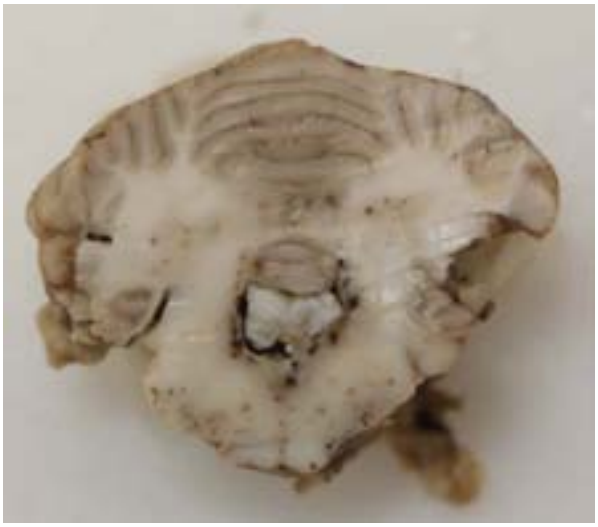

1-1. Cerebellum, pons, and fourth ventricle, dog: Arising from the wall of the fourth ventricle is an epidermoid cyst that assymetrically compresses the adjacent neuropil. There are multifocal random areas of hemorrhage throughout the midbrain. (Photo courtesy of: Diagnostic Services Unit, University of Calgary Veterinary Medicine, Clinical Skills Building, 11877 85 St. NW, Calgary AB T3R 1J3, http://vet.ucalgary.ca/)

Gross Pathology: Seven sections of brain were submitted in formalin for examination. There was moderate dilation of the lateral ventricles and marked dilation of the mesencephalic aqueduct and the most rostral aspects of the fourth ventricle. Occluding the lumen of the fourth ventricle there was a 0.8 cm, irregularly shaped, expansile, firm, opalescent mass. Multifocal areas of hemorrhage were noted in the adjacent cerebellum and brain stem.

Histopathologic Description: Brain, fourth ventricle: Filling approximately 80% of the fourth ventricle and in close association with the choroid plexus, there is a multilocular (not in all sections), expansile, unencapsulated and moderately well-defined mass. The wall of the mass is composed of well-differentiated stratified squamous epithelium which exhibits gradual

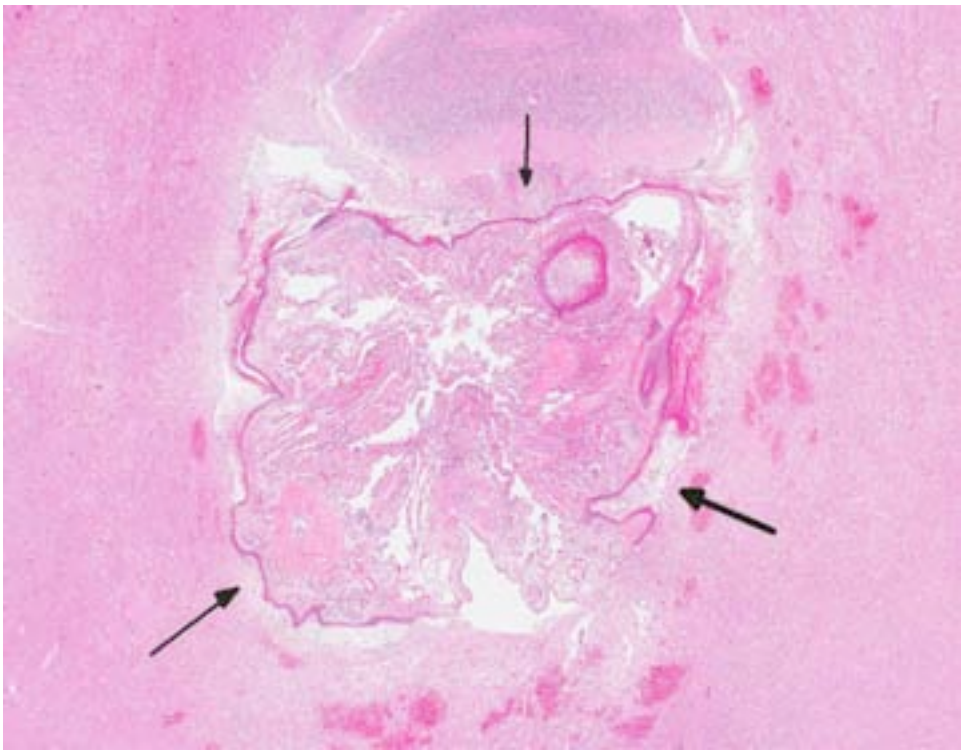

1-2. Cerebellum, pons, and fourth ventricle, dog: Within and expanding the fourth ventricle, incorporating and expanding the choroid plexus and compressing adjacent brainstem and cerebellum, there is an epithelial-lined cyst (arrows). (HE 8X)

keratinization through a granular cell layer resulting in the formation of multiple cysts filled with lamellar keratin. The cyst wall is discontinuous and free keratin spills into the lumen of the fourth ventricle. The squamous epithelium is supported by a moderate amount of fibrovascular stroma which frequently entraps the choroid plexus. In some areas the stroma is dense and brightly eosinophilic. Within the stroma there are modest numbers of inflammatory cells which mainly include lymphocytes and plasma cells. Infrequently there are stellate shaped cells with abundant dark brown, finely granular pigment which are interpreted to be melanocytes. Occasional hemosiderin laden macrophages are noted. There is marked rarefaction neuropil and hemorrhage. This is accompanied by numerous eosinophilic, spherical structures which are interpreted to be spheroids (swollen axons). Lining the lumen of the ventricle there are multiple round cells with abundant pale, foamy to slightly granular, eosinophilic cytoplasm, and one to multiple eccentric nuclei. These are interpreted to be gitter cells.

Intercellular bridges between keratinized cells are prominent. There are approximately five mitoses per 400x field with frequent bizarre mitotic figures. There is severe anisocytosis and anisokaryosis. Multifocally within the neoplasm there are large areas of necrosis, hemorrhage and a mixed inflammatory infiltrate of lymphocytes, plasma cells, neutrophils and some macrophages. Many submucosal and subserosal vessels contain clusters of neoplastic cells (tumor emboli) as well as fibrin thrombi. Overlying the ulcerated mucosa, there is abundant fibrillar eosinophilic material (fibrin exudation) and hemorrhage, admixed with cellular and karyorrhectic debris (necrosis) and bacterial colonies. Throughout the mass, but especially along the serosa, there are multiple nodules or bands of abundant fibrous connective tissue (scirrhous response).

Contributor's Morphologic Diagnosis: Brain, fourth ventricle: Epidermoid cyst with hemorrhage, malacia, and acquired obstructive hydrocephalus.

Contributor's Comment: The central nervous system (CNS) develops from specialized ectoderm (neuroectoderm) which lies dorsal to the notochord throughout the axis of the embryo. Invagination of the neuroectoderm forms the neural groove and lateral processes referred to as the neural folds. Fusion of the neural folds results in the formation of the neural tube with the latter forming the ventricular system and central canal of the CNS. At the time of neural tube closure, the neuroectoderm separates from the surface ectoderm to form two distinct layers. The layer of nonneural ectoderm gives rise to structures such as the epidermis. Epidermoid cysts of the CNS are congenital lesions that are thought to be the

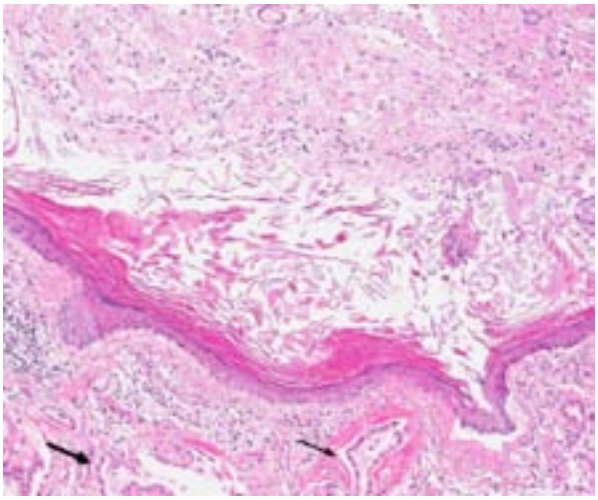

1-3. Midbrain and fourth ventricle, dog: The cyst is lined by one to three rows of stratified squamous epithelium which shows normal maturation and keratinization, to include the presence of a granular cell layer. Between the cyst lining and the entrapped choroid plexus (arrows), there is a layer of dense collagen containing small amounts of lymphocytic inflammation. (HE 200X) Exteriorly, there are layers of keratin in apposition to the wall of the fourth ventricle. (HE 200X)

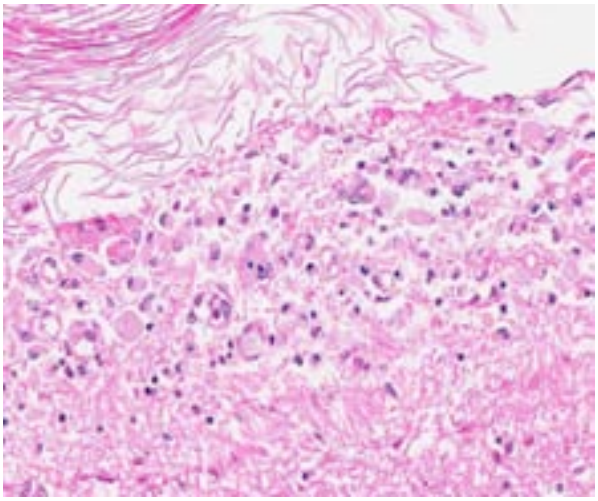

1-4. Fourth ventricle, dog: The neuropiladjacent to layers of free keratin contains numerous epithelioid (rarely multinucleate) macrophages. (HE 225X)

result of inappropriate inclusion of this nonneural ectoderm at the time of closure of the neural tube.[4]

In humans, intracranial epidermoid cysts are a well-recognized entity and are thought to comprise up to 1.8% of all intracranial masses.[7] Epidermoid cysts of the CNS are uncommon in domestic animals with a handful of cases being reported in dogs, horses, mice, and rats.[2,4,9,10] In dogs, epidermoid cysts have been reported within the cranial cavity[4,6,11,12] and within the vertebral canal.[1,4] Intracranial masses are most common.

There are too few reports of intracranial epidermoid cysts in dogs to reliably identify a breed or sex predilection. Dogs with intracranial epidermoid cysts have ranged in age from 3 months to 8 years with the majority of dogs being less than 2 years old.[4] These findings may suggest a predilection for young dogs, and could be consistent with the presence of a congenital lesion. Intracranial epidermoid cysts are slow growing masses and in people typically do not cause clinical signs until fifth decade of life.[4] The slow, linear growing pattern of these masses may explain the wide age range reported in dogs for a purportedly congenital lesion.

Intracranial epidermoid cysts exhibit an expansile growth pattern through desquamation and accumulation of keratin.[7] While these lesions may be found as incidental findings at necropsy,[4] intracranial epidermoid cysts may cause clinical signs referable to compression of adjacent structures resulting in focal neurologic dysfunction or obstruction of CSF resulting in hydrocephalus.[4,6,11,12] In both humans and dogs, epidermoid cysts have a predilection for the caudal fossa which may be a reflection of the initial closure of the neural tube in the rhombencephalon. In dogs, intracranial epidermoid cysts have been reported in the fourth ventricle and cerebellopontine angle.[4] Based on their location in the caudal fossa, canine epidermoid cysts are frequently associated with vestibular and occasionally cerebellar signs.[4,6] In addition to the space occupying nature of these lesions, other sequelae reported in people include the development of chemical meningitis, and rarely malignant transformation to squamous cell carcinoma.[7,8] Malignant transformation has not been reported in dogs, and in the current case there was no evidence of squamous cell carcinoma in the sections examined.

Pathologic features of intracranial epidermoid cysts are similar to those that are routinely encountered in the skin. Microscopic examination reveals the presence of a cyst lined by stratified squamous epithelium supported by connective tissue stroma and surrounding keratin. Portions of choroid plexus are often adhered to or are incorporated into the cyst.[4] Intracranial dermoid cysts have also been reported and also arise from the inappropriate inclusion of

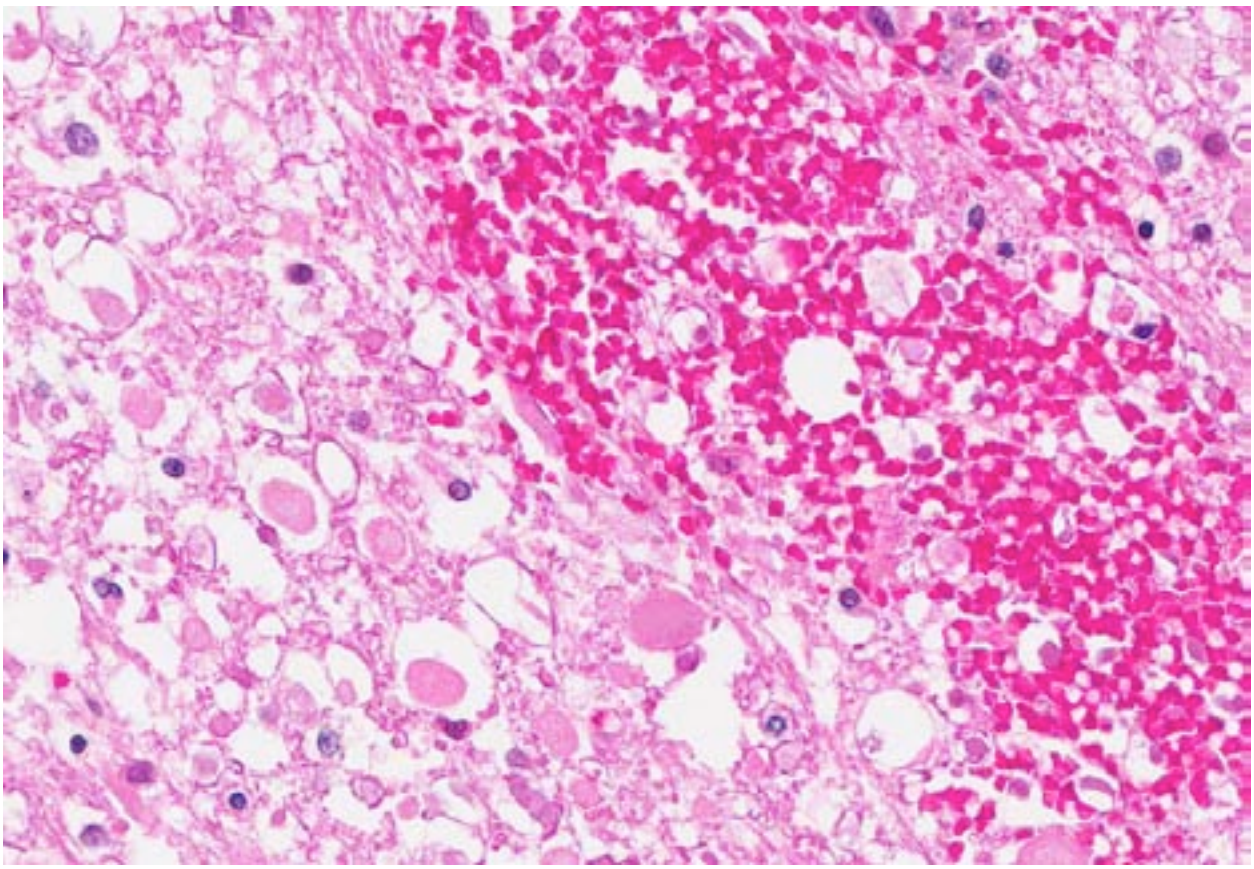

1-5. Midbrain, dog: Periventricular white matter contains numerous dilated myelin sheaths and swollen axons (spheroids), as well as multifocal hemorrhage. (HE 100X)

nonneural ectoderm in the CNS. Dermoid cysts can be differentiated from epidermoid cysts in that the former is lined by adnexal structures such as hair follicles, sebaceous glands, and sweat glands.[4] These features were not observed in the current mass favoring a diagnosis of epidermoid cyst over dermoid cyst.

JPC Diagnosis: Brain, 4th ventricle: Epidermoid cyst with granulomatous rhombencephalitis, encephalomalacia, edema and hemorrhage.

Conference Comment: Conference participants discussed the embryologic histogenesis and clinical signs of intracranial epidermoid cysts, as reviewed by the contributor in the above comments. Clinical signs of neurologic dysfunction are generally attributed to compression of adjacent neural structures[5]- indeed one of the more striking histologic features in this case is the degree of axonal degeneration and numerous, prominent spheroids noted within the adjacent neuropil. Cyst rupture with subsequent inflammation, known in human medicine as chemical meningoencephalitis, may also contribute to the clinical signs.[6] Although intracranial epidermoid cysts are more common (and of course, extracranial epidermoid cysts are the most common), intravertebral and intramedullary spinal cord cysts with progressive ataxia and paraparesis have also been described in dogs.[1,5]

Participants also examined dermoid cysts as a related, but more frequent finding in the CNS of dogs. Like their non-congenital, dermal counterparts, both epidermoid and dermoid intracranial cysts are lined by stratified squamous epithelium. Although they have a similar embryologic origin, the dermoid cyst is derived from a more pluripotent precursor cell and often produces adnexal structures, such as sebaceous glands, apocrine glands or hair follicles.[6] Additionally, Rhodesian ridgeback dogs that carry the autosomal dominant dorsal ridge trait have been shown to be predisposed to the congenital cutaneous defect known as dermoid sinus, which is a draining sinus at the dorsal midline that

occasionally communicates with the subarachnoid space.[3] Typically these dogs do not have any clinical problems.

Intracranial epidermoid cysts occur in other veterinary species; in mice they often occur within the leptomeninges of the lumbar/sacral spinal cord or (less commonly) associated with the fourth ventricle.[2] There are generally no clinical signs in mice or rats with this lesion, which may be an indication that the cysts do not grow large enough to compress adjacent structures.[2] Intracranial epidermoid cysts in mice are thought to be strain dependent and are typically interpreted as incidental findings. Conversely, dermoid cysts in mice have rarely been associated with clinical neurologic dysfunction.[2] Epidermoid cysts have not been reported in the CNS of hamsters or cats.

Contributing Institution: Diagnostic Services Unit
University of Calgary Veterinary Medicine
Clinical Skills Building
11877 85 St. NW
Calgary AB T3R 1J3
http://vet.ucalgary.ca/

References:

1. Capello R, Lamb CR, Rest JR. Vertebral epidermoid cyst causing hemiparesis in a dog. *Vet Rec*. 2006;158:865-867.
2. Hansmann F, Herder V, Ernst H, et al. Spinal epidermoid cyst in a SJL mouse: case report and literature review. *J Comp Pathol*. 2011;145:373-377.
3. Hillbertz NH, Andersson G. Autosomal dominant mutation causing the dorsal ridge predisposes for dermoid sinus in Rhodesian ridgeback dogs. *J Small Anim Pract.* 2006;47(4): 184-188.
4. Kornegay JN, Gorgacz EJ. Intracranial epidermoid cysts in three dogs. *Vet Pathol*. 1982;19:646-650.
5. Lipitz L, Rylander H, Pinkerton ME. Intramedullary epidermoid cyst in the thoracic spine of a dog. *J Am Anim Hosp Assoc*. 2011;47:e145-e149.
6. MacKillop E, Schatzburg SJ, de Lahunta A. Intracranial epidermoid cyst and syringohydromyelia in a dog. *Vet Radiol Ultrasound*. 2006;47:339-344.
7. Michael II LM, Moss T, Madhu T, et al. Malignant transformation of the posterior fossa epidermoid cyst. *Br J Neurosurg*. 2005;19:505-510.
8. Netsky MG. Epidermoid tumors. *Surg Neurol*. 1988;29:477-483.
9. Nobel TA, Nyska A, Pirak M, et al. Epidermoid cysts in the central nervous system of mice. *J Comp Pathol*. 1987;97:357-359.
10. Peters M, Brandt K, Wohlsein. Intracranial epidermoid cyst in a horse. *J Comp Pathol*. 2003;12:89-92.
11. Platt SR, Chrisman CL, Adjiri-Awere A, et al. Canine intracranial epidermoid cyst. *Vet Radiol Ultrasound*. 1999;40:454-458.
12. Steinberg T, Matiasek K, Bruhschwein A, et al. Imaging diagnosis-intracranial epidermoid cyst in a Doberman Pinscher. *Vet Radiol Ultrasound*. 2007;48:250-253.

CASE II: 10-461 (JPC 4031864).

Signalment: 10-year-old male neutered Staffordshire terrier dog, (Canis familiaris).

History: Urinary bladder mass, hematochezia, hematemesis.

Gross Pathology: The urinary bladder is 1 cm thick, has emphysema of the wall, and has multiple 0.5-1.0 cm red nodules in the mucosa.

Histopathologic Description: Urinary bladder: The urinary bladder has severe transmural emphysema, severe submucosal edema, mild multifocal submucosal hemorrhage, and a mild, diffuse submucosal inflammation of lymphocytes, plasma cells, eosinophils and macrophages containing hemosiderin. A few macrophages and multinucleate giant cells are present around the air spaces.

Contributor's Morphologic Diagnosis: Urinary bladder: Emphysematous cystitis.

Contributor's Comment: Emphysema of the urinary bladder has been reported in humans, dogs, cattle and cats.[1,2] It occurs with infection of the bladder by gas-producing bacteria that ferment glucose in the urine. E. coli, Pseudomonas, Klebsiella, Proteus, Enterobacter sp., and Clostridium sp. are bacteria that have been isolated from cases of emphysematous cystitis in dogs and humans.[1,2] Glucosuria caused by diabetes mellitus is the most common cause of urinary bladder emphysema. The condition also occurs in non-diabetic humans and dogs associated with chronic recurrent cystitis, cortisone administration and primary glucosuria.[1,2]

JPC Diagnosis: Urinary bladder: Emphysema, transmural, multifocal to coalescing, marked, with mild granulomatous and lymphoplasmacytic cystitis, and submucosal hemorrhage and edema.

Conference Comment: Conference participants explored various mechanisms contributing to glucosuria and emphysematous cystitis, as summarized above by the contributor. Although diabetes mellitus is the most common underlying cause, proximal renal tubular disorders also result in glucosuria, and may induce emphysematous cystitis in several breeds of dog, including Basenjis, Labrador retrievers, Norwegian elkhounds, schnauzers and Shetland sheepdogs.[4] In Basenjis, this renal tubular abnormality, known as canine Fanconi-like syndrome, is hereditary. It is characterized by impaired renal tubular reabsorption of glucose, phosphate, sodium, potassium, uric acid, amino acids and protein.[6] In humans, Fanconi-Bickel syndrome is due to a defect in the SLC2 gene, which results in defects of GLUT2, a member of the renal glucose

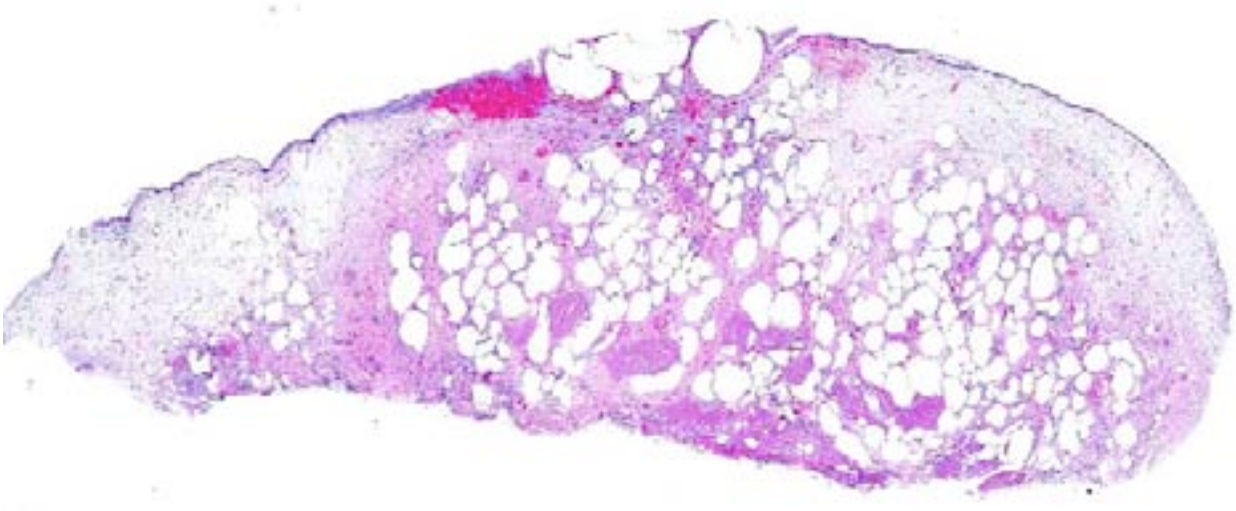

2-1. Urinary bladder, dog: The bladder wall is markedly expanded by discrete clear spaces (emphysema), as well as areas of subucosal pallor (edema). (HE 40X)

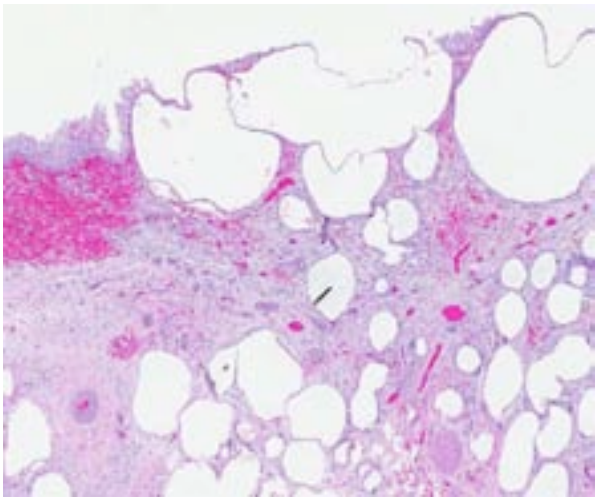

2-2. Urinary bladder, dog: Emphysematous spaces are present within the urothelium (top), as well as in the submucosa. There is multifocal hemorrhage and lymphoplasmacytic inflammation within the superficial submucosa. (HE 25X)

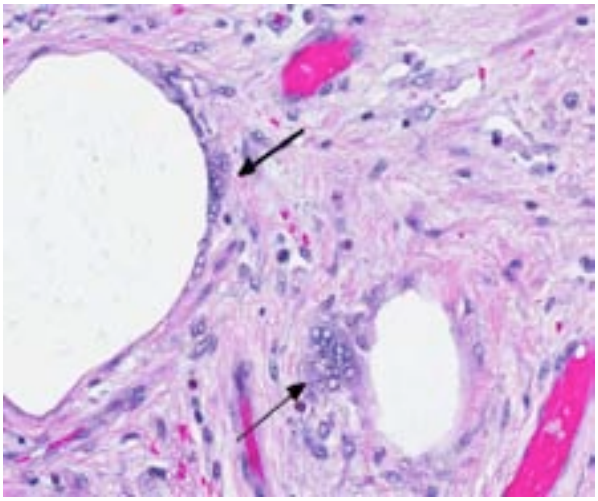

2-3. Urinary bladder, dog: Emphysematous spaces are surrounded and bordered by multinucleated giant cell macrophages. (HE 256X)

transporter protein family.[5] It is suspected that there is a similar underlying defect triggering canine Fanconi-like syndrome, but this has not been proven. Acquired Fanconi-like syndrome in dogs has been associated with several drugs and toxins, such as gentamicin and ethylene glycol. Whether congenital or acquired, Fanconi-like syndrome results in glucosuria (with normal blood glucose), phosphaturia, aminoaciduria and proteinuria.[4] Primary (type II) renal tubular acidosis may also occur due to impaired bicarbonate reabsorption in renal proximal convoluted tubules, which leads to secretional, hyperchloremic metabolic acidosis with normal anion gap and alkaline urine.[3]

Primary renal glucosuria (without other reabsorption abnormalities) is an inherited disorder of Norwegian elkhounds.[4] It is caused by defects in SGLT2, from the sodium-glucose cotransporter family of proteins that is encoded by SLC5 genes in people.[5] As with Fanconi-like syndrome, the underlying genetic defect in dogs has not been established. In addition to primary glucosuria and diabetes, treatment with exogenous corticosteroids, and the subsequent antagonism of insulin, can lead to glucosuria (and thus, emphysematous cystitis) as well; once the resorptive capacity of the proximal renal tubule is exceeded, at a blood glucose concentration greater than 180mg/dL in dogs, glucose spills over into the urine.[3] Glucosuria may also occur in cattle treated with intravenous glucose.

Participants also reviewed other pathologic processes resulting in tissue emphysema. Clostridia are probably the most well-known gas producing organisms, as exemplified by Clostridium chauvoei induced necrohemorrhagic and emphysematous myositis (blackleg). Pulmonary emphysema is a non-specific change due to alveolar rupture in downer cattle or those with dyspnea or increased respiratory effort. Subcutaneous emphysema in any species could be a sequela to tracheal, bronchial or pulmonary trauma. In swine, intestinal emphysema (pneumatosis cystoides intestinalis) is an idiopathic, incidental finding at slaughter. Fetal death with maceration and emphysema is a fairly well described condition in ruminants. So called "gas bubble disease" in fish is caused by supersaturated levels of dissolved oxygen or nitrogen in the water of the tank. Lesions are secondary to the accumulation of gas bubbles in blood vasculature and tissues. Finally, postmortem gas production is also a familiar occurrence in veterinary pathology; it can be distinguished from antemortem emphysema by the absence of an inflammatory reaction.

Contributing Institution: College of Veterinary Medicine
Virginia Tech
Blacksburg, VA 24061
www.vetmed.vt.edu

References:

1. Matsuo S, Hayashi S, Watanabe, T, et al. Emphysematous cystitis in a chemically-induced diabetic dog. *J Toxicol Pathol*. 2009;22:289-292.
2. Lobetti RG, Goldin JP. Emphysematous cystitis and bladder trigone diverticulum in a dog. *J Sm Anim Pract*. 1998;39:144-147.
3. Latimer KS, ed. *Duncan & Prasse's Veterinary Laboratory Medicine- Clinical Pathology*. 5th ed. Ames, IA: Wiley-Blackwell; 2011:163-165,193-194, 263.
4. Maxie MG, Newman SJ. Urinary system. In: Maxie MG, ed. *Jubb, Kennedy, and Palmer's Pathology of Domestic Animals*. 5th ed., vol. 2. St. Louis, MO: Elsevier Limited; 2007: 474.
5. Santer R, Calado J. Familial renal glucosuria and SGLT2: from a mendelian trait to a therapeutic target. *Clin J Am Soc Nephrol*. 2010;5(1):133-141.
6. Yearly JH, Hancock DD, Mealey KL. Survival time, lifespan, and quality of life in dogs with idiopathic Fanconi syndrome. *J Am Vet Med Assoc*. 2004;225(3):377-383.

CASE III: 55860 (JPC 4032564).

Signalment: 1-year-old female blackbuck, (Antilope cervicapra cervicapra).

History: This blackbuck was housed in a large, mixed species enclosure. Two days prior to death she was isolating herself from the group, with some head shaking and stretching. In the afternoon prior to death she delivered a stillborn calf. The blackbuck was found dead on the following morning.

Gross Pathology: The diaphragm is loosely adhered to the ventral serosal surface of the spleen with tan fibrinous material. A small amount of fibrin is present on multiple loops of small intestine. An approximately 20 cm long region of small intestine (jejunum) is dark red to purple, and friable. A moderate amount of fibrin is present in the lumen orad and aborad to the affected intestine, and the mucosal surfaces are mildly petechiated. A mesenteric lymph node adjacent to the most severely affected loop of intestine is pink with a few white foci scattered throughout. The uterus contains a small amount of tan to grey material adhered to the endometrium. The vagina and cervix are markedly dilated and have red to dark red mucosal surfaces.

Laboratory Results: Bacterial culture of intestinal content was performed with the following results: Yersinia pseudotuberculosis 2+, Escherichia coli 3+, normal gram-positive flora 2+. Campylobacter, Salmonella, Shigella, Pleisiomonas, Edwardsiella, and Aeromonas sp. not isolated.

Histopathologic Description: Small intestine with adjacent fat and lymph node: The intestinal mucosa and submucosa are necrotic with extensive hemorrhage, infiltrates of neutrophils, and large clusters of gram-negative bacterial rods. Crypts are identified in most sections, but are absent in many areas. The superficial mucosa has large amounts of fibrinous exudate and necrotic debris with bacteria of various types. Autolysis

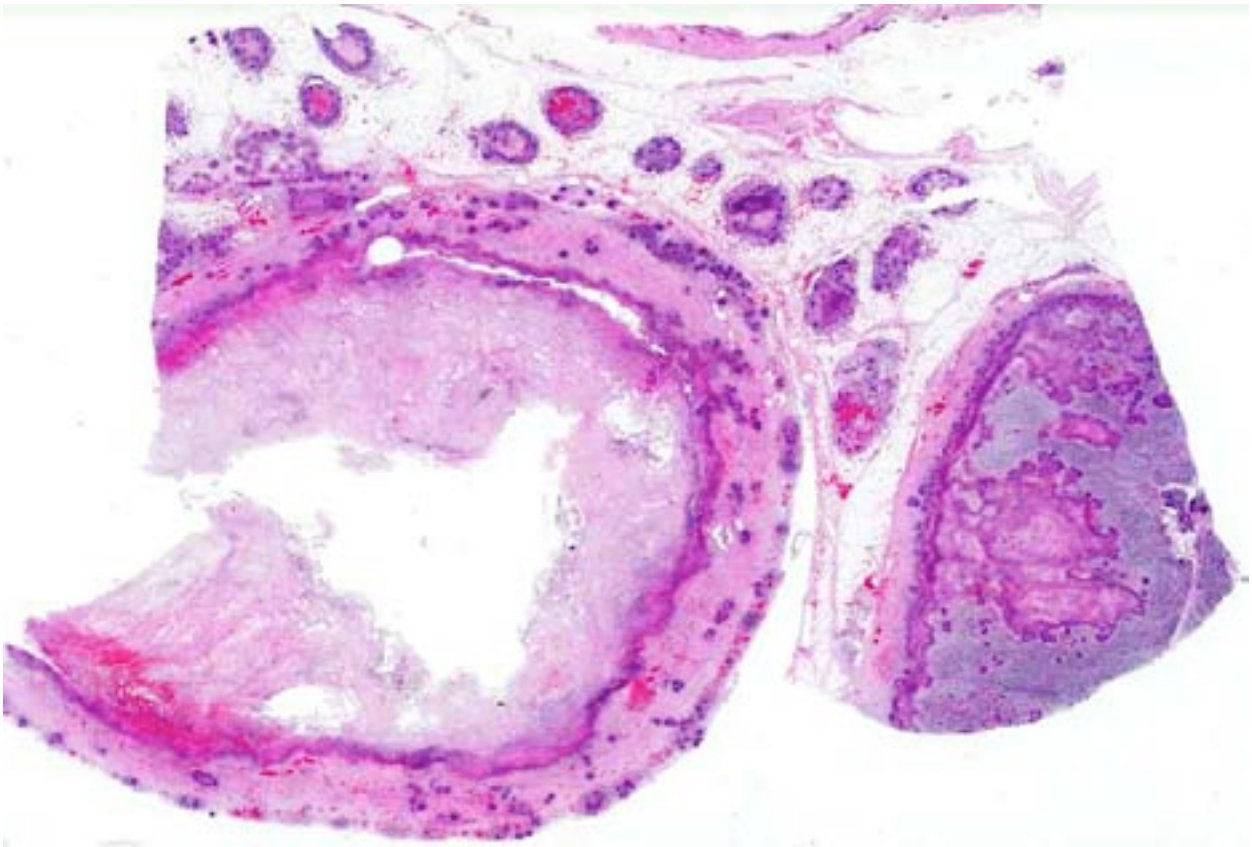

3-1. Jejunum and mesentery, black buck: There is diffuse circumferential lytic and coagulative necrosis of the intestinal mucosa (left); only eosinophilic necrotic remnants of villi remain, outlined at their base by hemorrhage and coalescing areas of lytic necrosis. There are numerous foci of lytic necrosis scattered throughout the adjacent layers of the intestine, mesentery, and mesenteric lymph node. (HE 0.63X)

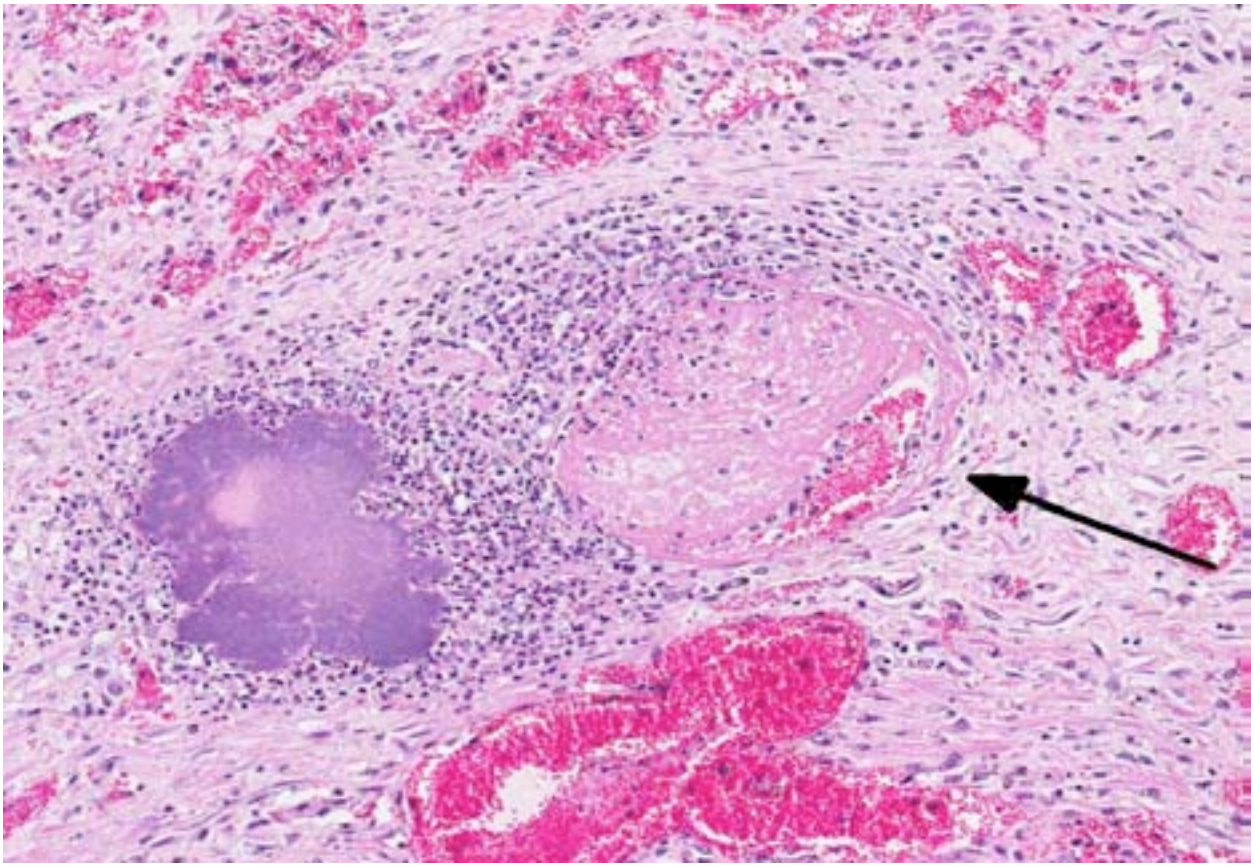

3-2. Jejunum, black buck: Foci of lytic necrosis throughout the slide contain large colonies of 2-3 µm bacilli, characteristic of Yersinia species. The submucosal veins within the jejunum often contain fibrin thrombi, and walls contain degenerate neutrophils and cellular debris (vasculitis). (HE 80X)

hinders detailed evaluation of the superficial mucosa. Fibrin thrombi are present in many vessels (probable lymphatics). Adipose tissue and lymph node have similar areas of necrosis with large numbers of bacteria.

Contributor's Morphologic Diagnosis: Small intestine, lymph node, adipose tissue: Severe regionally extensive acute necrotizing enteritis, lymphadenitis, and steatitis with intralesional bacteria (etiology: Yersinia pseudotuberculosis).

Contributor's Comment: Yersinia pseudotuberculosis (YPT) is a gram-negative facultative anaerobic intracellular bacterium that is found worldwide. It causes sporadic disease in domestic animals and humans, and has been isolated from a wide range of species in both captive situations and the wild. In domestic animals infection usually results in sporadic cases, with occasional outbreaks. In wild rodents and birds epidemics are common. YPT may cause abortion in cattle, sheep, and goats.[1,2]

YPT, Yersinia enterocolitica (YE) and Yersinia pestis (YP) share 97% of their genomes as well as a tropism for lymph nodes. Despite this, manifestations of disease can be quite different for the three bacteria, presumably due to a combination of shared and unique chromosomal and plasmid-derived virulence factors.[3]

Less is known specifically about the pathogenesis of YPT infections than that of its close relative YE. As demonstrated with YE, following ingestion of contaminated food or water, bacteria adhere to distal small intestinal epithelial cells, cross the intestinal barrier using M cells which leads to bacterial replication in Peyer's patches. Spread to mesenteric and other distant lymph nodes is common. There is little host response to bacterial replication in the first 36-48 hours following infection. Subsequently, an influx of activated phagocytes induces cytokine production and tissue necrosis. Septicemic spread from the distal ileum to the spleen and liver is relatively common.[3]

YPT is frequently isolated from feces of normal cattle. The organism may be shed in the feces by carrier animals in the group, or the environment may be contaminated by birds and rodents. The organism can survive and grow in cool environmental temperatures. Disease may be related to compromise of cell-mediated immunity and outbreaks may occur when animals are stressed (e.g., breeding, bad weather, poor nutritional condition). Clinical signs include mild diarrhea, severe hemorrhagic diarrhea, vague illness, or sudden death. Gross lesions may also be variable, with little noted in mild cases. More severe cases have hemorrhage in the intestine and enlarged hemorrhagic mesenteric lymph nodes. White foci of necrosis may be found in other organs, especially the liver and spleen.[1,2]

Diagnosis is based on the presence of characteristic lesions and isolation of the organism. Y. pseudotuberculosis prefers to grow at temperatures lower than the standard culture temperature of 37 degrees C, and since it may not be isolated using routine culture techniques, the laboratory should be notified when infection with this agent is suspected.[1,2]

Y. pseudotuberculosis also causes acute gastroenteritis and mesenteric lymphadenitis in humans. It is a food borne illness, and in the United States is much less common than Yersinia enterocolitica. In a review of FoodNet sites covering the period 1996-2007, 18 confirmed cases were identified, with an average annual incidence of 0.04 cases per 1,000,000 persons. Cases are probably underreported because less invasive forms are not recognized, and because of culture requirements for this organism. Infections in humans are less common in the United States than other countries.[4]

Our experience with this organism is similar to what is reported in the literature. We generally have seen sporadic cases, but this blackbuck was a case in an outbreak of 15 animals located in multiple enclosures, most of which are large and house multiple species. Attempts to isolate YPT from non-collection animals (e.g., wild rabbits and birds) were unsuccessful. In this blackbuck YPT was also isolated from the uterus, and mild fibrinous endometritis was present. Inflammation with bacteria was also seen in lung, liver, spleen, and urinary bladder.

JPC Diagnosis: Small intestine and mesenteric lymph node: Enteritis and lymphadenitis, necrosuppurative, subacute, diffuse, severe with mesenteric steatitis and numerous large colonies of bacilli.

Conference Comment: To open, participants conducted a cursory review of other types of pathogenic large colony-forming bacteria commonly encountered in veterinary medicine. Yersinia sp., Actinomyces sp., Actinobacillus sp., Corynebacterium sp., Staphylcoccus sp. and Streptococcus sp. are well known for the production of extensive bacterial colonies. Most are Gram-positive bacteria, with the exception of Yersinia sp. and Actinobacillus sp.

Next, the conference moderator expanded upon the contributor's adept description of the pathogenesis of Yersinia pseduotuberculosis (YPT) and participants further analyzed several of its virulence factors. Transmission of YPT is generally fecal-oral, with rare transmission via inhalation. Yersinia adhesion A protein, or YadA (encoded on the pYV virulence plasmid) and invasin (encoded by the chromosomal inv locus) facilitate bacterial contact for invasion of host small intestinal M-cells; YadA adheres to extracellular matrix proteins such as fibronectin, collagen and laminin, while invasin binds to host cell b1 integrins. Next, Yops (Yersinia outer membrane proteins) come into play. YopB & YopD form a pore in the host cell membrane which allows the type three secretion system (T3SS) injectisome, which is also encoded on the pYV virulence plasmid and has a structure similar to flagella, to inject effector Yops into the host cell.[3]

The RNA chaperone protein Hfq is important in the production of T3SS effectors as well as intracellular survival. The PhoP/Q system (chromosomally encoded) stimulates growth and survival in macrophages as well as delayed macrophage activation via reduction in the stimulatory capacity of LPS. Superantigenic toxin YPM contributes to systemic infection by inducing T-cell proliferation and cytokine production. Various Yop proteins inhibit the host inflammatory response via alteration of phagocyte function, inhibition of signal transduction and disruption of the cytoskeleton. YopM sequesters caspase-1, which blocks activation of pro-inflammatory cytokines and YadA inhibits the

classic complement and lectin pathways. YopP/J induces apoptosis of host cells by inhibiting the inflammatory and pro-survival actions of LPS and directly activating caspases. So, overall, YPT infections are characterized by an initial "quiet" 36–48 hour period of bacterial replication with apoptosis and minimal host response, followed by a flood of phagocytic cells and an acute inflammatory response characterized by cytokine production and tissue necrosis.[3] This is illustrated by the abundant necrosis and large colonies of bacilli exhibited histologically.

To close, participants briefly discussed the role of exogenous superantigen in infection and immunity (such as the YPM toxin produced by *Y. pseudotuberculosis* in this case). Superantingens, which are often produced by Gram-negative bacteria, bind the V_b domain of the T-lymphocyte receptor (TCR) with the a chain of a class II major histocompatibility complex (MHC). This occurs outside of the normal antigen binding site and results in polyclonal T-lymphocyte activation regardless of antigen specificity, as well as massive cytokine release.[5]

Contributing Institution: Wildlife Disease Laboratories
Institute for Conservation Research, San Diego Zoo Global
http://www.sandiegozooglobal.org

References:

1. Brown C, Baker DC, Barker IA. Alimentary system. In: Maxie, MG, ed. *Jubb, Kennedy, and Palmer's Pathology of Domestic Animals*. 5th ed., vol 2. Philadelphia, PA: Elsevier; 2007:204-205.
2. Valli VEO. Hematopoietic system. In: Maxie, MG, ed. *Jubb, Kennedy, and Palmer's Pathology of Domestic Animals*. 5th ed., vol 3. Philadelphia, PA: Elsevier; 2007:298-299.
3. Galindo CL, Rosenzweig JA, Kirtley ML, Chopra AK. Pathogenesis of Y. enterocolitica and Y. pseudotuberculosis in human yersiniosis. *J Pathog*. 2011:doi:10.4061/2011/182051.
4. Long C, Jones TF, et al. Yersinia pseudotuberculosis and Y. enterocolitica infections, FoodNet, 1996-2007. *Emerg Infec Dis*. 2010;16(3):566-567.
5. Snyder PW. Diseases of immunity. In: McGavin MD, Zachary JF, eds. *Pathologic Basis of Veterinary Disease*. 5th ed. St. Louis, MO: Mosby Elsevier; 2007:270.

CASE IV: DR30 (JPC 4032701).

Signalment: 11-year-old male rhesus macaque, (Macaca mulatta).

History: Presented for chronic weight loss (9% loss in previous 10 weeks) and past history of vaccination with commercial Fluvax® and trauma to the hand that required surgical repair.

Gross Pathology: Thin male monkey presented with a bulging multinodular mass on the anterior pole of the right kidney measuring 1x2.3 cm. Suppurative exudate was apparent on cut section.

Laboratory Results: Previous viral testing indicated positive tests for CMV, LCV, RRV, and SV40. All previous TB skin tests were negative. CBC and clinical chemistry were unremarkable. Routine culture of the mass identified a mixture, in order of most abundant, of hemolytic, coagulase negative staphylococcus, Streptococcus fecalis, gamma and alpha hemolytic streptococcus, and Corynebacterium sp. Stains of smears for AFB were negative.

Histopathologic Description: Kidney: The kidney contains multiple variably sized sometimes confluent pyogranulomas that compress and ablate parenchyma from the medulla to the capsule. Pyogranulomas have thin peripheral concentric fibrous rings infiltrated with lymphocytes and plasma cells that surround sheets of epithelioid macrophages, numerous multinucleated giant cells, and a central core filled with large numbers of neutrophils and eosinophils. Within many of the granulomas and often associated with giant cells are spherical yeast-like cells measuring 10-20 microns in diameter with double-contoured walls and a smaller dense granular central nucleoid. Rare budding forms are observed. GMS stain highlights the outer wall. Gram stain demonstrates gram positive cocci within phagocytic cells. Proximal tubules have swollen epithelium with granular sometimes vacuolated cytoplasm, while scattered groups of ectatic distal tubules contain hyaline protein and cellular casts.

Contributor's Morphologic Diagnosis: Rhesus macaque, kidney: Pyogranulomatous inflammation with intralesional Blastomyces dermatitidis and Staphylococcus sp. and with tubular degeneration and cast formation.

Contributor's Comment: Blastomycosis is a disseminated or localized mycotic infection of primarily man and dogs in the Ohio and Mississippi River basins of North America and in Africa, and is caused by Blastomyces dermatitidis.[1,2] It is a dimorphic fungus found in soil in mycelial form but transforms into a pathogenic yeast at body temperature and is transmitted by inhalation or inoculation.[3] Common sites of infection are lung, skin, bone, male urogenital system, particularly prostate and testis[4] with less frequent distribution to liver,

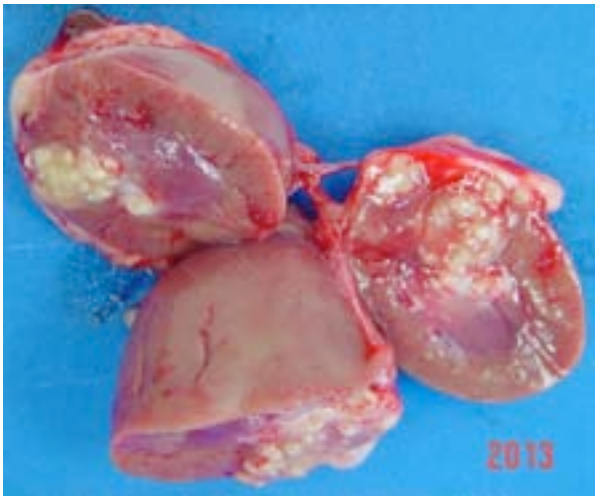

4-1. Kidney, rhesus macaque: This male monkey presented with a bulging multinodular mass on the anterior pole of the right kidney measuring 1x2.3 cm. Suppurative exudate was apparent on cut section. (Photo courtesy of: Tulane National Primate Research Center; Department of Comparative Pathology; 18703 Three Rivers Road; Covington, LA 70433)

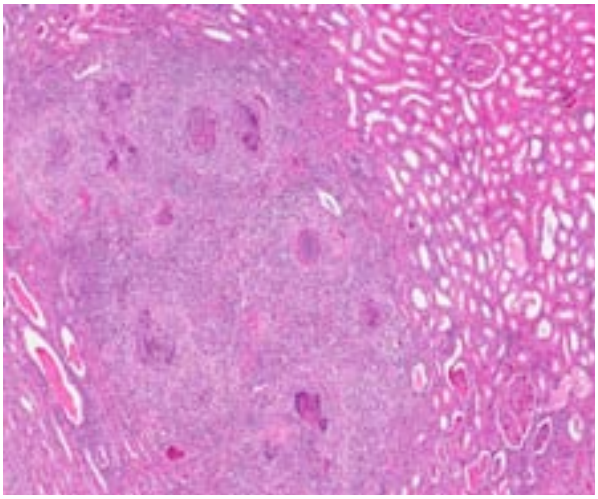

4-2. Kidney, rhesus macaque: Approximately 60% of the cortex is replaced by multifocal to coalescing pyogranulomas which contain large multinucleated giant cell macrophages which range up to 100 µm in diameter. (HE 63X)

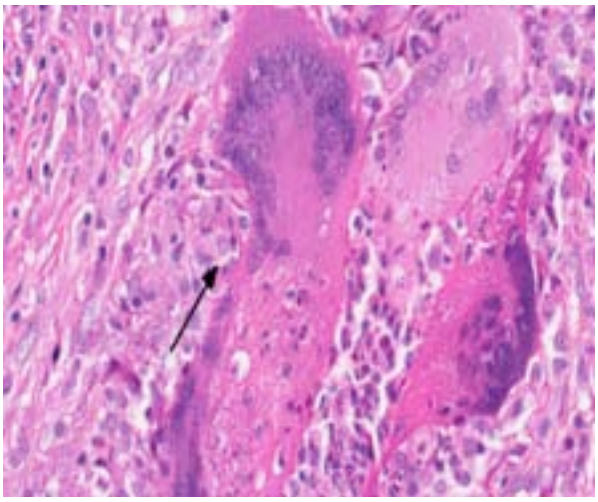

4-3. Kidney, rhesus macaque: The pyogranulomas are centered on moderate numbers of intra- and rarely extrahistiocytic yeasts (arrow) which measure 12-15 µm with a 2-3 µm clear cell wall (consistent with Blastomyces dermatitidis. (HE 400X)

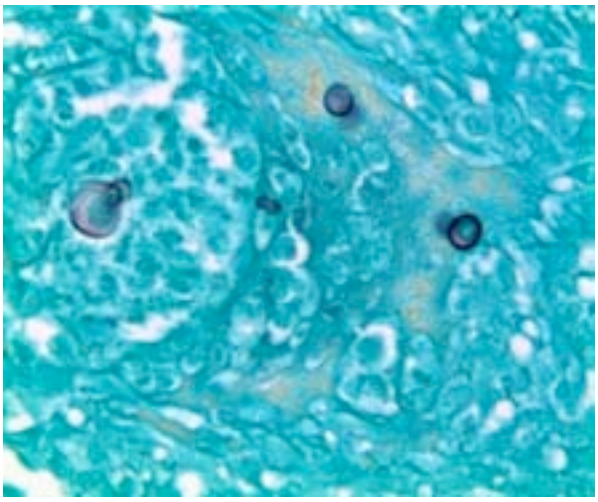

4-4. Kidney, rhesus macaque: Silver staining more clearly outlines the cell wall of Blastomyces dermatidis. (GMS 400X) (Photo courtesy of: Tulane National Primate Research Center; Department of Comparative Pathology; 18703 Three Rivers Road; Covington, LA 70433)

spleen, and lymph nodes.[5] It is rarely reported in monkeys; the first report in monkeys described an animal that originated from our colony.[6] We subsequently have seen several additional cases, which like the first report, developed lesions several years after leaving our breeding facility and contact with soil (Didier, unpublished). Serology[9] and PCR[11] may aid in the clinical diagnosis and recent work has associated clinical phenotypes of human infection with genetic variants of B. dermatitidis.[12]

JPC Diagnosis: Kidney: Pyogranulomas, multiple and coalescing, with renal capsular fibrosis, perirenal granulomatous steatitis and numerous yeasts, etiology consistent with Blastomyces dermatitidis.

Conference Comment: Participants summarized the key morphologic features used to differentiate Blastomyces dermatitidis from other pathogenic dimorphic fungi of veterinary significance, including Cryptococcus neoformans, Histoplasma capsulatum, Sporothrix schenckii, *Coccidioides immitis* and *posadasii* and *Penicillium marnefii*. B. dermatitidis appears in animal tissues, both extracellularly and intracellularly within macrophages and neutrophils, as an 8-20 µm round, yeast, with a double contoured, often refractile cell wall and broad-based budding. It stains with GMS, Gridleys and PAS. C. neoformans, which is also found in tissue in the yeast form, ranges from 2-20 µm and can be differentiated by its thick carminophilic capsule and narrow-based budding. Rare forms of *C. neoformans* lack a capsule, making definitive identification of these yeasts a challenge. H. capsulatum is smaller (2-6 µm) and typically intrahistiocytic, usually with many organisms in each macrophage and has narrow-based budding and a shrinkage-artifact "halo" on H&E sections; this yeast has no true capsule. S. schenckii appears in tissues as a 2-6 µm, pleomorphic, often cigar-shaped intracellular and extracellular yeast. It stains well with both PAS and GMS; however, yeasts are often difficult to see on H&E-stained sections in most species other than cats, in which they are usually readily visible. *C. immitis* and *posadasii* reproduce by endosporulation and have a characteristic tissue section appearance as 20-200 µm spherules, with a double-contoured wall and numerous 2-5 µm endospores.[2] As emphasized by one participant, *Coccidioides* sp. is another fungal organism occasionally encountered in research monkeys.[7] *Penicillium marnefii*, which is emerging as an important pathogen of immunosuppressed humans in Southeast Asia, has also been identified in animals. *P. marnefii* is found both intracellularly and extracellularly; yeasts are 2-3 µm and multiply by binary fission, so elongated cells up to 13 µm are occasionally present.[10]

The most important virulence factor associated with *B. dermatitidis* is the adhesin BAD1. BAD1 has multiple functions and is secreted exclusively by the yeast form of *Blastomyces*. It mediates adhesion to host macrophages via calcium-

dependent attachment to chitin in the yeast cell wall and binding to CR3 and CD14 on phagocytic cells. It also acts as an immunomodulator by suppressing the generation of TNF-α, a pro-inflammatory cytokine important in defense against fungal infections.[8]

One interesting aspect of this case is that this monkey developed clinical signs of blastomycosis several years after suspected exposure. Since the infective (mycelial) form of B. dermatitidis is generally found in soil, and this animal was housed entirely indoors, it is presumed that he was initially infected while housed outdoors at the breeding facility, and then harbored the organism for several years before developing clinical disease.[6] As pointed out by the contributor, there have been several similar reports, which suggest the potential for long periods of subclinical infection with *B. dermatitidis* before the manifestation of clinical disease.

Contributing Institution: Tulane National Primate Research Center
Department of Comparative Pathology
18703 Three Rivers Road
Covington, LA 70433
http://www.tnprc.tulane.edu/

References:

1. Bradsher RW. Histoplasmosis and blastomycosis. *Clin Inf Dis*. 1996;22(Suppl 2):S102-11.
2. Caswell JL, Williams KJ. Respiratory system. In: Maxie MG, ed. *Jubb, Kennedy, and Palmer's Pathology of Domestic Animals.* 5th ed., vol 2. St. Louis, MO: Elsevier Limited; 2007:523-653.
3. Khansari N, Segre D, Segre M. Diagnosis of histoplasmosis and blastomycosis by an antiglobulin hemagglutination test. *Am J Vet Res*. 1982;43(12):2279-2283.
4. Legendre AM. Canine blastomycosis: a review of 47 clinical cases. *J Am Vet Assoc*. 1981;178:1163-1168.
5. Motswaledi HM, Monyemangene FM, Maloba BR, et al. Blastomycosis: a case report and review of the literature. *Inter J Derm*. 2012;51:1090-1093.
6. Meece JK, Anderson JL, Gruszka S, et al. Variation in clinical phenotype of human infection among genetic groups of Blastomyces dermatitidis. *J Inf Dis*. 2013;207:814-822.
7. Mense MG, Batey KL, Estep S, Armstrong K, Fleurie G, Suttie AW. Disseminated Coccidiomycosis in a Cynomolgus Monkey (Macaca fasicularis). *J Primatol*. 2013;2(2):1-3.
8. Rappleye CA, Goldman WE. Defining virulence genes in the dimorphic fungi. *Annu Rev Microbiol.* 2006;60:281-303.
9. Sidamonidze K, Peck MK, Perez M, et al. Real-time PCR assay for identification of Blastomyces dermatitidis in culture and in tissue. *J Clin Microbio*. 2012;50(5):1783-1786.
10. Vanittanakom N, Cooper CR, Fisher MC, Sirisanthana T. *Penicillium marneffei* infection and recent advances in the epidemiology and molecular biology aspects. *Clin Microbiol Rev*. 2006;19(1):95-110.
11. Wilson RW, van Dreumel AA, Henry JNR. Urogenital and ocular lesions in canine blastomycosis. *Vet Pathol*. 1973;10:1-11.
12. Wilkinson LM, Wallace JM, Cline JM. Disseminated blastomycosis in a rhesus monkey (Macaca mulatta). *Vet Pathol*. 1999;36:460-462.

WEDNESDAY SLIDE CONFERENCE 2013-2014

Conference 2

18 September 2013

CASE I: C1707 (JPC 4033366).

Signalment: 11-month-old male Border Collie dog (*Canis familiaris*).

History: The dog had a history of poor growth, weight loss, chronic upper respiratory infection and cyclical pyrexia.

Gross Pathology: There were multifocal pale yellow to white firm irregular nodules (2-3 mm in diameter) within the myocardium and on the epicardial and endocardial surfaces. Similar nodules (1-2 mm in diameter) were present on the capsular and cut surfaces of both kidneys. The lungs were diffusely mottled dark red and there was a focal firm mass (1.5 x 1.5 x 1 cm) with a reddish grey cut surface within one lung lobe. On the meningeal surface of the brain, there were multiple pale red foci.

Laboratory Results: Fungal culture of lung and brain yielded *Scedosporium prolificans*.

Histopathologic Description: Heart: Within the myocardium, there are multiple 1-2 mm diameter foci of acute coagulative necrosis characterized by large aggregates of fibrin admixed with mostly degenerate neutrophils, fewer macrophages, karyorrhectic debris and numerous intralesional fungal hyphae. The hyphae are approximately 5 µm in diameter, septate, with parallel walls and haphazard or dichotomous branching; multifocally there are ovoid conidia (approximately 5 x 8 µm). Within these areas, cardiomyofibres are fragmented and exhibit deeply eosinophilic sarcoplasm with loss of cross-striations. Within the surrounding myocardium cardiomyofibres are frequently separated by clear spaces (edema), or dissected by abundant fibrin aggregates with scattered neutrophils and macrophages. Interstitial blood vessels are often lined by plump (reactive) endothelial cells.

Contributor's Morphologic Diagnosis: Heart: Myocarditis, suppurative and necrotizing, multifocal, moderate, acute with intralesional fungal hyphae (*Scedosporium prolificans*).

Contributor's Comment: Histological examination of further tissues from this case showed necrotic foci with fungal hyphae within the lungs, kidney, liver, pancreas, pituitary gland and cerebral cortex. The fungal morphology was compatible with *Scedosporium prolificans* as obtained by fungal culture from both lungs and brain.

Scedosporium prolificans (previously *Scedosporium inflatum*) is a filamentous fungus within the family

1-1. Heart, canine: Within the myocardium and on the epicardial and endocardial surfaces there were multifocal pale yellow to white firm irregular nodules (2-3 mm in diameter). (Photo courtesy of: The Royal Veterinary College, Department of Pathology and Pathogen Biology, Hawkshead Lane, Hatfield, AL9 7TA, United Kingdom, www.rvc.ac.uk)

1-2. Heart, canine: Areas of necrosis and inflammation are randomly scattered throughout the section. (HE 0.63X)

Microascaceae.[1] In the environment it has been isolated from soil and potted plants.[1] The organism is increasingly recognized as a cause of disseminated fungal infections in immunocompromised human patients. Treatment of infections is challenging due to the resistance of *S. prolificans* to most antifungal agents.[1] There are rare reports of *S. prolificans* infection in animals. In dogs *S. prolificans* has been isolated from a German Shepherd dog with a disseminated infection involving kidney, heart, bone marrow, skeletal muscle, liver, lung, spleen, lymph nodes and pancreas.[5] In addition one case has been reported of a beagle with osteomyelitis in which *S. prolificans* was found to have disseminated to the lungs.[7]

One case of *S. prolificans* infection in a horse associated with osteomyelitis and arthritis has also been described.[9] Musculoskeletal infections are also a common presentation in humans.[1] Further isolates characterized as *S. prolificans* were obtained from eye scrapings of two horses and from a draining sinus in a cat.[8]

In tissues the morphology of *Scedosporium* spp. is similar to that of *Aspergillus* spp. although *Scedosporium* spp. exhibit haphazard branching with less frequent dichotomous branching.[6] Culture of the fungus allows more definitive identification; the colonies grow rapidly and exhibit a moist, felty appearance with initially a white color that becomes olive-grey to black. Microscopically the conidiophores display distinctly swollen bases (hence the previous name *S. inflatum*) with ovoid conidia.

If material for culture is not available, identification of *Scedosporium* spp. by PCR is also possible.[4]

Disseminated infections with opportunistic fungi in dogs have been associated with a number of different fungal species. In particular, systemic infections with *Aspergillus terreus* have commonly been described in German Shepherd dogs. Breed-associated abnormalities in IgA levels or function have been reported but have not been conclusively proven to be the cause of the increased susceptibility to fungal infections.[2,11]

The Border collie presented in the current case had shown poor growth from birth and persistent upper respiratory disease; however, an underlying immunodeficiency was not established.

Other fungal species isolated from dogs with disseminated infections include *Penicillium* sp., *Paecilomyces* sp., *Chrysosporium* sp and *Pseudoallescheria boydii* or *Scedosporium apiospermum* (the asexual form of *P. boydii*).[10]

JPC Diagnosis: Heart: Myocarditis, necrotizing, acute, random, marked with numerous fungal hyphae and conidia.

Conference Comment: Fungi capable of causing disseminated disease are generally divided into two groups: the truly pathogenic, such as the dimorphic

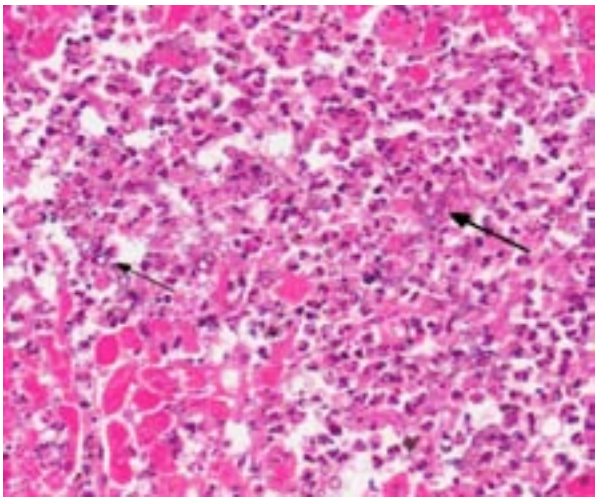

1-3. Heart, canine: Areas of necrosis contain numerous fungal hyphae (right) and conidia (left) which are admixed with numerous degenerate neutrophils and cellular debris. Adjacent myofibers are either degenerate or necrotic. (HE 400X)

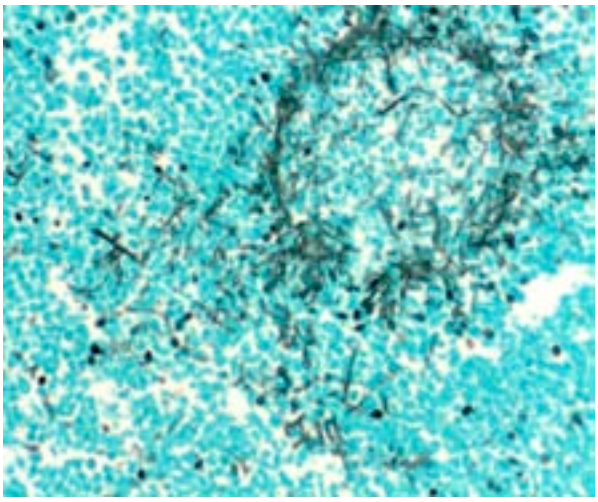

1-4. Kidney, canine: A Gomori methenamine silver stain demonstrates the fungi. Fungal hyphae measure 6-8 µm in diameter, pauciseptate, with non-parallel walls and dichotomous to right angle branching. There are numerous round 10 µm conidia intermixed among the hyphae, characteristic of Scedosporium prolificans.

fungi *Blastomyces dermatitidis*, *Histoplasma capsulatum* or *Coccidioides immitis*, and the opportunistic pathogens, such as *Aspergillus fumigatus* or *Candida albicans*. By and large, the opportunistic fungi are ubiquitous, saprophytic organisms which tend to cause disease in immunocompromised individuals.[10] As noted by the contributor, disseminated, opportunistic fungal infections in dogs (especially German shepherds), are generally attributed to *Aspergillus* sp., such as *Aspergillus terreus*, however in recent years *Scedosporium prolificans* has gained notoriety as an emerging opportunistic pathogen in both humans and animals. In addition to *Aspergillus* sp., other differential diagnoses for *S. prolificans* include: *Candida* sp., *Zygomycetes* such as *Absidia*, *Rhizopus* and *Mucor* sp., or non-fungal agents like *Pythium insidiosum*.

S. prolificans is a filamentous, non-pigmented, parallel-walled fungus with septate, 3-5 µm, haphazardly branching hyphae (sometimes described as a "letter-H" pattern) with lemon-shaped conidiophores from which a small cluster of single-cell conidia emerges.[1] *Scedosporium* will produce conidia in solid non-aerated tissues,[5] such as the myocardium in the present case. *Aspergillus* has a similar size and tissue morphology, and it also produces conidiophores, or fruiting bodies, but unlike *Scedosporium*, these are generally more round than lemon-shaped and they only occur in aerated tissues like ectatic bronchi or the surface of skin wounds.[6] *Candida* sp. appears in tissue in both hyphal and budding yeast forms, which could be confused with *Scedosporium*, however the presence of pseudohyphae is relatively common in candidiasis and rare in *S. prolificans* infection.[6] Like *S. prolificans,* zygomycete hyphae may also appear in a "letter-H" pattern,[6] though their hyphae are more broad (6-25 µm) and pauciseptate with non-parallel walls and non-dichotomous branching.[3] *S. prolificans* may also be mistaken for *Pythium insidiosum,* which, although it is an oomycete rather than a true fungus, produces 2-10 µm, pauciseptate hyphae with non-parallel walls and non-dichotomous branching.[3]

S. prolificans is resistant to many anti-fungal drugs and generally carries a grave prognosis, so differentiating it from other opportunistic fungi or fungal-like organism is imperative.[6] Although *Scedosporium* has several unique morphologic characteristics, definitive diagnosis with histopathology alone is often difficult to achieve, so culture and/or PCR are critical.

Contributing Institution: The Royal Veterinary College
Department of Pathology and Pathogen Biology
Hawkshead Lane
Hatfield
AL9 7TA
United Kingdom
www.rvc.ac.uk

References:

1. Cortez KJ, Roilides E, Quiroz-Telles F, et al. Infections caused by *Scedosporium* spp. *Clinical Microbiology Reviews*. 2008;21:157-197.
2. Day MJ, Penhale WJ, Eger CE, et al. Disseminated aspergillosis in dogs. *Aust Vet J*. 1986;63:55-59.
3. Ginn PE, Mansell JEKL, Rakich PM. Skin and appendages. In: Maxie MG, ed. *Jubb, Kennedy, and Palmer's Pathology of Domestic Animals*. Vol 1. 5th ed. Philadelphia, PA: Elsevier Saunders. 2007:695-708.
4. Harun A, Blyth CC, Gilgado F, Middleton P, Chen SC-A, Meyer W. Development and validation of a multiplex PCR for detection of *Scedosporium* spp. in respiratory tract specimens from patients with cystic fibrosis. *J Clin Microbiol*. 2011;49:1508-1512.
5. Haynes SM, Hodge PJ, Tyrrell D, Abraham LA. Disseminated *Scedosporium prolificans* infection in a German Shepherd dog. *Aust Vet J*. 2012;90:34-38.
6. Kimura M, Maenishi O, Ito H, Ohkusu K. Unique histological characteristics of *Scedosporium* that could aid in its identification. *Pathology International*. 2010;60:131-136.
7. Salkin IF, Cooper CR, Bartges JW, Kemna ME, Rinaldi MG. *Scedosporium inflatum* osteomyelitis in a dog. *J Clin Microbiol*. 1992;30:2797-2800.
8. Salkin IF, McGinnis MR, Dykstra MJ, Rinaldi MG. *Scedosporium inflatum*, an emerging pathogen. *J Clin Microbiol*. 1988;26:498-503.
9. Swerczek TW, Donahue JM, Hunt RJ. *Scedosporium prolificans* infection associated with arthritis and osteomyelitis in a horse. *Journal of the American Veterinary Medical Association*. 2001;218:1800-1802,1779.
10. Watt PR, Robins GM, Galloway AM, O'Boyle DA. Disseminated opportunistic fungal disease in dogs: 10 cases (1982-1990). *Journal of the American Veterinary Medical Association*. 1995;207:67-70.
11. Whitbread TJ, Batt RM, Garthwaite G. Relative deficiency of serum IgA in the German Shepherd dog: a breed abnormality. *Res Vet Sci*. 1984;37:350-352.

CASE II: NCAH 2013-2 (JPC 4033380).

Signalment: Adult male Jersey bull (*Bos Taurus*).

History: The bull was presented for slaughter at a US federally-inspected slaughter plant, passed ante-mortem inspection, and was retained for further diagnostic testing after lesions resembling tuberculosis were identified during post-mortem examination.

Gross Pathology: Multifocally within the lung there were firm, homogenous, white to tan nodules up to 2.5 cm in diameter scattered throughout the parenchyma. The medial retropharyngeal and thoracic lymph nodes were enlarged and edematous with multifocal to coalescing yellow caseous granulomas.

Laboratory Results: *Mycobacterium avium* complex was isolated by culture. PCR from formalin-fixed, paraffin-embedded tissue was negative for IS6110 (*Mycobacterium tuberculosis* complex), 16S rDNA (*M. avium* complex), and IS900 (*M. avium paratuberculosis*).

Histopathologic Description: Lung: Effacing 70-90% of the section are multiple, often coalescing, granulomas centered on homogenous eosinophilic cellular debris (caseous necrosis) that contain central basophilic granular material (mineral). Necrotic foci are surrounded by large numbers of epithelioid macrophages, multinucleated giant cells (Langhans' type), and smaller numbers of lymphocytes, plasma cells, and neutrophils. Langhans' giant cells range from 25 µm to over 100 µm in diameter and may contain over 50 nuclei. Granulomas are surrounded by fibrocytes, fibrous connective tissue, free erythrocytes, edema, and cellular debris. Similar inflammatory cells (without giant cells) and exudates expand alveolar septa and peribronchiolar areas. The interlobular septa and pleura are expanded by edema, and small amounts of inflammatory exudates. Very small numbers of acid-fast bacilli (AFB), up to 5 µ m long, were present within necrotic foci and the cytoplasm of multinucleated giant cells of New Fuchsin-stained sections; bacteria fluoresced in Acridine Orange/ Auramine O-stained sections.

Lymph node: Granulomatous lesions are similar to those described in the lung.

Contributor's Morphologic Diagnosis: Lung: Pneumonia, granulomatous, multifocal to coalescing, chronic, severe, with intra- and extra-histiocytic acid-fast bacilli.

Lymph node: Lymphadenitis, granulomatous, multifocal to coalescing, chronic, severe, with intra- and extra-histiocytic acid-fast bacilli.

Contributor's Comment: *Mycobacterium bovis* causes tuberculosis in many mammals, including cattle and humans and is a zoonotic disease. Cattle slaughtered in USDA-inspected abattoirs undergo inspection by Food Safety Inspection Service (FSIS) personnel to insure that resultant products are safe

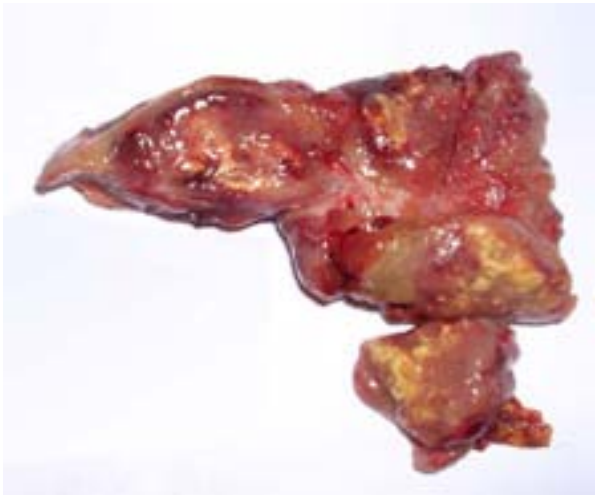

2-1. Thoracic lymph node, ox: The medial retropharyngeal and thoracic lymph nodes were enlarged and edematous with multifocal to coalescing yellow caseous granulomas. (Photo courtesy of: National Centers for Animal Health, 1920 Dayton Ave, Ames, IA 50010, http://www.aphis.usda.gov/animal_health/lab_info_services/about_nvsl.shtml)

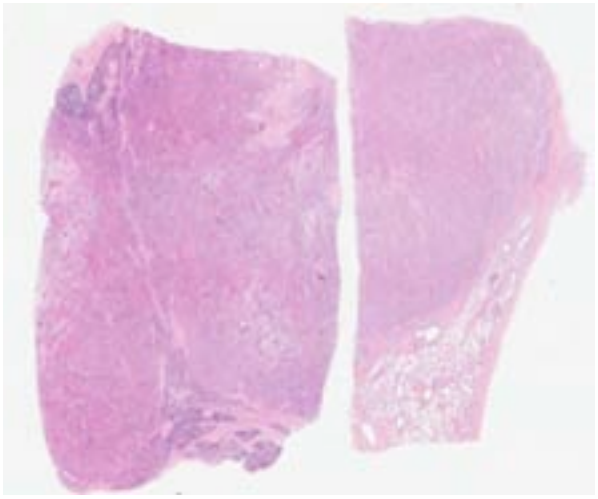

2-2. Lung and thoracic lymph node, ox: Approximately 95% of the lymph node (left) and 70% of the lung (right) is replaced by poorly formed granulomas. (HE 0.63X)

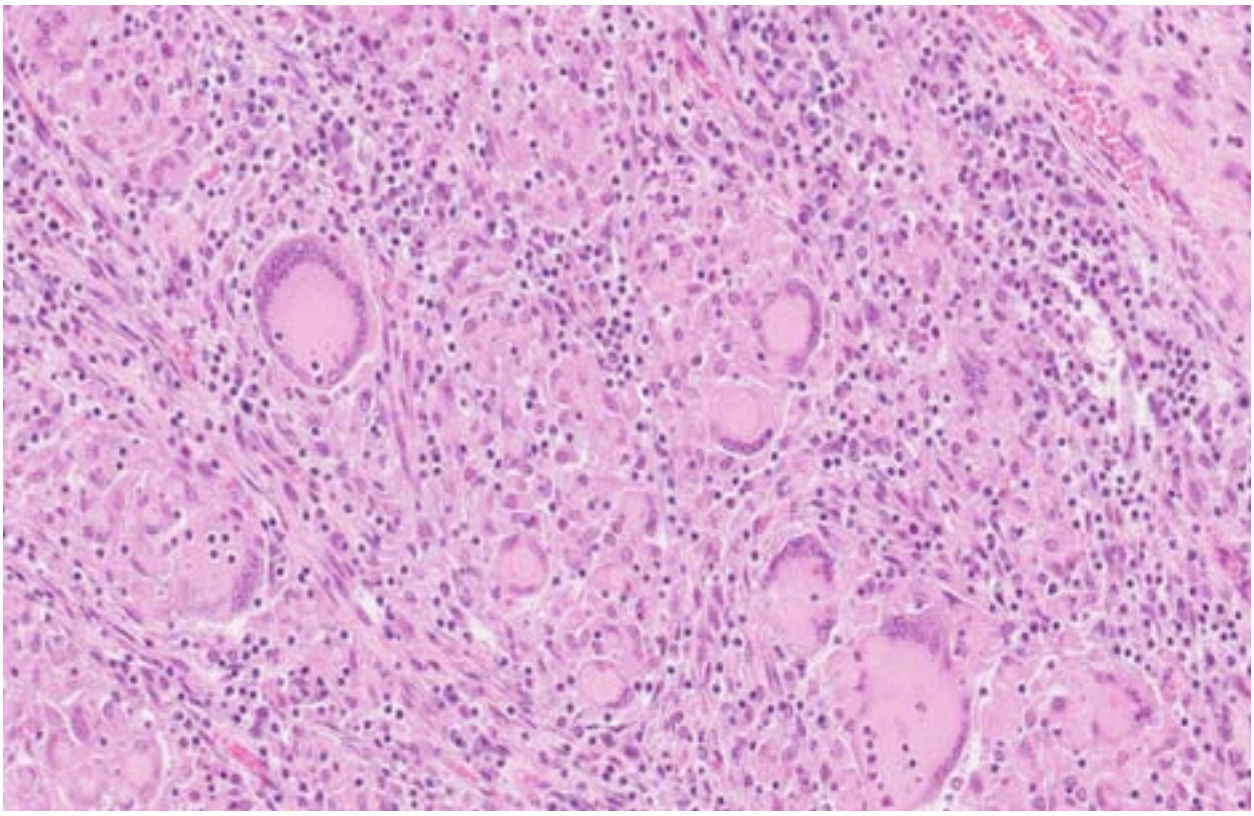

2-3. Lung, ox: Granulomas are poorly formed and contain numerous large (up to 75 µm) multinucleated giant cells of the Langhans type, lymphocytes, and plasma cells. (HE 220X)

and wholesome for entry into the retail market. In accordance with the USDA's Bovine Tuberculosis Eradication Program, FSIS personnel retain carcasses when granulomas resembling tuberculosis are identified. Suspect granulomas from these cattle are collected and submitted to the National Veterinary Services Laboratories (NVSL) for histopathology and culture.[12]

Microscopic lesions consistent with tuberculosis in cattle are often multicentric and coalescing with central areas of caseous necrosis and mineral. Epithelioid macrophages surround the necrosis and often included are small to moderate numbers of multinucleated giant cells with smaller numbers of lymphocytes, plasma cells, and occasional neutrophils.[2] The typical tuberculous lesion caused by *Mycobacterium bovis* has small to occasionally moderate numbers of acid fast bacteria present within the cytoplasm of macrophages and giant cells as well as areas of necrosis.[2]

Bovine cases fitting this description undergo additional testing using PCR on formalin-fixed, paraffin embedded (FFPE) tissue to test for mycobacterial DNA. Because the scope of the TB eradication program is focused on identifying *M. bovis*, primers used in the PCR are limited to those for *M. tuberculosis* complex (MTBC, of which M. bovis is a member), *M. avium* complex (MAC, common environmental mycobacteria) and *M. avium* subsp. *paratuberculosis* (MAP, the organism that causes Johne's disease in cattle). A recent report[12] of mycobacteria cultured from clinical samples submitted to the NVSL stated that the majority of mycobacteria cultured from cattle were *M. bovis* (32%) followed by *M. avium* complex (25.5%). The next most common species, *M. fortuitum*/*M. fortuitum* complex, comprised 10.1%.[12]

The microscopic features of the current case were consistent with bovine tuberculosis. FFPE tissue was tested by PCR for mycobacterial DNA using our primers for MTBC, MAC, and MAP, and tests were negative. False negative results for mycobacterial DNA can occur for a couple of reasons. First, formalin fixation causes irreversible cross-linking between DNA and protein, which increases as the tissue fixes over time. Over-fixation in formalin can reduce availability of DNA for the PCR, and result in a false negative finding.[5] Tuberculosis-suspect submissions from FSIS are

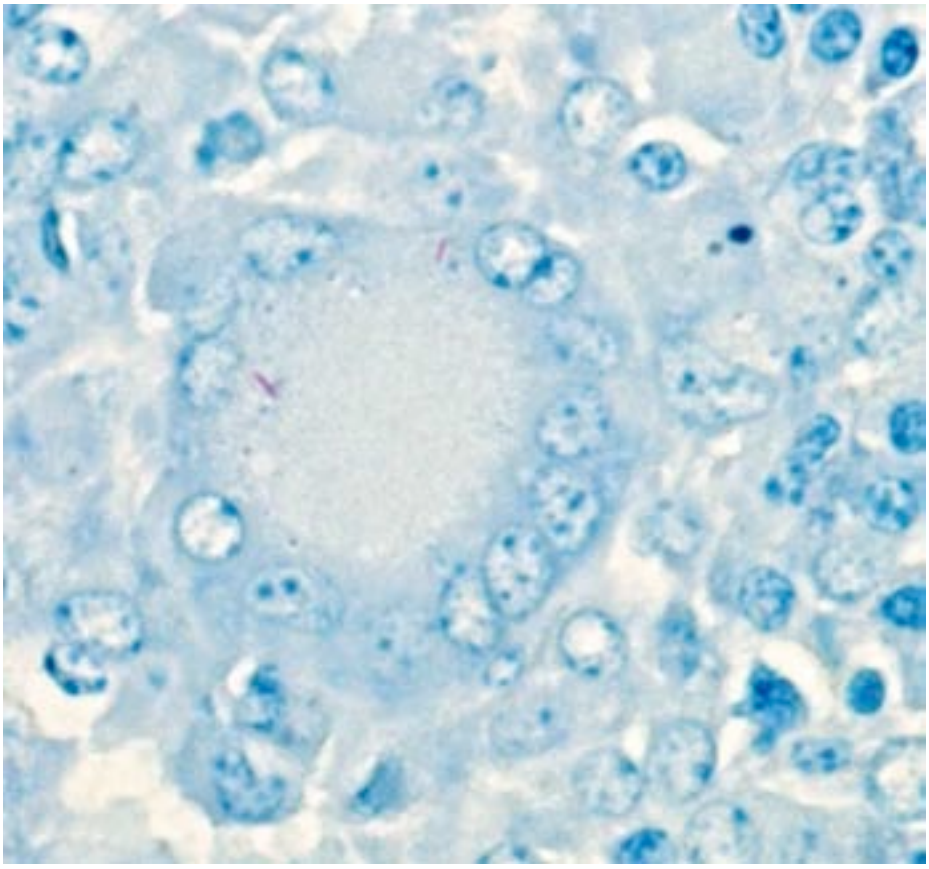

2-4. Lung, ox: Langhans cells contain few beaded acid-fast bacilli measuring up to 5 µm. (Fite-Furaco 400X)

shipped to the NVSL overnight; samples are cut-in immediately upon receipt and processed overnight for microscopic exam the next day. Because this case was an FSIS submission, over-fixation is unlikely as a cause for the false-negative PCR results. Second, false negative results may occur when there are extremely low numbers of AFB, as there were in this case.

M. avium complex was isolated from the tissues of this animal. Further subspeciation of the isolate was not performed. Culture is the gold standard for definitive diagnosis of bovine tuberculosis[1] and takes up to 10 weeks to complete with slow-growing mycobacteria.

Members of the *M. avium* complex are slow growing saprophytes commonly found in water, soil, and decaying vegetation.[4,6] MAC can cause tuberculosis-like disease in humans (particularly those who are immunocompromised) and birds.[4] Additionally, naturally occurring MAC infections have been reported in a tiger,[3] dogs,[7,9] pigs,[8] and a ferret with lymphoma.[10] Acid-fast bacilli are frequently numerous in lesions caused by MAC organisms,[6] but were uncommonly sparse in this case.

JPC Diagnosis: Lung and lymph node: Pneumonia and lymphadenitis, granulomatous, multifocal to coalescing, marked, with rare intra-histiocytic acid-fast bacilli.

Conference Comment: Although most sections contain vague, disorganized, poorly formed pulmonary granulomas, there is some slide variation, with the occasional presence of more distinct, classic granulomas. A classic granuloma has central core of necrosis, surrounded by epithelioid macrophages and multinucleated giant cells, variable numbers of lymphocytes and plasma cells, and a rim of reactive fibroblasts producing fibrous connective tissue.[1] One of the most striking features of this case is the massive size of the Langhans'-type multinucleated giant cells, which occasionally exceed 100 µm in diameter. Additionally, the few acid-fast bacilli present stain poorly with Ziehl-Neelsen and are more easily visualized with the modified acid-fast stain (Fite-Faraco), which the moderator noted is a common finding in mycobacteriosis.

Mycobacteria are broadly characterized as obligate and opportunistic pathogens. Obligate pathogens include the tuberculosis complex (MTBC: *M. tuberculosis* and *M. bovis*) and the leprosy group (*M. leprae* and *M. lepraemurium*), while opportunistic mycobacteria are subdivided into rapid-growing (e.g., *M. fortuitum*, *M. chelonae* and *M. smegmatis*) and slow-growing (e.g., *M. avium* complex (MAC)) mycobacteria.[1] Another classic taxonomic division, which excludes the tuberculosis complex, is the Runyon system. This divides mycobacteria into four groups based on pigment and growth rate; these are

summarized in Table 1. Mycobacteria have a protective lipid-rich cell wall with mycolic acid; once phagocytized, they inhibit phagosome-lysosome fusion, thus preventing oxygen radical formation, disrupting cytokine production, and avoiding proteolytic enzymes produced by the host cell.[8]

Some species, such as MTBC in cattle and *M. avium* subsp. *avium* in birds, generally produce a T_H1 (tuberculoid) reaction, which results in the formation of granulomas with low numbers of AFB (i.e., paucibacillary granulomas). The immunologic basis for this reaction is delayed-type (i.e., type IV) hypersensitivity, with a T_H1-type, or cell mediated lymphocytic response; in cattle, this often begins in the lungs, since the respiratory tract is the most common portal of entry for MTBC. Specifically, antigen presenting cells release IL-12, which induces naïve CD4+ T-lymphocytes to enter the T_H1 pathway. Once committed, T_H1 cells synthesize and release IL-2, which activates additional T_H1-lymphocytes; IFN-γ and TNF-β, which activates and attracts macrophages; and TNF-α, which promotes an inflammatory response. Interferon-γ also inhibits activation of the T_H2 pathway.[1] This T_H1 response results in "classical" macrophage activation, which influences the structure of the chronic inflammatory response. Specifically, classical macrophage activation via IFN-γ triggers the expression of MHC II, respiratory burst, and release of NO as well as the cytokines IL-1, IL-6 and TNF. The end result is microbial killing, granuloma formation, cellular immunity and delayed type hypersensitivity,[1] which accounts for the microscopic features observed in this case.

In contrast, some types of mycobacteriosis are characterized by a T_H2 (lepromatous) response; examples include leprosy (*M. leprae*) and Johne's disease (MAP). Here, commitment to the T_H2 immune response is induced by IL-4, and T_H2-lymphocytes release IL-4, IL-5, IL-10, IL-13, IL-17 and IL-19, which result in B-lymphocyte activation, antibody production (humoral immunity) and alternative macrophage activation. This is an ineffective method of killing mycobacteria, so histologically there is a multibacillary, disseminated granulomatous response, generally in the gastrointestinal tract and mesenteric lymph nodes.[1]

Although MAC can produce both multibacillary, lepromatous lesions and paucibacillary, tuberculoid lesions,[4] *M. bovis* is more commonly isolated from bovine pulmonary granulomas, so it is somewhat surprising that *M. avium* was isolated from the submitted tissue and that PCR for MTBC was negative. As the contributor noted, the gross and microscopic features of this case were more consistent with bovine tuberculosis.

Table 1: Runyan system of mycobacterial classification[11]

I	slow-growing photochromogens that turn yellow when exposed to light
II	slow-growing scotochromogens that appear yellow in the dark and after exposure to light
III	slow-growing non-photochromogens are non-pigmented
IV	rapid growers, which show visible growth within seven days

Contributing Institution: National Centers for Animal Health
http://www.ars.usda.gov/
http://www.aphis.usda.gov/

References:

1. Ackermann MR. Inflammation and healing. In: McGavin MD, Zachary JF, eds. *Pathologic Basis of Veterinary Disease*. 5th ed. St. Louis, MO: Mosby; 2012:122-128,1032.
2. Caswell JL, Williams KJ. Respiratory system. In: Maxie MG, ed. *Jubb, Kennedy, and Palmer's Pathology of Domestic Animals.* 5th ed. Vol. 2. St. Louis, MO: Saunders Elsevier; 2007:523-653.
3. Cho HS, Kim YH, Park NY. Disseminated mycobacteriosis due to *Mycobacterium avium* in captive Bengal tiger (*Panthera tigris*). *J Vet Diagn Invest.* 2006;18:312-314.
4. Coelho AC, Pinto MdL, Matos A, Matos M, Pires MA. *Mycobacterium avium* complex in domestic and wild animals. *Insights from Veterinary Medicine*. 2013:91-128.
5. Fang SG, Wan QH, Fujihara N. Formalin removal from archival tissue by critical point drying. *Biotechniques*. 2002;33:604-611.
6. Ginn PE, Mansell JEKL, Rakich PM. Skin and appendages. In: Maxie MG, ed. *Jubb, Kennedy, and Palmer's Pathology of Domestic Animals.* 5th ed. Vol. 1. St. Louis, MO: Saunders Elsevier; 2007:553-781.
7. Gow AG, Gow DJ. Disseminated *Mycobacterium avium* complex infection in a dog. *Vet Rec*. 2008;162:594-595.

8. Hibiya K, Kasumi Y, Sugawara I, Fujita J. Histopathological classification of systemic *Mycobacterium avium* complex infections in slaughtered domestic pigs. *Comp Immunol Microbiol Infect Dis*. 2008;31:347-366.
9. O'Toole D, Tharp S, Thomsen BV, Tan E, Payeur JB. Fatal mycobacteriosis with hepatosplenomegaly in a young dog due to *Mycobacterium avium*. *J Vet Diagn Invest.* 2005;17:200-204.
10. Saunders GK, Thomsen BV. Lymphoma and *Mycobacterium avium* infection in a ferret (*Mustela putorius furo*). *J Vet Diagn Invest*. 2006;18:513-515.
11. Stahl DA, Urbance JW. The division between fast- and slow-growing species corresponds to natural relationships among the mycobacteria. *J Bacteriol*. 1990;172(1):116-124.
12. Thacker T, Robbe-Austerman S, Harris B, Palmer MV, Waters WR. Isolation of mycobacteria from clinical samples collected in the United States from 2004 to 2011. *BMC Vet Res.* 2013;9:100.

CASE III: N2012AFIP938 (JPC 4032817).

Signalment: 1-year-4-month-old male rock hyrax (*Procavia capensis*).

History: This rock hyrax was found dead without premonitory signs. There were no other deaths in the group in the preceding four months. A second, four month old, rock hyrax was euthanized due to similar lesions 10 days after this individual died.

Gross Pathology: There are multifocal to coalescing, thick, tenacious, white to pale yellow plaques adhered to the mucosal surfaces of the aryepiglottic folds, the vocal folds, the laryngeal pouches and the nasopharynx and extending into tonsillar crypts. The aryepiglottic folds are markedly thickened, resulting in severe reduction in the diameter of the glottis (pinpoint). There is multifocal red discoloration of the mucosa in areas not covered by plaques. There were no other significant findings.

Laboratory Results: Aerobic culture, larynx: moderate coagulase negative *Staphylococcus* spp., moderate *Pasteurella multocida*

Anaerobic culture, larynx: Few *Prevotella* spp.

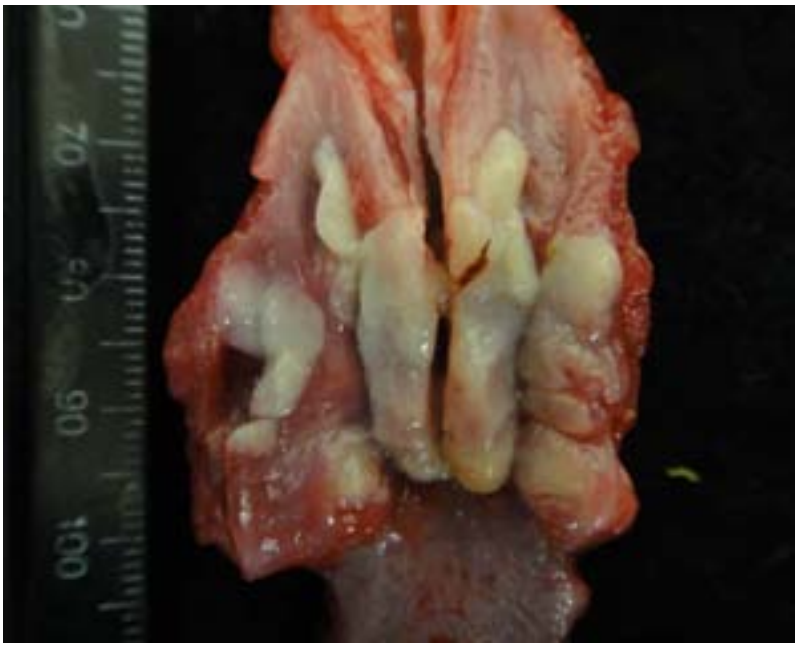

3-1. Larynx, rock hyrax: The laryngeal mucosa is covered by a fibrinonecrotic membrane with marked thickening of the aryepiglottic folds and severe reduction of the glottis. (Photo courtesy of: Wildlife Conservation Society, Zoological Health Program, Department of Pathology, www.wcs.org)

Histopathologic Description: Larynx/pharynx: There is multifocal and extensive ulceration of the laryngeal mucosa, a thick overlying pseudomembrane and dense inflammatory infiltrates in the submucosa. Intact epithelium adjacent to areas of ulceration is infiltrated by variable numbers of neutrophils, is mildly hyperplastic and expanded by edema. These areas often contain large syncytial cells which, in addition to individual epithelial cells, have large amphophilic intranuclear inclusion bodies that either fill the entire nucleus leaving a thin band of peripheralized chromatin, or are surrounded by a clear halo encircled by peripheralized chromatin. The overlying pseudomembrane is composed of fibrin, wispy basophilic material (mucin), viable and intact neutrophils, cellular debris, sloughed epithelial cells (occasionally with intranuclear inclusion bodies) and large, dense colonies of mixed bacteria which are most prevalent on the surface. Inflammation expanding the submucosa directly subtending ulcers is composed of predominantly neutrophils with fewer lymphocytes and plasma cells; the latter predominate in the deeper submucosa and more peripherally. There is multifocal marked submucosal edema and submucosal capillaries are markedly congested.

Contributor's Morphologic Diagnosis: Larynx/ Pharynx: Laryngitis/pharyngitis, fibrinosuppurative, ulcerative, subacute, multifocal to coalescing, extensive, marked, with intralesional intranuclear viral inclusion bodies, intralesional viral syncytia and superficial mixed bacteria.

Contributor's Comment: The histological findings in this case, specifically mucosal ulceration with intralesional intranuclear inclusion bodies and syncytia formation, were consistent with infection by the previously described hyrax herpesvirus.[1] The severity of lesions resulted in near-obstruction of the larynx and presumably contributed to the death of this hyrax.

Investigations into this virus performed by Galeota et al.[1], including biological behavior and molecular characteristics, supported the inclusion of hyrax herpesvirus in the *Alphaherpesvirinae* subfamily and *Simplexvirus* genus. At our

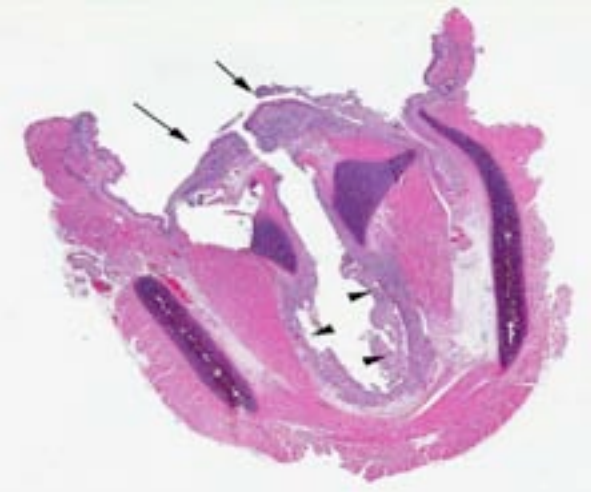

3-2. Larynx, rock hyrax: Approximately 25% of the pharyngeal stratified squamous epithelium (arrows, top), and 50% of the laryngeal respiratory epithelium (arrowheads, center) is ulcerated and replaced by a serocellular crust. (HE 0.63)

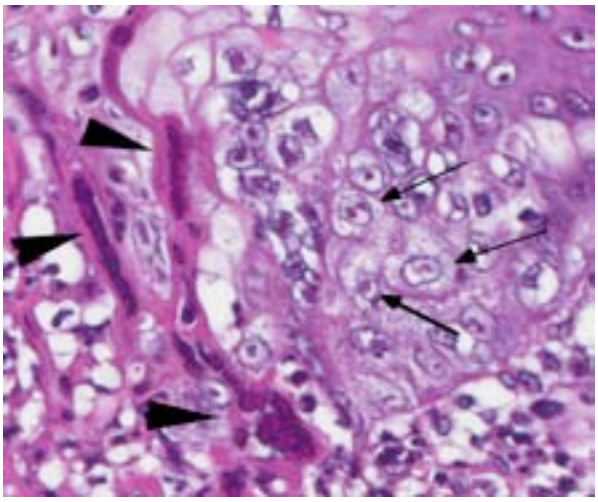

3-3. Larynx, rock hyrax: Within and adjacent to the ulcerated epithelium, mucosal epithelium contains 2-4 µm irregularly round intranuclear viral inclusions (arrows), as well as multinucleated viral syncytia (arrowheads). (HE 400X)

institutions we have seen oral ulcers on numerous occasions in rock hyraxes (often as incidental lesions), and previous molecular investigations from individuals in this colony have shown the offending organism to have 100% shared identity with published hyrax herpesvirus DNA polymerase gene sequences.

As with multiple other members of the *Alphaherpesvirinae*, lesions associated with the hyrax herpesvirus are the result of epithelial necrosis and ulceration with secondary inflammation and, in some cases, bacterial infection. Systemic lesions associated with this virus have not been confirmed, but one published case was described as having nonsuppurative meningoencephalitis[1] and we have seen neuronal necrosis in one of our cases. As with other herpes viruses, it is suspected that the hyrax herpesvirus causes long-term infection with occasional episodes of recrudescence. As no new animals were recently introduced into this group prior to the death of these two animals, recrudescence was suspected in these cases. The colony had recently been transferred to their indoor winter housing which likely introduced stressors and may have induced shedding of the virus in previously infected animals and overt lesions in these younger individuals.

JPC Diagnosis: Larynx/Pharynx: Laryngitis/ pharyngitis, ulcerative and fibrinosuppurative, acute, multifocal, marked, with eosinophilic intranuclear inclusion bodies, viral syncytial cells, submucosal edema and colonies of bacteria.

Conference Comment: Herpesviruses belong to the order Herpesvirales, which contains three families: *Herpesviridae* (herpesviruses of birds, mammals and reptiles), *Malacoherpesviridae* (oysters) and *Alloherpesviridae* (fish and frogs).[2] Herpesviruses are double-stranded, enveloped DNA viruses with worldwide distribution. Replication occurs within the nucleus, resulting in intranuclear inclusion bodies; the viral envelope is acquired via budding through the nuclear membrane. These viruses usually have a narrowly restricted host range and are known for the ability to establish latent infections. The family *Herpesviridae* is divided into three broad subfamilies: *alpha*, *beta* and *gammaherpesvirinae*.[2] Betaherpesviruses, also known as cytomegaloviruses, replicate slowly, have a highly restricted host range and often produce greatly enlarged cells. When latent, they are sequestered in secretory cells, lymphoreticular organs, and the kidney, however they are more associated with continuous viral shedding than periodic reactivation (as opposed to alphaherpesviruses).[2] Betaherpesvirus is normally found in many species, however it usually only causes disease in immunosuppressed individuals, such as SIV infected monkeys. Betaherpesviruses also cause inclusion body rhinitis in swine (suid herpesvirus 2) and salivary gland inclusions and cytomegaly in guinea pigs (caviid herpesvirus 2).[2] Gammaherpesviruses, such as ovine herpesvirus-2 and alcephaline herpesvirus-1 (causative agents of malignant catarrhal fever) or saimiriine herpesvirus 2 (*Herpesvirus saimiri*) replicate in lymphoblastic cells and induce lymphoproliferative response.[2]

Table 1: Alphaherpesviruses of veterinary importance.[2,4]

Bovine herpesvirus 1	Infectious bovine rhinotracheitis, infectious pustular vulvovaginitis
Bovine herpesvirus 2	Bovine mammillitis/pseudo-lumpy skin disease
Bovine herpesvirus 5	Bovine herpes meningoencephalitis
Porcine herpesvirus 1	Pseudorabies/Aujeszky's Disease
Equine herpesvirus 1	Equine abortion
Equine herpesvirus 3	Equine coital exanthema
Equine herpesvirus 4	Equine rhinopneumonitis
Equine herpesvirus 5	Multinodular pulmonary fibrosis
Gallid herpesvirus 1	Avian infectious laryngotracheitis
Gallid herpesvirus 2	Marek's disease
Psittacid herpesvirus	Pacheco's disease
Anatid herpesvirus 1	Duck Plague
Feline herpesvirus 1	Feline viral rhinotracheitis
Canine herpesvirus 1	Canine herpesviral disease
Macacine herpesvirus 1	B-virus of macaques
Saimiriine herpesvirus 1	Herpes tamarinus

Alphaherpesviruses tend to lyse host cells and typically result in widespread or localized necrosis, as in this case. They grow rapidly, producing Cowdry type-A intranuclear inclusion bodies (and viral syncytial cells) and establishing lifelong latent infections in both the lymphoreticular system and the trigeminal ganglion.[4] Gallid herpesvirus 2 (Marek's disease) is a rare example of an alphaherpesvirus which acts more like a gammaherpesvirus in that it induces a lymphoproliferative response.[2] Table 1 summarizes other alphaherpesviruses of veterinary importance.[2,4]

Directional spread of alphaherpesviruses within the nervous system and the establishment of latency is a critical component of the viral lifecycle. The virus initially replicates peripherally in the skin or mucus membranes, where the innate immune response provides the first line of defense. Toll-like receptors (TLRs) recognize pathogen-associated molecular patterns (PAMPs) expressed by the virus. Activated TLRs result in the production of cytokines, which recruit macrophages and/or induce proteins that degrade mRNA and inhibit translation. The adaptive immune response also works to prevent viral spread via viral specific CD8+ cytotoxic T-cells.[3] Although the initial infection is typically cleared within a few weeks, the virus spreads along axons to the sensory nerve ganglion, where the viral genome is maintained indefinitely. During latency, normally productive viral genes are quiescent and unproductive and LATs (latency associated RNA transcripts) accumulate in neuronal nuclei. LATs are Bcl-2 analogs (Bcl-2 is an anti-apoptotic regulator protein) that confers resistance to apoptosis, allowing viral persistence in sensory neurons.[5] Thus, in times of stress or immune suppression, the virus can reactivate and cause clinical disease.

Contributing Institution: Wildlife Conservation Society
Zoological Health Program
Department of Pathology
www.wcs.org

References:

1. Galeota J, Napier J, Armstrong D, Riethoven J, Rogers D. Herpesvirus infections in rock hyraxes (*Procavia capensis*). *J Vet Diagn Invest*. 2009;21:531-535.
2. MacLachlan NJ, Dubovi EJ eds. *Fenner's Veterinary Virology*. 4th ed. London, UK; 2011:179-201.
3. Kramer T, Enquist LW. Directional spread of alphherpesvirus in the nervous system. *Viruses*. 2013;5:678-707.
4. Zachary JF. Mechanisms of microbial infections. In: McGavin MD, Zachary JF, eds. *Pathologic Basis of Veterinary Disease*. 5th ed. St. Louis, MO: Mosby; 2012:212-238.
5. Zerboni L, Che X, Reichelt M, Qiao Y, Gu H, Arvin A. Herpes simplex virus 1 tropism for human sensory ganglion neurons in the severe combined immunodeficiency mouse model neuropathogenesis. *J Virol.* 2013;87(5):2791-2802.

CASE IV: 2105011 (JPC 4017829).

Signalment: 13-year-old neutered female Labrador retriever dog (*Canis familiaris).*

History: This dog had a two-day history of rear limb edema and an activity level that had declined over several months. Abdominal ultrasound revealed 2 large masses in the region of the liver, one of which was compressing the vena cava. It was suspected that postcaval compression by this mass had caused the limb edema.

Gross Pathology: Bilaterally, the subcutaneous tissues of the rear limbs are thickened up to 1.5 cm by gelatinous pale yellow fluid, and this fluid became red, with discoloration of the adjacent tissue below the hock. A 13x12x8cm firm red mass is present on the left lateral liver lobe, and a smaller similar mass is present on the left medial lobe. The liver weighed 6.3% of the body weight. An externally firm 8x7x5 cm mass is present on the right lobe of the pancreas. When sectioned, the mass is soft and dark red continuing several pale nodules that measure 0.5 cm or less in diameter. The pancreatic lymph nodes were firm, tan and measure 3 cm in length.

Histopathologic Description: Pancreas: Compressing the adjacent pancreatic parenchyma and expanding the fibrous capsule is a multi-lobular, moderately cellular mass arranged in acini and tubules. These are separated by fibrovascular stroma that is expanded by amorphous eosinophilic hyaline material. Individual neoplastic cells are cuboidal or polygonal, with distinct cytoplasmic borders and abundant amphophilic to granular eosinophilic cytoplasm. The basal nuclei are round, possessing finely stippled chromatin and a variably distinct nucleolus. No mitotic figures are found in ten 400X fields. Focal necrosis is apparent. Neoplastic cells do not infiltrate the capsule of the organ, but lymphatic emboli occurred in some sections.

Contributor's Morphologic Diagnosis: Pancreas: Exocrine pancreas: adenocarcinoma, hyalinizing.

Contributor's Comment: The pancreatic mass is consistent with pancreatic exocrine adenocarcinoma of hyalinizing type. Overall, exocrine pancreatic

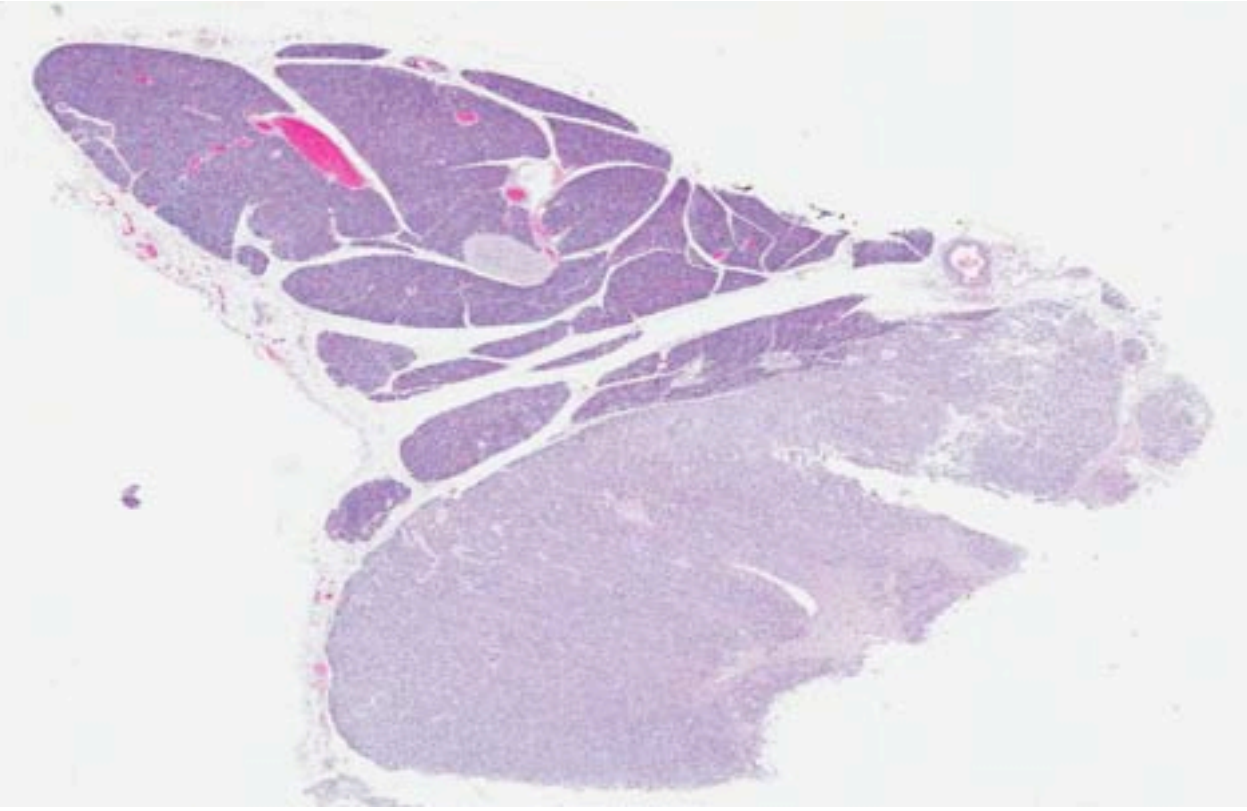

4-1. Pancreas, canine: Approximately 50% of the section is effaced by a well-demarcated, unencapsulated, moderately cellular neoplasm. (0.63X)

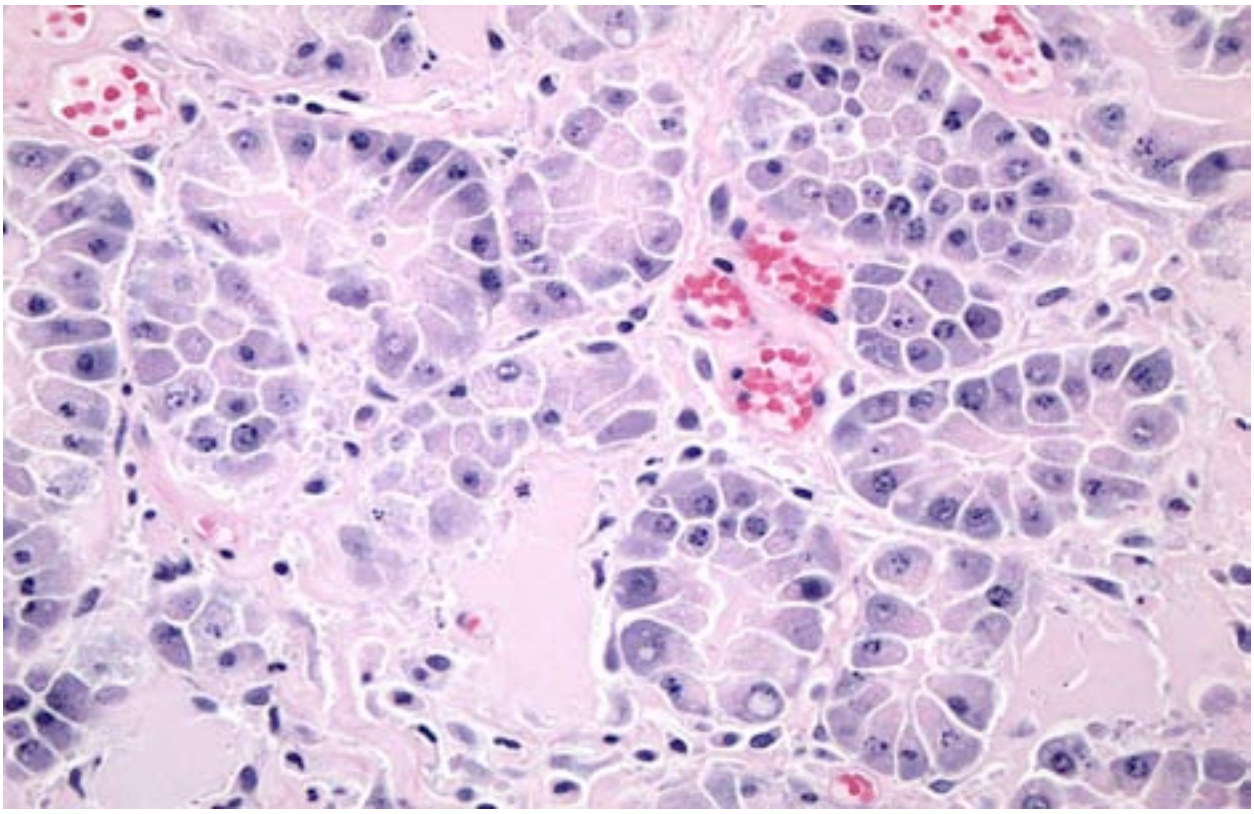

4-2. Pancreas, canine: Neoplastic polygonal cells are arranged in poorly-formed acini, with small amounts of pale zymogen granules in their apical cytoplasm. There is mild anisocytosis and extensive apoptosis. Acini of neoplastic cells are surrounded and often infiltrated by large amounts of homogenous hyaline material. (HE 400X) (Photo courtesy of: Veterinary Medical Diagnostic Laboratory, University of Missouri, 1100 East Rollins Street, Columbia, MO 65211)

tumors are most frequent in dogs amongst the domestic species, with a higher prevalence in older females according to some studies. Extensive implantation and metastases to lymph nodes and liver are often evident by the onset of clinical signs.

Carcinomas may be manifest as single or multiple masses in the organ. They are histologically variable and are classified as acinar, which look like normal exocrine tissue, tubular, which appear more similar to ducts, or undifferentiated, when cells occur in sheets. Hyalinizing carcinomas contain interstitial glassy eosinophilic matrix in tubular lumina or expanding the matrix.[1] This substance is not congophilic and fails to stain immunohistochemically with reagents to serum amyloid A, amylin, α1-antitrypsin or immunoglobulin light chain. The nature of this matrix is not known. In a small case series, these carcinomas tended to favor the acinar pattern and patients that were not euthanized immediately after surgery had a somewhat longer survival than expected.[1] A case with clear cell morphology and similarly increased interstitial matrix has been recently reported in a dog, in which the matrix was PAS+.[4] Our case has a mixed pattern with sheets of undifferentiated cells as well as acini.

Cytokeratin labeling has been disappointing[2] for use in identifying pancreatic carcinomas in dogs, and has the draw-back of staining cytokeratin on other organs when utilized to identify metastases. In cats pancreatic exocrine neoplasms are often positive for one or both reagents, as is normal pancreas. In dogs, pancreatic ducts are reported to express cytokeratin 7, but acini were negative, while acinar tissue reacted with neither reagent. Four pancreatic exocrine neoplasms tested in this series were also uniformly negative. Recently claudin-4 has been suggested as a reagent useful in negative poorly differentiated exocrine tumors and ductular tumors from between differentiated acinar neoplasms, which are positive.[3]

The patient had very severe rear leg swelling with marked subcutaneous edema, which histologically was found to contain numerous neutrophils. Two of the cases in reference 1 also had one or more areas

of suppurative panniculitis, although the lesions were in other locations. This patient had severe postcaval compression from one of its hepatocellular carcinomas, and this may have been the cause of edema.

JPC Diagnosis: Exocrine pancreas: Hyalinizing pancreatic adenocarcinoma.

Conference Comment: The most notable characteristic of this neoplasm, and the feature that distinguishes it from the more common variants of canine exocrine pancreatic carcinoma (EPC), is the extensive extracellular deposition of homogenous to globular eosinophilic material.[1] This substance is consistent with the microscopic appearance of amyloid, however, as noted by the contributor, it is generally not congophilic or birefringent and is immunohistochemically negative for serum amyloid A, amylin, α1-antitrypsin and immunoglobulin light chain; the origin of this material remains unknown.[1] Interestingly, in this case, the application of Masson's trichrome stained the hyaline eosinophilic material blue.

Canine hyalinizing pancreatic adenocarcinoma is a well-differentiated, solitary mass most commonly seen in the right limb of the pancreas. The most frequent clinicopathological abnormalities are elevated serum amylase and lipase.[1] Hyalinizing pancreatic adenocarcinoma is a form of EPC, and the main differential diagnoses are other variants of EPC, such as anaplastic (undifferentiated) EPC or pancreatic acinar or ductal carcinomas.[4] Pancreatic acinar cell carcinomas are further classified histologically as well-differentiated, which are less invasive, or poorly-differentiated, which tend to metastasize or invade adjacent tissue. One recent report found that loss of expression of claudin-4, a tight junction integral protein normally expressed in canine pancreatic acinar cell membranes, may lead to cellular detachment, disorientation and invasion in poorly-differentiated EPCs. The same study suggested immunohistochemical staining for claudin-4 as a marker to distinguish well-differentiated from poorly-differentiated acinar cell carcinomas.[3] Canine hyalinizing pancreatic adenocarcinomas behave less aggressively than the other, more common variants of canine EPC. Dennis, et al. speculate that this more benign behavior may be secondary either to the hyaline matrix material mechanically or biochemically impeding malignancy, or to the degree of tumor differentiation (or both).[1]

In the sections submitted for the conference, there is a diffuse loss of cellular detail and differential staining within the tumor, and because the contributor observed that some sections contained neoplastic emboli within lymphatics this led several conference participants to speculate that the entire neoplasm could be infarcted.

Contributing Institution: Veterinary Medical Diagnostic Laboratory and Department of Veterinary Pathobiology
University of Missouri
http://www.cvm.missouri.edu/vpbio

References:

1. Dennis MM, O'Brien TD, Wayne T, Kuipel M, Powers BE. Hyalinizing pancreatic adenocarcinoma in 6 dogs. *Vet Pathol.* 2008;45:475-483.
2. Espinosa de los Monteros A, Fernádez A, Millán MY, Rodriguez F, Herráez P, Martin de las Mulas J. Coordinate expression of cytokeratins 7 and 20 in feline and canine carcinomas. *Vet Pathol.* 1999;36:179-190.
3. Jakab CS, Rusvai M, Demeter Z, Gálfi P, Szabó Z, Kulka J. Expression of claudin-4 molecule in canine exocrine pancreatic acinar cell carcinomas. *Histol Histopathol.* 2011;26:1121-1126.
4. Pavone S, Manuali E. Eleni C, Ferrari A, Bonano E, Carioli A. Canine pancreatic clear acinar cell carcinoma showing unusual mucinous differentiation. *J Comp Path.* 2011;145:355-358.

WEDNESDAY SLIDE CONFERENCE 2013-2014

Conference 3

26 September 2013

CASE I: 04135-11 (JPC 4032910).

Signalment: 16-year-old male cynomolgus macaque (*Macaca fascicularis*).

1-1. Multiple organs, cynomolgus monkey: a) Variably sized, up to 1 cm diameter, pale green to yellow abscesses were visible on the serosal surface of the liver. b) More caseous foci were present in the kidneys (c, d). The left lobe of the seminal vesicle was enlarged to approximately twice normal owing to extensive abscessation. (Photo courtesy of: Wake Forest University Health Sciences, Animal Resources Program, Medical Center Boulevard, Winston-Salem, NC 27157 http://www.wfubmc.edu/schoolOfMedicine/schoolOfMedicine_default.aspx?id=26651)

History: This animal arrived at Wake Forest University from Indonesia in 2003, and for 1 year was relatively healthy. On the day before death, it presented non-weight bearing on the left rear limb and on the following day was reluctant to move, hypothermic (84.6 F), dehydrated and had mild bradycardia. Radiographs disclosed radiopacity of the left leg proximal to the stifle joint. Blood work revealed anemia (HCT- 22%), a high normal white blood cell count (8,000/ml) with a degenerative left shift, azotemia (creatinine-7.59 mg/dl, BUN- 68 mg/dl), hyperproteinemia (7.5 g/dl), hyperphosphatemia (7.9 g/dl), and mild elevations of the liver enzymes (ALP-311 U/l, GGT-108 U/l). The animal died despite supportive care.

Gross Pathology: A 5.25kg cynomolgus macaque was submitted for necropsy. The subcutaneous tissue surrounding and adjacent to the left tibiotarsal joint was swollen and the joint contained viscous, tan pus. Variably sized, up to 1 cm diameter, pale green to yellow abscesses were visible on the serosal surface of the liver with extension into the parenchyma. Similar lesions were present in the spleen and mesentery. More caseous foci were present in the kidneys. About 2 mL of pus was present in the urinary bladder, and the left lobe of the seminal vesicle was enlarged to approximately twice normal owing to extensive abscessation.

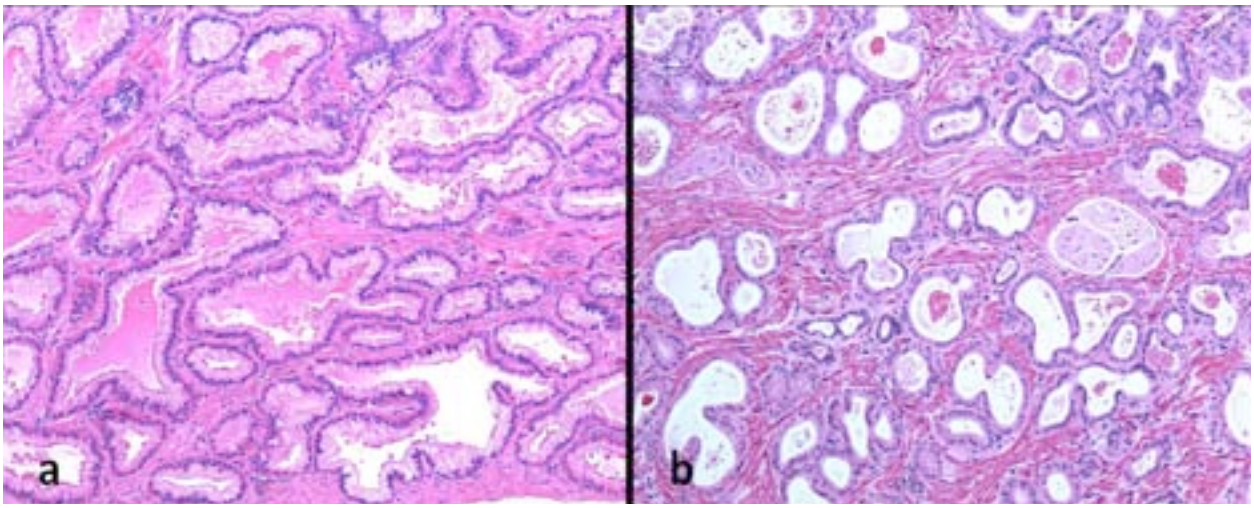

1-2. Prostate gland, cynomolgus monkey: Normal cranial (a) and caudal (b) prostate from a 16-year-old rhesus macaque (Macaca mulatta). The cranial prostate has larger, irregular glands with tall columnar epithelium. The caudal prostate has smaller glands with low columnar to cuboidal epithelial cells. (HE 10X) (Photo courtesy of: Wake Forest University Health Sciences, Animal Resources Program, Medical Center Boulevard, Winston-Salem, NC 27157 http://www.wfubmc.edu/schoolOfMedicine/schoolOfMedicine_default.aspx?id=26651)

Laboratory Results: *Burkholderia pseudomallei* cultured from urinary bladder, and renal and hepatic abscesses.

Histopathologic Description: Caudal prostate gland: Extensive abscessation effaces and compresses the glands of the caudal prostate. This reaction is composed of abundant neutrophils, many degenerate, admixed with eosinophilic amorphous material, karyorrhectic debris, fibrin and small accumulations of extravascular erythrocytes (hemorrhage). Adjacent prostatic glands are filled with similar material. In some sections, lymphocytes are present in the prostatic stroma, while in others, there is a suppurative exudate present within the urethral lumen.

Contributor's Morphologic Diagnosis: Prostatitis, multifocal, suppurative, subacute, severe.

Contributor's Comment: In humans, the three pathologic processes that most commonly affect the prostate are inflammation, benign nodular enlargement and neoplasia. In nonhuman primates, inflammation is more common.[7] In humans, acute bacterial prostatitis is typically caused by bacteria that cause urinary tract infections, including *Escherichia coli*, other gram-negative rods, enterococci and staphylococci. Bacteria become implanted in the prostate by intraprostatic reflux of urine from the urethra or the urinary bladder. Occasionally bacteria may spread to the prostate via

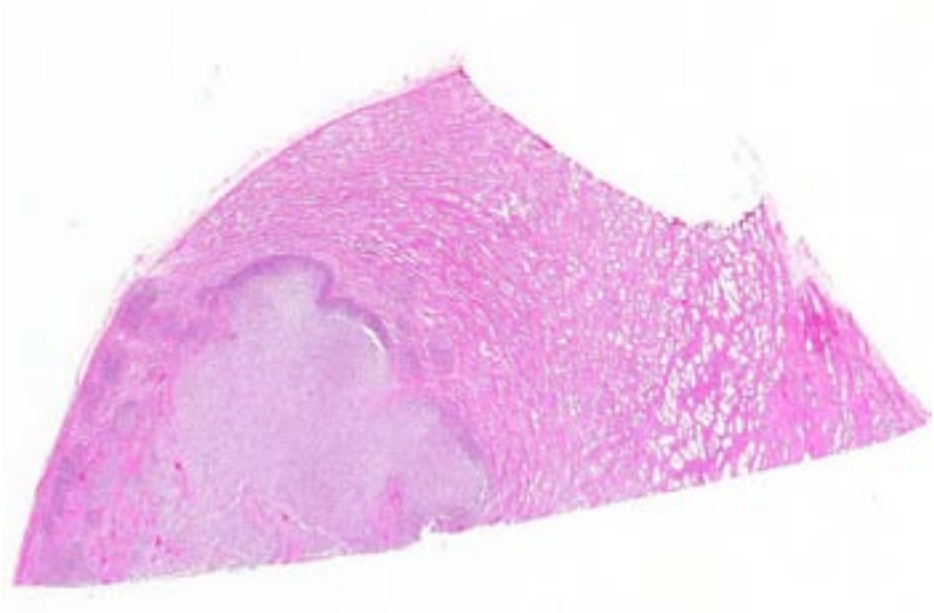

1-3. Prostate gland, cynomolgus monkey: 33% of the prostate gland is effaced by lytic necrosis. Adjacent less affected glands are compressed by the abscess and multifocally contain cellular and necrotic debris. (HE 0.63X)

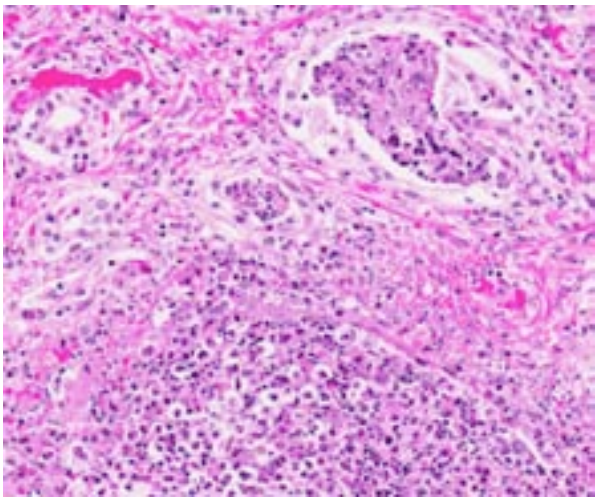

1-4. Prostate gland, cynomolgus monkey: Adjacent to large areas of lytic necrosis (center), adjacent prostate glands are expanded by degenerate neutrophils and cellular debris. (HE 216X)

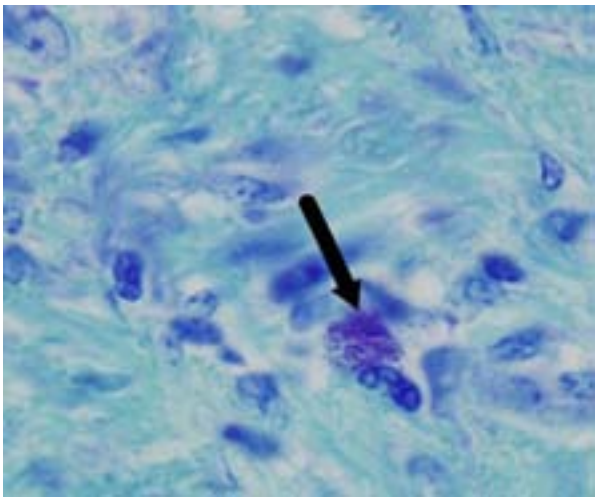

1-5. Prostate gland, cynomolgus: Intracytoplasmic B. pseudomallei within a macrophage. The bacterium is rod-shaped with rounded ends and is often described as having a "safety pin" appearance on electron microscopy. (Giemsa 1000X)

lymphohematogenous routes from distant sites of infection.[4] In this macaque, either route could have caused the inflammation in the prostate, but as widespread abscessation had occurred, it is more likely that the prostate was affected by hematogenous spread of *Burkholderia pseudomallei*.

Burkholderia pseudomallei is a facultative anaerobic, saprophytic, gram-negative bacterium that causes melioidosis, a zoonotic multisystemic disease. The bacterium is rod-shaped with rounded ends and is often described as having a "safety pin" appearance.[4] It can survive hostile environmental conditions including acidic environments, wide temperature ranges, nutrient deficiencies and dehydration.[3] The disease is spread through inhalation, contamination of skin wounds, or ingestion from the environment. Direct transmission from infected to naïve animals and vertical transmission are rare.[9] It is designated as a Tier 1 select agent (requiring biosafety level 3 containment) by the US Centers for Disease Control due to its natural resistance to antibiotics, potential for easy dissemination and high mortality in humans and animals.[8,9] Sporadic cases of melioidosis have been reported in Central and South America but the disease is rare in North America.[9,12] As it is endemic in Southeast Asia, northern Australia and the Indian subcontinent,[9,12] melioidosis should be a differential diagnosis for nonhuman primates imported from Asia which develop abscesses or nonspecific signs of infectious disease, regardless of the time since importation.[9] The animal presented here had been considered healthy for 1 year before presentation.

Burkholderia pseudomallei is an opportunistic pathogen, affecting many mammalian and non-mammalian species. The clinical signs and lesions of melioidosis are variable, and while septicemia is common, multisystemic suppurative or caseous inflammatory lesions are also characteristic.[9] The disease is best described in ruminants and swine where it may result in subclinical to disseminated fatal disease, depending on the route of infection, infectious dose, strain virulence, and host immune status.[12] In nonhuman primates, including rhesus, stumptail and pigtail macaques, chimpanzees and orangutans,[9,10] the most common clinical signs include anorexia, wasting, listlessness, intermittent cough, nasal discharge and mild respiratory disease that can result in bronchopneumonia, and generalized weakness. Multisystemic abscessation is common.[10] Nerve damage and necrotizing osteomyelitis have also been described.[9] In horses, donkeys and mules, a closely related bacterium, *B. mallei*, causes pyogranulomatous lymphangitis of the respiratory tract and skin,[14] commonly called glanders and farcy, respectively. It primarily occurs in Africa, Asia, the Middle East and South Africa, and human infections are often fatal if not treated.[2]

In nonhuman primates the prostate is divided into the cranial and caudal regions which are labeled according to their proximity to the urinary bladder and seminal vesicles,[7] and have distinct histological characteristics. In humans, the prostate is divided into 4 regions: the peripheral, central and transitional zones, and the anterior fibromuscular stroma.[4,6] Since proliferative lesions differ between the regions

of the human prostate, for example, carcinomas occur more frequently in the peripheral zone,[4,6] it is important to differentiate between the lobes of the prostate. In macaques, the cranial and caudal lobes of the prostate are analogous to the central and peripheral zones of the human prostate, respectively.[6,7] In addition to these anatomical similarities, some nonhuman primates (macaques, orangutans, chimpanzees, gorillas) express the prostate specific antigen (PSA), a marker of prostatic health in humans, enabling value as natural models for human prostatic disease.[5,6,7]

JPC Diagnosis: Prostate gland: Prostatitis, necrosuppurative, multifocal to coalescing, subacute, marked.

Conference Comment: *Burkholderia pseudomallei,* which has changed names numerous times, was first described in 1911 by Captain Alfred Whitmore, in a population of morphine users in Southeast Asia who developed multi-organ abscesses and septicemia. Noting its similarity to equine glanders (*Bacillus mallei*), Whitmore originally named it *Bacillus pseudomallei*, however it was also known as "Whitmore's disease" and "morphine injector's septicemia." Sporadic infections occurred in US and Japanese soldiers in World War II, and by the Vietnam War, the etiologic agent of melioidosis had been reclassified as *Pseudomonas pseudomallei*. Although less than 300 cases occurred during the conflict, many additional cases surfaced years later, which led to the nickname "the Vietnam Time Bomb."[11]

Given that *B. pseudomallei* is a zoonotic and potentially deadly disease as well as a potential bioterrorist threat, a significant amount of research is currently being conducted with regards to the pathogenesis, treatment and prevention of melioidosis. A recent study explored the role of toll-like receptors in the immune response and morbidity/mortality of the disease. Toll-like receptors are surface pattern recognition receptors expressed by various cells that recognize exogenous microbial products and signal the presence of infection to the host. The binding of pattern-associated molecular patterns (PAMPs) to TLRs initiates transmembrane signaling, generally utilizing the MyD88 protein, which leads to the activation of NF kappa β transcription factors, MAPK signaling, the expression of inflammatory cytokines and activation of the innate and adaptive immune systems.[1] TLR2 and TLR4, which bind bacterial lipoprotein and lipopolysaccharide (LPS) respectively, have previously been shown to regulate host innate immune responses in humans with *B. pseudomallei*.[13] TLR5, which binds flagellin, is defective in a small subset of people with a specific genetic defect resulting in ineffective signaling; carriers of this defect have recently been shown to have improved survival in melioidosis. This has led to the supposition that melioidosis may induce a TLR5-dependent innate immune response, with the release of IL-10, IL-8 and IL-6, among other cytokines, and that people with non-functional TLR5 have reduced sepsis and lower mortality due to an impairment of this inflammatory response.[13]

In closing, conference participants briefly discussed one possible differential diagnosis for melioidosis in a non-human primate: *Klebsiella pneumonia*, sometimes referred to as the "shipping fever of monkeys," can also cause abscess in multiple organs; however, the bacteria are usually evident microscopically.

Contributing Institution: Wake Forest University Health Sciences
Animal Resources Program
Medical Center Boulevard
Winston-Salem, NC 27157
http://www.wfubmc.edu/schoolofmedicine/

References:

1. Ackerman MR. Inflammation and healing. In: McGavin MD, Zachary JF, eds. *Pathologic Basis of Veterinary Disease*. 5th ed. St. Louis, MO: Elsevier; 2012:111-113.
2. Balder R, Lipski S, Lazarus JJ, et al. Identification of *Burkholderia mallei* and *Burkholderia pseudomallei* adhesions for human respiratory cells. *BMC Microbiology*. 2010;10:250. [accessed 11 June 2013].
3. Cheng AC, Currie BJ. Melioidosis: epidemiology, pathophysiology, and management. *Clin Microbiol Rev* 2005;18(2):383–416.
4. Epstein, JI. The lower urinary tract and male genital system. In: KumarV, Abbas AK, Fausto N, eds. *Robbins and Cotran Pathologic Basis of Diseases*. 8th ed. Philadelphia, PA: Saunders Elsevier; 2010:971-1004.
5. Lewis RW, Kim JCS, Irani D, et al. The prostate of the nonhuman primate: normal anatomy and pathology. *The Prostate*. 1981;2:51-70.

6. McNeal JE. Anatomy of the prostate: a historical survey of divergent views. *The Prostate*. 1980;1:3-13.
7. Mubiru JN, Hubbard GB, Dick EJ Jr., et al. Nonhuman primates as models for studies of prostate specific antigen and prostatic disease. *The Prostate*. 2008;68:1546-1554.
8. Peacock SJ, Schweizer HP, Dance DAB, et al. Management of accidental laboratory exposure to *Burkholderia pseudomallei* and *B. mallei* [online report]. *Emerg Infect Dis* [serial on the Internet]. 2008;14(7) [accessed: 11 June 2013] http://wwwnc.cdc.gov/eid/article/14/7/07-1501_article.htm
9. Ritter JM, Sanchez S, Jones TL, et al. Neurologic melioidosis in an imported Pigtail Macaque. *Vet Pathol*. Published online 10 April 2013 [accessed 11 June 2013].
10. Sprague LD, Neubauer H. Melioidosis in animals: a review on epizootiology, diagnosis and clinical presentation. *J Vet Med B*. 2004;50:305-320.
11. Vietri, NJ, Deshazer D. Melioidosis. In: *Medical Aspects of Biological Warfare*. United States Department of Defense: Walter Reed Army Medical Center Borden Institute; 2008:147-150.
12. Warawa JM. Evaluation of surrogate animal models of melioidosis. *Front Microbiol*. 2010;1:141.
13. West TE, Chantratita N, Chierakul W, et al. Impaired TLR5 functionality is associated with survival in melioidosis. *J Immunol*. 2013;190(7): 3373-3379.
14. Zachary JF. Mechanisms of microbial infections. In: McGavin MD, Zachary JF, eds. *Pathologic Basis of Veterinary Disease*. 5th ed. St. Louis, MO: Elsevier; 2012:147-241.

CASE II: DX12-72 (JPC 4017832).

Signalment: Adult female grey short-tailed opossum (*Monodelphis domestica*).

History: The animal was found dead.

Gross Pathology: The left ventricle was dilated with a cauliflower mass involving the aortic valves and the base of the aorta at the level of the branching of the coronary arteries from the aorta.

Laboratory Results: Gram stain: Gram-positive small cocci suggestive of *Streptococcus sp*.

Histopathologic Description: Heart: There is a mixed inflammatory infiltrate consisting predominately of neutrophils admixed with large colonies of bacterial cocci that are attached to and destroying the aortic valves.

Contributor's Morphologic Diagnosis: Heart, aortic valve: Bacterial vegetative myocardial valvulitis.

Contributor's Comment: Bacterial vegetative endocarditis is a common spontaneous occurrence in the Virginia opossum (*Didelphis virginiana*) and this marsupial has been used as an experimental animal model for *Streptococcus* bacterial endocarditis. Although cardiovascular diseases are the second most common cause of death of the laboratory grey short-tailed opossum (*Monodelphis domestica*)[1], to the contributor's knowledge, bacterial vegetative valvular endocarditis has not been previously reported in the laboratory grey short-tailed opossum.

Bacterial endocarditis primary arises from adhesion of the microorganisms to the endocardium, leading to death of the endothelium and formation and adherence of a thrombus within which large colonies of bacteria proliferate. Such proliferative growths and thrombus are called vegetative endocarditis. Although not observed in the opossum, pieces of the vegetation may break free and circulate to other organs, causing septic infarcts or abscesses. It is not uncommon for valvular endocarditis to cause cardiac dysfunction leading to congestive heart failure.

JPC Diagnosis: Heart: Valvulitis, arteritis and endocarditis, fibrinosuppurative, multifocal to coalescing, subacute, severe with fibrin thrombi, myocardial degeneration and necrosis and numerous Gram-positive bacterial cocci.

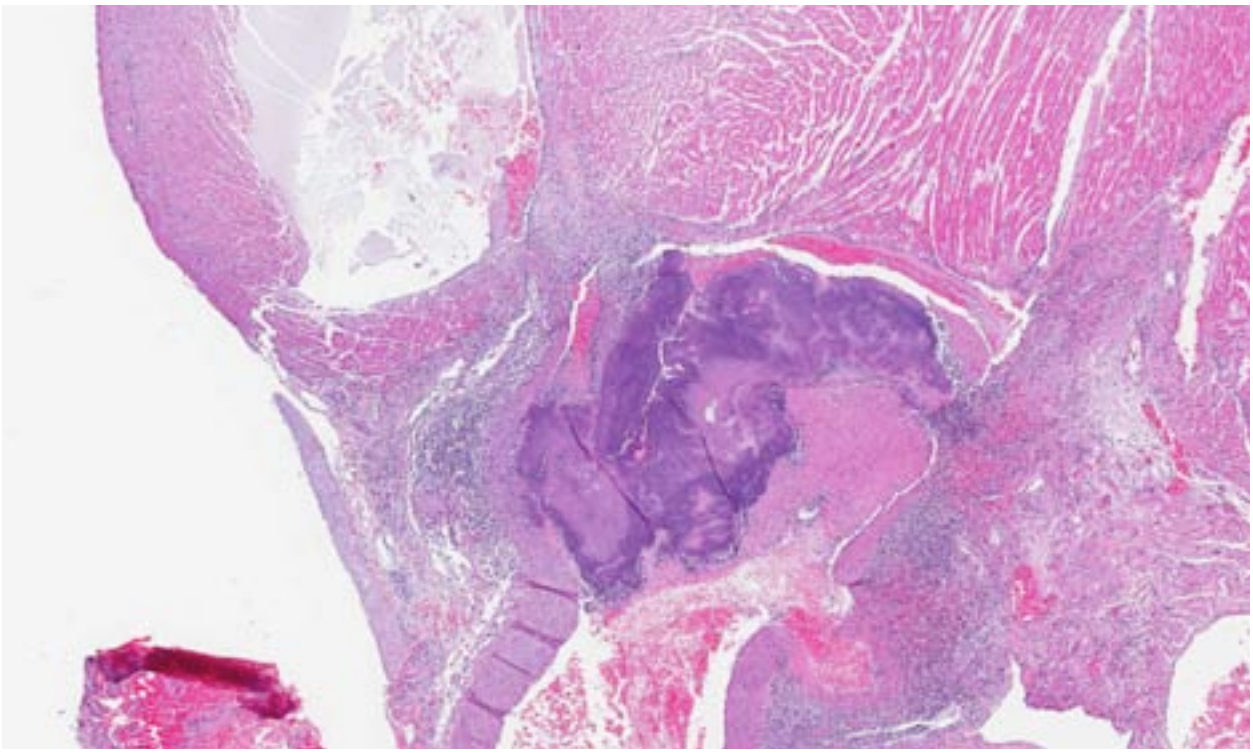

2-1. Heart, short-tailed possum: The aortic valve is effaced and the aorta lumen occluded by a septic thrombus. The inflammation extends through and beyond the wall of the aorta and dissects into the subendocardial myocardium and the base of the left atrium. (HE 10X)

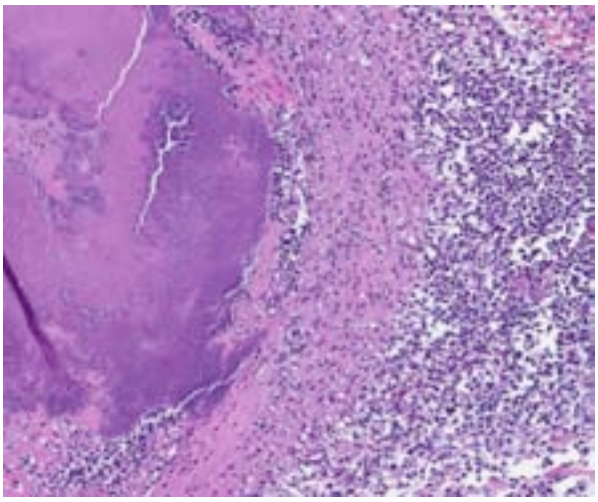

2-2. Aorta, short-tailed possum: Necrosuppurative inflammation extends from the septic thrombus through the aortic wall, into the aortic adventitia. (HE 116X)

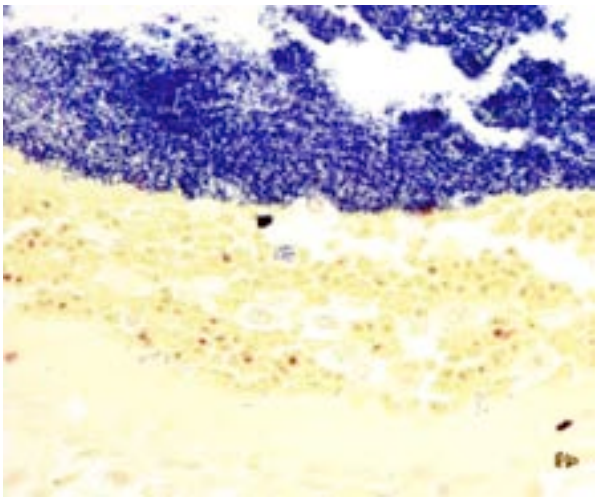

2-3. Aorta, short-tailed possum: The thrombus contains numerous gram-positive cocci. Unfortunately, the bacteria in this case were not cultured. (Brown-Brenn 1000X)

Conference Comment: In recent years, the grey short-tailed opossum has become the most commonly utilized marsupial in biomedical research, owing to its small size, docile nature, rapid growth, high fertility and relative ease of husbandry.[3] The young are not fully developed at birth, but born at a stage somewhat comparable to 40-day-old human embryos. Thus this species is often used in reproductive research.[5] *M. domestica* is also routinely used in the study of UV light-induced skin and eye neoplasia, such as melanoma. Although *M. domestica* is a hardy species with few documented parasitic or specific infectious diseases, several spontaneous pathologic conditions are reported. Most are associated with the digestive system, including rectal prolapse, which occurs primarily in females, likely related to parturition. Dermatitis, and cardiovascular disease with secondary pulmonary lesions, are also described. Pituitary adenoma is reported as the most common neoplasm in *M. domestica*, followed by uterine leiomyoma and cutaneous lipoma.[1]

Spontaneous bacterial endocarditis in the Virginia opossum (*Didelphis virginiana*) is typically due to *Streptococcus viridans* or *Staphylococcus aureus*.[4] Although culture was not performed in this case, a tissue Gram stain reveals numerous intralesional Gram-positive cocci, supporting a similar etiology in this case. In research species, bacterial endocarditis has been associated with the use of vascular access ports and intravenous catheters. Vegetative valvular endocarditis is also seen in ruminants, swine, dogs, and rarely in cats and horses. *Streptococcus* sp., *Staphylococcus* sp. and *E. coli* are frequently implicated as the etiologic agents in many species. Additionally, *Erysipelothrix rhusiopathiae* is often isolated in pigs and (occasionally) dogs, while *Bartonella* sp. is more specific to the dog or the cat. *Arcanobacterium pyogenes* is a common pathogen in cattle and *Actinobacillus equuli* can occasionally cause valvular endocarditis in horses.[2] Regardless of the inciting cause, this condition can result in valve damage and the development of congestive heart failure, or detachment of the vegetations with subsequent embolic disease.[2] In this case, because the lesion is located in the left heart at the aortic valve, the kidney would be a likely anatomic location for secondary embolic lesions.

Contributing Institution: St. Jude Children's Research Hospital
Department of Pathology
Jerold.rehg@stjude.org

References:

1. Hubbard, GB, Mahaney MC, Gleiser CA, Taylor DE, VandeBerg JL. Spontaneous pathology of the gray short-tailed opossum. *Laboratory Animal Science*. 1997;47:19-26.
2. Maxie MG, Robinson WF. Cardiovascular system. In: Maxie MG, ed. *Jubb, Kennedy and Palmer's Pathology of Domestic Animals*. 5th ed. Vol. 3. Philadelphia, PA: Elsevier Saunders; 2007:27-29.
3. Samollow PB. The opossum genome: insights and opportunities from an alternative mammal. *Genome Res.* 2008;18(8):1199-1215.
4. Sherwood BF, Rowlands MD, Vakilzadeh J, LeMay JC. Experimental bacterial endocarditis in

the Opossum (*Didelphis virginiana*). *Am J Pathol*. 1971;64(3):513-520.
5. Xie Q, Mackay S, Ullmann SL, Gilmore DP, Payne AP, Gray C. Postnatal development of Leydig cells in the opossum (*Monodelphis domestica*): an immunohistochemical and endocrinological study. *Biol Reprod*. 1998;58(3):664-669.

CASE III: PV00129C1 (JPC 4032440).

Signalment: Adult female mixed breed 4-year-old canine (*Canis lupus familiaris*).

History: This dog presented to the Center for Zoonoses Control in Natal, Brazil with anorexia, cachexia, exudative dermatitis, facial edema, and keratoconjunctivitis.

Gross Pathology: Necropsy was performed immediately after humane euthanasia. The body condition of this dog was thin with minimal subcutaneous and abdominal adipose tissue. Externally, the skin had multifocal to coalescing regions of crusting with seborrheic exudate, the muzzle of the face was markedly edematous, and the eyes had amucopurulent palpebritis and keratoconjunctivitis. There was a significant burden of ticks within the ears of the dog. The spleen was enlarged to 1.5 times normal size with a mottled irregular appearance. The liver was mildly enlarged and mottled in appearance. The kidneys were bilaterally pale and mildly enlarged with a mottled appearance and an undulating cortical surface. The bladder contained cloudy urine with numerous protein casts.

Histopathologic Description: Section of kidney with marked multifocal infiltrates of inflammatory cells including large numbers of plasma cells, macrophages, and lymphocytes. These cellular infiltrates were primarily located in perivascular and periglomerular areas of the cortical and medullary interstitium. Large foamy macrophages containing 1-3 small 1.5-3 micron amastigotes with an occasionally visible kinetoplast perpendicular to the protozoal nucleus were commonly found within areas of inflammation. Glomeruli were diffusely altered, with 10-15% being shrunken and hypocellular with increased collagen both within the glomerular tuft and Bowman's capsule (sclerosis), and others with the glomerular mesangium diffusely expanded by streaks of eosinophilic collagen with marked mesangial and endocapillary hypercellularity (membranoproliferative glomerulonephritis). Synechiae were numerous, often with the formation of glomerular crescents. Bowman's capsule was similarly expanded to 3-6 times its normal thickness by eosinophilic material in most affected nephrons. The tubular interstitium was prominently expanded by the inflammatory cell infiltrates as well as the deposition of fibrillar eosinophilic material (collagen). Distal medullary tubules were ectatic and contained hyper-eosinophilic proteinaceous concretions.

Contributor's Morphologic Diagnosis: Kidney: Glomerulonephritis, membranoproliferative, chronic, diffuse/global, severe, with prominent glomerulosclerosis and multifocal to coalescing lymphoplasmacytic and histiocytic interstitial nephritis with intra-histiocytic protozoal amastigotes; morphology consistent with *Leishmania* species *(Leishmania infantum* (synonym *chagasi))*.

Contributor's Comment: Canine leishmaniasis, primarily caused by *Leishmania infantum,* is a progressive and fatal disease with public health significance in endemic areas.[6] These endemic regions include the Mediterranean basin, northern and sub-Saharan Africa, Central and South America, and northern and northwestern China.[6] Additionally, within the United States, canine leishmaniasis is endemic with the American Foxhound breed, with sporadic occurrence in the Neapolitan Mastiff, Italian Spinone, other European origin breeds, and military service animals from the Middle East. Transmission is via one of numerous phlebotomine sandflies in endemic regions and vertical transmission independent of vector species has been documented. Dogs are also susceptible to cutaneous leishmaniasis caused by a variety of species including *L. braziliensis* and *L. panamensis.*[6]

Leishmania species have a unique pathogenesis and means of persistence within host cells enabling the establishment of long-term chronic infection. After a sandfly bite, an influx of both neutrophils and macrophages occurs, even in the absence of parasites. Parasites are able to survive within neutrophils due to the ability to inhibit the acidification of the phagosome, but have not been shown to transform into amastigotes or proliferate within in the neutrophil.[9] At the time of neutrophil apoptosis, surviving parasites are phagocytosed by resident and infiltrating macrophages, where the parasites will transform into amastigotes, replicate, and establish long-term infection. Dermal dendritic cells also become infected at the site of inoculation, becoming mature and migrating to the lymph node. *Leishmania* are resistant to acidification as amastigotes, and persist in these compartments which are late endosome associated LAMP1, Rab7 positive vacuoles.[13]

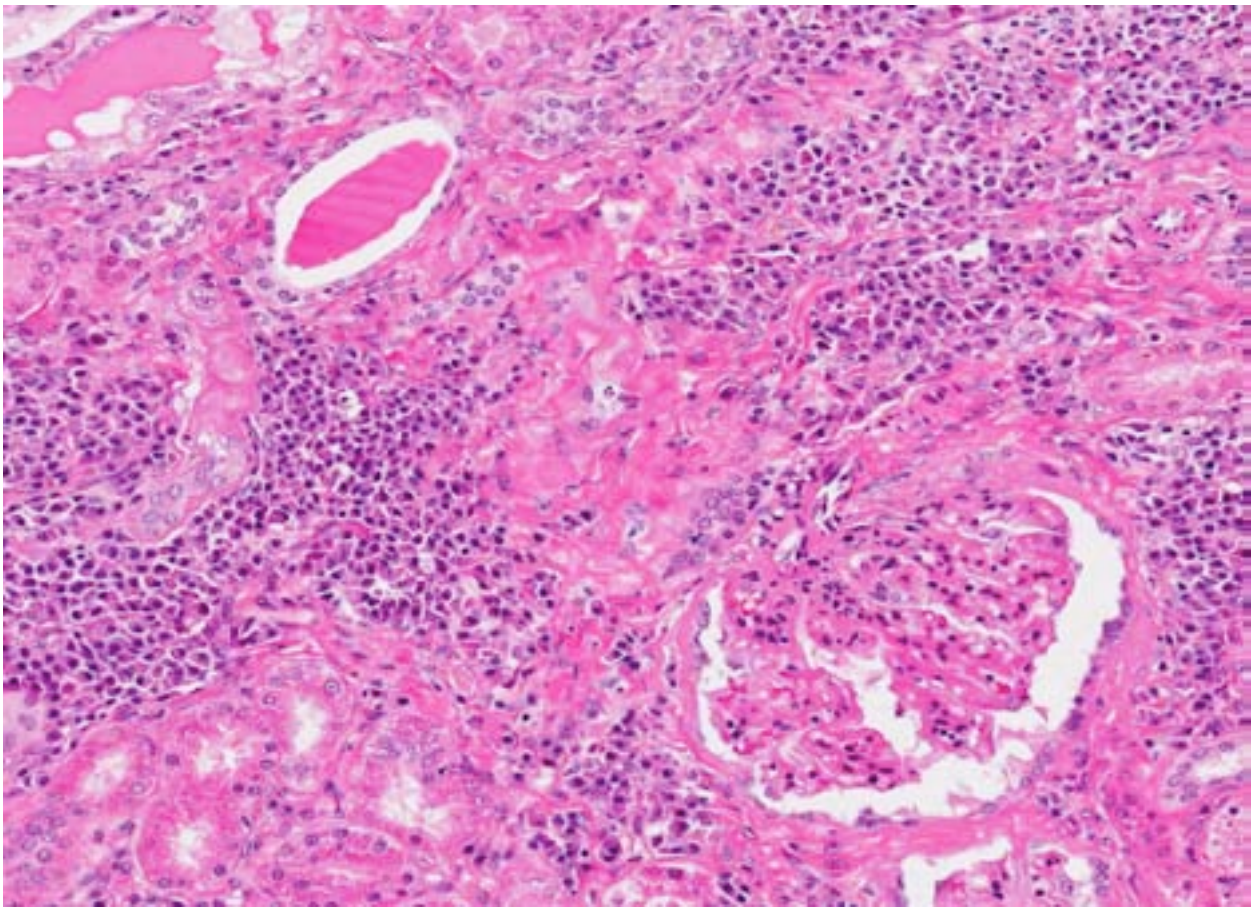

3-1. Kidney, dog: The interstitium is expanded by large numbers of plasma cells and rare histiocytes. Glomeruli are enlarged and hypercellular, and tubules are often ectatic with brightly eosinophilic protein within their lumen. (HE 144X)

The immune response to all *Leishmania* species as an intracellular pathogen is dependent upon a timely and appropriate Th1 response including IL-12 production by dendritic cells and macrophages, efficient MHC II presentation, and subsequent IFNy production from T cell populations. Parasite killing is dependent primarily upon intracellular killing via superoxide and nitric oxide within phagolysosomes of infected macrophages. *Leishmania* utilize a number of immune evasion strategies to inhibit the immune response including the interruption of DC maturation, the stimulation of anti-inflammatory cytokines such as TGF-p and IL-10, the interruption of cellular signaling of the STAT pathways necessary for IFNy production, and through the induction of CD25+, FoxP3+ T regulatory cells.

Clinical presentation varies and includes dermal lesions, splenomegaly, generalized lymphadenopathy, cachexia, anorexia, muscle wasting, polyuria and polydipsia, proteinuria, keratoconjunctivitis, nail overgrowth, and hematologic abnormalities.[2,8,14] Splenic and hepatic lesions typically consist of granulomatous splenitis characterized by variable numbers of amastigote-infected macrophages, and lymphoplasmacytic and granulomatous portal and periportal hepatitis.[14] Skin lesions are one of the most common presenting signs in endemic regions and can include nonpruritic dermatitis, ulcerative dermatitis, focal or multifocal nodular dermatitis, proliferative dermatitis, or mucocutaneous ulcerative or proliferative dermatitis.[14] With these lesions, secondary bacterial pyoderma is the most common complicating co- morbidity.[8] Histologically, these lesions are granulomatous or pyogranulomatous with acanthosis, orthokeratotic and hyperkeratotic hyperkeratosis, and ulceration with serocellular crust formation.[8] Lymphoplasmacytic vasculitis and perivasculitis may also be present. Ocular lesions may also occur in approximately 16% of patients, depending on disease severity.[11] Common manifestations are conjunctivitis, blepharitis, and anterior uveitis.[11]

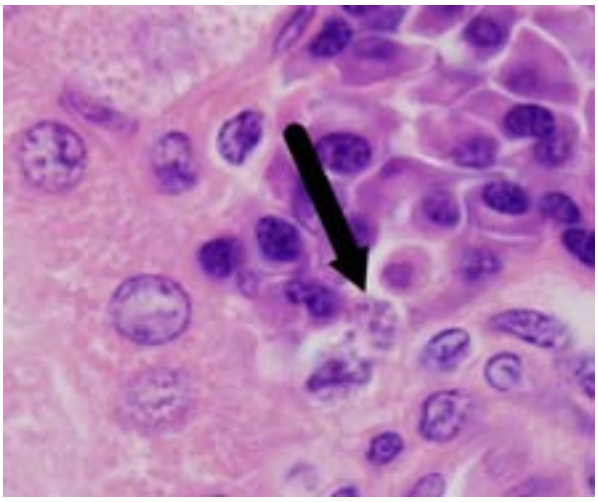

3-2. Kidney, dog. Histiocytes contain intracytoplasmic 2-4 µm round amastigotes with a central dark nucleus and a single rod-shaped kinetoplast. (HE 1000X)

Renal disease due to glomerulonephritis and interstitial nephritis is a common clinical sign of canine leishmaniasis due to *Leishmania infantum,* occurring in greater than 96% of symptomatic dogs. Alterations in renal function during active VL are generally reversible with *anti-Leishmania* therapy with antimonials or amphotericin B.[1,7] However, VL-associated kidney disease is progressive and without therapy can result in end stage renal disease (>25% of canine cases).[7,12] Renal lesions due to visceral leishmaniasis have been previously characterized as progressive glomerulonephritis including mesangial proliferative, membranoproliferative (MPGN), focal segmental glomerulosclerosis, and minimal change glomerulonephritis, and a smaller percentage with crescentic glomerulonephritis.[4,5] Multiple studies have evaluated the morphology and ultrastructural characteristics of renal lesions due to canine leishmaniasis.[4,5] Previous characterizations described a wide array of morphologic changes, primarily of a membranoproliferative and mesangial proliferative type.[4,5]

Dogs with symptomatic VL typically have a hypergammaglobulinemia and a high degree of circulating parasite antigen.[3] It is logical that immune complexes comprise glomerular deposits responsible for VL-associated MPGN. However, studies evaluating the proteins associated with these glomerular deposits have had conflicting results, with either presence or absence of lgG, lgM, or C3b in glomerular deposits.[5,10] All studies found a significant increase in the amount of *L. infantum* antigen and inflammatory cells within the glomerular basement membrane and mesangium.[4,5] Increased numbers of CD4+ T cells within the glomerulus of affected animals as well as increased expression of adhesion molecules ICAM-1 and P-Selectin have been characterized.[5]

JPC Diagnosis: Kidney: Glomerulonephritis, membranoproliferative, diffuse, severe, chronic, with multifocal to coalescing lymphoplasmacytic and histiocytic interstitial nephritis and intra-histiocytic protozoal amastigotes.

Conference Comment: The contributor does an excellent job of summarizing the epidemiology, pathogenesis, clinical appearance and gross/ histologic features of canine leishmaniasis. *Leishmania* sp. produces three general types of disease in veterinary medicine: cutaneous, mucocutaneous and visceral. VL has both anthroponotic (*L. donovani*) and zoonotic (*L. infantum*) forms- dogs are the primary reservoir of zoonotic leishmaniasis.[6] VL has received a significant amount of media attention in recent years, owing to hundreds of reported cases of Old World cutaneous and (less frequently) visceral leishmaniasis in US soldiers and military working dogs deployed to Iraq or Afghanistan.[15]

While there are numerous potential clinical presentations of canine leishmaniasis, diffuse mesangioproliferative or membranoproliferative glomerulonephritis and interstitial nephritis are the most common renal manifestations.[1,4] As noted by the contributor, although a type III hypersensitivity mechanism has historically been accepted as the primary mechanism of VL glomerulopathy, there is new evidence to suggest that migration of CD4+ T-cells and increased expression of adhesion molecules such as ICAM-1 and P-Selectin are also involved, while decreased apoptosis may play a role in the proliferative pattern of MPGN.[5] The basic pathogenesis of type III hypersensitivity and immune mediated glomerulonephritis involves persistent antigenemia with a slight antigen excess, which results in circulating soluble immune complexes that deposit in glomerular capillaries. These antigen-antibody complexes activate the complement cascade via the classical pathway, which induces production of C3a, C5a and C5-9 (the membrane attack complex or MAC). C5a is chemotactic for neutrophils, which release toxic proteinases, arachidonic acid metabolites and oxygen free radicals, while both C3a and C5a are potent anaphylatoxins. Additionally, the MAC is

capable of directly damaging the glomerular capillaries and mesangium.[16]

Contributing Institution: Department of Veterinary Pathology
College of Veterinary Medicine
Iowa State University
Ames, Iowa 50010-1250

References:

1. Aresu L, Benali S, Ferro S, et al. Light and electron microscopic analysis of consecutive renal biopsy specimens from Leishmania-Seropositive dogs. *Vet Pathol.* 2013;50(5):753-60.
2. Baneth G, Koutinas AF, Solano-Gallego L, et al. Canine leishmaniosis – new concepts and insights on an expanding zoonosis: part one. *Trends Parasitol.* 2008;24:324-330.
3. Boggiatto PM, Ramer-Tait AE, Metz K, et al. Immunologic indicators of clinical progression during canine *Leishmania infantum* infection. *Clin Vaccine lmmunol.* 2010;17:267-273.
4. Costa FA, Goto H, Saldanha LC, et al. Histopathologic patterns of nephropathy in naturally acquired canine visceral leishmaniasis. *Vet Pathol.* 2003;40:677-684.
5. Costa FA, Prianti MG, Silva TC, et al. T cells, adhesion molecules and modulation of apoptosis in visceral leishmaniasis glomerulonephritis. *BMC Infect Dis.* 2010;10:112.
6. Esch KJ, Petersen CA. Transmission and epidemiology of zoonotic protozoal diseases of companion animals. *Clin Microbial Rev.* 2013;26:58-85.
7. lkeda-Garcia FA, Lopes RS, Ciarlini PC, et al. Evaluation of renal and hepatic functions in dogs naturally infected by visceral leishmaniasis submitted to treatment with meglumine antimoniate. *Res Vet Sci.* 2007;83:105-108.
8. Koutinas AF, Polizopoulou ZS, Saridomichelakis MN, et al. Clinical considerations on canine visceral leishmaniasis in Greece: a retrospective study of 158 cases (1989-1996). *J Am Anim Hosp Assoc.* 1999;35:376-383.
9. Laufs H, Muller K, Fleischer J, et al. Intracellular survival of Leishmania major in neutrophil granulocytes after uptake in the absence of heat-labile serum factors. *Infect lmmun.* 2002;70:826-835.
10. Nieto CG, Navarrete I, Habela MA, et al. Pathological changes in kidneys of dogs with natural Leishmania infection. *Vet Parasitol.* 1992;45:33-47.
11. Pena MT, Naranjo C, Klauss G, et al. Histopathological features of ocular leishmaniosis in the dog. *J Comp Pathol*. 2008;138:32-39.
12. Plevraki K, Koutinas AF, Kaldrymidou H, et al. Effects of allopurinol treatment on the progression of chronic nephritis in Canine leishmaniosis (*Leishmania infantum*). *J Vet Intern Med*. 2006;20:228-233.
13. Rodriguez NE, Gaur Dixit U, Allen LA, et al. Stage-specific pathways of *Leishmania infantum chagasi* entry and phagosome maturation in macrophages. *PLoS One.* 6:e19000, 2011.
14. Solano-Gallego L, Koutinas A, Miro G, et al. Directions for the diagnosis, clinical staging, treatment and prevention of canine leishmaniosis. *Vet Parasitol.* 2009;165:1-18.
15. Weina PF, Neafie RC, Wortmann G, Polhemus M, Aronson NE. Old world leishmaniasis: an emerging infection among deployed US military and civilian workers. *Clin Infect Dis*. 2004;39(11): 1674-1680.
16. Zachary JF, McGavin MD, eds. *Pathologic Basis of Veterinary Disease*. 5th ed. St. Louis, MO: Elsevier; 2012:104-106,263-266,620-622.

CASE IV: G8745 (JPC 4033559).

Signalment: 3-year-old intact male ring-tailed lemur (*Lemur catta*).

History: The lemur was part of the breeding group of the German Primate Center (GPC), kept in a partly indoor and partly outdoor facility. Until found in an ill condition, the animal was an active part of his social group. He was found in the morning, apart from his family with signs of abdominal tumefaction, pressing and passive behavior. Treatment with Butylscopolamin, Metamizole and Dexamethasone followed. The general condition declined two days later, so blood samples were taken, the medical treatment was sustained and an intravenous drip was administered for rehydration.

The next day, ultrasonic examination of the abdomen was made without proper results, so a laparotomy was performed. Within the abdomen there was ascites and severe multifocal necrotizing hepatitis, so a biopsy of the liver was taken. One day after the surgery the ring-tailed lemur was found dead in his cage.

Gross Pathology: At necropsy, the lemur was in good nutritional condition. The main pathologic finding was severe hepatomegaly. The liver parenchyma was diffusely interspersed with small partly confluent whitish lesions. The spleen was enlarged and a serofibrinous peritonitis was manifest, accompanied by ascites. Parts of the small intestine, mesentery and pancreas were clotted together. In addition the mesenteric lymph nodes were hyperplastic. Focal petechial hemorrhage was found in parts of the duodenum and ileum. There was also severe, diffuse edema in the lung.

Laboratory Results: AST (392 U/L) and LDI (2079 U/L) were markedly increased. BUN (72 mg/dl) and creatinine (1.66 mg/dl) were moderately increased.

Listeria monocytogenes was isolated from heart, lung, liver, spleen, kidney and central nervous system by bacteriological culture and confirmed by PCR.

Immunohistochemistry using a polyclonal anti-*Listeria monocytogenes*-antibody revealed a positive reaction in liver, gallbladder, spleen, kidney, urinary bladder, large and small intestine, mesentery, pancreas, palatine tonsil, mesenteric lymph nodes and periorchium.

Histopathologic Description: Liver: Within the parenchyma there are numerous multifocal to coalescing areas of necrosis and inflammation, characterized by karyorrhectic debris, degradation of cells and a mild infiltration of leukocytes. The foci are sharply bounded from healthy liver tissue and randomly scattered throughout the liver.

Contributor's Morphologic Diagnosis: Liver: Necrotizing hepatitis, acute, multifocal to coalescing, with necrotizing serositis, ring-tailed lemur (*Lemur catta*), nonhuman primate.

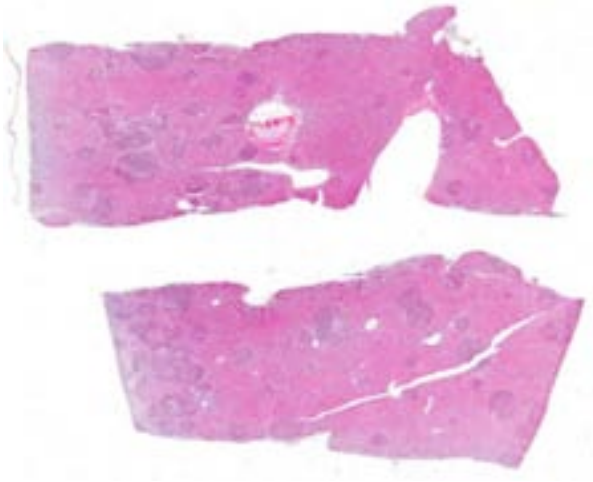

4-1. Liver, ring-tailed lemur: There are multifocal to coalescing random areas of hepatocellular necrosis that often efface portal, central veins, and vasculature. (HE 0.63X)

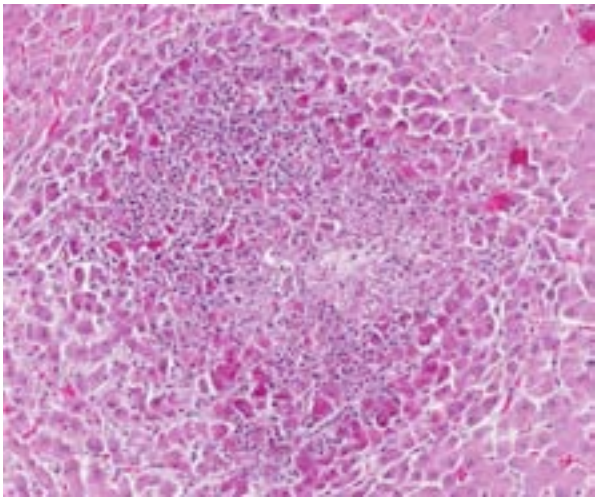

4-2. Liver, ring-tailed lemur: Areas of lytic necrosis are surrounded by darkly eosinophilic shrunken, degenerating hepatocytes. (HE 80X)

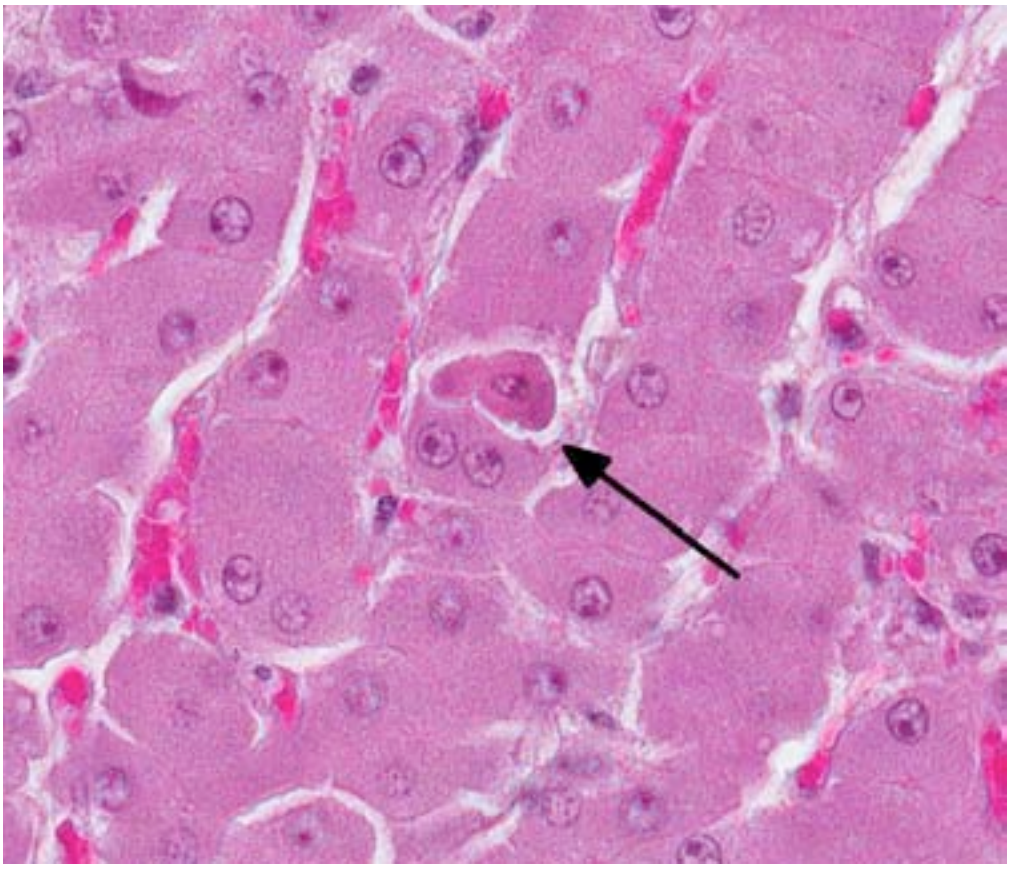

4-3. Liver, lemur: In less affected areas, there are individual hepatocytes that are rounded up, with darkly eosinophilic cytoplasm. (HE 400X)

Contributor's Comment: Listeriosis is an important foodborne disease, found in a large range of species. It is most frequently apparent in ruminants, but it is also an important issue in human medicine, especially in geriatrics, neonatology and diseases of immunocompromised patients.

The disease is caused by *Listeria monocytogenes*, a facultative anaerobic, gram-positive, rod-shaped bacterium which has the ability to invade cells and duplicate in the cytoplasm. *Listeria monocytogenes* is a ubiquitous pathogen; it is found in the natural microbial flora in ruminants, in the feces of birds and wild animals and it persists in the environment as a saprophyte, especially on decaying vegetation, such as inadequately soured silage. *Listeria monocytogenes* is known to cause three different clinical presentations. The cerebral form, with meningitis and encephalitis, is the most common in sheep. The pregnancy-associated form leads to stillbirths, abortion and premature birth. The third form is the septicemic form. Most cases of listeriosis remain clinically silent in healthy individuals.

Relatively few cases of listeriosis are reported in nonhuman primates (NHP) and there are no case reports in ring-tailed lemurs. Most of the reported incidences in NHP are accompanied by reproductive failure with abortion, stillbirth or neonatal death due to septicemia or cerebral complications.[1,6,11] There is one report of a free-living guereza in Kenya with similar pathologic findings to this case.[8]

The severe nature and rapid progression of the disease in the present case could be secondary to immune suppression, as lymphoid depletion is noted in multiple lymph nodes throughout the body.

JPC Diagnosis: Liver: Hepatitis, necrotizing, acute, multifocal to coalescing, moderate, with hepatocellular dissociation and individual hepatocyte necrosis.

Conference Comment: *Listeria monocytogenes* is most notorious in veterinary medicine for its effects in the CNS and reproductive system, although a septicemic form appears to be the culprit in this case. In ruminants and horses, unilateral or bilateral rhombencephalitis (and occasional meningitis/ meningoencephalitis), with microabscessation, is the typical clinical manifestation of listeriosis, however this bacterium can also localize to the pregnant uterus, causing sporadic abortion and stillbirth.[10] Abortion due to *Listeria* has also been reported in rabbits,[7] and listeriosis has become an increasingly significant cause of reproductive failure and fetal septicemia in non-human primates.[2] Additionally,

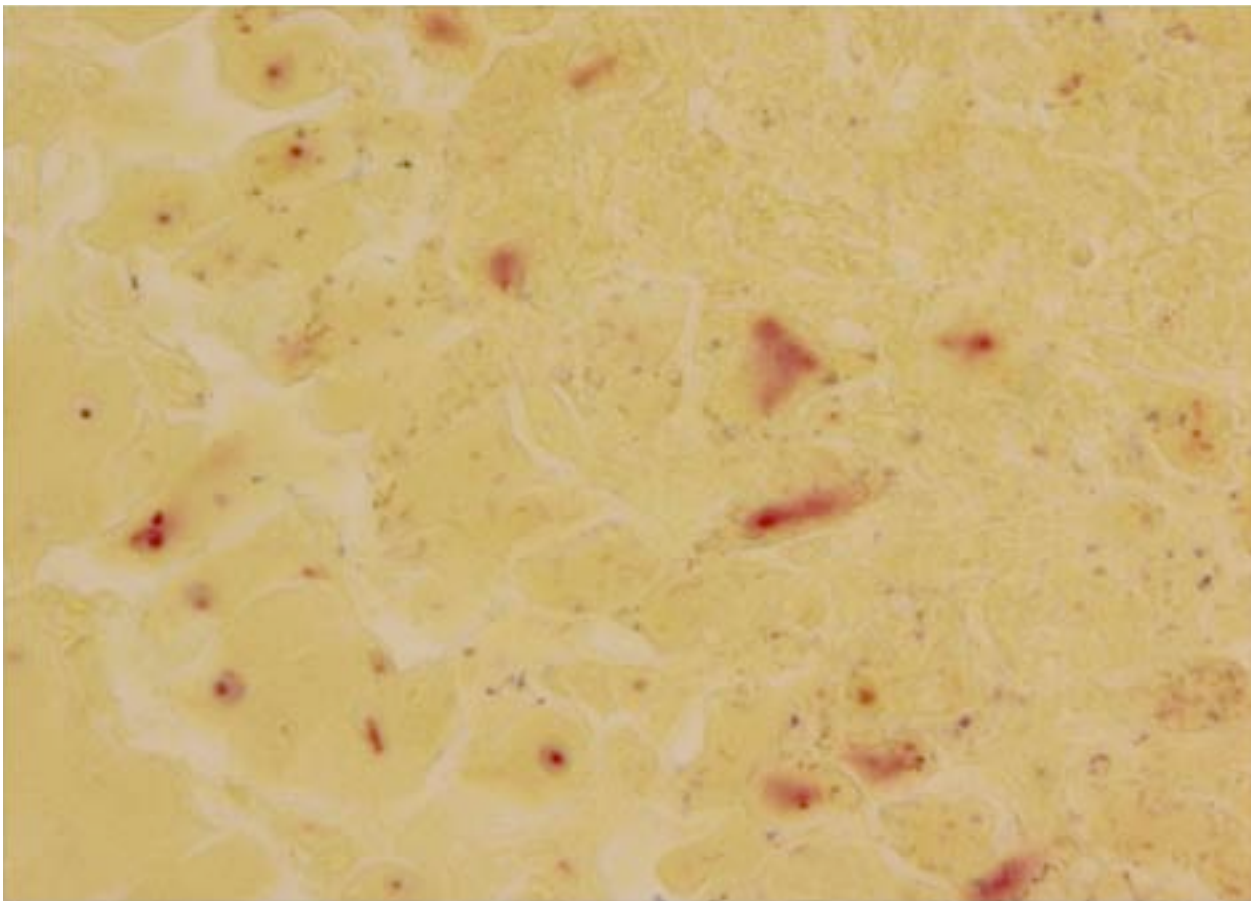

4-4. Liver, lemur: Few gram-positive L. monocytogenes bacilli are present at the periphery of necrotic foci. (BB 1000X)

there is at least one report of spontaneous meningoencephalitis in an immunocompetent rhesus macaque,[7] and enteric listeriosis, though infrequent, has been reported in New Zealand sheep.[4]

There is evidence that *Listeria* localizes to the ruminant brainstem via retrograde axonal migration along cranial nerve branches after crossing the oral epithelium, with potential spread into more rostral brain regions by intracerebral axonal migration. This is in contrast to human CNS infections where a hematogenous route is hypothesized.[3] It has also been suggested that E-cadherin (expressed by oral epithelium and Schwann cells) could bind internalin on the surface of *Listeria* to facilitate entry into the brainstem, however this has not yet been demonstrated.[3,4] Listerial abortions in ruminants occur during the last trimester of pregnancy with fetal infection or septicemia caused by hematogenous spread from the placenta. If the dam is infected at the beginning of the last trimester, there is rapid fetal infection and abortion with only mild maternal disease. If the infection occurs closer to parturition, dystocia with severe metritis, placentitis and septicemia are more likely.[10]

Histologic lesions of listeriosis are typically characterized by necrosis with a mild neutrophilic infiltrate.[8] Conference participants explored several potential differential diagnoses for necrotizing hepatitis in a NHP, briefly discussing *Francisella tularensis*, *Clostridium piliforme* and alphaherpesviruses. Hepatic conditions specifically reported in lemurs include cirrhosis, hemochromatosis and hepatocellular carcinoma.[5,8]

Contributing Institution: German Primate Center, Pathology Unit
Kellnerweg 4, 37077
Göttingen, Germany
http://dpz.eu

References:

1. Chalifoux LV, Hajema EM. Septicemia and meningoencephalitis caused by *Listeria*

monocytogenes in a neonatal *Macaca fascicularis*. *J Med Primatol*. 1981;10(6):336-339.
2. Cline JM, Brignolo L, Ford EW. Urogenital system. In: Abee CR, Mansfield K, Tardif S, Morris T, eds. 2nd ed. *Nonhuman Primates in Biomedical Research: Diseases*. San Diego, CA: Academic Press; 2012:524-525.
3. Disson O, Lecuit M. Targeting of the central nervous system by *Listeria monocytogenes*. *Virulence*. 2012;3(2):213-221.
4. Heldstab A, Rüedi D. Listeriosis in an adult female chimpanzee (*Pan troglodytes*). *J Comp Pathol*. 1982;92(4):609-612.
5. Fairley RA, Pesavento PA, Clark RG. *Listeria monocytogenes* infection of the alimentary tract (enteric listeriosis) of sheep in New Zealand. *J Comp Path*. 2012;146(4)308-313.
6. Glenn KM, Campbell JL, Rotstein D, Williams CV. Retrospective evaluation of the incidence and severity of hemosiderosis in a large captive lemur population. *Am J Primatol*. 2006;68(4):369-81.
7. Heldstab A, Rüedi D. Listeriosis in an adult female chimpanzee (*Pan troglodytes*). *J Comp Pathol*. 1982;92(4):609-612.
8. Lemoy MJ, Lopes DA, Reader JR, Westworth DR, Tarara RP. Meningoencephalitis due to *Listeria monocytogenes* in a pregnant rhesus macaque (*Macaca mulatta*). *Comp Med*. 2012;62(5):443-447.
9. Kock ND, Kock RA, Wambua E, et al. Listeriosis in a free-ranging colobus monkey (*Colobus guerezacaudatus*) in Kenya. *Vet Rec*. 2003;152(5): 141-142.
10. Nemeth NM, Blas-Machado U, Cazzini P, et al. Well-differentiated hepatocellular carcinoma in a ring-tailed lemur (*Lemur catta*). *J Comp Pathol*. 2013;148(2-3):283-287.
11. Schlafer DH, Miller RB. Female genital system. In: Maxie MG, ed. *Jubb, Kennedy and Palmer's Pathology of Domestic Animals*. 5th ed. Vol. 3. Philadelphia, PA: Elsevier Saunders; 2007:492-493.
12. Simmons J, Gibson S. Bacterial and mycotic diseases of nonhuman primates. In: Abee CR, Mansfield K, Tardif S, Morris T, eds. 2nd ed. *Nonhuman Primates in Biomedical Research: Diseases*. San Diego, CA: Academic Press; 2012:105-172.

WEDNESDAY SLIDE CONFERENCE 2013-2014

Conference 4

09 October 2013

CASE I: C13-122 (JPC 4032962).

Signalment: 4-year-old, 1.4 kg castrated male ferret (*Mustela putorius furo*).

History: The ferret presented for an approximately 2-month history of difficulty ambulating, progressive ataxia, and proprioceptive deficits in all limbs. MRI and CT identified a non-resectable mass at the level of C1 to C2. Fine needle aspirational cytology was performed. The animal was euthanized approximately 2 months later after failing to improve neurologically after attempting definitive radiation therapy.

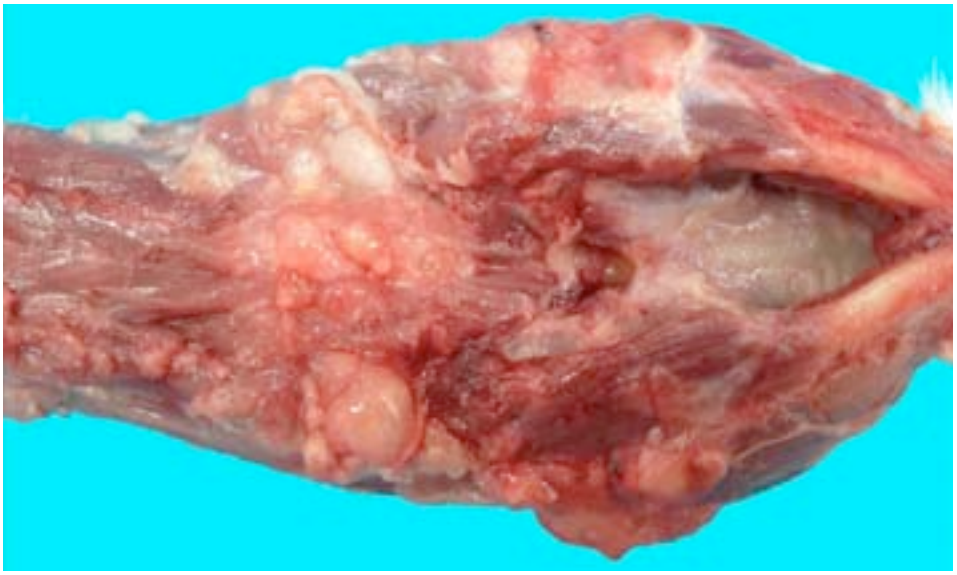

1-1. Cervical vertebrae, ferret: An approximately 2 x 1.8 x 1 cm, multinodular, translucent white neoplasm infiltrates the atlas and extends ventrally into the cervical musculature, dorsally into the spinal canal and extends craniad into the foramen magnum. (Photo courtesy of: Tufts Cummings School of Veterinary Medicine, Department of Biomedical Sciences, Section of Pathology. http://www.tufts.edu/vet/dbs/pathology.html)

Gross Pathology: An approximately 2 x 1.8 x 1 cm, multi-nodular, clear and gelatinous to hard and white mass effaced the C1 vertebra, extended ventrally into the cervical musculature and projected dorsally into the spinal canal and extended cranially into the foramen magnum along the ventral aspect of the brainstem. There was marked, segmental compression of the cervical spinal cord and brainstem.

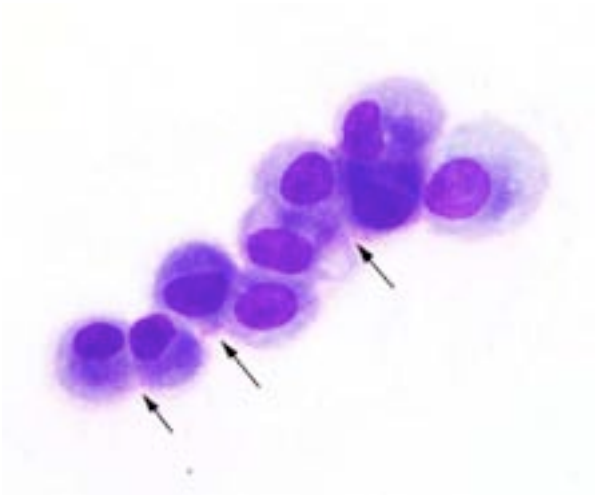

1-2. Fine needle aspirate, cervical mass: Clusters of neoplastic cells are composed of 10 µm polygonal cells with dark blue cytoplasm, indented nuclei with ropy chromatin, and one prominent nucleolus. A thin layer of bright pink matrix (arrows) separates neoplastic cells. (Wright-Giemsa 400X). (Photo courtesy of: Tufts Cummings School of Veterinary Medicine, Department of Biomedical Sciences, Section of Pathology. http://www.tufts.edu/vet/dbs/pathology.html)

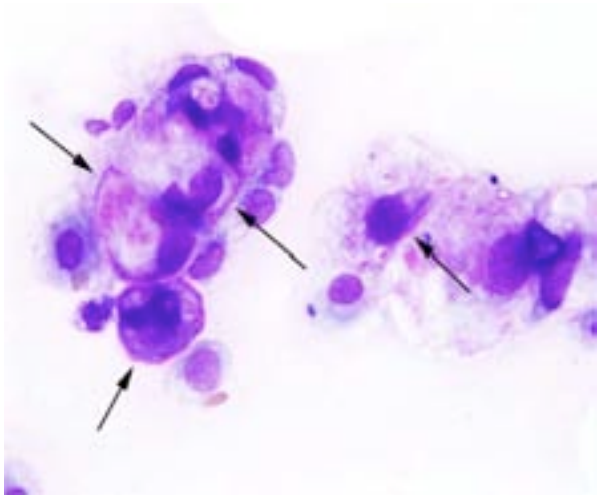

1-3. Fine needle aspirate, cervical mass: In some clusters, neoplastic cells (physaliferous cells) are binucleate, range up to 75 µ m, have vacuolated cytoplasm and often contain pink cytoplasmic granules that range up to 5 µm. Bright pink eosinophilic matrix (arrows) is visible. (Wright 400X). (Photo courtesy of: Tufts Cummings School of Veterinary Medicine, Department of Biomedical Sciences, Section of Pathology. http://www.tufts.edu/vet/dbs/pathology.html)

Cytologic Description: Fine needle aspirate, cervical mass: The sample is of good quality with minimal hemodilution. There are moderate numbers of nucleated cells on a moderately thick, grainy, eosinophilic background. Nucleated cells are present individually or in small clusters, showing marked (up to 5-fold) anisocytosis. The smaller cells are approximately 10 microns in diameter with a small amount of basophilic cytoplasm. The larger cells (physaliphorous cells) are markedly distended up to approximately 80 microns by cytoplasmic vacuolation that is clear or contains pink, grainy material. Nuclei are round to oval and often eccentric, with reticular chromatin, typically lacking obvious nucleoli. Mitotic figures are not observed.

Contributor's Morphologic Diagnosis: Cervical mass: Chordoma.

Contributor's Comment: The chordoma was confirmed by histopathology and immunohistochemistry following postmortem examination. Histopathology revealed an unencapsulated, multilobulated, moderately cellular neoplasm that effaced the first cervical vertebra and was composed of polygonal cells arranged in solid sheets supported by a moderate amount of fibrous to myxomatous to chondromatous stroma. These cells were often markedly vacuolated, typical of the physaliphorous cells described in chordomas. No mitoses were observed. Immunohistochemistry for cytokeratin and vimentin expression was performed on decalcified sections of the neoplasm, resulting in weak to moderate, patchy, cytoplasmic expression of both markers.

Chordomas are the most common neoplasm of the musculoskeletal system of the ferret,[4] but have also been described in other species, such as rats,[11] cats,[2] humans,[10] mink[6] and dogs.[8] The embryonic notochord degenerates early in fetal development and remains as the nucleus pulposus within intervertebral disks.[7] In some cases, residual notochord cells remain outside the intervertebral disks and may become a chordoma.

In ferrets, chordomas arise primarily in or adjacent to the caudal vertebra,[4] but they also have been described elsewhere along the spine.[9,12] Chordomas are locally aggressive, destroy the vertebral body, and invade adjacent tissues. Cutaneous metastases of chordomas have been reported in ferrets.[7,12] Although chordomas of the tail may be treated by amputation, at other locations along the axial skeleton, chordomas may not be amenable to surgical therapy and can cause spinal cord compression, as seen in this case.

The main differential diagnosis for a chordoma is chondrosarcoma. The large, severely vacuolated, physaliphorous cells of chordomas are not a feature of chondrosarcoma;[8] however, differentiation of these tumors is further aided by immunohistochemistry. Chordomas express

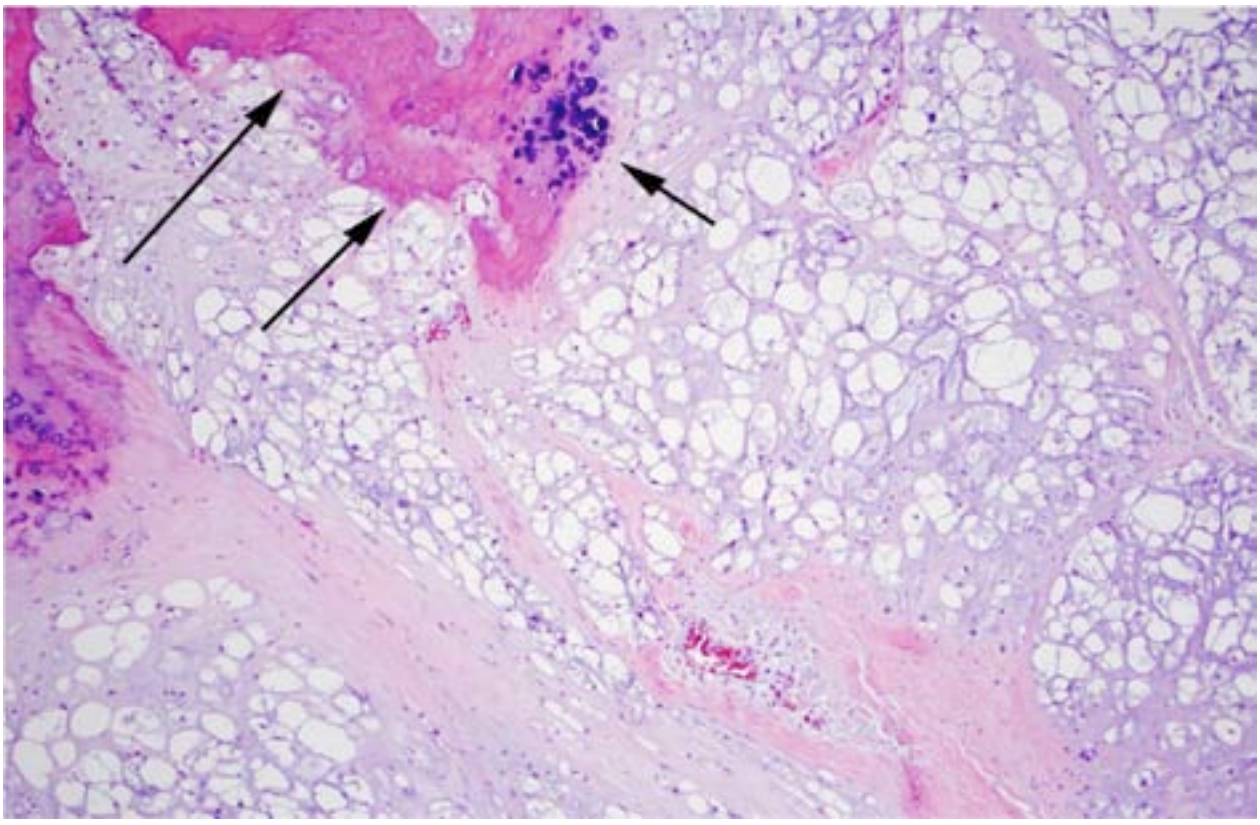

1-4. Cervical vertebrae, ferret: The neoplasm is primarily composed of physaliferous cells in a blue intracellular matrix, through which are interspersed trabeculae of cartilage (short arrow) and bone (large arrows). (HE 200X) (Photo courtesy of: Tufts Cummings School of Veterinary Medicine, Department of Biomedical Sciences, Section of Pathology. http://www.tufts.edu/vet/dbs/pathology.html)

vimentin, cytokeratin, and S-100 protein, while chondrosarcomas do not express cytokeratin. Combining the midline location of the tumor, cytological criteria such as physaliphorous cells, and immunohistochemical expression of cytokeratin confirms a diagnosis of chordoma.

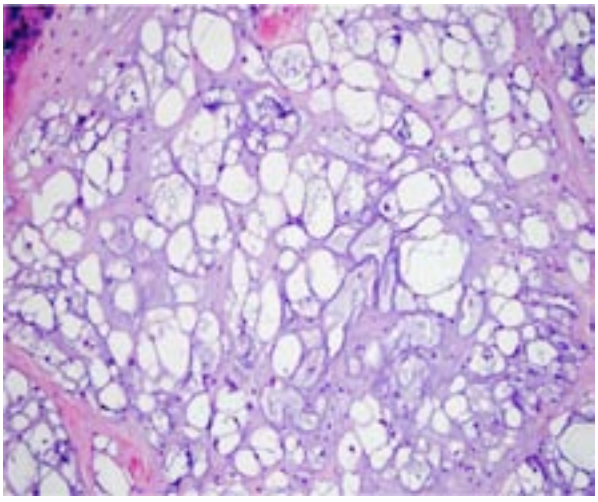

1-5. Cervical vertebrae, ferret: Neoplastic cells are markedly vacuolated, typical of the physalipherous cells in chordomas. (HE 400X) (Photo courtesy of: Tufts Cummings School of Veterinary Medicine, Department of Biomedical Sciences, Section of Pathology. http://www.tufts.edu/vet/dbs/pathology.html)

JPC Diagnosis: Cervical vertebrae: Chordoma.

Conference Comment: Chordomas are fairly well described in humans; however, they are rare in domestic animals, with the exception of ferrets.[9] In both humans and rats, chordomas are more common in aged males.[2,11] In humans they can occur anywhere along the vertebral column, often extend into soft tissue, and are divided into three types: conventional, chondroid and dedifferentiated.[3] Conventional chordomas are slow-growing, but locally invasive with a high rate of recurrence, especially in those that arise from the sacrococcygeal region or the vertebrae. Chondroid chordomas tend to originate from the spheno-occipital region and generally behave more benignly.[1] Conversely, dedifferentiated chordomas are rare (less than 5% of cases), with histologic features of a high-grade spindle cell sarcoma and aggressive biologic behavior. The distinction between conventional, chondroid and dedifferentiated types is important prognostically as

survival rates are up to three times higher with chondroid chordomas.[3]

Conference participants briefly discussed the occurrence of chordomas in various veterinary species. In ferrets, the most common location is on the tip of the tail; however, in most domestic species, chordomas tend to occur in the sacrococcygeal and cervical regions. In dogs, chordomas have also been reported in the brain, spinal cord, and skin.[5] Of the two reported cases of feline chordoma, one was initially diagnosed as chronic granulomatous inflammation due to the interpretation of the characteristic physaliphorous cells as atypical, foamy macrophages, but was later shown to be a classic chordoma, which subsequently metastasized to multiple lymph nodes.[2] The second feline case was classified histologically and immunohistochemically as a chondroid chordoma.[1] Chondroid chordomas similar to the human subtype have been reported in ferrets, mink, cats and dogs.[1,5] Similarly to human medicine, the distinction between conventional and chondroid chordomas may also have some degree of prognostic significance in animals. Although all chordomas are potentially locally invasive, chondroid chordomas in ferrets, dogs and cats have not been reported to metastasize, while conventional chordomas in rats[11] and cats[2] (but not dogs)[5] seem to have a higher rate of metastasis. Additionally, chordomas arising from the tail appear to have a good prognosis in all cases.[1]

An alternate spelling of "physaliferous" may be seen in the literature, and is considered a correct spelling as well.

Contributing Institution: Tufts Cummings School of Veterinary Medicine
Departement of Biomedical Sciences, Section of Pathology
http://www.tufts.edu/vet/dbs/pathology.html

References:

1. Carminato A, Marchioro W, Melchiotti E, Vascellari M, Mutinelli F. A Case of coccygeal chondroid chordoma in a cat: morphological and immunohistochemical features. *J Vet Diagn Invest.* 2008;20(5):679-681.
2. Carpenter JL, Stein BS, King NW Jr, Dayal YD, Moore FM. Chordoma in a cat. *J Am Vet Med Assoc.* 1990;197:240-242.
3. Chugh R, Tawbi H, Lucas DR, et al. Chordoma: the nonsarcoma primary bone tumor. *The Oncologist*. 2007;12(11):1344-1350.
4. Dunn DG, Harris RK, Meis JM, Sweet DE. A histomorphologic and immunohistochemical study of chordoma in twenty ferrets (*Mustela putorius furo*). *Vet Pathol.* 1991;28(6):467-473.
5. Gruber A, Kneissi S, Vidoni B, Url A. Cervical spinal chordoma with chondromatous component in an dog. *Vet Pathol*. 2008;45(5):650–653.
6. Hadlow WJ. Vertebral chordoma in two ranch mink. *Vet Pathol.* 1984;21(5):533-536.
7. Munday JS, Brown CA, Richey LJ. Suspected metastatic coccygeal chordoma in a ferret (*Mustela putorius furo*). *J Vet Diagn Invest.* 2004;16(5): 454-458.
8. Munday JS, Brown CA, Weiss R. Coccygeal chordoma in a dog. *J Vet Diagn Invest.* 2003;15(3): 285-288.
9. Pye GW, Bennett RA, Roberts GD, Terrell SP. Thoracic vertebral chordoma in a domestic ferret (*Mustela putorius furo*). *J Zoo Wildl Med*. 2000;31(1):107-111.
10. Rich TA, Schiller A, Suit HD, Mankin HJ. Clinical and pathologic review of 48 cases of chordoma. *Cancer.* 1985;56(1):182-187.
11. Stefanski SA, Elwell MR, Mitsumori K, Yoshitomi K, Dittrich K, Giles HD. Chordomas in Fischer 344 rats. *Vet Pathol.* 1988;25(1):42-47.
12. Williams BH, Eighmy JJ, Berbert MH, Dunn DG. Cervical chordoma in two ferrets (*Mustela putorius furo*). *Vet Pathol.* 1993;30(3):204-206.

CASE II: N12-247 (JPC 4032703).

Signalment: 1-year-old male rat snake (*Pantherophis* sp.)

History: Presented for inappetence and weight loss.

Gross Pathology: The mucosal surface of the stomach is diffusely tan and appears moderately thickened with a wall thickness of approximately 5 mm and increased prominence of rugal folds.

Histopathologic Description: The gastric mucosa is diffusely moderately to markedly thickened, with prominent rugal folds. Gastric pits lined by luminal epithelial cells are moderately to markedly elongated and frequently mildly dilated and branched or irregularly shaped. There is moderate to marked proliferation (hyperplasia) of mucus neck cells and aggregates of mucus neck cells multifocally replace granular cells within deeper portions of gastric glands disrupting the normal glandular architecture. There is multifocal piling (hyperplasia) of luminal epithelial and mucus neck cells and low numbers of mitotic figures are observed within these cell populations (averaging one per 400X field) and these mitotic figures extend to the luminal aspect of gastric pits. Low to moderate numbers of gastric glands are mildly dilated. Low numbers of gastric glands lined by remaining granular cells have multifocal attenuation (atrophy) of the glandular epithelium. Large numbers of approximately 3-6 µm diameter protozoa with amphophilic cytoplasm and distinct basophilic nuclei are adherent to the luminal epithelium and epithelium lining gastric pits and glands and are frequently admixed with small amounts of mucin and low numbers of necrotic epithelial cells. The lamina propria is diffusely expanded by mildly to moderately increased amounts of fibrous connective tissue that separates adjacent glands. Low to moderate numbers of lymphocytes and plasma cells and low numbers of heterophils are scattered within the lamina propria and are present in multifocal, nodular aggregates that surround gastric glands. Low numbers of lymphocytes and plasma cells are present within the luminal and glandular epithelium. The submucosa is multifocally expanded by small to moderate amounts of pale amphophilic granular to wispy material (edema), mildly increased amounts of fibrous connective tissue and small numbers of similar inflammatory cells.

2-1. Stomach, rat snake: The stomach wall is diffusely thickened and thrown into prominent rugal folds. (HE 0.63X)

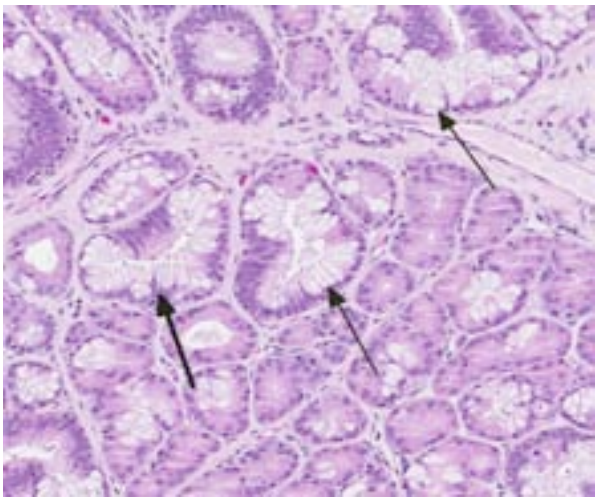

2-2. Stomach, rat snake: In addition to diffuse hyperplasia of mucus cells within gastric glands, there is also mucus cell metaplasia, in which mucus cells replace atrophic granular cells deep within crypts (arrows). (HE 120X)

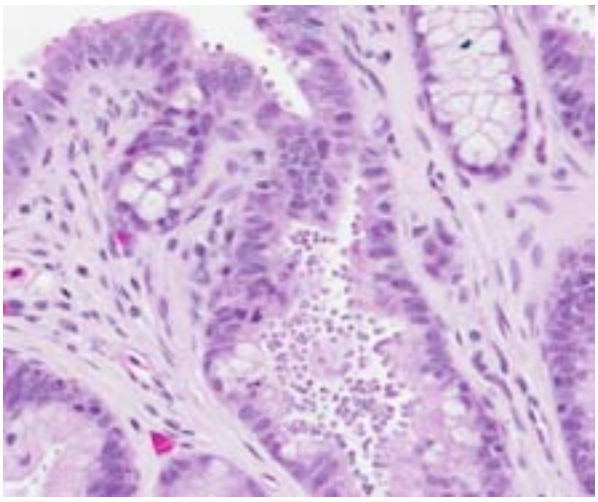

2-3. Stomach, rat snake: Moderate numbers of 4-6 µm apicomplexan schizonts, consistent with Cryptosporidium serpentis, line the luminal and glandular mucosal epithelium. (HE 400X)

Contributor's Morphologic Diagnosis: Stomach: Hypertrophic gastritis, diffuse, moderate, chronic, with myriad intraluminal protozoa consistent with *Cryptosporidium* sp.

Contributor's Comment: A number of *Cryptosporidium* sp. infect reptiles, including *C. serpentis*, *C. varanii* (*saurophilum*), and other unidentified species of *Cryptosporidium.*[9] Despite this, each species of *Cryptosporidium* is relatively species-specific; species from mammals do not infect snakes with experimental transmission.[6] *Cryptosporidium* infection commonly causes proliferative gastritis, progressive weight loss, and eventual death.[4] In lizards, enteritis is more common, although gastritis can occur as well.

Histopathology is considered the gold standard for diagnosis, as it enables differentiation of pathogenic cryptosporidia from those ingested with prey, which makes fecal testing difficult. However, recent advances in molecular biology make fecal testing more useful.[9]

JPC Diagnosis: Stomach: Gastritis, proliferative, diffuse, moderate, with marked mucus cell hyperplasia and metaplasia, rare mucosal epithelial necrosis and numerous intraepithelial and luminal apicomplexan schizonts.

Conference Comment: Cryptosporidia are obligate intracellular coccidians of the phylum *Apicomplexa*. Apicomplexans are so named because the sporozoites possess an "apical complex," containing rhoptries, micronemes, a conoid and a polar ring associated with microtubules, all of which are evident ultrastructurally.[2] These organisms reside within parasitophorous vacuoles along the epithelial microvillus border, and thus occupy an intracellular yet extracytoplasmic domain; at the junction with the host cell there are finger-like folds of parasitic cytoplasm formed within an electron dense attachment zone, known as the "feeder organelle."[8] Infected hosts shed sporulated, thick-walled fecal oocyts that contain four sporozoites and can remain viable for several months. Upon ingestion, sporozoites excyst and invade the microvillus border of gastrointestinal, biliary, or respiratory epithelial cells, where they undergo asexual multiplication (schizogony/merogony) and gametogeny resulting in macro- and microgamonts. Finally, fertilization produces two types of oocysts, which sporulate within the host. Thick-walled oocysts exit the host, while thin-walled oocysts are involved in autoinfection; this ability to self-infect accounts for the chronicity and severity observed in some cases of cryptosporidiosis.[1]

Cryptosporidium infects both immune-competent and immune-suppressed animals.[3] Some cryptosporidia of veterinary importance are listed in table 1.[3,8,9] *Cryptosporidium* spp. have a comparatively low minimum infective dose, are relatively resistant to normal concentrations of chlorination and can cause life-threatening diarrhea in immune-deficient humans.[5] Several species, most notoriously *C. parvum*, are zoonotic; however the most frequent mode of human transmission is

actually human-to-human.[7] Whereas dairy calves are an important potential source of *C. parvum*, adult cattle typically shed non-zoonotic species. *C. meleagridis*, especially from turkeys, has also been identified as zoonotic. *C. hominis* and *C. parvum* are the most commonly identified species in humans.[5] Interestingly, *Cryptosporidium* sp. instigated the largest ever recorded waterborne disease outbreak, affecting 400,000 people (approximately one quarter of the population) in Milwaukee, Wisconsin in 1993.[7] Initially, contamination of the municipal drinking water was blamed on contaminated run-off from nearby cattle farms and abbatoirs; however *C. hominis* was the primary isolate from water samples, with lower concentrations of *C. parvum*, suggesting that the majority of the contamination was likely secondary to human sewage.[5]

Table 1. Selected *Cryptosporidium* sp.[3,8,9]

Species	**Major Host**
C. parvum	Mammals (human and bovine genotypes)
C. hominis	Humans
C. andersoni	Cattle, camels
C. suis	Pigs
C. felis	Cats
C. canis	Dogs
C. muris	Rodents, camels
C. wrairi	Guinea pigs
C. cuniculus	Rabbits
C. baileyi, C. meleagridis	Birds
C. serpentis, C. crotali	Snakes
C. varanii	Lizards, snakes
C. ducismarci	Tortoises
C. molnari	Fish
C. fayeri, C. macropodum	Kangaroos

Contributing Institution: Department of Infectious Diseases and Pathology
University of Florida
P.O. Box 110880
Gainesville, FL 32611-0880
http://idp.vetmed.ufl.edu/

References:

1. Bowman DD, ed. *Georgis' Parasitology for Veterinarians*. 9th ed. St. Louis, MO: Elsevier; 2009:99-101.
2. Brogden KA. Cytopathology of pathogenic prokaryotes. In: Cheville NF, ed. *Ultrastructural Pathology: The Comparative Cellular Basis of Disease*. 2nd ed. Ames, IA: Wiley-Blackwell; 2009:538-558.
3. Brown CC, Baker DC, Barker IK. Alimentary system. In: Maxie MG, ed. *Jubb, Kennedy, and Palmer's Pathology of Domestic Animals*. 5th ed. Vol. 2. Philadelphia, PA: Elsevier; 2007:274-276.
4. Brownstein DG, Strandberg JD, Montali RJ, Bush M, Fortner J. *Cryptosporidium* in snakes with hypertrophic gastritis. *Vet Pathol*. 1977;14(6): 606-617.
5. Chako CZ, Tyler JW, Schultz LG, Chiguma L, Beerntsen BT. Cryptosporidiosis in people: it's not just about the cows. *J Vet Intern Med*. 2010;24(1): 37-43.
6. Graczyk TK, Cranfield MR. Experimental transmission of *Cryptosporidium* oocyst isolates from mammals, birds and reptiles to captive snakes. *Vet Res*. 1998;29(2):187-195.
7. Leav BA, Mackay M, Ward HD. *Cryptosporidium* species: new insights and old challenges. *CID*. 2003;36(7):903-908.
8. Pohlenz J, Bemrick WJ, Moon HW, Cheville NF. Bovine Cryptosporidiosis: a transmission and scanning electron microscopic study of some stages in the life cycle and of the host-parasite relationship. *Vet Pathol.* 1978;15(3):417-427.
9. Richter B, Nedorost N, Maderner A, Weissenbock H. Detection of *Cryptosporidium* species in feces or gastric contents from snakes and lizards as determined by polymerase chain reaction analysis and partial sequencing of the 18S ribosomal RNA gene. *J Vet Diagn Invest*. 2011;23(3):430-435.
10. Richter B, Rasim R, Globokar Vrhovec M, Nedorost N, Pantchev N. Cryptosporidiosis outbreak in captive chelonians (*Testudo hermanni*) with identification of two *Cryptosporidium* genotypes. *J Vet Diagn Invest*. 2012;24(3):591-595.

CASE III: WSC 2012 #1 (JPC 4019387).

Signalment: 8-week-old male Flemish Giant rabbit (*Oryctolagus cuniculus*).

History: A 400-animal rabbitry experienced a mortality of 20 rabbits in one month. Clinical signs included sudden onset of marked lethargy and head tilt. Rabbits died 24-48 hours after showing signs of illness. Clinical signs were observed in all age groups, although mostly young rabbits were affected. The breeder was treating the herd with sodium sulfamethazine and amprolium solution in water for coccidiosis.

Gross Pathology: Five, 8-week-old rabbits (3 male, 2 female) were submitted for necropsy. The rabbits were in poor body condition, e.g. were very thin and lacked body fat. There was tan/red mottling of the renal cortices, and the cortical surfaces of the kidneys were irregular. The cut surfaces of kidneys had many pale areas extending from the cortex to the medulla. The lungs were moderately congested and edematous. The spleen was moderately enlarged and the liver was moderately congested. The stomach contained a small amount of green mucoid material. In many areas, the mucosa of the small and large intestine was moderately congested.

Laboratory Results: Fecal flotation was positive for *Eimeria* sp. oocysts.

Aerobic bacterial culture of the kidney yielded *E. coli*.

A sample of frozen kidney was positive by PCR testing for *Encephalitozoon cuniculi*.

Histopathologic Description: Kidney: In many areas of the cortex and medulla there are interstitial infiltrates of moderate to large numbers of macrophages and lymphocytes and plasma cells. These interstitial infiltrates frequently surround ectatic tubules, which are lined by attenuated, degenerate, or necrotic epithelium; occasionally, tubules are lined by swollen renal tubular epithelial cells that contain numerous, intracytoplasmic, 1.5 x 3 µm refractile spores. Often the lumina of affected tubules contain sloughed tubular epithelial cells, cellular debris, and numerous intracellular and extracellular 1.5 x 3 µm refractile spores. Moderate numbers of tubules have cellular casts in their lumina.

Affecting the gray and white matter of the cerebrum and the cerebellum (slide not provided), there are scattered, nodular infiltrates of moderate numbers of macrophages (which contain 1.5 x 3 µm refractile spores in their cytoplasm) and activated microglia, few lymphocytes and plasma cells, and rare neutrophils together with small amounts of necrotic debris. Rarely there are 10-100 µm in diameter cysts which contain numerous, 1.5 x 3 µm refractile spores; these cysts are present both in areas of inflammation and in areas free of inflammation. The leptomeninges in many areas are moderately expanded by a similar inflammatory infiltrate. Vessels are lined by reactive endothelium and there

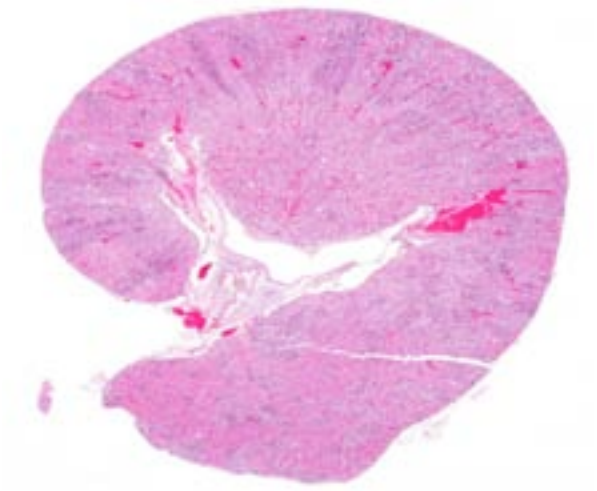

3-1. Kidney, rabbit: The cortical interstium is expanded by pyramidal rays of basophilic inflammatory cells. Vasculature is congested. Renal tubules are ectatic multifocally. (HE 0.63)

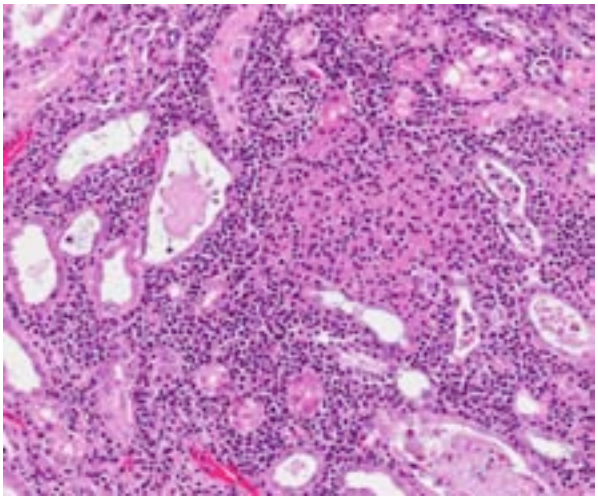

3-2. Kidney, rabbit: Tubules are multifocally necrotic, and the intervening interstitium is expanded by aggregates of macrophages surrounded by large numbers of lymphocytes and plasma cells. (HE 256X)

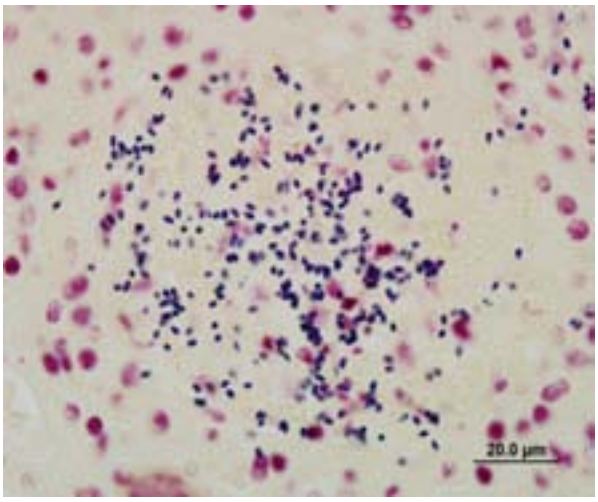

3-3. Kidney, rabbit: A tissue Gram stain reveals numerous 2 X 3 µm intra- and extracellular microsporidian spores consistent with Encephalitozoon cuniculi. (Brown and Brenn 1000X)

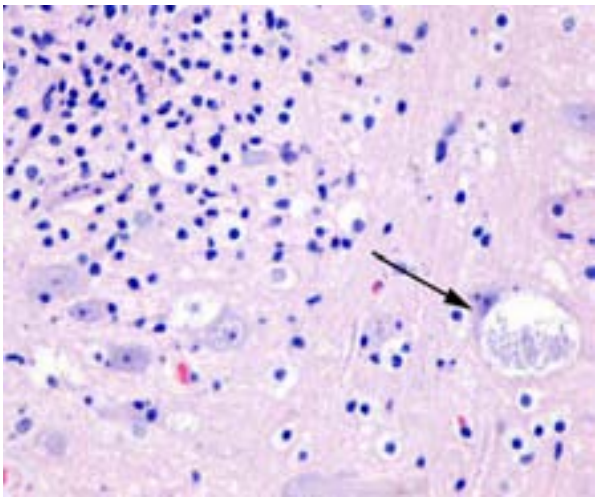

3-4. Cerebrum, rabbit: Mature spores are present within a vacuolated neuron (arrow). (Photo courtesy of: University of Connecticut, Connecticut Veterinary Medical Diagnostic Laboratory, Department of Pathobiology and Veterinary Science. www.patho.uconn.edu) (HE 1000X)

is a small amount of hemorrhage in the leptomeninges.

The spores in the kidney and the brain stained gram positive with the Brown and Brenn's gram stain and faintly acid-fast-positive with Ziehl-Neelsen acid-fast stain.

Contributor's Morphologic Diagnosis: Kidney: Marked, multifocal, granulomatous, interstitial nephritis, with tubular ectasia, degeneration and necrosis, and intralesional microsporidial spores, etiology consistent with *Encephalitozoon cuniculi.*

Contributor's Comment: In this case, 4 out of 5 rabbits had kidney and brain lesions that were similar and severe; one had mild lesions but had severe enteric coccidiosis. A Gram stain was used to assist in identifying spores and their features, which were compatible with those of microsporea. PCR was performed on a sample of frozen kidney from one of the rabbits to confirm the presence of DNA of *Encephalitozoon cuniculi*.

Encephalitozoon cuniculi is a microscopic parasite that belongs to the phylum Microspora, which encompasses obligate intracellular, spore-forming, single-celled parasites with a direct life cycle.[5,9] Microsporidia are characterized by a severe reduction, or even absence, of cellular components typical of eukaryotes such as mitochondria, Golgi apparatus and flagella. This simplistic cellular organization has made it difficult to infer the evolutionary relationship of Microsporidia to other eukaryotes. It is now widely acknowledged that features of Microsporidia previously recognized as primitive are instead highly derived adaptations to their obligate parasitic lifestyle.[2] Microsporidia were initially thought to be protozoa but subsequent molecular biological evidence suggests that they are more closely related to fungi than protozoa.[10] These findings include the presence of a particular mitochondrial heat shock protein more closely related to that of fungi, alpha- and beta-tubulins that are closely related in composition to those of fungi, and the presence of chitin and trehalose, which are typical components of fungi.[6,10]

Encephalitozoon cuniculi infections have been reported in many mammalian species, e.g. rabbits, SCID mice, guinea pigs, alpacas, neonatal foxes, neonatal dogs, and immune compromised people. Severe disease is rare except in immune compromised mammals.[5,7,10,11] Three strains have been identified: strain I was found in rabbits and humans, strain II in rodents and blue foxes, and strain III in dogs and humans. Identification of strains in humans and animals suggest possible zoonotic transmission. Although strain III of *E. cuniculi* is found in humans and dogs, no direct evidence suggests that dogs can transmit the disease to humans.[3]

Encephalitozoon cuniculi transmission occurs through ingestion, by inhalation of contaminated urine or feces shed by infected hosts, transplacentally, and rarely by penetration across

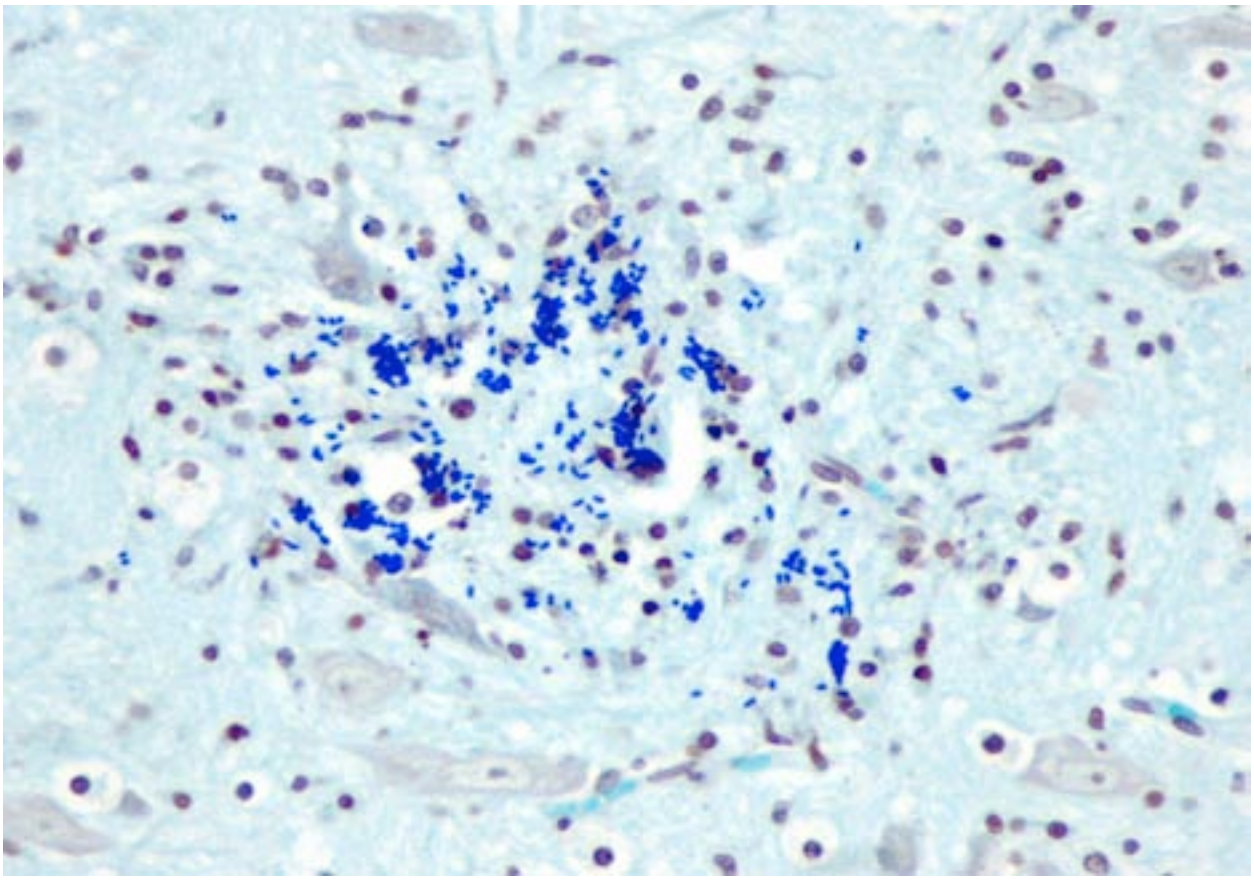

3-5. Cerebrum, rabbit: Mature spores are present intra-and extracellularly within areas of cerebral inflammation. (Photo courtesy of: University of Connecticut, Connecticut Veterinary Medical Diagnostic Laboratory, Department of Pathobiology and Veterinary Science. www.patho.uconn.edu) (Gram 1000X)

injured epithelium.[8,10] Microsporidia extrude a polar tube and inject the infective sporoplasm into the host cell in response to the appropriate environmental stimuli from the host. Subsequently, development proceeds by two processes, i.e. merogony and sporogony. During merogony the sporoplasm divides and generates numerous proliferative forms called meronts. Sporogony produces intermediate stages known as sporonts, which produce sporoblasts that will mature into spores and eventually be released into extracellular space.[12]

In naturally infected rabbits, *E. cuniculi* infections are often subclinical. Occasionally infected rabbits will display neurologic signs of ataxia, opisthotonos, torticollis, hyperaesthesia, or paralysis.[4] This is especially true in young rabbits. Dwarf rabbits are also especially susceptible.[10] Focal, irregular, depressed areas in the renal cortex can be seen in chronically infected rabbits; however, gross lesions are usually absent in infected rabbits.[4] The parasite is able to infect a large variety of cell types, such as neurons, epithelial cells of ependyma and choroid plexus, renal tubular epithelium, endothelium and macrophages.[10] Characteristic foci of granulomatous inflammation and organisms are observed in brain, kidney, lung, adrenal gland, and liver.[5] Histologically, multifocal nonsuppurative meningoencephalitis with astrogliosis and perivascular lymphocytic infiltration and focal to segmental lymphocytic-plasmacytic interstitial nephritis with variable amounts of fibrosis are reported. Early lesions in the kidney display focal to segmental granulomatous interstitial nephritis with degenerated epithelial cells and mononuclear cell infiltration. Lesions minimally involve glomeruli. In the lung, focal to diffuse interstitial pneumonia with mononuclear cell infiltration may occur. Hepatic lesions are characterized by a focal granulomatous inflammatory response with periportal lymphocytic infiltration. Multifocal lymphocytic infiltrates may also occur in the myocardium. With the Gram stain parasites are seen as gram-positive, 1.3-1.5 µm, rod-shaped organisms in the intracellular parasitophorous vacuoles of cells. Encephalitozoonosis in rabbits should be

differentiated from infection by *Pasteurella multocida, Listeria monocytogenes*, and *Toxoplasma gondii*.[8,10] Electron microscopy can reveal the organisms in parasitophorous vacuoles as well as the distinctive polar filaments.[3]

The incidence of encephalitozoonosis is on the decline in many areas, particularly in well-managed rabbitries. Regular serological testing will readily identify infected animals. Since seroconversion precedes renal shedding, infected animals can be identified before they are shedding organisms in the urine.[8]

JPC Diagnosis: Kidney: Nephritis, tubulointerstitial, histiocytic & lymphoplasmacytic, chronic, multifocal, moderate with intratubular microsporidian spores.

Conference Comment: As noted in the contributor's thorough examination of the life cycle and pathogenesis of E. cuniculi, microsporidia are obligate intracellular, unicellular eukaryotes that are most closely related to fungi, specifically zygomycetes. They have one of the smallest known genomes and exist extracellularly only as small, thick-walled spores with a coiled polar filament.[6] Developing spores can be packaged within a parasitophorous vacuole (*Encephalitozoon* spp.) or can remain within the cytoplasm (*Enterocytozoon bieneusi, Nosema* spp.).[10] The first recorded microsporidian parasite, *Nosema bombycis*, devastated the European silk-worm industry in the 1850s,[2] while currently, *Nosema apis* is a significant problem in honey bees, *Enterocytozoon salmonis* causes disease in chinook salmon[6] and *Encephalitozoon hellum* affects pigeons and exotic birds such as budgerigars and parrots.[7] Several other microsporidian species, including *Encephalitozoon intestinalis, E. hellum, Enterocytozoon bieneusi*, and *Vittaforma cornea* have been identified as opportunistic pathogens of humans, especially immunocompromised patients.[10] Additionally, a recent study suggests that Crohn's disease (CD) patients are at risk for microsporidiosis and that microsporidiosis may be involved in the etiology of CD.[1]

Contributing Institution: University of Connecticut
Connecticut Veterinary Medical Diagnostic Laboratory
Department of Pathobiology and Veterinary Science
www.patho.uconn.edu

References:

1. Andreu-Ballester JC, Garcia-Ballesteros C, Cuellar C. Microsporidia and its relation to Crohn's disease: a retrospective study. *PLoS ONE*. 2013;8(4):e62107.
2. Corradi N, Keeling PJ. Microsporidia: a journey through radical taxonomical revisions. *Fungal Biology Reviews*. 2009;23:1-8.
3. Didier PJ, Snowden K, Alvarez X, Didier ES. Microsporidiosis. In: Green CE, ed. *Infectious Diseases of the Dog and Cat*. 3rd ed. St. Louis, MO: Saunders; 2006:711-716.
4. Flatt RE, Jackson SJ. Renal nosematosis in young rabbits. *Vet Pathol.* 1970;7(6):492–497.
5. Fuentealba IC, Mahoney NT, Shadduck JA, Harvill J, Wicher V, Wicher K. Hepatic lesions in rabbits infected with *Encephalitozoon cuniculi* administered per rectum. *Vet Pathol.* 1992;29(6): 536-540.
6. Keeling PJ, McFadden GI. Origins of microsporidia. *Trends Microbiol.* 1998;6(1):19–23.
7. Lallo MA, Calabria P, Milanelo L. *Encephalitozoon* and *Enterocytozoon* (Microsporidia) spores in stool from pigeons and exotic birds: microsporidia spores in birds. *Vet Parasitol.* 2012;190(3-4):418-22.
8. Percy DH, Barthold SW. Rabbit. In: *Pathology of Laboratory Rodents and Rabbits*. 3rd ed. Ames, IA: Blackwell Publishing; 2007:290-294.
9. Szabo JR, Shadduck JA. Experiemental encephalitozoonosis in neonatal dogs. *Vet Pathol.* 1987;24(2):99-108.
10. Wasson K, Peper RL. Mammalian microsporidiosis. *Vet Pathol.* 2000;37(2):13-28.
11. Webster JD, Miller MA, Vemulapalli R. *Encephalitozoon cuniculi*-associated placentitis and perinatal death in an alpaca (*Lama pacos*). *Vet Pathol.* 2008;45(2):255–258.
12. Weidner E. Ultrastructural study of microsporidian invasion into cells. *Z Parasitenkd.* 1972;40(3):227–242.

CASE IV: 12-0399 (JPC 4025191).

Signalment: 2-year-old female goat, breed unspecified (*Capra hircus*).

History: Two female goats presented with multifocal to coalescing progressive ulcerative and crusting lesions on the commissures of the lips. Both goats were recently sent to another farm to be bred. The owner reports no change in appetite or behavior.

Gross Pathology: Portions of the lip were submitted for histopathological evaluation. Gross lesions consisted of multifocal to coalescing proliferative and ulcerative cheilitis.

Histopathologic Description: Haired skin, lip: There was extensive multifocal epidermal hyperplasia with acanthosis up to 10 times normal thickness with elongated, anastomosing rete ridges. Multifocally within the stratum, spinosum, keratinocytes were markedly swollen and often contained clear intracytoplasmic vacuoles (ballooning degeneration) and pyknotic nuclei. Multifocally, rare keratinocytes contained one or more 2-6 µ m, round to oval, eosinophilic intracytoplasmic inclusion bodies. Within the superficial stratum spinosum and stratum corneum, there was neutrophilic transmigration and multifocally there were microabscesses composed of aggregates of degenerate neutrophils admixed with eosinophilic cellular and karyorrhectic debris and abundant serum. There was multifocal spongiosis of the epidermis. Overlying the affected epidermis was a thick serocellular crust composed of keratin, proteinaceous fluid, degenerate neutrophils, and rare mixed bacteria. Within the dermis there were numerous dilated small caliber blood vessels separated by increased clear space and fibrin (edema), and moderate numbers of perivascular neutrophils, histiocytes, and lymphocytes.

Contributor's Morphologic Diagnosis: Haired skin, lip: Cheilitis, proliferative and necrotizing, focally extensive, severe, with epidermal hyperplasia, hyperkeratosis, rare epidermal eosinophilic intracytoplasmic inclusion bodies, and intraepidermal and intracorneal microabscesses, breed unspecified, caprine.

Contributor's Comment: Contagious ecthyma, also called contagious pustular dermatitis, is a zoonotic disease with worldwide distribution that affects sheep, goats, and man.[1-9,13,14,16,17] The causative agent is a dsDNA parapoxvirus (PPV).[1,3,5-9,16] PPV, also known as orf virus, gains entry through abraided skin and replicates in epidermal cells.[1,3,6-9,16,17] Skin lesions progress in an orderly fashion through multiple stages: erythema, macule, papule, vesicle, pustule, scab, and scar.[1-6,8,9,13,16,17] Infection is confined to the squamous epithelium and may involve the oral cavity, eyelids, teats, and coronary band, and predispose affected animals to secondary infections.[1,2,4,13,14,16,18] Very rarely, lesions extend to the squamous epithelium of the esophagus, rumen and omasum, causing ulcerative gastroenteritis.[1,2,4,18] Residual skin lesions are not infective once the scab falls off, but substantial amounts of infective virus are shed within scabs which can remain infective for years.[1,3-8,16] The disease has high morbidity and low mortality but can cause significant debilitation due to the inability of affected animals to suckle or graze.[4,6-9,13] Nursing animals often transfer the virus to adults, typically affecting the teats and udder.[1,3,4,6,7,9,13,14,17] There are several commercial vaccines for orf virus which contain virulent virus.[8,13] These vaccines are valuable because they limit the severity of disease, but they do not prevent infection, induce lesions, and contribute to maintenance of infective virus in the environment, so are only recommended for use in endemically infected herds.[8,13]

Gross lesions are characterized by multifocal to coalescing proliferative and ulcerative dermatitis which is localized to mucocutaneous junctions, particularly around the mouth and nares.[1,3,5,9,14] Histologic lesions are characterized by ballooning degeneration, exuberant epidermal hyperplasia with intracorneal pustules, and eosinophilic intracytoplasmic inclusion bodies within the stratum spinosum that are only briefly detectable at the vesicular stage.[1,3,4,8,9,17] There are frequently superimposed bacterial infections in the affected skin.[13]

Sheep previously exposed to orf virus can be repeatedly infected although the severity of the lesions and time to resolution diminishes with each subsequent infection.[1,6,8,13] This indicates that the host immune response can control the severity of disease but cannot prevent reinfection.[6] The reason is due, at least in part, to the presence of at least five immunomodulatory proteins expressed by orf virus that subvert or suppress elements of the host immune and inflammatory response, including:[2,5-8,11]

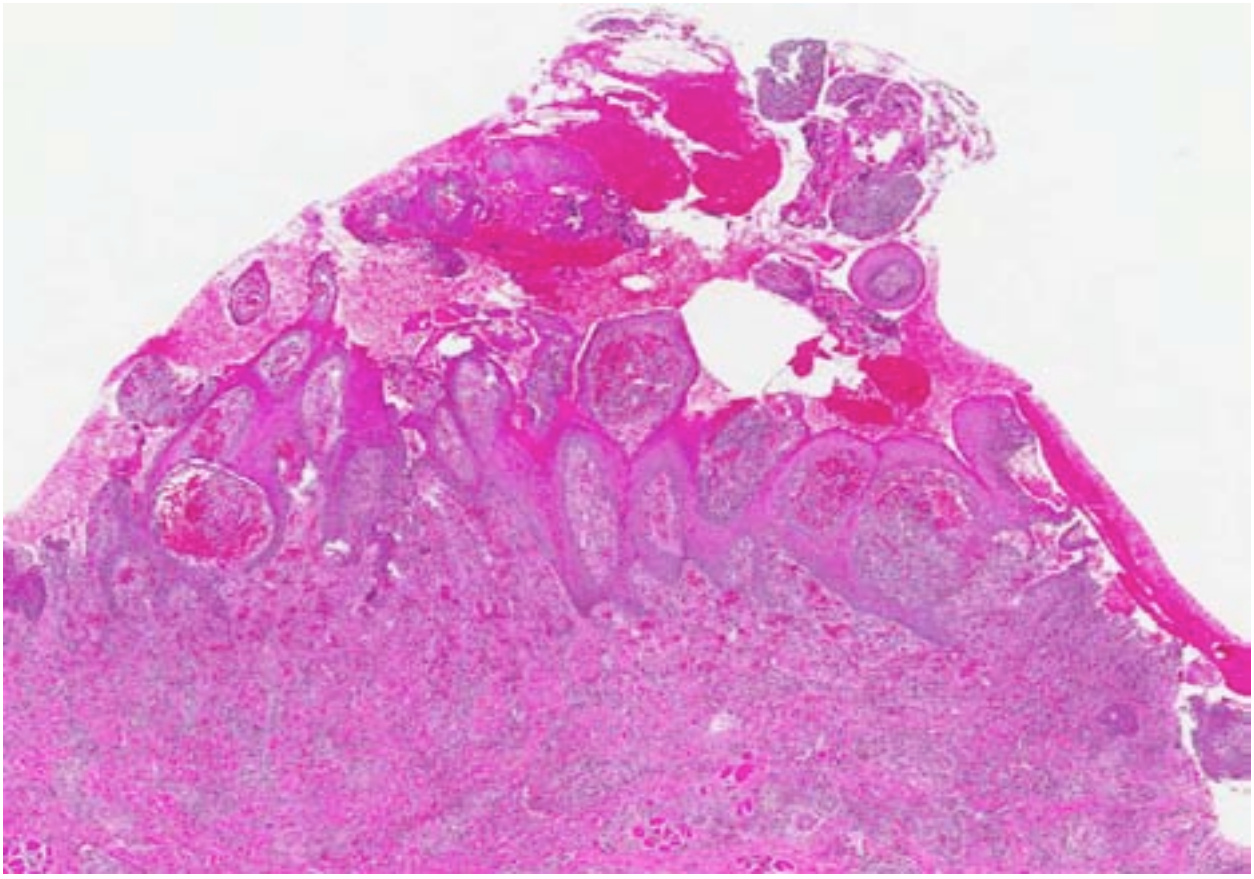

4-1. Lip, goat: At one edge of the section, the multifocally ulcerated epithelium is markedly hyperplastic and thrown into papillae. (HE 0.63X)

(1) **Orf virus interferon resistance protein (OVIFNR):** Host cells generally attempt to stop viral replication through interferon-induced activation of the double stranded RNA-dependent kinase (PKR) pathway.[5,7,8] In the presence of viral double-stranded RNA, the PKR pathway is induced by interferon and binds to viral dsRNA which inhibits virus (and host cell) protein translation, effectively blocking virus replication.[5-8] The orf virus encodes a protein, OVIFNR, which is a homologue of vaccinia virus E3L gene product, competitively binds to dsRNA and disallows activation of PKR, which ultimately promotes a permissive state for viral replication, leading to sustained protein synthesis and completion of the virus life cycle.[5-8] In other words, the OVIFNR protein prevents activation of PKR and protects the virus from the antiviral effects of interferons, allowing viral replication.[5-8]

(2) **Granulocyte/macrophage colony-stimulating factor (GM-CSF) inhibitory factor (GIF):** GIF binds to and inhibits the biological activity of the cytokines GMCSF and interleukin2 (IL-2).[2,5-7] In non-hematopoietic tissues, GMCSF is involved in the recruitment and activation of macrophages and neutrophils.[6,8] GMCSF also supports the recruitment and antigen-presenting function of dendritic cells (DC).[6,8] IL2 is required for T cell proliferation and activation, for example, the augmentation of T cell IF gamma production and to expand CTL and NK cell populations.[6] Inhibition of these two important cytokines significantly impedes the development of both innate and acquired immune responses.

(3) **Orf viral interleukin 10 (ORFV-IL-10):** The initiation of an acquired immune response to a virus requires that antigen be taken up by DC at the periphery, and then processed and transported to lymphoid tissue to be presented to T cells.[7,11] For this to occur, DC must first be activated by signals transmitted through the interaction of viral products with pattern recognition receptors expressed on the surface of the DC.[11] DC therefore form the vital bridge between the innate and acquired arms of the immune response.[11] IL-10 is an immunoregulatory cytokine that inhibits both innate and adaptive

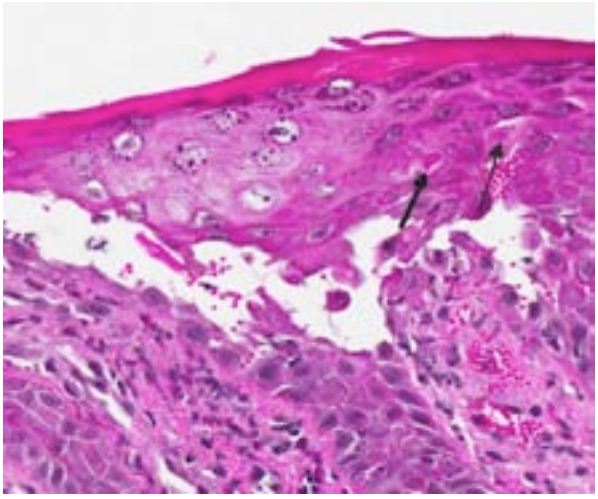

4-2. Lip, goat: At left, keratinocytes within the stratum spinosum undergo marked intracytoplasmic swelling ("ballooning degeneration"), at right several irregular 2-4 µ m intracytoplasmic poxviral inclusions are present (arrows). (HE 230X)

immune responses and is produced by macrophages and dendritic cells in response to microbial products.[17] It is produced by multiple T cell subsets, including all three populations of helper T cells (Th1, Th2, and Th17).[17] IL10 is able to down regulate MHC class II and co-stimulatory molecule expression on DC and macrophages, thus decreasing antigen presentation.[7,17] Orf virus-encoded interleukin-10 (ORFVIL10), a homologue of IL-10, has specifically been shown to suppress the migration of Langerhans cells (LC) and inhibit DC function in addition to suppressing inflammation and the innate immune response.[11] ORFV-IL-10 has the capacity to impair the initiation of an acquired immune response and hence inhibit the generation of immunological memory necessary for immunity of subsequent exposure.[11] ORFV-IL-10 may be capable of inhibiting the activation of memory cells recruited to infected skin following reinfection, as well as having the potential to inhibit the activation of naïve T cells that would otherwise be brought about by activated LC trafficking to the draining lymphoid tissue.[11] The implications of this are that on repeated cycles of infection, the virus can replicate, shed, and be transmitted to other hosts before elimination by the acquired immune response.[11]

(4) **Orf virus chemokine-binding protein (CBP):** Orf virus produces a novel CBP that binds CC chemokines such as monocyte chemotactic protein-1, macrophage inflammatory protein-1-alpha and RANTES (regulated upon activation normal T cell expressed and secreted) that control monocyte/macrophage and T cell recruitment to sites of infection.[5] Orf virus CBP also binds lymphotactin, a C chemokine that recruits T cells, B cells and neutrophils through the XCR1 receptor.[5] This provides further evidence that orf virus has evolved to inhibit important cellular elements of an anti-viral immune response.[5]

(5) **Orf virus vascular endothelial growth factor (VEGF):** Orf virus VEGF functions in the same way as cellular VEGFs, causing vascular proliferation and angiogenesis.[5,6,8,16] Orf virus lesions in sheep are characterized by vascular proliferation and dilation as well as epidermal proliferation.[5,8,16] The induction of epidermal proliferation by orf virus is probably important in supplying an abundance of target epidermal cells for virus replication.[5,8,16] Additionally, host cell VEGF has the ability to inhibit the development and maturation of dendritic cells.[5,8] If viral VEGF also has this ability, it would benefit the virus because of the important role that dendritic cells play in the generation and maintenance of immune responses.[5]

JPC Diagnosis: Mucocutaneous junction: Epithelial hyperplasia, diffuse, severe, with marked acanthosis, focally extensive necrosis, ballooning degeneration and rare intracytoplasmic viral inclusions.

Conference Comment: The contributor provides an excellent, comprehensive review of parapoxviruses. This genus causes epitheliotropic disease in a number of species of veterinary importance, in addition to sheep and goats. Papular stomatitis virus causes proliferative to ulcerative lesions on the lips and oral mucosa of cattle, while pseudocowpox virus causes similar lesions on the teats of dairy cattle and on the muzzles and mouths of nursing calves.[13] A parapoxvirus has been blamed for the sporadic occurrence of pustular facial dermatitis in camels[13] as well as New Zealand farmed red deer.[10] Additionally, outbreaks of contagious ecthyma have resulted in serious economical loss in Norwegian reindeer.[10] Sealpox virus, which produces self-limiting ulcerative dermal nodules in some pinniped species, has also been tentatively classified as a parapoxvirus.[15] The red squirrel population in the United Kingdom has been devastated by what was initially classified as a parapoxvirus, but is more likely a closely related poxvirus from the subfamily *Chordopoxvirinae*. American grey squirrels, which are relatively resistant to this virulent squirrelpox virus, likely

serve as a reservoir for disease in the more susceptible red squirrel population.[12]

Contributing Institution: Walter Reed Army Institute of Research
503 Robert Grant Avenue
Silver Spring, MD 20910
http://wrair-www.army.mil/

References:

1. Anderson DE, Rings DM, Pugh DG. Diseases of the integumentary system. In: Pugh DG, ed. *Sheep and Goat Medicine*. Philadelphia, PA: W.B. Saunders Company; 2002:203-204.
2. Deane D, McInnes CJ, Percival A, et al. Orf virus encodes a novel secreted protein inhibitor of granulocyte-macrophage colony-stimulating factor and interleukin-2. *J Virol*. 2000;74(3):1313-1320.
3. Gelberg HB. Alimentary system and the peritoneum, omentum, mesentery, and peritoneal cavity. In: Zachary JF, McGavin MD, eds. *Pathologic Basis of Veterinary Disease*. 5th ed. St. Louis, MO: Elsevier; 2012:326-327.
4. Ginn PE, Mansell JEKL, Rakich PM. Skin and appendages. In: Maxie MG, ed. *Jubb, Kennedy, and Palmer's Pathology of Domestic Animals*. 5th ed. Vol. 1. Philadelphia, PA: Elsevier; 2007:664-666.
5. Haig DM. Orf virus infection and host immunity. *Curr Opin Infect Dis*. 2006;19(2):127-131.
6. Haig DM. Subversion and piracy: DNA viruses and immune evasion. *Res Vet Sci*. 2001;70(3): 205-219.
7. Haig DM, McInnes CJ, Thomson J, et al. The orf virus OV20.0L gene product is involved in interferon resistance and inhibits an interferon-inducible, double-stranded RNA-dependent kinase. *Immunology*. 1998;93(3):335-340.
8. Haig DM, Mercer AA. Orf. *Vet Res*. 1998;29(3-4):311-326.
9. Hargis AM, Ginn PE. The integument. In: Zachary JF, McGavin MD, eds. *Pathologic Basis of Veterinary Disease*. 5th ed. St. Louis, MO: Elsevier; 2012:1023.
10. Klein J, Tryland M. Characterization of parapoxviruses isolated from Norwegian semi-domesticated reindeer (*Rangifer tarandus tarandus*). *Virology Journal*. 2005;2:79-89.
11. Lateef Z, Fleming S, Halliday G, et al. Orf virus-encoded interleukin-10 inhibits maturation, antigen presentation and migration of murine dendritic cells. *J Gen Virol*. 2003;84(Pt 5):1101-1109.
12. McInnes CJ, Wood AR, Thomas K, et al. Genomic characterization of a novel poxvirus contributing to the decline of the red squirrel (*Sciurus vulgaris*) in the UK. *J Gen Virol*. 2006;87(8):2115-2125.
13. Murphy FA, Gibbs EPJ, Horzinek MC, Studdert MJ. Poxviridae. In: *Veterinary Virology*. 3rd ed. San Diego, CA: Academic Press; 1999:289-291.
14. Navarre CB, Lowder MQ, Pugh DG. Oral-esophageal diseases. In: Pugh DG, ed. 1st ed. *Sheep and Goat Medicine*. Philadelphia, PA: W.B. Saunders Company; 2002:66-67.
15. Roess AA, Levine RS, Barth L, et al. Sealpox virus in marine mammal rehabilitation facilities, North America, 2007-2009. *Emerg Infect Dis*. 2011;17(12):2203-2208.
16. Savory LJ, Stacker SA, Fleming SB, et al. Viral vascular endothelial growth factor plays a critical role in orf virus infection. *J Virol*. 2000;74(22): 10699-10706.
17. Tizard IR. Regulation of adaptive immunity. In: *Veterinary Immunology*. 9th ed. St. Louis MO: Elsevier; 2013:217.
18. Zachary JF. Mechanisms of microbial infections. In: Zachary JF, McGavin MD, eds. *Pathologic Basis of Veterinary Disease*. 5th ed. St. Louis, MO: Elsevier; 2012:210.

Joint Pathology Center
Veterinary Pathology Services

WEDNESDAY SLIDE CONFERENCE 2013-2014

Conference 5

16 October 2013

CASE I: N12-191 (JPC 4019350).

Signalment: 5-week-old male Yorkshire cross, (*Sus scrofa domesticus*).

History: Three days before submission, the piglet became listless, developed a head tilt, ataxia, hind limb paresis and was circling. The piglet was treated with oral meloxicam and subcutaneous ceftiofur. On the day of submission, the piglet was recumbent with generalized muscle tremors. Additional piglets in this litter were less severely affected; however, one additional piglet from this litter was submitted for necropsy 2 days later with a similar clinical history.

1-1. Cerebrum at level of lateral ventricle, pig: At subgross inspection, the lateral ventricle is markedly expanded, contains an exudate, and there is rarefaction in the periventricular white matter. (HE 0.63X)

Gross Pathology: There are small, multifocal, perivascular white to tan plaques on the surface of the cerebral cortex. The lateral ventricles are moderately dilated and contain light yellow, clear fluid.

Histopathologic Description: Brain: Within the parenchyma and surrounding vessels around the ventricle, there are low to moderate numbers of lymphocytes, macrophages, plasma cells, neutrophils and few eosinophils. Low numbers of neutrophils, lymphocytes, plasma cells and macrophages infiltrate the ependymal layer, which is disorganized, as well as

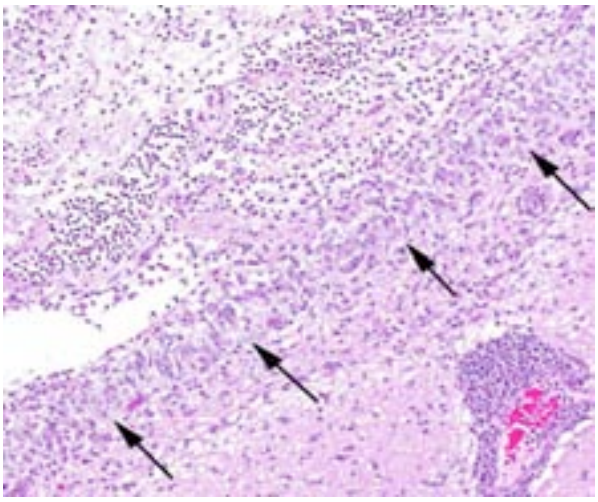

1-2. Cerebrum at level of lateral ventricle, pig: The ependyma is hypercellular with transmigrating inflammatory cells. At upper left, the ventricular exudate is composed of abundant fibrin and a mixed inflammatory population of numerous neutrophils, and fewer macrophages, eosinophils, lymphocytes, and plasma cells. At lower left, periventricular vessels are cuffed by moderate numbers of histiocytes, lymphocytes, and plasma cells. (HE 40X)

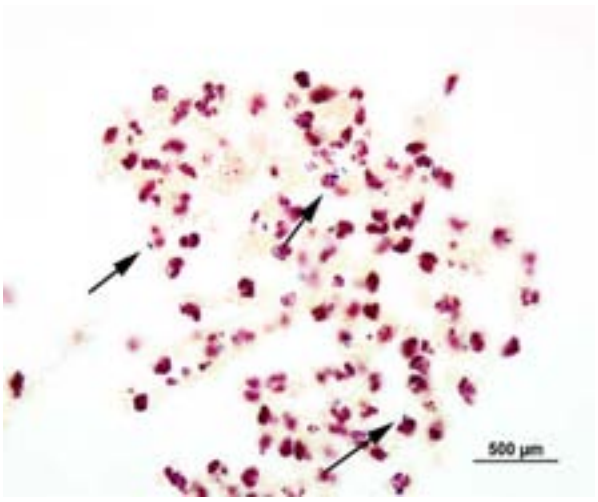

1-3. Lateral ventricle, pig: 1-2 µm Gram-positive paired cocci, consistent with Streptococcus suis, are present within phagocytes and adhered to necrotic debris. (Brown and Brenn 1000X)

the underlying parenchyma. The parenchyma surrounding the ventricle is edematous, and blood vessels with perivascular cuffs are lined by plump endothelial cells. The leptomeninges multifocally contain few to low numbers of lymphocytes, fewer macrophages and rare eosinophils and neutrophils. The ventricular lumen contains aggregates of fibrin, moderate numbers of neutrophils and macrophages, few multinucleated giant cells and rare eosinophils. Occasionally admixed with inflammatory cells and fibrin are Gram-positive cocci that are multifocally arranged in short chains.

Contributor's Morphologic Diagnosis: Brain: Meningoencephalitis and ventriculitis, neutrophilic, lymphohistiocytic and eosinophilic to pyogranulomatous, subacute, multifocally extensive, moderate, with intralesional gram-positive cocci.

Contributor's Comment: The cause for the neurologic signs was a meningoencephalitis that was localized primarily around and within the ventricles and choroid plexus. Multifocally within the ventricles, there were occasional clusters of intralesional gram-positive cocci arranged in short chains. Aerobic bacterial culture of the brain yielded *Streptococcus suis*, confirming suspicion of a streptococcal infection. The distribution of the inflammation was similar to what is described in association with this bacterium,[13] although the presence of multinucleated giant cells and eosinophils has not been reported within cases of streptococcal meningoencephalitis. This may speculatively have been due to an unusual serotype of the bacterium or an unidentified co-infection. The lesions in the other piglet submitted from this group the following week were similar.

Streptococcus suis is a gram-positive, facultative anaerobic, α-hemolytic streptococcus belonging to Lancefield group D.[3,11] More than 30 serotypes have been identified, and most infections in pigs in most countries are caused by serotype 2.[3] Disease is mainly seen in weanlings and growing pigs, with incidence peaking at weaning, and may include septicemia, serositis, meningitis, polyarthritis, pneumonia, abortions, abscesses and endocarditis.[3,11]

Outbreaks of *S. suis* generally have low morbidity and mortality ranging from 0-20%, depending on treatment.[11] Carriers are significant factors in disease transmission, and outbreaks may occur in closed herds.[11] Stress can predispose to infection, and concurrent infections increase morbidity.[11]

JPC Diagnosis: Cerebrum, lateral ventricle: Ventriculitis and paraventriculitis, fibrinosuppurative, granulomatous and eosinophilic, with mild to moderate meningitis

and intra-ventricular and intra-neutrophilic gram-positive cocci.

Conference Comment: *Streptococcus* species are catalase-negative, opportunistic pathogens affecting multiple organ systems in various species. They are generally categorized on the basis of their hemolytic pattern on blood agar as α, β or γ (non)-hemolytic. α- and γ-hemolytic streptococci are often normal inhabitants of the upper respiratory and lower urinary tracts, as well as the skin and gastrointestinal tract, while pathogenic species are usually β-hemolytic. *Streptococcus* species can be further designated into Lancefield groups A-V (excluding I and J) based on their cell wall polysaccharides.[5] *S. suis*, considered one of the most important bacterial pathogens of swine, has several important virulence factors, including its capsular polysaccharide and virulence-related proteins such as muramidase-released protein, extracellular protein factor and hemolysin. Hemolysin (or suilysin), is thought to enhance bacterial invasion and lysis of host cells. Suilysin is expressed by many strains of *S. suis* and has been associated with high virulence.[14]

There are several *Streptococcus* species of veterinary importance in addition to *S. suis*. *S. canis* infection in neonatal and adult dogs (and less commonly cats) has been associated with pneumonia, abortion, septicemia, endocarditis, necrotizing fasciitis, keratitis, lower urinary tract infections, cholangiohepatitis, prostatic abscesses, mastitis, arthritis and meningoencephalitis.[5] *S. equi* subsp. *equi* causes equine strangles, a contagious infection of the upper respiratory tract and local lymph nodes;[12] it has also been linked with immune mediated vasculitis and purpura hemorrhagica.[7] *S. equi* subs. *zooepidemicus* and *S. equisimilis* are associated with equine reproductive disease, but have also been isolated from the lung, liver, brain, kidney and joints.[8,12] *S. equi* subs. *zooepidemicus* also causes bursitis or fistulous withers in horses,[7] and was implicated in an outbreak of acute hemorrhagic pneumonia in more than 1,000 shelter dogs in California.[2] *S. agalactiae* (and less commonly *S. dysgalactiae* and *S. uberis*) are important causes of bovine mastitis.[9] *S. iniae* is a significant aquatic pathogen of tilapia and other reef fish, which causes necrosis, inflammation and vasculitis.[4] Furthermore, several species of *Streptococcus* are zoonotic, including *S. canis*,[5] *S. equi* sub. *zooepidemicus*,[12] *S. iniae*[4] and *S. suis*.[11,14]

Conference participants outlined several potential causes for the gross and histologic lesions associated with *S. suis* in swine. The fibrinous polyserositis often noted grossly at necropsy[11] could also occur secondary to *Hemophilus parasuis* or *Mycoplasma hyorhinus* infection.[1] Ruleouts for the microscopic lesions of meningoencephalitis and ventriculitis include salt toxicity, edema disease and postweaning multisystemic wasting syndrome (PMWS). Salt toxicity is characterized by cortical laminar necrosis/malacia with eosinophilic meningoencephalitis.[7] Shiga-toxin producing *E. coli* (STEC), the etiologic agent of porcine edema disease, induces fibrinoid vascular change and necrotizing vasculitis with subsequent edema in various tissues, including the brain.[6] Cerebellar spongiosis, necrotizing vasculitis, edema and hemorrhage are occasionally described in conjunction with porcine circovirus type 2 and PMWS.[10] However, as noted by the contributor, the ventricular localization and fibrinosuppurative character of the lesions in this case are fairly specific for *S. suis*.[11]

Contributing Institution: Department of Infectious Disease and Pathology
University of Florida College of Veterinary Medicine
http://idp.vetmed.ufl.edu/

References:

1. Brown CC, Baker DC, Barker IK. Alimentary system. In: Maxie MG, ed. *Jubb, Kennedy, and Palmer's Pathology of Domestic Animals*. 5th ed. Vol. 2. Philadelphia, PA: Elsevier; 2007:228, 288.
2. Erol E, Locke SJ, Donahe JK, Mackin MA, Carter CN. Beta-hemolytic *Streptococcus* spp. from horses: a retrospective study (2000-2010). *J Vet Diagn Invest*. 2012;24(1):142-147.
3. Kahn CM, ed. *Streptococcus suis* infection. In: *The Merck Veterinary Manual*, 9th ed. Whitehouse Station, NJ: Merck & Co, Inc.; 2011. Retrieved from <http://www.merckvetmanual.com/mvm/index.jsp?cfile=htm/bc/54302.htm>.
4. Keirstead ND, Brake JW, Griffin MJ, Halliday-Simmonds I, Thrall MA, Soto E. Fatal septicemia caused by the zoonotic bacterium Streptococcus iniae during an outbreak in Caribbean reef fish.

Vet Pathol. 2013 Sep 27. [Epub ahead of print]. Accessed 19 October 2013.
5. Lamm CG, Ferguson AC, Lehenbauer TW, Love BC. Streptococcal infection in dogs: a retrospective study of 393 cases. *Vet Pathol*. 2010;47(3):387-395.
6. Matise I, Sirinarumitr T, Bosworth T, Moon HW. Vascular ultrastructure and DNA fragmentation in swine infected with Shiga toxin-producing *Escherichia coli*. *Vet Pathol*. 2000;37(4):318-327.
7. Maxie MG, Youssef S. Nervous system. In: Maxie MG, ed. *Jubb, Kennedy, and Palmer's Pathology of Domestic Animals*. 5th ed. Vol. 1. Philadelphia, PA: Elsevier; 2007:173, 257, 358.
8. Pesavento PA, Hurley KF, Bannasch MJ, ARtiushin S, Timoney JF. A clonal outbreak of acute fatal hemorrhagic pneumonia in intensively housed (shelter) dogs caused by *Streptococcus equi* subsp. *zooepidemicus*. *Vet Pathol*. 2008;45(1):51-53.
9. Schlafer DH, Miller RB. Female Genital System. In: Maxie MG, ed. *Jubb, Kennedy, and Palmer's Pathology of Domestic Animals*. 5th ed, Vol. 3. Philadelphia, PA: Elsevier; 2007: 552-554.
10. Seelinger FA, Brugmann ML, Greiser-Wilke I, Verspohl J, Segales J, et al. Porcine circovirus type 2-associated cerebellar vasculitis in postweaning multisystemic wasting syndrome (PMWS)-affected pigs. *Vet Pathol*. 2007;44(5): 621-634.
11. Staats JJ, Feder I, Okwumabua O, Chengappa MM. *Streptococcus suis*: past and present. *Vet Res Comm.*1997;21:381-407.
12. Timoney, JF. The pathogenic equine streptococci. *Vet Res*. 2004;35(4):397-409.
13. Vasconcelos D, Middleton DM, Chirino-Trejo JM. Lesions caused by natural infection with *Streptococcus suis* type 9 in weaned pigs. *J Vet Diagn Invest.* 1994;6:335-341.
14. Zheng P, Zhao YX, Zhang AD, Kang C, Chen HC, et al. Pathologic analysis of the brain from *Streptococcus suis* type 2 experimentally infected pigs. *Vet Pathol*. 2009;46(3):531-535.

CASE II: D120073 (JPC 4032261).

Signalment: Wild-caught juvenile male raccoon, (*Procyon lotor*).

History: A juvenile male raccoon exhibiting neurological deficits was found by a member of the public and submitted to a wildlife rehabilitation facility in northern California in January 2012. The raccoon had wounds on the tail, pale mucous membranes, ataxia, head tremors, mild inappetence and an initial exacerbated startle response. The animal could never right himself, rolled over and was uncoordinated. Palliative treatment with meloxicam (Metacam®, 0.2 mg/kg subcutaneously q24h), procaine G penicillin (20,000 Units/kg subcutaneously q24h), iron dextran (10 mg/kg intramuscularly once) and vitamin B complex (30 mg/kg subcutaneously once), did not ameliorate the clinical signs. The raccoon was humanely destroyed and submitted to the California Animal Health and Food Safety Laboratory, Davis, California, for necropsy examination.

Gross Pathology: The raccoon had adequate fat stores. The liver was diffusely and markedly enlarged and pale with irregular, undulating surfaces. The spleen was also markedly enlarged and meaty. All lymph nodes noted were very pale and enlarged. The lungs were collapsed and there were occasional pinpoint pale subpleural foci. The gastrointestinal tract contained scant contents with a small amount of dry fecal matter in the distal large intestine.

Histopathologic Description: In the section of cerebellum the neuronal as well as glial cell cytoplasm was markedly distended (up to 3 times normal size) by aggregates of delicate clear round vacuoles (approximately 1µm in diameter). These aggregates occasionally displaced the nucleus to the periphery of the cell. Multifocally swollen eosinophilic axons were observed in the granular layer.

In the section of the spleen, foamy macrophages expanded the germinal centers and formed extensive sheets that replaced and effaced the red pulp.

Laboratory Results:

Test	Result
Aerobic culture- lung, liver, mesenteric lymph node	Mixed growth
Fecal PCR for *Salmonella* sp.	*Salmonella arizonae*
Fecal flotation	Negative
Serology for *Toxoplasma* sp.	Negative
Heavy/trace mineral analysis (lead, manganese, iron, zinc, arsenic, cadmium, molybdenum, copper, mercury, selenium)	Within normal limits
Rabies testing via fluorescent antibody testing on brain tissue	Negative
Lysosomal enzyme analysis	See Table 1
Special stains: Oil red O (on formalin fixed frozen sections), PAS, Sudan Black, Luxol fast blue and acid fast	- Multifocal endothelial cell intra-cytoplasmic accumulation of Oil red O-positive material - Affected neurons and macrophages were Oil red O, PAS, Sudan Black, Luxol fast blue and acid fast negative
Autofluorescence (via UV scope)	Negative

Contributor's Morphologic Diagnosis: Cerebellum: Severe diffuse neuronal and glial cell vacuolation and swelling with occasional multifocal spheroids (suspect storage disease).

Spleen: Germinal centers and red pulp severe diffuse histiocytosis (suspect storage disease).

Contributor's Comment: In addition to the cerebellum and spleen, multiple tissues were infiltrated and expanded by aggregates or sheets of previously described foamy macrophages. These include multiple lymph nodes; lamina propria of the tongue, intestine, colon; portal areas of the liver; and around the pulmonary vessels, in the alveolar spaces and subpleurally in the lung. Additionally, cerebral neurons and glial cells as well and peripheral ganglia neurons were similarly affected. Various degrees of cytoplasmic foaminess were also observed in the epithelial cells of the renal tubules, parietal glomerular cells and hepatocytes.

Transmission electron microscopy revealed lysosomal accumulations of floccular variably electron dense and frequently concentrically arranged lamellar material consistent with lysosomal storage disease. However, ultrastructural analysis is relatively non-specific regarding type of storage.

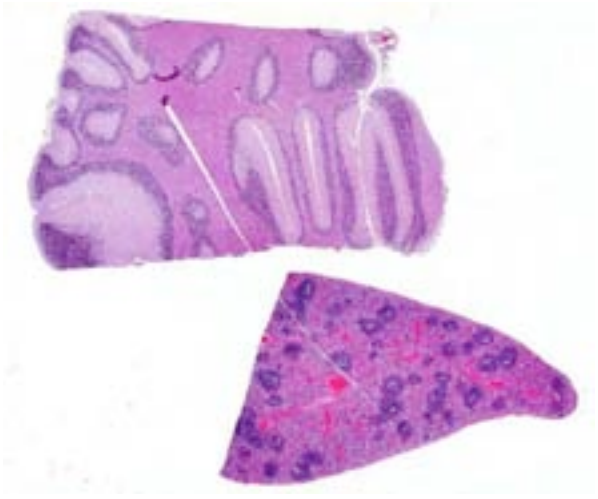

2-1. Cerebellum with medulla and spleen, raccoon: The granular layer of the cerebellum appears attenuated and the red pulp of the spleen is markedly expanded. The splenic white pulp appears hyperplastic. (HE 0.63X)

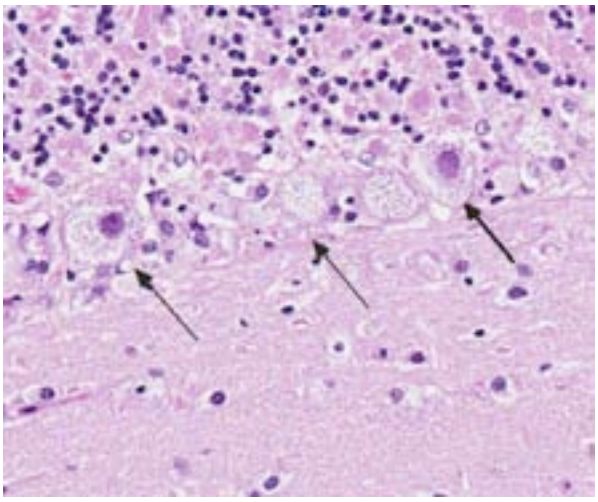

2-2. Cerebellum with medulla, raccoon: Purkinje cells (arrows) and smaller neurons within the granular cell layer are markedly swollen and contain large numbers of discrete clear vacuoles within their cytoplasm. (HE 250X)

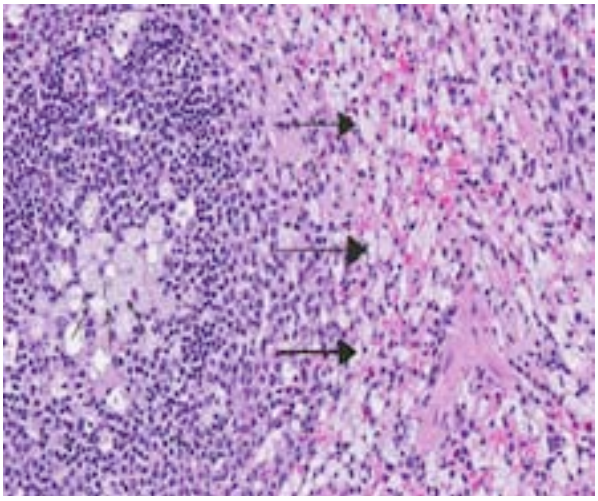

2-3. Spleen, raccoon: Macrophages with abundant foamy cytoplasm expand the germinal centers of splenic white pulp (small arrows) and greatly expand the red pulp (large arrows). (HE 250X)

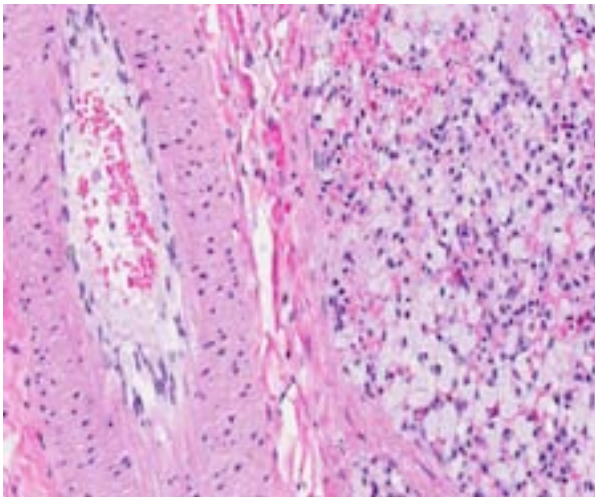

2.4. Spleen, raccoon: Endothelial cells also contain numerous discrete vacuoles within their cytoplasm. (HE 400X)

Measurement of lysosomal enzyme activity including sphingomyelinase, β-galactosidase, β-hexosaminidase and β-hexosaminidase A and B was performed in water homogenates of the brain samples from affected and age-matched non-affected raccoon[8] (Table 1). This assay revealed complete absence of sphingomyelinase activity. The absence of sphingomyelinase activity is a criterion for the diagnosis of sphingomyelin lipidosis (also known as Niemann – Pick disease (NPD)).[7]

Sphingomyelin lipidosis belongs to a large group of sphingolipidosis lysosomal storage diseases that also includes GM1 and GM2 gangliosidosis and globoid cell leukodystrophy, to name a few. In sphingolipidoses the spectrum of affected organs is wide and often includes viscera and macrophages because the substrate is derived from all cell membranes.[3] The involvement of neurons in most LSDs is due to both the high metabolic activity of these cells and their long life span, which allows the gradual accumulation of undegraded substrate.[3] Ultrastructural pathology offers useful information in the diagnosis of LSDs and helps categorize the type of LSD. In diseases accumulating sphingolipids, storage bodies are characterized by membranous material arranged

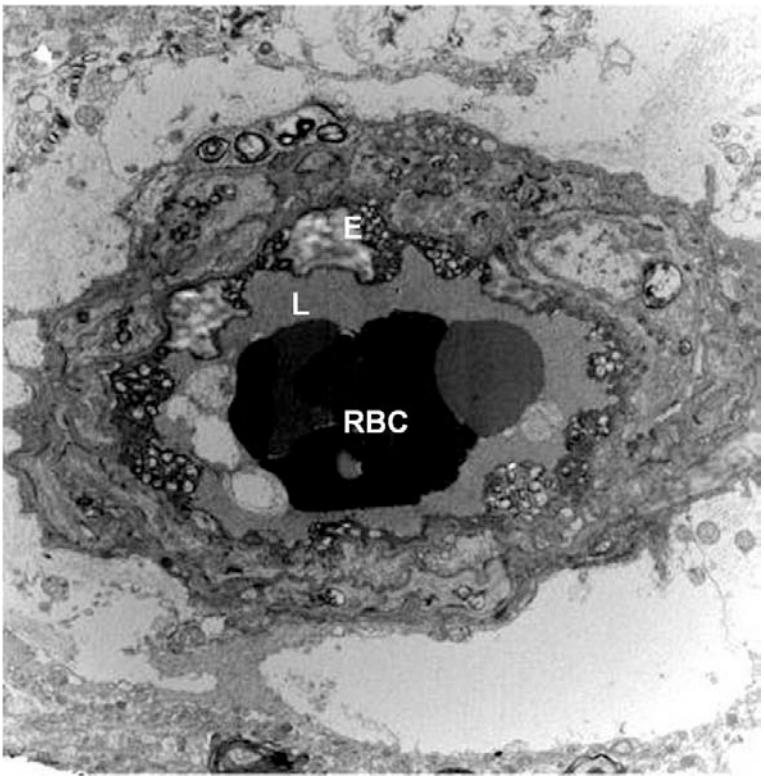

2-5. Spleen, raccoon: Ultrastructural analysis of endothelial cells of a capillary reveals the presence of numerous lysosomes filled with lamellar material (E). Unfortunately, electron microscopy is useful only for identify lysosomal storage diseases, but poor in determining which type.

concentrically (membranous cytoplasmic bodies). None of these forms is specific for a given disease, but concentric lamellae are most common in GM1 and GM2 gangliosidoses. In the present case the storage bodies were poorly defined, concentrically arranged lamellar whorls. Histochemistry, immunohistochemistry and fluorescence microscopy may also be of use in identifying storage material, but definitive and gold standard for diagnosis is by means of biochemical analysis.[3]

There is no single presentation common to all lysosomal storage diseases; the clinical and gross pathological manifestations are dependent on the deficient enzyme and the outcome of the deficiency in the organs that utilize the enzyme. Microscopically, LSDs are characterized by accumulation of enlarged lysosomes containing uncatabolized substrate in solution or complexed with related chemical species, which will be partially or wholly removed during fixation and preparation of the paraffin wax-embedded sections. If the substrate is soluble in water or lipid solvents, there will be a vacuolated appearance of the affected cells.[3]

Sphingolipids are an important group of structural lipids in which the unifying compound, ceramide, is esterified to sialyloligosaccharides to form gangliosides, to other saccharides to form neutral glycolipids such as globoside, or to phosphocholine to form sphingomyelin.[3]

The primary metabolic defect in Niemann–Pick disease (NPD) types A and B in man is the lack of sphingomyelinase enzyme that catalyzes the hydrolytic cleavage of sphingomyelin to ceramide and phosphocholine.[3] The reduced or absent enzyme activity results in accumulation of sphingomyelin in lysosomes.[7] Similarly to humans, an autosomal recessive mode of inheritance has been demonstrated in a cat and a dog.[2,8]

Similar histological and ultrastructural features to those in this case were reported affecting neurons, oligodendroglial cells, macrophages, renal epithelial cells, endothelium and pericytes in the CNS, PNS, spleen, liver, lung and kidney in a cat,[1] a dog and a Hereford calf.[6] Consistent with the present case, these animals presented as juveniles, had neurological signs and virtually no sphingomyelinase activity was detected in the brain and liver compared with normal controls. Autofluorescence by UV light was reported in a dog with NPD,[2] but was not found in the present case.

JPC Diagnosis: Cerebellum: Neuronal, glial cell and endothelial cytoplasmic vacuolation, diffuse, marked, with gliosis.
Spleen: Histiocytosis, diffuse, marked with cytoplasmic vacuolation.

Conference Comment: Conference participants briefly reviewed select inherited (see Table 2) and acquired lysosomal storage diseases of veterinary importance. Sphingolipidoses result from defective catabolism of normal cell membrane

Table 1: Lysosomal enzyme activities in brain homogenates from the affected and a normal raccoon

Enzyme activity (nmol/ h/mg protein	Affected Raccoon	Normal Raccoon
Beta-galactosidase[a]	64.0	22.6
Beta-hexosaminidase A[b]	81.4	28.9
Beta-hexosaminidase A and B[c]	611.1	118.0
Sphingomyelinase[d]	0.13 (3X)	5.2

a- measured using 4MU-β-galactoside
b- measured using 4MU-β-N-acetylglucosaminideSO4
c- measured using 4MU-β-N-acetylglucosaminide
d- measured using 14C-sphingomyelin; 3x means measured three times

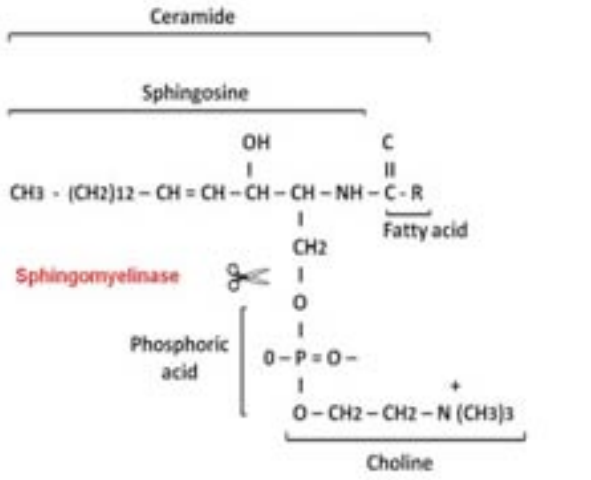

2-6. Derivation of sphingolipids (see contributor's comments for discussion.)

constituents known as glycosphingolipids, and exhibit autosomal recessive inheritance. This case is an excellent example of sphingomyelinosis, or Niemann-Pick disease, the pathogenesis of which is thoroughly described in the contributor's comment. GM_1 gangliosidosis has been described in dogs, cats, Friesian cattle and sheep. Accumulation of lysosomal GM_1 ganglioside occurs due to a deficiency in β-galactosidase, though GM_1 gangliosidosis in Suffolk sheep is actually due to deficiencies in both β1-galactosidase and α-neuraminidase. GM_2 gangliosidosis results from insufficient activity of hexosaminidase (which exists as an αβ- or ββ-dimer) or its activator protein. This condition is reported in domestic shorthair and Korat cats, German shorthaired pointers and golden retrievers due to a β-subunit deficiency, while in Japanese spaniel dogs and Yorkshire pigs there is an activator protein deficiency. Tay-Sachs and Sandhoff diseases are examples of GM_2 gangliosidosis in humans. As in sphingomyelinosis, neurons in GM_1/GM_2 gangliosidosis are expanded by abundant, foamy, PAS-positive cytoplasm, with faint granules; ultrastructurally lysosomal granules are composed of concentric membranous whorls. Glial cells and macrophages are also affected. Glucocerebrosidosis, which is similar to Gaucher disease in humans, has been reported in Sydney Silky Terriers, and results from deficient glucocerebrosidase, the catalyst for conversion of glucocerebroside to ceramide. Microscopically, glucocerebrosidosis manifests in hepatic and lymph node sinusoidal macrophages, as well as some neurons, but not in Purkinje cells or the spinal cord. Ultrastructurally, storage material appears twisted or branching.[5]

Globoid cell leukodystrophy, also known as galactocerebrosidosis, is an autosomal recessive disorder reported in dogs, cats and polled Dorset sheep. It is classified within the sphingolipidosis group of storage diseases and results from deficient activity lysosomal galactocerebrosidase, an enzyme which normally catalyzes the breakdown of galactocerebrosides. Galactocerebrosides are important components of myelin, but at high concentrations are cytotoxic; excessive accumulation in oligodendrocytes and Schwann cells causes extensive cellular degeneration and necrosis, halting active myelination. This combined with the degeneration of existing myelin, results in demyelination and axonal loss. Phagocytic macrophages, however, are unable to degrade galactocerebroside, and thus appear microscopically as characteristic swollen, PAS-positive "globoid cells," which exhibit perivascular cuffing within the white matter. In contrast to many of the other lysosomal storage diseases, neurons are not typically involved in the accumulation of excess storage material in galactocerebrosidosis.[5]

Glycoproteinoses, such as α- and β-mannosidosis, or α-L-fucosidosis, are characterized by defective degradation of the carbohydrate component of N-linked glycoproteins. In α-mannosidosis, a historically important entity in Angus cattle, a

Table 2: Select inherited lysosomal storage diseases[5]

Condition	Enzyme Defect	Storage Material	Inheritance/species
GM_1 gangliosidosis	β-galactosidase	GM_1 ganglioside in lysosomes of neurons, glial cells, macrophages	- autosomal recessive - dogs, cats, Friesian cattle; - suffolk sheep- deficiencies in β1-galactosidase AND α-neuraminidase.
GM_2 gangliosidosis (Tay-Sachs and Sandhoff diseases)	-hexosaminidase (αβ- or ββ-dimer) -activator protein	GM_2 ganglioside in lysosomes of neurons, glial cells, macrophages	- autosomal recessive 1. domestic and Korat cats, German shorthaired pointers, golden retrievers: β-subunit deficiency 2. Japanese spaniel dogs, Yorkshire pigs: activator protein deficiency
Sphingomyelinosis (Niemann-Pick disease)	sphingomyelinase	sphingomyelin in lysosomes of neurons and macrophages	- autosomal recessive in cat and dog
Globoid cell leukodystrophy (glactocerebrosidosis)	galactocerebrosidase	galactocerebrosides in oligodendrocytes/Schwann cells, globoid cell macrophages (NOT in neurons)> demyelination, axonal loss	- autosomal recessive - dogs, cats and polled Dorset sheep
Glucocerebrosidosis (Gaucher disease)	glucocerebrosidase	glucocerebroside in lysosomes of hepatic/lymph node sinusoidal macrophages, some neurons (NOT in Purkinje cells or the spinal cord)	- Sydney Silky Terriers
α-Mannosidosis	α-mannosidase	mannose/N-acetylglucosamine oligosaccharide in lysosomes of neurons, macrophages, secretory epithelial cells	- Angus cattle
β-Mannosidosis	β-mannosidase	oligosaccharides in lysosomes of neurons, macrophages, secretory epithelial cells	- Salers cattle and Nubian goats
MPS I	α-L-iduronidase	mucopolysaccharide storage in mesoderm derived cells	- domestic shorthair cats and Plott hounds
MPS III	N-acetylglucosamine-6-sulfatase	heparan sulfate in mesoderm-derived cells; neurons contain gangliosides	- Nubian goats
MPS VI	arylsulfatase-B	mucopolysaccharide storage in mesoderm derived cells; neuronal storage does not occur	- Siamese and domestic shorthair cats
MPS VII	β-glucuronidase	widespread neurovisceral storage	- dogs and cats
Glycogenosis (type II in humans)	α-1,4-glucosidase	widespread glycogen storage within lysosomes and intracytoplasmically; including neurons	- autosomal recessive in shorthorn and Brahman beef cattle

defective enzyme leads to decreased lysosomal α-mannosidase activity in all cells except hepatocytes, which leads to widespread mannose/N-acetylglucosamine oligosaccharide deposition. β-mannosidosis due to β-mannosidase deficiency is reported in Salers cattle and Nubian goats. In both α- and β-mannosidoses, neurons, macrophages and secretory epithelial cells are most severely affected, although storage material is typically lost during tissue processing so vacuoles appear empty on standard H&E slides. In α-L-fucosidosis deficient activity of α-L-fucosidase leads to a similar histological appearance; this condition is autosomal recessive in English springer spaniels.[5]

Mucopolysaccharidoses are distinguished by defective catabolism of glycosaminoglycans, so skeletal and connective tissue abnormalities such as deformities, degenerative joint disease, and thickening of the heart valves or leptomeninges are often observed; neurons can be involved as well. Deficiency in α-L-iduronidase, known as mucopolysaccharidosis type I (MPS I) in humans, is reported in domestic shorthair cats and Plott hounds. Storage primarily occurs in mesoderm-derived cells. Deficiency in N-acetylglucosamine-6-sulfatase leads to the veterinary counterpart of human MPS III, which has been described in Nubian goats. Mesoderm-derived cells are packed with heparan sulfate, while neurons contain gangliosides, which

accumulate due to interference with neuraminidase activity. Siamese and domestic shorthair cats occasionally have a deficiency in arylsulfatase-B, a disorder known as MPS VI in humans. Mucopolysaccharidosis VI differs from MPS I and II in that neuronal storage does not occur. Finally, the counterpart to human MPS VII is reported in dogs and cats secondary to a lack of β-glucuronidase. Again, microscopic findings are similar to those described above; however, there is also widespread neurovisceral storage.[5]

Glycogenoses result from defective glycogen catabolism. α-1,4-glucosidase deficiency, an autosomal recessive condition documented in shorthorn and Brahman beef cattle, leads to widespread glycogen storage, both within lysosomes and intracytoplasmically. In contrast, other types of glycogen storage diseases are concentrated primarily within the liver and muscle. Since the excess storage material is composed of glycogen, it is PAS-positive and diastase-sensitive. Neurons are severely affected in this disease.[5]

Acquired lysosomal storage diseases often follow the ingestion of toxic plants, or, less commonly, drug administration. Swainsonine is an indolizidine alkaloid found in several plant species, such as locoweed (*Astragalus, Oxytropis* sp.). Ingestion of swainsonine by grazing livestock causes inhibition of α-mannosidase, inducing a form of α-mannosidosis. Ingestion by pregnant sheep can also result in abortion and fetal malformation. Ingestion of *Trachyandra divaricata* or *T. laxa* causes excessive storage of lipofuscin in central and peripheral neurons of South African/Australian livestock.[5] Aminoglycosides, such as gentamicin, accumulate within lysosomes of renal proximal tubular cells where they inhibit lysosomal phospholipases, producing aggregates of phospholipid-containing myeloid bodies. As lysosomes become progressively distended with myeloid bodies, they rupture, releasing acid hydrolases as well as high concentrations of aminoglycosides into the cytoplasm, further damaging the cell.[4]

Regardless of the underlying genetic or acquired cause, most lysosomal storage diseases in veterinary species are characterized clinically by an early onset of neurologic impairment. Considering the similarity of clinical signs as well as the frequent overlap of the gross and microscopic lesions in many types of lysosomal storage diseases, electron microscopy and especially measurement of lysosomal enzyme activity are often necessary to elucidate a specific etiology.

Contributing Institution: College of Veterinary Medicine
UC Davis
1 Garod Drive
Davis, CA 95616
http://www.vetmed.ucdavis.edu/pmi/

References:

1. Baker HJ, Wood PA, Wenger DA, Walkley SU, Inui K, Kudoh T, et al. Sphingomyelin lipidosis in a cat. *Vet Pathol.* 1987;24:386-391.
2. Bundza A, Lowden JA, Charlton KM. Niemann-Pick disease in a poodle dog. *Vet Pathol*. 1979;16:530-538.
3. Jolly RD, Walkley SU. Lysosomal storage diseases of animals: an essay in comparative pathology. *Vet Pathol*. 1997;34:527-548.
4. Kaloyanides GJ. Drug-phospholipid interactions: role in aminoglycoside nephrotoxicity. *Ren Fail*. 1992;14(3):351-357.
5. Maxie MG, Youssef S. Nervous system. In: Maxie MG, ed. *Jubb, Kennedy and Palmer's Pathology of Domestic Animals*. 5th ed. Vol 1. St. Louis, MO: Elsevier; 2007:322-332, 381.
6. Saunders GK, Wenger DA. Sphingomyelinase deficiency (Niemann-Pick disease) in a Hereford calf. *Vet Pathol*. 2008;45:201-202.
7. Stanbury JB, Wyngaarden JB, Fredrickson DS. *The Metabolic Basis of Inherited Disease*. 3rd ed. New York, NY: McGraw-Hill; 1972.
8. Wenger DA, Sattler M, Kudoh T, Snyder SP, Kingston RS. Niemann-Pick disease: a genetic model in Siamese cats. *Science*. 1980;208:1471-1473.

CASE III: 11-342 (JPC 4032320).

Signalment: 11-year-old female spayed Maine coon cat, (*Felis catus*).

History: The cat was presented to a local emergency clinic for acute onset of tetraplegia. Neurologic examination revealed normal cranial nerve function, deep pain sensation in all limbs, hindlimb hyperreflexia, and forelimb hyporeflexia, consistent with a C6-T2 spinal cord lesion. The neck was non-painful with normal range of motion. Cervical and thoracic radiographs were unremarkable. The cat's neurologic status deteriorated overnight, with worsening forelimb hyporeflexia and loss of deep pain sensation in the left forelimb. A guarded prognosis was given, and the owners elected euthanasia and subsequent necropsy.

Gross Pathology: Transverse sectioning of the spinal cord revealed multiple asymmetric brown-grey foci of malacia and hemorrhage, extending from C4-T2. The vertebrae and intervertebral discs were grossly normal.

Laboratory Results: Brain slices tested negative for rabies virus antigen via immunofluorescence.

Histopathologic Description: Spinal cord, caudal cervical to cranial thoracic: Affecting up to 75% of the grey and white matter, and most severely affecting the ventral horns and ventral funiculi, are multiple asymmetric foci of malacia characterized by parenchymal vacuolation, hemorrhage, and neuronal necrosis and loss (infarcts). The ventral spinal artery and numerous intramedullary arteries and veins contain luminal amorphous blue-grey material (fibrocartilaginous emboli). Vessel walls are rarely disrupted by brightly eosinophilic fibrillar material and cellular debris (fibrinoid vascular necrosis). Within malacic areas, blood vessels are surrounded by low to moderate numbers of neutrophils that multifocally extend into the surrounding meninges and neuroparenchyma (neutrophilic meningomyelitis) and glial cells are mildly increased in number. Adjacent white matter tracts contain large regions of myelin sheath dilation with numerous swollen axons (spheroids) and rare myelomacrophages (Wallerian degeneration). Within the ventral dura mater are multifocal basophilic concretions (dural mineralization).

Contributor's Morphologic Diagnosis: Spinal cord (caudal cervical to cranial thoracic): Severe multifocal acute myelomalacia with intravascular fibrocartilaginous emboli, secondary neutrophilic meningomyelitis, gliosis, and Wallerian degeneration.

Contributor's Comment: Fibrocartilaginous embolism (FCE), though well-documented in dogs, is considered an uncommon cause of spinal cord disease in cats[4] and has been reported in numerous other species including sheep, pigs, horses, turkeys, mustelids, and humans.[2] Affected cats are non-painful and develop peracute to acute, usually asymmetric, spinal cord-related signs that are non-progressive beyond the first

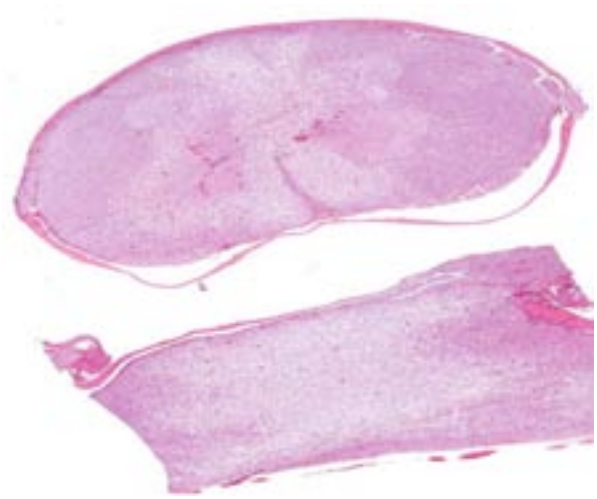

3-1. Cervical spinal cord, cat: Subgross inspection reveals asymmetric pallor (malacia) affecting the grey matter as well as all funiculi within the spinal white matter. (HE 0.63X)

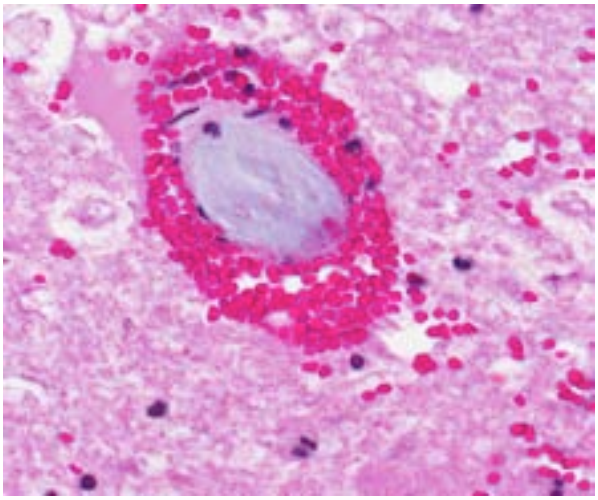

3-2. Cervical spinal cord, cat: Multiple veins within the grey matter and white matter contain emboli of fibrocartilage. (HE 200X)

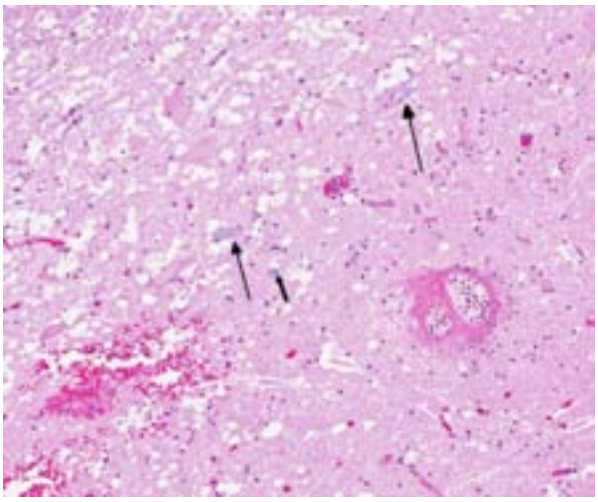

3-3. Cervical spinal cord, cat: Areas of infarction include white matter (upper left), multiple vessels containing fibrocartilaginous emboli (arrows), hemorrhage, and vessels with necrotic walls (lower right). (HE 220X)

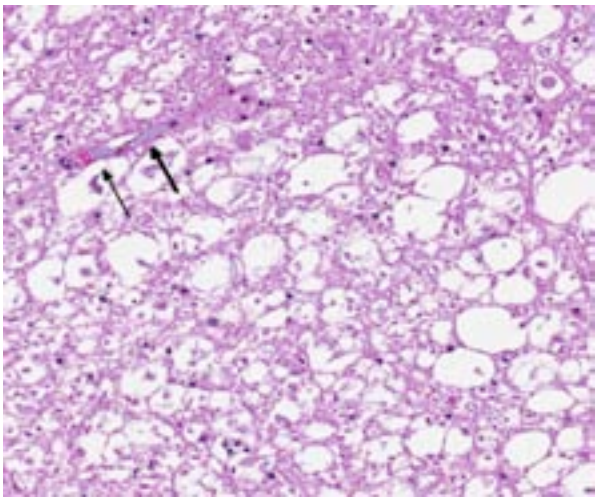

3-4. Cervical spinal cord, cat: Within the dorsal funiculus, axons in proximity of vessels with fibrocartiaginous emboli (arrows) exhibit degenerative changes such as dilated myelin sheaths, swollen axons, and axonophagia by Gitter cells. (HE 320X)

24-48 hours.[2,5,7] While definitive diagnosis requires histopathologic examination, a presumptive diagnosis may be made antemortem based on history, clinical examination and MRI findings, and exclusion of other causes of myelopathy. Resolution of clinical signs, in the absence of specific therapy, is also highly suggestive of FCE.[4]

The myelomalacia seen in cases of FCE results from occlusion of the blood supply to the spinal cord by fibrocartilaginous emboli, which are thought to originate from the nucleus pulposus of the intervertebral disk.[4,5,7] It is uncertain how the disk material enters the vasculature. Several theories have been proposed, including: 1) penetration of disk material into spinal vessels (e.g. due to trauma), 2) entry into a common blood supply of the intervertebral disk and spinal cord (e.g. remnant embryonic vessels or neovascularization), 3) entry into an anomalous arteriovenous communication, or 4) herniation of disk material into an adjacent vertebral body, allowing entry into the vertebral venous sinus.[1,2,4,5,7] The distribution and extent of the myelomalacia depends on the size, location, and number of affected blood vessels. Spinal arteries have extensive anastomoses, thus the presence of spinal cord infarcts is consistent with simultaneous occlusion of multiple vessels.[6] Typical histopathologic findings, as seen in this case, include myelomalacia and fibrocartilaginous emboli within leptomeningeal and/or intramedullary blood vessels. Fibrocartilaginous emboli have been described in both arteries and veins, though often the type of vessel affected cannot be definitively identified.[6] While emboli may be evident on routine histologic examination, their identification can be enhanced with Giemsa, toluidine blue, or alcian blue histochemical stains.[7]

JPC Diagnosis: Spinal cord: Infarcts, multifocal to coalescing, extensive, with wallerian degeneration, hemorrhage and numerous fibrocartilagenous emboli.

Conference Comment: The contributor provides a concise, thorough summary of the clinical presentation and pathogenesis of fibrocartilagenous embolism. Although FCE is definitively diagnosed via histopathology, a presumptive diagnosis can sometimes be made on the basis of history, clinical signs, a thorough physical and neurologic examination and imaging such as MRI. Differential diagnoses for FCE include causes of acute, asymmetrical paresis such as trauma, spinal cord or vertebral neoplasia, diskospondylitis, intervertebral disk disease, aortic thromboembolism and bacterial, viral or parasitic infections.[1,2,8] In contrast to most of these conditions, however, animals with FCE are typically non-painful on spinal palpation and clinical signs are non-progressive after the first 24-48 hours.[1,2,4]

Metabolic and degenerative disorders as well as toxicities that affect the brain and spinal cord and may result in a similar clinical presentation, but

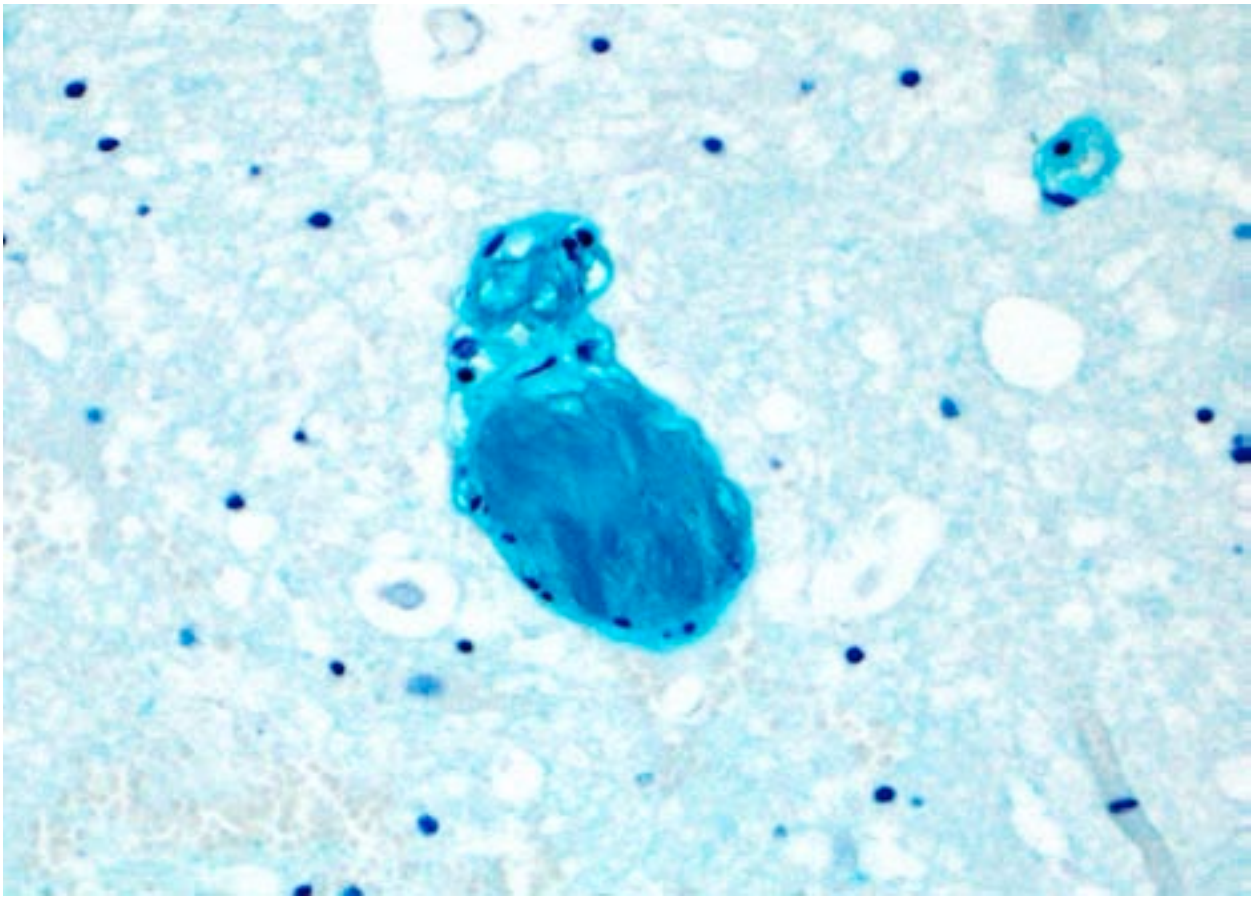

3-5. Cervical spinal cord, cat: Fibrocartilaginous matrix appears bright blue-green when stained with Alcian Blue. (Alcian Blue 2.0, 400X) (Photo courtesy of: Laboratory of Pathology and Toxicology, University of Pennsylvania, School of Veterinary Medicine, Philadelphia, PA USA. http://www.vet.upenn.edu/)

unlike FCE, these conditions generally exhibit a symmetrical distribution. For example, bilaterally symmetrical polioencephalomalacia is observed secondary to dietary thiamine deficiency in carnivores, while lead toxicity can occasionally cause symmetrical laminar cortical necrosis in cattle. A focal, symmetrical poliomyelomalacia of unknown etiology is reported in sheep, goats, pigs and Ayrshire calves, while polioencephalomalacia (PEM) is well described in ruminants; salt toxicity in swine also causes similar lesions. In horses the ingestion of neurotoxin repin, from the yellow star thistle (*Centauea solstitialis*) or Russian knapweed (*Centaurea repens*), induces symmetrical malacia of the pallidus and substantia nigra, while thiaminase from bracken fern (*Pteridium* sp.) and horsetail (*Equisetum arvense*) results in bilaterally symmetrical necrosis of the periventricular gray matter.[3]

Contributing Institution: Laboratory of Pathology and Toxicology, University of Pennsylvania, School of Veterinary Medicine, Philadelphia, PA, USA. http://www.vet.upenn.edu/

References:

1. Abramson CJ, Platt SR, Stedman NL. Tetraparesis in a cat with fibrocartilagenous emboli. *J Am Anim Hosp Assoc*. 2002;38:153-156.
2. Coradini M, Johnstone I, Filippich LJ, Armit S. Suspected fibrocartilaginous embolism in a cat. *Aust Vet J*. 2005;83:550-551.
3. Maxie MG, Youssef S. Nervous system. In: Maxie MG, ed. *Jubb, Kennedy, and Palmer's Pathology of Domestic Animals*. 5th ed. Vol. 1. Philadelphia, PA: Elsevier; 2007:283-455.
4. Mikszewski JS, Van Winkle TJ, Troxel MT. Fibrocartilaginous embolic myelopathy in five cats. *J Am Anim Hosp Assoc*. 2006;24:226-233.
5. Negrin A, Schatzberg S, Platt S. The paralyzed cat: neuroanatomic diagnosis and specific spinal

cord diseases. *J Feline Med Surg*. 2009;11:361-372.
6. Summers BA, Cummings JF, de Lahunta A. Degenerative diseases of the central nervous system. In: *Veterinary Neuropathology*. St. Louis, MO: Mosby; 1995:246-249.
7. Vandevelde M, Higgins RJ, Oevermann A. Vascular disorders. In: *Veterinary Neuropathology: Essentials of Theory and Practice*. Ames, IA: Wiley-Blackwell; 2012:44-45.

CASE IV: L11-8963 (JPC 4019357).

Signalment: 9-month-old male C57BL/6 TRAMP mouse, (*Mus musculus*).

History: This mouse was a control animal that was part of a novel imaging modality study. No clinical signs reported.

Gross Pathology: This mouse was presented alive in good body condition. There is a focally extensive, 1.2 x 1.0 x 1.0 cm, mottled pale tan to red, firm, somewhat circumscribed mass around the neck of the urinary bladder. All other organs and tissues are within normal gross limits.

Histopathologic Description: Prostate gland: There is a regionally extensive, invasive, unencapsulated mass arising from and replacing most of the anterior prostate lobe, with infiltration and effacement of other prostate lobes and the urinary bladder. The mass is comprised of sheets and anastomosing lobules of cells with scant fibrovascular stroma. The cells are pleomorphic (polygonal, elongated, round) with poorly defined cell borders enclosing small amounts of eosinophilic cytoplasm. The nuclei are round to ovoid with coarsely clumped chromatin and single inconspicuous nucleoli. A range of 15 to 25 and an average of 20 mitoses per 400X field is noted. Anisocytosis and anisokaryosis is marked (>3 fold). Apoptosis/single cell necrosis is noted throughout the mass, and there is multifocal to coalescing central lytic necrosis with hemorrhage throughout the mass. Within most remaining glands of the anterior lobe and the other lobes of the prostate gland, there are changes consistent with prostatic intraepithelial neoplasia (PIN), including areas of epithelial stratification,

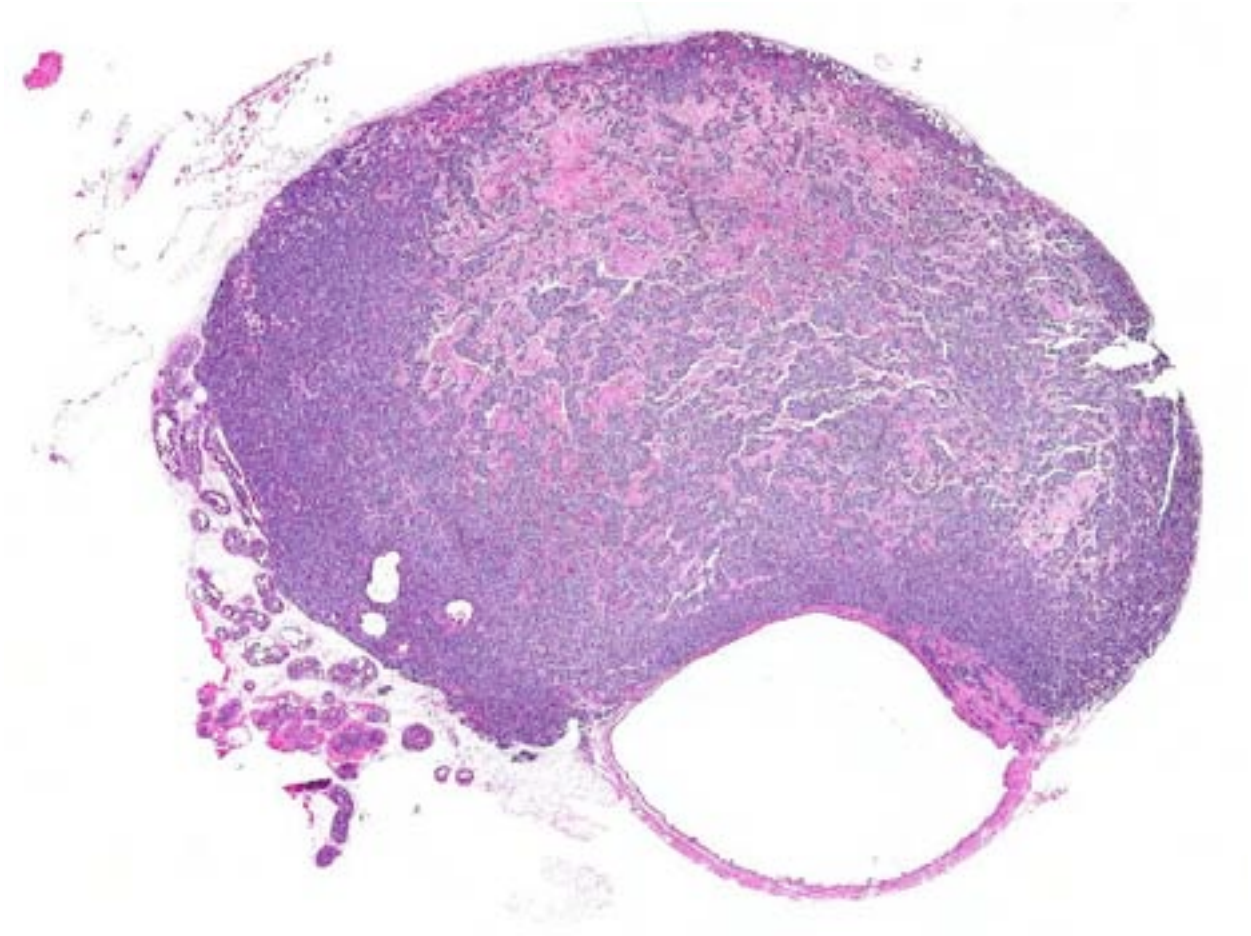

4-1. Prostate, TRAMP mouse: The anterior lobe of the prostate is enlarged up to 1.3 cm and effaced by an infiltrative neoplasm that compresses the adjacent urinary bladder. (HE 0.63X)

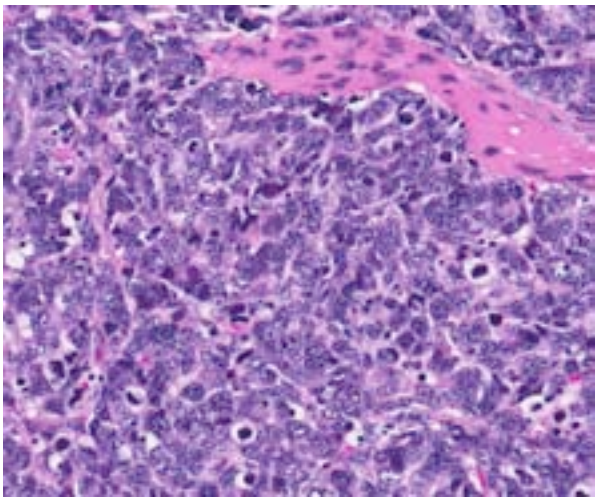

4-2. Prostate, TRAMP mouse: Neoplastic cells are polygonal and pleomorphic, forming sheets rather than acinar structures. There are large numbers of mitotic figures as well as apoptotic neoplastic cells. (HE 300X)

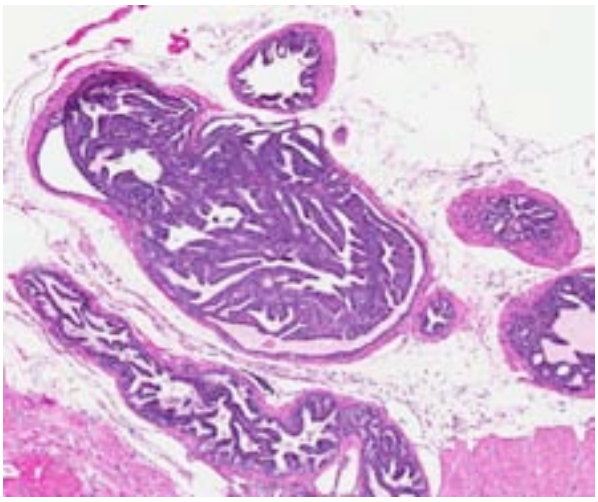

4-3. Prostate, TRAMP mouse: Adjacent glands show a disorderly array of columnar cells in contiguous acini, rather than the typical single layer. This preneoplastic change is referred to as prostatic intraepithelial neoplasia (PIN). (HE 35X)

micropapillary formation, and cribriform structure formation.

Contributor's Morphologic Diagnosis: 1. Prostate gland (anterior lobe), poorly-differentiated prostatic carcinoma.
2. Prostate gland (all lobes), high-grade prostatic intraepithelial neoplasia (PIN).

Contributor's Comment: Transgenic adenocarcinoma of mouse prostate (TRAMP) is a transgenic mouse engineered to express the SV40 virus large T and small t oncoproteins in the secretory epithelial cells of the prostate under the control of the androgen-responsive minimal rat probasin promoter.[1,3,4] Expression of these transgenes results in inhibition of p53 and Rb tumor suppressor function.[1]

The TRAMP model has been based on either C57BL/6 or C57BL/6 TRAMP x FVB hybrid mouse strains.[1,3,4] The prostate tumors observed in male TRAMP mice progress in a stepwise fashion through different preneoplastic and neoplastic lesions, which is a feature of prostate tumors in humans.[1,3] In TRAMP mice, commonly observed lesions include:[1]

1. *6- to 12-week-old mice:* hyperplastic epithelial lesions or prostatic intraepithelial neoplasia (PIN).
2. *12- to 24-week-old mice:* well-differentiated prostatic adenocarcinoma.
3. *>24-week-old mice:* poorly-differentiated prostatic adenocarcinoma, with development of metastases (commonly iliac lymph nodes and lungs).
4. *33- to 52-week-old mice:* death.

TRAMP prostate tumors share other similarities with human prostate tumors, including metastases to distant sites, development of androgen independence, and neuroendocrine differentiations.[1,3] As such, TRAMP mice have been extensively used to study the molecular events important in prostate cancer progression in humans.

The classification and grading of lesions in transgenic mouse models of prostatic tumors (including and mainly those observed in TRAMP mice) can be confusing and controversial. The most widely used scheme for classifying such tumors originates from the 2004 Bar Harbor Meeting of the Mouse Models of Human Cancer Consortium Prostate Pathology Committee.[4] This classification scheme refined and stressed the importance of PIN lesions based on a wide body of published work. Recently, a grading scheme was proposed that incorporates some data and concepts developed and published since the 2004 Bar Harbor classification scheme, which in summary includes:[1]

- *Grade 0: Normal.* Prostate glands lined by a monolayer of cuboidal to columnar epithelium with basally-oriented nuclei.
- *Grade 1: Low-grade PIN.* Crowding and occasional stratification of prostate epithelial cells, with increased nuclear to cytoplasmic ratio.
- *Grade 2: Moderate-grade PIN.* Similar to low-grade PIN, but there is more frequent stratification.

- *Grade 3: High-grade PIN.* Similar to moderate-grade PIN, but hyperplastic epithelial cells can form papillary projections and/or cribriform patterns.
- *Grade 4: Phyllodes-like tumor.* Consists of papillary projections of loose stroma with loosely-arranged stellate mesenchymal cells.
- *Grade 5: Well-differentiated adenocarcinoma*. Invasive tumor consisting primarily of well-differentiated tubules or acini. There is marked cellular and nuclear atypia, and high mitotic indices.
- *Grade 6: Moderately-differentiated adenocarcinoma.* Invasive tumor that consists of a mass of epithelial cells, some of which form recognizable acini or tubules. There is marked cellular and nuclear atypia, and high mitotic indices.
- *Grade 7: Poorly-differentiated carcinoma (neuroendocrine type).* Invasive tumors composed of solid sheets of polygonal to elongated cells. There is marked cellular and nuclear atypia, and high mitotic indices.

JPC Diagnosis: Prostate gland: Prostatic carcinoma, high grade, with adjacent prostatic intraepithelial neoplasia (PIN).

Conference Comment: The contributor has given a comprehensive overview of this important mouse model and given a clear summary of the different classification schemes. We concur with the contributor's use of the 2012 proposed grading scheme, which classifies the intraepithelial proliferative lesions as PIN rather than atypical hyperplasia for this model because, as the authors note, PIN lesions in TRAMP mice are clearly precursors of more invasive and aggressive carcinomas.[1]

Physicians from the Joint Pathology Center (JPC) Genitourinary subspecialty were consulted on this case. These pathologists were impressed by the striking lack of differentiation within this aggressive tumor and noted that the histological features closely approximate the neuroendocrine phenotype described as a "grade 7" in the paper previously referenced. Apparently this microscopic appearance is rare in human prostatic carcinomas, which are generally diagnosed and treated well before reaching this stage. JPC pathologists also expressed agreement that the changes in the remaining glands of the prostate gland are consistent with high-grade prostatic intraepithelial neoplasia, which represents an intermediate stage between normal epithelium and invasive malignant carcinoma. In human medicine, PIN is clinically significant in that it provides relatively early identification of patients at risk for malignancy.[2]

Contributing Institution: Veterinary Services Center
Department of Comparative Medicine
Stanford School of Medicine
http://med.stanford.edu/compmed/

References:

1. Berman-Booty LD, Sargeant AM, Tosol TJ, et al. A review of the existing grading schemes and a proposal for a modified grading scheme for prostatic lesions of TRAMP mice. *Toxicol Pathol*. 2012;40:5-17.
2. Brawer MK. Prostatic intraepithelial neoplasia: an overview. *Rev Urol*. 2005;7(suppl 3);11-18.
3. Chiaverotti T, Couto SS, Donjacour A, et al. Dissociation of epithelial and neuroendocrine carcinoma lineages in the transgenic adenocarcinoma of mouse prostate model of prostate cancer. *Am J Pathol*. 2008;172:236-246.
4. Schappell SB, Thomas GV, Roberts RL, et al. Prostate pathology of genetically engineered mice: definitions and classification. The consensus report from the Bar Harbor Meeting of the Mouse Models of Human Cancer Consortium Prostate Pathology Committee. *Cancer R*es. 2004;64:2270-2305.

Joint Pathology Center
Veterinary Pathology Services

WEDNESDAY SLIDE CONFERENCE 2013-2014

Conference 6

23 October 2013

CASE I: WSC 2013, Case #2 (4032579).

Signalment: 6-month-old female Nubian goat, (*Capra hircus*).

History: This goat belonged to a small (<20) flock of sheep and goats at a newly developed community supported agriculture farm. Animals were acquired from multiple sources. This goat had a two-week history of respiratory tract infection, corneal edema, blindness and weakness of the hind end. The animal was euthanized.

Gross Pathology: The goat was in poor body condition. There was cloudiness of the cornea of each eye. Approximately 70 % of the cranioventral regions of the lungs were dark red and consolidated, and there was abundant white froth in the lumen of the trachea. Multiple segments of the small intestine had a reddened

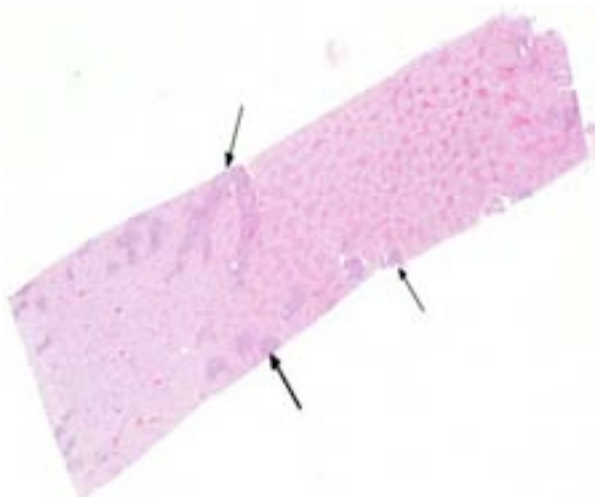

1-1. Kidney, goat: Renal vessels of various sizes are surrounded by a dense cellular infiltrate. (HE 0.63X)

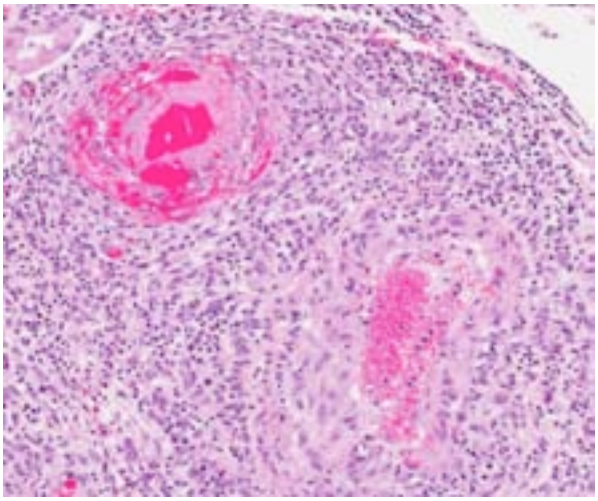

1-2. Kidney, goat: Brightly eosinophilic protein, hemorrhage, and cellular debris expands the wall of the arteriole at upper left (fibrinoid necrosis), the wall of both vessels is further expanded by disorganized smooth muscle, fibroblasts, and infiltrating lymphocytes. (HE 64X)

serosa. There were multiple, pinpoint, white foci on the liver surface and throughout the parenchyma. White pulp was prominent on the cut surface of the spleen. The mesenteric and sublumbar lymph nodes were moderately enlarged.

Laboratory Results: Capnophilic [10 %] culture of the lung yielded *Mycoplasma* sp. There was no bacterial growth on capnophilic [10 %] culture of the liver. A sample of kidney was submitted to the National Veterinary Services Laboratory, Ames, IA for testing by nested polymerase chain reaction (PCR) for the presence of alcelaphine herpesvirus 1 (AlHV-1) and ovine herpesvirus 2 (OvHV-2) DNA. OvHV-2 DNA was detected in the sample.

Histopathologic Description: Kidney: Affecting multiple blood vessels, predominantly arteries, in the cortex, corticomedullary junction (including arcuate and interlobular arteries) and pelvis, there is necrotizing vasculitis, characterized by marked expansion and disruption of one to all tunicae of vessel walls by an infiltrate composed of large numbers of lymphocytes together with lesser numbers of macrophages and lymphoblasts, and occasional plasma cells. These infiltrates often involve the outer margin of the media and the adventitia, and markedly expand the perivascular interstitium, occasionally surrounding glomeruli or tubules. In the tunica media of some affected arteries, the cellular infiltrate is admixed with homogeneous to fibrillar to beaded eosinophilic material, and pyknotic and karyorrhectic debris. There is disruption of the intima and/or hypertrophy of endothelium in affected vessels; rare fibrin thrombi partially occlude the lumen of several vessels (variation among the slides). Multifocally in the cortex, there is infiltration by low to medium numbers of lymphocytes, lesser numbers of macrophages and plasma cells in the interstitium. There is a small proportion of tubules that are moderately ectatic and contain aggregates of degenerate cells and necrotic cellular debris in the lumen or are lined by epithelial cells that contain cytoplasmic eosinophilic droplets. A loosely organized infiltrate of low to medium numbers of lymphocytes is present subjacent to the urothelium of the pelvis (variation among slides). There is moderate congestion, and occasional small hemorrhages in some areas.

Contributor's Morphologic Diagnosis: Kidney: Severe, multifocal, lymphohistiocytic and lymphoblastic, chronic necrotizing vasculitis and perivasculitis with mild multifocal lymphocytic interstitial nephritis, tubular degeneration and necrosis.

Contributor's Comment: This case is a rare example of malignant catarrhal fever (MCF) in a goat, which highlights the susceptibility of goats to clinical disease from OvHV-2 infection, albeit very uncommon.

Malignant catarrhal fever is a herpesviral disease with a worldwide distribution that affects certain wild and domestic species of the order *Artiodactyla*.[2] It is caused by closely related viruses in the genus *Macavirus* (sigla for malignant catarrhal fever virus) in the subfamily Gammaherpesvirinae.[4] The International Committee on Taxonomy of Viruses (ICTV) currently recognizes 9 species in the genus,[7] of which probably the best known are alcelaphine herpesvirus 1 and ovine herpesvirus.[2] Gammaherpesviruses have a propensity to become latent. As a result, the gammaherpesviruses have co-evolved with their natural hosts. Unless natural hosts are immunodeficient, gammaherpesviruses are normally carried asymptomatically. However, natural hosts act as reservoirs and are sources of infection to susceptible cloven-hoofed species that are not as highly adapted to the virus.[1]

Molecular phylogenetic analysis of a portion of the DNA polymerase gene that is relatively conserved among herpesviruses has revealed two major groups of MCF viruses. This is relevant not only because viruses within each group have similar biological properties, but also because it is suggestive of a shared epidemiology.[8] Most MCF viruses are named after their reservoir hosts, and the two aforementioned groups are the following (note: this analysis included viruses not yet classified by the ICTV):[7]

The alcelaphinae/hippotragine group, which includes AIHV-1, the virus responsible for wildebeest-associated MCF; alcelaphine herpesvirus 2 (AIHV-2), hippotragine herpesvirus 1 (HiHV-1) and MCF virus oryx (MCFV-oryx) which are carried asymptomatically by hartebeest, roan antelope and oryx, respectively, have not yet been associated with disease.[8]

The caprine group, which includes MCF virus-white tailed deer (MCFV-WTD) of unknown origin that causes disease in white-tailed deer; MCF virus carried by ibex (MCFV-ibex), which is responsible for disease in bongo antelope and anoa; MCF virus in muskox (MCFV-muskox) and aoudad (MCF-aoudad), which are carried asymptomatically and have not yet been associated with disease; caprine herpesvirus 2 (CpHV-2) which is endemic in goats and has been associated with disease in sika deer, white-tailed deer and pronghorn antelopes; and OvHV-2.[8]

OvHV-2 is one of the most characterized causative agents of MCF. The virus is endemic in most domesticated sheep.[8,11] MCF-like disease has been experimentally induced in sheep by aerosol inoculation with high doses of OvHV-2; however, the disease is uncommon or non-existent under natural conditions.[10] The susceptibility of ruminant species to development of MCF varies significantly. Père David's deer, banteng (aka Bali cattle), and bison are most susceptible to disease, followed by water buffalo. Domestic cattle (*Bos taurus* and *Bos indicus*) are comparatively resistant; for example, bison are 1000 times more susceptible to clinical MCF than cattle. The reason for this range in susceptibility is not known. Sheep-associated MCF has occasionally been reported in moose and pigs.[13]

There are few reports of sheep-associated MCF in domestic goats in Europe (Germany and United Kingdom). In two published cases, the most common clinical presentation included pyrexia and neurological signs, predominantly ataxia and tremors.[6,14] Necropsy examination of three goats in Germany revealed enlargement of lymph nodes and visceral organs with minute white-spots in the liver and kidney. One goat had erosions and ulcerations of the esophagus, and another had bilateral corneal opacity.[6] Microscopically, goats in the published reports[6,14] had characteristic multisystemic lymphohistiocytic necrotizing vasculitis with fibrinoid necrosis, predominantly of medium-sized arteries. In the present case, neurologic signs were observed and included weakness of the hind end. Similarly, gross findings included bilateral corneal opacity, swollen lymph nodes and multiple, pinpoint, white foci in the liver, along with splenomegaly and prominent white pulp; erosions or ulcers in the alimentary tract were not observed in this goat. As in previous reports, the salient histopathologic finding was lymphohistiocytic necrotizing vasculitis, which was observed in the kidney, urinary bladder, spleen, lymph nodes, thymus, bone marrow, alimentary tract, liver and lung of this goat. Furthermore, meningoencephalitis as a result of vasculitis, marked hyperplasia of the splenic white pulp and of T-cell dependent areas of several lymph nodes were noted in this goat, which is also consistent with MCF. As with other cases, demonstration of OvHV-2 DNA by PCR in lesioned tissues, i.e. the kidney of this goat, supported the diagnosis of MCF.[6,14]

Vasculitis is rare in goats, and the lymphohistiocytic and necrotizing nature observed in MCF has been proposed to originate from a cell-mediated and cytotoxic process. MCF virus-infected CD8+ T lymphocytes have a tropism for blood vessels, where they infiltrate vascular walls and perivascular spaces. These lymphocytes express viral glycoproteins, which can in turn recruit lymphocytes and macrophages, and produce pro-inflammatory cytokines which are cytotoxic and cause injury to vascular cells.[15] This results in lymphoproliferative and necrotizing vasculitis.

The cutaneous form of MCF has been reported in one goat. That doe had multiple erythematous papules on the distal limbs that progressed to widespread erythema, localized scaling, and thinning of the hair coat, together with focal and moderate scaling and crusting of the peribuccal skin, nares and pinnae. Microscopically, granulomatous mural folliculitis was present, resembling that reported in two Sika-deer associated with a CpHV-2 infection. MCF-like cutaneous lesions, along with PCR analysis, were considered compelling evidence to associate it with an OvHV-2 infection. Sheep-associated MCF with generalized cutaneous disease, in the absence of other 'classical' features, has been reported in cattle.[5]

In the published cases discussed above and in the present case, the affected goats were kept with sheep and other goats. Data on the OvHV-2 status of the sheep and unaffected goats in the herds was not available in any of the cases.[5,6,14] However, the source of infection was tentatively attributed to contact with sheep,[5,14] as they are the recognized reservoir host for OvHV-2.[7] Although goats are the endemic carriers for CpHV-2,

OvHV-2 DNA sequences have been detected in 9% of goats in North America, suggesting that goats can also be infected asymptomatically with OvHV-2.[11] The transmission from a herd of OvHV-2-positive sheep to naïve goats has been demonstrated in a study involving a low number of animals. On the contrary, transmission from a herd of OvHV-2 infected goats did not occur during close contact with other goats over a one year period.[9]

JPC Diagnosis: Kidney: Vasculitis, lymphoblastic, necrotizing, multifocal, severe, with fibrinoid change, lymphoplasmacytic interstitial nephritis and tubular degeneration and necrosis.

Conference Comment: The contributor provides an excellent, comprehensive assessment of the epidemiology, pathogenesis and clinical presentation of malignant catarrhal fever in various species. Following a brief overview of classification schemes and general characteristics of the *Herpesviridae* family (see WSC 2013-14 conference 2, case 3), conference participants discussed two broad categories of vasculitis: infectious and non-infectious.[14] The etiologic agents of infectious vasculitis, such as bacteria (*Erysipelothrix rhusiopathiae, Salmonella* sp.), fungi (*Aspergillus* sp.), rickettsial organisms (*Ehrlicia* sp.), helminths (*Strongylus vulgaris, Dirofilaria immitis*) and viruses (African swine fever virus, Equine infectious anemia virus), directly damage vessels.[12] Non-infectious vasculitis may also be associated with infectious agents, via immune-mediated processes, or it can be secondary to toxins as in drug reactions and uremia. Causes of immune-mediated, non-infectious vasculitis include immune complex deposition associated with type III hypersensitivity reactions, cytotoxic type II hypersensitivity reactions against the endothelium, or various inflammatory mediators.[12] The cause of the vascular damage in MCF is not fully understood, but recent work suggests the possibility of direct cytotoxicity of virus infected, dysregulated cytotoxic T cells. CD8+ T-cells and MHC-unrestricted natural killer cells (large granular lymphocytes) are two of the major inflammatory cell types implicated in MCF vasculitis. Interestingly, large granular lymphocytes generally carry the highest load of viral antigen in MCF.[6,13] Additionally, in this case, there appeared to be a fibrinoid component to the vasculitis, so participants examined a PTAH stain in order to confirm the presence of fibrin. PTAH is normally used to highlight skeletal muscle cross striations; however, it can also be used to identify fibrin. Affected vessel walls from this goat multifocally stained deep purple, providing convincing evidence of fibrinoid change.

There are five clinical patterns of MCF: peracute, head and eye, alimentary, neurological, and cutaneous. Most of the clinical patterns, with the exception of the cutaneous form, are associated with lymphoproliferation and/or vasculitis with subsequent necrosis in various tissues. The head and eye forms, characterized by ocular and nasal discharge, with lesions such as petechial hemorrhages and necrosis on the muzzle and in the mouth, are the most common forms in cattle. Diarrhea occurs in both the alimentary, and occasionally in the peracute form. The cutaneous form is distinguished grossly by alopecia with erythematous papules and crusts and microscopically by granulomatous mural folliculitis. It has been reported in cattle and one goat.[5,13] Rule outs for MCF include Jembrana disease, pestivirus, orbivirus, morbillivirus, or vesicular diseases.[2,13] Jembrana disease in Bali cattle (banteng) is caused by a lentivirus. Its principal lesion is a large number of intravascular macrophages filling and surrounding small to medium pulmonary arteries and veins.[3] Pestivirus (bovine viral diarrhea, border disease), morbillivirus (rinderpest, peste-des-petits), orbivirus (bluetongue, epizootic hemorrhagic disease, Ibaraki disease), herpesvirus (infectious bovine rhinotracheitis) and vesicular stomatitides such as rhabdovirus (vesicular stomatitis) and aphthovirus (foot and mouth disease) can all cause oral/enteric ulceration in ruminants; however, they are not generally associated with lymphoid proliferation and vasculitis.[2] Due to the variability in clinical presentation as well as its similarity to other enteric and vesicular diseases, laboratory confirmation of MCF, via PCR, ELISA or indirect immunofluorescence, is essential.[13]

Contributing Institution: Department of Pathobiology and Veterinary Science
Connecticut Veterinary Medical Diagnostic Laboratory
University of Connecticut
www.patho.uconn.edu

References:

1. Ackermann M. Pathogenesis of gammaherpesvirus infections. *Vet Microbiol*. 2006;113:211-222.
2. Brown CC, Baker DC, Barker IK. The alimentary system. In: Maxie MG, ed. *Jubb, Kennedy and Palmer's Pathology of Domestic Animals*. 5th ed. Vol 2. Philadelphia, PA: Elsevier Saunders; 2007:135-137, 140-148, 152-161.
3. Budiarso IT, Rikihisa Y. Vascular lesions in lungs of Bali cattle with Jembrana disease. *Vet Pathol.* 1992;29(3):210-215.
4. Davidson AJ, Eberle R, Ehlers B, et al. The order Herpesvirales. *Arch Virol*. 2009;154:171-177.
5. Foster AP, Twomey DF, Monie OR, et al. Diagnostic exercise: generalized alopecia and mural folliculitis in a goat. *Vet Pathol*. 2010;47(4):760-763.
6. Jacobsen B, Thies K, Von Altrock A, et al. Malignant catarrhal fever-like lesions associated with ovine herpesvirus-2 infection in three goats. *Vet Microbiol*. 2007;124:353-357.
7. King AMQ, Lefkowitz E, Adams MJ, Carstens EB, eds. *Virus Taxonomy: Ninth Report of the International Committee on Taxonomy of Viruses*. London, UK: Elsevier/Academic Press; 2011:119-120.
8. Li H, Cunha CW, Taus NS. Malignant catarrhal fever: understanding molecular diagnostics in context of epidemiology. *Int J Mol Sci*. 2011;12:6881-6893.
9. Li H, Keller J, Knowles DP, et al. Transmission of caprine herpesvirus 2 in domestic goats. *Vet Microbiol*. 2005;107:23-29.
10. Li H, O'Toole D, Kim O, et al. Malignant catarrhal fever-like disease in sheep after intranasal inoculation with ovine herpesvirus-2. *J Vet Diagn Invest*. 2005;17:171-175.
11. Li H, Keller J, Knowles DP, et al. Recognition of another member of the malignant catarrhal fever virus group: an endemic gammaherpesvirus in domestic goats. *J Gen Virol*. 2001;82:227:232.
12. Maxie MG, Robinson WF. Cardiovascular system. In: Maxie MG, ed. *Jubb, Kennedy and Palmer's Pathology of Domestic Animals*. 5th ed. Vol. 3. Philadelphia, PA: Elsevier; 2007:69-72.
13. Russell GC, Stewart JP, Haig DM. Malignant catarrhal fever: A review. *Vet J*. 2009;179(3): 324-335.
14. Twomey DF, Campbell I, Cranwell MP, et al. Multisystemic necrotising vasculitis in a pygmy goat (*Capra hircus*). *Vet Rec*. 2006;158:867-869.
15. Zachary JF. Mechanisms of microbial infections. In: Zachary JF, McGavin MD, eds. *Pathologic Basis of Veterinary Disease*. 5th ed. St Louis, Missouri: Mosby Elsevier; 2012:219.

CASE II: 10-1729 NCSU-CVM (JPC 4004353).

Signalment: 9-year-old female spayed Pomeranian dog, (*Canis familiaris*).

History: This dog presented to the North Carolina State University College of Veterinary Medicine (NCSU-CVM) Neurology service in July 2010 for further evaluation of a two-week history of a head tilt.

Gross Pathology: In the subdural region of both cerebral hemispheres, the leptomeninges appear cloudy and multifocally contain a moderate hemorrhage in the form of petechiae and ecchymoses.

There are two sharp lines of demarcation, one that is noted at the beginning of the duodenum near the termination of the pylorus, and the other line is noted near the beginning of the jejunum. That area, which encompasses the duodenum, measures 15 cm in length, is diffusely dark red to black, and on cut surface, there is diffuse serosal and mucosal hemorrhage. The jejunum, ileum, cecum, and colon contain multifocal dark red hemorrhagic areas on the serosa that measure 1.0 cm to 2.0 cm in diameter and contain a moderate amount of hemorrhagic luminal content.

Laboratory Results:
CBC: mildly decreased hemoglobin (11.7 g/dl, reference range: 12.1-20.3 g/dl) and mild thrombocytopenia (99 x 10^3/UL, reference range 170-400 x10^3/UL).
Blood smear: unremarkable.

The neurological exam findings included the following: depressed, dull mental status; right-sided head tilt and circling to the right; mild amount of pain elicited on palpation of cranial cervical region; no vestibulo-ocular response present; positional ventral strabismus OD; and anisocoria (L>R). Lesion localization was central vestibular disease (vestibular signs with altered mentation).

Tick panel, 4 DX (*Ehrlichia*, *Anaplasma*, Heartworm, Lyme), and *Cryptococcus* antibody: all negative.

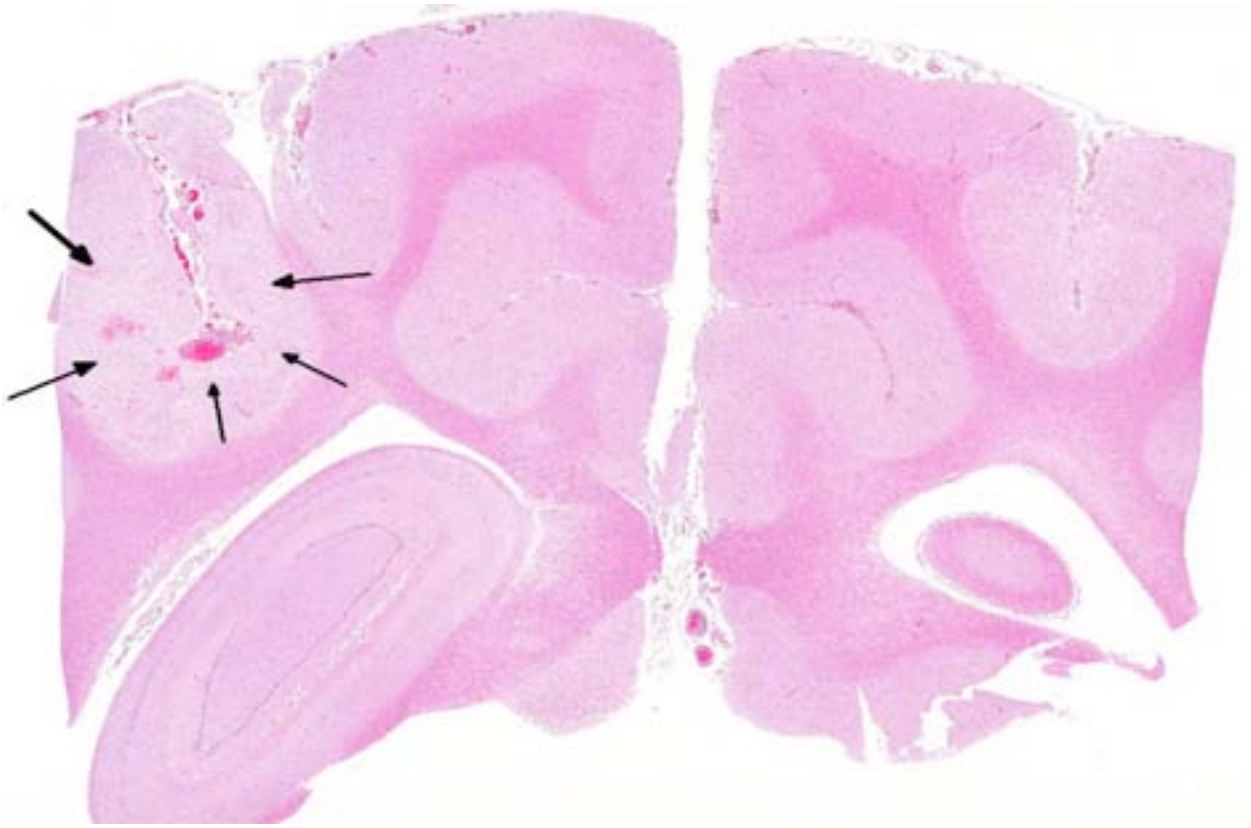

2-1. Cerebrum at level of hippocampus, dog: Meningeal vessels and vessels in the neuropil are expanded by thrombi induced by neoplastic round cells, resulting in infarction and rarefaction of the neuropil. (HE 0.63X)

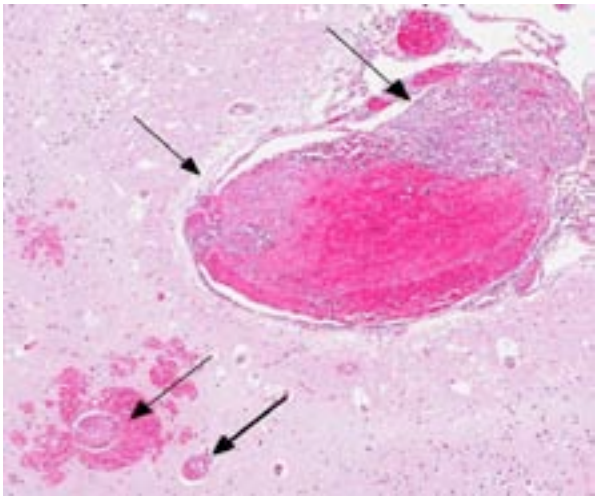

2-2. Within this area, numerous vessels contain fibrin thrombi, which are occasionally attached to vessel walls (upper left). (HE 46X)

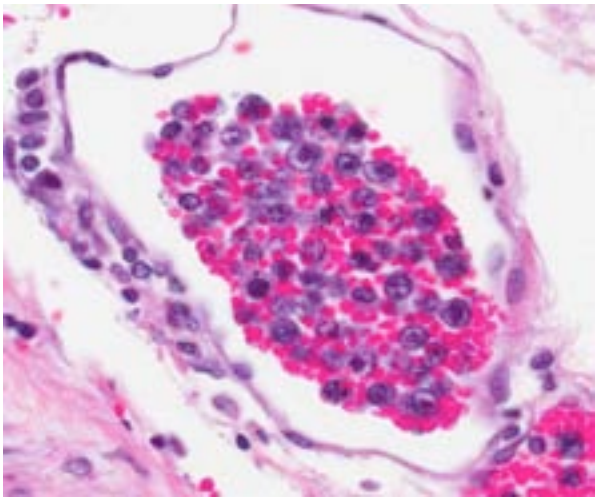

2-3. Cerebrum at level of hippocampus, dog: Neoplastic lymphocytes are present solely within vessels within the meninges and neuropil. Neoplastic cells range from 7-20 µ m, with abundant granular eosinophilic cytoplasm, irregularly round nuclei, prominent nuclei, and exhibit moderate anisocytosis and anisokaryosis. (HE 400X)

MRI: multifocal regions of parenchymal T2 hyperintensity and increased meningeal enhancement with evidence of parenchymal hemorrhage consistent with a severe meningoencephalitis, and focal regions of compensatory hydrocephalus consistent with prior parenchymal necrosis, and left otitis media.

CSF analysis: mononuclear pleocytosis (NCC 19).

Otic cytology: septic suppurative inflammation.

Otic culture: *Staphylococcus pseudintermedius.*

CD3 and CD79a immunohistochemical stains were applied to the tissue sections of cerebrum. The positive controls worked well and internal control lymphocytes were positive. CD3 immunostain revealed minimal to mild, occasional membrane staining of individual neoplastic cells within vessels. The CD79a immunostain was negative.

PARR (PCR for antigen receptor rearrangement) results for cerebrum: TCRγ PARR produced a crisp band in duplicate of the appropriate size that persisted upon heteroduplex analysis. BCR PARR was negative. PARR interpretation: These results should raise your suspicion of T cell neoplasia.

Histopathologic Description: Cerebrum: Multifocally, variably sized blood vessels within the parenchymal and meningeal layer contain neoplastic round cells. Neoplastic cells have large, round to oval nuclei, abundant coarsely clumped chromatin, sparse to moderate lightly basophilic cytoplasm, and 1-2 nucleoli. There is marked anisocytosis and ansiokaryosis and occasionally cells appear binucleated. Mitotic figures are occasionally seen. Multifocally, vessels that contain neoplastic cells also are partially occluded by fibrin thrombi that are composed of brightly eosinophilic, homogenous to beaded material and are admixed with scattered pyknotic and karyorrhectic cellular debris. Fibrin and necrotic cell debris multifocally expands and replaces the walls of scattered vessel profiles. Multifocally, expanding the meninges is a moderate cellular infiltrate that consists predominantly of lymphocytes, plasma cells, and macrophages. Multifocally, within the white matter, there are small aggregates of gitter cells. Multifocally, within the gray matter, there is a mild amount of vacuolation and a moderate amount of hemorrhage. Multifocally, admixed with the cellular infiltrate in the meninges is a moderate amount of hemosiderin laden macrophages and bright, yellow pigment consistent with hematoidin.

Additional findings (not included in slide set): The same neoplastic population of cells was seen within vascular lumens in the following organs:

Table 1: Select endothelial cell and leukocyte adhesion molecules[1]

Endothelial Molecule	Leukocyte Receptor	Major Role
P-selectin	PSGL-1 (a Sialyl-Lewis-X glycoprotein)	Rolling (neutrophils, monocytes, lymphocytes)
E-selectin	ESL-1 (a Sialyl-Lewis-X glycoprotein); Sialyl-Lewis A glycoprotein	Slow rolling, adhesion to active endothelium (neutrophils, monocytes, T-cells) Important in homing of effector & memory T-cells, especially to skin
ICAM-1	β_2-integrins: LFA-1 (CD11a/CD18), Mac-1 (CR3; CD11b/CD18); gp150,95 (CR4; CD11c/CD18)	Adhesion, stable adhesion, transmigration (all leukocytes)
VCAM-1	β_1-integrins: VLA-4 ($\alpha4\beta1$; CD49d/CD29), LPAM-1 ($\alpha4\beta7$)	Adhesion (eosinophils, monocytes, lymphocytes) VLA-4 mediates homing of lymphocytes to endothelium at peripheral sites of inflammation
GlyCAM-1; MadCAM-1; CD34	L-selectin	Rolling; lymphocyte homing to high endothelial venules (HEV) Also serves to bind neutrophils to activated endothelium
PECAM (CD31)	PECAM (CD31)	Transmigration; Leukocyte migration through endothelium
CD99	CD99	Transmigration
JAM-A	JAM-A, LFA-1	Transmigration
JAM-C	JAM-B, Mac-1	Transmigration

cervical and thoracic spinal cord, left and right bulla, liver, spleen, lung, lymph node, adrenal glands, and duodenum. Other histological findings in this animal included: moderate lymphoplasmacytic and neutrophilic cellular infiltrate within the epithelium of the middle ear of the left bulla; diffuse submucosal hemorrhage in the right bulla; diffuse hemorrhagic pancreatic necrosis; transmural duodenal hemorrhage, and multifocal mucosal hemorrhage in the remainder of the intestinal tract.

Contributor's Morphologic Diagnosis: Brain with systemic organ involvement: intravascular lymphoma with multifocal vascular thrombosis.

Contributor's Comment: The histological findings and special testing in this case are most consistent with intravascular lymphoma (IVL), also known as malignant angioendotheliomatosis, intravascular lymphomatosis, and angiotropic large-cell lymphoma.[3] This neoplasm is defined by a proliferation of neoplastic lymphocytes within vessels of organs with a lack of a primary extravascular neoplasm or circulating neoplastic cells or leukemia.[3] The location of the neoplastic cells causes secondary occlusion of the vessel, which then can lead to thrombosis, hemorrhage, and infarction,[2] as in this case. In order to distinguish IVL from disseminated lymphoma and leukemia, one publication suggests that the following criteria can be used: inability to locate neoplastic cells in blood smears, lack of a primary extravascular mass, and absence of bone marrow involvement,[4] which were all consistent findings in this case. The neoplasm is predominantly of T-lymphocyte origin in dogs.[3]

Table 2: Select leukocyte integrins and extra-cellular matrix components involved in leukocyte chemotaxis[1]

Leukocyte Integrin	ECM Component
VLA-1, 2	Collagen
VLA-3, 5	Fibronectin
VLA-6	Laminin

Although this neoplasm is rare, the disease in dogs has been reported to have a predilection for CNS, lung, and less commonly skin.[3,4] One retrospective review of cases of canine IVL found that the most common clinical presentation in dogs included spinal cord ataxia, seizures, vestibular disease, and posterior paralysis.[4] The laboratory findings (CBC, chemistry panel) in the dogs in this study, as well as the dog in this case, were non-specific. Intravascular lymphoma appeared to affect mostly large breed dogs with an average age of six years.[4] The diagnosis of IVL is predominantly a postmortem diagnosis; however, there is one report of an antemortem diagnosis achieved by CT-guided biopsy of a brain lesion.[2] Intravascular lymphoma is typically rapidly progressive; death is reported to occur from 20 days to six months after the first reported clinical signs.[2]

Although the reason for the tendency of neoplastic cells to remain within vessels has not been definitively proven in dogs, several human studies have demonstrated an absence of leukocyte adhesion molecules such as CD11a/CD18[5,7] and CD29,[6] in neoplastic cells. Based on the findings, it was hypothesized that due to the lack of adhesion molecules, the neoplastic cells could not extravasate.

JPC Diagnosis: 1. Cerebrum: Intravascular lymphoma.
2. Midbrain, gray matter and meninges: Vascular necrosis and thrombosis, multifocal, severe with infarction.

Conference Comment: In human intravascular lymphoma, which is usually of B-cell origin, several studies have demonstrated β_1 (CD29) or β_2-integrin (CD18) deficiencies.[4,5] β-integrins are important in the leukocyte adhesion cascade, enabling leukocytes to exit blood vessels and migrate through tissue in order to participate in inflammation. Once activated, all stages of the leukocyte adhesion cascade (i.e., margination, rolling, stable adhesion, locomotion and transmigration) occur concurrently. Initial vasodilation leads to decreased hydrostatic pressure and a slowing of blood flow. Leukocytes exit laminar flow due to decreased vessel wall shear stress, and move toward the endothelial cell surface (margination). Initial rolling is mediated by selectins; low affinity binding between selectins and their receptors allows leukocytes to "roll" along the endothelium. Leukocytes in some species express L-selectin, which binds to GlyCam-1/CD34 and MadCAM-1on endothelial cells; P-selectin glycoprotein ligand-1 (PSGL-1) which is a sLe-X glycoprotein that binds to P-selectin released from endothelial Weibel-Palade bodies; and a sLe-X type protein receptor which binds E-selectin expressed by endothelial cells (Table 1). Expression of adhesion molecules is enhanced by inflammatory mediators released from mast cells, endothelial cells and macrophages in response to infection or injury. For instance, TNF and IL-1 induce endothelial cells of post-capillary venules to express E-selectin and ligands for L-selectin, while histamine, thrombin and platelet activating factor stimulate the release of P-selectin from storage within the Weibel-Palade bodies of endothelial cells.[1]

Integrins mediate stable adhesion, which must be preceded by activation, margination and rolling. Leukocytes that normally express integrins in low affinity state are activated by chemokines, while L-selectins are cleaved from the neutrophil surface by A Disintegrin and Metalloproteinase 17 (ADAM17). This results in the conversion of β_1–integrins, such as VLA-4 ($\alpha_4\beta_1$, CD49d/CD29), and β_2–integrins, such as LFA-1 (CD11a/CD18), Mac-1 (CD11b/CD18, CR3), gp150, 95 (CD11c/CD18, CR4) and $\alpha_d\beta_2$ (CD11d/CD18) to a high-affinity state. Inflammatory mediators also induce endothelial expression of ligands for β_1/β_2-integrins. These ligands generally belong to the immunoglobulin superfamily. Most β_2-integrins on appropriately stimulated leukocytes firmly adhere to ICAM-1 (CD-54) on endothelial cell; $\alpha_d\beta_2$, on the other hand, binds ICAM-3. Alternatively, β_1–integrins on lymphocytes, monocytes and high endothelial venules (HEVs) bind VCAM-1 on endothelial cells (Table 1).[1]

During transmigration, leukocytes emigrate between endothelial cells, primarily at intercellular junctions in post-capillary venules. This is mediated by adhesion molecules, which vary slightly depending on the leukocyte and tissue type. PECAM-1 (CD31) and CD99 on leukocytes bind homotypically to PECAM-1 and CD99, respectively on endothelial cells. Additionally, leukocyte junctional adhesion molecules JAM-A and JAM-B can bind to JAM-A and JAM-C at endothelial cell junctions. Leukocyte integrins also play a role in transmigration. Leukocytes extend pseudopodia between endothelial cells to interact with basement membrane laminins and collagen as well as extracellular matrix proteins such as proteoglycans, fibronectin and vitronectin. Leukocyte binding to these proteins, primarily via β_1-integrins, enables leukocytes to transmigrate into perivascular tissue, from which they can migrate along chemotactic gradients toward the area of injury. Whether endogenous (e.g., cytokines, C5a, arachidonic acid metabolites) or exogenous (e.g., bacterial) substances, chemotactic agents bind to specific G-protein coupled receptors and activate second messengers, which induces actin polymerization and allows filopodia to pull the cell into the area of inflammation. In connective tissue, leukocytes can adhere to the extracellular matrix and advance via β_1-integrins (Table 2).[1]

Deficiencies in β_1 (CD29) or β_2-integrins (CD18) have been reported in the neoplastic cells in human intravascular lymphoma. Although other defects are likely involved as well, this lack of leukocyte adhesion molecules may render neoplastic lymphocytes unable to successfully exit the blood vessel, resulting in the intravascular cellular accumulation characteristically noted in this neoplasm. A similar leukocyte adhesion deficiency has not yet been demonstrated in canine intravascular lymphoma, and its molecular basis remains unknown.[4,5,6]

Contributing Institution: North Carolina State University, College of Veterinary Medicine, Department of Population Health and Pathobiology
http://www.cvm.ncsu.edu/ed/res_ap.html or
http://www.cvm.ncsu.edu/

References:

1. Ackermann MR. Inflammation and healing. In: Zachary JF, McGavin MD, eds. *Pathologic Basis of Veterinary Disease*. 5th ed. St. Louis, MO: Elsevier; 2012:96-98.
2. Bush WW, Throop JL, McManus PM, et al. Intravascular lymphoma involving the central and peripheral nervous systems in a dog. *J Am Anim Hosp Assoc*. 2003;39(1):90-96.
3. Ginn PE, Mansell JEKL, Rakich PM. Skin and appendages. In: Maxie, MG, ed. *Jubb, Kennedy, and Palmer's Pathology of Domestic Animals*. 5th ed. Vol. 1. Philadelphia, PA: Elsevier; 2007:775.
4. McDonough SP, Van Winkle TJ, Valentine BA, et al. Clinicopathological and immunophenotypical features of canine intravascular lymphoma (Malignant Angioendotheliomastosis). *J Comp Pathol*. 2002;126(4):277-288.
5. Ossege LM, Postler E, Pleger B, et al. Neoplastic cells in the cerebrospinal fluid in intravascular lymphomatosis. *J Neurol*. 2000;48(8):656-658.
6. Ponzoni M, Ferreri AJM. Intravascular lymphoma: a neoplasm of "homeless" lymphocytes? *Hematol Oncol*. 2006;24(3): 105-112.
7. Valli VEO. Hematopoietic system. In: Maxie MG, ed. *Jubb, Kennedy, and Palmer's Pathology of Domestic Animals*. 5th ed. Vol. 3. Philadelphia, PA: Elsevier;2007:183.

CASE III: T11-09742 (JPC 4002867).

Signalment: 8-month-old female spayed domestic shorthair cat, (*Felis catus*).

History: An oral mass was noted when the cat yawned.

Gross Pathology: As per the clinician: the mass is "red, inflamed and appears to extend along the gumline."

Histopathologic Description: Gingiva: The tissue is composed of a mass that is characterized by fronds and islands of odontogenic epithelium that are separated by and often cradling loose or compact mesenchymal tissue. In some areas the mesenchymal tissue is forming compact round aggregates and these are the areas in which the epithelium appears to form a rim or cradle around the mesenchymal tissue. The epithelial fronds are lined by columnar cells with basal nuclei and tend to have prominent intercellular bridges. Mitotic cells are rare and primarily seen in the more compact areas of both the mesenchymal and the epithelial components. The overlying oral epithelium is segmentally ulcerated. Large numbers of neutrophils were present in the subjacent necrotic stroma and infiltrated the mesenchymal tissue of the neoplastic mass.

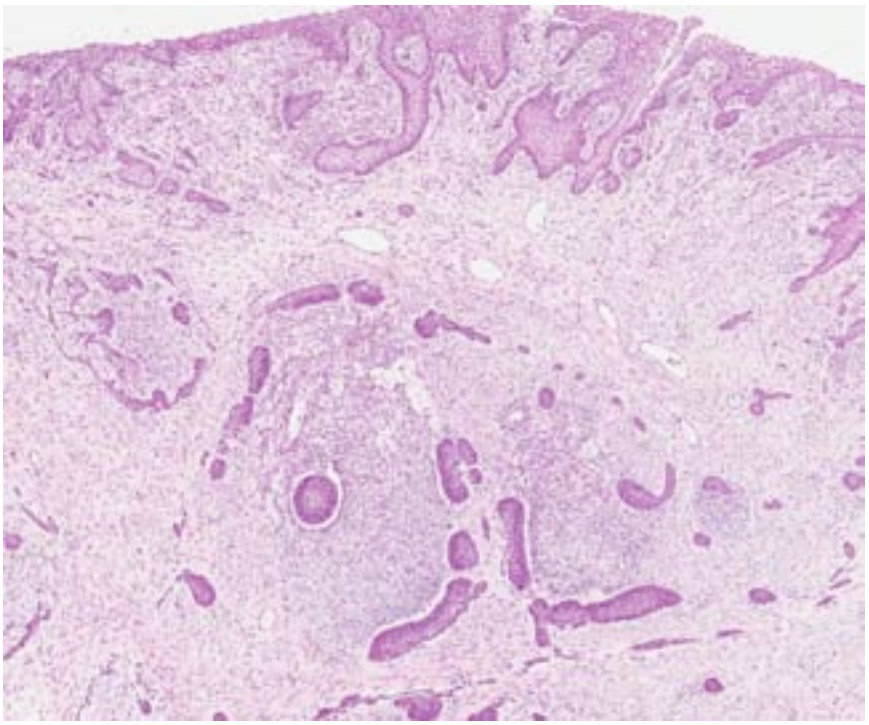

3-1. Gingiva, cat: The gingiva is expanded by an infiltrative, unencapsulated neoplasm composed of trabeculae of odontogenic epithelium and primitive mesenchyme. The overlying epithelium is ulcerated, eroded and hyperplastic. (HE 0.63X)

Contributor's Morphologic Diagnosis: Gingiva: Feline inductive odontogenic tumor (Feline inductive fibroameloblastoma).

Contributor's Comment: Feline inductive odontogenic tumor (also known as inductive fibroameloblastoma) is grouped as part of feline ameloblastic fibroma, which is characterized by epithelial and mesenchymal proliferation as a manifestation of the inductive properties of the odontogenic epithelium. Ameloblastic fibroma consists of poorly organized and more or less diffuse mesenchymal induction around the epithelial islands. A subtype of ameloblastic fibroma is the inductive fibroameloblastoma, characterized by well-formed cup-shaped epithelial structures that partially encircle stroma that resembles dental pulp.[10] The terminology "inductive" is used based on the resemblance of the epithelial islands to the cup stage of odontogenesis in which the dental lamina has an inductive effect on the stroma producing dental pulp.[6]

Feline inductive odontogenic tumors (FIOT) are rare dental tumors specific to cats.[6,7] The neoplasm is the most common dental tumor of young kittens of either sex.[10] Feline inductive odontogenic tumor is described exclusively in cats under 3 years of age[1] and is most often found on the rostral maxilla,[7,10] occasionally causing tooth loss or partial distortion. It has been confused with ameloblastoma in cats.[5] Unlike FIOT, which occurs in young cats, up to three years of age with most being younger than 18 months,[6] ameloblastomas occur in adult cats, chiefly over the age of six years and affects the maxilla and the mandible.[6]

Feline inductive odontogenic tumor is a rare and interesting

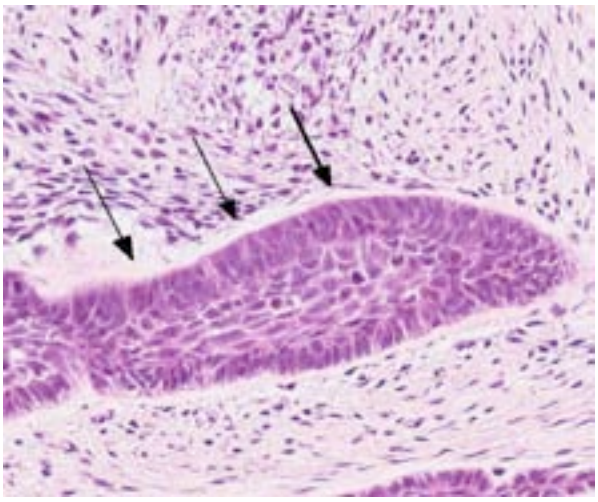

3-2. Gingiva, cat: Odontogenic epithelium is columnar, palisades along a basement membrane, and has prominent intercellular bridges. (HE 252X)

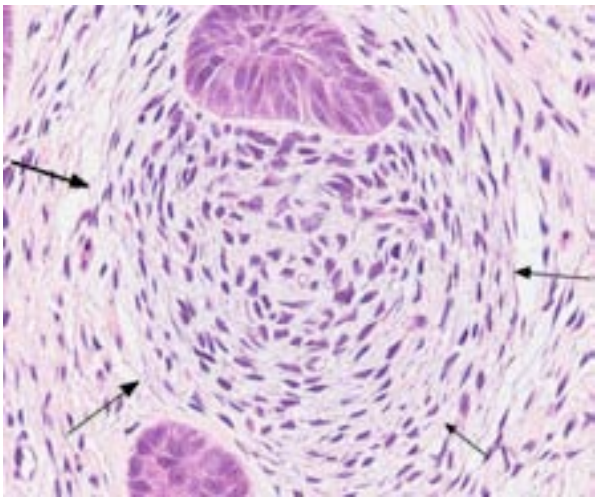

3-3. Gingiva, cat: Trabeculae of odontogenic epithelium encircle condensations of primitive mesenchyme, recapitulating dental pulp. (HE 400X)

odontogenic neoplasm in which the odontogenic epithelium has inductive potential to form aggregated foci of dental pulp-like mesenchymal cells.[9] Its biological behavior is not well elucidated. The neoplasm is thought to have a benign behavior. Some studies indicate that Type IV collagen and laminin were constantly positive around the foci of epithelial cells, and Ki-67 positive indices were extremely low. These findings are consistent with the benign clinical presentation.[9] Although, it is a benign neoplastic mass histopathologically, feline inductive odontogenic tumor grows by expansion and can infiltrate the underlying bone and cause considerable local destruction.[1] Local recurrence has been reported in incompletely excised masses; however, metastasis does not appear to occur. This tumor differs microscopically from human ameloblastic fibromas in that it is not well-circumscribed but rather originates multifocally within the supporting connective tissue as characteristic, spherical condensations of fibroblastic connective tissue (ectomesenchyme) associated with islands of odontogenic epithelium.[6]

JPC Diagnosis: Gingiva: Feline inductive odontogenic tumor.

Conference Comment: Understanding normal tooth development is helpful in understanding the various odontogenic tumors and their classifications. Teeth develop from two embryonic tissues: the buccal cavity squamous epithelium (BCSE) and the embryonic mesenchyme (EM). BCSE invaginates into the EM to become the dental lamina, which develops into the enamel organ. The enamel organ is composed of the outer enamel epithelium, inner enamel epithelium, stellate reticulum and stratum intermedium. Ameloblasts originate from the inner enamel epithelium and form a cap enclosing a nodule of mesenchyme, known as the dental papilla. Ameloblasts induce the dental papilla mesenchyme to condense at the site of the future tooth and differentiate into odontoblasts. Odontoblasts produce dentin, and dentin production re-induces ameloblasts to synthesize enamel. Dentin formation always precedes enamel formation. Odontoblasts, which initially lay down pre-dentin and then move backward toward the pulp cavity as they produce dentin, remain active throughout life, so the process of making dentin continues after eruption and the pulp cavity shrinks as the animal ages. Ameloblasts, induced by odontoblasts, differentiate as a row of palisading columnar cells facing the odontoblasts. They lay down an uncalcified matrix, and then harden it, backing away as the enamel layer is built up. In brachydonts, cementum covers dentin where it is not covered by enamel. Cementum formation over the root occurs when there is degeneration of Hertwig's epithelial root sheath allowing mesenchymal cells to come in contact with dentin. Those epithelial cells differentiate into cemtoblasts which produce cementum. In brachydonts, such as dogs and cats, once the tooth erupts through the gumline, the cells of the stellate reticulum die and the stimulus is lost,

hence the ameloblasts die and enamel can't be renewed. On the other hand, in hypsodont teeth, found in ruminants, rodents and horses, ameloblasts survive and enamel is continuously renewed. Overall, odontoblasts, dentin, cementum and pulp derive from EM (mesenchyme), while ameloblasts and enamel derive from epithelium (BCSE). The periodontal ligament, which anchors teeth into alveolar bone, is produced by ligament fibroblasts which stem from dental follicle cells.[2,3,11]

Odontogenic epithelium is characterized by 1) peripheral palisading of columnar epithelial cells, 2) apical hyperchromatic nuclei with basilar cytoplasmic clearing and 3) prominent intercellular bridging between internal epithelial cells (stellate reticulum).[2] Tumors of odontogenic epithelium are broadly divided into two categories: non-inductive tumors without odontogenic mesenchyme, including ameloblastoma, amyloid-producing odontogenic tumor and canine acanthomatous ameloblastoma, and inductive tumors with the presence odontogenic mesenchyme, including feline inductive odontogenic tumor, ameloblastic fibroma, complex odontoma and compound odontoma.[2,8,9,10]

Ameloblastoma, the least differentiated of the non-inductive odontogenic tumors, has been reported in dogs, cats, horses and humans. Ameloblastoma is classified as central (within the bone) or peripheral (within the gingival soft tissue) and is characterized by islands of poorly differentiated odontogenic epithelium, occasionally admixed with foci of metaplastic bone. Ameloblastic epithelial cells often undergo squamous differentiation and tumors are occasionally so heavily keratinized that it becomes difficult to differentiate ameloblastoma from squamous cell carcinoma. Central ameloblastomas are more common in animals.[2,8,10] The neoplastic islands of odontogenic epithelium in amyloid-producing odontogenic tumors (APOT) are separated by abundant waxy eosinophilic material (amyloid) which exhibits strong apple-green birefringence under polarized light when stained with Congo red. Recent studies have suggested the protein in APOT is not actually amyloid, but is derived from an ameoblastin-like peptide, or AAmel. Ameloblastin (formerly known as sheathlin) is an enamel matrix protein that is essential for enamel formation. Ameloblastin and another enamel protein, amelogenin, are both produced by ameloblasts during amelogenesis (see WSC 2012-13, conference 8, case 2).[2,4] Canine acanthomatous ameloblastoma is more locally aggressive than the other non-inductive odontogenic tumors and, like the ameloblastoma, is generally composed of interconnecting cords and sheets of odontogenic epithelium. It can be differentiated from ameloblastoma by an increased amount of stroma with abundant fibrillar collagen, regularly-positioned stellate mesenchymal cells, and regularly dispersed empty blood vessels, reminiscent of periodontal ligament connective tissue (see WSC 2012-13, conference 8, case 1). Cyst formation is common in acanthomatous ameloblastomas, however, in contrast to ameloblastomas, keratinization is rare.[2,8] A comprehensive review of feline inductive odontogenic tumors is provided above by the contributor. Another inductive odontogenic tumor, ameloblastic fibroma, is composed of islands and cords of odontogenic epithelium on an abundant, collagen-poor fibrous stroma resembling dental pulp (see WSC 2011-12, conference 1, case 4). This is the most common odontogenic tumor in cattle, but has also been reported in young horses and dogs.[2,7] Complex/compound odontomas, the most differentiated odontogenic tumors, are composed of tooth-like structures known as denticles. Denticles contain enamel, dentin, cementum and pulp, arranged in a manner similar to a normal tooth; discrete islands of odontogenic epithelium are not present. These are reported in dogs, horses and cattle and can disrupt surrounding, normal teeth.[2]

Contributing Institution: The University of Georgia
Veterinary Diagnostic and Investigational Laboratory
Tifton, GA 31793
http://www.vet.uga.edu/dlab/tifton/index.php

References:

1. Beatty JA, Charles JA, Malik R, France MP, Hunt GB. Feline inductive odontogenic tumour in a Burmese cat. *Aust Vet J*. 200;78(7):452-455.
2. Brown CC, Baker DC, Barker IK. The alimentary system. In: Maxie MG, ed. *Jubb, Kennedy and Palmer's Pathology of Domestic Animals*, 5th ed. Vol 2. Philadelphia, PA: Elsevier Saunders; 2007:5-7, 24-28.

3. Caceci T. Digestive System I: Oral Cavity & Associated Structures. VM8054: Veterinary Histology website. http://www.vetmed.vt.edu/education/Curriculum/VM8054/Labs/labtoc.htm. Accessed October 29, 2013.
4. Delaney MA, Singh K, Murphy CL, Solomon A, Nel S, Boy SC. Immunohistochemical and biochemical evidence of ameloblastic origin of feline amyloid-producing odontogenic tumors in cats. *Vet Pathol*. 2013;50(2):238-242.
5. Gardner DG. Ameloblastomas in cats: a critical evaluation of the literature and the addition of one example. *J Oral Pathol Med*. 1998;27(1):39-42.
6. Gardner DG, Dubielzig RR. Feline inductive odontogenic tumor (inductive fibroameloblastoma) – a tumor unique to cats. *Journal of Oral Pathology & Medicine*. 1995;24:185–190.
7. Head KW, Else RW, Dubielzig RR. Tumors of the alimentary tract. In Meuten DJ, ed. *Tumors in Domestic Animals*. 4th ed. Ames, IA: Iowa State Press; 2002:401-481.
8. Head KW, et al. Tumors of odontogenic epithelium without odontogenic mesenchyme. In: *Tumors of the Alimentary System of Domestic Animals*. Washington DC: AFIP and CL Davis DVM Foundation and WHO Collaborating Center for Worldwide Reference on Comparative Oncology; 2003:49-51.
9. Hiroki Sakai, Takashi Mori, Tsuneyoshi Iida, Yanai Tokuma, Kouji Maruo and Toshiaki Masegi. Immunohistochemical features of proliferative marker and basement membrane components of two feline inductive odontogenic tumours. *Journal of Feline Medicine & Surgery.* 2008;10(3):296-299.
10. Poulet FM, Valentine BA, Summers BA. A Survey of epithelial odontogenic tumors and cysts in dogs and cats. *Vet Pathol*. 1992;29:369-380.
11. Tutt C. Tooth development (odontogenesis). In: *Small Animal Dentistry: A Manual of Techniques*. 2006:1-32.

CASE IV: 11-0193-1/2 (4035415).

Signalment: Adult male rhesus macaque, (*Macaca mulatta*).

History: This animal was euthanized for research purposes.

Gross Pathology: Postmortem examination revealed an adult male rhesus macaque in good body condition with excess subcutaneous and mesenteric adipose stores. The liver was markedly enlarged, friable, and mottled dark brown, olive, and pale yellow. Sections of liver were submitted in 10% neutral buffered formalin and post-fixed in 2.5% glutaraldehyde for transmission electron microscopy.

Electron Microscopic Description:
11-0193-1:

This electron micrograph contains portions of 5 large polygonal cells, 4 of which converge to form a 2 µm diameter channel lined by a microvillous brush border (bile canaliculus). The cell in the center of the image is 22 µ m in greatest dimension and contains abundant, medium-electron dense, bland cytoplasm, and 2 round nuclei with prominent nucleoli and peripherally condensed heterochromatin (binucleate hepatocyte). The cells are bordered by a 15 µm wide branching sinusoid which is filled with large numbers of densely packed, pale, randomly-oriented and interlacing, non-branching, ~10nm diameter fibrils (amyloid).
11-0193-2:

This electron micrograph contains 2 distinct types of extracellular fibrillar material. Centrally there is a 3 µm wide bundle of ~50nm diameter, banded fibrils arranged in regular parallel arrays (collagen). Above and below the collagen bundle, there are large numbers of densely packed, medium-electron dense, randomly-oriented and interlacing, non-branching, ~10nm diameter fibrils (amyloid). A small portion of a cell is visible at the bottom of the image.

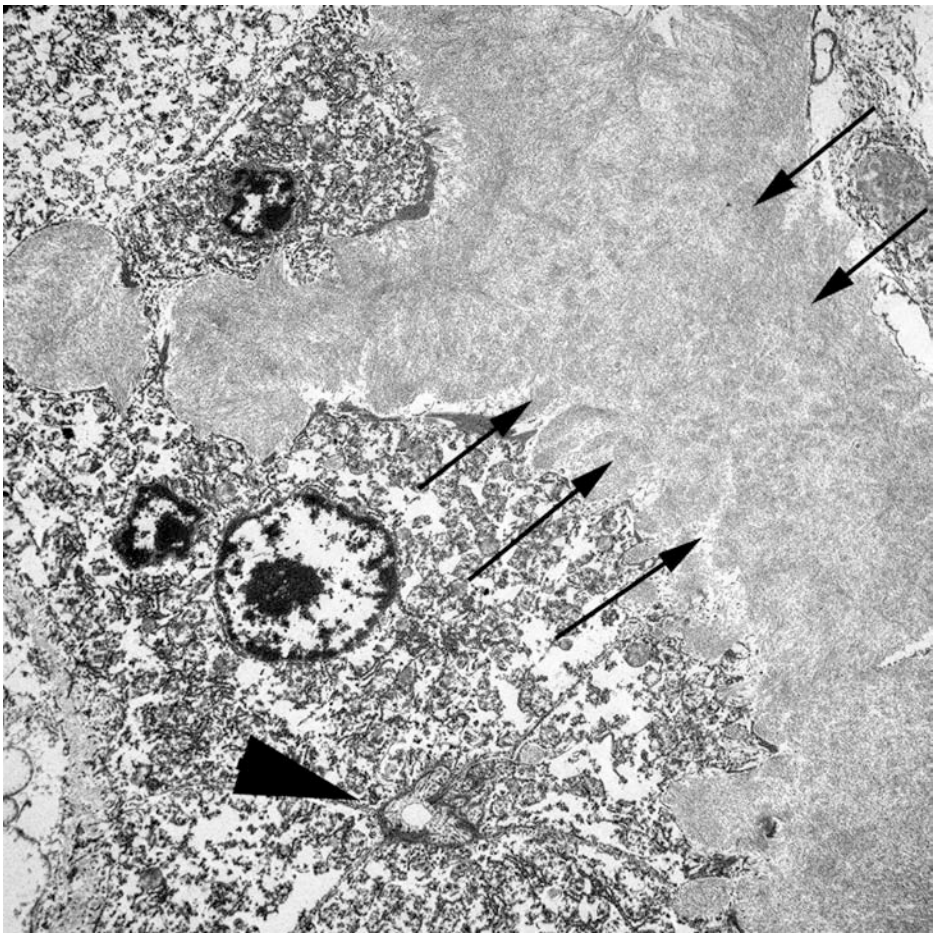

4-1. Liver, rhesus macaque: Several compressed (atrophic) hepatocytes surround a bile canaliculus (arrowhead) and are separated and surrounded by a loosely and haphazardly arranged fibrillar material amyloid. (Photo courtesy of: Integrated Research Facility, Division of Clinical Research, NIAID, NIH, 8200 Research Plaza, Fort Detrick, Frederick, MD 21702, Srikanth.yellayi@nih.gov) (Electron Microscopy)

Contributor's Morphologic Diagnosis: Liver: Amyloidosis, sinusoidal, with focal fibrosis.

Contributor's Comment: Amyloid is an extracellular proteinaceous material composed of approximately 95% fibrillar proteins, and 5% amyloid P protein, proteoglycans, and glycosaminoglycans.[12] Conformationally, the fibrils form regular arrays of β-pleated sheets which allows for

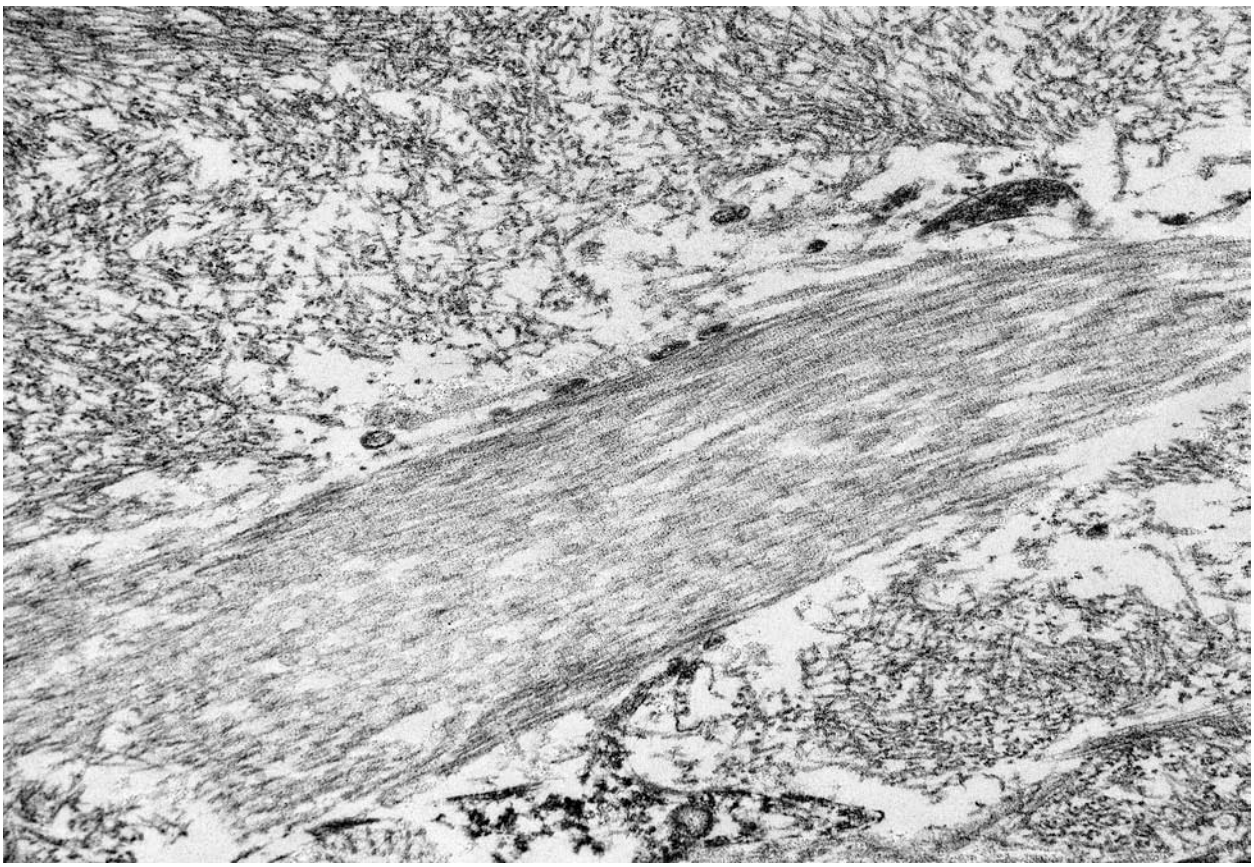

4-2. Liver, rhesus macaque: A 3 µm wide bundle of collagen (arranged in parallel and with an obvious periodicity – center) divides the loosely and haphazardly arranged amyloid fibrils (upper left and bottom right). (Photo courtesy of: Integrated Research Facility, Division of Clinical Research, NIAID, NIH, 8200 Research Plaza, Fort Detrick, Frederick, MD 21702, Srikanth.yellayi@nih.gov). (Electron Microscopy)

positive Congo Red staining and a characteristic green birefringence when viewed under polarized light.[12] Numerous biochemical forms of amyloid have been identified. The amyloid light chain (AL) form is composed of intact or fragmented immunoglobulin light chains, and is associated with immune cell dyscrasias (primary amyloidosis).[12] The amyloid-associated (AA) form is derived from the acute phase protein, serum amyloid A, and is associated with chronic inflammation (secondary amyloidosis).[12] Other commonly recognized types include Aβ amyloid and islet amyloid, which are associated with cerebral amyloid angiopathy of Alzheimer's disease, and Type II diabetes mellitus, respectively.[15,16]

Amyloidosis is the pathologic accumulation of amyloid in tissues and can be systemic or localized. It has been identified in mammals, reptiles, and birds and is a well-recognized condition in rhesus monkeys and other macaques.[1,7,8,17]

By light microscopy, amyloid has a homogenous eosinophilic hyaline appearance which can be similar to other extracellular fibrillar proteinaceous deposits, such as collagen or fibrin. Ultrastructurally, however, it has a distinct appearance and can be readily differentiated, as seen in this case. When viewed with transmission electron microscopy, amyloid fibrils are non-branching, 7.5-10nm in diameter, and randomly-oriented and interlacing.[3] This is in contrast to collagen which has larger fibrils (~50nm in diameter) that are banded and arranged in regular parallel arrays; and fibrin, the strands of which vary in diameter and form dense irregularly-branching mats, generally in the vicinity of platelets.[4,5]

JPC Diagnosis: Liver, space of Disse: Amyloidosis with hepatocellular compression.

Conference Comment: Amyloidogenic proteins have a tendency toward misfolding which leads to the formation of unstable, self-associated fibrils.[12]

Reactive systemic (secondary) amyloidosis is the most common form of amyloidosis in domestic animals. Tissue accumulations is caused by overproduction of AA amyloid, in combination with reduced destruction, and is often associated with chronic inflammatory or neoplastic diseases.[7,9] The precursor to AA, serum amyloid A (SAA), is an acute phase protein produced by the liver during inflammatory conditions under the influence of IL-6 and IL-1. SAA is normally degraded by the monocyte-macrophage system,[12,13] however, a prolonged increase in SAA alone is not sufficient to induce amyloidosis. Several explanations for the development of reactive amyloidosis have been proposed, including a defective SAA degradation system and an inherent alteration in quality of SAA, which renders it resistant to complete degradation.[12]

Systemic AA amyloidosis can also be inherited in humans (familial Mediterranean fever), Chinese Shar-Pei dogs (autosomal recessive Familial AA amyloidosis), Abyssinians (autosomal dominant with incomplete penetrance) and Siamese cats. In Shar-Peis with inherited amyloidosis, amyloid is preferentially deposited in the renal medullary interstitium, while in Abyssinian cats, deposition is glomerular and in Siamese cats amyloid deposits accumulate in the hepatic space of Disse. Whether reactive or inherited, clinical signs in systemic amyloidosis are generally secondary to dysfunction of adjacent organs and pressure atrophy in areas adjacent to amyloid accumulation.[12,13]

In dogs, AA amyloidosis is usually idiopathic, but it has also been associated with *Hepatozoon americanum*, *Ehrlichia canis* and other causes of chronic suppurative/granulomatous inflammation. Canine AA amyloidosis lesions usually occur within renal glomeruli, which leads to proteinuria and progressive renal insufficiency.[13] In contrast, feline amyloidosis primarily affects the renal medulla, so proteinuria is not a typical clinical finding.[13] Equine systemic AA amyloidosis is a well-recognized hepatic lesion in horses used to produce hyperimmune serum.[13] Glomerular amyloidosis, with accompanying proteinuria, occurs occasionally in ruminants. Swine rarely develop amyloidosis.[13] Much like the other forms of reactive amyloidosis described above, avian amyloidosis tends to develop after a period of chronic inflammation and occurs most frequently in waterfowl, although it has also been reported in chickens (amyloid arthropathy).[9] Conversely, reactive amyloidosis is rarely reported in reptiles (snakes and tortoises).[17]

Reactive amyloidosis has been described in the Patas monkey, squirrel monkey, mandrill, chimpanzee, barbary ape and cynomolgus and rhesus macaques; incidence generally increases with age, likely due to cumulative exposure to parasites, infectious agents and injury.[7] Non-human primates with reactive amyloidosis often have concurrent arthritis and/or enterocolitis. Deposition typically occurs in the large or small intestine, or less commonly in the spleen, lymph node, liver, adrenal glands or stomach.[1,7] Affected animals often display elevated levels of alkaline phosphatase, aspartate aminotransferase, lactate dehydrogenase and serum amyloid A, in combination with decreased albumin and cholesterol on serum chemistry profiles.[8] Additionally, the cynomolgus macaque, rhesus macaque, squirrel monkey, gray mouse lemur and common marmoset have all been used as models for cerebral amyloidosis.[7]

Amyloidosis is a common age related change in laboratory mice, especially in CD-1 strains.[14] Mouse amyloidosis is typically composed of AA amyloid or AapoAII (senile amyloid) deposits, but mice are also subject to several localized forms of amyloidosis involving the brain or endocrine tumors. In contrast to AA amyloid, AapoAII deposition is less marked in the liver and spleen, with more deposition in adrenals, intestine, heart, lungs, thyroid and gonads. CBA and B6 mice are most susceptible to reactive (AA) amyloidosis, while A/J mice are resistant, and A/J and SJL mice are predisposed to AapoAII amyloidosis.[11] In hamsters, as in many other species, the incidence of amyloidosis increases with age. Interestingly, females are three times more likely to develop amyloidosis than males, likely due to a "hamster female protein," which is similar to amyloid P. The liver, kidneys and adrenal glands are the most frequently involved organs.[11] Amyloidosis in gerbils has been experimentally associated with filariid infection, but it also occurs spontaneously in older animals. Similarly, renal amyloidosis is reported in aged rabbits, especially those that have been hyperimmunized for antibody production.[11]

As noted by the contributor, primary amyloidosis with AL amyloid is often associated with immune

cell dyscrasias. Cutaneous amyloidosis occurs in approximately 10% of dogs and cats with extramedullary plasmactyomoas. Cutaneous amyloidosis in dogs is also associated with dermatomyositis and monoclonal gammopathy. In horses, the cause of nodular AL amyloid deposition within the skin and upper respiratory tract is unknown.[6]

In addition to AA, AL and Aβ amyloid discussed above, islet amyloid is significant in several veterinary species. Islet amyloid polypeptide (IAPP) produced by pancreatic islet β-cells in some species of mammals, birds and fishes. Although the exact pathogenesis is still unknown, IAPP can be deposited in pancreatic islets as amyloid in cats, non-human primates and humans, resulting in type 2 diabetes.[16] Endocrine disorders of the pancreas have been associated with amyloid deposits in the cynomolgus macaqe,[10] rhesus macaqe,[5] baboon, Celebes crested macaque, and Formosan rock macaque.[7]

Contributing Institution: Integrated Research Facility
Division of Clinical Research, NIAID, NIH
8200 Research Plaza
Fort Detrick
Frederick, MD 21702

References:

1. Blanchard JL, Baskin GB, Watson EA. Generalized amyloidosis in rhesus monkeys. *Vet Pathol*. 1986;23(4):425-430.
2. Cheville NF. Extracellular substances, pigments, and crystals. In: Cheville NF, ed. *Ultrastructural Pathology: An Introduction to Interpretation*. Ames, Iowa: Iowa State University Press; 1994:304-308.
3. Cheville NF. Extracellular Substances, Pigments, and Crystals. In: Cheville NF, ed. *Ultrastructural Pathology: An Introduction to Interpretation*. Ames, Iowa: Iowa State University Press; 1994:279.
4. Cheville NF. Blood and hemostasis. In: Cheville NF, ed. *Ultrastructural Pathology: An Introduction to Interpretation*. Ames, Iowa: Iowa State University Press; 1994:407.
5. De Koning EJ, Bodkin NL, Hansen BC, Clark A. Diabetes mellitus in *Macaca mulatta* monkeys is characterised by islet amyloidosis and reduction in beta-cell population. *Diabetologia*. 1993;36(5): 378-384.
6. Ginn PE, Mansell JEKL, Rakich PM. Skin and appendages. In: Maxie MG, ed. *Jubb, Kennedy, and Palmer's Pathology of Domestic Animals*. 5th ed. Vol. 1. Philadelphia, PA: Elsevier; 2007:662, 776.
7. Hukkanen RR, Liggitt HD, Anderson DM, et al. Detection of systemic amyloidosis in the pig-tailed macaque (*Macaca nemestrima*). *Comp Med*. 2006;56(2):119-27.
8. MacGuire JG, Christe KL, Yee JL, et al. Serologic evaluation of clinical and subclinical secondary hepatic amyloidosis in rhesus macaque (*Macaca mulatta*). *Comp Med*. 2009;59(2): 168-73.
9. Murakami T, Inoshima Y, Sakamoto E, et al. AA amyloidosis in vaccinated growing chickens. *J Comp Pathol*. 2013;149(2-3);291-297.
10. O'Brien TD, Wagner JD, Litwak KN, et al. Islet amyloid and islet amyloid polypeptide in cynomolgus macaques *(Macaca fascicularis):* An animal model of human non-insulin-dependent diabetes mellitus. *Vet Pathol*. 1996;33(5):479-485.
11. Percy DH, Barthold SW, eds. *Pathology of Laboratory Rodents and Rabbits*. 3rd ed. Ames, IA: Blackwell Publishing; 2007:93-94, 200-201, 301.
12. Snyder PW. Diseases of immunity. In: McGavin MD, Zachary JF, eds. *Pathologic Basis of Veterinary Disease*. 5th ed. St. Louis, Missouri: Mosby Elsevier; 20012:37-38, 284-288.
13. Stalker MJ, Hayes MA. Liver and biliary system. In: Maxie MG, ed. *Jubb, Kennedy and Palmer's Pathology of Domestic Animals*, 5th ed. Vol 2. Philadelphia, PA: Elsevier Saunders; 2007:315-316, 463-464, 532.
14. Thoolen B, Maronpot RR, Harada T, et al. Proliferative and nonproliferative lesions of the rat and mouse hepatobiliary system. *Toxicol Pathol*. 2010;38(7 suppl):5S-81S.
15. Uno H, Alsum PB, Dong S, et al. Cerebral amyloid angiopathy and plaques, and visceral amyloidosis in aged macaques. *Neurobiol Aging*. 1996;17(2):275-281.
16. Westermark P, Andersson A, Westermark GT. Islet amyloid polypeptide, islet amyloid, and diabetes mellitus. *Physiol Rev*. 2011;91(3): 795-826.
17. Zschiesche W, Jakob W. Pathology of animal amyloidoses. *Pharmac Ther*. 1989;41(1-2):49-83.

Joint Pathology Center
Veterinary Pathology Services

WEDNESDAY SLIDE CONFERENCE 2013-2014

Conference 7

30 October 2013

CASE I: CSUVTH Sheep (JPC 4032698).

Signalment: 13-month-old Hampshire-cross castrated ram (*Ovis aries*).

History: The animal had a 5-7 day history of progressive ill thrift, and was subsequently euthanized due to poor quality of life.

Gross Pathology: Bilaterally, the cranioventral lung lobes were markedly firm on palpation. Multifocally visible in the immediate subpleural parenchyma of all lung lobes were numerous, coalescing, white, non-raised, nodular foci. On cut section the parenchyma was consolidated, mottled pale tan to dark red to brown, and displayed an increased prominence of cross-sectional profiles of small to medium caliber airways due to circumscription by dense cuffs of moderately firm white tissue.

Laboratory Results: PCR of lung tissue was positive for *Mycoplasma* spp. and was confirmed as *Mycoplasma ovipneumoniae* by genetic sequencing. PCR for Maedi-Visna virus (MVV; Ovine Progressive Pneumonia) was negative. Routine aerobic culture from the lung yielded heavy growth of *Mannheimia haemolytica.*

Histopathologic Description: Lung: Affecting 60-100% of the parenchyma within submitted sections, alveolar lumina are variably filled by large numbers of neutrophils and macrophages admixed with marked amounts of edema, and lesser amounts of fibrin. Frequently, macrophages contain abundant foamy cytoplasm, with rare multi-nucleate giant cells present. Multifocally, moderate numbers of affected alveoli are lined by plump, cuboidal epithelial cells (type II pneumocyte hyperplasia). Diffusely, the lumens of bronchi and bronchioles are also filled with variable numbers of neutrophils admixed with fewer macrophages, sloughed epithelial cells, moderate amounts of fibrin, and rare clusters of coccobacilli. Frequently, the submucosa of bronchi and bronchioles, as well as the adventitia of blood vessels, are expanded by cuffs of lymphocytes and plasma cells up to 10 cell layers thick, occasionally which are arranged in more follicular aggregates. Segmentally, there is hyperplasia of the respiratory epithelium of affected bronchi and bronchioles characterized by crowding and piling up of epithelial cells. Multifocally, interlobular septa are also expanded by ectatic lymphatics, edema, and lesser amounts of fibrin. Within some sections, rare bronchiolar lumens are partially occluded by nodular protrusions of fibrous connective tissue which are

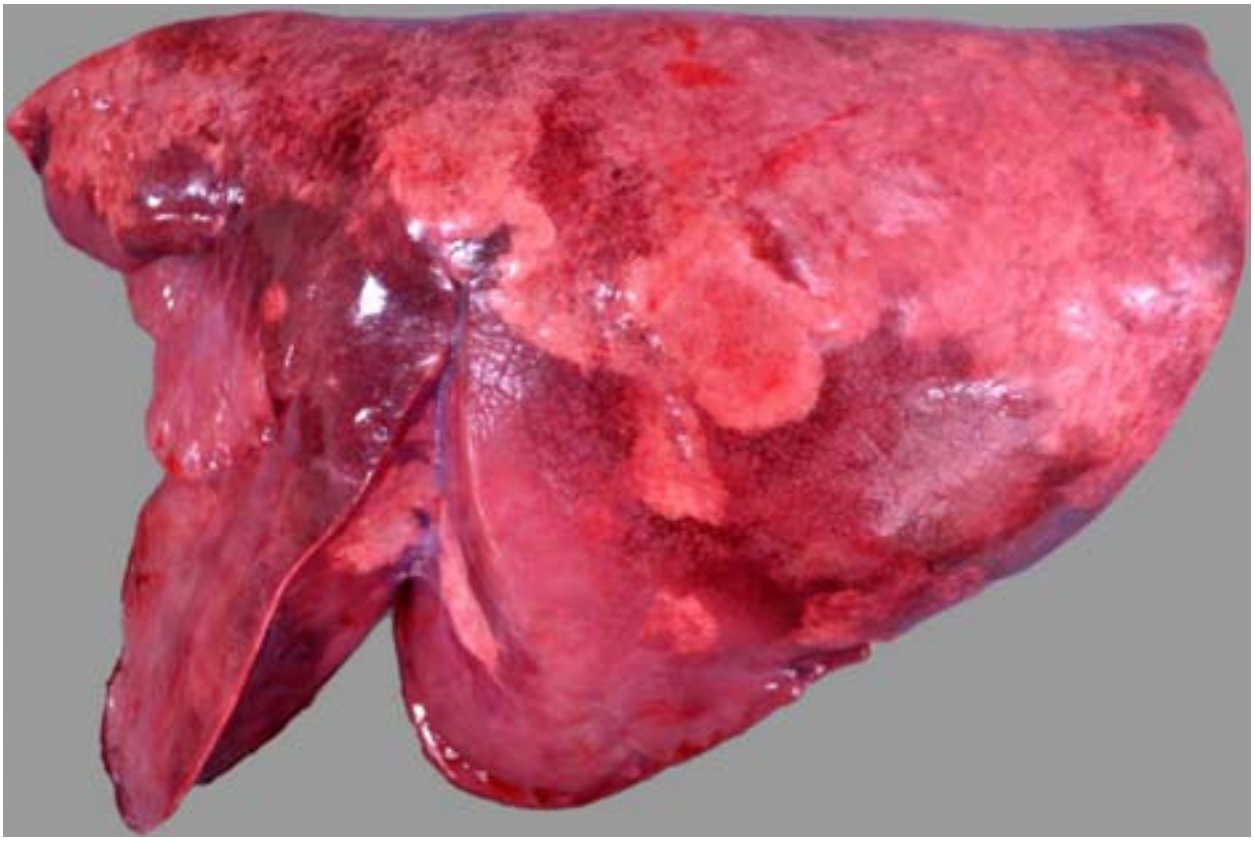

1-1. Lung, sheep: Cranioventral lung lobes were firm, mottled pale tan to dark red to brown and contained numerous white coalescing foci. On cut section the parenchyma displayed an increased prominence of cross-sectional profiles of small to medium caliber airways surrounded dense cuffs of moderately firm white tissue. (Photo courtesy of: Colorado State University, College of Veterinary Medicine and Biomedical Sciences, Dept. of Microbiology, Immunology, and Pathology/Diagnostic Medicine Center, Fort Collins, CO 80524, www.cvmbs.colostate.edu)

lined by hypertrophied epithelial cells (nodular hyaline casts).

Contributor's Morphologic Diagnosis: Lung; bronchopneumonia, suppurative and histiocytic, chronic-active, diffuse, severe, with bronchial epithelial and type II pneumocyte hyperplasia, and perivascular and peribronchiolar lymphofollicular proliferation.

Contributor's Comment: Numerous *Mycoplasma* spp. have been documented to cause disease in small ruminants including *M. mycoides* ssp. *Mycoides,* large colony type (LC), *M. mycoides* ssp. *capri, M. capricolum* ssp. *capricolum*, *M. putrefaciens*, *M. agalactiae, M. capricolum* ssp. *capripneumoniae* (the causative agent of contagious caprine pleuropneumonia (CCPP), and *M. ovipneumoniae*.[2] Similar to cattle, other domestic animal species, and laboratory rodents, these mycoplasmas cause a wide range of pathologic conditions not only including pneumonia/pleuropneumonia, but also polyarthritis, septicemia/polyserositis, keratitis/conjunctivitis, and mastitis.[2,5,10] Specifically in sheep, *Mycoplasma ovipneumoniae* is the primary etiologic agent involved in the condition known as "chronic enzootic pneumonia" or "chronic non-progressive pneumonia", a multi-factorial disease complex which typically affects lambs of 1 year of age or less.[2,5,10,12] *M. ovipneumoniae* infection is typically subclinical, frequently only causing a mild, non-fatal pneumonia that results in poor growth rates, until it becomes compounded by additional risk factors such as stress, poor air quality, adverse weather conditions, respiratory syncytial or parainfluenza viral infections, and secondary bacterial infections, which combine to cause overt clinical respiratory disease.[2,5,10,12]

The spectrum of histological lesions present in this animal are a good representation of the pathogenesis of this disease syndrome, as the prominent lymphoid cuffing and bronchial epithelial hyperplasia are consistent with histological findings previously reported for *M.*

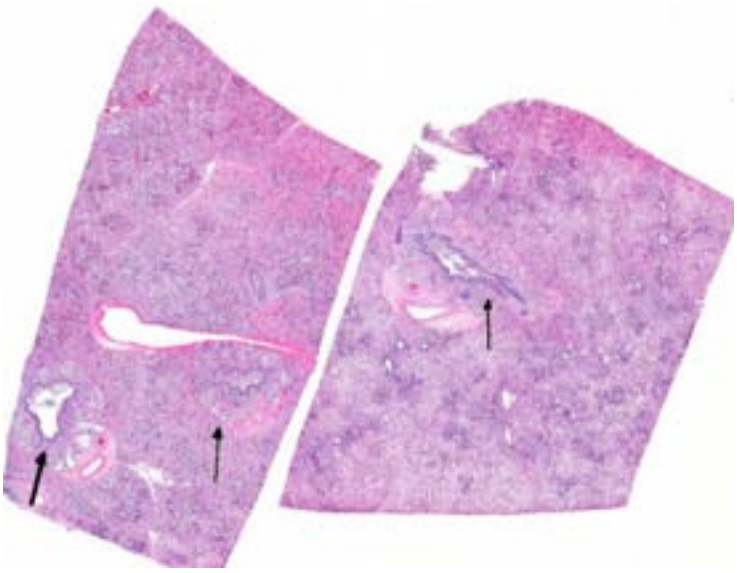

1-2. Lung, sheep: The lung is diffusely consolidated, and airways (arrows) are filled with refluxed exudate. (HE 0.63X)

ovipneumoniae, and typify mycoplasmal pneumonias, while the suppurative inflammation is reflective of the secondary *Mannheimia haemolytica* infection and not of *M. ovipneumoniae* infection.[2,12] Besides *M. haemolytica*, other secondary bacterial infections reported with ovine pulmonary mycoplasmosis include *Pasteurella multocida* and *Bibersteinia trehalosi* (formerly *Pasteurella haemolytica* biotype T).[5] In addition to domestic sheep, *M. ovipneumoniae* has also been reported to cause similar lesions in Bighorn sheep (*Ovis canadensis canadensis*), as well as predispose them to secondary, fatal *M. haemolytica* pneumonia.[1,3]

Colonization of the ciliated respiratory epithelium and induction of ciliostasis are shared pathogenic features of *Mycoplasma* spp. pneumonia, factors which are thought, at least in part, to prevent clearance of the organism from the respiratory tract by the innate defense system of the mucociliary escalator.[4,7] While unique, these features are also characteristic of *Bordetella bronchiseptica* and cilia-associated respiratory bacillus (CAR bacillus), both important bacterial causes of respiratory disease in numerous laboratory and domestic animal species.[10,11] Specifically, investigations into the ability of *M. ovipneumoniae* to persist in the respiratory tract of sheep have shown that this persistence may be due to a combination of: 1) an initial aberrant immune response to the organism and 2) delayed generation of a protective systemic humoral immune response.[9] Experimental evidence corroborating this includes the presence of ciliary autoantibodies in acutely infected sheep, and the resolution of late clinical disease following systemic generation of antigen-specific IgG antibodies.[8,9] It is speculated that this delayed development of protective humoral immunity results from a marked variation in antigenicity between organisms, as well as expression of a polysaccharide capsule.[4,9]

JPC Diagnosis: Lung: Bronchopneumonia, neutrophilic and histiocytic, focally extensive, moderate with peribronchial, peribronchiolar, and perivascular lymphoplasmacytic proliferation.

Conference Comment: A tissue Gram stain revealed moderate numbers of gram-negative coccobacilli within peribronchial glands, interpreted as secondary bacterial colonization. Although none were isolated, conference participants speculated upon the presence of an initiating viral agent, which may have created ideal physiologic conditions for subsequent bacterial infection. Potential etiologic agents include bovine parainfluenza virus 3, bovine respiratory syncytial virus, Maedi-Visna virus, and (less likely) peste des petits ruminants virus. Both bovine parainfluenza virus 3 and bovine respiratory syncytial virus are members of the family *Paramyxoviridae*. Alone, they are unlikely to cause respiratory disease; however, they are commonly associated with both shipping fever and bovine respiratory disease complex, which frequently induce secondary bronchopneumonia due to bacterial agents such as *Mannheimia haemolytica*. Both of these syndromes are characterized by respiratory signs such as nasal discharge, tachypnea, anorexia, fever and general malaise, as exhibited in this case.[6] Maedi-Visna virus, the cause of ovine progressive pneumonia, is a lentivirus from the family *Retroviridae*, which is closely related to caprine arthritis-encephalitis virus.[6] Discovered in Iceland, this disease was historically distinguished by clinical signs indicating both respiratory and central nervous system lesions (*maedi* means "dyspnea" and *visna* means "fading away" in Icelandic); however, currently, the most common presentation is a slowly progressive pneumonia, which often

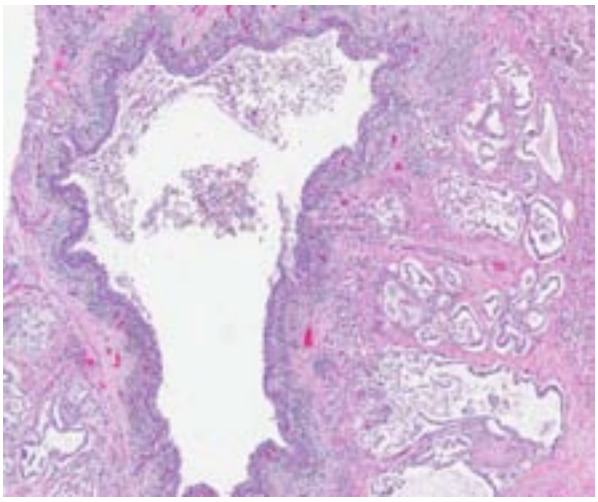

1-3. Lung, sheep: Bronchioles are ectatic and filled with refluxed exudate. Airway epithelium is hyperplastic, and is surrounded by large numbers of lymphocytes and plasma cells. Adjacent submucosal glands are often necrotic. (HE 40X)

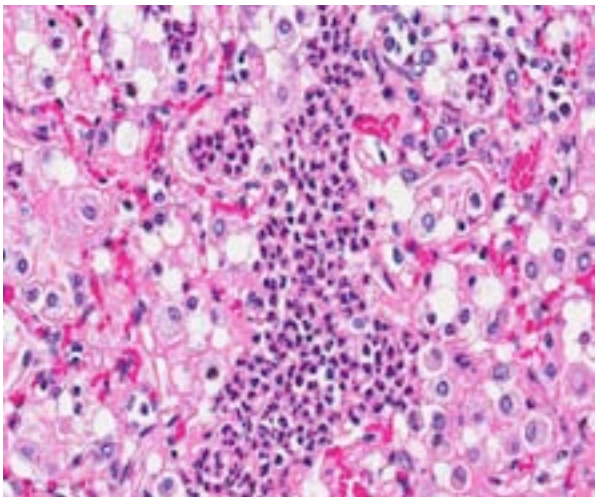

1-4. Lung, sheep: Alveoli are filled with viable and degenerate neutrophils and abundant foamy macrophages. Alveolar septa appear congested and surrounded by proteinaceous exudate (fibrin and edema). (HE 400X)

predisposes secondary bacterial infection.[2] Peste des petits ruminants virus is a morbillivirus which, although not endemic to North America, can also cause respiratory disease in small ruminants.[6]

In this case, PCR analysis implicates *Mycoplasma ovipneumoniae* as the inciting agent. Mycoplasmas, the smallest known bacteria, are obligate parasites that lack a cell wall and have a protein- and lipid-rich plasma membrane. They have a relatively small genome and a propensity for genomic rearrangement, leading to frequent variations in cell surface antigens. These characteristics likely result in an innate ability to evade the host immune response. In addition to ciliostasis, other pathogenic mechanisms of mycoplasmas include alteration of prostaglandin synthesis and induction of lymphocyte apoptosis. Additionally, mycoplasmal membranes contain superantigens, which generate a substantial nonantigen-specific immune response; this is the likely cause of the characteristic peribronchiolar lymphoid cuffing often associated with pulmonary mycoplasmosis.[2] Superantingens bind the V_{β} domain of the T-lymphocyte receptor (TCR) with the α-chain of a class II major histocompatibility complex (MHC). This occurs outside of the normal antigen binding site and results in polyclonal T-lymphocyte activation regardless of antigen specificity, as well as massive cytokine release (see 2013-14 WSC conference 1, case 3). In lambs, infection with M. *ovipneumoniae* and *M. arginini* can induce paroxysmal coughing of such severity as to induce rectal prolapse, known as "coughing syndrome."[8]

Contributing Institution: Colorado State University
College of Veterinary Medicine and Biomedical Sciences
Dept. of Microbiology, Immunology, and Pathology/Diagnostic Medicine Center
Fort Collins, CO 80524
www.cvmbs.colostate.edu

References:

1. Besser TE, Cassirer EF, Potter KA, et al. Association of *Mycoplasma ovipneumoniae* infection with population-limiting respiratory disease in free-ranging Rocky Mountain bighorn sheep (*Ovis canadensis canadensis*). *J Clin Microbiol*. 2007;46:423-430.
2. Caswell JL, Williams KJ. Respiratory system. In: Maxie MG, ed. *Jubb, Kennedy, and Palmer's Pathology of Domestic Animals*. 5th ed. Vol. 2. Philadelphia, PA: Elsevier; 2007:579-650.
3. Dassanayake RP, Shanthalingam S, Herndon CN, et al. *Mycoplasma ovipneumoniae* can predispose bighorn sheep to fatal *Mannheimia haemolytica* pneumonia. *Vet Microbiol*. 2010;145:354-359.
4. Howard CJ, Taylor G. Immune responses to mycoplasma infections of the respiratory tract. *Vet Immunol Immunopathol*. 1985;10:3-32.
5. Lopez A. Respiratory system, mediastinum, and pleurae. In: Zachary JF, McGavin MD, eds.

Pathologic Basis of Veterinary Disease. 5th ed. St. Louis, MO: Elsevier; 2012:458-538.
6. MacLachlan NJ, Dubovi EJ, eds. *Fenner's Veterinary Virology*. 4th ed. London, UK: Elsevier; 2011:267-268,308-323.
7. Minion FC. Molecular pathogenesis of mycoplasma animal respiratory pathogens. *Front Biosci*. 2002;7:1410-1422.
8. Niang M, Rosenbusch RF, Andrews JJ, Lopez-Virella J, Kaeberle ML. Occurrence of autoantibodies to cilia in lambs with a 'coughing syndrome'. *Vet Immunol Immunopathol*. 1998;64:191-205.
9. Niang M, Rosenbusch RF, Lopez-Virella J, Kaeberle ML. Differential serologic response to *Mycoplasma ovipneumoniae* and *Mycoplasma arginini* in lambs affected with chronic respiratory disease. *J Vet Diagn Invest*. 1999;11:34-40.
10. Percy DH, Barthold SW, eds. *Pathology of Laboratory Rodents and Rabbits*. 3rd ed. Ames, IA: Blackwell Publishing; 2007:64, 132, 141-143, 211, 226-228, 267-268.
11. Schoeb TR, Davidson MK, Davis JK. Pathogenicity of cilia-associated respiratory (CAR) bacillus isolates for F344, LEW, and SD rats. *Vet Pathol*. 1997;34:263-270.
12. Sheehan M, Cassidy JP, Brady J, et al. An aetiopathological study of chronic bronchopneumonia in lambs in Ireland. *Vet J*. 2007;173:630-637.

CASE II: 13-3472 (JPC 4032481).

Signalment: 2.5-year-old intact female Bernese Mountain dog (*Canis familiaris*).

History: The owners had intended to use the bitch for breeding. Multiple breedings never resulted in pregnancy. Ovariohysterectomy was performed in March of 2013. Uterus and ovaries were submitted for histopathology to determine the cause of infertility.

Gross Pathology: At surgery, the midbody of the right uterine horn had a circular 'lump'. Both ovaries had multiple dark nodules.

Macroscopically, the mid-region of the uterine mucosa of both horns was multifocally and segmentally expanded by a few, nodular, firm masses. There was one mass in the right uterine horn (3.0 x 2.5 x 1.5 cm, partially bisected by submitter) and two smaller masses in the left uterine horn (1.8 cm and 1.5 cm diameter), all of which oozed moderate amounts of clear fluid on sectioning.

Histopathologic Description: In the affected uterine segments, the endometrium was disrupted by discreet, multilayered masses. Within these focal enlargements, deep endometrial glands were lined by a single layer of cuboidal epithelial cells, contained variable amounts of globular to homogeneous, proteinaceous material, and were separated by a fine collagenous stroma, reminiscent of the deep glandular layer of the placenta. This layer of dilated glands was covered by a thin band of fibrous tissue, reminiscent of the supraglandular layer of the placenta. Luminal to the band of fibrous tissue was a second segment composed of folds and small villi of columnar endometrial epithelial cells with weakly eosinophilic to vacuolated cytoplasm, reminiscent of the outer layer of the placenta. The third, and most luminal layer was composed of many, large, irregularly sized papillary projections and cysts filled with mucus and protein and lined by pseudostratified, flattened to cuboidal to columnar epithelial-like cells, reminiscent of the placental labyrinth. These cells had moderate to marked anisokaryosis with rare multinucleated cells. The projections and cysts protruded into and partially occluded the uterine lumen. Abundant karyorrhectic and hypereosinophilic debris was scattered among the inner endometrial mucosa. The smooth muscle bundles of the inner and outer myometrium were flanked and mildly separated by increased amounts of collagen bundles.

The mucosa distal and proximal to the uterine masses described above contained pools of erythrocytes, and endometrial glands were nested and separated by moderate amounts of collagenous stroma. Luminal epithelium was tall columnar with plump cytoplasm containing numerous cytoplasmic vacuoles.

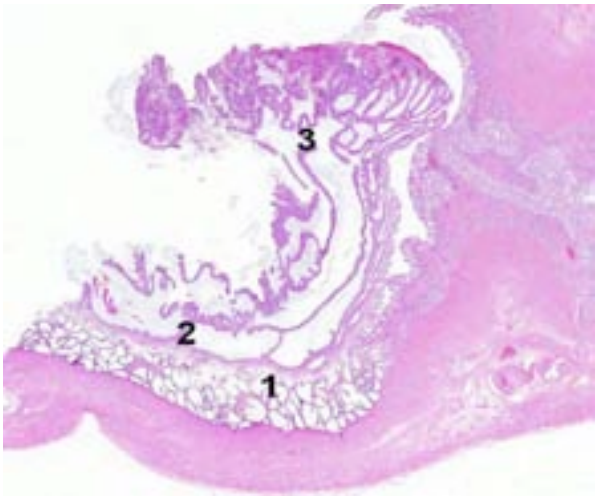

2-1. Uterus, dog: Segmentally, the hyperplastic endometrium exhibits a three-layer appearance reminiscent of placental formation, known as "pseudoplacentational endometrial hyperplasia". #1 is the deep glandular region, #2 is a linear strip of dense collagen separating glandular layers, and #3 is a layer of villous proliferation resembling the junctional zone. (HE 4X)

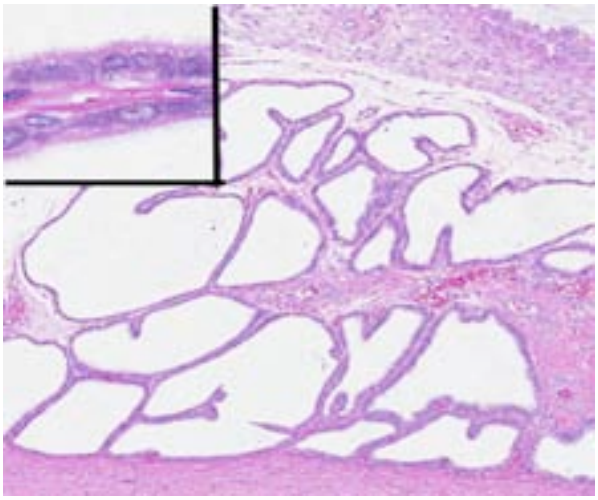

2-2. Uterus, dog: The deep glandular regional consists of cystic glands lined by attenuated ciliated cuboidal cells with indistinct cell borders and a moderate amount of eosinophilic granular cytoplasm (inset). (HE 40X)

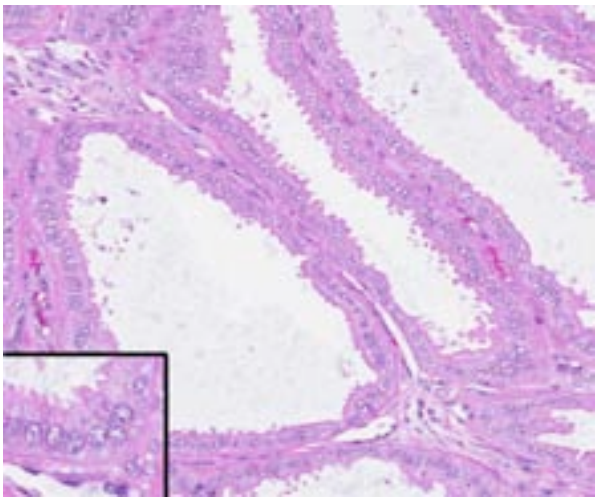

2-3. Uterus, dog: The innermost layer of the junctional zone is composed of large dilated glands lined by columnar epithelium (inset) which contain abundant basophilic mucin. (HE 40X)

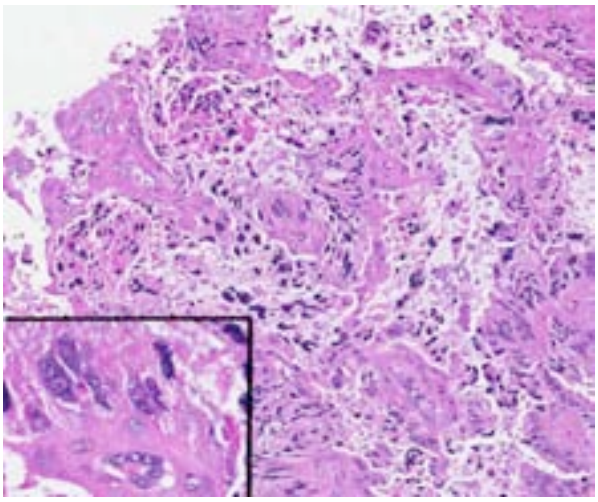

2-4. Uterus, dog: The outermost layer of the junctional zone is composed of papillary projections of endometrial cells, of which over 50% are necrotic. Multinucleated cells are commonly seen in this area (inset). (HE 40X)

Ovaries: In two cross-bisected sections, approximately 40 to 60% of the right and left ovaries were composed of large corpora lutea. The remaining portions of the ovaries had follicles in various developmental stages.

Contributor's Morphologic Diagnosis: 1. Uterus: Segmental endometrial hyperplasia (pseudo-placentational endometrial hyperplasia). 2. Ovary: Multiple ovarian corpora lutea.

Contributor's Comment: Endometrial hyperplasia is a proliferative condition of the uterine mucosal epithelium that is generally considered to be caused by abnormal elevations in either estrogen or progesterone, or both. In the bitch, the normal estrous cycle includes differentiation and proliferation of endometrial glands under estrogen influence during proestrus, and more extensive proliferation and coiling of glands during estrus and metestrus/diestrus under the influence of rising progesterone levels. As progesterone levels fall during late diestrus, the endometrium regresses to a quiescent/atrophic state during anestrus.[3]

In females of most domestic species (especially mares, sows and cows), the pathologic condition of endometrial hyperplasia is associated with hyperestrogenism.[8] Endogenous estrogen from cystic follicles or granulosa cell tumors and ingestion of exogenous estrogenic plants have been implicated. In the bitch and the queen, the condition usually referred to as cystic endometrial hyperplasia (CEH)-pyometra complex has been attributed to diffuse cystic proliferation of endometrial glands under prolonged progesterone influence after estrogen priming. Although some authors have argued that CEH and pyometra are not necessarily linked,[1] it is generally accepted that the same prolonged high progesterone levels that cause endometrial gland proliferation also increase susceptibility of the uterus to infection.[3] Besides the CEH-pyometra complex, McKentee described 3 other forms of endometrial hyperplasia in the bitch: 1) estrogen-induced CEH, 2) focal endometrial polyps and 3) endometrial hyperplasia associated with psuedopregnancy; the latter is the subject of this report.

Segmental endometrial hyperplasia, also called pseudo-placentational endometrial hyperplasia (PEH) and deciduoma, is a condition of the canine uterus not always associated with psuedopregnancy.[2,7] Although the cause of spontaneous cases is unknown, the condition has been induced by intraluminal stimulation of the canine uterus in the luteal phase of the estrous cycle.[5,6] Clinically it has been associated, along with CEH and endometritis, with infertility and pregnancy loss in the bitch.[4] The term 'deciduoma' as used by some authors is derived from conditions in primates and rodents and is less accurate in that it implies a neoplastic rather than hyperplastic lesion.[9]

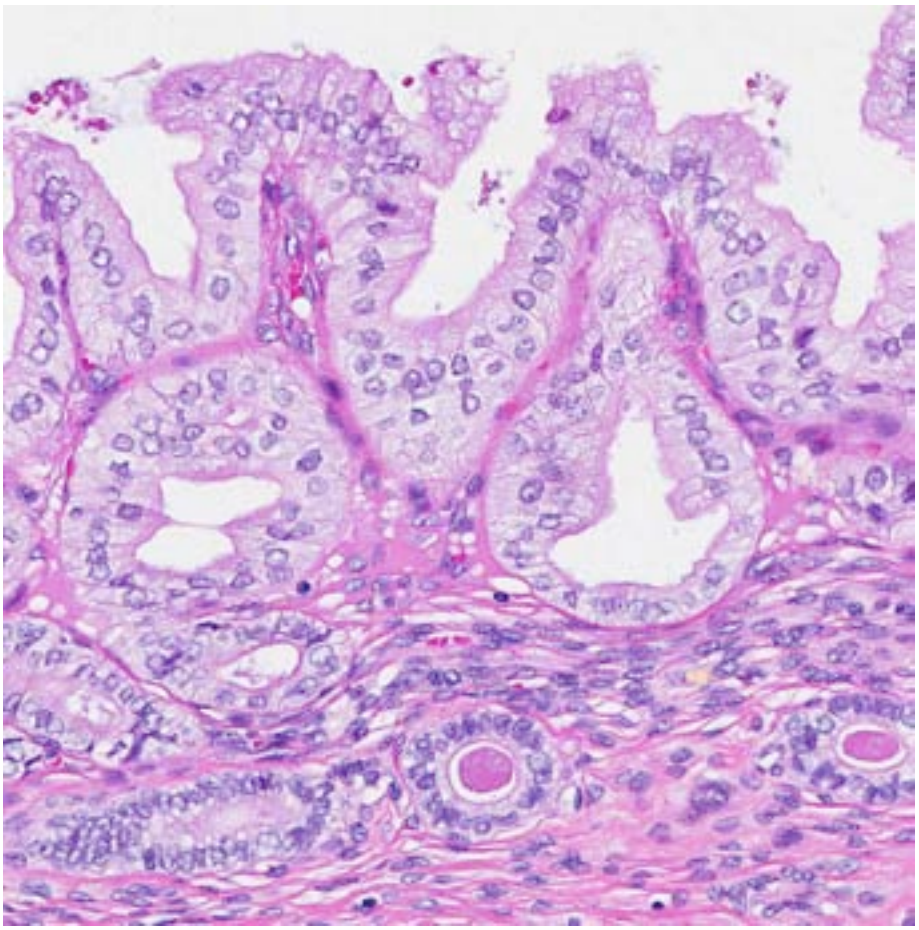

2-5. Uterus, dog: Adjacent to the segmental area of hyperplasia, endometrial cells demonstrate progestational change. (HE 100X)

PEH is clearly distinguishable from CEH both grossly and histologically.[9] While CEH is generally a diffuse reaction involving the entire endometrium, PEH is a characterized by focal or multifocal masses mimicking placentation sites. Histologically, the masses are characterized by the 3 distinct zones mimicking the normal maternal placenta.[2] The deepest, outermost zone, also called the stratum spongiosum, is composed of dilated glandular structures. That zone is separated from the highly folded luminal epithelium by a dense connective tissue band. The luminal surface consists of pseudostratified epithelium with scattered necrotic syncytia formation; fetal remnants and membranes are not identified.[9]

McKentee described regression of similar lesions in cases of psuedocyesis,[3] presumably as a result of falling progesterone levels. In a study of infertility in bitches, PEH was identified by uterine biopsy at various stages of the estrous cycle, but hormone levels were not recorded.[4] In the case of the young bitch in this report, presence of multiple corpora lutea in the ovaries at the time of ovariohysterectomy suggests that the lesions formed or at least were maintained in the presence of high circulating progesterone; whether the lesions would have regressed as CLs regressed is unknown. The fact that the dog had documented infertility, however, suggests the PEH may have been interfering with fertility in this case.

JPC Diagnosis: Uterus, endometrium: Hyperplasia, pseudoplacentational, focally extensive.

Conference Comment: The contributor provides an excellent review of pseudo-placentational endometrial hyperplasia (PEH). Some conference participants identified a number of multinucleated syncytia within the luminal epithelium, suggesting the possibility of syncytiotrophoblast formation and true placentation in this case.

Dr. Robert Foster of the University of Guelph was consulted on this possible interpretation. Dr. Foster confirmed that the presence of syncytia in the outermost layer is an expected finding in PEH, and the lack of multinucleated cells within deeper layers argues against the possibility that they are true syncytiotrophoblasts.

In this case, the corpora lutea are considered essentially normal, the cellular atypia seen within the largest nodule is considered to be within acceptable morphologic limits. In the area of the endometrium adjacent to PEH, the progestational effects (vacuolation of endometrial cells,

tortuosity of glands, and presence of secretory material within deep glands) of these corpora lutea is seen.

Contributing Institution: Department of Veterinary Microbiology and Pathology
College of Veterinary Medicine
Washington State University
Pullman, WA 99164-7040
www.vetmed.wsu.edu

References:

1. DeBosschere H, Ducatelle R, Verrneirsch H, et al. Cystic endometrial hyperplasia-pyometra complex in the bitch: should the two entities be disconnected? *Theriogenol*. 2001;55:1509-1519.
2. Koguchi A, Nomura K, Fujiwara T, et al. Maternal placenta-like endometrial hyperplasia in a Beagle dog (canine deciduoma). *Exp Anim*. 1995;44:251-253.
3. McKentee K. The uterus: atrophic, metaplastic and proliferative lesions. In: *Reproductive Pathology of Domestic Animals*. San Diego, CA: Academic Press; 199:171-175.
4. Mir F, Fontaine E, Albaric O, et al. Findings in uterine biopsies obtained by laparotomy from bitches with unexplained infertility or pregnancy loss: an observational study. *Theriogenol*. 2013;79:312-322.
5. Nomura K. Induction of canine deciduoma in some reproductive stages with different conditions of the corpora lutea. *J Vet Med Sci*. 1997;59:185-190.
6. Nomura K, Makino T. Effect of ovariectomy in the early first half of the diestrus on induction or maintenance of canine deciduoma. *J Vet Med Sci*. 1997;59:227-230.
7. Sato Y. Psuedo-placentational endometrial hyperplasia in a dog. *J Vet Diag Invest*. 2011;23:1071-1074.
8. Schlafer DH, Miller RB. Pathology of the genital system of the nongravid female. In: Maxie MG, ed. *Jubb, Kennedy and Palmer's Pathology of Domestic Animals*. 5th ed. Vol. 3. Philadelphia, PA: Saunders Elsiever; 2007:462-463.
9. Schlafer DH, Gifford AT. Cystic endometrial hyperplasia, psuedoplacentational endometrial hyperplasia and other cystic conditions of the canine and feline uterus. *Theriogenol*. 2008;70:349-358.

CASE III: H11-0101-A (JPC 4006298).

Signalment: Dog 1: 7-year-old female spayed Cavalier King Charles Spaniel (*Canis familiaris*). Dog 2: 12-year-old female spayed miniature Poodle (*Canis familiaris*).

History: Four dogs presented to our referral hospital over a seven-week period with clinical signs of severe liver disease (including one or more of: inappetence, lethargy, vomiting, diarrhoea, polyuria and polydipsia). All four dogs had a common history of consuming a cooked commercial camel meat and sweet potato diet as a novel protein for management of suspected allergic skin disease. Two of these dogs subsequently deteriorated despite supportive therapy and were euthanized. Dog 1 was submitted for a full necropsy examination whereas surgical biopsy specimens of liver and pancreas were collected from dog 2 two days prior to euthanasia.

Gross Pathology: Post mortem examination of dog one revealed generalized jaundice and widespread petechial and ecchymotic haemorrhages on mucosal and serosal surfaces. The liver was small with a rough, granular to nodular surface and the pancreas was also irregularly thickened and firm. A necropsy examination was not performed on dog 2, and only limited information on the gross appearance of the liver (or pancreas) was provided by the surgeon, who simply noted that the liver demonstrated "severe liver changes with minimal normal hepatic tissue identified".

Laboratory Results:

Dog 1

	Day 1	Day 13	Day 18	Day 19	Reference range
Lipase	1500	-	-	2500	13-200 U/L
Amylase	2200	-	-	3500	65-1140 U/L
ALT	1100	1500	-	1455	21-142 U/L
ALP	550	1000	-	900	20-184 U/L
AST	N	290	-	-	10-60 U/L
GGT	13	30	-	-	
Bilirubin	N	36	-	181	0-8 umol/L
Cholesterol	9.6	10	-	10	3.3-6.9 mmol/L
Urea	N	-	-	1.9	3.6-10.0 mmol/L
PT	-	-	19.4	-	5.1-7.9 secs
APTT	-	-	24.8	-	8.6-12.9 secs

Serum biochemistry:

*N = within the reference range

(-) = not performed or result not provided

Dog 2:

	Day 1	Day 5	Day 6	Day 7	Day 8	Reference range
ALT	3120	3200	-	1960	1460	21-142 U/L
ALP	136	633	-	561	531	20-184 U/L
AST	926	956	-	687	577	10-60 U/L
Bilirubin	8	134	-	144	123	0-8 umol/L
Cholesterol	5.3	6.0	-	4.6	4.1	3.3-6.9 mmol/L
Urea	4.1	4.5	-	2.3	3.7	3.6-10.0 mmol/L
PT	-	-	18.5	-	-	5.1-7.9 secs

*N = within the reference range

(-) = not performed or result not provided

Toxicology: Indospicine was subsequently detected in the serum or plasma of both dogs as well as in samples of liver and skeletal muscle of dog 1. Detection of indospicine in a sample of the cooked camel meat and sweet potato diet fed to one of the dogs, as well as in samples of camel meat provided by the manufacturer, confirmed the source of the toxin. Aflatoxins B1, B2, G1 & G2 were not detected in either of these samples.

Indospicine was also detected in the serum of the other two dogs that developed clinical signs of hepatic disease, although these dogs subsequently recovered with supportive therapy and have remained well for the duration of follow up. In addition, indospicine was similarly detected in the serum of 15 other dogs known to have been consuming the diet. 3/15 of these dogs had increased serum ALT activity, although with the exception of one dog, none developed clinical signs of liver disease. One dog however subsequently went on to develop clinical signs of severe liver disease, despite withdrawal of the contaminated diet 5 months prior and was euthanized.

Histopathologic Description: A section of liver from each dog is present on the submitted slides. These two sections of liver have been included in order to demonstrate the range of hepatic changes that may be observed as a result of the hepatotoxic effects of indospicine.

Dog 1, liver (larger section of tissue): This section demonstrates extensive disruption of the hepatic

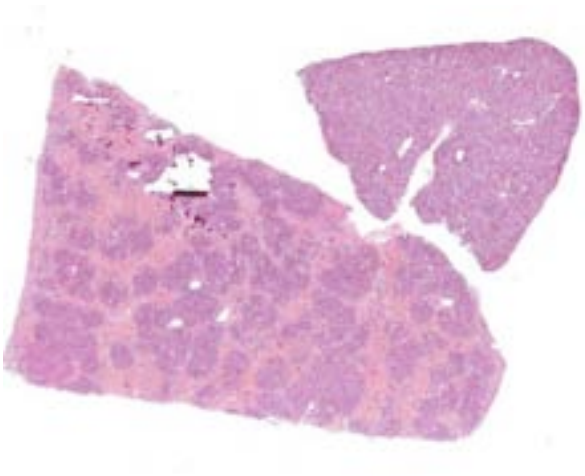

3-1. Liver, dog: There are sections from two different dogs on this slide, suggesting different dosage. A larger section with centrilobular to massive necrosis suggests a higher, more acute dose than the smaller section, in which bridging fibrosis, but little necrosis, suggests a more chronic low-grade exposure to the toxin. (HE 0.63X)

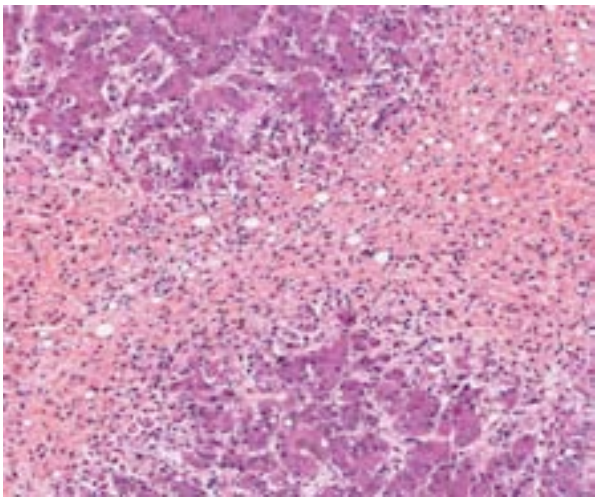

3-2. Liver, dog: Centrilobular hepatocytes are diffusely necrotic, and bands of necrotic hepatocytes bridge between central veins. In some lobules, necrosis extends to midzonal and even portal hepatocytes (massive necrosis). (HE 100X)

architecture by diffuse, centrilobular to massive zonal hepatocyte loss and haemorrhage. Numerous macrophages containing erythrocytes or a fine, golden to coarse dark brown granular cytoplasmic pigment are scattered extensively throughout the areas of hepatocyte loss and haemorrhage, and to a lesser extent the intact hepatic parenchyma. The majority of the cytoplasmic granules stain blue with a Perl's Prussian Blue (haemosiderin). Infiltrating portal triads and scattered throughout the areas of haemorrhage, are frequent clusters of lymphocytes and plasma cells accompanied by fewer neutrophils and macrophages. Within the residual clusters of hepatocytes there are often plugs of bile within distended canaliculi. Bile ducts are often distended by variably cellular casts. The remaining hepatocytes demonstrate moderate anisocytosis, often associated with cytoplasmic macro- and microvesicular vacuolation. There are also scattered individually necrotic hepatocytes. Subcapsular and portal lymphatics are often ectatic. Histochemical staining with Martius Scarlett Blue highlighted the presence of a mild increase in fibrous connective tissue surrounding the portal triads. A thin strand of fibrous connective tissue also dissects between individual hepatocytes in the centrilobular regions.

Dog 2, liver (smaller section of tissue): The architecture of the liver is disrupted by mild to moderate, diffuse bridging fibrosis which connects central veins. Associated with the fibrosis is a moderate, multifocal, mixed infiltrate of haemosiderophages (confirmed with a Perls stain for iron), lymphocytes and plasma cells and frequent dilated lymphatics. Portal triads are also expanded by mild to moderate fibrosis, mild biliary hyperplasia and an infiltrate of modest numbers of haemosiderophages, lymphocytes and occasional neutrophils. Associated with the centrilobular and portal fibrosis, there is moderate variation in hepatic lobule size, which is attributable to a combination of hepatocyte degeneration, atrophy and loss particularly surrounding the central veins. Remaining hepatocytes also demonstrate moderate to marked anisocytosis associated with cytoplasmic macrovesicular and microvesicular vacuolation. Occasional hepatocytes are binucleate and some have prominent, multiple nucleoli. There is also occasional single cell necrosis of hepatocytes. The undulating appearance of the capsular surface is attributable to the predominately centrilobular hepatocyte loss, lobular collapse and fibrosis.

Pancreas (sections not included): Examination of the pancreas of both dogs reveals multifocal to coalescing foci of pancreatic fibrosis with degeneration, atrophy and loss of adjacent exocrine pancreatic acini. These changes are accompanied by variably extensive foci of peripancreatic fat necrosis and a neutrophilic infiltrate; minimal and focal in dog 1 but severe and reasonably extensive in dog 2.

Contributor's Morphologic Diagnosis:
Dog 1 (larger tissue section):

1. Liver:
    a. Severe, diffuse, subacute to chronic, centrilobular to massive hepatic necrosis and loss, with marked haemorrhage and haemosiderosis.
    b. Mild to moderate, multifocal, chronic, mixed hepatitis.
    c. Mild, periportal to dissecting, subacute, hepatic fibrosis.
    d. Mild, multifocal, subacute to chronic vacuolar hepatopathy.

Dog 2: (smaller tissue section)

1. Liver:
    a. Mild to moderate, chronic, centrilobular to bridging fibrosis, haemorrhage and haemosiderosis.
    b. Moderate, diffuse subacute to chronic vacuolar hepatopathy.
    c. Mild to moderate, subacute to chronic, multifocal lymphoplasmacytic hepatitis.

Contributor's Comment: Indospicine (6-amidino-2-amino-hexanoic acid) is a toxic amino acid of plant origin that is found in several species of the plant genus *Indigofera*, many of which are found extensively across the sub-tropical and arid regions of Australia.[1,7] The toxin was first isolated from the seed and leaf of *I. spicata*,[9] after this plant species was shown to be hepatotoxic in a range of species including chicks, sheep, cattle, rabbits and mice.[4,10,11] Hepatotoxicosis was subsequently induced in rats and mice following oral or parenteral administration of purified indospicine.[5,8] In addition to being a hepatotoxin, indospicine has also been demonstrated to be teratogenic in cattle, rats, mice and rabbits.[14] Extremely similar in structure to the essential amino acid arginine, indospicine is not metabolized by arginine and is unusual in that it is not incorporated into protein. Rather, it accumulates in body tissues as the free amino acid.[15] Indospicine has been shown to competitively block the incorporation of arginine and subsequently other amino acids into rat liver protein in vitro.[5,13] Whilst the exact mechanism of toxicity remains unknown, it is thought that these antimetabolite properties may contribute to the hepatotoxicity of indospicine.

Mammals appear to have a poor ability to metabolize or excrete indospicine, and experimentally levels have been shown to persist in the tissues (including skeletal muscle) of horses, goats, cattle and rabbits for several months following cessation of *Indigofera* spp. intake.[6] Such indospicine residues have the potential to cause secondary toxicosis in carnivores consuming contaminated meat and severe, sometimes fatal hepatotoxicosis has been reported in dogs consuming contaminated horse and camel meat. There is, however, marked species variability in susceptibility to indospicine hepatotoxicosis with dogs being particularly sensitive.[6,7] Cattle and sheep are unaffected under normal grazing conditions; however, liver damage

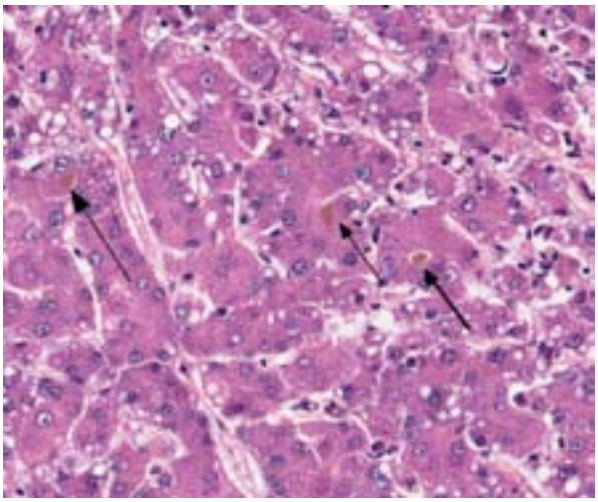

3-3. Liver, dog: Bile canaliculi (arrows) are markedly dilated and filled with bile (cholestasis). Throughout the section, bile ducts are dilated and filled with mucin. (HE 288X)

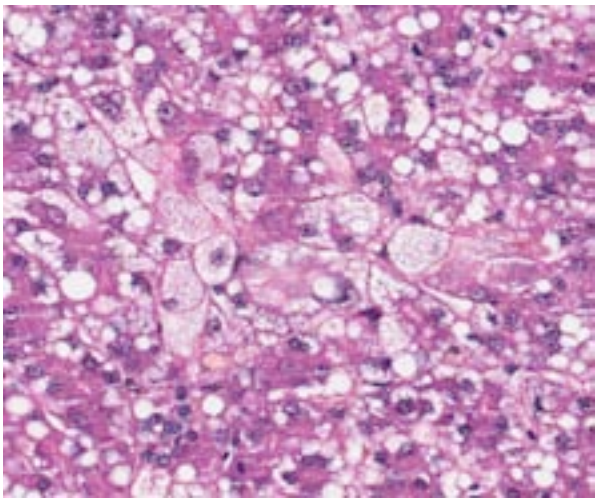

3-4. Liver, dog: In the second ("more chronic") section, hepatocytes are swollen with accumulation of both large (macrovesicular) and small discrete (microvesicular) fat droplets within the cytoplasm. (HE 320X)

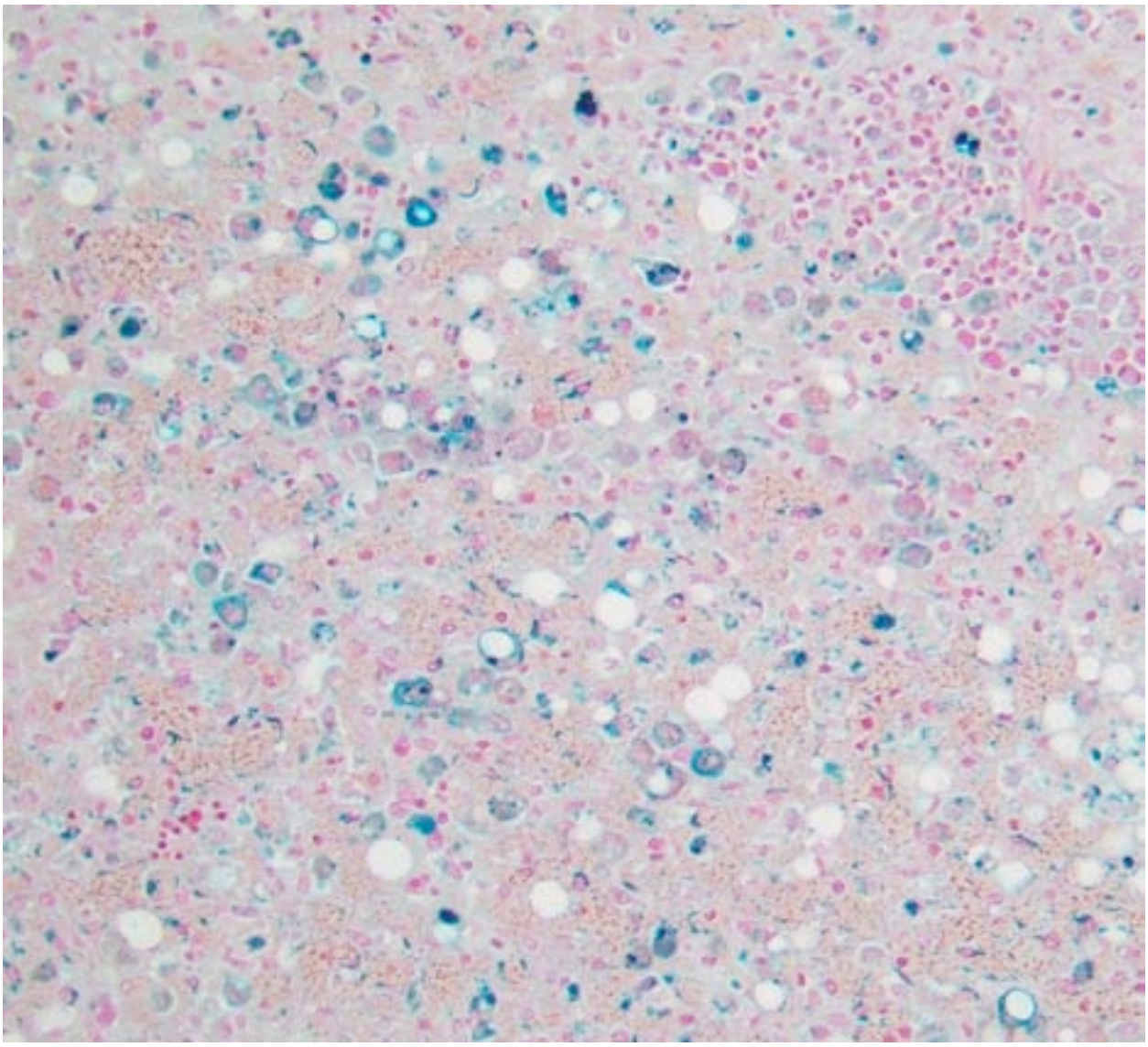

3-5. Liver, dog: Scattered Kupffer cells contain intracytoplasmic hemosiderin granules. (Perl's Prussian Blue, 20X) (Photo courtesy of: Murdoch University, Department of Anatomic Pathology, School of Veterinary and Biomedical Sciences, Faculty of Health Sciences. South Street, Murdoch, Perth, Western Australia, 6150, AUSTRALIA. http://www.vetbiomed.murdoch.edu.au/)

has been experimentally induced under conditions of high *Indigofera* spp. intake.[6] Horses appear resistant to the hepatotoxic effects of indospicine; however, horses grazing *I. linnaei* (Birdsville indigo) may suffer from a neurological disturbance known as Birdsville horse disease,[3] presumably due to co-occuring esters of 3-nitropropanoic acid.[17] There are no reports of indospicine or *Indigofera*-associated toxicosis in camels, although the remote location of these animals in the arid regions of Australia generally limits close observation.[6]

The reason behind the species variability and apparently unique susceptibility of dogs to the hepatotoxic effects of indospicine is similarly unknown. Indospicine is also not a predictable hepatotoxin in dogs, although the characteristic lesions of hepatocellular vacuolation, necrosis, haemorrhage and mononuclear inflammatory cell infiltration primarily seem to target the centrilobular hepatocytes. Note that the cause of the concurrent pancreatic inflammation and fibrosis seen in both of these dogs is unknown,[7] as it has not been previously reported in cases of indospicine toxicosis in animals, despite the pancreas having the highest levels of indospicine in a variety of tissues tested.[12,17] The trends seen in naturally occurring cases,[6,7] as well the results of experimental trials in dogs[12,17] show a high

degree of variability in the susceptibility of individual dogs to indospicine hepatotoxicosis, with liver failure only occurring in a small proportion of dogs exposed.[6,7,12,17] These findings have led the suggestion that an idiosyncratic response to the toxin may occur, perhaps in addition to a more consistent toxic effect. The nature of the inflammatory response has also led to postulation that an immune-mediated mechanism may be involved.[16] Whatever the exact mechanism of liver injury, the available evidence suggests that indospicine is not a rapidly necrotizing hepatotoxin. Based on the results of previous experimental studies, prolonged exposure (4 days) is seemingly required for development of clinical disease, with no dogs in short term trials (dosed over four consecutive days) developing signs of liver disease.[2,7,17]

JPC Diagnosis: 1. Liver: Necrosis, centrilobular to massive, bridging, severe, with marked cholestasis and macro and microvesicular hepatocellular lipidosis.
2. Liver, hepatocytes: Macro and micronodular lipidosis with multifocal hepatocyte necrosis, and loss, mild bridging fibrosis and mild cholestasis.

Conference Comment: Conference participants conducted a comprehensive assessment of the clinical-pathologic findings for this case. Alanine aminotransferase (ALT), aspartate aminotransferase (AST), alkaline phosphatase (ALP) and bilirubin were markedly elevated in both dogs, while urea and cholesterol were decreased. Additionally, prothombin time (PT) and activated partial thromboplastin time (APTT) were significantly prolonged. These are expected findings in cases of massive hepatic necrosis with secondary cholestasis.[2]

Although the most striking microscopic lesions in this case are the massive hepatocellular necrosis and loss along with cholestasis and lipidosis, there is also mild bridging fibrosis in dog 2, which was demonstrated with a Masson's stain. This subtle suggestion of chronicity supports the contributor's supposition that indospicine toxicity is likely not a peracute/acute hepatotoxin. Given that indisopicine containing species such as *Indigofera* are not generally found in North America, most conference participants formulated a list of alternative hepatoxins that could potentially induce similar lesions dogs, including aflatoxicosis, pyrrolizidine alkaloid toxicosis, sago palm toxicity, blue-green algae toxicity, copper toxicosis, iron overload and amanita toxicity.

Contributing Institution: Murdoch University, Department of Anatomic Pathology
School of Veterinary and Biomedical Sciences, Faculty of Health Sciences
South Street, Murdoch, Perth, Western Australia, 6150
http://www.vetbiomed.murdoch.edu.au/

References:
1. Aylward JH, Court RD, Haydock KP, Strickland RW, Hegarty MP. *Indigofera* species with agronomic potential in the tropics. Rat toxicity studies. *Aust J Agric Res*. 1987;38:177-186.
2. Bain PJ. Liver. In: Latimer KS, ed. *Duncan and Prasse's Veterinary Laboratory Medicine Clinical Pathology*. 5th ed. Ames, IA: John Wiley & Sons; 2011:134-136, 211-225, 274-277, 416.
3. Bell AT, Everist SL. *Indiogofera enneaphylla*: a plant toxic to horses (Birdsville disease). *Aust Vet J.* 1951;27:185-188.
4. Britten EJ, Palofox AL, Frodyma MM, Lynd FT. Level of 3-nitropropanoic acid in relation to toxicity of *Indigofera spicata* in chicks. *Crop Sci.* 1963;3:415-416.
5. Christie GS, Wilson M, Hegarty MP. Effects on the liver in the rat of ingestion of *Indigofera spicata*, a legume containing an inhibitor of arginine metabolism. *J Pathol.* 1975;117:195-205.
6. FitzGerald LM, Fletcher MT, Paul AEH, Mansfield CS, O'Hara A. Hepatotoxicosis in dogs consuming a diet contaminated with indospicine. *Aust Vet J.* 2011;89: 95-100.
7. Hegarty MP, Kelly WR, McEwan D, Williams OJ, Cameron R. Hepatotoxicity to dogs of horse meat contaminated with indospicine. *Aust Vet J.* 1988;65:337-340.
8. Hegarty MP, Pound AW. Indospicine, a hepatotoxic amino acid from *Indigofera spicata*: isolation, structure, and biological studies. *Aust J Biol Sci.* 1970;23:831-842.
9. Hegarty MP, Pound AW. Indospicine, a new hepatotoxic amino acid from *Indigofera spicata*. *Nature* . 1968;217:354-355.
10. Hutton EM, Windrum GM, Kratzing CC. Studies on the toxicity of *Indigofera endecaphylla*: II. Toxicity for mice. *J Nutr.* 1958;65:429-440.
11. Hutton EM, Windrum GM, Kratzing CC. Studies on the toxicity of *Indigofera*

endecaphylla: I. Toxicity for rabbits. *J Nutr.* 1958;64:321-337.
12. Kelly WR, Young MP, Hegarty MP, Simpson GD. The hepatotoxicity of indospicine in dogs. In: James LF, Keeler RF, Bailey EM, Cheeke PR, Hegarty MP, eds. *Poisonous Plants*. Ames, Iowa: Iowa State University Press; 1992:126-130.
13. Madsen NP, Hegarty MP. Inhibition of rat liver homogenate arginase activity in vitro by the hepatotoxic amino acid indospicine. *Biochem Pharmacol.* 1970;19:2391-2393.
14. Pearn J. An experimental study of the embryopathic effects of indospicine: with particular reference to the production of cleft palate. MD thesis, University of Queensland, St. Lucia, Brisbane, 1967. Cited in: Young MP: Investigation of the toxicity of horsemeat due to contamination by indospicine. PhD thesis, *School of Veterinary Science*, University of Queensland, Brisbane; 1992:28-30.
15. Pollitt S, Hegarty MP, Pass MA. Analysis of the amino scid indospicine in biological samples by high performance liquid chromatography. *Nat Toxins.* 1999;7:233-240.
16. Stalker MJ, Hayes MA. Liver and biliary system. In: Maxie, MG, ed. *Jubb, Kennedy, and Palmer's Pathology of Domestic Animals*. 5th ed. Vol. 1. Philadelphia, PA: Elsevier; 2007:376-378.
17. Young MP. Investigation of the toxicity of horsemeat due to contamination by indospicine. PhD thesis, *School of Veterinary Science*, University of Queensland, Brisbane, 1992.

CASE IV: NIAH 2013 2 (JPC 4035422).

Signalment: Four-week-old domestic duck, a crossbreed of wild mallard and domesticated duck *(Anas platyrhynchos)*.

History: This domestic duck was inoculated intravenously with H5N1 highly pathogenic avian influenza (HPAI) virus. The bird showed severe neurological symptoms from day 3 postinoculation (PI) and died on day 5 PI.

Gross Pathology: At necropsy, white multiple foci were found in the pancreas. Skin and feathers appeared normal.

Laboratory Results: By virus isolation using eggs, influenza viruses were re-isolated from organs including calami of plucked feathers.

Histopathologic Description: There were many developing feathers in the dermis of the skin. Focal to diffuse epidermal necrosis was observed in some feathers. Lesions were accompanied by mild to severe heterophilic infiltration. The affected feather epidermis rarely had the vesicular formation. Phagocytic cells containing melanin pigments were present in some lesions. The feather pulp of some feathers exhibited heterophilic inflammation, blood congestion, hemorrhage and edematous change. Depending on the section, there were crust formation on the skin epidermis and small aggregates of lymphocytes around the small vessels of the dermis.

Immunohistochemical analysis to detect type A influenza virus revealed that influenza virus matrix antigens were present in the feather epidermal cells with/without necrotic changes. Few fibroblasts in the feather pulp were also positive for viral antigens. No relation was found between the virus antigen distribution and foci of lymphocytes in the dermis. Other major pathological findings in this case were non-suppurative encephalomyelitis, myocarditis, pancreatic necrosis, myositis, keratitis and focal epithelial necrosis of the beak, tongue and legs.

Contributor's Morphologic Diagnosis: Feathered skin: Epidermal necrosis of feathers with heterophilic infiltration.

Contributor's Comment: Since 1997, an epidemic of Asian lineage H5N1 subtype HPAI virus has spread from Asia to the Eurasian continent, causing fatal infections in poultry, wild birds, mammals, and humans.[1] Interestingly, this virus can cause clinical symptoms and pathological lesions to waterfowl which have been considered natural reservoirs of avian influenza virus in nature.[6] However, in contrast to chickens which usually result in fatal outcome after infection, ducks can exhibit asymptomatic clinical course and shed the virus into the environment.[2] Asymptomatically infected domestic ducks contributed to the viral spread in Southeast Asia.[2]

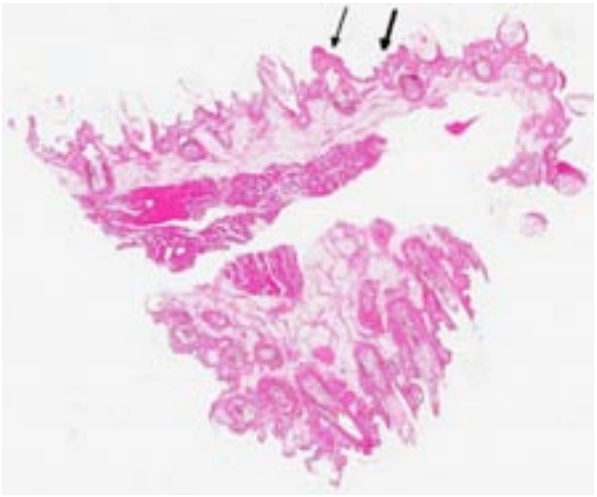

4-1. Feathered skin, duck: The epidermis has a serocellular crust and intracorneal pustule (arrows). Multifocal feather follicles are similarly affected by necrotizing folliculitis. (HE 0.63X)

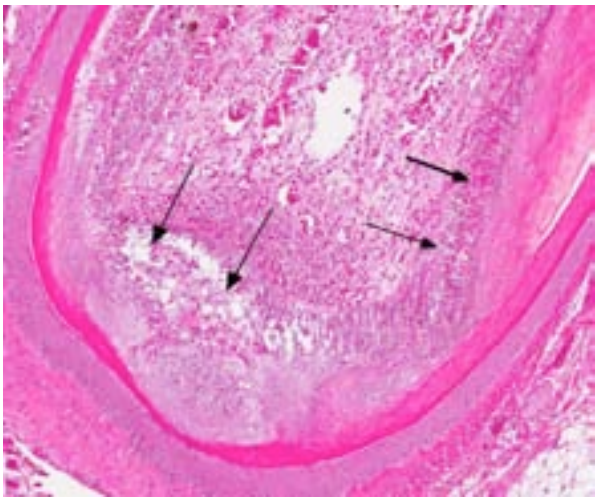

4-2. Feathered skin, duck: There is lytic necrosis of the epithelium of the outer root sheath with vesicle formation. The outer root sheath and pulp are infiltrated by large numbers of heterophils. (HE 40X)

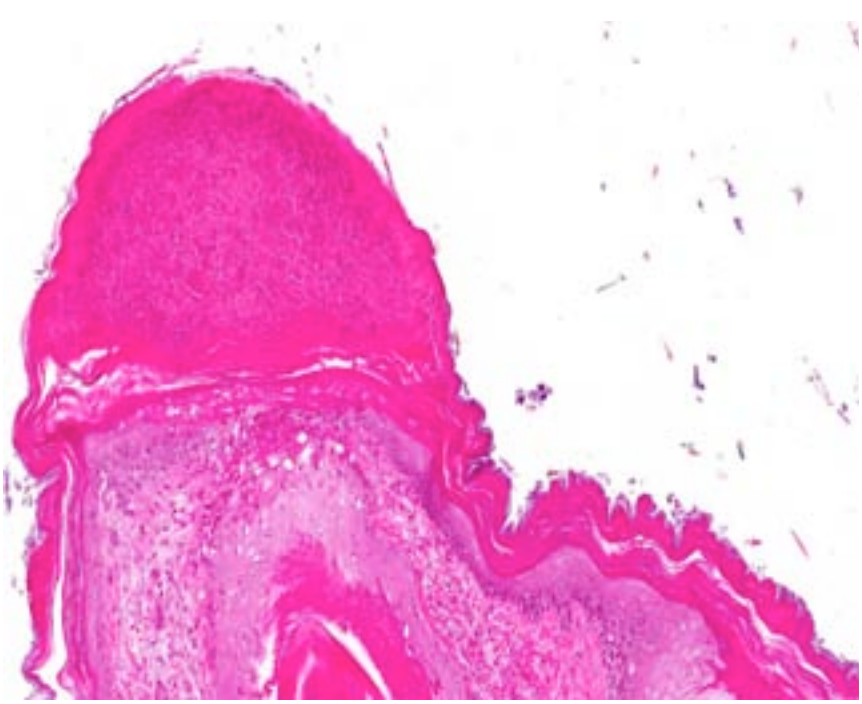

4-3. Feathered skin, duck: There are multiple heterophilic pustules within the epidermis as well as heterophilic infiltration of the underlying dermis. (HE 140X)

Histopathological findings in waterfowl infected with Asian H5N1 HPAI virus are frequently found in the central nervous system, heart and pancreas.[5] In addition, virus replication in the feather epidermis is one of the characteristic findings in waterfowl infected with H5N1 HPAI virus.[7] This microscopic feather lesion was reported in domestic ducks, geese and wild swans.[3,7,8] Even asymptomatic ducks had the feather lesions in the experimental infection.[7] Spherical virions were observed in the feather epidermis by electron microscopic examination.[7] These findings raise the possibility that H5N1 HPAI viruses may be released from feathers of infected waterfowl to the environment and that feathers could become potential sources of infection along with their feces and respiratory secretions.

JPC Diagnosis: Skin, feather follicle: Folliculitis, necrotizing and heterophilic, multifocal, moderate, with heterophilic pustular dermatitis and pulpitis.

Conference Comment: Highly pathogenic avian influenza virus, a single stranded RNA virus, is a member of the family *Orthomyxoviridae*, which contains three genera: *Influenzavirus A*, *B* and *C*. Influenzaviruses that are pathologic to domestic animals, including avian influenza, make up the *Influenzavirus A* genus, although some of these can cross over to humans as well.[8] Influenza B viruses primarily affect humans, while influenza C viruses, which lack neuraminidase, infect humans. Swine are susceptible to both influenza A and influenza C viruses.[4] Influenza viruses are sensitive to heat, acid and lipid solvents; thus they are quite labile within the environment.[4] Currently influenza A viruses are classified into 16 hemagglutinin (H) and 9 neuraminidase (N) types, and further categorized as high or low pathogenicity.[1] The virus strain naming convention provides a great deal of information and consists of the virus type (A, B, C), geographic origin, strain number, year of isolation and hemagglutinin/ neuraminidase subtypes.[1,4] For example "A/ chicken/Scotland/1959 (H5N1)" was the first reported high-pathogenicity H5 avian influenza virus, in Scotland.[4]

The influenza A subtypes most frequently implicated in animal infections include: H5 and H7 in poultry, which can be highly pathogenic; H7N7 and H3N8 (equine influenza viruses 1 and 2), which cause respiratory disease in horses; enzootic H1N1, H1N2 and H3N2, which affect swine; H7N7 and H4N5 in seals; sporadic H10N4 in mink; H1N1, H2N2, H3N2 (historically endemic) and H5N1, H7N3, H7N7 and H9N2 (more recent) in humans; and H3N8 and H3N2 which cause respiratory disease in dogs.[4]

Highly pathogenic avian influenza (HPAI) is confined to subtypes H5 and H7, and is generally introduced into poultry flocks via wild birds (especially ducks).[4] Low-pathogenicity avian influenza (LPAI), replicates in the gastrointestinal tracts of waterfowl, who shed high concentrations of the virus in feces and have been implicated as an important viral reservoir.[3] LPAI infections in domestic birds are typically subclinical (with occasional mild respiratory signs or decreased egg production), however ,mutation to highly

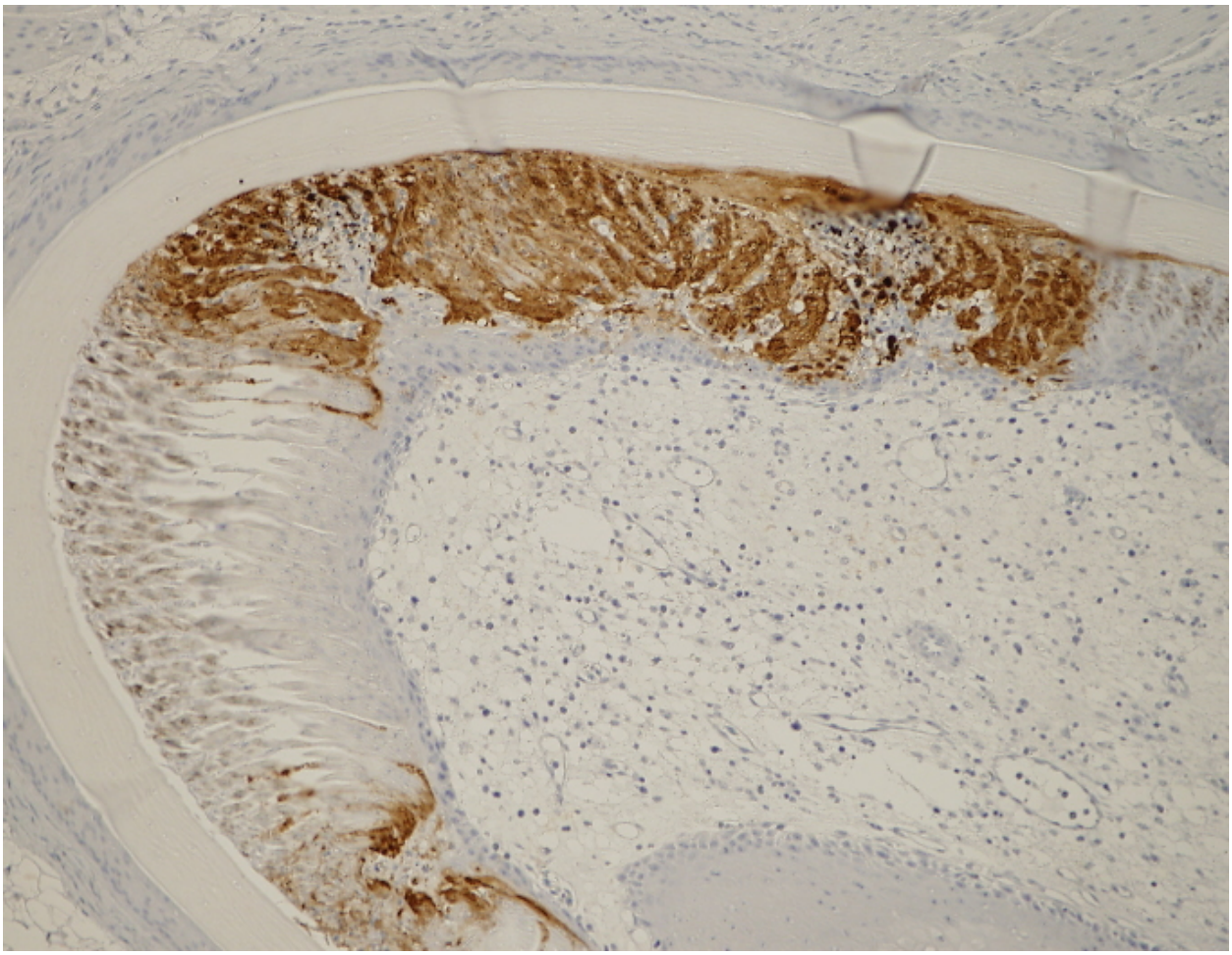

4-4. Feather follicle, duck: Feather epithelium shows immunopositive against Type A influenza virus matrix antigens. (IHC HPAI, 80X) (Photo courtesy of: National Institute of Animal Health, Japan, http://www.naro.affrc.go.jp/org/niah)

pathogenic avian influenza can occur, with devastating economic affects.[5] Resulting HPAI viruses can cause severe systemic disease in chickens, with necrosis and inflammation in the skin, viscera and brain. In general, the emergence of new and varied influenza viruses depends on genetic drift (point mutations) as well as genetic shift (genomic segment reassortment).[4] An important virulence determinant in avian influenza is the amino acid sequence at the hemagglutinin protein cleavage site. Low pathogenicity strains of virus have a single, basic amino acid (arginine) at the cleavage site; insertions, deletions or point mutations resulting in changes to this cleavage site can significantly alter pathogenicity.[4]

In poultry, following binding of hemagglutinin to host cell α2,3-glactose receptors and the subsequent induction of receptor-mediated endocytosis, avian influenza virus replicates in (and is shed from) both the respiratory and gastrointestinal tracts. Cell damage occurs secondary to direct virus replication, inflammatory mediators and/or vascular thrombosis and ischemia.[5] Depending on the host, HPAI can be epitheliotropic, endotheliotropic, neurotropic or pantropic.[5] The presence of gross findings depends upon the strain and virulence of the virus, and may include ruffled feathers; edema of the comb, wattles, periorbital areas and legs, subcutaneous hemorrhage; multifocal visceral and mucosal hemorrhage and necrosis; pulmonary edema and hemorrhage; pancreatic necrosis; and intestinal lymphoid necrosis.[5] Microscopic lesions are more frequent than gross lesions and consist primarily of necrosis and inflammation within multiple organs, especially the skin/feather follicles, pancreas, brain, heart, lungs, adrenal glands and primary/secondary lymphoid organs.[5] Central nervous system involvement can occur

after direct viral spread from the nasal cavity to the brain via olfactory nerves, hematogenous spread, or infection of ependymal cells with subsequent ventriculitis/periventriculitis.[5] Death can be peracute, or it may follow multi-organ failure; extremely virulent strains of avian HPAI virus can cause up to 75% or even 100% mortality.[4,5] Similar morbidity and mortality has also been reported in turkeys, quail, guineafowl and pheasants.[5]

Early research demonstrated that HPAI viruses rarely produced fulminant disease in wild birds; however, since 2002 a new Eurasian-African lineage of H5N1 HPAI virus has been reported to cause clinical disease and death in ducks under both natural and experimental conditions.[3,5,6] As noted by the contributor, lesions in waterfowl infected with HPAI virus frequently occur in the brain, heart and pancreas, with characteristic virus replication in the feather epidermis,[7,8] as demonstrated in this case.

Contributing Institution: National Institute of Animal Health, Japan
http://www.naro.affrc.go.jp/org/niah/

References:

1. Alexander DJ, Brown IH. History of highly pathogenic avian influenza. *Rev Sci Tech*. 2009;28:19-38.
2. Gilbert M, Chaitaweesub P, Parakamawongsa T, Premashthira S, Tiensin T, Kalpravidh W, Wagner H, et al. Free-grazing ducks and highly pathogenic avian influenza, Thailand. *Emerg Infect Dis*. 2006;12:227-234.
3. Löndt BZ, Nunez A, Banks J, Nili H, Johnson LK, Alexander DJ. Pathogenesis of highly pathogenic avian influenza A/turkey/Turkey/1/2005 H5N1 in Pekin ducks (*Anas platyrhynchos*) infected experimentally. *Avian Pathol*. 2008;37:619-627.
4. MacLachlan NJ, Dubovi EJ, eds. *Fenner's Veterinary Virology*. 4th ed. London, UK: Elsevier; 2011:353-368.
5. Pantin-Jackwood MJ, Swayne DE. Pathogenesis and pathobiology of avian influenza virus infection in birds. *Rev Sci Tech*. 2009;28:113-136.
6. Sturm-Ramirez KM, Ellis T, Bousfield B, Bissett L, Dyrting K, Rehg JE, Poon L, et al. Reemerging H5N1 influenza viruses in Hong Kong in 2002 are highly pathogenic to ducks. *J Virol*. 2004;78:4892-4901.
7. Yamamoto Y, Nakamura K, Okamatsu M, Yamada M, Mase M. Avian influenza virus (H5N1) replication in feathers of domestic waterfowl. *Emerg Infect Dis*. 2008;14:149-151.
8. Yamamoto Y, Nakamura K, Yamada M, Ito T. Zoonotic risk for influenza A (H5N1) infection in wild swan feathers. *J Vet Med Sci*. 2009;71:1549-1551.

Joint Pathology Center
Veterinary Pathology Services

WEDNESDAY SLIDE CONFERENCE 2013-2014

Conference 8

06 November 2013

CASE I: MLP12093 (JPC 4035110).

Signalment: 14-week-old male Sprague Dawley rat (*Rattus norvegicus*).

History: This rat was a clinically normal animal in an experimental drug study.

Gross Pathology: Both kidneys were moderately enlarged and when sectioned contained multiple, variably-sized (up to 3.0 mm diameter), fluid-filled spaces involving most of the renal parenchyma. The liver was slightly enlarged and had an irregular surface (Figure 1), which corresponded with spaces, similar to those seen in the kidneys, when sectioned. There were no gross abnormalities in other organs or tissues.

Laboratory Results: Routine hematology and clinical chemistry analysis were within normal limits.

1-1. Liver, rat: The liver was slightly enlarged and had an irregular surface with numerous capsular depressions. (Photo courtesy of: Pfizer Inc, Worldwide Research and Development, 588 Eastern Point Rd, Groton, CT 06340, www.pfizer.com)

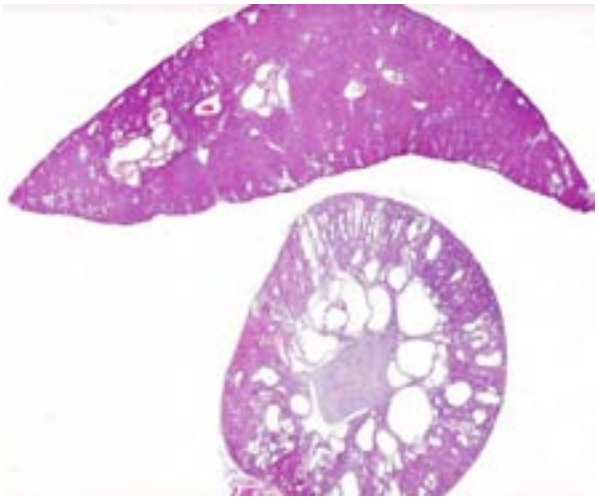

1-2. Kidney and liver, rat: Cysts in the liver and kidney range up to 5mm. In the liver, cysts primarily involve the portal areas; in the kidney, cysts affect more distal segments of the renal tubules. (HE 0.63X)

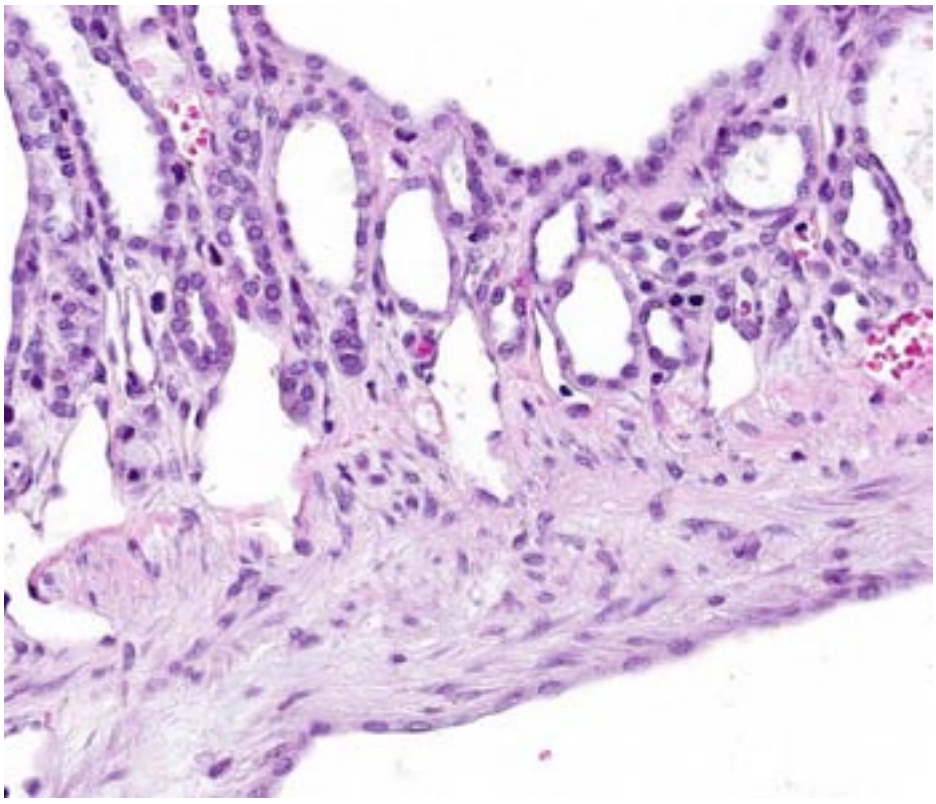

1-3. Kidney, rat: The medulla is expanded by numerous cystic tubules which are bordered by low to moderate amounts of fibrous connective tissue. (HE 140X)

Histopathologic Description: Kidney: Both the cortex and the medulla contained numerous dilated tubules lined by variably squamous to cuboidal to columnar epithelium (cysts), with rare papillary projections. Many of these cysts were distended by pale amphophilic fluid admixed with necrotic cellular debris, scant macrophages, and/or degenerate neutrophils. Between the cysts, some areas of the interstium were expanded by loose connective tissue which often contained a few residual tubules of relatively normal caliber and/or a mixed inflammatory cell infiltrate. Occasional glomeruli had a slightly thickened basement membrane and the urothelium was slightly thickened.

Liver: There are multiple individual to coalescing spaces that were lined by variably attenuated cuboidal epithelial cells (cysts) and surrounded by a band of collagenous tissue. In the adjacent hepatic parenchyma, there was slight atrophy of hepatic cords, proliferation of bile ducts, and minimal mixed inflammatory cell infiltrate in periportal regions.

Contributor's Morphologic Diagnosis: 1. Kidney: Severe multifocal renal tubular dilatation and ectasia with mild interstitial fibrosis.
2. Liver: Marked multifocal biliary duct hyperplasia and ectasia with mild portal fibrosis.

Contributor's Comment: The gross and histopathologic findings in the kidney and liver are consistent with congenital polycystic kidney disease (PKD). PKD is a cystic genetic disorder of the kidneys which has been associated with cystic bile ducts, bile duct proliferation, and/or cystic pancreatic ducts.

In humans, there are two types of PKD: autosomal dominant polycystic kidney disease (ADPKD) and autosomal recessive polycystic kidney disease (ARPKD). In the more common form, ADPKD, the parenchyma is extensively replaced by cysts that originate from all segments of the nephron, collecting tubules, and ducts. In humans with ADPKD, there is an association with cysts in other organs, most often the liver. Other abnormalities that can be coupled with ADPKD include: cardiac valvular anomalies, intracranial aneurysms, and colonic diverticula. In ARPKD, cysts arise from only dilated collecting tubules and ducts and in most cases there is also biliary dysgenesis and hepatic fibrosis.[1,3]

In veterinary medicine, PKD has been recognized in many species including horses, pigs, lambs, calves, dogs, cats, and rodents. In domestic animals, PKD is most often consistent with ARPKD in that the disease manifests as stillbirths or death within the first few weeks of life due to renal failure. Syndromes resembling both recessive and dominant PKD have been described in domestic dogs and cats.[4,7]

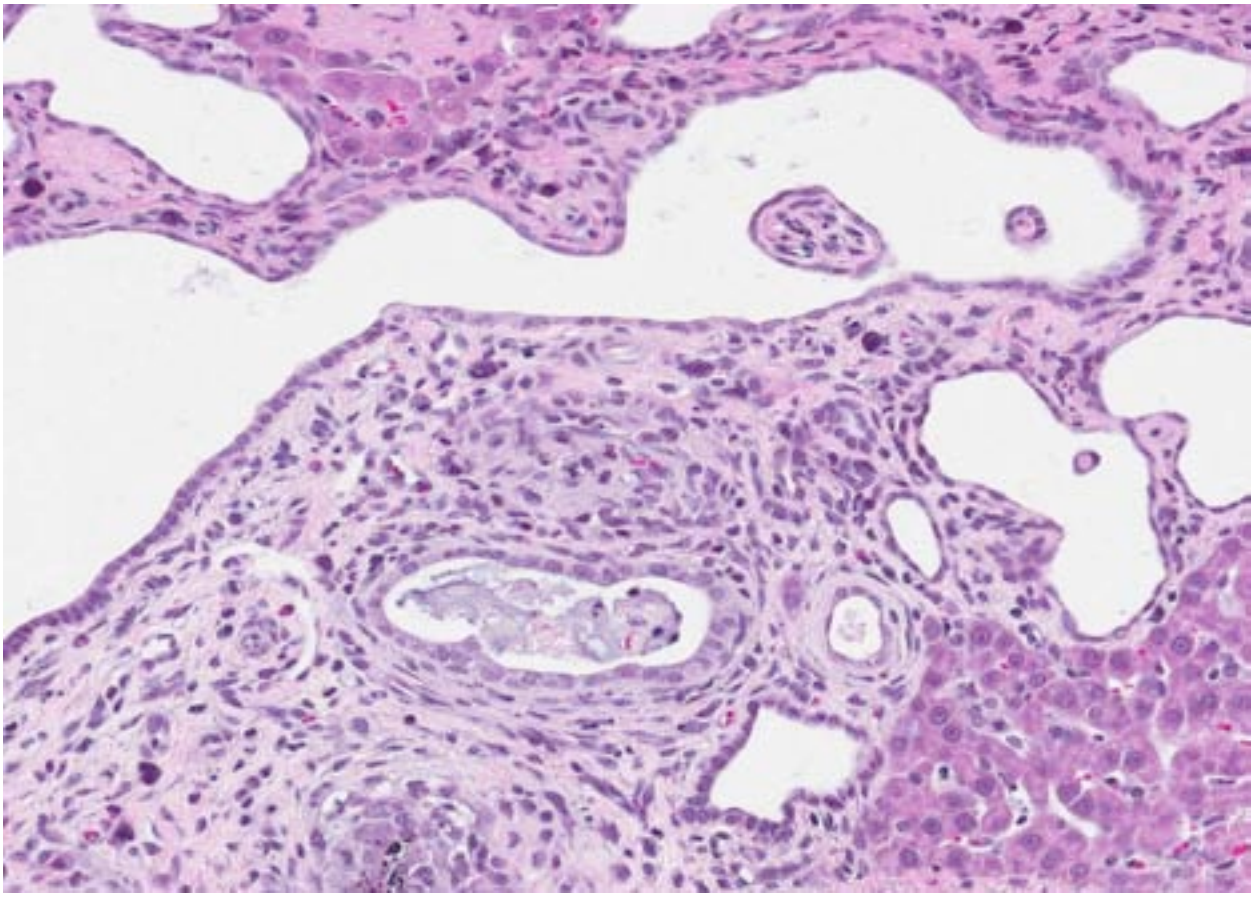

1-4. Liver, rat: Portal areas are fibrotic and expanded by numerous biliary profiles, which are often ectatic. Biliary ducts are also dilated and filled with mucin. (HE 140X)

Caroli's disease is a rare inherited disorder characterized by dilation of the intrahepatic bile ducts which is associated with liver failure and polycystic kidney disease. In the simple form, only bile ducts are affected. The more complex form, also known as Caroli Syndrome, is also linked with portal hypertension and congenital hepatic fibrosis. The differences between the causes of the two forms have not yet been discovered.[2,9]

Recently, a PKD rat, which is a spontaneous mutant derived from a colony of crj:CD rats, was found to also have polycystic lesions in the liver. Because this may represent an animal model of Caroli's disease, it has been well characterized and studied as a model of ADPKD. The mutation arose spontaneously, and initial analysis indicated inheritance as an autosomal recessive trait.[2,8]

The findings presented in this write up describe a case of polycystic kidney disease in a Sprague Dawley rat with involvement of the liver. The involvement of multiple organs suggests that the lesions resulted from a genetic or developmental process rather than an acquired process. Furthermore, the subclinical nature of the disorder and the large size of the kidneys at the time of necropsy suggest that the renal disease was progressive in nature.

JPC Diagnosis: 1. Kidney, tubules: Ectasia, multifocal, marked, with tubular degeneration, loss and mild lymphoplasmacytic interstitial nephritis.
2. Liver, bile ducts and ductules: Ectasia, diffuse, moderate to severe, with biliary ductular reaction.

Conference Comment: Polycystic kidney disease is a label used to refer to several pathologic entities, including incidental renal cysts and hereditary, developmental or acquired renal cysts. Four major mechanisms of cyst formation include: 1) obstruction of nephrons with increased intraluminal pressure and subsequent dilation, 2) changes in ECM and cell-

matrix interactions resulting in a weakened renal tubular basement and the formation of saccular dilations of the tubules, 3) disordered growth of tubular epithelial cells leading to focal hyperplastic lesions and cyst formation, and 4) dedifferentiation of tubular epithelial cells with loss of cell polarity, abnormal tubular arrangement, decreased tubular absorption and dilation of tubules. Often, several of these mechanisms occur concurrently to create renal cysts.[7] Incidental renal cysts, which do not cause renal dysfunction, are fairly common in pigs and calves.[4] Interstitial fibrosis or intratubular obstruction can result in acquired renal cysts (as well as hydronephrosis), which generally arise within the renal cortex.

In contrast, polycystic kidneys contain numerous cysts involving multiple nephrons.[7] In veterinary species, inherited PKD can be autosomal dominant or autosomal recessive; lesions are generally bilateral and cysts may affect any part of the nephron. ADPKD is described in bull terrier dogs and adult Persian cats. It can affect both proximal and distal convoluted tubules and typically results in chronic nephritis and renal failure.[4] ADPKD may be associated with mutations of PKD1 and/or PKD2 genes, which result in defective polycystin 1 and/or polycystin 2, respectively.[4] Polycystin 1 is a component of desmosomes that is important in cell adhesion and signaling; its loss may ultimately result in impairment of normal tubulogenesis.[7] Polycystin 2, on the other hand, functions as a plasma membrane calcium channel.[7] ARPKD, reported in Persian kittens, sheep, lambs, and West Highland white and cairn terrier puppies, is caused by a mutation on the PKHD1 gene encoding fibrocystin, which is a receptor protein.[5] In adult Persian cats and West Highland white terrier puppies with PKD, there are often concurrent hepatic cysts.[4] Congenital PKD, with inheritance that is not fully characterized, occurs in pigs, lambs, calves, kids, puppies, kittens and foals. The most common manifestation of this condition is stillbirth or neonatal/infant death.[5]

PKD has also been reported in Brazilian agoutis (*Dasyprocta leporina)*, springboks (*Antidorcas marsupialis),* an adult raccoon (*Procyon lotor*), rhesus macaques (*Macaca mulatta*), slender lorises (*Loris lydekkerianus*), and a stillborn white-tailed deer (*Odocoileus viriginianus*).[5] Two separate conditions resulting in polycystic kidneys are reported in goldfish. Infection with the myxosporidian protozoan *Mitraspora cyprini* causes a condition known as "kidney bloater disease," characterized by marked renal tubular hyperplasia and ectasia, with sparing of the glomeruli. Conversely, goldfish polycystic kidney disease primarily involves glomeruli. It is distinguished by severe dilation of the subcapsular space, with the thin connective tissue wall of Bowman's capsule overlying a layer of squamous parietal epithelium. The etiology of this lesion is unknown.[6]

Contributing Institution: Pfizer Inc
Worldwide Research and Development
588 Eastern Point Rd
Groton, CT 06340
www.pfizer.com

References:

1. Flaherty L, Bryda EC, Collins D, Rudofsky U, Montogomery JC. New mouse model for polycystic kidney disease with both recessive and dominant gene effects. *Kidney Int.* 1995;47(2): 552-558.
2. Katsuyama M, Masuyama T, Komura I, Hibino T, Takahashi H. Characterization of a novel polycystic kidney rat model with accompanying polycystic liver. *Exp Anim*. 2000;49(1):51-55.
3. Martinez JR, Grantham JJ. Polycystic kidney disease: etiology, pathogenesis, and treatment. *Dis Mon. Review*.1995;41(11):693-765.
4. Maxie MG, Newman SJ. Urinary system. In: Maxie MG, ed. *Jubb, Kennedy, and Palmer's Pathology of Domestic Animals*. 5th ed. Vol. 2. St. Louis, MO: Elsevier Limited; 2007:439-444.
5. Muller DWH, Szentiks CA, Wibbelt G. Polycystic kidney disease in adult Brazilian agoutis (*Dasyprocta leporina*). *Vet Pathol*. 2009;46(4):656-661.
6. Munkittrick KR, MOccia RD, Leatherland JF. Polycystic kidney disease in goldfish (*Carassius auratus*) from Hamilton Harbour, Lake Ontario, Canada. *Vet Pathol*. 1985;22(3):232-237.
7. Newman SJ. Urinary system. In: McGavin MD, Zachary JF, eds. *Pathologic Basis of Veterinary Disease*. 5th ed. St. Louis, MO: Elsevier; 2007:618-620.
8. Sanzen T, Harada K, Yasoshima M, Kawamura Y, Ishibashi M, Nakanuma Y. Polycystic kidney rat is a novel animal model of Caroli's disease associated with congenital hepatic fibrosis. *Am J Pathol*. 2001;158(5):1605-1612.

9. Taylor AC, Palmer KR. Caroli's disease. *Eur J Gastroenterol Hepatol*. 1998;10(2):105-108.

CASE II: KM07/13A342 (JPC 4032702).

Signalment: Full term fetus, male rhesus macaque (*Macaca mulatta*).

History: Found dead.

Gross Pathology: Male fetus presented with swollen face and extremities. Dystocia suspected. Both testicles were intra-abdominal. The left testicle was swollen, cystic, and measured 1.5x2cm.

Histopathologic Description: The polycystic mass is composed of variably sized, fluid-filled cysts with a thin outer rim of immature testis and solid areas with mature ectodermal and endodermal structures. At the periphery, clusters of seminiferous tubules with a single and multiple layers of Sertoli cells are located around cuboidal cell-lined channels of the rete testis. Protein filled cysts are lined by single and sometimes multiple layers of keratinized squamous to cuboidal epithelium.

Ectodermal components include scattered nests of squamous epithelium with peripheral basal layers, central stratum lucidum, and inner stratum corneum and a central keratin core. Some sections contain haired skin with keratinized epidermis, hair follicles and shafts, dermal vasculature and fat, and clusters of adnexal glands. Mesodermal components include scattered islands of cartilage, rare spicules of new bone formation, and rudimentary tooth formation. Endodermal components consist of cystic spaces lined by complex cuboidal to columnar epithelium mixed with goblet cells that cover papillary villous-like projections and has a submucosa with lymphoid aggregates.

Contributor's Morphologic Diagnosis: Testis: Teratoma.

Contributor's Comment: Neoplasia of the gonad in non-human primates is extremely rare. In our colony we have only seen three teratomas (one testicular and two ovarian), a dysgerminoma, and one interstitial cell tumor over the last 25 years.

Teratomas of the human testis can be classified as solid or cystic, and mature or immature, based on whether components have adult or embryonic features; the tumors often have features of both.[7] In animals, teratomas are most frequently found in the horse, the majority in cryptorchid testes.[3] In the fetus, teratoma formation probably prevents normal descent.[12] Human cases with undescended testes are 5-48 times more likely to be neoplastic[12], but neoplasia after surgical reduction (orchiopexy) and in the other normally descended testis is also reported.[1]

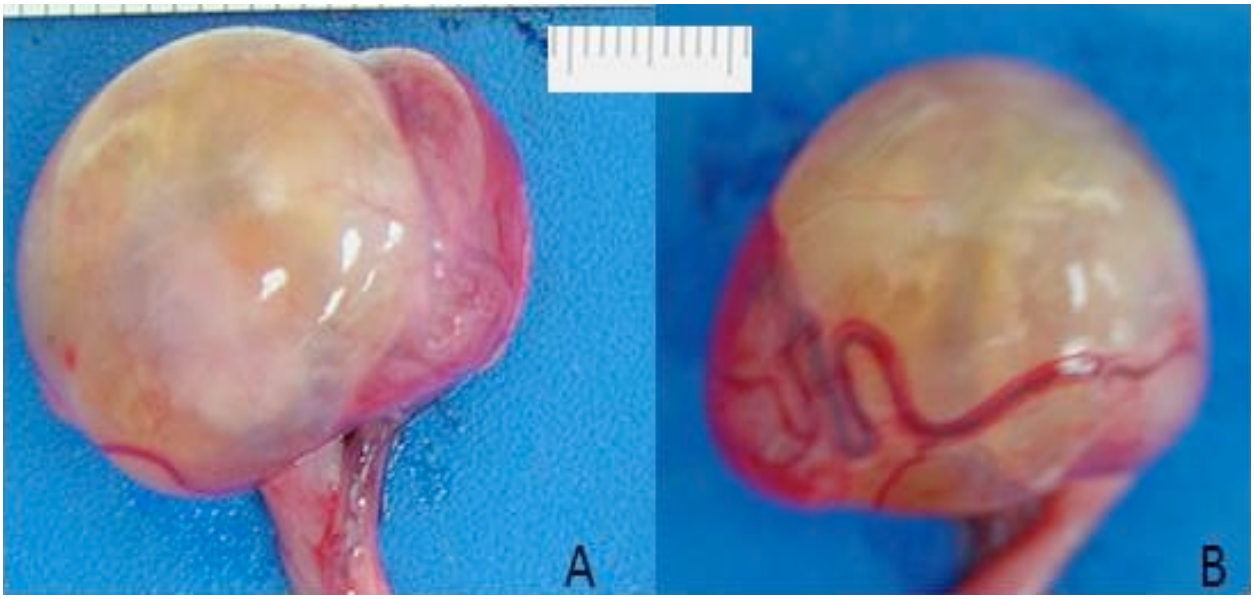

2-1. Testis, rhesus macaque: The left testis is enlarged, measuring 1.5x2cm, and the vaginal tunic is distended by abundant fluid. (Photo courtesy of: Tulane National Primate Research Center, Department of Comparative Pathology, 18703 Three Rivers Road, Covington, La 70433, pjdidier@tulane.edu)

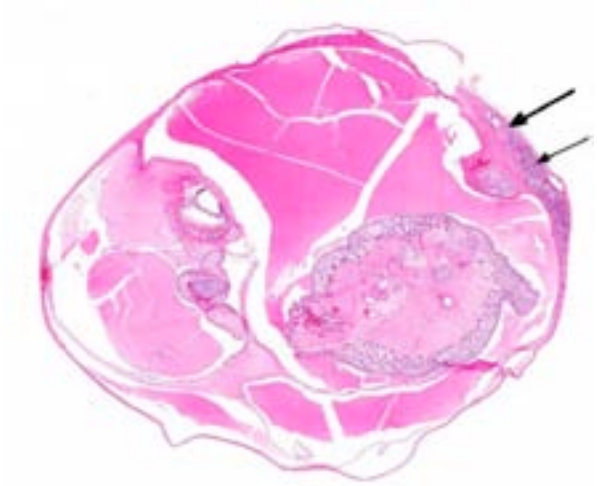

2-2. Testis, rhesus macaque: 95% of the testis is effaced by a multicystic neoplasm. A thin rim of atrophic seminiferous tubules remains at the periphery (arrows). (HE 0.63X)

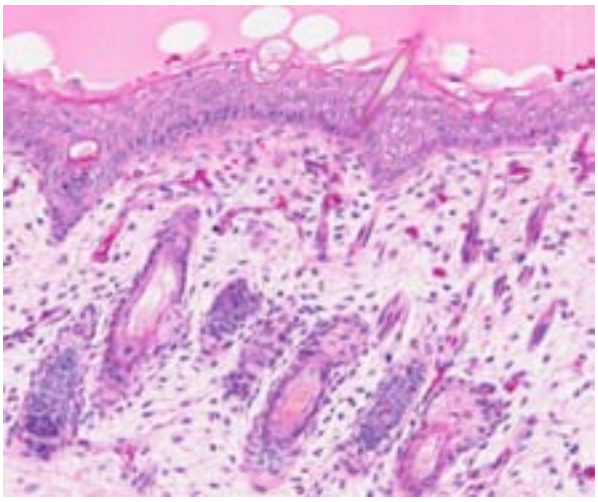

2-3. Testis, rhesus macaque: Among the ectodermal elements in the neoplasm is an extensive area which contains well differentiated haired skin, included stratified squamous epithelium, follicles with hair shafts, and dermis with adipose tissue. (HE 168X)

In animals most teratomas are benign, as are most ovarian teratomas in women, whereas most post pubertal testicular tumors in men are malignant (except those occurring in childhood), suggesting origin from benign and malignant cells respectively.[6] The difference may be based on the human female's tolerance for parthenogenetic development of immature somatic ova cells into three germ layers while suppressing neoplastic cells, in contrast to the human male that differentiates malignant immature somatic cells less efficiently in the embryo.[11] Why this hypothesis does not appear to extend to animals is unexplained.

Table 1: Embryonic germ cell layers and selected tissue derivatives.[2,10]

Ectoderm	Mesoderm	Endoderm
• Epidermis of skin and its derivatives (sweat glands, hair follicles, and sensory receptors) • Epithelial lining of mouth and anus • Cornea and lens of eye • Nervous system • Adrenal medulla • Tooth enamel • Epithelium of pineal and pituitary glands	• Notochord • Musculoskeletal system • Muscular layer of stomach and intestine • Excretory system • Circulatory and lymphatic systems • Reproductive system (except germ cells) • Dermis of skin • Adrenal cortex	• Epithelial linings (digestive tract, respiratory system, urethra, urinary bladder, and reproductive system) • Liver • Pancreas • Thymus • Thyroid and parathyroid glands

JPC Diagnosis: Testis: Teratoma.

Conference Comment: Totipotential primordial germ cells can give rise to several types of tumors, including relatively undifferentiated embryonal carcinomas, and more differentiated yolk sac tumors and choriocarcinomas. Additionally, they may differentiate along somatic cell lines to form teratomas.[4,9] The term "teratoma" is derived from the Greek word "teraton" meaning "a monster."[6] These tumors are classically defined as having at least two of the three embryonic layers (i.e., endoderm,

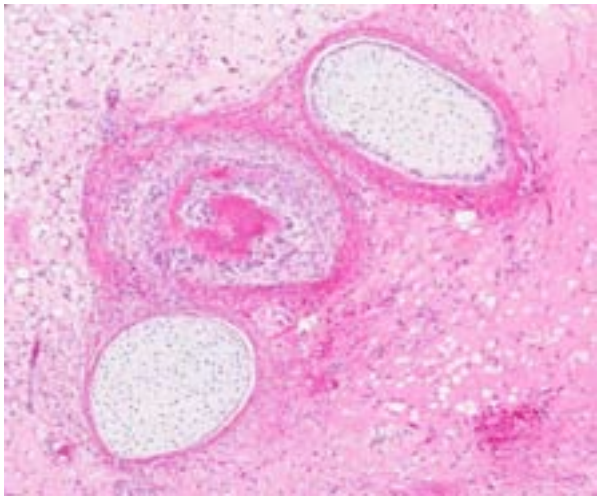

2-4. Testis, rhesus macaque: Mesodermal elements include scattered islands of cartilage and bone (center). (HE 63X)

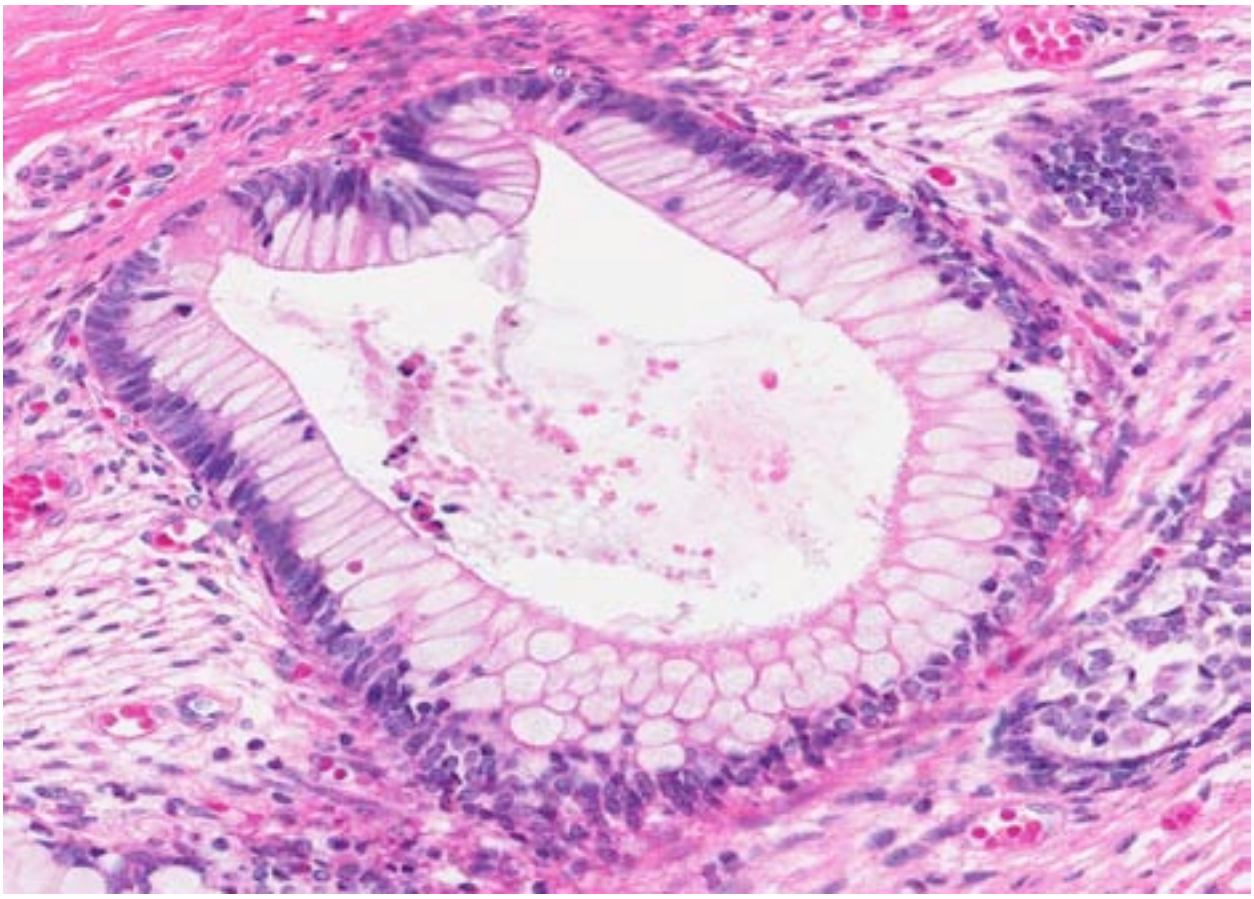

2-5. Testis, rhesus macaque: Endodermal elements consist of cystic spaces lined by goblet cells, recapitulating digestive epithelium. (HE 100X)

mesoderm, and ectoderm),[2] however, recent classifications also include monodermal types.[6,9] See Table 1 for the tissue derivatives of these embryonic layers.[2,10] Teratomas have been reported in horses, cattle, dogs, mice, ferrets and some wildlife species, such as roe deer, a giraffe and a great blue heron.[4,5,8,9] They occur most frequently in the gonads; however, these tumors can also develop at extragonadal locations, usually along the midline.[5] The most plausible rule-out for a well differentiated teratoma is a dermoid or epidermoid cyst. Both are benign, cystic tumors, lined by stratified squamous epithelium and often filled with lamellations of keratin; however, the dermoid cyst may also produce adnexal structures such as hair follicles, sebaceous glands, and sweat glands (see WSC 2013-14, conference 1, case 1).

For comparison to the testicular teratoma, conference participants examined a mouse ovarian teratoma, provided by the moderator. The ovarian teratoma was composed of haphazard regions of neuroectoderm, vague glandular/ductular components, poorly differentiated muscle (mesoderm) and respiratory epithelium (endoderm), consistent with an immature teratoma.

Contributing Institution: Tulane National Primate Research Center
Department of Comparative Pathology
18703 Three Rivers Road
Covington, LA 70433

References:

1. Banks K, Tuazon E, Berhane K, et al. Cryptorchism and testicular germ cell tumors: comprehensive meta-analysis reveals that association between these conditions diminished over time is modified by clinical characteristics. *Frontiers Endo.* 2013;3:1-11.
2. Foster RA. Male reproductive system. In: McGavin MD, Zachary JF, eds. *Pathologic Basis of Veterinary Disease*. 5th ed. St. Louis, MO: Elsevier; 2012:1142-1143.

3. Foster RA, Ladd PW. Male genital system. In: Maxie MG, ed. *Jubb, Kennedy, and Palmer's Pathology of Domestic Animals*. 5th ed. Vol. 3. St. Louis, MO: Elsevier Limited; 2007:565-619.
4. Jamadagni SB, Jamadagni PS, Lacy SH, et al. Spontaneous nonmetastatic choriocarcinoma, yolk sac carcinoma, embryonal carcinoma, and teratoma in the testes of a Swiss albino mouse. *Toxicol Pathol*. 2013; 41(3):532-536.
5. Keller DL, Schneider LK, Chamberlin T, Ellison M, Steinberg H. Intramedullary teratoma in a domestic ferret. *J Vet Diagn Invest*. 2012;24(3):621-624.
6. Lakhoo, K. Neonatal teratomas. *Early Hum Develop*. 2010;86:643-647.
7. Moulton JE. Tumors of the genital system. In *Tumors of Domestic Animals*. 2nd ed. Berkely, CA: University of California Press; 1978:309-345.
8. Murai A, Yanai T, Kato M, Yonemaru K, Sakai H, Masegi T. Teratoma of the umbilical cord in a giraffe (*Giraffa camelopardalis reticulata*). *Vet Pathol*. 2007;44(2):204-206.
9. Robinson NA, Manivel JC, Olson EJ. Ovarian mixed germ cell tumor with yolk sac and teratomatous components in a dog. *J Vet Diagn Invest*. 2013;25(3):447-452.
10. Schlafer DH, Miller RB. Female genital system. In: Maxie MG, ed. *Jubb, Kennedy, and Palmer's Pathology of Domestic Animals*. 5th ed. Vol. 2. Philadelphia, PA: Saunders Elsevier; 2007:450, 453-4.
11. Ulbright TM. Germ cell tumors of the gonads: a selective review emphasizing problems in differential diagnosis, newly appreciated, and controversial issues. *Modern Path*. 2005;18:S61-S79.
12. Yam B, Georgiou NA, Khullar P, et al. Radiology-Pathology conference: mature teratoma arising from an intra-abdominal undescended testis in a 7-month-old infant. *Clin Imaging*. 2010;34:466-471.

CASE III: MK12-3255 (JPC 4036188).

Signalment: 17-year-old male rhesus macaque (*Macaca mulatta*).

History: In 1998, the macaque underwent total body irradiation followed by autologous bone marrow transplantation to track the development of peripheral blood cells from retrovirus-marked stem cells. The bone marrow was successfully engrafted and the macaque was considered to be immunocompetent.[11] Fourteen years later, the animal presented acutely with coughing and hemoptysis and was sedated for evaluation. The animal was in thin body condition with pale mucous membranes. Lung sounds were judged to be harsh but heart sounds were normal. Radiographs revealed consolidation of the left lung field and aerophagia of the esophagus and stomach. The monkey was subsequently euthanized.

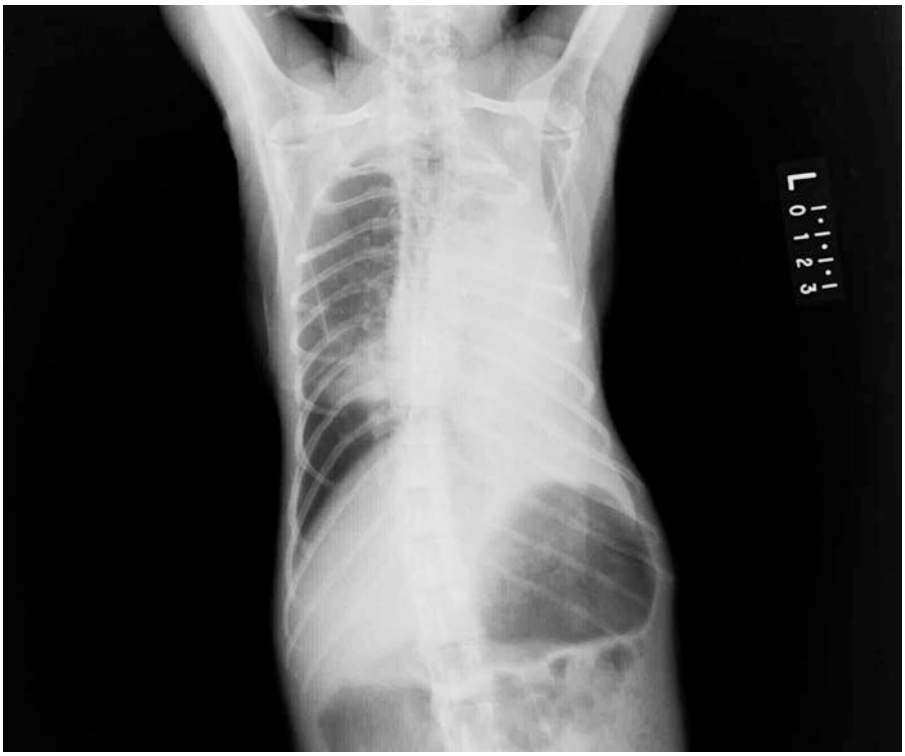

3-1. Chest and proximal abdomen, dorsoventral view, rhesus macaque: Radiographs reveal consolidation of the left lung field and aerophagia of the esophagus and stomach. (Photo courtesy of: Division of Veterinary Resources, National Institutes of Health, 9000 Rockville Pike, Bethesda, MD 20892)

Gross Pathology: The left lung lobes were consolidated and diffusely and firmly adhered to the pleural wall. Within the cranial left thoracic cavity, there was a small amount of thin, serosanguineous fluid. When the left lung lobes were incised, there was abundant, red/brown/dark yellow viscous fluid. There were yellow nodular areas (abscesses) in the caudal left lung lobes. The right lung lobes also were consolidated but not as severely as the left and, when incised, also had viscous fluid. Samples of the pleural fluid, abscesses and consolidated lung were collected for bacterial culture. The mediastinal, sternal and thoracic lymph nodes were moderately - markedly enlarged. Sections of lung and tracheobronchial lymph nodes were collected for PCR for mycobacterium. No other significant gross changes were noted.

Laboratory Results:

- *Klebsiella pneumoniae* was cultured from the pleural effusion, one of the nodules and a section of left lung lobe.
- Sections of lung and thoracic lymph nodes were negative for *Mycobacteria sp*. by PCR.
- Gram stain revealed numerous gram-negative rods.
- Fungal cysts, consistent with *Pneumocystis* spp., were not found with GMS stain.
- *Mycobacteria* spp. were not seen with Acid Fast stain.

Histopathologic Description: Lung: Bronchi contained neutrophils and macrophages admixed with extra and intracellular bacterial rods. Alveoli were lined by hypertrophied type II pneumocytes and were expanded by numerous neutrophils, macrophages with fewer multinucleate giant cells. Within macrophages and multinucleate giant cells, the bacteria were surrounded by clear spaces (capsule). Connective tissue around bronchi was edematous with fibrin deposition and scattered inflammatory cells.

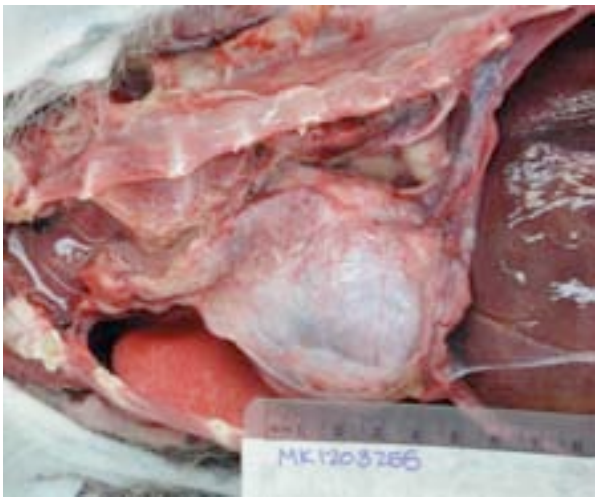

3-2. Lung, rhesus macaque: Within the cranial left thoracic cavity, there was a small amount of thin, serosanguineous fluid. The left lung lobes were consolidated and diffusely and firmly adhered to the pleural wall. (Photo courtesy of: Division of Veterinary Resources, National Institutes of Health, 9000 Rockville Pike, Bethesda, MD 20892)

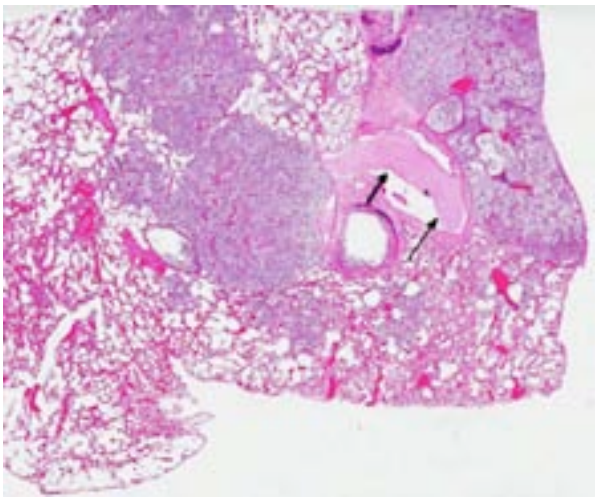

3-3. Lung, rhesus macaque: Inflammatory nodules efface 50% of the lung. Inflammatory exudate fills alveoli and airways within these areas; numerous vessels contain large fibrin clots (arrows). (HE 0.63X)

There was pleuritis composed of small aggregates of neutrophils, bacteria and fibrin.

Contributor's Morphologic Diagnosis: Lung: Bronchopneumonia multifocal and focally extensive, suppurative, moderate – marked, acute with gram-negative rods and mild pleuritis.

Contributor's Comment: Other lesions included:

- Pancreas islet cell hyalinization, multifocal, mild
- Heart, myocardial degeneration, loss and fibrosis, multifocal, minimal - mild
- Kidney, cyst, focal, mild
- Lymph node, lymphoid hyperplasia, moderate

Klebsiella pneumoniae is a gram-negative, non-spore-forming, facultative, anaerobic, nonmotile rod with a prominent capsule. Non-pathogenic strains can be found in soil, water, man and mammals; the bacteria colonize mucosal surfaces. *Klebsiella pneumoniae* afflicts the debilitated, immunosuppressed and those in hospitals and long-term care facilities and is the most frequent case of gram-negative pneumonia. Intravenous catheters and surgical sites may also serve as sources of infection.[4,10,13]

Disease in nonhuman primates may be associated with such stressors as shipping, quarantine and overcrowding. In New World monkeys and Old World monkeys, *Klebsiella pneumoniae* infection has been associated with septicemia, air sacculitis, pneumonia, pulmonary abscess, peritonitis, cystitis and meningitis. Vaccination with killed whole bacterin in owl monkeys, capsular polysaccharide in squirrel monkeys, and autogenous vaccines in marmosets have been used to reduce morbidity and mortality due to *Klebsiella pneumoniae* infection.[14]

Klebsiella pneumoniae in lab animals is a rare cause of enterotyphlitis, septicemia and necrotizing bronchopneumonia in rabbits; septicemia, bronchopneumonia, pericarditis, pleuritis and peritonitis in guinea pigs; lymph node and kidney abscesses as well as rhinitis in rats. In mice, cervical lymphadenopathy, liver and kidney abscesses, empyema, endo- and myocarditis and thrombosis are associated with, but not diagnostic for, *Klebsiella pneumoniae* infection.[6,7,8,9] In domestic animals, *Klebsiella pneumoniae* has been isolated from mares with endometritis and abortion and from foals with pneumonia and septicemia.[2,12]

A hypermucoviscous (HMV) variant of *Klebsiella pneumoniae* (HMV-KP) has been identified in humans and subsequently in animals. The virulence of HMV is thought to be due, in part, to capsular serotypes (K1 and K2) that carry genes MagA (mucoviscosity-associated gene/K1 specific capsular polymerase gene) and rmpA (regulator of mucoid phenotype) which make the bacteria more invasive and more resistant to

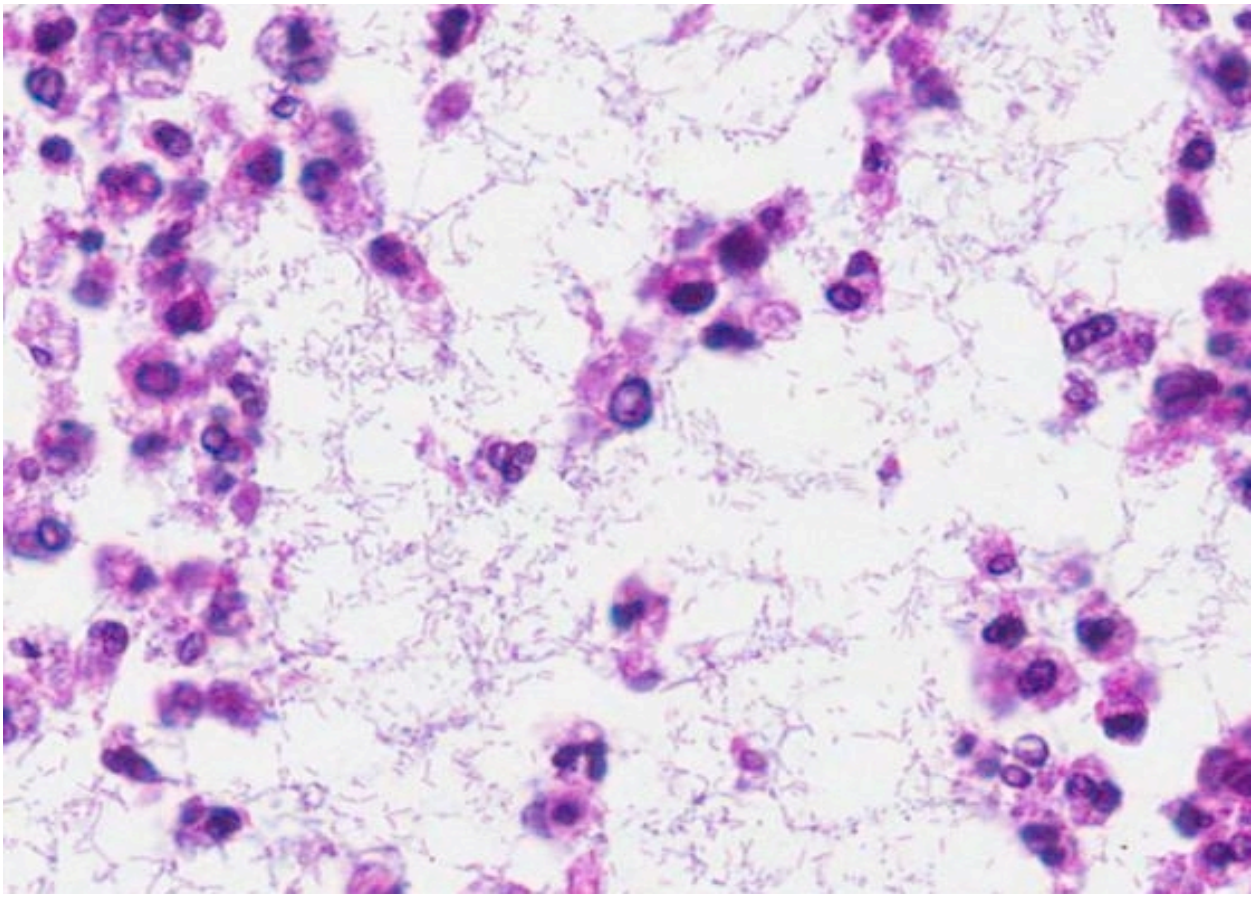

3-4. Lung, rhesus macaque: Alveoli contain abundant viable and degenerate neutrophils, foamy macrophages, and innumerable intra- and extracellular 2-3 µm bacilli that are separated and surrounded by a clear capsule, consistent with Klebsiella pneumoniae. (HE 400X)

phagocytosis.[13,15] Bacterial colonies appear mucoid and have a positive string test (an inoculation loop is pulled through the bacterial colony and the resulting string formed is greater than 5mm). In humans, HMV infection is unusual in that it infects healthy individuals and causes liver abscesses, pneumonia, meningitis, and endophthalmitis. The mode of infection is unknown but is thought to be via the intestine.[12,13]

Klebsiella pneumoniae with an HMV phenotype has been identified in African green monkeys in which abscesses were found in the abdomen, lungs, cerebellum and skin. The masses appeared to be centered on lymph nodes and there was associated peritonitis and adhesions to the intestines. Oral and rectal swabs of macaques in the same facility identified animals that were subclinically infected.[1,16]

Klebsiella pneumoniae HMV has been cultured from California sea lions dying shortly after being observed to be ill. Many of the animals were in good body condition but had bronchopneumonia, fibrinous pleuritis and abscess. Sea lions may serve as a potential source of zoonotic disease for swimmers.[5]

The HMV phenotype can be detected by rapid real-time PCR assays that target rmpA and magA genes. RAPD (rapid amplification of polymorphic DNA) can then be used to determine genetic variability between isolates.[3]

JPC Diagnosis: Lung: Bronchopneumonia, suppurative, multifocal to coalescing, severe, with numerous intra- and extracellular bacilli.

Conference Comment: The contributor provides an excellent summary of *Klebsiella pneumoniae* infection in humans and veterinary species. *Klebsiella* can affect a variety of organ systems, including the respiratory and urinary tracts, which differ considerably with respect to host defense mechanisms. As a result, virulence factors can differ between bacterial strains. Current research

has demonstrated important pathogenicity factors of *Klebsiella* spp. including the polysaccharide capsule, the lipopolysaccharide O antigens, pili/fimbriae, and siderophores.[10]

The polysaccharide capsule is essential for *Klebsiella* virulence. It prevents phagocytosis, suppresses the activation of complement components (especially C3b), and may inhibit macrophage differentiation.[10] *Klebsiella* spp. have developed resistance to the host serum bactericidal effect, normally mediated by complement proteins. This resistance likely involves two factors: 1) capsular polysaccharide, which may mask LPS and prevent complement activation and 2) the structure of lipopolysaccharide (LPS). It is hypothesized that the O antigens of LPS extend through the capsule layer, where complement protein C3b is fixed preferentially to the longest O-polysaccharide side chains. This binding fixes C3b far enough away from the bacterial cell membrane that the formation of the lytic membrane attack complex (C5b–C9) is prevented.[10] Pili, or fimbriae, are nonflagellar, filamentous bacterial surface projections that act as adhesions to bind host cells. Type 1 pili mediate bacterial colonization of mucus or epithelial cells of the urogenital, respiratory, and intestinal tracts, while type 3 pili adhere to endothelial cells, respiratory and urinary epithelium, tubular basement membranes, Bowman's capsules, and renal vessels.[10] Finally, since iron availability is a limiting factor for bacterial growth, *Klebsiella* spp. secrete siderophores, such as enterobactin and aerobactin. Siderophores are high-affinity, low-molecular-weight iron chelators that are capable of competitively taking up iron bound to host proteins.[10]

Contributing Institution: Division of Veterinary Resources
National Institutes of Health
9000 Rockville Pike
Bethesda, MD 20892

References:

1. Burke RL, Whitehouse CA, Taylor JK, Selby EB. Epidemiology of invasive *Klebsiella pneumoniae* with hypermucoviscosity phenotype in a research colony of nonhuman primates. *Comp Med*. 2009;59:6, 589–597.
2. Caswell JL, Williams KJ. The respiratory system. In: Maxie MG, ed. *Jubb, Kennedy and Palmer's Pathology of Domestic Animals*. 5th ed. Vol 2. Philadelphia, PA: Elsevier Limited; 2007:632.
3. Hartman LJ, Selby EB, Whitehouse CA, Coyne SR, Jaissle JG, Twenhafel NA, et al. Rapid real-time PCR assays for detection of *Klebsiella pneumoniae* with the rmpA or magA genes associated with the hypermucoviscosity phenotype - screening of nonhuman primates. *J Mol Diagn*. 2009;11(5):464–471.
4. Husain A, Kumar V. The lung. In: Kumar V, Abbas AK, Fausto N, eds. *Pathologic Basis of Disease*. 7th ed. London, UK: Saunders/Elsevier; 2005:748.
5. Jang S, Wheeler L, Carey RB, Jensen B, Crandall CM, Schrader KN, et al. Pleuritis and suppurative pneumonia associated with a hypermucoviscosity phenotype of *Klebsiella pneumoniae* in California sea lions (*Zalophus californianus*). *Vet Microbiol*. 2010;141(1-2): 174-177.
6. Percy DH, Barthold SW. The guinea pig. In: *Pathology of Laboratory Rodents and Rabbits*. 3rd ed. Ames, IA: Blackwell Publishing; 2007:222.
7. Percy DH, Barthold SW. The mouse. In: *Pathology of Laboratory Rodents and Rabbits*. 3rd ed. Ames, IA: Blackwell Publishing; 2007:64.
8. Percy DH, Barthold SW. The rabbit. In: *Pathology of Laboratory Rodents and Rabbits*. 3rd ed. Ames, IA: Blackwell Publishing; 2007:275.
9. Percy DH, Barthold SW. The rat. In: *Pathology of Laboratory Rodents and Rabbits*. 3rd ed. Ames, IA: Blackwell Publishing; 2007:152.
10. Podschun R, Ullmann U. *Klebsiella* spp. as nosocomial pathogens: epidemiology, taxonomy, typing methods, and pathogenicity factors. *Clin Microbiol Rev*. 1998;11(4):589-603.
11. Schmidt M, Zickler P, Hoffmann G, Haas S, Wissler M, Muessig A, et al. Polyclonal long-term repopulating stem cell clones in a primate model. *Blood*. 2002;100(8):2737-2743.
12. Shlafer DH, Miller RB. The female genital system. *Jubb, Kennedy and Palmer's Pathology of Domestic Animals*. 5th ed. Vol 3. Philadelphia, PA: Elsevier Limited; 2007:507.
13. Shon AS, Bajwa RP, Russ, TA. Hypervirulent (hypermucoviscous) *Klebsiella pneumoniae*: a new and dangerous breed. *Virulence*. 2013;4(2): 107-118.
14. Simmons J, Gibson S. Bacterial and mycotic diseases of nonhuman primates In: Abee CR, Mansfield K, Tardiff S, Morris T, eds. *Nonhuman*

Primates in Biomedical Research. 2nd ed. London, UK: Elsevier; 2012:128-130.
15. Soto E, LaMon V, Griffin M, Keirstead N, Palmour, R. Phenotypic and genotypic characterization of *Klebsiella pneumoniae* isolates recovered from nonhuman primates. *J Wildl Dis*. 2012;48(3):603-611.
16. Twenhafel NA, Whitehouse CA, Stevens EL, Hottel HE, Foster CD, Gamble S, et al. Multisystemic abscesses in African green monkeys (*Chlorocebus aethiops*) with invasive *Klebsiella pneumoniae*-identification of the hypermucoviscosity phenotype. *Vet Pathol*. 2008;45:226-231.

CASE IV: MK12-557 (JPC 4036187).

Signalment: 6-year-old male rhesus macaque (*Macaca mulatta*).

History: This macaque was inoculated intravascularly with SHIV in April 2010. The macaque tested negative for Herpes B, measles virus, SRV, STLV-1, and SIV one year prior to experimental infection. The macaque was relatively healthy for approximately 2 years post-infection, but several months prior to necropsy developed a nasal discharge and was treated with antibiotics over this period. The macaque became acutely hypoactive and lethargic and euthanasia was performed.

Gross Pathology: The macaque was somewhat thin but relatively well muscled and contained a small amount of body fat. Within the pinna of the left ear, there was a focal area of ulceration with a superficial scab measuring approximately 1.5 cm in diameter. There was a focal slightly elevated tan-white lesion measuring approximately 1 cm in greatest dimension on the tip of the left side of the tongue. The remainder of the tongue and oral cavity appeared normal.

The mesenteric lymph node was severely enlarged and measured 5.0 x 3.5 x 2.0 cm, and was tan to white on cut surface. A focal tan-white lesion was present within the jejunum with prominent thickening of the wall over a length of 4.5 cm. The colonic and pancreatic lymph nodes were moderately enlarged. The spleen was mildly enlarged and there were multiple nodules within the parenchyma which were irregular, tan-white and up to 1.5 cm in diameter. The wall of the gallbladder was moderately to severely thickened and was white to tan. These lesions were consistent with lymphoma.

The heart, kidneys, stomach, duodenum, ileum, cecum, colon and testes appeared normal. Several adhesions were present between the right caudal lung lobe and thoracic wall. The lungs otherwise appeared grossly normal.

Laboratory Results: Total lymphocyte counts averaged 1145/ uL over the last six months of life. CD4 counts were less than 200/uL over the same period. The macaque maintained a high level of viremia for SHIV during this period.

Histopathologic Description: The submitted slide is a section from the left ear pinna. The epidermis is focally ulcerated with an overlying serocellular crust, comprised primarily of degenerative neutrophils. The epidermis at the lateral margins of the lesion is irregular, with disarray and ballooning of epithelial cells, admixed with degenerative neutrophils. Many epithelial cells along the margin have enlarged nuclei with marginated chromatin and prominent amphophilic intranuclear inclusion bodies. Several syncytial cells are evident, containing intranuclear inclusions. Some of the adjacent sebaceous glands have similarly affected

4-1. Pinna, rhesus macaque: Within the pinna of the left ear, there was a focal area of ulceration with a superficial scab measuring approximately 1.5 cm in diameter. (Photo courtesy of: Division of Veterinary Resources, National Institutes of Health, 9000 Rockville Pike, Bethesda, MD 20892)

4-2. Tongue, rhesus macaque: There was a focal slightly elevated tan-white lesion measuring approximately 1 cm in greatest dimension on the tip of the left side of the tongue. (Photo courtesy of: Division of Veterinary Resources, National Institutes of Health, 9000 Rockville Pike, Bethesda, MD 20892)

4-3. Mesenteric lymph nodes, rhesus macaque: Mesenteric lymph nodes are diffusely enlarged as a result of concomitant granulomatous inflammation resulting from colonic M. avium infection. (Photo courtesy of: Division of Veterinary Resources, National Institutes of Health, 9000 Rockville Pike, Bethesda, MD 20892)

4-4. Pinna, rhesus macaque: The glabrous skin of the pinna is multifocally ulcerated (arrows). (HE 0.63X)

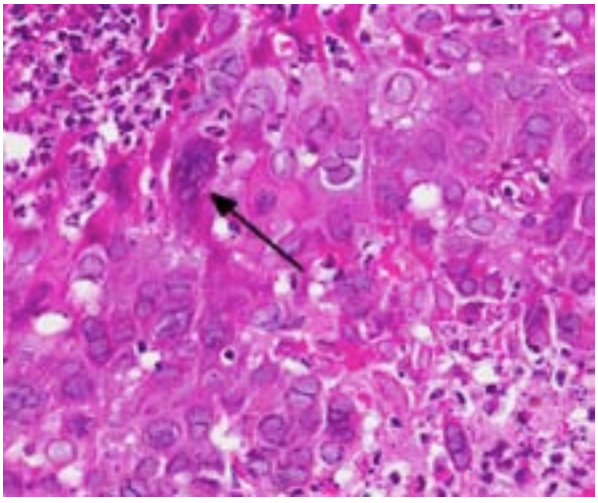

4-5. Pinna, rhesus macaque: Within the necrotic epidermis, numerous keratinocyte nuclei are expanded by a glassy intranuclear viral inclusion. Multinucleated viral syncytia are scattered throughout the epithelium (arrow). (HE 280X)

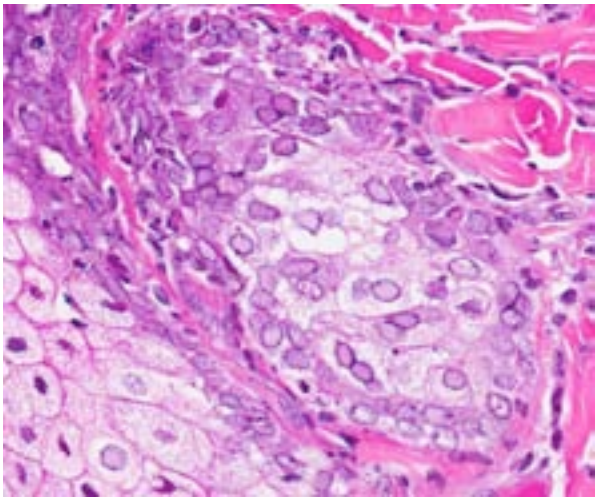

4-6. Pinna, rhesus macaque: Sebocytes are similarly infected, and display intranuclear viral inclusions. (HE 400X)

epithelium with cells containing prominent intranuclear inclusion bodies.

Examination of the tongue (not submitted) revealed an acute focal ulcerative glossitis with the margins of the lesion containing epithelial cells with prominent amphophilic intranuclear inclusion bodies. Transmission electron microscopy from a section of tongue revealed intranuclear icosahedral viral nucleocapsid particles measuring approximately 100 nm, and enveloped particles approximately 160 nm in diameter in the cytoplasm, consistent with herpesviral particles.

Other significant findings in this case included lymphoblastic lymphoma affecting the spleen, jejunum, gall bladder, adrenal gland, and mesenteric, perisplenic, pancreatic and colonic lymph nodes. Additionally, there was a granulomatous colitis and lymphadenitis affecting a portion of the colon and associated lymph nodes due to mycobacterial infection, with large numbers of acid fast bacilli evident in macrophages in the affected tissue. Mild to moderate multifocal interstitial pneumonia and fibrosis were evident in the lung.

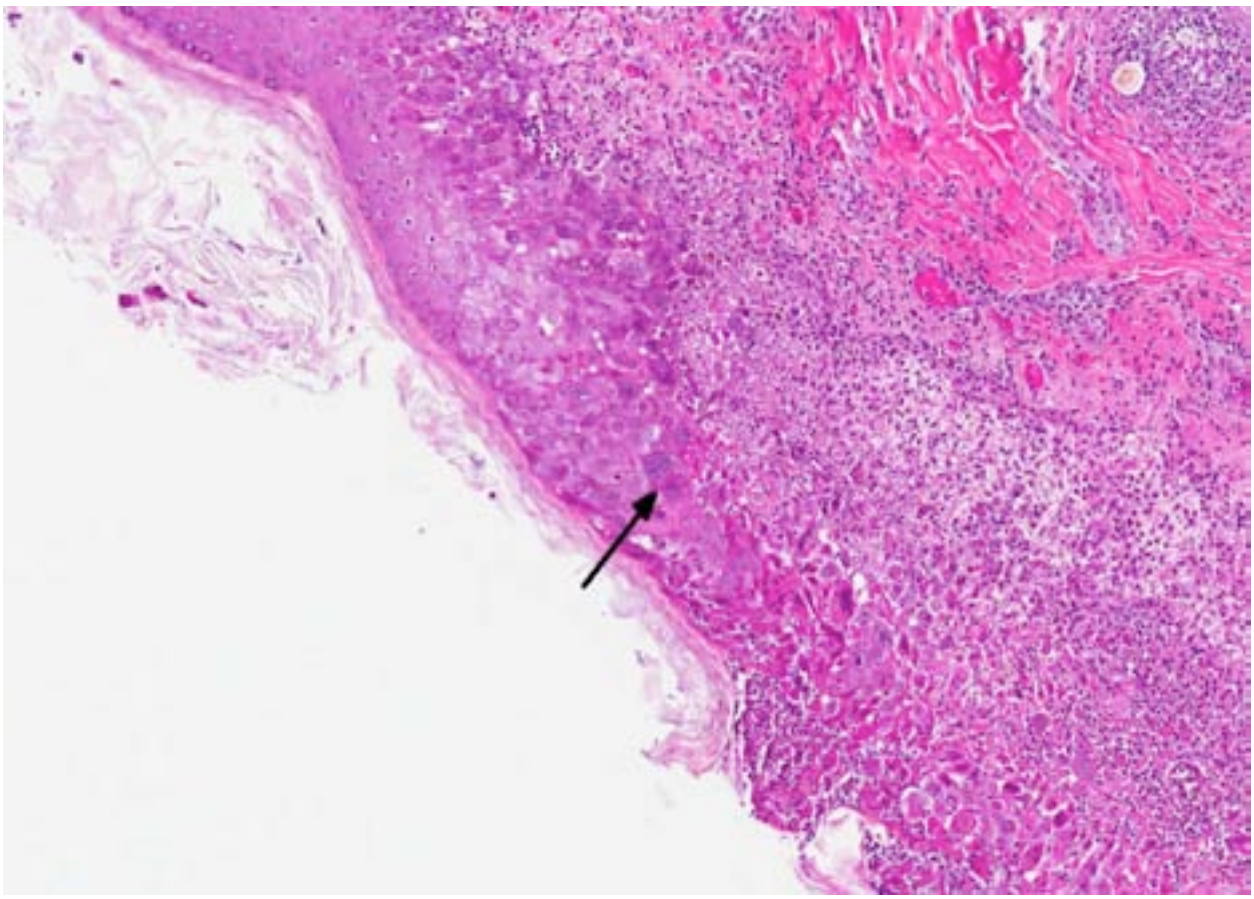

4-7. Pinna, rhesus macaque: Nuclei of infected cells contain icosahedral viral nucleocapsid particles measuring approximately 100 nm, and enveloped particles approximately 160 nm in diameter are visible within the cytoplasm. The characteristic "bulleye" appearance of enveloped particles within the cytoplasm is characteristic of herpesviruses.

Contributor's Morphologic Diagnosis: External ear, otitis externa, acute, focal, ulcerative, with intranuclear inclusion bodies, consistent with alpha herpesvirus.

Contributor's Comment: This macaque developed several disease conditions related to immunosuppression from experimental infection with SHIV. The principal presenting signs were upper respiratory and were likely related to the findings of pulmonary fibrosis and multifocal interstitial pneumonia. The macaque had lymphoma affecting multiple organs. Additionally, there was granulomatous colitis multifocally due to infection with mycobacteria. The findings of herpetic lesions involving the tip of the tongue and the left ear also reflect the ongoing immunosuppressive state in this macaque. The external pinna is an unusual location for active herpesviral infection, with the lingual lesion being more typical. No other lesions were noted systemically due to herpesviral infection. While the herpesviral infection is likely due to macacine herpesvirus-1 in this case, the possibility of infection with herpes simplex virus-1 cannot be ruled out. This macaque had tested previously negative by serology for herpes B and this may represent a false negative result. While the macaque may have become infected subsequent to experimental SHIV inoculation, this is less likely as these macaques were singly housed following inoculation.

Macacine herpesvirus-1, previously known as Cercopithecine herpesvirus-1, Herpesvirus simiae and Herpes B virus is a common alpha herpesvirus infection affecting Old World macaques. It has been documented in rhesus macaques (*Macaca mulatta*), cynomolgus macaques (*M. fascicularis*), stumptail macaques (*M. artoides*), pigtailed macaques (*M. nemestrina*), Japanese macaques (*M. fuscata*), bonnet macaques (*M. radiata*) and Taiwan macaques (*M. cyclopis*). Natural infection in

macaques is usually asymptomatic, with localized mucosal lesions occurring infrequently. Transmission is horizontal between macaques with most animals acquiring the infection by 2-4 years of age. Lesions when present typically involve the oral and gingival mucosa, tongue and conjunctiva. Genital lesions are generally not observed.[5] Infection of New World monkeys, while uncommon, is also possible. Asymptomatic natural infection with macacine herpesvirus-1 has been documented in a colony of brown capuchin monkeys (*Cebus apella*).[3]

Macacine herpesvirus-1 has typical morphology for alpha-herpesviruses and is composed of double stranded DNA, with a 40 nm core, icosahedral nucleocapsid approximately 100 nm in diameter and enveloped particles of 160-180 nm in the infected cell cytoplasm. Host cell infection occurs by fusion of viral envelope with host cell plasma membranes, penetration of nuclear pores by viral capsids with release of viral DNA in the nucleus, leading to viral replication.[6]

Transmission typically occurs via exposure of oral, ocular or genital mucous membranes from an infected animal shedding virus most commonly in saliva. The virus replicates locally, enters sensory nerves and is transmitted intra-axonally where it can remain latent in sensory ganglia, protected from host immune responses. Reactivation can occur periodically from the latent state, with virus being transported down axons to mucosal tissues. The majority of reactivated infections are asymptomatic. Virus carriers generally have a low rate of shedding, however, stress associated with transportation, changes in social groupings and immunosuppression can lead to reactivation and viral shedding.[4]

While generally not a significant clinical disease entity for immunocompetent macaques, cases of systemic infection have been documented in cynomolgus macaques causing necrosis of lung, liver, spleen, pancreas, and adrenal glands.[2,7] In one of these cases infection with Simian retrovirus type D was noted as the likely cause of immunosuppression leading to pathogenic herpesvirus infection.[2]

Macacine herpesvirus is an extremely important zoonotic agent. Human exposure to an infected macaque shedding virus can result in a highly pathogenic infection leading to CNS involvement and a fatality rate greater than 70% in individuals who are not treated aggressively with antiviral drugs.[1,4] Universal precautions with appropriate PPE are required when working with nonhuman primates. Any exposure by scratch, bite, needle stick injury or any other exposure of mucous membranes or an open skin wound require immediate attention and consultation with occupational medical specialists.

JPC Diagnosis: Haired skin, pinna: Dermatitis, necrotizing, multifocal, severe, with folliculitis, furunculosis, and numerous intraepithelial intranuclear viral inclusions and syncytia.

Conference Comment: The contributor has provided an excellent review of macacine herpesvirus-1. In addition to the section of ulcerated pinna, the contributor/moderator provided conference participants with the opportunity to examine multiple tissues from this animal, both microscopically and grossly (via photographs). Lesions in the tongue were similar to those described in the pinna, with focally extensive glossal ulceration, a marked neutrophilic infiltrate, large eosinophilic intra-nuclear inclusion bodies within epithelial cells and occasional viral syncytia. Transmission electron microscopy of the tongue was also consistent with α-herpesviral infection (see contributor's histopathologic description). The spleen, liver, gallbladder, multiple lymph nodes and a focal area of the jejunum were grossly thickened/enlarged. Microscopically, these tissues were infiltrated by a monomorphic population of mononuclear cells with large nuclei and prominent nucleoli, interpreted as disseminated lymphoblastic lymphoma. Neoplastic lymphocytes demonstrated strong cytoplasmic immunoreactivity for anti-CD79a, suggesting B-cell origin, although there were scattered CD3-positive T-cells within the neoplasm. There was also marked granulomatous lymphadenitis and colitis. Several mesenteric lymph nodes and sections of colon were effaced by numerous epithelioid macrophages, with abundant intra-histiocytic acid-fast bacilli, consistent with *Mycobacterium avium*. Interestingly, despite this considerable microscopic evidence of mycobacteriosis, PCR for *Mycobacteria* spp. was negative.

Overall, this rhesus macaque had lymphoma, α-herpesviral glossitis and otitis externa, granulomatous lymphadenitis/colitis (likely secondary to *M. avium*) and alveolitis, interstitial pneumonia and fibrosis.

Contributing Institution: National Institutes of Health
Division of Veterinary Resources, Pathology Service
9000 Rockville Pike, Building 28A/115, Bethesda, MD 20892

References:

1. Bailey CC, Miller AD. Ulcerative cheilitis in a rhesus macaque. *Vet. Pathol.* 2012;49(2):412-415.
2. Carlson CS, O'Sullivan MG, Jayo MJ, et al. Fatal disseminated cercopithecine herpesvirus 1 (herpes B infection in cynomolgus monkeys (*Macaca fascicularis*). *Vet. Pathol.* 1997;34(5): 405-14.
3. Coulibaly C, Hack R, Seidl J, et al. A natural asymptomatic herpes B virus infection in a colony of laboratory brown capuchin monkeys (*Cebus apella*). *Lab. Anim.* 2004;38(4):432-8.
4. Elmore D, Eberle R. Monkey B virus (Cercopithecine herpesvirus 1). *Comp. Med.* 2008;58(1):11-21.
5. Huff JL, Barry PA. B virus (Cercopithecine herpesvirus 1) infection in humans and macaques: potential for zoonotic disease. *Emerg. Infect. Dis.* 2003;9(2): 246-50.
6. Jainkittivong A, Langlais RP. Herpes B virus infection. *Oral Surg. Oral Med. Oral Pathol. Oral Radiol. Endod.* 1998;85(4):399-403.
7. Simon MA, Daniel MD, Lee-Parritz D, et al. Disseminated B virus infection in a cynomolgus monkey. *Lab. Anim. Sci.* 1993;43(6):545-50.

Joint Pathology Center
Veterinary Pathology Services

WEDNESDAY SLIDE CONFERENCE 2013-2014

Conference 9

04 December 2013

CASE I: TVMDL 2012-02 (JPC 4018680).

Signalment: Six-month-old female Meerkat (*Suricata suricatta*).

History: The animal presented with one week history of visual impairment, intention tremor, head tilt, circling to right, absent menace reflex, and lack of proprioception of the pelvic limbs. The animal was treated with clindamycin, dexamethasone, and vitamin B with no clinical improvement. Euthanasia was opted due to poor prognosis.

Gross Pathology: None reported.

Histopathologic Description: The submitted slides contain sections of either the left or right cerebellar hemisphere, along with part of the vermis, and the underlying segment of the medulla. The main histologic lesions affected the folia of both hemispheres and the cerebellar vermis. These were characterized by areas of normal-appearing cerebellar folia that abruptly presented extensive and segmental Purkinje cell depletion. Affected areas were characterized by loss of neuronal bodies (empty baskets) that were surrounded by a proliferation of large numbers of astrocytes (Bergmann astrocytes). Cerebellar nuclei, the molecular layer, and the white matter presented variable gliosis with occasional vacuolation of the latter. These were the main features in the submitted sections. Additional changes affecting Purkinje cells that are variably present in the slides include shrunken and hypereosinophilic cells showing an occasionally vacuolated perikaryon. A few cells had a swollen cytoplasm with dispersion of the Nissl bodies and displacement of the nucleus to the periphery (central chromatolysis). The sections of cerebellum of this meerkat were compared with an age-matched control that died of an unrelated cause. An apparent increase in the number of granular neurons was noticed in this animal, which also presented markedly increased numbers of astrocyte cell processes demonstrated with GFAP immunostaining. Astrocytic processes extended into both the molecular and granular layers. In the former, the processes presented a vague segmental distribution that corresponded to areas lacking Purkinje cells. GFAP also demonstrated marked astrocytosis and astrogliosis in the cerebellar nuclei.

Contributor's Morphologic Diagnosis: Cerebellum: Multifocal, marked, Purkinje cell degeneration and loss with vacuolation, chromatolysis, astrocytosis, and astrogliosis.

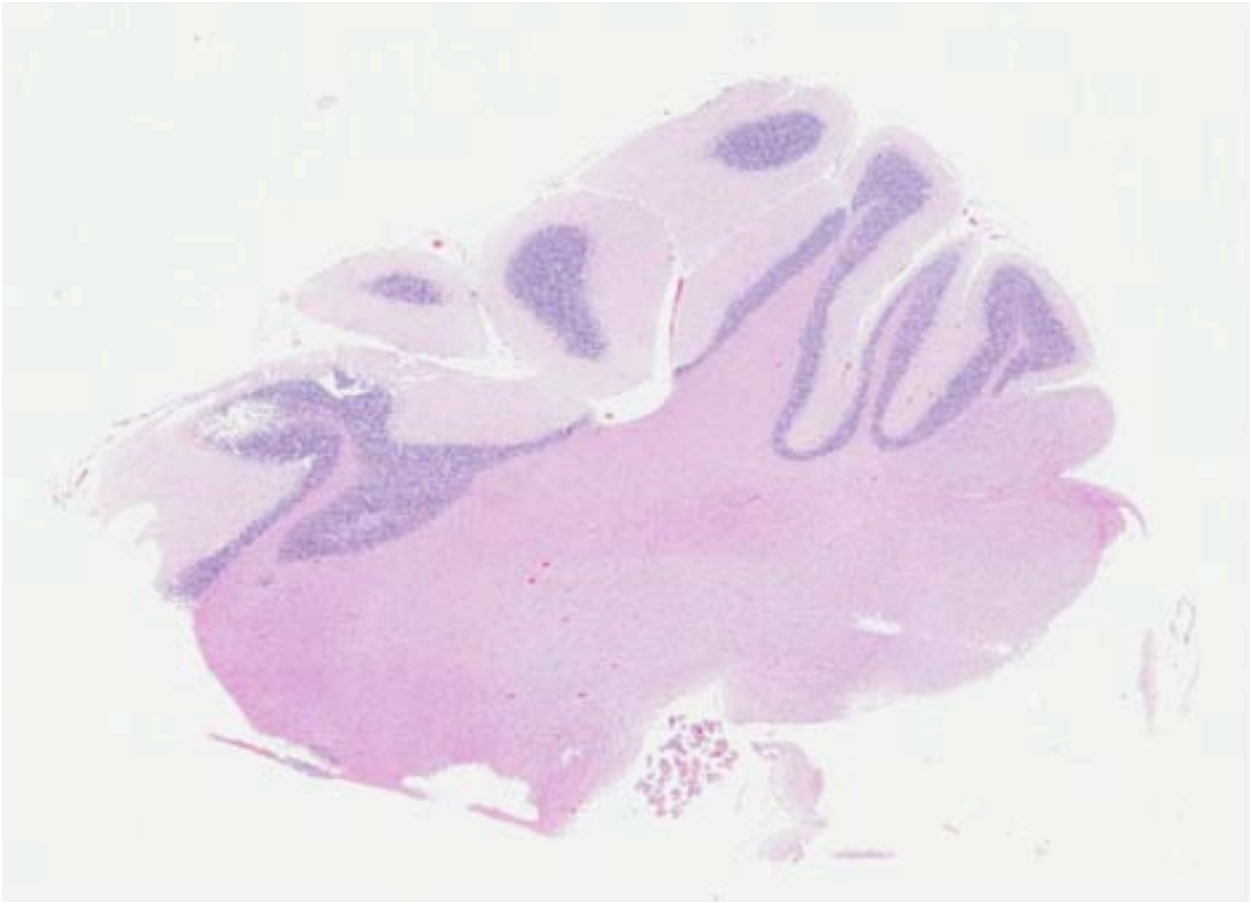

1-1. Cerebellum, meerkat: The cerebellar folia are diffusely flattened and the granular layer appears hypocellular. (HE 0.63X)

Contributor's Comment: The clinical history and histopathologic findings in the cerebellum of this meerkat are compatible with cerebellar abiotrophy. This term, which literally means lack of a life-sustaining nutritive factor, is used to denote diseases in veterinary neuropathology that share clinicopathological features with these seen in this case.[10] This condition has been described in several breeds of dogs, in horses, bovine, sheep, pigs, cats, in rabbits, and in an alpaca.[5,6,7,8,10] Reports of neurologic disease in meerkats are rare and confined to a case series of cholesterol granulomas and disseminated toxoplasmosis.[9,10] To our knowledge, cases of abiotrophy have not been reported in this species.

As the term abiotrophy implies, the microscopic lesions are not considered the result of an acquired insult (e.g. infectious disease or intoxication), but rather is the consequence of an intrinsic metabolic disorder with a suspected hereditary basis of transmission. Besides this animal, two other meerkats from the same zoo (three and six-months of age) presented with similar clinicopathologic findings suggesting an inherited disease. These animals belong to a small colony, in which inbreeding is very common. No histologic evidence of an infectious disease was detected in the examined sections of all three animals.

Abiotrophy is characterized by the spontaneous degeneration and loss of neurons prematurely, and it is viewed as affecting the organ after it has developed its full cellular component.[2,10] This differs from hypoplasia, in which the cerebellum fails to form completely during development as the result of infectious diseases (e.g. feline panleukopenia, bovine viral diarrhea, classical swine fever), toxicities (e.g. organophosphate trichlorfon in piglets), and malnutrition (e.g. hypocuprosis in goat kids and lambs).[5]

Most commonly, animals with abiotrophy are neurologically normal at birth but will progressively develop cerebellar deficits in the

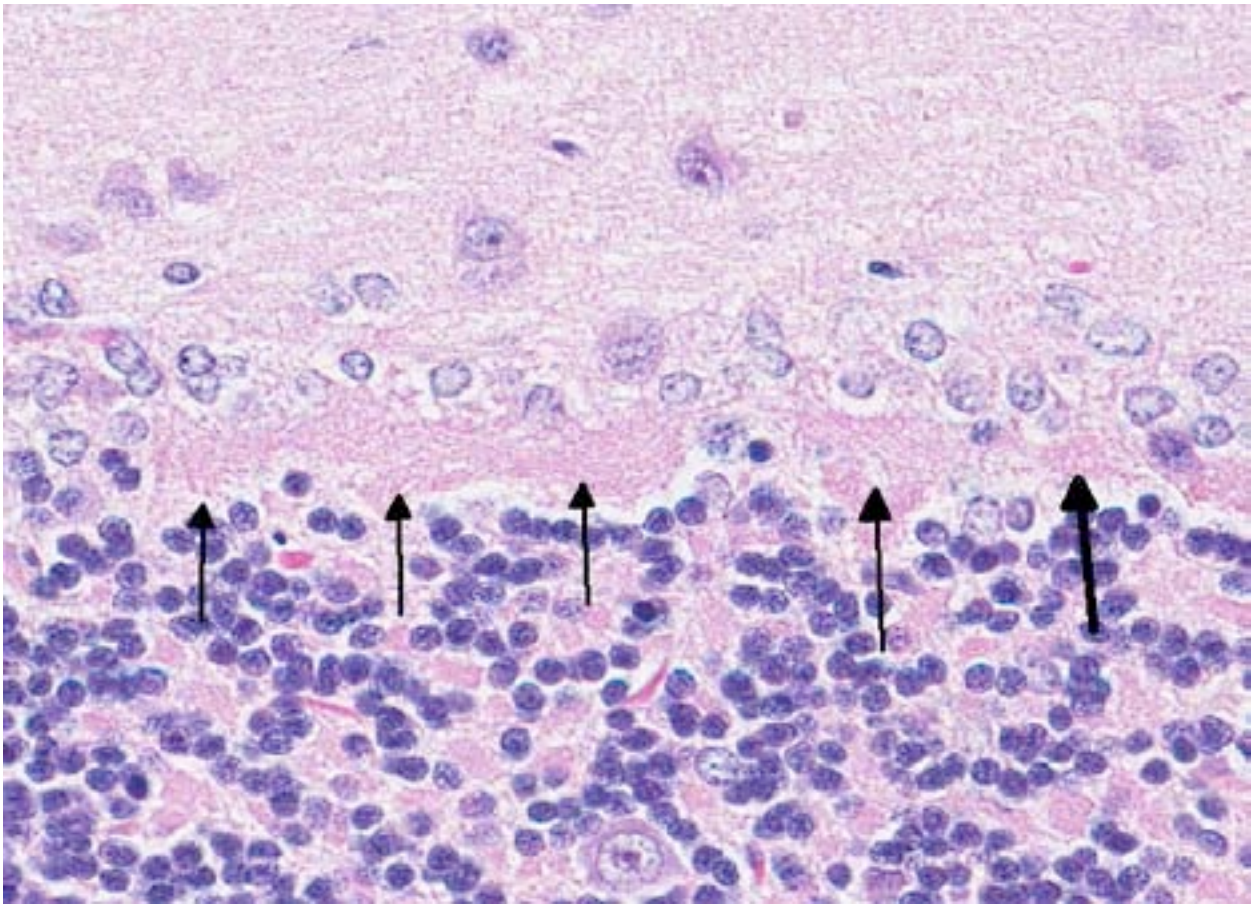

1-2. Cerebellum, meerkat: There is segmental and extensive loss of Purkinje cells, with "empty baskets" formed by the filling in of spaces previously occupied by Purkinje cells with a dense mat of astroglial fibers (arrows). Above the empty baskets are numerous large Bergmann astrocytes. (HE 192X)

postnatal period. However, some animal species may present a neonatal syndrome in which clinical signs are manifested in the immediate postnatal period (bovine and ovine) or can be delayed until time of ambulation (dog).[2,6] In postnatal syndromes, the onset and progression of clinical signs varies from a few days to months with a static course or slow progression.[3] Cerebellar ataxia, head tremor, truncal ataxia, symmetrical hypermetria, spacity, broad-based stance, and loss of balance are the most commonly described clinical manifestations in animals with cerebellar abiotrophy.[3] Besides visual and impaired proprioceptive positioning that were described by the field veterinarian, all the clinical signs evident in this meerkat are compatible with cerebellar disease.[3]

Grossly, the cerebellum can be normal or smaller, which is usually seen later in the course of the disease.[10] In animals that present gross changes of abiotrophy, cerebellar shrinkage can be noticeable with failure to fill the caudal part of the cranial vault, as well as with diminution of individual cerebellar folia, and broadening of sulci.[10] The involvement of the cerebellum is usually not uniform.[10] The cerebellum of the animal of this case was grossly unremarkable.

Microscopically, the distribution and characteristics of lesions vary depending on the species and breed of animals affected, but include: degeneration and loss of Purkinje cells, swelling of Purkinje cell axons, astrogliosis, gliosis of cerebellar nuclei, Wallerian degeneration of the white matter of the folia, and spheroids.[6,10] Proliferation of Bergmann astrocytes is seen in folia where significant Purkinje cell loss has occurred.[10] Because the integrity of the granule cell neuron is dependent on its synaptic relationship with the dendritic zone of the Purkinje neuron, loss of the latter is followed by reduction of the granule cell neurons.[2] The animal in this case presented an apparent increase in the number of granular neurons that was evident when compared with the cerebellum of

the age-matched control. The cause for this finding is undetermined. However, the other two meerkats that were diagnosed with cerebellar abiotrophy presented a decreased cellularity of the granular cell layer when compared with the control. Massive loss of Purkinje cells, which is accompanied by gliosis in the molecular layer, and atrophy of both molecular and granular layers are also features of poisoning in livestock that ingest several species of plants of the genus *Solanum*.[6] The consistency in the age of onset of clinical signs in these meerkats supported the diagnosis of abiotrophy. Extracerebellar lesions of abiotrophy have been described in the cerebellar cortex in the miniature Poodle, spinal Wallerian degeneration in rough-coated and Border Collies, and in Merino sheep.[6] The other sections of the CNS of all three meerkats were histologically normal.

JPC Diagnosis: Cerebellum: Purkinje cell loss, segmental, moderate, with Bergmann's astrocytosis.

Conference Comment: At the start of the conference, the moderator pointed out that most histological findings within the nervous system are, in reality, artifact. He cautioned participants that Purkinje cell degeneration, necrosis and chromatolysis are challenging to definitively identify, as Cytoplasmic darkening, unevenly dispersed Nissl substance and vacuolation are common artifacts in Purkinje cells. Participants briefly discussed the difficulty in differentiating normal gaps in Purkinje cells, which often exhibit irregular spacing, from the true loss observed in cerebellar abiotrophy. A key feature is the presence of increased numbers of Bergmann's astrocytes surrounding empty spaces where Purkinje cells are lost ("empty baskets"). Cerebellar astrocytes are classified broadly as bushy/velate protoplasmic (granular layer), smooth protoplasmic (granular and molecular layers) and Bergmann glial cells.[11] Bergmann glial cells are unipolar protoplasmic astrocytes located around Purkinje cells with long radial processes that enfold the synapses on Purkinje cell dendrites and traverse the molecular layer, terminating on the pial surface; their differentiation, migration and maturation is closely linked with that of the nearby Purkinje cells.[11] Immunohistochemical staining, specifically GFAP, is useful in demonstrating the "empty baskets" surrounded by Bergmann's gliosis that are often evident in cases of cerebellar abiotrophy.[5,11] Conference participants also debated the presence of decreased cellularity of the granular cell layer of the cerebellum, however they were subsequently informed that the contributor actually noted an apparent increase in the number of granular neurons when compared with the cerebellum of an age-matched meerkat control. This is an unexpected finding, as neurons of the granular cell layer are generally lost following the Purkinje cell degeneration and necrosis that characterizes cerebellar abiotrophy.

The contributor provides an excellent summary of cerebellar abiotrophy in various species of veterinary interest. Ruleouts for meerkat cerebellar abiotrophy include cerebellar hypoplasia due to in-utero/perinatal viral infection or toxin ingestion, neuroaxonal dystrophy and lysosomal storage diseases. Feline parvovirus, bovine pestivirus and ovine pestivirus have been shown to cause necrosis of the granular cell layer with resultant cerebellar hypoplasia in kittens, calves and lambs, respectively;[5] however, these viruses are not reported in meerkats. Additionally, when endogenous or exogenous factors such as infectious agents or toxins result in damage to fetal cerebellar components, the animal is typically affected at birth. On the other hand, with cerebellar abiotrophy the animal usually has normal cerebellar components at birth, but is subject to early-onset, hereditary, progressive cerebellar degeneration postnatally,[8] although as noted by the contributor there are exceptions to this generalization. Neuroaxonal dystrophy, reported in dogs, cats, horses and sheep, is a degenerative condition that occasionally affects the cerebellum and is characterized by nerve fiber degeneration and formation of large spheroids.[1,8] Lysosomal storage diseases occur when a lack of specific lysosomal enzymes causes various materials to accumulate in nerve cells and macrophages.[8] Neuroaxonal dystrophy and lysosomal storage diseases have not been reported in meerkats.

Contributing Institution: Texas Veterinary Medical Diagnostic Laboratory
Pathology Section
Drawer 3040
College Station, TX 77841
http://tvmdl.tamu.edu

References:

1. Aleman M, Finno CJ, Higgins RJ, et al. Evaluation of epidemiological, clinical, and pathological features of neuroaxonal dystrophy in Quarter horses. *J Am Vet Med Assoc.* 2011;239(6): 823-833.
2. de Lahunta A. Abiotrophy in domestic animals: a review. *Can J Vet Res.* 1990;54:65-76.
3. de Lahunta A, Glass E. Cerebellum. In: de Lahunta A, Glass E. eds. *Veterinary Neuroanatomy and Clinical Neurology*. 3rd ed. St. Louis, MO: Saunders Elsevier; 2009:348-388.
4. Juan-Salles C, Prats N, Lopez S, Domingo M, Marco AJ, Moran JF. Epizootic disseminated toxoplasmosis in captive slender-tailed meerkats (*Suricata suricatta*). *Vet Pathol.* 1997;34:1-7.
5. Maxie MG, Youssef S. Nervous system. In: Maxie MG, ed. *Jubb, Kennedy, and Palmer's Pathology of Domestic Animals*. 5th ed. Vol. 1. Philadelphia, PA: Elsevier; 2007:281-487.
6. Zachary JF. Central nervous system. In: McGavin MD, Zachary JF, eds. *Pathologic Basis of Veterinary Disease*. 4th ed. St. Louis, MO: Mosby Elsevier; 2007:833-953.
7. Mouser P, Levy M, Sojka JE, Ramos-Vara JA. Cerebellar abiotrophy in an alpaca (*Lama pacos*). *Vet Pathol.* 2009;46:1133-1137.
8. Sato J, Sasaki S, Yamada N, Tsuchitani M. Hereditary cerebellar degenerative disease (cerebellar cortical abiotrophy) in rabbits. *Vet Pathol.* 2012;49(4):621-628.
9. Sladky KK, Dalldorf FG, Steinberg H, Wright JF, Loomis MR. Cholesterol granulomas in three meerkats (*Suricata suricatta*). *Vet Pathol*. 2000;37:684-686.
10. Summers BA, Cummings JF, de Lahunta A. Degenerative diseases of the central nervous system. In: Summers BA, Cummings JF, de Lahunta A, eds. *Veterinary Neuropathology*. 1st ed. St. Louis, MO: Mosby-Yearbook, Inc; 1995:300-307.
11. Yamada K, Watanabe M. Cytodifferentiation of Bergmann glia and its relationship with Purkinje cells. *Anatomical Science International*. 2002;77:94-108.

CASE II: B10-1823-2L (JPC 4032319).

Signalment: 11-year-old male castrated Saint Bernard (*Canis lupus familiaris*).

History: The dog failed to recover normally following general anesthesia for a dental procedure. Upon presentation to an overnight care facility, he was non-ambulatory, minimally responsive, and sedate. Overnight, he had a generalized tonic/clonic seizure and developed anisocoria. By morning, he remained stuporous and unable to rise, but was transiently able to lift his head. Neurologic examination findings were consistent with lesions in the cerebrum and brainstem. MRI and CSF analysis were not performed due to anesthetic concerns. Previous bloodwork revealed severe hypothyroidism.

After weeks of supportive care and physical therapy, the dog was able to eat on his own. He continued to improve at home, though he lacked a menace response in the left eye and intermittently circled to the left. After five months, his neurologic status rapidly deteriorated, with incessant circling, hypersalivation, and multiple seizures. The owners elected euthanasia and histopathologic evaluation of the brain.

Gross Pathology: There was marked atrophy of the entire left cerebral hemisphere, with the rostral portion most severely affected. Blood vessels along the ventral surface of the left side of the brain were markedly thickened, white-tan, and gritty upon sectioning.

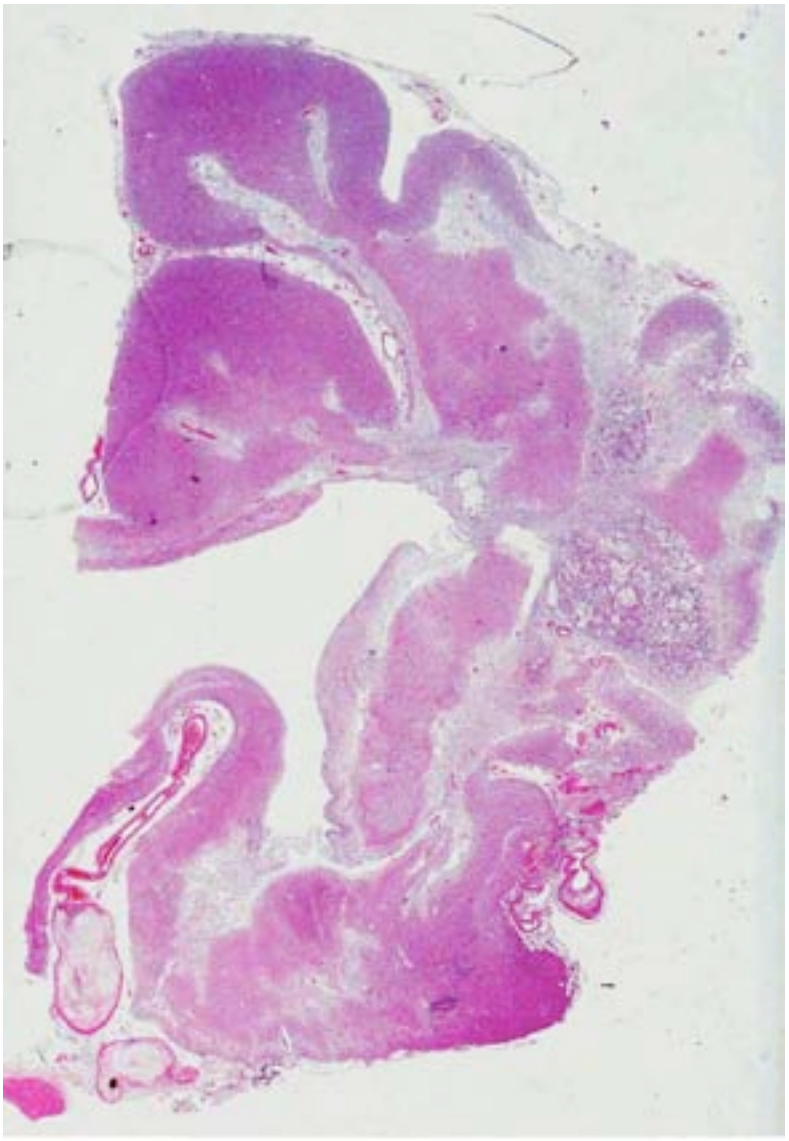

2-1. Cerebrum, cross section at level of putamen, dog: There are multifocal to coalescing areas of pallor (necrosis) within both the gray and white matter, affecting up to 40% of the section, and the lateral ventricle is mildly dilated. (HE 0.63X)

Histopathologic Description: Cerebral hemispheres: Affecting up to 40% of the grey and white matter of the left hemisphere are multiple coalescing foci of malacia, characterized by parenchymal loss with replacement by gitter cells, multinucleated giant cells, acicular (cholesterol) clefts, and scattered mineral (chronic infarcts). The white matter tracts are most severely affected. Adjacent to the malacic foci, the parenchyma is often vacuolated with increased numbers of glial cells (including reactive astrocytes), scattered necrotic neurons, and rare spheroids. The lateral ventricles are dilated (*hydrocephalus ex vacuo*), particularly the left. Within both the left and right hemispheres leptomeningeal blood vessels are often irregularly dilated. The tunica intima and media are expanded by cholesterol clefts and lipid-laden macrophages and leiomyocytes (foam cells) in a fibrous to amorphous eosinophilic fibrillar stroma (atherosclerotic plaques) that narrow the vascular lumina. Within these plaques are occasional foci of

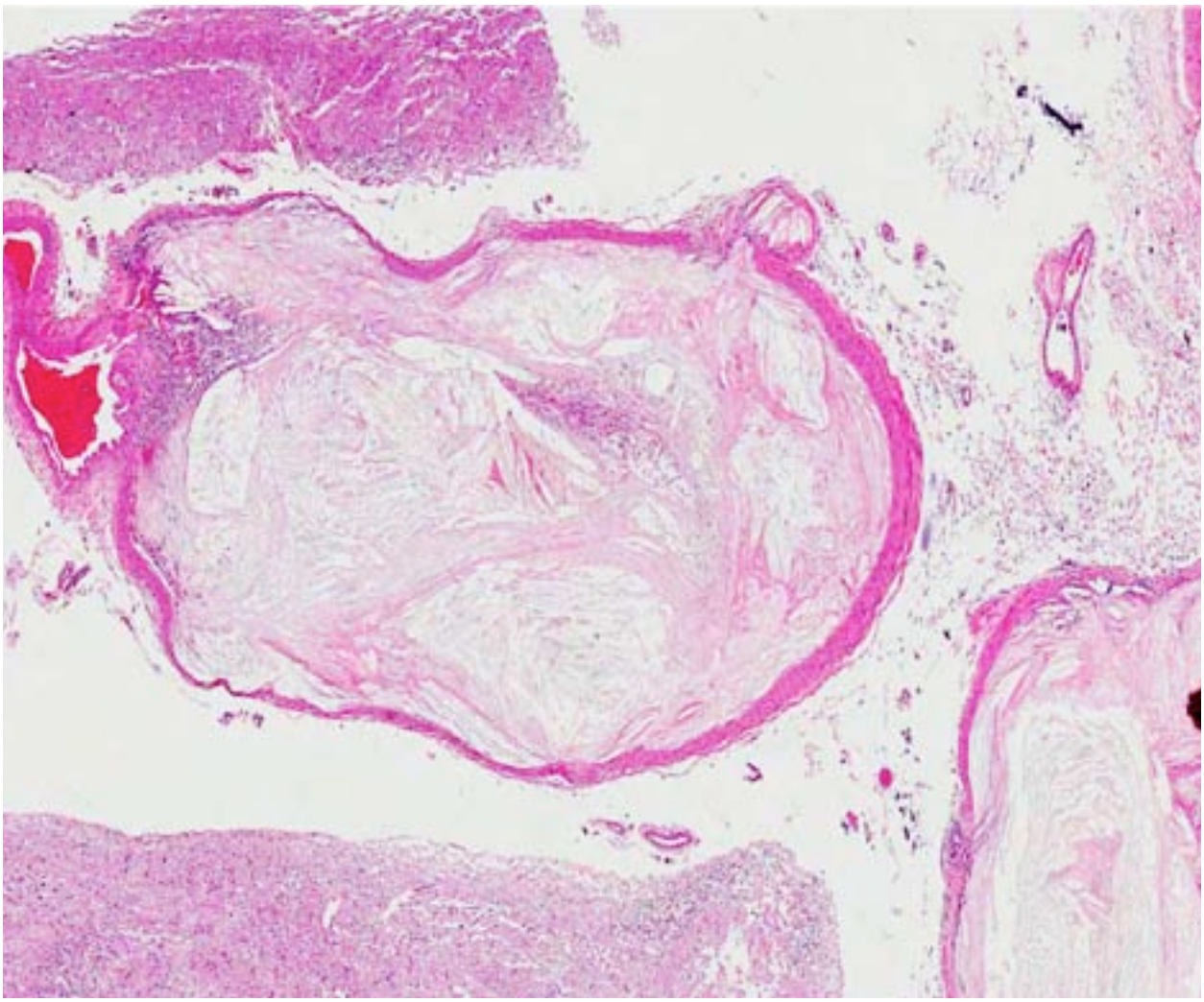

2-2. Cerebrum, cross section at level of putamen, dog: The walls of meningeal arteries at the base of the brain are markedly expanded, effacing the arterial lumens. (HE 23X)

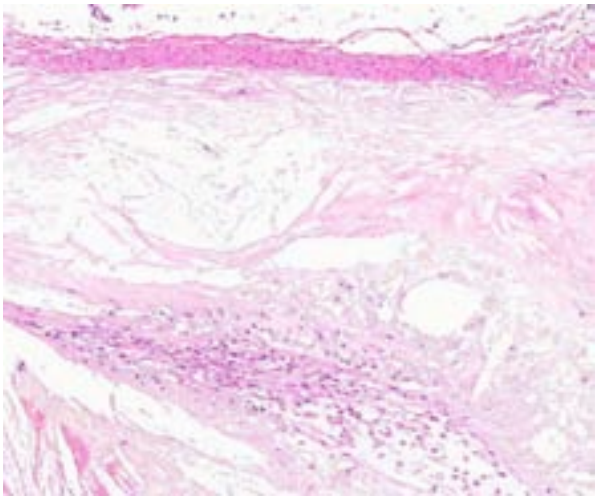

2-3. Cerebrum, cross section at level of putamen, dog: The arterial wall is effaced by abundant lipid, cholesterol clefts, and lipid laden histiocytes ("foam cells"). (HE 120X)

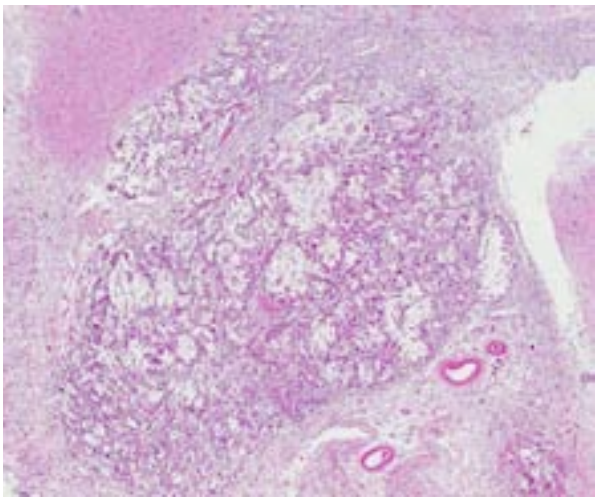

2-4. Cerebrum, cross section at level of putamen, dog: Occasionally, malacic areas are replaced by large cellular cholesterol granulomas. (HE 100X)

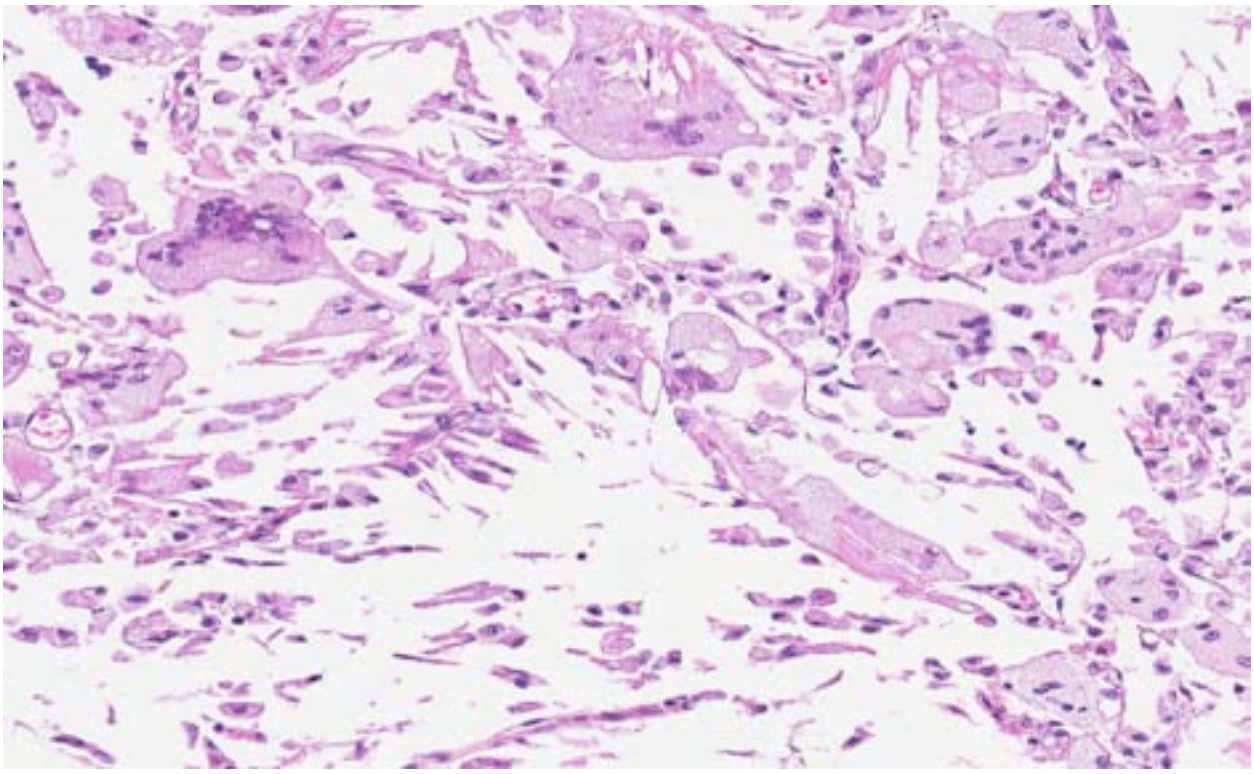

2-5. Cerebrum, cross section at level of putamen, dog: Higher magnification of one of the cholesterol granulomas, exhibit numerous multinucleated foamy macrophages admixed with numerous cholesterol clefts. (HE 300X)

hemosiderin- and hematoidin-laden macrophages and mineral. Low numbers of foamy macrophages, lymphocytes, and plasma cells are within the tunica adventitia and surrounding leptomeninges.

Contributor's Morphologic Diagnosis: Cerebral hemisphere (left): severe multifocal chronic encephalomalacia with cholesterol clefts, gitter cells, and multinucleated giant cells (chronic infarcts).

Leptomeningeal blood vessels: severe multifocal chronic atherosclerosis.

Contributor's Comment: The encephalomalacia in this case is consistent with an infarct secondary to severe atherosclerosis and luminal narrowing of the cerebral arteries, particularly the left rostral cerebral artery. Atherosclerosis is a vascular disease characterized by the formation of atheromas, or atherosclerotic plaques, in the vessel wall.[12] Atherosclerosis and its sequelae, including stroke, myocardial infarcts, and peripheral vascular disease, are leading causes of morbidity and mortality in humans.[10] However, atherosclerosis is infrequent in domestic animals. The disease has been reproduced experimentally in pigs, chickens, and rabbits by feeding high cholesterol diets, but other species (including bovids, goats, cats, dogs, and rats) are considered resistant.[10,11] Naturally-occurring atherosclerosis has been described in aged pigs, birds, and dogs.[11]

Lesions in dogs have been described within the aorta and within small muscular arteries in a variety of organs, including the heart, lung, alimentary tract, spleen, eye, and urogenital and endocrine organs.[6,8] Arteries in the heart, brain, and kidneys are usually most severely affected. Clinical disease is rare and occurs when, as in humans, the atheromas occlude or rupture into the lumen, leading to ischemia, thrombosis, and/or lipid embolism.[10]

On gross examination, affected arteries are yellow-white with thick, irregularly nodular walls and narrowed lumina. Microscopically, early lesions consist of lipid-laden macrophages and leiomyocytes (foam cells) admixed with degenerating leiomyocytes within the tunica media.[8] With progression, the media becomes thicker with replacement of the normal architecture by intra- and extracellular lipid,

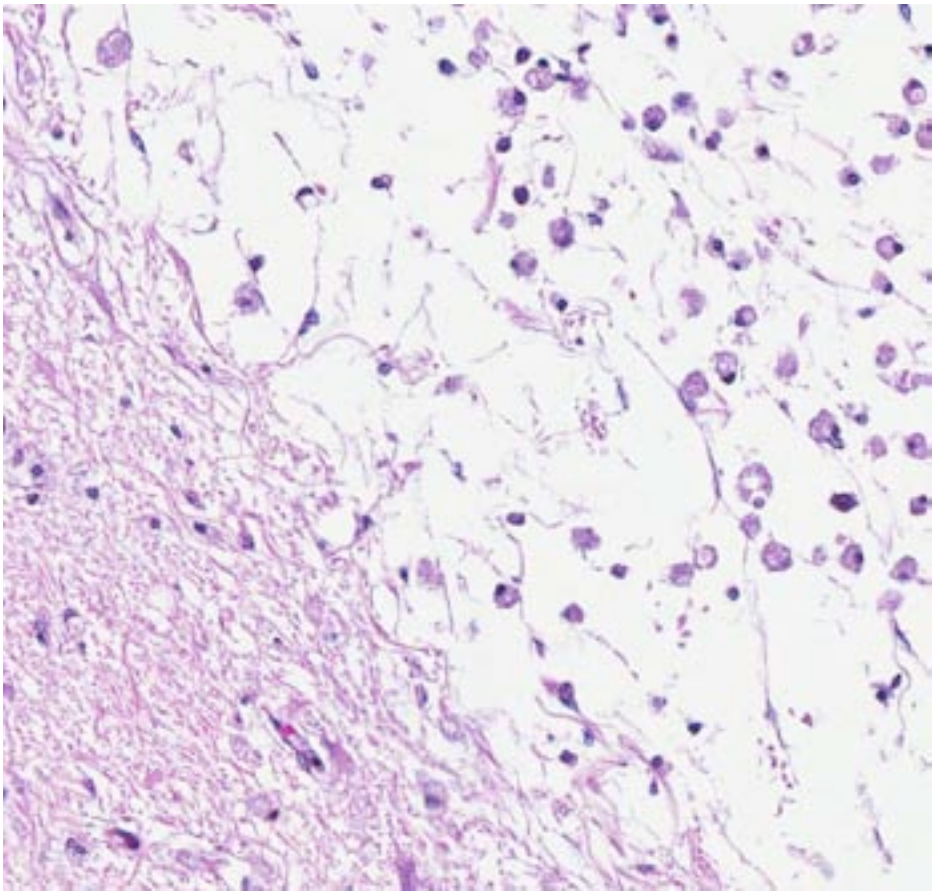

2-6. Cerebrum, cross section at level of putamen, dog: Within the cerebral white matter tracts there are large areas of liquefactive necrosis containing moderate numbers of Gitter cells. (HE 140X)

cholesterol clefts, mineral, cellular debris, and fibrous connective tissue that may become hyalinized.[6,8,10] Severe lesions lead to extension into the adventitia, as well as disruption of the internal elastic lamina and extension into the intima. This is in contrast to human atherosclerosis, where lipid deposition occurs primarily in the intima.[10]

In almost all canine cases, atherosclerosis occurs in association with hypothyroidism and/or diabetes mellitus.[10] Hypercholesterolemia is a common finding in both of these endocrinopathies and is thought to lead to the development of atherosclerosis in affected dogs.[5,10] However, in some dogs, serum cholesterol is normal and no endocrinopathy can be identified.[5] Furthermore, some thyroidectomized dogs on a high-cholesterol diet do not develop atherosclerosis.[10] Thus, other factors, such as genetics, may play a role in the development of canine atherosclerosis. In humans, a genetic predisposition to hyperlipidemia has been shown to increase the risk of atherosclerosis. While certain dog breeds, such as miniature schnauzers and Shetland sheepdogs, have a genetic predisposition to hyperlipidemia, additional studies are needed to determine the risk of atherosclerosis in these dogs.[5]

JPC Diagnosis: Cerebrum at the level of the putamen, gray and white matter: Necrosis, multifocal to coalescing, severe with cholesterol granulomas.

Brain, cerebral arteries: Atherosclerosis, diffuse, severe.

Conference Comment: Spontaneous, diet-induced atherosclerosis is a common condition in pet birds, especially psittacines, White Carneau pigeons and Japanese quails.[2] It is also occasionally reported in captive reptiles.[13] Additionally, the Watanabe heritable hyperlipidaemic (WHHL) rabbit strain, which has a heritable gene mutation that results in hypercholesterolemia and atherosclerosis, has been developed as a model for human atherosclerosis.[1] Atherosclerosis is rare in dogs and it is typically associated with hypercholesterolemia or hyperlipidemia; its development is thought to result from abnormal lipid metabolism, although the exact pathogenesis has not been determined.[8]

There are five major plasma lipids in domestic animals: cholesterol, cholesterol esters, triglycerides and phospholipids are transported as lipoproteins, while nonesterified fatty acids are bound to albumin for transportation.[4] In mammals, dietary lipid is digested by pancreatic lipase and emulsified by bile acids into monoglycerides and free fatty acids. Micelles,

which are formed from monglycerides, fatty acids, cholesterol, bile salts and fat soluble vitamins, are absorbed by jejunal enterocytes, where they are degraded.[4] Chylomicra are synthesized within enterocytes from triglycerides (formed from glycerol and fatty acids), cholesterol esters, cholesterol, phospholipid and apolipoprotein. These chylomicra are then secreted into intestinal lacteals, and they eventually reach the plasma via lymphatics and the thoracic duct. Chylomicra are hydrolyzed by lipoprotein lipase to fatty acids and glycerol, which are absorbed by adipocytes/hepatocytes and stored as triglycerides.[4] Lipid is transported in plasma bound to apolipoprotein, which is synthesized and secreted by the liver. Lipoproteins are classified (with increasing density) as chylomicra, very low density (VLDL), intermediate density (IDL), low density (LDL) or high density (HDL) lipoprotein.[4]

Very low density lipoprotein is synthesized in the liver; in addition to triglyceride, cholesterol and phospholipid (in a ratio of 4:1:1), it has three apolipoproteins: B-100, C and E. ApoC and ApoE are acquired from HDL. The primary function of VLDL is to deliver triglycerides to adipose tissue and striated muscle.[4,13] Within the capillaries of these tissues, VLDL is cleaved by lipoprotein lipase, producing IDL, which retains ApoE and ApoB-100; IDL can then follow two possible pathways: 1) the hepatocyte LDL receptor recognizes ApoB-100 or ApoE, allowing hepatic uptake and recycling to form VLDL, or 2) conversion to LDL by hepatic lipase (in hepatic sinusoidal capillaries) with removal of ApoE and most of the triglyceride. The LDL can then be cleared by the liver via LDL receptor recognition of ApoB-100, or it can be cleared by other methods, especially the monocyte/macrophage system, which contributes to the pathogenesis of atherosclerosis.[4,7,13] Defects in the LDL receptor, such as the inherited LDL receptor defect in Watanabe rabbits or in people with familial hypercholesterolemia,[1] result in increased monocyte/macrophage-mediated clearance of excess LDLs, promoting the formation of xanthogranulomas and atherosclerosis.

Hepatic LDL receptor binding occurs within a clathrin-coated pit where LDL is internalized within a vesicle that fuses with the lysosome, resulting in degradation of ApoB-100 to its constituent amino acids, and the catabolism of cholesterol esters into free cholesterol.[7] The LDL receptor is subsequently recycled to the surface, while free cholesterol exits the lysosome via a process mediated by NPC1 and NPC2. This free cholesterol plays several roles in lipid metabolism. It can be utilized to form cell membrane components, steroid hormones and/or bile salts; it also activates acyl-coenzyme A, which leads to esterification and storage of excess cholesterol.[7] Free cholesterol within hepatocyte cytoplasm also inhibits LDL receptor synthesis, and inhibits HMG CoA reductase, which is the rate-limiting enzyme in cholesterol synthesis.[7]

In humans most cholesterol is transported as LDL, the plasma concentration of which is the most important risk factor for development of atherosclerosis.[14] The lipoprotein profile of swine bears the closest resemblance to that of humans, while dogs and cats have a higher proportion of HDL; as a result dogs and cats are generally considered to be resistant to atherosclerosis.[4] The exact pathogenesis of atherosclerosis in association with canine hypothyroidism has not yet been characterized.[14]

New data suggest an important role for chemokines and chemokine receptors in atherosclerosis,[13] and a recent study showed that advanced glycation end products (AGEs) may play a role in the pathogenesis of atherosclerosis in humans and dogs. Advanced glycation end products belong to group of compounds resulting from glycation and oxidation of proteins, lipids and nucleic acids; specifically, hyperglycemia and oxidant stress contribute to increased formation of AGEs.[3] In humans and dogs, deposition of AGEs has been demonstrated immunohistochemically in atherosclerotic lesions and it has been suggested that AGEs may contribute to the development of atherosclerosis via effects on lipoproteins, extracellular matrix proteins, inflammatory mediators, smooth muscle and vascular endothelial cells.[3] Advanced glycation end products may also suppress cellular antioxidants and induce expression of two important oxidized LDL (OxLDL) receptors: macrophage scavenger receptors class A and CD36. Increased expression of these receptors leads to enhanced uptake of OxLDLs, resulting in the transformation of macrophages to foam cells.[3]

Rule-outs for canine atherosclerosis include arteriosclerosis (i.e., age related, often incidental

intimal fibrosis of large elastic arteries), arterial calcification (e.g., due to renal disease, vitamin D toxicosis, ingestion of calcinogenic plants or infectious diseases) or lysosomal storage diseases such as Mucopolysaccharidosis-I (MPS-I). Mucopolysaccharidosis-I is an inherited, autosomal recessive deficiency of α-L-iduronidase that causes lysosomal accumulation of glycosaminoglycans (GAGs) in a variety of cell types, including those within the vascular system (see WSC 2013-14, conference 5, case 2).[9] A similar disease (i.e., Hurler/Scheie syndrome) affects humans.[7] Some dogs with MPS-I develop occlusive plaques affecting the tunica intima of medium to large arteries near branch points, or areas of low shear stress, such as the distal aorta or coronary and mesenteric arteries.[9] Histologically, intimal plaques consist of abundant extracellular matrix admixed with foamy (i.e., GAG-laden) macrophages, fibroblasts and smooth muscle cells.[9]

Contributing Institution: Laboratory of Pathology and Toxicology
University of Pennsylvania
School of Veterinary Medicine
Philadelphia, PA USA
http://www.vet.upenn.edu/

References:

1. Alley G, Burnstock G. Watanabe rabbits with heritable hypercholesterolemia: a model of atherosclerosis. *Histol Histopathol.* 1998;13(3): 797-817.
2. Beaufrere H, Nevarez JG, Wakamatsu N, Clubb S, Cray C, Tully TN. Experimental diet-induced atherosclerosis in Quaker parrots (*Myiopsitta monachus*). *Vet Pathol*. 2013;50(6):1116-1126.
3. Chiers K, Vandenberge V, Ducatelle R. Accumulation of advanced glycation end products in canine atherosclerosis. *J Comp Pathol*. 2010;143(1):65-69.
4. Evans EW. Proteins, lipids and carbohydrates. In: Latimer KS, ed. *Duncan and Prasse's Veterinary Laboratory Medicine Clinical Pathology*. 5th ed. Ames, IA: John Wiley and Sons; 2011:183-191.
5. Hess RS, Kass PH, Van Winkle, TJ. Association between diabetes mellitus, hypothyroidism or hyperadrenocorticism, and atherosclerosis in dogs. *J Vet Intern Med*. 2003;17:489-494.
6. Kagawa Y, Hirayama H, Uchida E, Izumisawa Y, Yamaguchi M, Kotani T, et al. Systemic atherosclerosis in dogs: histopathological and immunohistochemical studies of atherosclerotic lesions. *J Comp Path*. 1998;118:195-206.
7. Kumar V, Abbas AK, Fausto N, Aster JC, eds. Genetic disorders. In: *Robbins and Cotran Pathologic Basis of Disease*. 8th ed. Philadelphia, PA: Saunders Elsevier; 2010:147-150.
8. Liu S, Tilley LP, Tappe JP, Fox PR. Clinical and pathologic findings in dogs with atherosclerosis: 21 cases (1970-1983). *J Am Vet Med Assoc*. 1986;2:227-232.
9. Lyons JA, Dickson PL, Wall JS, et al. Arterial pathology in canine mucopolysaccharidosis-I and response to therapy. *Lab Invest*. 2011;91(5): 665-674.
10. Maxie MG, Robinson WF. Cardiovascular system. In: Maxie MG, ed. *Jubb, Kennedy, and Palmer's Pathology of Domestic Animals.* 5th ed. Vol 3. St. Louis, MO: Saunders Elsevier; 2007:57-59.
11. Miller LM, Van Vleet JF, Gal A. Cardiovascular system and lymphatic vessels. In: Zachary JF, McGavin MD, eds. *Pathologic Basis of Veterinary Disease*. 5th ed. St. Louis, MO: Elsevier; 2012:560-561.
12. Mitchell RN, Schoen FJ. Blood vessels. In: Kumar V, Abbas AK, Fausto N, Aster JC, eds. *Robbins and Cotran Pathologic Basis of Disease*. 8th ed. Philadelphia, PA: Saunders Elsevier; 2010:496.
13. Schillinger L, Lemberger K, Chai N, Bourgeois A, Charpentier M. Atherosclerosis associated with pericardial effusion in a central bearded dragon (*Pogona vitticeps*). *J Vet Diagn Invest*. 2010;22:789-792.
14. Vitale CL, Olby NJ. Neurologic dysfunction in hypothyroid, hyperlipidemic Labrador retrievers. *J Vet Intern Med*. 2007;21(6): 1316-1322.

CASE III: NIAH 2013 1 (JPC 4035522).

Signalment: 110-days of gestation male mixed-breed stillbirth fetus, pig (*Sus scrofa domesticus*).

History: From September to October 2005, a total of 6 sows in a herd of 13 aborted. On the morning of October 12, 2005, a litter of 19 piglets from one sow was found as stillbirth feti, including two cases of mummification. Two of those stillborn piglets were in fair postmortem condition and were submitted for necropsy. Sows had been vaccinated for Aujeszky's disease virus (ADV) but not for Japanese encephalitis virus (JEV).

Gross Pathology: The brain was slightly swollen and edematous at necropsy. No obvious gross abnormalities were seen in other examined organs.

Laboratory Results:

- No significant bacteria or viruses were isolated from the fetus.
- JEV Hemagglutination inhibition (HI) titers from the body fluid of stillborn piglets: ~10 to~640.
- JEV HI titers from sows that aborted: ~640 to ~5120.
- Serological tests for porcine reproductive respiratory syndrome virus (PRRSV), porcine parvovirus (PPV), ADV and toxoplasmosis were all negative.
- PCR for PRRSV and PPV were negative.

Histopathologic Description: Cerebrum: There was nonsuppurative encephalitis characterized by perivascular cuffing with mononuclear cells, multifocal gliosis and severe neuronal necrosis. Mild meningitis was also observed in the cerebral hemisphere. In the brainstem, there was severe multifocal necrosis with hemorrhage in addition to the nonsuppurative inflammation. Basophilic granular material was noted multifocally within necrotic lesions. These basophilic granules stained black with Von Kossa and were identified as calcification. JEV antigen was immunohistochemically detected in the cytoplasm of nerve cells within the lesions.

Spinal cord (not included): There was nonsuppurative poliomyelitis characterized by perivascular cuffing with mononuclear cells, diffuse and multifocal gliosis and severe neuronal necrosis. JEV antigen was immunohistochemically detected in the cytoplasm of nerve cells within the lesions.

Histological lesions and viral antigen were restricted to the central nervous system. There were no lesions in the other examined organs including the liver, spleen, kidney, heart, lung and lymph node.

Contributor's Morphologic Diagnosis: Cerebrum: Meningioencephalitis, nonsuppurative, necrotizing, diffuse, moderate to severe, Japanese encephalitis, stillbirth fetus, pig.

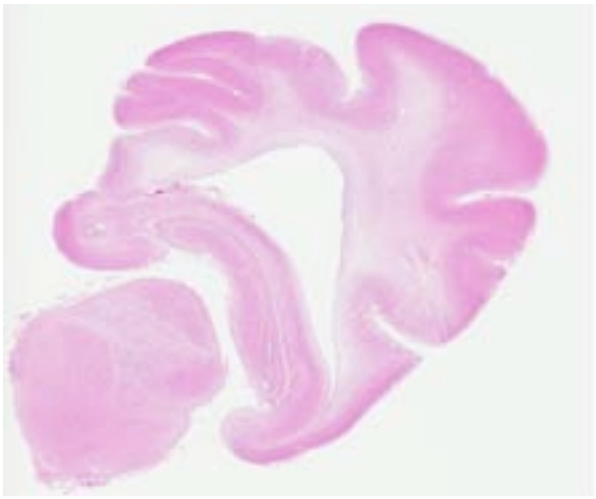

3-1. Cerebrum at level of hippocampus, one-day old piglet: At subgross inspection there is marked pallor of the cerebral white matter. This is considered an appropriate level of myelination at this age. (HE 0.63X)

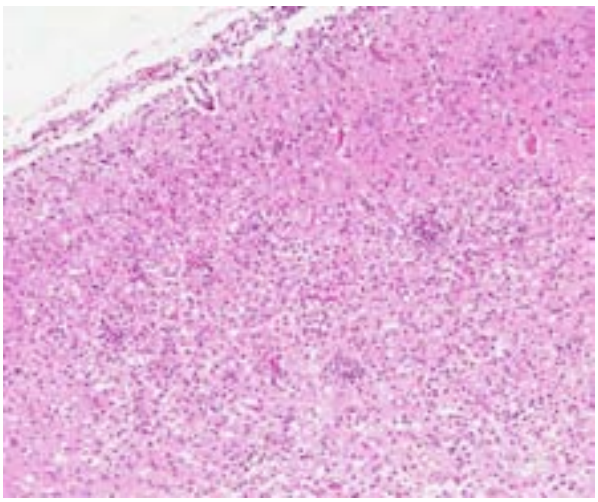

3-2. Cerebrum at level of hippocampus, one-day old piglet: There is marked inflammation of the superficial cortex as well as the overlying meninges. (HE 140X)

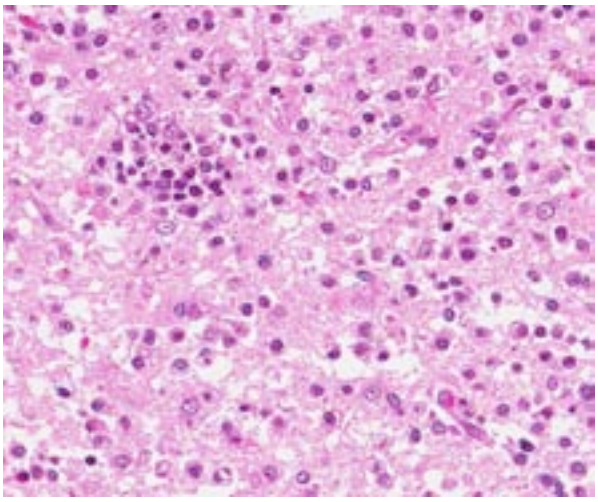

3-3. Cerebrum at level of hippocampus, one-day old piglet: Within areas of inflammation, neutopil is spongiotic and infiltrated with low to moderate numbers of histiocytes and lymphocytes, which are concentrated in perivascular areas. There are also increased numbers of reactive astrocytes within these areas. (HE 325X)

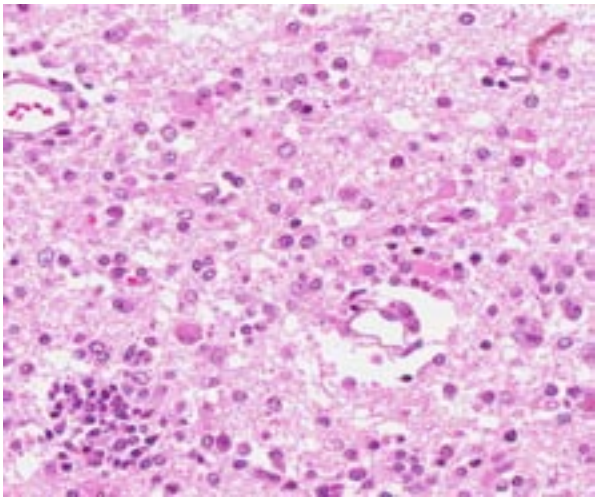

3-4. Cerebrum at level of hippocampus, one-day old piglet: Within areas of inflammation there are numerous reactive astrocytes with abundant eosinophilic cytoplasm (gemistocytes). (HE 400X)

Contributor's Comment: Japanese encephalitis virus (JEV) is one of four major encephalitic flaviviruses of public health importance; the other three are West Nile virus (WNV), St. Louis encephalitis virus (SLEV) in North America, and Murray Valley encephalitis virus (MVEV) in Australasia.[6] JEV is transmitted by mosquitoes of the genus *Culex*.[3,10] A wide range of domestic and wild avian and mammalian species including humans, horses, and swine are infected in nature.[10] Pigs are considered to be amplifier hosts with viremia that makes the virus available to mosquitoes.[3] Adult, non-pregnant swine typically do not exhibit overt signs of infection.[10] Reproductive failure may occur in non-immune females that become infected prior to 60-70 days gestation.[10] Pregnant sows may abort, produce mummified fetuses or give birth to stillborn or weak piglets.[10] Nonsuppurative fetal encephalitis has been described in cases of JEV abortion.[1]

In the present case, JEV antigen was immunohistochemically detected in the cytoplasm of intralesional nerve cells. An immunohistochemical method for diagnosing JEV in formalin-fixed tissues from infected pigs would be useful as a simple and rapid diagnostic test. JEV antigen was immunohistochemically detected in the nerve cells within areas of nonsuppurative encephalitis in 3-week-old pigs experimentally infected with JEV.[12,13] However, postmortem changes prevent immunohistochemical detection of viral antigen in many cases of aborted fetuses. Therefore, there are limited reports of immunohistochemical detection of JEV antigen in aborted fetuses. The present case shows that immunohistochemical detection of JEV antigen is also of diagnostic importance in those aborted fetuses with a relative lack of postmortem change.

In the present case, the virus was not isolated from stillbirth fetus. It appears that successful isolation of JEV from pigs of abnormal litters is dependent on the time that pigs were exposed to the virus in utero. It was reported that JEV was successfully isolated from feti of 3 litters that were collected at 7 to 22 days after experimental inoculation of sows with JEV, but not from affected pigs of 2 litters that were collected 62 and 84 days after infection of sows.[11] Detection of JEV specific antibody in body fluids of aborted fetuses by HI is a useful method for diagnosis.[10] The present case was diagnosed as Japanese encephalitis based on clinical history, histopathological findings, detection of JEV specific antibody by HI and immunohistochemical detection of JEV antigen in the brain lesions.

JPC Diagnosis: Cerebrum at the level of the hippocampus: Meningoencephalitis, necrotizing, nonsuppurative, focally extensive, marked, with gliosis.

Conference Comment: The family *Flaviviridae* is composed of three genera: Flavivirus, Pestivirus and Hepacivirus.[7] The genus

Flavivirus contains multiple viruses of veterinary importance, many of which are mosquito or tick-borne, including Japanese encephalitis virus, West Nile virus, Wesselsbron virus, and several less well-described flaviviruses in central Europe and South America.[7] Other flaviviruses of public health significance include Yellow-fever virus, dengue virus, St. Louis encephalitis virus, and Murray Valley encephalitis virus.[7] The flaviviral genome is composed of positive-sense ssRNA with a 5' terminal cap structure.[7]

As its name implies, Japanese encephalitis virus primarily occurs in Asia and Southeast Asia, especially in areas with extensive freshwater marshes or irrigated rice fields. The primary vector is the *Culex* mosquito.[7] Swine do not typically develop clinical disease when infected with this flavivirus (with exceptions as noted by the contributor); they function as disease amplifiers and they are often used as sentinels for monitoring Japanese encephalitis virus in endemic areas. In addition to swine, wild birds have been implicated as amplifying hosts in virus transmission.[3] Viral titers in horses and humans are likely insufficient for re-infection of mosquito vectors, so these species are considered dead-end hosts.[3] Japanese encephalitis virus is one of the most frequent causes of human encephalitis in Asia[3] and it can also cause fatal encephalitis in horses.[12] Routes of flaviviral neuroinvasion remain somewhat controversial. Historically, hematogenous spread to the CNS was the presumed route of infection, however recent studies also support retrograde axonal transport via olfactory nerves.[2,13]

West Nile virus is also transmitted by *Culex* mosquitoes, with wild birds functioning as the primary amplifying hosts.[4] American crows and other corvids (blue jays, magpies), passerines, raptors, shorebirds and flamingos are highly susceptible, while domestic poultry and psittacines are generally resistant to fatal infection with WNV.[8] Common histopathological findings in WNV infected wild birds include meningoencephalitis, myocarditis, splenic and bone marrow necrosis; viral antigen is most commonly detected in the kidney, brain and heart.[4] In contrast to the high-titer viremia and widespread necrosis and inflammation found in wild birds, horses tend to have a transient, low-titer viremia with primarily central nervous system involvement.[4] Histological lesions in equids typically include lymphocytic polioencephalomyelitis, predominantly within the lower brain stem and ventral horns of the thoracolumbar spinal cord, with perivascular cuffing and scattered hemorrhage.[2] In addition to wild birds, horses, mules, donkeys and pigs,[5] clinical disease due to WNV has also been reported in reindeer,[9] and Eastern fox squirrels and humans.[5]

Wesselsbron virus, a flavivirus transmitted by *Aedes* mosquitoes, is important in sub-Saharan Africa, where it causes acute disease resembling Rift Valley fever in sheep.[7] Wesselsbron disease causes high mortality in newborn lambs and kids, with subclinical infection or sporadic abortions in adults.[7]

The mosquito-born flaviviruses described above are typically neurotropic, however yellow fever virus and Dengue virus, which affect humans and monkeys, are viscerotropic, causing hemorrhagic fever rather than encephalitis.[4] Yellow fever virus was originally transported (via its *Aedes* mosquito vector) to the "New World" on slave ships, where it decimated the populations of many coastal cities in the 18th and 19th centuries.[7] Disease is biphasic, beginning with fever, headache and nausea, followed by eventual hepatic and renal failure. The widespread icterus often observed with this disease led to the name "yellow fever."[7] Old world monkeys tend to have subclinical infections, while New World monkeys develop clinical disease with high mortality.[7] Infection is characterized by widespread midzonal hepatic necrosis, acute renal tubular necrosis and multifocal lymphoid necrosis. Dengue fever is one of the most important viral arthropod-borne hemorrhagic diseases in the world today. African monkeys have been implicated as the original reservoir of the dengue virus, and may still play a role in transmission, however the urban mosquito *Aedes aegypti/albopictus* is currently the most widely recognized vector in most outbreaks.[7]

Contributing Institution: National Institute of Animal Health, Japan
http://www.naro.affrc.go.jp/org/niah/

References:

1. Burns KF. Congenital Japanese B encephalitis infection of swine. *Proc Soc Exp Biol Med.* 1950;75:621-625.

2. Cantile C, Del Piero F, Di Guardo G, Arispici M. Pathologic and immunohistochemical findings in naturally occurring West Nile virus infection in horses. *Vet Pathol.* 2001;38(4):414-421.
3. Endy TP, Nisalak A. Japanese encephalitis virus: ecology and epidemiology. *Curr Top Microbiol Immunol*. 2002;267:11-48.
4. Kimura T, Sasaki M, Okumura M, Kim E, Sawa H. Flavivirus encephalitis: pathological aspects of mouse and other animal models. *Vet Pathol*. 2010;47(5):806-818.
5. Kiupel M, Simmons HA, Fitzgerald SD, et al. West Nile virus infection in Eastern fox squirrels (*Sciurus niger*). *Vet Pathol*. 2003;40(6):750-752.
6. Mackenzie JS, Barrett, AD, Deubel V. The Japanese encephalitis serological group of flaviviruses: a brief introduction to the group. *Curr Top Microbiol Immunol*. 2002;267:1-10.
7. MacLachlan NJ, Dubovi EJ, eds. *Fenner's Veterinary Virology*. 4th ed. London, UK; 2011:467-475.
8. Maxie MG, Youssef S. Nervous system. In: Maxie MG, ed. *Jubb, Kennedy, and Palmer's Pathology of Domestic Animals.* 5th ed. Vol 1. St. Louis, MO: Saunders Elsevier; 2007:421-422.
9. Palmer MV, Stoffregen WC, Rogers DG, et al. West Nile virus infection in reindeer (*Rangifer tarandus*). *J Vet Diagn Invest*. 2004;16(3): 219-222.
10. Platt KB, Joo HS. Japanese encephalitis and West Nile virus. In: Straw BE, Zimmerman JJ, D'Allaire S, Taylor DJ, eds. *Disease of Swine*. 9th ed. Ames, IA: Iowa state University Press; 2006:359-365.
11. Shimizu T, Kawakami Y, Fukuhara S, Matsumoto M. Experimental stillbirth in pregnant swine infected with Japanese encephalitis virus. *Jpn J Exp Med*. 1954;24:363-375.
12. Yamada M, Nakamura K, Yoshii M, Kaku Y. Nonsuppurative encephalitis in piglets after experimental inoculation of Japanese encephalitis flavivirus isolated from pigs. *Vet Pathol*. 2004;41:62-67.
13. Yamada M, Nakamura K, Yoshii M, Kaku Y, Narita M. Brain lesions induced by experimental intranasal infection of Japanese encephalitis virus in piglets. *J Comp Pathol.* 2009;141:156-162.

CASE IV: F1021947 (JPC 4002855).

Signalment: 11-year-old spayed female Pembroke Welsh Corgi dog (*Canis lupus familiaris*).

History: One year duration of immune-mediated hemolytic anemia (IMHA) with recent resolution of pneumonia. The dog presented to Colorado State University Veterinary Teaching Hospital for acute onset of panting and reluctance to move.

Gross Pathology: The abdomen is pendulous with approximately 20 milliliters of brown, thick fluid which is confined to the left cranial dorsal quadrant. This fluid corresponds to a full thickness, elliptical perforation of the gastric fundus measuring 1 ½ cm in length with regional serosal fibrinous adhesions to the omentum. There are multifocal hemorrhages within the greater leaf of the omentum and greater curvature of the stomach. The liver is mild to moderately enlarged diffusely with rounded edges and contains multiple tan, soft, round nodules that exude thick viscous material and measuring 1mm-2cm in diameter. Within the left frontal lobe there is a moderately well demarcated, soft, gelatinous, gray to tan foci measuring no more than 2cm in diameter. There are multifocal renal, capsular pits which correspond with collapse and loss of cortical parenchyma.

Laboratory Results:

Complete blood count:

Parameter	**Result**	**Reference Range**
Nucleated cells	2.9 x 10^3/µl	4.5-15.0 x10^3/µl
Segmented neutrophils	1.9x10^3/µl	2.6-11.0x10^3/µl
Lymphocytes	0.2x10^3/µl	1.0-4.8x10^3/µl
Eosinophils	0.1x10^3/µl	0.1-1.2x10^3/µl
nRBCs	0.1 x10^3/µl	0.0x10^3/µl
RBC	4.1x10^3/µl	5.5-8.5x10^3/µl
HGB	9.7 g/dl	13.0-20.0 g/dl
PCV	30.0%	40.0-55.0%
MCV	75.0 fl	62.0-73.0 fl
MCHC	32.0 g/dl	33.0-36.0 g/dl
Reticulocytes	85,050/µl	0.0-60,000/µl

Serum chemistry:

Parameter	**Result**	**Reference Interval**
Total protein	7.3 gm/dl	5.3-7.2 gm/dl
Globulin	3.9 gm/dl	2.0-3.8 gm/dl
ALP	437 IU/l	20-142 IU/l
ALT	179 IU/l	10-110 IU/l
GGT	68 IU/l	0-9 IU/l
Glucose	534 mg/dl	75.0-130.0 mg/dl
Anion gap	26	13-22

Blood gas (venous):

Parameter	**Result**	**Reference Interval**
pH	7.119	7.3-7.5
pCO2	40.3 mmHG	24.0-39.0 mmHG
pO2	166.0 mmHG	67.0-92.0 mmHG
HCO3	12.5 mm/L	15.0-24.0 mm/L
Anion gap	24 mEq/l	13.0-22.0 mEq/l

Histopathologic Description: Brain: Focally expanding approximately 25% of the section there is rarefaction and effacement of the neuropil by marked numbers of inflammatory cells, karyorrhectic debris and abundant numbers of brown pigmented fungal hyphae. Hyphae have parallel walls and are occasionally septate and

branching. Inflammatory infiltrates consist primarily of epithelioid macrophages, occasionally multinucleated cells and intact and degenerative neutrophils. Hyphae are typically extracellular but a few are intimately associated with multinucleated cells. Vessels within this region are lined by prominent, hypertrophied endothelium, surrounded and disrupted by macrophages, lymphocytes, plasma cells and lesser neutrophils. Multifocally there are patches of perivascular fibrin exudate. At the periphery of this region there are scattered neurons with pale nuclei and dispersion of Nissl substance (chromatolysis). The leptomeninges contain moderate perivascular lymphocytes and plasma cells.

Contributor's Morphologic Diagnosis: Brain: Pyogranulomatous encephalitis, focally extensive, marked with intralesional dematiaceous fungal hyphae and vasculitis.

Contributor's Comment: Phaeohyphomycosis in domestic animals is an uncommon, opportunistic infection caused by a variety of fungal species.[4] Characteristic of phaeohyphomycotic fungi is the presence of variable melanin pigment in the cell wall giving it a distinct brown color.[4] Production of melanin pigment is thought to contribute to the organism's virulence.[4,9] DHN-melanin (1, 8-dihydroxynaphthalene) and DOPA-melanin (L-3, 4-dihydroxyphenylalanine) are two specific melanin pigments thought to play a role in the pathogenicity of dematiaceous fungi.[9] The role of such pigment has been implicated in contributing to organism's resistance to ultraviolet radiation, extreme temperature variation, oxidation, enzymatic degradation, as well as structural functions and guarding against desiccation.[2,9,14]

The various fungal species are not morphologically distinct on routine H&E histologic examination.[4] Culture, fungal morphology or molecular techniques are generally required for speciation.[6] Organisms in general have a dark brown to light yellow pigment, although degree of pigmentation can vary, and

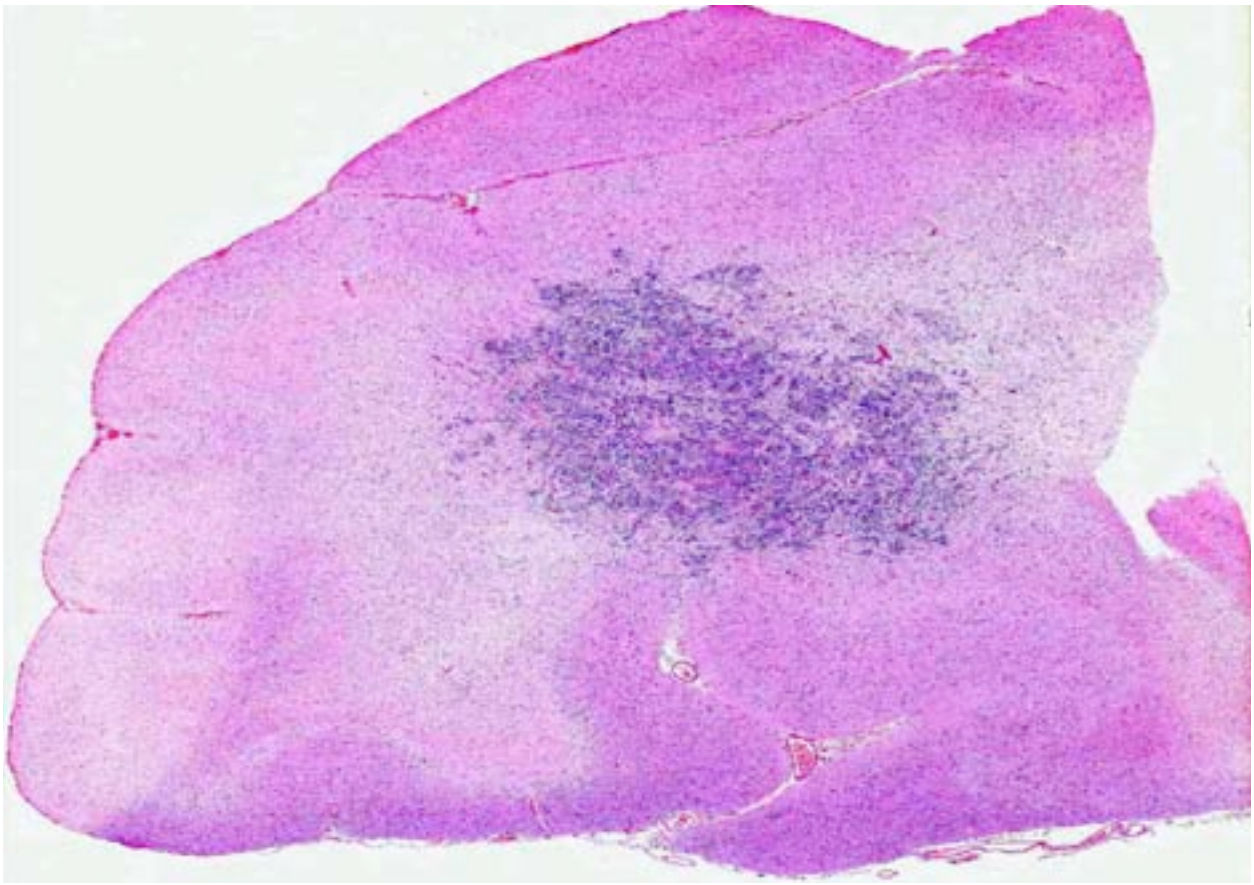

4-1. Cerebrum, dog: Within the frontal lobe there is a focally extensive area of inflammation and necrosis. (HE 0.63X)

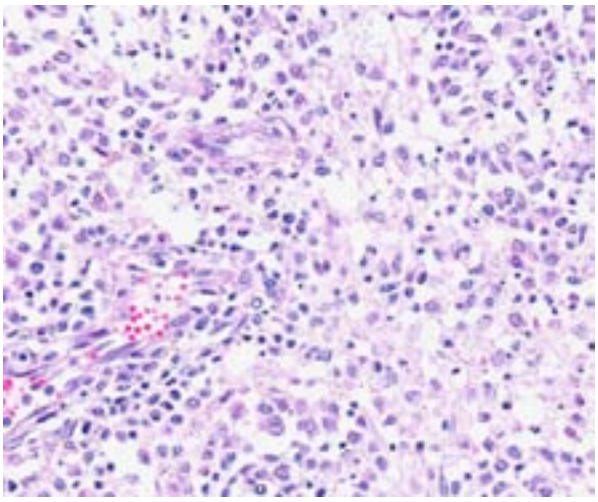

4-2. Cerebrum, dog: Necrotic foci are infiltrated by large numbers of histiocytes, moderate numbers of neutrophils, and rare multinucleated macrophages. Inflammation is concentrated in perivascular areas; vascular endothelium is markedly hypertrophic. (HE 200X)

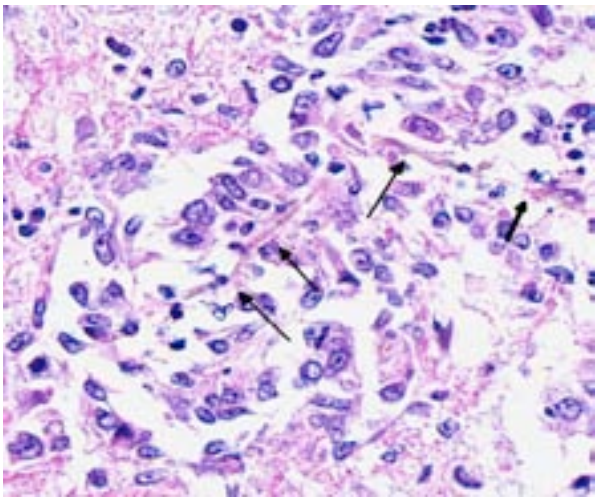

4-3. Cerebrum, dog: Scattered throughout areas of necrosis and inflammation are rare 3-5 diameter, pauciseptate, lightly pigmented fungal hyphae with parallel walls, consistent with dematiaceous fungi. (HE 400X)

have 2-6 µm in width septate hyphae that can be branched or unbranched.[4,7] If melanin pigment is not identifiable, Fontana-Masson histochemical stain may assist in identification of subtle pigment.[4,7]

Phaeohyphomycotic fungi are composed of more than 100 different dematiaceous species presenting clinically as cutaneous, central nervous system and disseminated infections.[6,14,16] Reported most frequently in cats, phaeohyphomycosis has been occasionally documented in horses, dogs, cattle and goats.[5,7,12,15] Typically feline infections are limited to subcutaneous tissues although disseminated and cerebral forms do occur and are most often associated with immunologic compromise.[14,16] Cutaneous forms are thought to occur due to introduction of the organism via a penetrating wound.[14,16] Specifically, *Cladophialophora bantiana*, (also known as *Cladosporium bantianum*, *Cladosporium trichoides*, and *Xylohypha bantiana)* has a tropism for nervous tissue and has been reported as a cause for cerebral phaeohyphomycosis in both dogs and cats.[11,12]

Immunosuppression likely contributed to the pathogenesis of cerebral phaeohyphomycosis in this dog with a history of cyclosporine and prednisone administration for treatment of IMHA. Route of infection was unclear at the time of necropsy although ultimately hematogenous dissemination was suspected due to the presence of fungal organisms within the liver. Cutaneous infection may have been the route of entry although lesions were absent at necropsy examination. Ingestion of the fungus and entry via the compromised stomach was considered but unlikely due the absence of histologic identification of the organism within sections of the stomach at the location and distant to the perforation.

JPC Diagnosis: Cerebrum: Encephalitis, necrotizing and granulomatous, multifocal to coalescing, severe, with vasculitis, mild lymphohistiocytic meningitis and rare dematiaceous fungal hyphae.

Conference Comment: Several species of dematiaceous fungi demonstrate a predilection for the central nervous system and phaeohyphomycosis (cerebral and/or disseminated) has been reported in an alpaca, a snow leopard, reptiles, including a tortoise and an iguana and leafy and weedy seadragons,[1,3,8,13] in addition to the domestic species previously listed.

As noted in the summary, immunosuppression secondary to repeated administration of cyclosporine and prednisone for treatment of immune mediated hemolytic anemia likely predisposed this dog to fungal infection. With that in mind, conference participants briefly discussed the clinical pathologic findings in this case, which were consistent with the history of treatment for IMHA and the diagnosis of disseminated phaeohyphomycosis. Macrocytic,

hypochromic, regenerative anemia is an expected finding in dogs with IMHA.[10] Corticosteroid treatment typically induces lymphopenia, and while neutrophilia is a common finding in cases of hemolysis and corticosteroid administration, the neutropenia observed in this case probably occurred due to the disseminated fungal infection.[10] Globulin concentration also increases in infection and inflammation.[10] Anemia induced hypoxic injury to centrilobular hepatocytes may result in elevation of ALT, while increased ALP and GGT may occur following corticosteroid-induced hepatocellular glycogen accumulation.[10] Corticosteroids also induce hyperglycemia.[10]

Contributing Institution: Colorado State University
Diagnostic Medicine Center
300 West Drake Road
Fort Collins, CO 80523-1644
www.dlab.colostate.edu

References:

1. Bonar CJ, Garner MM, Weber ES 3rd, et al. Pathologic findings in weedy (*Phyllopteryx taeniolatus) and leafy (Phycodurus eques)* seadragons. *Vet Pathol*. 2013;50(3):368-376.
2. Fothergill AW. Identification of dematiaceous fungi and their role in human disease. Clinical Infectious Diseases. 1996;22(8uppl 2): 8179-8184.
3. Frank C, Vemulapalli R, Lin T. *Cerebral phaeohyphomycosis due to Cladophialophora bantiana* in a Huacaya alpaca (*Vicugna pacos*). *J Comp Pathol*. 2011;145(4):410-413.
4. Ginn PE, Mansell JEKL, Rakich PM. Skin and appendages. In: Maxie MG, ed. *Jubb, Kennedy and Palmer's Pathology of Domestic Animals*. 5th ed. Vol. 1. Philadelphia, PA: Elsevier Inc; 2007:702-703.
5. Giri DK, Sims WP, Sura R, Cooper JJ, Gavrilov BK, et al. Cerebral and renal phaeohyphomycosis in a dog infected with *Bipolaris* species. *Vet Pathol*. 2011;48:754-757.
6. Grooters AM, Foil CS. Miscellaneous Fungal Infections. In: Greene CE ed.
Infectious Disease of the Dog and Cat. 3rd ed. Elsevier Inc; 2006:647-649.
7. Herra´ez P, Rees C, Dunstan R. Invasive phaeohyphomycosis caused by *Curvularia* species in a dog. *Vet Pathol*. 2001;38:456–459.
8. Janovsky M, Grone A, Ciardo D, Vollm J, Burnens A, Fatzer R, et al. Phaeohyphomycosis in a snow leopard (*Uncia uncia*) due to *Cladophialophora bantiana*. *J Comp Pathol*. 2006;134(2-3):245-248.
9. Langfelder K, Streibel M, Jahn B, Haase G, Brakhage AA. Biosynthesis of fungal melanins and their importance for human pathogenic fungi. *Fungal Genetics and Biology*. 2003;38:143–158.
10. Latimer KS, ed. *Duncan and Prasse's Veterinary Laboratory Medicine Clinical Pathology*. 5th ed. Ames, IA: John Wiley and Sons; 2011:65,178-179,386-388.
11. Lavely J, Lipsitz D. Fungal infections of the central nervous system in the dog and cat. *Clin Tech Small Anim Pract*. 2005;20:212-219.
12. Migaki G, Casey HW, Bayles WB. Cerebral phaeohyphomycosis in a dog. *J Am Vet Med Assoc*. 1987;191: 997-998.
13. Olias P, Hammer M, Klopfleisch R. Cerebral phaeohyphomycosis in a green iguana (*Iguana iguana*). *J Comp Pathol*. 2010;143(1):61-64.
14. Revankar SG, Patterson JE, Sutton DA, Pullen R, Rinaldi MG. Disseminated Phaeohyphomycosis: Review of an emerging mycosis. *Clinical Infectious Diseases*. 2006;34:467–476.
15. Singh K, Flood J, Welsh RD, Wickoff III JH, Snider TA, Sutton DA. Fatal systemic phaeohyphomycosis caused by *Ochroconis gallopavum* in a dog (*Canis familaris*). *Vet Pathol*. 2006;43:988–992.
16. Swift, IM, Griffin A, Shipstone MA. Successful treatment of disseminated cutaneous phaeohyphomycosis in a dog. *Australian Veterinary Journal*. 2006;84:431-435.

Joint Pathology Center
Veterinary Pathology Services

WEDNESDAY SLIDE CONFERENCE 2013-2014

Conference 10

10 December 2013

CASE I: TP-10-016 (JPC 4019883).

Signalment: Five-year-old female cynomolgus macaque (*Macaca fasicularis*).

History: The animal presented with a clinical history of lethargy and anorexia. The neurologic examination revealed mild intention tremors, anisocoria, ataxia, and left-sided facial paralysis.

Gross Pathology: At necropsy, there was a tan to gray, granular, soft, irregularly-shaped mass that extended from the base of the skull at the level of the sella turcica, through the cribiform plate, to the upper areas of the nasal cavity and paranasal sinuses. The tumor compressed the ventral aspect of the brain from the frontal lobes to the midbrain.

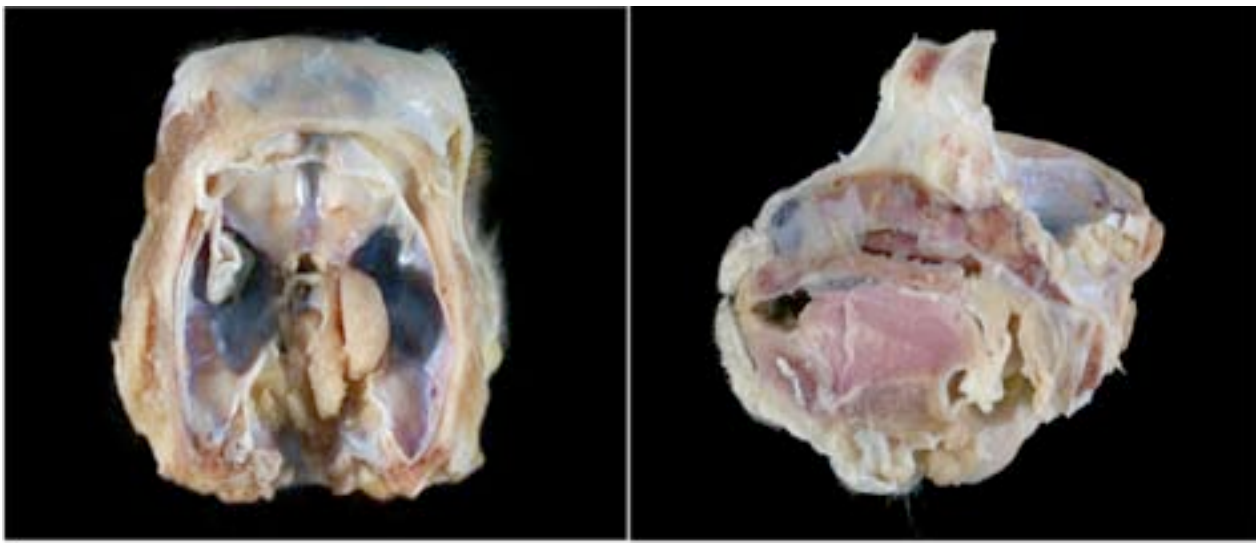

1-1. Skull and nasal cavity, cynomolgus monkey: At necropsy, there was a tan to gray, granular, soft, irregularly-shaped mass that extended from the base of the skull at the level of the sella turcica (left), through the cribiform plate, to the upper areas of the nasal cavity and paranasal sinuses (right). (Photo courtesy of: Pfizer Inc. Global Research and Development, Groton/New London Laboratories, Eastern Point Road MS 8274-1330, Groton, CT. Phone: 860-715-1086, www.pfizer.com)

Histopathologic Description: Slides from two different blocks of this tumor were submitted. This neoplasm infiltrated the nasal mucosa and propria submucosa, nasal septum (turbinate bone), flat bone (cribiform plate) and soft tissue/skeletal muscle. Sections of tongue, oral mucosa, and olfactory nerve were on some but not all slides. This infiltrative and non-encapsulated mass was composed of neoplastic cells arranged in solid clusters, sheets, and lobules that were separated by delicate fibrovascular connective tissue. Tumor cells frequently formed true rosettes or pseudorosettes and had a primitive appearance. Neoplastic cells had small, round to polygonal, hyperchromatic nuclei and scant eosinophilic cytoplasm. Mitotic figures, as well as large foamy cells (nasal clear cells), and areas of hemorrhage and necrosis were commonly observed throughout the mass.

Multiple immunohistochemical (IHC) stains of this tumor were performed including ubiquitin carboxyl-terminal hydrolase L1 (PGP 9.5 neuron specific protein), CD56 (neuronal cell adhesion molecule), S-100, neuron specific enolase (NSE) and vimentin. The expression of PGP 9.5, CD56, S-100, NSE and vimentin, along with the gross and histopathologic findings, confirmed that this neoplasm was an olfactory neuroblastoma and ruled out other neoplasms such as malignant pituitary tumor, lymphosarcoma, meningioma, suprasellar germ cell tumor and intracranial schwannosarcoma.

Contributor's Morphologic Diagnosis: Olfactory neuroblastoma.

Contributor's Comment: Olfactory neuroblastomas are uncommon neuroectodermal tumors that may arise within the nasal cavity.[9] The morphology of this neoplasm is heterogenous and the histogenic origin is unclear, resulting in many different names including, but not limited to, olfactory neuroblastoma, esthesioneuroblastoma, and olfactory neuroepithelioma.[4,9] One paper describing a prospective study in humans suggests that the term "olfactory neuroblastoma" might be the most reflective of both the origin and nature of the neoplasm.[8] This neoplasm has been described in humans,[5] dogs,[9] rats,[6] cats,[4] cows,[1] a horse[11] and a cynomolgus monkey.[3] Interestingly, olfactory neuroblastomas are chemically induced in rats,[7] as opposed to other animal species and humans where this tumor is typically of spontaneous origin. Some examples of chemicals that induce olfactory neuroblastomas in rats include 1-nitrosopiperazine and nitrosomorpholine.[6] The development of olfactory neuroblastomas in rats is not related to the route of administration of the chemical but it is directly associated with chemical metabolism in nasal basal cells that leads to neoplastic transformation.

The differential diagnoses for this mass consisted of esthesioneuroblastoma (olfactory neuroblastoma), lymphosarcoma, suprasellar germ cell tumor, meningioma, intracranial

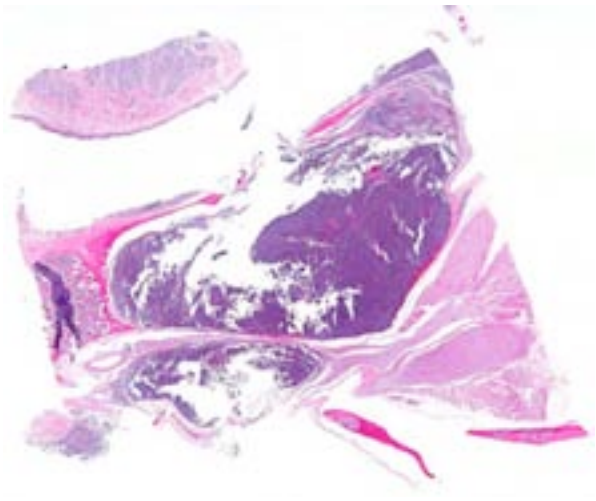

1-2. Skull and nasal cavity, cynomolgus monkey: A densely cellular neoplasm infiltrates and effaces bones of the nasal cavity and skull, as well adjacent skeletal muscle and large nerves. (HE 0.63X)

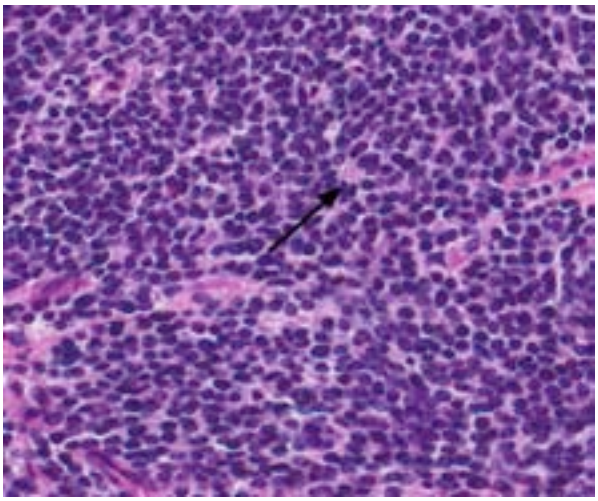

1-3. Skull and nasal cavity, cynomolgus monkey: The neoplasm is composed of densely packed polygonal cells with large oval nuclei and small amounts of cytoplasm which often form rosettes (arrows). (HE 324X)

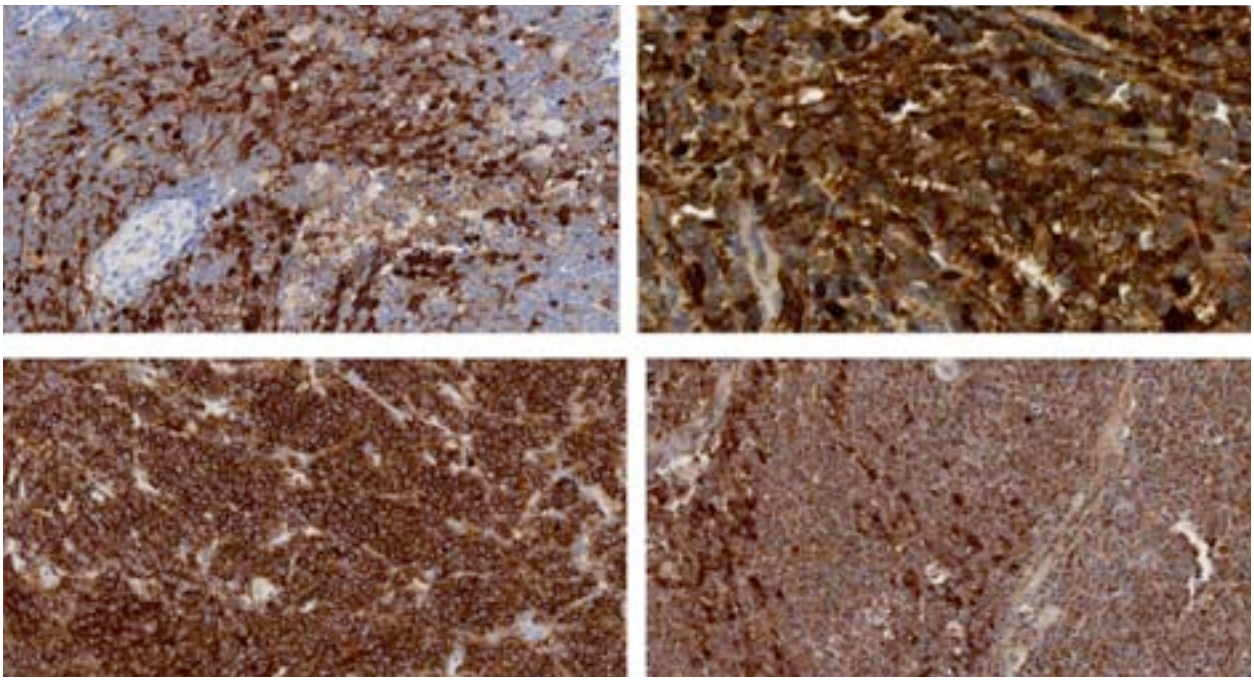

1-4. Skull and nasal cavity, cynomolgus monkey: Neoplastic cells are immunopositive for (clockwise from upper left): NSE (200X), S-100 (400X), CD56 (200X), and PGP 9.5(200X). (Photo courtesy of: Pfizer Inc. Global Research and Development, Groton/New London Laboratories, Eastern Point Road MS 8274-1330, Groton, CT. Phone: 860-715-1086, www.pfizer.com)

schwannosarcoma, and malignant pituitary gland tumor. Since olfactory neuroblastomas originate from the olfactory epithelium, it is important to split the cranium along the midline into two sagittal half sections to locate the origin of the tumor in the nasal cavity with infiltration into the base of the cranial cavity.

This case was presented at the 2011 annual National Toxicology Program (NTP) Satellite Symposium, entitled *Pathology Potpourri* that was held in Denver, Colorado in advance of the Society of Toxicologic Pathology's 30th Annual Meeting, and published by Boorman G, et al. in the *Journal of Toxicologic Pathology*.[2]

JPC Diagnosis: Skull, nasal cavity and paranasal sinus: Olfactory neuroblastoma.

Conference Comment: Key histological features of this case include the arrangement of neoplastic cells into parallel arrays and the presence of pseudorosettes and occasional Homer-Wright type rosettes.[5] Homer-Wright rosettes are composed of neoplastic cells surrounding a central lumen of fiber-rich neuropil. They are one of the major distinguishing characteristics of medulloblastomas, but also occur in primitive neuroectodermal tumors (PNETs) and pineoblastomas.[10] Pseudorosettes, on the other hand, are formed by neoplastic cells palisading around a centrally placed vessel.[10] Perivascular pseudorosettes are less specific than Homer-Wright rosettes in that they are also encountered in medulloblastomas, PNETs, central neurocytomas, glioblastomas and other tumors. Even with these characteristic lesions olfactory neuroblastomas can display a wide range of microscopic appearances with a large differential diagnosis. Immunohistochemically, these tumors are usually positive for some, or all, of the following: S-100 and neuroendocrine markers such as neuron-specific enolase (NSE), synaptophysin, chromagranin and CD56.[5]

Contributing Institution: Pfizer Inc.
Global Research and Development
Groton/New London Laboratories
Eastern Point Road MS 8274-1330
Groton, CT
Phone: 860-715-1086
www.pfizer.com

References:

1. Anderson BC, Cordy DR. Olfactory neuroblastoma in a heifer. *Vet Pathol*. 1981;18:536-540.

2. Boorman G, Crabbs TA, Kolenda-Roberts H, et al. Proceedings of the 2011 national toxicology program satellite symposium. *Toxicol Pathol*. 2012;40:321-344.
3. Correa P, Dalgard DW, Adamson RH. Olfactory neuroepithelioma in a cynomolgus monkey (*Macaca fascicularis*). *J Med Primatol.* 1975;4:51-61.
4. Cox NR, Powers RD. Olfactory neuroblastomas in two cats. *Vet Pathol*. 1989;26:341-343.
5. Faragalla H, Weinreb I. Olfactory neuroblastoma: a review and update. *Adv Anat Pathol.* 2009;16:322-331.
6. Garcia H, Keefer L, Lijinsky W, Wenyon CE. Carcinogenicity of nitrosothiomorpholine and 1-nitrosopiperazine in rats. *Z Krebsforsch*. 1970;74:179-184.
7. Long PH, Herbert RA, Peckham JC, Grumbein SL, Shackelford CC, Abdo K. Morphology of nasal lesions in F344/N rats following chronic inhalation exposure to naphthalene vapors. *Toxicol Pathol.* 2003;31:655-664.
8. Lund VJ, Howard D, Wei W, Spittle M. Olfactory neuroblastoma: past, present, and future? *The Laryngoscope.* 2003;113:502-507.
9. Mattix ME, Mattix RJ, Williams BH, Ribas JL, Wilhelmsen CL. Olfactory ganglioneuroblastoma in a dog: a light, ultrastructural, and immunohistochemical study. *Vet Pathol*. 1994;31:262-265.
10. Wippold II FJ, Perry A. Neuropathology for the neuroradiologist: rosettes and pseduorosettes. *Am J Neuroradiol*. 2006;27:488-492.
11. Yamate J, Izawa T, Ogata K, Kobayashi O, Okajima R, Kuwamura M, et al. Olfactory neuroblastoma in a horse. *J Vet Med Sci.* 2006;68:495-498.

CASE II: E 1242/12 (JPC 4033368).

Signalment: 1-day-old chickens (*Gallus gallus domesticus*), male and female.

History: Numerous one-day-old chickens in a hatchery were found in a weakened state.

Gross Pathology: Necropsy did not reveal any significant lesions.

Laboratory Results: ELISA yielded in the detection of antibodies against avian encephalomyelitis virus.

Histopathologic Description: Brain, longitudinal section (including cerebrum with brainstem and cerebellum): Multifocally, predominantly affecting large nuclei in the brainstem and the cerebellar Purkinje cells, there is neuronal degeneration characterized by marked dispersion of Nissl substance (central chromatolyis). Less commonly, neuronal necrosis is evident with neuronal hypereosinophilia, shrunken or swollen cell bodies, karyopyknosis, karyorrhexis and karyolysis.

With some slide variation, few neuronal cell bodies are surrounded by low numbers of astrocytes (satellitosis). Occasionally, macrophages phagocytosing cellular and karryorhectic debris (neuronophagia) as well as discrete nodules composed of low numbers of glial cells and fewer lymphocytes replacing neurons (glial nodules) can be observed. Scattered minimal to mild predominantly perivascular lymphocytic and histiocytic infiltrates (lymphohistiocytic cuffing) are present.

Contributor's Morphologic Diagnosis: Brain: Neuronal degeneration and necrosis, mild to moderate, acute, multifocal with minimal satellitosis, neuronophagia glial nodules and minimal to mild, acute, multifocal, lymphohistiocytic encephalitis.

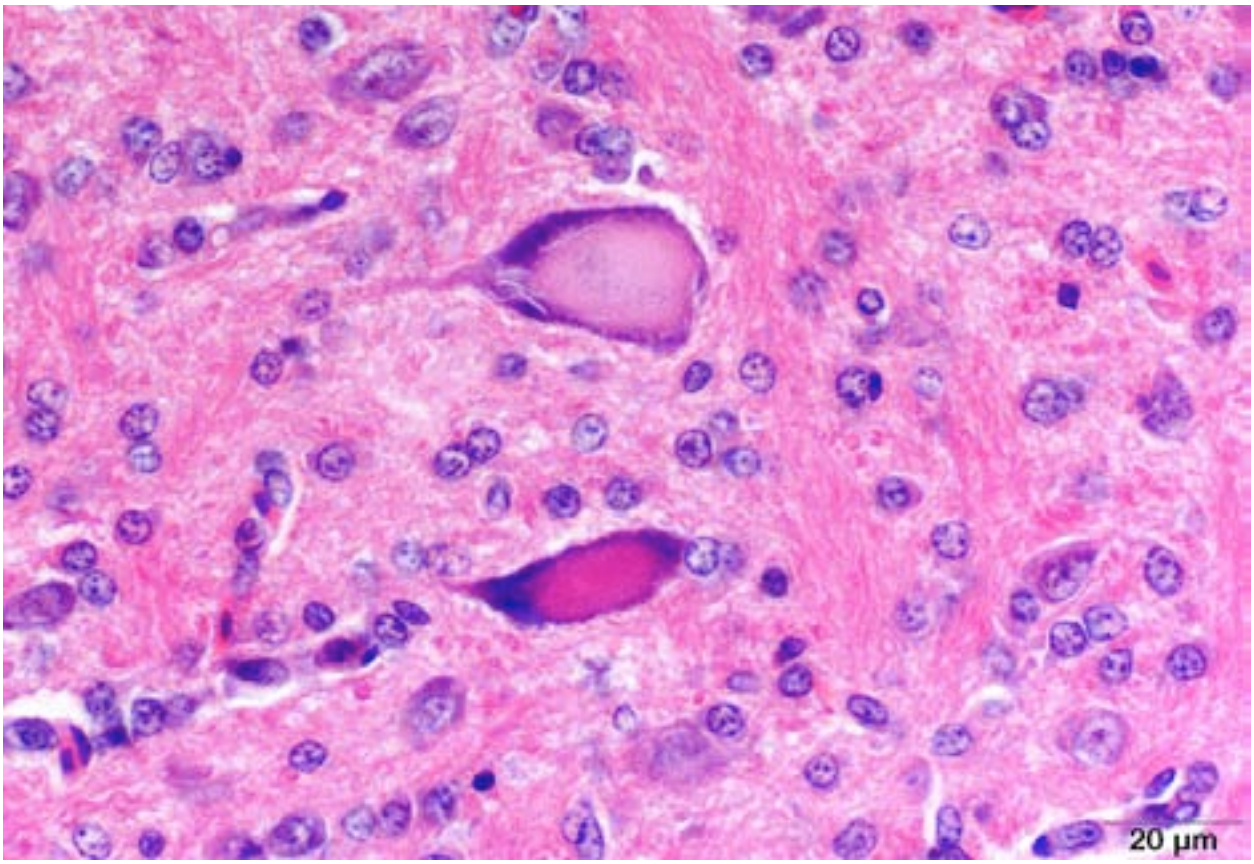

2-1. Brain, 1-day-old chicken: Multifocally, and most visibly in the brainstem nuclei, neurons exhibit central chromatolysis, a characteristic finding in avian encephalomyelitis. (Photo courtesy of: Department of Veterinary Pathology, Freie Universität Berlin, Germany, http://www.vetmed.fu-berlin.de/en/einrichtungen/institute/we12/index.html)

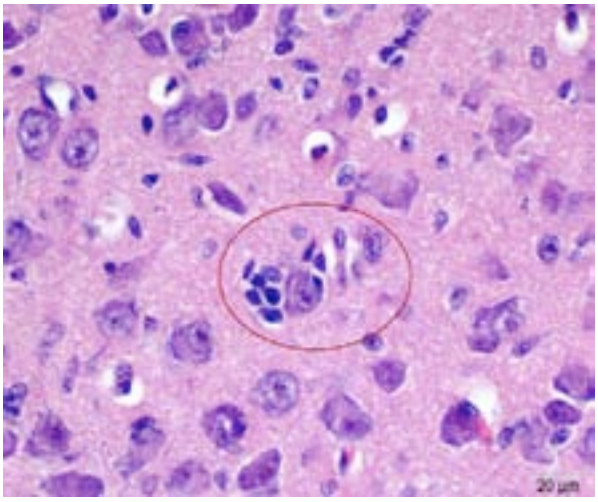

2-2. Brain, 1-day-old chicken: Rarely, neurons are surrounded by numerous glial cells (satellitosis). (Photo courtesy of: Department of Veterinary Pathology, Freie Universität Berlin, Germany, http://www.vetmed.fu-berlin.de/en/einrichtungen/institute/we12/index.html)

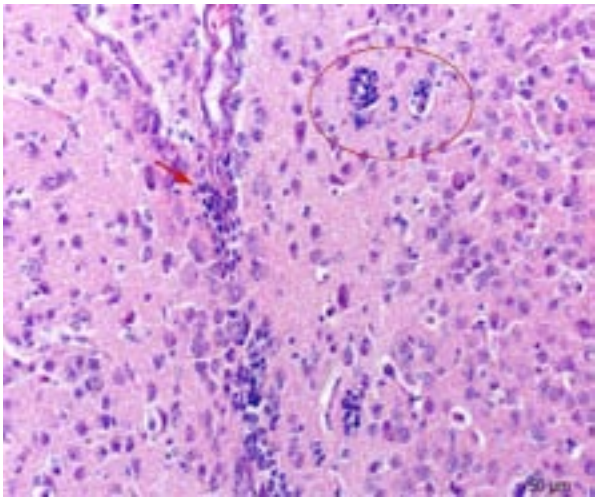

2-3. Brain, 1-day-old chicken: Rarely, there are low numbers of lymphocytes and histiocytes within perivascular areas and the meninges (arrow). (Photo courtesy of: Department of Veterinary Pathology, Freie Universität Berlin, Germany, http://www.vetmed.fuberlin.de/en/einrichtungen/institute/we12/index.html)

Contributor's Comment: Avian encephalomyelitis (AE) was first reported in 1932 as a nervous disorder of chickens with pronounced and rapid tremor of the head and neck with, in some cases, ataxia. The symptoms worsened when the chickens were excited and disappeared in sleep.[3] The causative agent, avian encephalomyelitis virus (AEV), belongs to the *Hepatovirus* genus of the *Picornaviridae* family and transmission occurs via the oral-fecal and vertical routes. Avian encephalomyelitis affects chickens, turkeys, and quails.[5] Synonyms for AE include "infectious avian encephalomyelitis" and "epidemic tremor."

Clinically, outbreaks occur in young birds, less than six (typically 1-3) weeks of age. The animals develop ataxia with possible progression to paralysis or tremor of the head and neck (i.e., epidemic tremor). In general, the severity of the disease depends on the age and immunological status of the bird. Whereas clinical signs might be present at the time of hatching, they are usually evident between 1-2 weeks of age. There seems to be a marked resistance if exposure is after 2-3 weeks of age. Adult birds show a drop in egg production for no more than two weeks.[1,2]

Gross lesions are commonly absent, especially in adult chickens. Whitish areas in the ventriculus muscle due to massive lymphocytic infiltration may occur.[1,2] Histologically, lesions may be lacking in the peracute stage. Typical lesions of acute AE include central chromatolysis of neurons in the brainstem (medulla oblongata) and of Purkinje cells. The neuronal nuclei isthmi, ruber, reticularis, rotundus and cerebellaris as well as the ventral horns of the spinal cord are primary targets. A disseminated lymphoplasmahistiocytic encephalomyelitis with ganglionitis of the dorsal root ganglia can be detected in more subacute to chronic cases. In addition, nodular microgliosis, predominantly in the cerebellar molecular layer, may be observed. Multifocal microgliosis of the Purkinje cell layer, with triangular or flame-like extensions into the molecular layer are also suggestive of AE. Additionally, aggregates of lymphocytes appear within the muscular wall of the ventriculus, the pancreas and myocardium.[1,2]

Differential diagnoses include Marek's disease virus, which causes lymphoid infiltrates in the peripheral nerves and lymphomatosis of the viscera (not seen in AE), Newcastle disease virus, with peripheral chromatolysis rather than the central chromatolysis of AE, and Avian influenza virus.[1,2]

JPC Diagnosis: Brainstem nuclei: Central chromatolysis, multifocal, mild.

Conference Comment: The contributor provides a thorough overview of avian encephalomyelitis virus. Clinical disease due to AE has also been described in pheasants, partridges and turkeys,[6]

though these species appear to be less susceptible than chickens.

The *Picornaviridae* family is composed of eight genera: *Aphthovirus, Enterovirus, Teschovirus, Cardiovirus, Erbovirus, Kobuvirus, Hepatovirus and Parechovirus*. Picornaviruses are non-enveloped, icosahedral, single stranded, RNA virions.[4] Diseases of veterinary importance caused by picornaviruses include foot-and-mouth disease (*Aphthovirus*), encephalomyocarditis virus and Theiler's mouse encephalomyelitis virus (*Cardiovirus*), swine vesicular disease (*Enterovirus*), porcine teschovirus 1 (*Teschovirus*) and avian encephalomyelitis virus. Originally classified in the genus *Enterovirus* and later reclassified into the genus *Hepatovirus*, AEV has recently been considered for classification into a new genus within the *Picornaviridae* family, *Tremovirus*.[4]

The striking feature of this case is the paucity of microscopic lesions, consistent with the peracute disease course described in this case. Conference participants debated the presence of Purkinje cell degeneration and central chromatolysis, however a consensus was not reached. The hypercellularity of the submitted specimen also confounded uniform diagnosis in this case, as development of the brain is still ongoing in a 1-day-old chick, and differentiation of maturing, migrating, and developing cells of neural and glial origin from those associated with viral infection.

Contributing Institution: Department of Veterinary Pathology
Freie Universität Berlin
Germany
http://www.vetmed.fu-berlin.de/en/einrichtungen/institute/we12/index.html

References:

1. Avian Disease Manual. 6th ed. Athens, GA: American Association of Avian Pathologists; 2006:12-14.
2. Avian Histopathology. 3rd ed. Madison, WI: American Association of Avian Pathologists; 2008:265-266.
3. Jones EE. An encephalomyelitis in the chicken. *Science*. 1932;76:331-332.
4. MacLachlan NJ, Dubovi EJ, eds. *Fenner's Veterinary Virology*. 4th ed. London, UK: Academic Press; 2011:425-441.
5. Tannock GA, Shafren DR. Avian encephalomyelitis: a review. *Avian pathology: Journal of the WVPA*. 1994;23:603-620.
6. Welchman DdeB, Cox WJ, Gough RE, et al. Avian encephalomyelitis virus in reared pheasants: a case study. *Avian Pathol*. 2009;38(3): 251-256.

CASE III: UFSM-2 (JPC 4034401).

Signalment: 5-year-old female mixed-breed domestic pig (*Sus scrofa domesticus*).

History: A mixed-breed pig in good plane of nutrition and with no detectable clinical abnormalities was sent to slaughter. The federal meat inspector detected "areas of green discoloration in the carcass" and sent large tissue samples from several organs to be examined at our lab.

Gross Pathology: Grossly, over the ribs and beneath the parietal pleura there were green, smooth, and opaque, irregularly contoured, non-circumscribed, soft, homogenous areas. Light green masses that partially or completely obliterated the bone marrow architecture were observed at the cut surfaces of some ribs and several vertebrae and sternebrae. In all lumbosacral vertebrae, typically a subperiosteal presentation was observable. In the cut surface of long bones (femora and humeri), the same pattern of presentation was observed in the metaphysis. In the kidneys, there were multiple, 1-3 mm in diameter pink to light green, soft, irregularly shaped nodules. There was a homogeneous aspect to the cut surface of these nodules. At cut surfaces of popliteal and iliac lymph nodes, there were pink or light green areas. In one of the lymph nodes (internal iliac), the cut surface was diffusely light green and crisscrossed by red serpiginous lines.

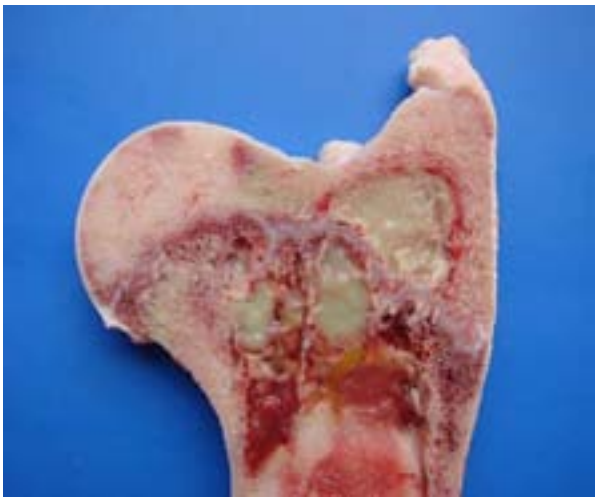

3-1. Vertebra, pig: At autopsy, several well-demarcated light green masses efface the metaphyseal bone. (Photo courtesy of: Departamento de Patologia, Universidade Federal de Santa Maria, 97105-900 Santa Maria, RS, Brazil. http://www.ufsm.br/lpv)

Laboratory Results: Cytological examination of the mass revealed large numbers of round cells approximately 20-30 µm. These round cells had round, oval, or reniform nuclei that contained slightly clumped chromatin and did not display prominent nucleoli. The cytoplasm was scant, and a fine eosinophilic granularity could be observed in the cytoplasm of some neoplastic cells but not in others. Such cells were interpreted as myelocytes belonging to the eosinophil lineage.

Histopathologic Description: Histologically, a sheet of round cells with a virtually imperceptible stroma obliterated the bone marrow. The bone marrow tissue surrounding these cellular sheets was replaced by fibroblasts and collagen (myelofibrosis). At these sites, there was reabsorption of compact bone and moderate periosteal reaction. Non-circumscribed foci of myeloid cells were observed dissecting, and at times replacing, the renal tubules. Sections of these areas revealed that the neoplastic cell cytoplasm stained red by the Sirius red eosinophil technique and demonstrated strong cytoplasmic positivity for myeloperoxidase by the immunohistochemistry stain. All sections were negative for all the other immunohistochemical markers (lysozyme, CD 117, CD3 and CD79) used.[1]

Contributor's Morphologic Diagnosis: Bone marrow, vertebral body: eosinophilic granulocytic sarcoma.

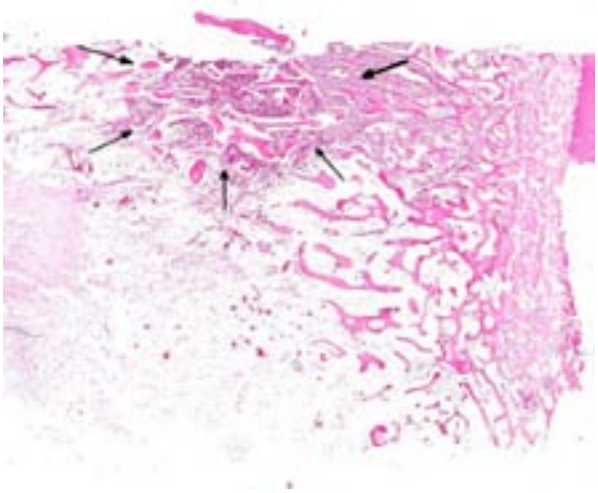

3-2. Vertebra, pig: A poorly circumscribed, well-demarcated mass infiltrates the subperiosteal bone marrow. (HE 0.63X)

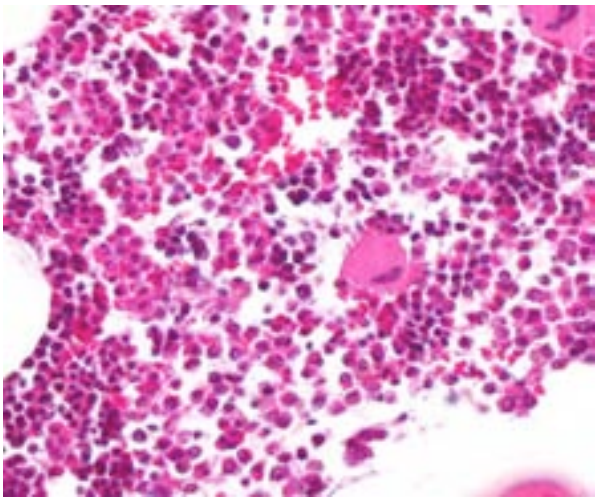

3-3. Vertebra, pig: The bone marrow is infiltrated by large numbers of neoplastic eosinophils often with large round nuclei and few to moderate numbers of eosinophilic granules. (HE 400X)

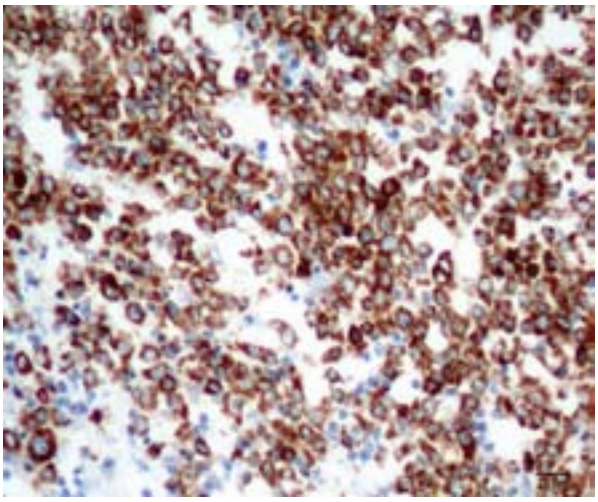

3-4. Vertebra, pig: Neoplastic cells exhibit strong cytoplasmic immunoreactivity for myeloperoxidase. (Photo courtesy of: Departamento de Patologia, Universidade Federal de Santa Maria, 97105-900 Santa Maria, RS, Brazil. http://www.ufsm.br/lpv)

Contributor's Comment: Granulocytic sarcoma is a morphologic presentation of myeloid sarcoma, a hematopoietic neoplasm affecting bones or extramedullary sites; in this latter case, the growth is also referred to as extramedullary myeloid tumor, myeloblastoma, or myelosarcoma. Granulocytic sarcomas may originate from variably differentiated precursors, from both neutrophilic and eosinophilic lineages. Such sarcomas tend to occur grossly as characteristic green masses; therefore, the sobriquet "chloroma," derived from the Latin transliteration of the Greek *khlorós,* meaning green, was given to the neoplasm.

In humans, granulocytic sarcomas precede or occur concomitantly with acute myeloid leukemia, chronic myeloproliferative disorders, or myelodysplastic syndromes but are also described without association with any other hematologic disturbance. In the veterinary literature, granulocytic sarcomas are mentioned affecting dogs, cats, cattle,[12] a rabbit,[9] and a pig.[5] In dogs and cats, the more consistently involved organs are the lungs, intestine, skin, lymph nodes and liver. In one of the few reports found in the veterinary literature, this tumor is mentioned as a mass in the neck of a Bull Terrier dog. In cattle, skeletal muscle is characteristically affected. In the case reported in a rabbit, the granulocytic sarcoma involved the skin, subcutaneous tissue, and skeletal muscle of the perineum.[9] In the reported case in the pig, the tumor involved liver, kidneys, and mesenteric lymph nodes.[5] Differently from what occurs in human patients, animals affected by granulocytic sarcomas are almost always aleukemic; however, progression to a leukemia may occur. The current report describes gross findings, cytology, histopathology, histochemistry, and immunohistochemistry of a multicentric eosinophilic granulocytic sarcoma affecting a pig.

Granulocytic sarcoma was suspected in the current case based on the presence of light green masses in the gross inspection of the carcass and viscera, a typical aspect of this tumor. The anatomical distribution of the lesions observed in the current case is quite similar to that described for human granulocytic sarcomas, in which the occurrence is primarily subperiosteal and involves mainly the ribs, sternum, and pelvis. The microscopic presentation pattern observed both at cytological and histological examination consisting predominantly of precursor cells with myelocyte differentiation, allowed the presumptive diagnosis of well-differentiated granulocytic sarcoma. Immunohistochemistry results established the cell origin as of the granulocytic lineage, and histochemistry determined that the cells were possibly of eosinophil lineage, definitively confirming the diagnosis suspected at gross examination.

The definitive diagnosis of myeloid sarcomas is based on the association of phenotypic (cytology, histology, cytochemistry, and histochemistry) and immunophenotypic (immunocytochemistry and

immunohistochemistry) aspects. An immune phenotype of neoplastic cells positive for myeloperoxidase is the hallmark for granulocytic sarcoma. Other antibody markers have reportedly yielded positive results when applied to human cases of granulocytic sarcoma, including CD13, CD33, CD117, CDl5, CD68, CD43,[7] and lysozyme.[8] However, lysozyme and CD68 are also marked in cases of monoblastic sarcoma, a less common form of myeloid sarcoma.

In the porcine tumor described here, the negative staining for CD117 could be explained by both the predominance of myelocytes and absence of myeloblasts, which are precursor cells that express this antigen. The negative staining for lysozyme was somewhat expected because swine granulocytes have been described as negative for this marker,[3] whereas porcine monocytes and/or macrophages are strongly positive,[4] similar to what is described in humans, a species in which lysozyme is the choice marker for monocytes and/ or macrophages. Based on this species-specific feature, the negative reaction to lysozyme further helps to differentiate granulocytic sarcoma from monoblastic sarcoma.

In human patients, several different forms of lymphoma presentation are often confused with myeloid sarcoma[7] and thus should be the main tumors to be included in the differential diagnosis. In the current case, the differentiation was made based on the following aspects: histological evidence of cytoplasmic eosinophilia, fine granularity observed in the cytoplasm of neoplastic cells when examined in cytological preparations, occurrence within the neoplasm of more mature eosinophil precursors amidst myeloblasts, and the immunohistochemistry results. Furthermore, the observation of light green masses that partially obliterated the bone marrow of several flat and long bones prompted the suspicion of granulocytic sarcoma, as this is the only hematopoietic neoplasm that expresses this typical color grossly. The green discoloration observed in fresh tissue specimens is due to the presence of myeloperoxidase and substantially helps in the diagnosis of granulocytic sarcoma.

Few lesions could grossly resemble granulocytic sarcoma. Such lesions include chlorellosis, a granulomatous algal infection observed in human beings and animals,[6] and eosinophilic myositis, which is frequently associated with *Sarcocystis* spp. infection in cattle[11] and has been described in a pig. The association of gross examination, cytology, histology, histochemistry, and immunohistochemistry findings is consistent with a diagnosis of eosinophilic granulocytic sarcoma.

JPC Diagnosis: Bone marrow, vertebral body: Eosinophilic granulocytic sarcoma.

Conference Comment: As noted in the comprehensive contributor's comment, cytoplasmic myeloperoxidase positivity provides an immunohistochemical indication of the myeloid origin of granulocytic sarcoma, while the cytological characteristics, including the presence of reniform nuclei and faint eosinophilic cytoplasmic granules that stain with the Sirius red technique, specifically confirm eosinophilic lineage. Myeloperoxidase is a lysosomal enzyme found in myeloblasts, immature myeloid cells and the primary granules of mature neutrophils,[1,12] while the Sirius red eosinophil technique stains eosinophilic cytoplasmic granules strongly red.[2] McGavin and Zachary[1] and Latimer[15] provide detailed lists of specific leukocyte granules, however this is a rapidly developing field of research and there is substantial inter-species variation, so most lists of leukocyte granules are not all-inclusive. Conference participants had some difficulty in distinguishing eosinophilic cytoplasmic granules in this case, which was likely due to a loss of cytologic detail secondary to decalcification of these sections of bone.

Contributing Institution: Departamento de Patologia
Universidade Federal de Santa Maria
97105-900 Santa Maria, RS, Brazil
http://www.ufsm.br/lpv

References:

1. Ackermann MR. In: Zachary JF, McGavin MD, eds. *Pathologic Basis of Veterinary Disease*. 5th ed. St. Louis, MO: Elsevier; 2012: e14 (chapter 3, Web Box 3-1).
2. Brum JS, Lucena RB, Martins TB, Fighera RA, Barros CSL. Eosinophilic granulocytic sarcoma in a pig. *J Vet Diagn Invest*. 2012;24:807-811.
3. Chianini F, Majó N, Segalés J, Dominguéz J, Domingo M. Immunohistological study of the immune system cell in paraffin-embedded tissues of conventional pigs. *Vet Immunol Immunopathol*. 2001;82:245-255.

4. Evensen O. An immunohistochemical study on the cytogenetic origin pulmonary multinucleate giant cells in porcine dermatosis vegetans. *Vet Pathol*, 1993;30:162-170.
5. Fisher LF, Olander HL. Spontaneous neoplasms of pigs-a study of 31 cases. *J Comp Pathol*. 1978;88:505-517.
6. Haenichen T, Facher E, Wanner G, Hermanns W. Cutaneous ch1orellosis in a gazelle *(Gazella dorcas*). *Vet Pathol*. 2002;39:386-389.
7. Menasce LP, Banerjee SS, Beckett E, Harris M. Extramedullary myeloid tumour (granulocytic sarcoma) is often misdiagnosed: a study of 26 cases. *Histopathology*. 1999;34:391-398.
8. Neiman RS, Barcos M, Berard C, Bonner H. Mann R, Rydell RE, et al. Granulocytic sarcoma: a clinicopathologic study of 61 biopsied cases. *Cancer*. 1981;48:1426-1437.
9. Perkins SE, Murphy JC, Alroy J. Eosinophil granulocytic sarcoma in a New Zealand white rabbit. *Vet Pathol*. 1996;33:89-91.
10. Valli VE. The hematopoietic system. In: Maxie MG. ed. *Jubb, Kennedy, and Palmer's Pathology of Domestic Animals*. 5th ed. Vol. 3. Philadelphia, PA: Elsevier; 2007:107-324.
11. Vangeel L, Houf K, Geldhof P, Nollet H, Vercruysse J, Ducattle R, et al. lntramuscular inoculation of cattle with *Sarcocystis* antigen results in focal eosinophilic myositis. *Vet Parasitol*. 2012;183:224-230.
12. Webb JL, Latimer KS. Leukocytes. In: Latimer KS, ed. *Duncan and Prasse's Veterinary Laboratory Medicine Clinical Pathology*. 5th ed. Ames, IA: John Wiley and Sons. 2011:45-58.

CASE IV: H11-164 (JPC 4007419).

Signalment: 1-week-old male Charolais (*Bos taurus*).

History: The calf had a history of hemorrhage from the rectum, injection sites and ear-tag site.

Gross Pathology: Carcass described by submitting veterinarian as markedly anaemic with widespread mucosal and serosal ecchymoses/ petechiae and diffuse splenic congestion. Formalin-fixed sections of bone marrow from the sternum, femur and ribs were submitted for histopathological examination.

Laboratory Results: PCR on spleen for bovine pestivirus (bovine viral diarrhea virus – BVDV) was negative. No significant bacterial isolates from tissues.

Histopathologic Description: Sternebra: There is diffuse hypoplasia of all three marrow hematopoietic cell lines with less than 10% cellularity (i.e. hematopoietic tissue as a percentage of the total of hematopoietic and adipose tissue). Multifocal, variably-sized aggregates of myeloid and erythroid precursors; megakaryocytes are absent. Multifocally, adipocytes are separated by small areas of hemorrhage and by fine, fibrillar, eosinophilic material (gelatinous transformation).

Contributor's Morphologic Diagnosis: Sternebral marrow: Trilineage hypoplasia of hematopoietic cells, severe.

Contributor's Comment: The trilineage hypoplasia in the bone marrow (aplastic pancytopenia) together with the clinical history, post-mortem findings, age of calf and the absence of BVDV are consistent with a diagnosis of bovine neonatal pancytopenia (BNP).[9] This condition was first described in Germany in 2007 but has since been reported in many European countries.[9] The condition is characterized by multiple (external and internal) hemorrhages, thrombocytopenia, leukopenia and bone marrow

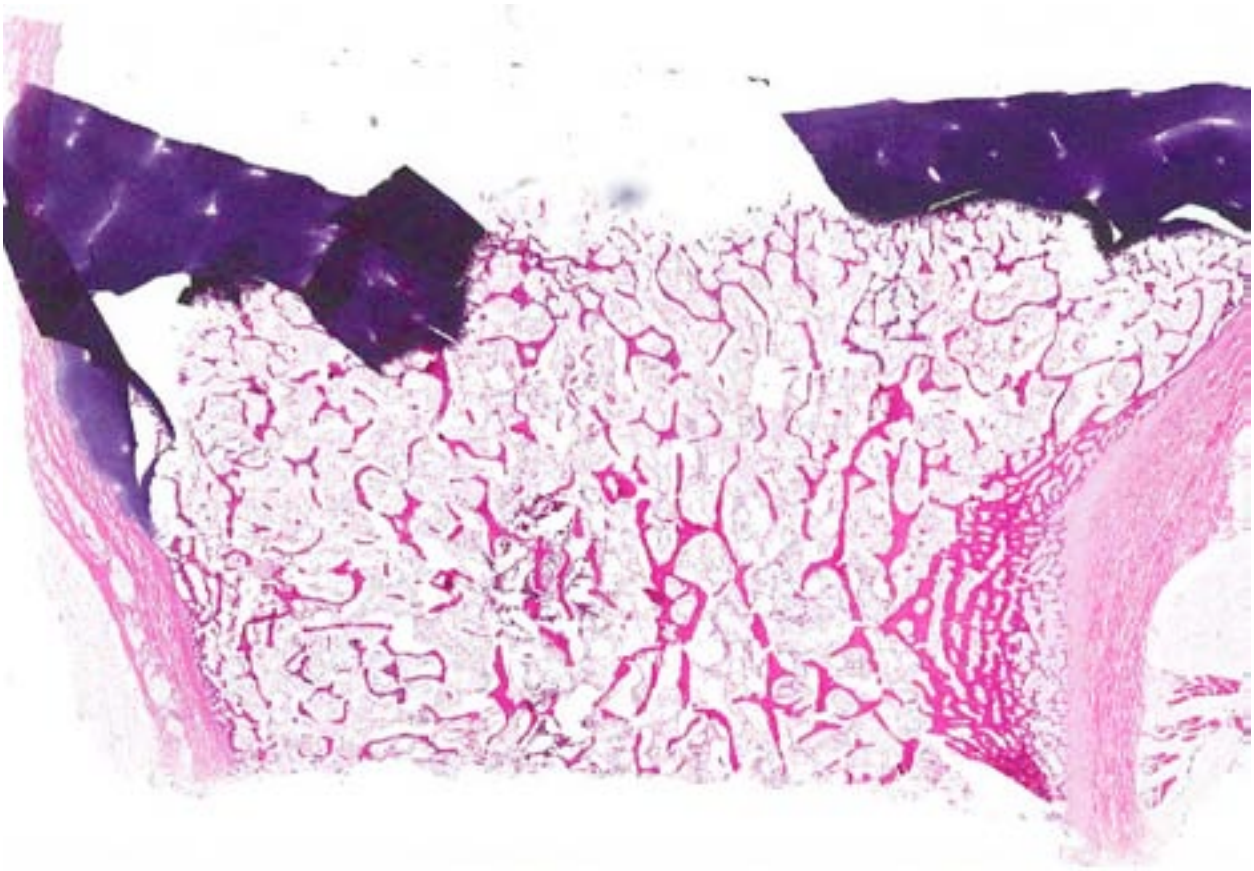

4-1. Sternebra, marrow, 1-week-old calf: The marrow cavity of this 1-week-old calf is markedly hypocellular. (HE 0.63X)

depletion in calves less than 4 weeks of age.[2,9] It has been postulated that BNP occurs as a result of an isoimmune reaction mediated by maternal antibodies in colostrum.[4] The occurrence of the disease has been linked to maternal vaccination with a particular BVDV vaccine,[1] to such an extent that the European Commission suspended marketing of this vaccine in 2010. A vaccination history was not available for this animal.

Aplastic pancytopenia has historically been uncommon in cattle but has been documented in association with infection with BVDV type 2.[11] BVDV type 1 has been isolated from cases of fatal hemorrhagic thrombocytopenia but experimental infection has failed to replicate the condition.[7] Fatal hemorrhagic pancytopenia has also been reported in cattle due to ingestion of bracken fern[10] and of T-2 mycotoxins.[8]

JPC Diagnosis: Bone marrow, sternebra: Trilineage pancytopenia, diffuse, severe.

Conference Comment: A study examining the pathogenesis of BNP found that dams vaccinated with a particular BVDV vaccine produce alloreactive antibodies that cross react with the bovine kidney cell line used in vaccine production. These maternal autoantibodies, passed to their calves in colostrum, bind to leukocyte surface antigens, leading to opsonization, subsequent phagocytosis by macrophages and, ultimately, trilineage bone marrow hypoplasia.[1]

Alloimmune phenomena are also described in several other species, including foals, humans and piglets. Neonatal isoerythrolysis (NI) in foals, a common alloimmune disease in foals, is a type II hypersensitivity reaction caused by the presence of anti-erythrocyte antibody complexes in the colostrum of the dam and results in destruction of erythrocytes.[3] This condition occurs in horses because of exposure to an incompatible blood type from the stallion. NI has also been reported in cattle and cats.[6] In neonatal alloimmune thrombocytopenia (NAIT), women homozygous for a certain genetic trait, who are carrying a fetus with heterozygous platelet antigens partially inherited from the father, may develop anti

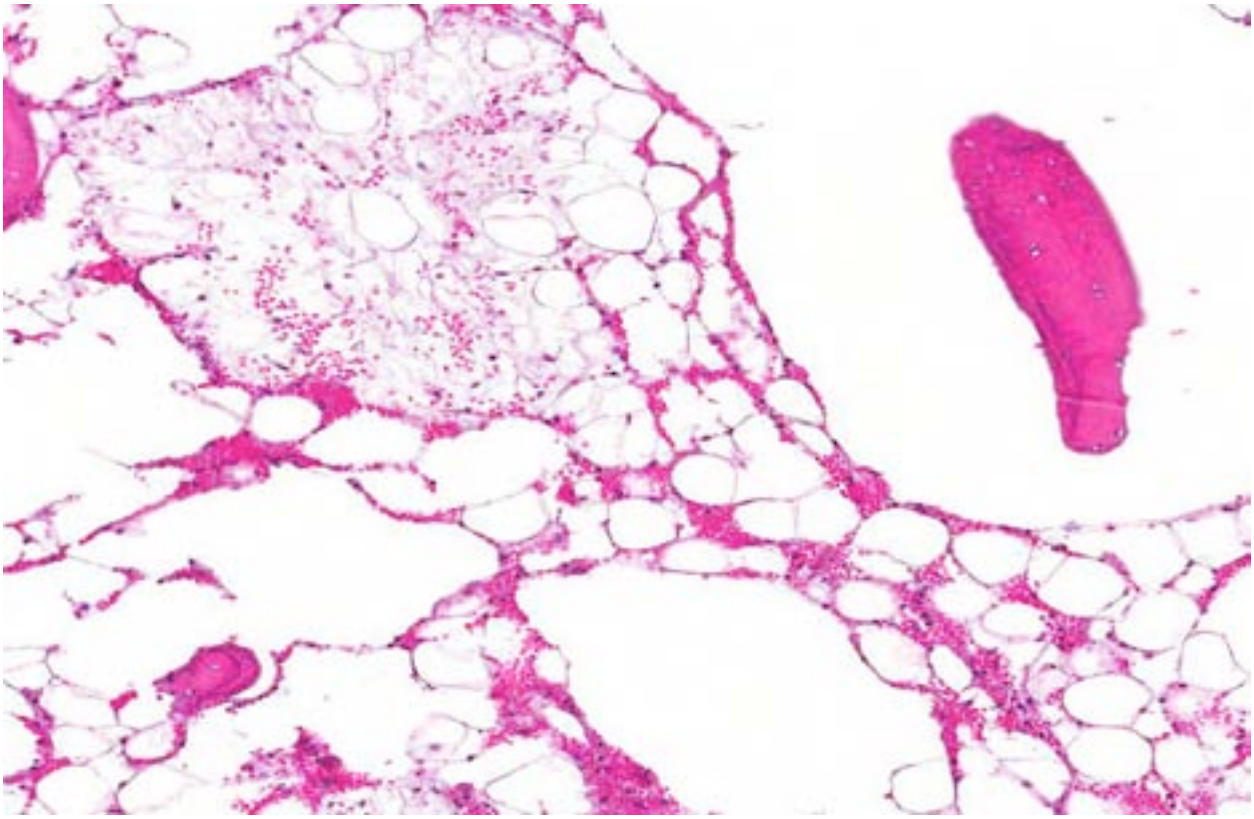

4-2. Sternebra, marrow, 1-week-old calf: Higher magnification of metaphyseal marrow spaces – the marrow lacks erythropoietic cells of all lineages. (HE 200X)

Human Platelet Antigen 1 antibodies. These antibodies pass through the placenta, causing fetal thrombocytopenia and subsequent intracranial hemorrhage.[1] NAIT has also been described in foals and piglets. In foals, it is hypothesized that the mare's plasma and milk contains antibodies reactive to foal platelet antigens inherited from the sire.[5] In contrast to BNP, which affects all hematopoietic cell lines, these conditions target one cell line; NI impacts erythrocytes while NAIT targets platelets, resulting in hemolytic anemia and thrombocytopenia respectively.[1,5]

In general, viruses and toxins are the most common causes of pancytopenia. In addition to those infectious/toxic agents described by the contributor, further potential causes of pancytopenia include radiation, chemotherapeutic agents, estrogen toxicity, stachybotryotoxicosis, infectious agents and myelophthisis.[10,11] Chemotherapy induced myelosuppression is the most common cause of canine pancytopenia, and is typically associated with doxorubicin administration.[11] Estrogen compounds, which may originate from iatrogenic administration or hormone overproduction, are also myelotoxic. Disease is typically characterized by irreversible pancytopenia with widespread hemorrhage.[10] Stachybotryotoxicosis is a pancytopenic disease of horses and ruminants that occurs due to ingestion of feed contaminated with the fungus *Stachybotrys alternans*.[10] Feline and canine parvoviruses target proliferating cells, such as epithelial cells within intestinal crypts or hematopoietic cells within the bone marrow, resulting in pancytopenia.[10,12] Myelophthisis refers to replacement of normal hematopoietic bone marrow elements with abnormal tissue, usually neoplastic cells or fibrous connective tissue.[6] Bone marrow neoplasia can be primary (multiple myeloma, leukemia, lymphoma) or metastatic.[6] Malignant histiocytosis has also been associated with canine pancytopenia, likely due to a combination of decreased marrow production and cytophagia.[12] Bone marrow fibrosis, or myelofibrosis, is most commonly reported in dogs, and may occur with sepsis, neoplasia, drug toxicity and immune-mediated disease.[6]

Contributing Institution: Veterinary Sciences Centre, Room 012
School of Veterinary Medicine, University College Dublin
Belfield, Dublin 2, Ireland
http://www.ucd.ie/vetmed/

References:

1. Bastian M, Holsteg M, Hanke-Robinson H, Duchow K, Cussler K. Bovine neonatal pancytopenia: is this alloimmune syndrome caused by vaccine-induced alloreactive antibodies? *Vaccine*. 2011;29:5267-5275.
2. Bell CR, Scott PR, Sargison ND, Wilson DJ, Morrison L, Howie F, et al. Idiopathic bovine neonatal pancytopenia in a Scottish beef herd. *Vet Rec*. 2010;167:938-940.
3. Boyle AG, Magdesian KG, Ruby RE. Neonatal isoerythrolysis in horse foals and a mule foal: 18 cases (1988-2003). *J Am Vet Med Assoc*. 2005;227(8):1276-1283.
4. Bridger PS, Bauerfeind R, Wenzel L, Bauer N, Menge C, Thiel H-J, et al. Detection of colostrum-derived alloantibodies in calves with bovine neonatal pancytopenia. *Vet Immunol Immunopathol*. 2011;141:1-10.
5. Buechner-Maxwell V, Scott MA, Godber L, Kristensen A. Neonatal alloimmune thrombocytopenia in a Quarter horse foal. *J Vet Int Med*. 1997;11(5):304-308.
6. Fry MM, McGavin MD. Bone marrow, blood cells, and the lymphatic system. In: Zachary JF, McGavin MD, eds. *Pathologic Basis of Veterinary Disease*. 5th ed. St. Louis, MO: Elsevier; 2012:704-734.
7. Hamers C, Couvreur B, Dehan P, Letellier C, Lewalle P, Pastoret PP, et al. Differences in experimental virulence of bovine viral diarrhoea viral strains isolated from haemorrhagic syndromes. *Vet J*. 2000;160:250-258.
8. Hsu IC, Smalley EB, Strong FM, Ribelin WE. Identification of T-2 toxin in moldy corn associated with a lethal toxicosis in dairy cattle. *Appl Microbiol*. 1972;24:684-690.
9. Pardon B, Steukers L, Dierick J, Ducatelle R, Saey V, Maes S, et al. Haemorrhagic diathesis in neonatal calves: an emerging syndrome in Europe. *Transbound Emerg Dis*. 2010;7:135–146.
10. Valli VEO. Hematopoietic system. In: Maxie MG, ed. *Jubb, Kennedy, and Palmer's Pathology of Domestic Animals*. 5th ed. Vol. 3. Philadelphia, PA: Elsevier; 2007:216-220.
11. Walz PH, Bell TG, Steficek BA, Kaiser L, Maes RK, Baker JC. Experimental model of type II bovine viral diarrhea virus-induced thrombocytopenia in neonatal calves. *J Vet Diagn Invest*. 1999;11:505-514.

12. Weiss DJ, Evanson OA, Sykes J. A retrospective study of canine pancytopenia. *Vet Clin Pathol*. 1999;28(3):83-88.

Joint Pathology Center
Veterinary Pathology Services

WEDNESDAY SLIDE CONFERENCE 2013-2014

Conference 11

08 January 2014

CASE I: A12-5214 (JPC 4017804).

Signalment: 4-year-old male domestic shorthaired cat (*Felis catus*).

History: An abdominal mass was palpated in a cat with anorexia and weight loss. The cat was serologically negative for feline leukemia virus and feline immunodeficiency virus. Eosinophilia was detected by complete blood count. At exploratory laparotomy, a solitary, infiltrative, 3 cm x 3 cm x 8 cm jejunal mass was treated by resection and anastomosis. No evidence of metastatic disease was observed grossly or by thoracic radiography. The resected segment of jejunum and a biopsy specimen of mesenteric lymph node were submitted in formalin to the Animal Disease Diagnostic Laboratory at Purdue University.

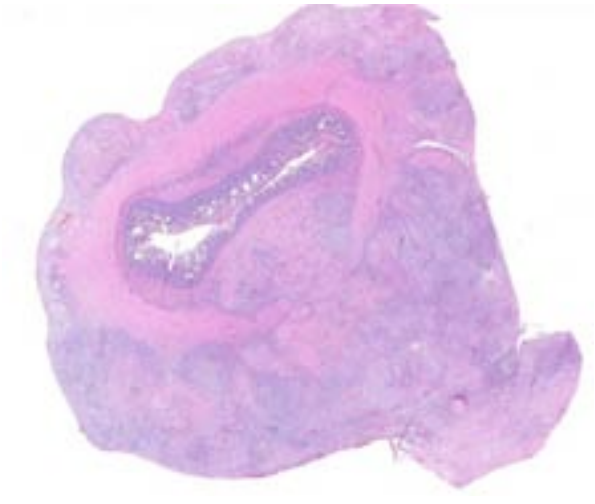

1-1. Small intestine, cat: The submucosa, muscularis, and serosa are markedly, circumferentially and asymmetrically expanded by fibrous connective tissue throughout which is scattered multiple foci or granulomatous inflammation. (HE 0.63X)

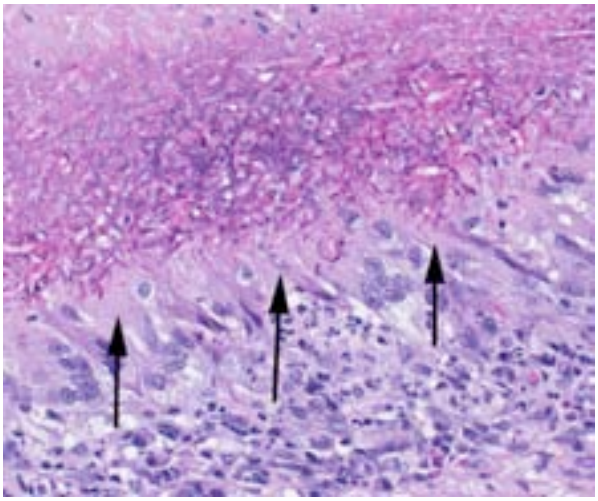

1-2. Small intestine, cat: Necrotic foci contain numerous outlines of non-septate hyphae which have non-parallel walls and measure 6-8 µm in diameter. These foci are surrounded by elongate epithelioid macrophages (below). (HE 340X)

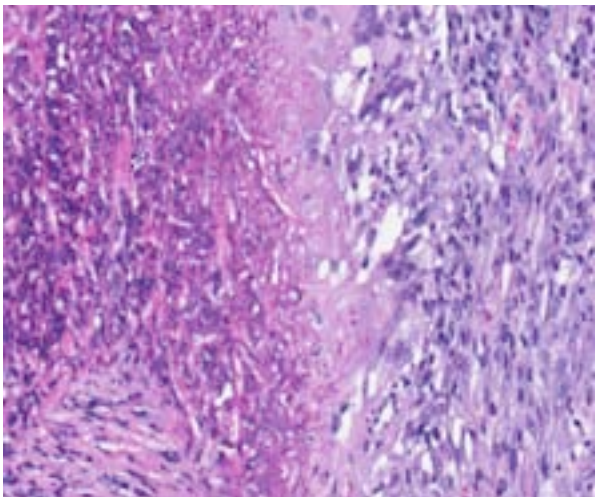

1-3. Small intestine, cat: Scattered throughout the section, arterial walls are necrotic and contain masses of hyphae in negative relief. (HE 370X)

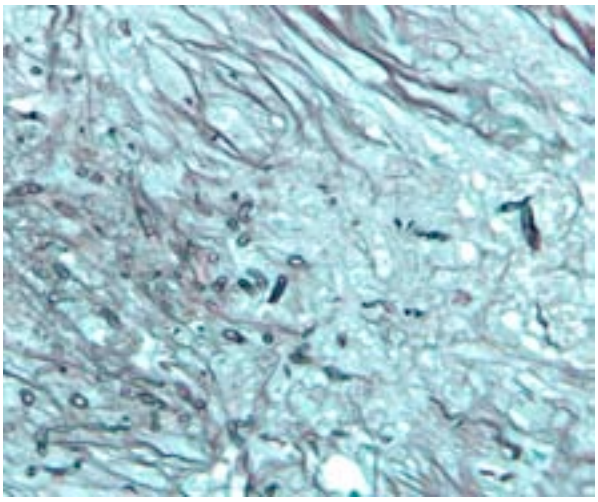

1-4. Small intestine, cat: A GMS stain demonstrates the lack of parallel walls, septations, and the non-dichotomous branching. (Photo courtesy of: Purdue University, Animal Disease Diagnostic Laboratory: http://www.addl.purdue.edu/)

Gross Pathology: A solitary, infiltrative, 3 cm x 3 cm x 8 cm jejunal mass was detected at laparotomy.

Laboratory Results: Infection with *Pythium insidiosum* was confirmed by PCR and gel electrophoresis on DNA extracted from formalin-fixed paraffin-embedded tissue sections.

Histopathologic Description: In a cross-section of resected jejunum, the mucosa was generally spared, except for mild to moderate increase in the number of lamina proprial eosinophils. In contrast, the submucosa and especially the tunica muscularis were almost circumferentially expanded by hypertrophied and hyperplastic fibroblasts in ample to abundant collagenous stroma with diffuse inflammation in which macrophages predominated, but eosinophils were multifocally numerous. The fibroblasts and the macrophages had 0 to 2 mitotic figures per 400x field. The fibroplasia and leukocytic infiltration extended into the serosa and mesentery, but lesional tissue was not evident in the surgical margins of the resection specimen. Although discrete well-organized granulomas were not observed, hyphal 'ghosts' were apparent, especially in foci of necrosis with heavy eosinophil infiltration in the outer layer of the tunica muscularis. Hyphae were easier to see with Gomori's methenamine silver (GMS), and were 2.5-7.5 µm in diameter with nonparallel walls, few septa and few branches. Hyphae and leukocytes were in the wall of a few vessels, mainly arteries. There were increased numbers of eosinophils in sinuses of the mesenteric lymph node biopsy specimen, but granulomatous lymphadenitis was not evident.

Contributor's Morphologic Diagnosis: Jejunum: Eosinophilic granulomatous mural enteritis with sclerosing fibroplasia.

Contributor's Comment: Although the intestinal mass looked like a neoplasm at surgery, the histologic impression was inflammation, with features like those of feline gastrointestinal eosinophilic sclerosing fibroplasia.[1] However, though intralesional bacteria were found in about half the cases, hyphae were not found with GMS in any of the 25 cats in that multi-institutional study. The presence of hyphae in this case expanded the differential diagnosis to include zygomycosis and pythiosis. Infection with *Pythium insidiosum* was confirmed by PCR and gel electrophoresis on DNA extracted from formalin-fixed paraffin-embedded tissue sections. The location of the lesion and the eosinophilic nature of the granulomatous inflammation were similar to gastrointestinal pythiosis in dogs.

Mammalian pythiosis, caused by *Pythium insidiosum,* is mainly a disease of horses, dogs, and humans in tropical, subtropical and temperate regions of the world.[2,3] Whereas equine pythiosis is usually a cutaneous infection, dogs are more likely to develop the gastrointestinal form. Most reported feline cases have been cutaneous or

subcutaneous, rather than intestinal infections.[3] However, intestinal pythiosis has been reported in 2 cats.[5] Interestingly, the prognosis after surgical resection of intestinal pythiosis may be much better in cats than in dogs. The invasive nature in most canine cases of gastrointestinal pythiosis hinders complete excision. In the reported cases, both cats became clinically normal after surgical resection of the intestinal mass and treatment with itraconozole.[5] Pythiosis is rare in Indiana, and is less common in cats than in dogs. In this cat, surgical margins were histologically free of hyphae or the eosinophilic and sclerosing inflammation. In addition to surgical resection of the affected jejunal segment, the cat was treated with prednisolone for the peripheral eosinophilia. Five months after excision of its intestinal mass, the owner reported that the cat had gained weight and was seemingly healthy.

JPC Diagnosis: Small intestine, submucosa, tunica muscularis, serosa and attached mesentery: Enteritis and peritonitis, granulomatous and eosinophilic, circumferential, chronic, diffuse, severe with marked fibrosis and hyphae.

Conference Comment: As noted by the contributor, *Pythium insidiosum* typically produces cutaneous lesions in cats, so with a clinical history of peripheral eosinophilia and palpation of an abdominal mass, pythiosis was not initially suspected. Potential causes of peripheral eosinophilia in a cat include parasitism, hypersensitivity, fungal infection, drug reactions, hyperthyroidism, hypereosinophilic syndrome, gastrointestinal eosinophilic sclerosing fibroplasia and neoplasia, specifically mast cell tumor, T-cell lymphoma, fibrosarcoma, thymoma, various carcinomas and eosinophilic leukemia.[6] Grossly, the jejunal mass was suggestive of alimentary lymphoma, intestinal adenocarcinoma, and feline gastrointestinal eosinophilic sclerosing fibroplasia. One of the most striking histological features in this case is the abundant, circumferential fibrosis, affecting the intestinal submucosa, muscularis and serosa, as well as the adjacent mesentery. This, in combination with the moderate numbers of infiltrating eosinophils, is somewhat reminiscent of feline gastrointestinal eosinophilic sclerosing fibroplasia; however, the presence of hyphae do not fit with this diagnosis.[1]

Pythium species belong to the class *Oomycetes* and are found in warm stagnant water, primarily in tropical to subtropical regions. Oomycetes are not true fungi, although they also produce characteristic hyphae. In contrast to true fungi, oomycetes have cell walls that contain cellulose and β-glucan but lack chitin, and ergosterol is not a significant component of the cell membrane.[4] Most species of *Pythium* are plant pathogens; however, *Pythium insidiosum* is pathogenic to several mammalian species.[4] The infective stage of the oomycete is a motile, biflagellate zoospore that is chemotactically attracted to injured tissue, such as damaged skin or gastrointestinal mucosa, resulting in the classically described cutaneous or enteric lesions.[4] Microscopically, pythiosis must be differentiated from lagenidiosis and zygomycosis. *Lagenidium* sp. is the only other known pathogenic oomycete, and has rarely been described in dogs; it is morphologically indistinguishable from *P. insidiosum*.[4] Although rarely described in cats and dogs, true fungi belonging to the class *Zygomycetes*, such as *Basidiobolus* and *Conidiobolus* sp., also produce hyphae with rare septae. Occasionally, on H&E stained sections, fungal hyphae are surrounded by a 2.5-25 μm eosinophilic "sleeve," which helps differentiate zygomycosis from pythiosis and lagenidiosis.[4]

Contributing Institution: Purdue University
Animal Disease Diagnostic Laboratory: http://www.addl.purdue.edu/
Department of Comparative Pathobiology: http://www.vet.purdue.edu/cpb/

References:

1. Craig LE, Hardam EE, Hertzke DM, Flatland B, Rohrbach BW, et al. Feline gastrointestinal eosinophilic sclerosing fibroplasia. *Vet Pathol*. 2009;46:63-70.
2. Gaastra W, Lipman LJA, De Cock AWAM, Exel TK, Pegge RBG, et al. *Pythium insidiosum*: an overview. *Vet Microbiol.* 2010;146:1-16.
3. Grooters AM. Pythiosis, lagenidiosis, and zygomycosis in small animals. *Vet Clin Small Anim Pract*. 2003;33:695-720.
4. Jang SS, Walker RL. Fungal and algal diseases. In: Greene CE, ed. *Infectious Diseases of the Dog and Cat*, 4th ed. St. Louis, MO: Elsevier; 2012:677-684.
5. Rakich PM, Grooters AM, Tang K-N. Gastrointestinal pythiosis in two cats. *J Vet Diagn Invest*. 2005;17:262-269.
6. Webb JL, Latimer KS. Leukocytes. In: Latimer KS, ed. *Duncan and Prasse's Veterinary Laboratory Medicine Clinical Pathology*. 5th ed. Ames, IA: John Wiley & Sons; 2011:74-75.

CASE II: 11-37333 (JPC 4009691).

Signalment: 11-year-old female spayed West-Highland white terrier dog (*Canis familiaris*).

History: This dog had chronic diarrhea for more than 30 days, which was non-responsive to antibiotics. Exploratory surgery revealed numerous small pin-point pale proliferative lesions within the mesentery and on the enteric serosa. The patient was euthanized due to poor prognosis.

Gross Pathology: Four images were submitted along with the biopsy by the referring clinician. These images reveal severely thickened and turgid enteric wall. On cut section (upper-right hand), there is marked transmural edema involving predominantly mucosa. The mucosa is diffusely rough, pink and has Turkish-towel-like appearance due to chyle-filled lacteals. Multiple, pale, pin-point, discrete, raised, and sharply demarcated granulomas are present on the enteric serosal surface and in the mesentery (lower left and right-hand images).

Laboratory Results: Hypoproteinemia.

Histopathologic Description: Small intestine - The lacteals are markedly dilated and the lamina propria is expanded by edema. Lymphatics within the submucosa, adventitia, muscularis, and mesentery are dilated and are surrounded by vacuolated lipid-laden macrophages with necrotic cores, rare neutrophils and fibrous connective tissue (lipogranulomas). Fibrosis, neutrophils, lymphocytes, and plasma cells are scattered within the mesentery.

Contributor's Morphologic Diagnosis: Small intestine: Severe chronic lymphangiectasia with pyogranulomatous non-mucosal enteritis and lymphangitis.

Contributor's Comment: Lymphangiectasia syndrome is a common cause of malabsorption and protein losing enteropathy in dogs. It is characterized by chronic diarrhea, wasting, hypoproteinemia, hypocalcemia, lymphopenia, and hypocholesterolemia. Anorexia, weight loss and steatorrhea are also observed. Yorkshire terriers and Norwegian Lundehunds are predisposed. The lesions of this syndrome grossly resemble an intestinal neoplasm because of the proliferative nature. Patients with this syndrome are often difficult to treat because of the poorly delineated pathogenesis of this condition; typically, these patients have a poor prognosis. The pathogenesis of this syndrome remains unknown. No congenital or acquired cause of lymphatic obstruction is observed in this case. Lipogranulomas are an inconsistent finding considered to be secondary to chronic leakage of lipid-laden chyle. These lesions can secondarily block lymphatics and add to the edema. Malabsorption of lipid from the gut causes diarrhea through the effects of fatty acids on colonic secretion. Hypocalcemia can be due to

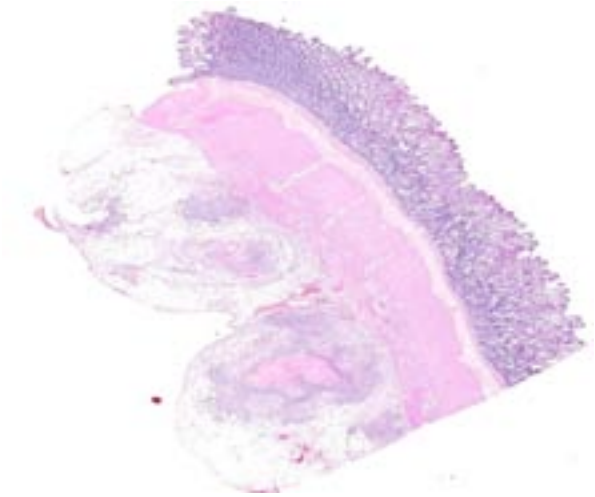

2-1. Small intestine, dog: Subgross inspection of the section demonstrates moderate mucosa and submucosal edema, and the presence of necrotizing and granulomatous inflammation surrounding lymphatics in the serosa and attached mesentery. (HE 0.63X)

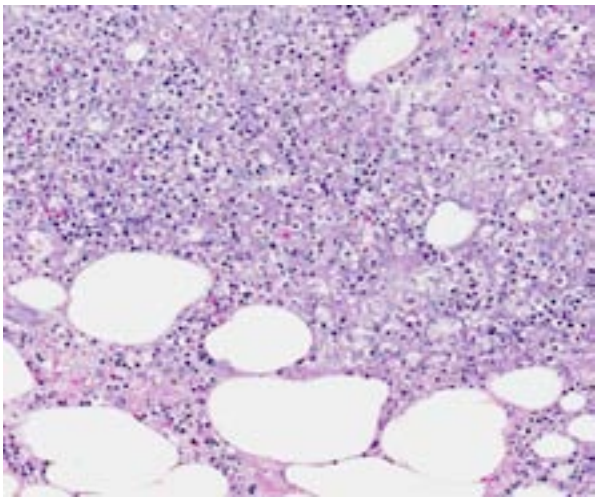

2-2. Small intestine, dog: Foci of lipogranulomatous inflammation within the mesentery are centered on necrotic fat and contain numerous, often degenerate neutrophils and lipophages. (HE 150X)

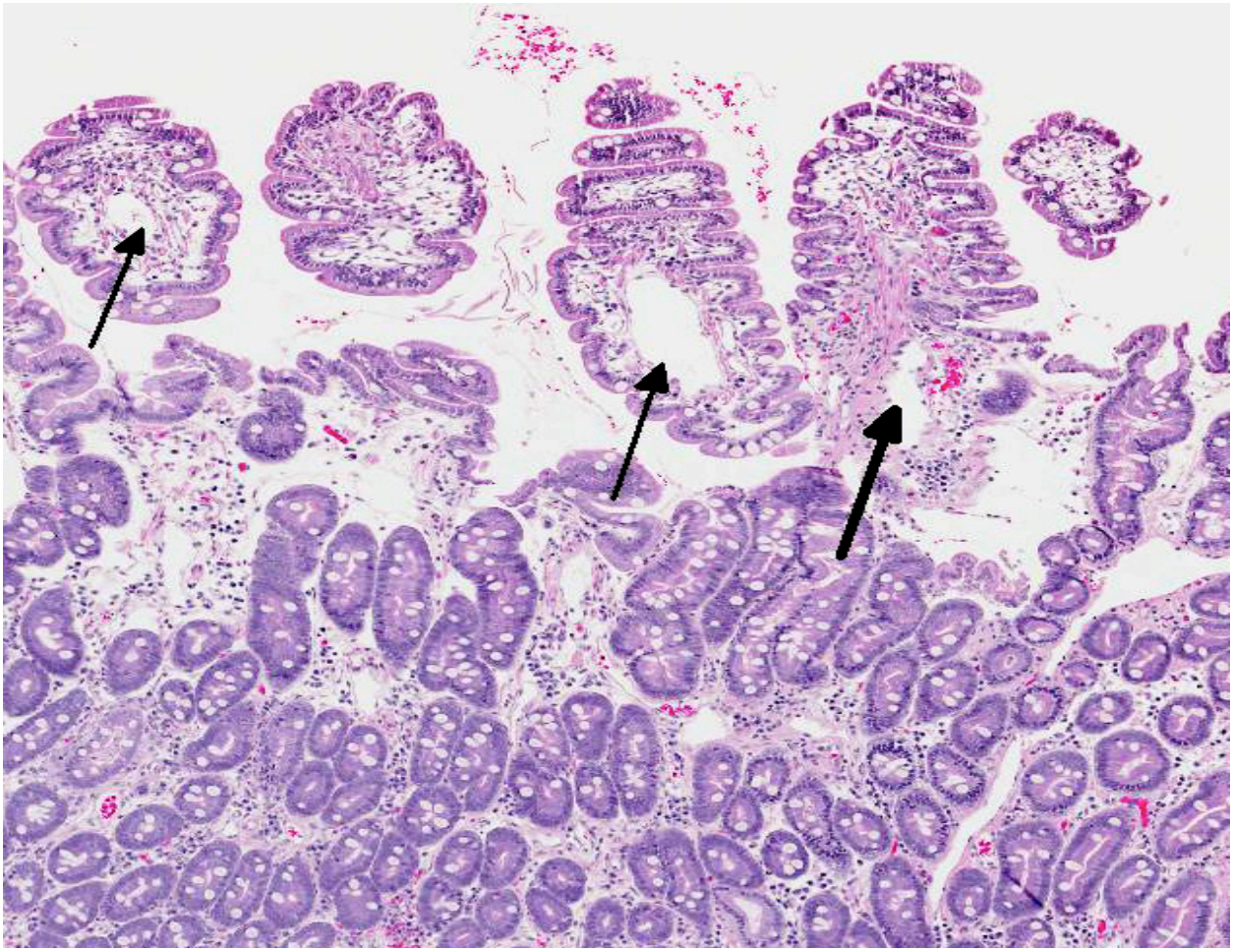

2-3. Small intestine dog: Lymphatics are markedly dilated at the villar tips (arrows), and the lamina propria is distended by clear edema fluid. (HE 50X)

loss of mineral bound albumin and perhaps due to vitamin D malabsorption or binding of calcium with esterified fatty acids. Lipid malabsorption causes hypocholesterolemia, while lymphopenia is due to loss of lymphocyte-rich lymph into the intestine.[1]

JPC Diagnosis: Small intestine, submucosa, tunica muscularis, serosa, and mesentery: Lymphangitis, lipogranulomatous, multifocal to coalescing, severe, with lymphangiectasia and edema.

Conference Comment: A distinguishing feature of lymphangiectasia, which is readily apparent in this case, is the even distribution of histological lesions; intestinal lymphatics and lacteals are generally diffusely affected. In contrast, there are few reports focal lipogranulomatous lymphangitis with lymphangiectasia, which manifests as localized masses rather than disseminated intestinal disease. In most of these cases, there is no laboratory evidence of protein losing enteropathy (PLE) and surgical excision appears curative; however, some affected animals do develop signs consistent with PLE, indicating the possibility of disease progression. Both presentations have an unknown pathogenesis and tend to affect older animals, producing vomiting, weight loss, and diarrhea.[3]

In addition to the idiopathic lymphangiectasia syndrome diagnosed in this case, canine PLE has been associated with alimentary lymphoma, inflammatory bowel disease and infectious agents such as *Giardia, Ancylostoma, Histoplasma, Prototheca* or *Pythium* sp.[2] Gross, histological and clinicopathologic findings, which are comprehensively reviewed above, can help differentiate between these conditions; there are also reports of dogs affected with multiple concurrent causes of PLE.

Contributing Institution: University of Illinois Veterinary Diagnostic Laboratory
http://vetmed.illinois.edu/vdl/index.html

References:
1. Brown CC, Baker DC, Barker IK. Alimentary system. In: Maxie MG, ed. *Jubb, Kennedy, and Palmer's Pathology of Domestic Animals*. 5th ed. Vol. 2. Philadelphia, PA: Elsevier Limited; 2007:103-104.
2. Tarpley HL, Bounous DI. Digestive system. In: Latimer KS, ed. *Duncan and Prasse's Veterinary Laboratory Medicine Clinical Pathology*. 5th ed. Ames, IA: John Wiley & Sons; 2011:244-245.
3. Watson VE, Hobday MM, Durham AC. Focal intestinal lipogranulomatous lymphangitis in 6 dogs (2008-2011). *J Vet Intern Med*. 2013 Nov 7. doi: 10.1111/jvim.12248. [Epub ahead of print]. Accessed January 11 2014.

CASE III: 111156-15 (JPC 4018123).

Signalment: 15-year-old female spayed domestic short hair cat (*Felis catus*).

History: This cat presented with a history of lethargy, anorexia, and vomiting of bile. Physical exam revealed a 1-pound weight loss within the past 4 months, grade 2-3 heart murmur, and doughy, slightly painful abdomen. Abdominal and thoracic radiographs showed no significant findings. An in-house CBC/serum chemistry/ urinalysis panel showed mild azotemia, hypercalcemia, hyperproteinemia, hyperglobinemia and slight increase in ALT. The cat was hospitalized and started on fluid therapy and anti-emetics. Additional clinical samples were then collected and sent out to a commercial laboratory for CBC, routine serum chemistry, urinalysis, serum ionized Ca, serum protein electrophoresis, serum parathyroid hormone related protein (PTHrP) and serum parathyroid hormone (PTH) analyses (see included table). After the results of these tests were known, the owners elected to euthanize the cat upon hearing the presumptive diagnosis (multiple myeloma).

Gross Pathology: A partial necropsy was performed by the clinician with no gross abnormalities noted. Samples of femur bone marrow, spleen, kidney, liver and sections of small intestine were collected for histopathological examination.

Laboratory Results:

Tests	**Results**	**Reference Range**	**Units**
Total Protein	10.7 (HIGH)	5.2-8.8	g/dL
Globulin	7.4 (HIGH)	2.3-5.3	g/dL
AST	152 (HIGH)	10-100	U/L
AST (ALT?)	155 (HIGH)	10-100	U/L
Urea Nitrogen	52 (HIGH)	14-36	mg/dL
Creatinine	2.6 (HIGH)	0.6-2.4	mg/dL
CPK	1109 (HIGH)	56-529	U/L
Calcium, ionized	2.20 (HIGH)	1.16-1.34	µmol/L
Calcium (verified)	18.3 (HIGH)	8.2-10.8	mg/dL
Protein Electrophoresis, serum			
Total Protein	10.7 (HIGH)	5.2-8.8	g/dL
Gamma	4.83 (HIGH)	0.50-1.90	g/dL
PTHrP	0.0	Less than 1.0	pmol/L
PTH	4.0	4-25	pg/ml

- CBC: WNL
- Platelet count: 56 (LOW); due to platelet clumping.
- Urinalysis (cystocentesis): Light yellow, clear, SG – 1.038, pH – 6.0, proteinuria (3+), hematuria (3+) and >50 RBC. Glucose, ketone, bilirubin were negative. No casts, crystals or bacteria. WBC and squamous epithelial cells were WNL.
- Urine microalbumin (feline): 7.4 (HIGH) indicating microalbuminuria.

Histopathologic Description: Bone marrow: The bone marrow is 60% effaced and replaced by an unencapsulated, poorly circumscribed, infiltrative, highly cellular neoplasm. The neoplasm is composed of round cells arranged in sheets supported on a pre-existing fibrovascular stroma. Neoplastic cells have fairly distinct cell borders and moderate amounts of eosinophilic cytoplasm. Nuclei are round to oval, occasionally eccentrically placed, with coarsely stippled chromatin and up to three indistinct nucleoli. Mitoses average five per high power field. There is mild anisokaryosis and anisocytosis, and scattered multifocal single-cell necrosis. There are adequate numbers of megakaryocytes and adipocytes.

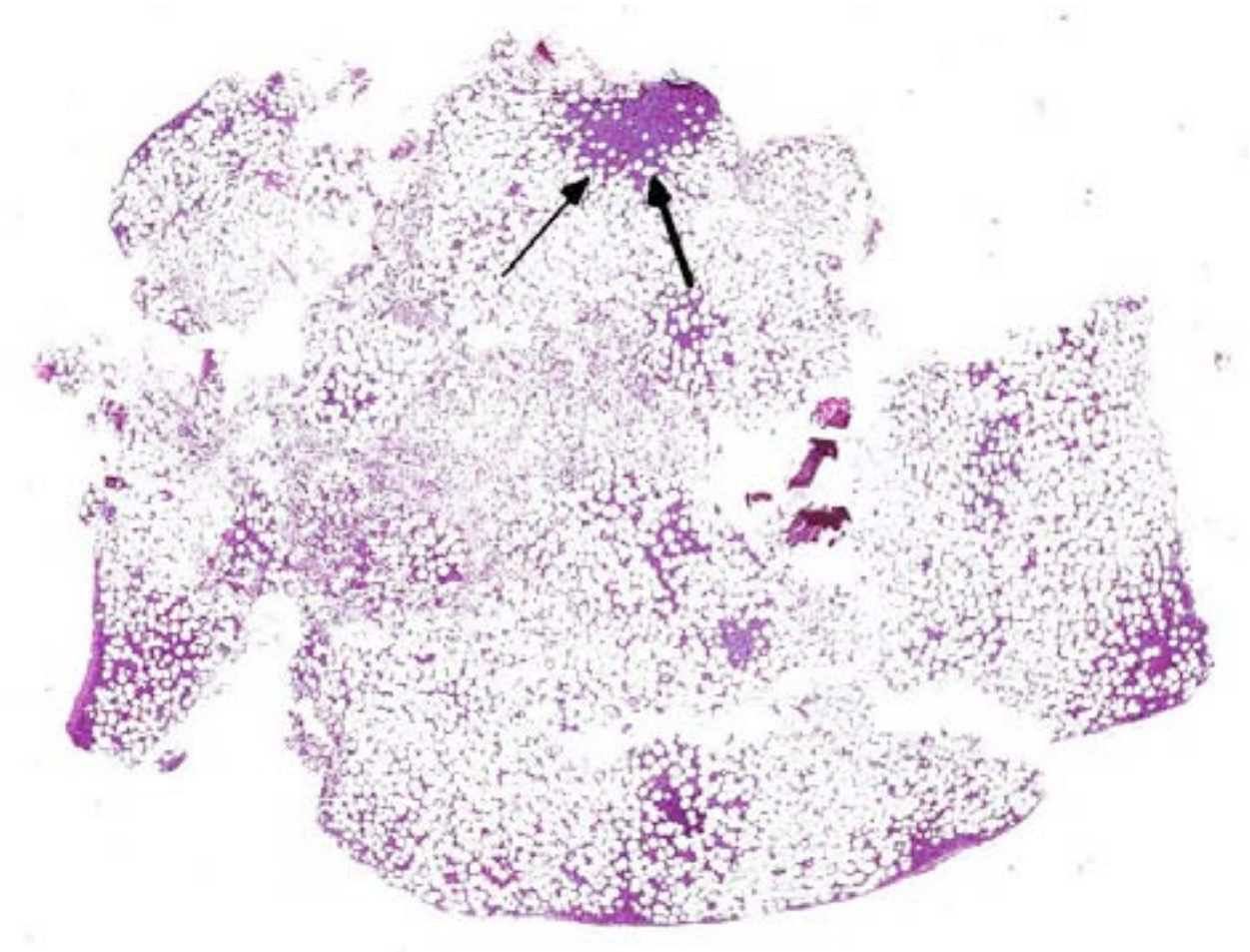

3-1. Bone marrow, cat: Bone marrow is subjectively normocellular at low magnification with adequate marrow fat. At one edge, there is a well-demarcated neoplastic focus (arrows). (HE 0.63X)

Contributor's Morphologic Diagnosis: Bone marrow (femur): Plasma cell myeloma, domestic short hair cat, feline.

Contributor's Comment: Plasma cell neoplasms originate from terminally differentiated B lymphocytes that have undergone malignant transformation. The two main recognized forms of plasma cell neoplasm in veterinary species are multiple myeloma and plasmacytoma. This case is a classical presentation of multiple myeloma, which refers to diffuse disease and, clinically, is the most important plasma cell neoplasm.

In animals, multiple myeloma is a rare, malignant tumor that arises in the bone marrow. It has a slowly progressive clinical course and sites of metastasis include the spleen, liver, lymph nodes and kidneys. Though rare, it has been reported in horses, cattle, cats and pigs, but it is seen more frequently in older dogs with a mean age of 8-9 years.[1,12] In cats, the median age is 12-14 years and there is possibly a male predisposition.[2,6-8] The cause in domestic animals is unknown, but in people, plasma cell neoplasms are associated with working in agriculture, exposure to petroleum products, and chronic exposure to an antigenic stimulus.[3,9-11] There is no evidence that feline immunodeficiency virus, feline leukemia virus, or feline infectious peritonitis virus infections are related to the development of multiple myeloma in cats.[7]

Neoplastic plasma cells usually secrete large amounts of immunoglobulin (Ig), and the hallmark laboratory finding is hyperglobulinemia. This homogeneous protein fraction is often called paraprotein or M-protein.[5]

Diagnosis of multiple myeloma is based on a minimum of two of the following abnormalities:[1,4-6,12-13]

1. Marked increase in numbers of plasma cells in the bone marrow (at least 30% of the nucleated cells are plasma cells which may be well differentiated to poorly differentiated cells with visible nucleoli, marked anisokaryosis and anisocytosis and multinucleation).
2. Monoclonal gammopathy because of clonal production of Ig or Ig fragments by the neoplastic cells. This is demonstrated by serum electrophoresis and can be characterized further using immunodiagnostic techniques. Most of the Igs migrate in the ***gamma***-region, but some may migrate to the *beta*-region (particularly IgA and IgM), hence the usage of the term monoclonal ***gammo***pathy. Note that monoclonal gammopathy is not specific to multiple myeloma and has been reported in cases of B lymphocyte lymphoma and some nonneoplastic conditions such as canine ehrlichiosis or leishmaniasis.
3. Radiographic evidence of osteolysis.
4. Light-chain proteinuria: Bence Jones proteins are free Ig light chains of low molecular weight that pass through the glomerular filter in the urine. These proteins do not react with urine dipstick protein indicators and are specifically detected by electroelectrophoresis and immunoprecipitation.

Patients with multiple myeloma often present with other pathologic findings including:[1,4-6,12-13] 1) hypercalcemia, due to neoplastic cell production of osteoclastic-activating factors

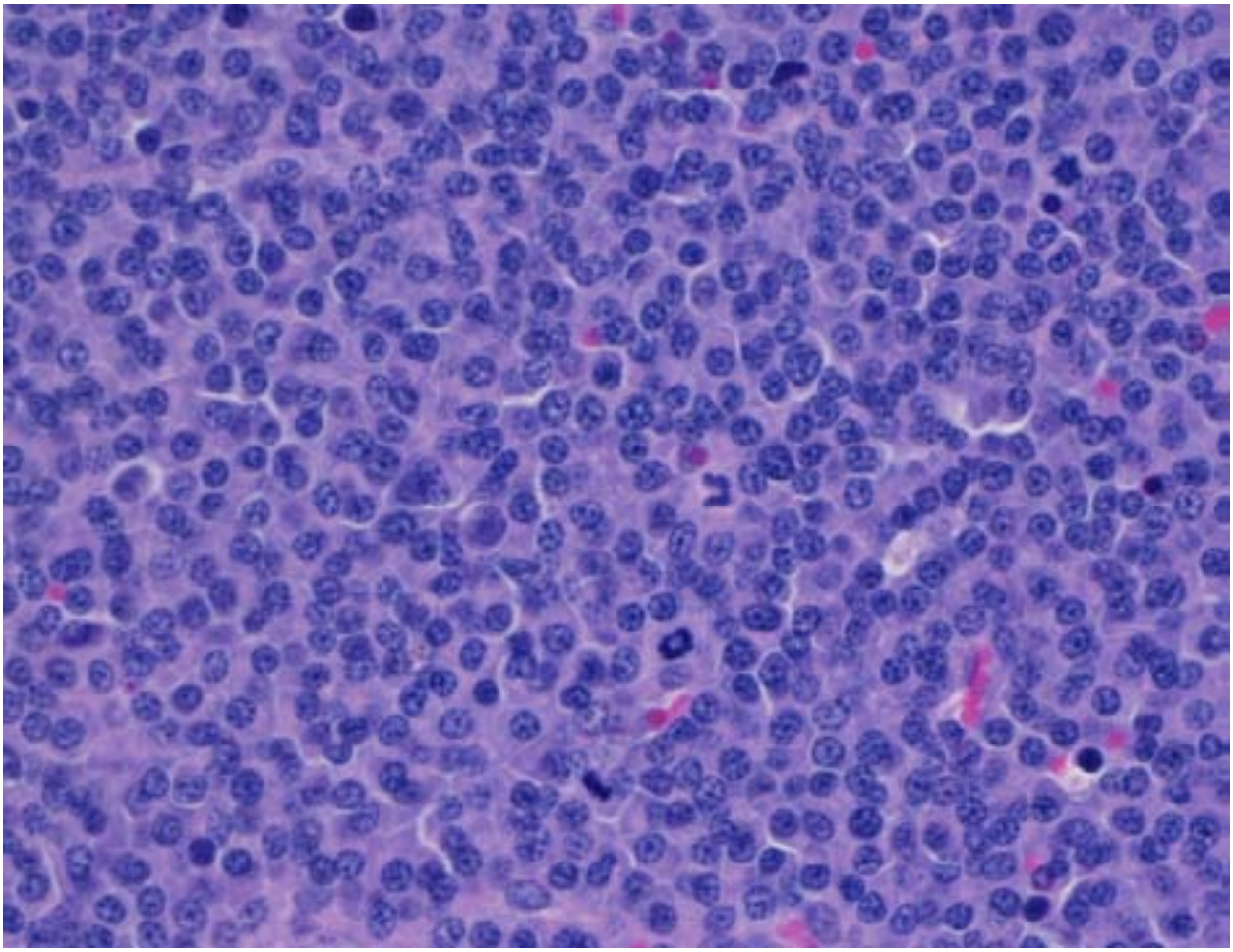

3-2. Bone marrow, cat: Neoplastic round cells exhibit plasma cell differentiation with abundant dark blue cytoplasm, eccentric nuclei and occasionally a perinuclear hoff. In some fields, mitotic figures averaged 5/hpf. (HE 400X) (Photo courtesy of: US Army Medical Research Institute of Infectious Diseases, Pathology Division, Fort Detrick, MD http://www.usamriid.army.mil/)

(RANKL) resulting in resorption of bone,
2) hemorrhage that is caused by secondary platelet dysfunction due to the binding of the paraprotein to platelets (decreased aggregation),
3) hyperviscosity syndrome (IgM and IgA dimers cause an increased viscosity of blood resulting in tissue ischemia and hemorrhage),
4) cytopenias caused by high numbers of neoplastic cells displacing normal bone marrow elements, and
5) renal disease, which develops from nephrocalcinosis secondary to chronic hypercalcemia, hypoxic damage from hyperviscosity, renal toxicity of light chains and neoplastic cell infiltration into the kidney and/or renal amyloidosis.

In this rare feline case of multiple myeloma, the diagnosis was made based on the hallmark laboratory finding of hyperglobulinemia and having two out of the four abnormalities for multiple myeloma: marked increase in numbers of plasma cells in the bone marrow and monoclonal gammopathy. In addition, there was metastasis to the spleen, kidney and liver. Hyperparathyroidism was ruled out based on PTHrP and PTH laboratory findings within normal limits.

Acknowledgment: The author thanks Dr. Lynn Facemire for contributing the clinical case history and the tissue samples for histopathology.

JPC Diagnosis: Bone marrow: Plasma cell myeloma.

Conference Comment: In the histopathologic description, the contributor noted that 60% of the bone marrow nucleated cell population was replaced by neoplastic plasma cells, however, in conference it appeared that plasma cells accounted for a significantly smaller proportion of bone marrow, and neoplastic cells were largely confined to one or two foci within the section. Despite this disparity, conference participants agreed that plasma cells did constitute greater than 30% of the nucleated cell population, which, in combination with the laboratory finding of hypergammaglobulinemia, supports a definitive diagnosis of plasma cell myeloma. Evidence of osteolysis was not reported and there was no history of Bence-Jones proteinuria, the two other diagnostic criteria for diagnosing plasma cell myeloma. Other causes of monoclonal gammopathy in cats and dogs include lymphoma, leukemia, amyloidosis, ehrlichiosis, visceral leishmaniasis, feline infectious peritonitis and plasmacytic gastroenterocolitis.[5] The azotemia and proteinuria/microalbuminuria observed in this case are likely secondary to renal damage, which is a relatively common finding in plasma cell myeloma.[5] Hypercalcemia typically occurs due to neoplastic plasma cell production of osteoclastic-activating factors, which induce bone resorption and subsequent release of calcium.[5] The underlying cause of the elevations in ALT and AST (both of which are hepatocellular leakage enzymes) is not clear, but may be related to tumor metastasis and resultant hepatocellular injury.

Contributing Institution: US Army Medical Research Institute of Infectious Diseases
Pathology Division
Fort Detrick, MD
http://www.usamriid.army.mil/

References:

1. Fry MM, McGavin MD. Bone marrow, blood cells and the lymphatic system. In: McGavin MD, Zachary JF, eds. *Pathologic Basis of Veterinary Disease*. 5th ed. St. Louis, MO: Elsevier; 2012:729-730.
2. Hanna F. Multiple myelomas in cats. *J Feline Med Surg*. 2005;7(5):275-287.
3. Imahori S, Moore GE. Multiple myeloma and prolonged stimulation of reticuloendothelial system. *NY State J Med*. 1972;72(12):1625-1628.
4. Kumar V, Abbas AK, Fausto N, Aster JC. Diseases of white blood cells, lymph nodes, spleen and thymus. In: Kumar V, Abbas AK, Fausto N, Aster JC, eds. *Robbins and Cotran Pathologic Basis of Disease*. 8th ed. Philadelphia, PA: Elsevier Saunders; 2009:609-610.
5. Latimer KS. Hematopoietic neoplasia. In: Latimer KS, ed. *Duncan and Prasse's Veterinary Laboratory Medicine Clinical Pathology*. 5th ed. Ames, IA: Wiley-Blackwell; 2011:93-95,173-181.
6. Mellor PJ, Haugland S, Smith KC, et al. Histopathologic, immunohistochemical, and cytologic analysis of feline myeloma-related disorders: further evidence for primary extramedullary development in the cat. *Vet Pathol*. 2008;45(2):159-173.
7. Mellor PJ, Haugland S, Murphy S, et al. Myeloma-related disorders in cats commonly present as extramedullary neoplasms in contrast to myeloma in human patients: 24 cases with

clinical follow-up. *J Vet Intern Med.* 2006;20(6): 1376-1383.
8. Patel RT, Caceres A, French AF, et al. Multiple myeloma in 16 cats: a retrospective study. *Vet Clin Pathol*. 2005;34(4):341-352.
9. Penny R. Hughes S. Repeated stimulation of the reticuloendothelial system and the development of plasma-cell dyscrasia. *Lancet*. 1970;1(7637):77-78.
10. Rosenblatt J, Hall CA. Plasma-cell dyscrasia following prolonged stimulation of reticuloendothelial system. *Lancet*. 1970;1(7641): 301-302.
11. Speer SA, Semenza JC, Kurosaki T, et al. Risk factors for acute myeloid leukemia and multiple myeloma: a combination of GIS and case control studies. *J Environ Health*. 2002;64(7):9-16.
12. Valli VE. Hematopoietic system. In: Maxie MG, ed. *Jubb, Kennedy and Palmer's Pathology of Domestic Animals*. Vol. 3. 5th ed. Philadelphia, PA: Elsevier Ltd; 2007:107-324.
13. Valli VE, Jacobs RM, Parodi AL, Vernau W, Moore PF. *Histological Classification of Hematopoietic Tumors of Domestic Animals.* 2nd Series, Vol. VIII. Washington DC: Armed Forces Institute of Pathology; 2002.

CASE IV: 2013KSUVDL-2 (JPC 4032561).

Signalment: 3-month-old mixed breed male puppy (*Canis familiaris*).

History: This puppy presented for a complete necropsy following euthanasia. It had a 1.5 week history of myoclonus and tested positive for canine distemper virus on PCR. This puppy was previously vaccinated twice with standard puppy vaccines (DH2PP) and housed with six other puppies who were also positive for canine distemper virus.

Gross Pathology: The puppy was thin, had a body condition score of 2/5 and was in fair post-mortem condition. The lungs failed to fully collapse after opening the thoracic cavity. Diffusely, lung lobes were pale pink and rubbery to firm when palpated. Multifocally, there were variably sized, yellow to greenish firm slightly raised areas of consolidation. Sectioned pulmonary parenchyma bulged and oozed small amounts of serous fluid. The trachea contained moderate amounts of serosanguineous fluid mixed with mucus. Teeth were grossly normal.

Histopathologic Description: Teeth, alveolar bone and gingiva: Each section has deciduous and developing permanent teeth. In the permanent tooth, ameloblasts lining enamel are multifocally swollen, hypereosinophilic, and have fragmented to vacuolated cytoplasm (degeneration). Frequently, ameloblasts contain intracytoplasmic and intranuclear 3-5 µm diameter, round to irregular, bright eosinophilic inclusions. Syncytia with 5-20 nuclei and abundant eosinophilic cytoplasm are multifocally present and contain similar intracytoplasmic inclusions. Ameloblasts are occasionally disorganized with loss of cell polarity and are piled 5-6 cell layers deep. Rarely, there is individual cell necrosis of ameloblasts characterized by shrunken cells, loss of cellular details and pyknotic nuclei. (The dentin and/or enamel are artifactually dislocated in some sections.)

Findings in other tissues (not submitted) include necrosuppurative bronchopneumonia, demyelination of cerebellum and brain stem, neuronal degeneration and necrosis of cervical, thoracic, and lumbar spinal cord segments, myocardial degeneration and necrosis, and lymphoid depletion of the spleen, lymph nodes and tonsils. Similar inclusions were present in the respiratory epithelium of the lung and trachea, mucosal epithelium of the renal pelvis and urinary bladder, astrocytes of the cerebrum and cerebellum and neurons of the spinal cord.

Contributor's Morphologic Diagnosis: Teeth, ameloblasts: degeneration and necrosis, multifocal, moderate to severe, with syncytia and

4-1. Lungs, 3-month old dog: At autopsy, the puppy's lungs were runbbery and failed to collapse. This patchy suppurative interstitial pneumonia is strongly suggestive of canine distemper. (Photo courtesy of: Department of Diagnostic Medicine and Pathobiology, Kansas State Veterinary College of Veterinary Medicine, 1800 Denison Avenue, Manhattan, KS 66506 http://www.vet.k-state.edu/depts/dmp/index.htm)

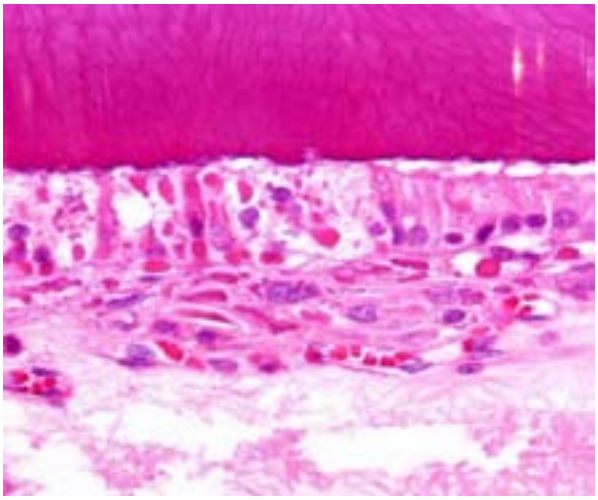

4-2. Developing permanent tooth (tooth bud), 3-month old dog: Degenerate ameloblasts exhibit marked cytoplasmic swelling and numerous 2-4 µm irregular eosinophilic intracytoplasmic viral inclusions, characteristic of canine morbillivirus. (Photo courtesy of: Department of Diagnostic Medicine and Pathobiology, Kansas State Veterinary College of Veterinary Medicine, 1800 Denison Avenue, Manhattan, KS 66506 http://www.vet.k-state.edu/depts/dmp/index.htm)

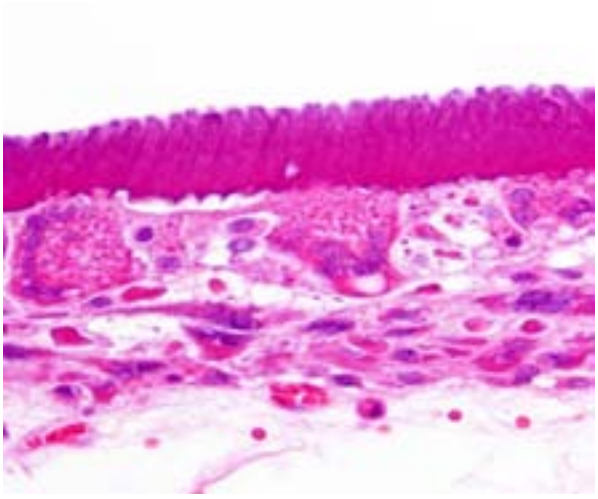

4-3. Developing permanent tooth (tooth bud), 3-month old dog: Numerous multinucleated viral syncytial cells which contain intracytoplasmic viral inclusion bodies are present within the ameloblast layer. (Photo courtesy of: Department of Diagnostic Medicine and Pathobiology, Kansas State Veterinary College of Veterinary Medicine, 1800 Denison Avenue, Manhattan, KS 66506 http://www.vet.k-state.edu/depts/dmp/index.htm)

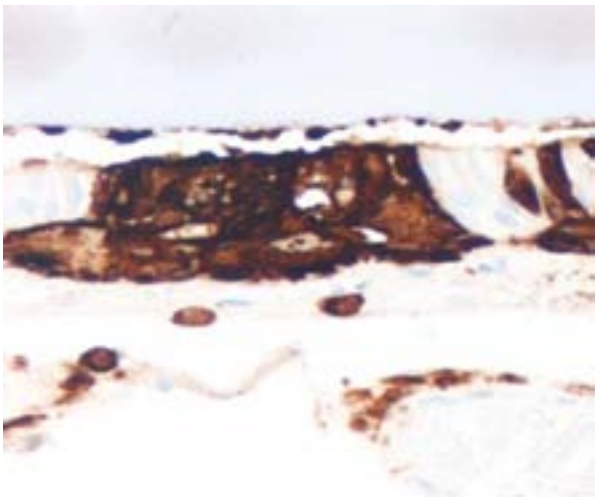

4-4. Developing permanent tooth (tooth bud), 3-month old dog: Ameloblasts show multifocal strong cytoplasmic immunoreactivity for canine morbillivirus antigen. (Photo courtesy of: Department of Diagnostic Medicine and Pathobiology, Kansas State Veterinary College of Veterinary Medicine, 1800 Denison Avenue, Manhattan, KS 66506 http://www.vet.k-state.edu/depts/dmp/index.htm)

eosinophilic intranuclear and intracytoplasmic inclusions.

Contributor's Comment: Canine distemper virus (CDV) is known to cause systemic disease in dogs, fox, coyotes, ferrets and other animals worldwide due to its ability to infect a variety of cell types, including neuroendocrine, epithelial, mesenchymal, and hematopoietic.[1,6] CDV is in the *Morbillivirus* genus and is closely related to measles virus and rinderpest virus.[3,6] The virus is described as a 150-250 nm diameter enveloped virion containing a single negative-sense RNA strand that encodes for various glycoproteins.[3,6] The H glycoprotein is likely used for attachment to the host cell during initial infection, therefore adequate immune response against H protein may lessen or prevent disease.[6]

Transmission of CDV occurs via nasal or oral routes where the virus replicates immediately in the lymphoid tissue causing marked immunosuppression.[1,3,6] Depending on the host response, age and virus strain, the animal will either clear the infection or develop systemic disease. The virus has a propensity to infect epithelial cells in various organs, especially the central nervous system.[3,6] Dogs with partial immunity can be viremic and shed virus for an extended period of time in secretions; clinical signs in these animals are minor to absent and can later manifest as hyperkeratosis of the foot pad and nose.[3,6] Disease following vaccination with modified live CDV vaccine has been occasionally reported;[3,6] however, widespread use of prophylactic vaccination has successfully controlled the disease and is currently uncommon in vaccinated dog populations.[3] A rare condition caused by CDV infection in mature vaccinated dogs is a progressive chronic encephalomyelitis known as old dog encephalitis.[1,3,6]

Clinical signs manifest as respiratory, neurologic, and/or enteric disease. Less commonly, young dogs can develop dental lesions, ocular lesions, and neonatal myocardial degeneration and necrosis.[3] Dental lesions following infection may include necrosis and cystic degeneration of ameloblasts, formation of syncytia, disorganization of ameloblasts, and prominent eosinophilic cytoplasmic viral inclusions.[3,5] Delayed changes in the enamel occur in animals that survive infection and are described as focal defects in the enamel, which appear as depressions (pits) or well-delineated areas of hypoplasia.[3,4] This occurs because the virus directly infects ameloblasts and causes disruption of enamel formation.[4] Other dental abnormalities attributed to CDV include dental impaction, partial eruption, and oligodontia.[2] In the present case, the puppy was euthanized before gross or microscopic evidence of enamel hypoplasia could be detected.

CDV can be diagnosed by a variety of methods; however, molecular assays such as reverse transcriptase polymerase chain reaction (RT-PCR) and real-time RT-PCR are considered sensitive and specific.[6] Distinction between field and vaccine strains is possible via nested RT-PCR assays. Postmortem diagnosis is achieved when there is evidence of systemic or CNS disease and the presence of characteristic inclusion bodies supported by positive immunohistochemistry (IHC) or other ancillary tests. Ameloblasts in the present case had intense multifocal cytoplasmic staining for CDV, which correlated with histologic findings. Additionally, cerebrum and brainstem were IHC positive for CDV. In this case, an unequivocal diagnosis of CDV was made due to the spectrum of gross and microscopic lesions seen along with CDV positive ameloblasts and the reported clinical history.

JPC Diagnosis: Developing tooth, ameloblasts; stratum intermedium: Degeneration and necrosis, multifocal, moderate, with eosinophilic intracytoplasmic viral inclusions and multinucleated viral syncytial cells.

Conference Comment: Conference participants agreed that this is an excellent case, providing a unique microscopic view of a lesion that most pathologists have only seen as a gross photograph.

The contributor provides a thorough review of the pathology of canine distemper virus. In addition to canine distemper, measles and rinderpest virus, the genus *Morbillivirus* comprises peste-des-petits-ruminants virus of goats and sheep, dolphin/porpoise morbillivirus, and phocine distemper virus.[1] Canine distemper virus has a broad host range; besides canids, infection has also been demonstrated in mustelids (ferrets, mink), raccoons, collared peccaries, non-human primates, seals, and felids, including lions, tigers, lynx, bobcat and even domestic cats.[1,6,7]

The signaling lymphocyte activation molecule (SLAM) is a receptor used by morbilliviruses to invade immune cells.[7] Variations in species specificity and infection of "aberrant" species with canine distemper virus was historically thought to result from amino acid alterations in SLAM and/or the hemagglutinin (HA) protein that binds SLAM; however, recent studies suggest that variability of the hemagglutinin protein is less important in determining infectivity and pathogenicity in various host species than was previously believed. Regardless, CDV has emerged as a potentially devastating pathogen in certain wild felid populations.[7]

Although morbilliviruses are notable for producing both intracytoplasmic and intranuclear viral inclusions, conference participants observed that, in this case, intranuclear inclusions were poorly discernible, possibly as a result of the decalcification process.

Contributing Institution: Department of Diagnostic Medicine and Pathobiology
Kansas State Veterinary College of Veterinary Medicine
1800 Denison Avenue
Manhattan, KS 66506
http://www.vet.k-state.edu/depts/dmp/index.htm

References:

1. Beineke A. Pathogenesis and immunopathology of systemic and nervous canine distemper. *Vet Immunol Immunopathol.* 2009;127:1-18.
2. Bittegeko SB, Arnbjerg J, Nkya R, Tevik A. Multiple dental developmental abnormalities following canine distemper infection. *J Am Animal Hospital Assoc*. 1995;31:42-45.
3. Caswell JL Williams KJ. Respiratory System. In: Maxie MG, ed. *Jubb, Kennedy, and Palmer's Pathology of Domestic Animals*, 5th ed. Vol. 2. Philadelphia, PA: Elsevier Saunders; 2007:635-638.
4. Dubielzig RR. The effect of canine distemper virus on the ameloblastic layer of the developing tooth. *Vet Pathol.* 1979;16:268-270.
5. Dubielzig RR, Higgins RJ, Krakowka S. Lesions of the enamel organ of developing dog teeth following experimental inoculation of gnotobiotic puppies with canine distemper virus. *Vet Pathol.* 1981;18:684-689.
6. Martella V. Canine distemper virus. *Vet Clin North Am Small Anim Pract.* 2008;38:787-797.
7. Terio KA, Craft ME. Canine distemper virus (CDV) in another big cat: should CDV be renamed carnivore distemper virus? *MBio*. 2013;4(5):e00702-13.

Joint Pathology Center
Veterinary Pathology Services

WEDNESDAY SLIDE CONFERENCE 2013-2014

Conference 12

15 January 2014

CASE I: 12-1353 (JPC4033123).

Signalment: Adult male Djungarian hamster (*Phodopus sungorus*).

History: Four adult dwarf hamsters with no significant prior medical history were on display at a museum petting exhibit. The animals were in the process of being retired from the exhibit with the intention of adoption when skin lesions were noticed on two hamsters. A male hamster described to have one necrotic pinna was culled and both pinnae were submitted for biopsy. Within one week of receiving biopsy results, a second male adult hamster with an abdominal skin lesion was culled and submitted for autopsy. The submitted tissue section is from the second hamster.

Gross Pathology: A 50g adult male hamster is presented for postmortem examination. The carcass is in good postmortem condition with a

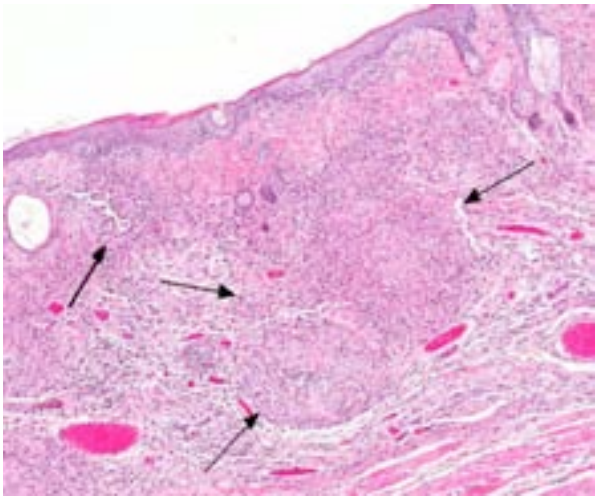

1-1. Haired skin, hamster: The superficial dermis is expanded by multifocal to coalescing aggregates of foamy macrophages. (HE 88X)

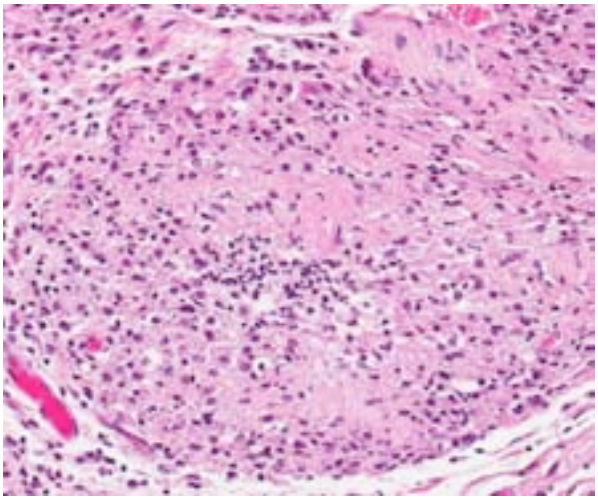

1-2. Haired skin, hamster: Some of the granulomas have a central core of viable neutrophils. (HE 120X)

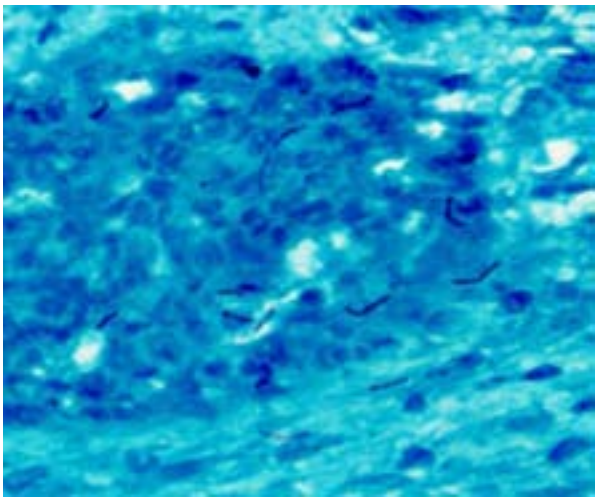

1-3. Haired skin, hamster: Scattered within granulomas are low numbers of filamentous, beaded, acid-fast bacilli. (Fite-Furaco 400X)

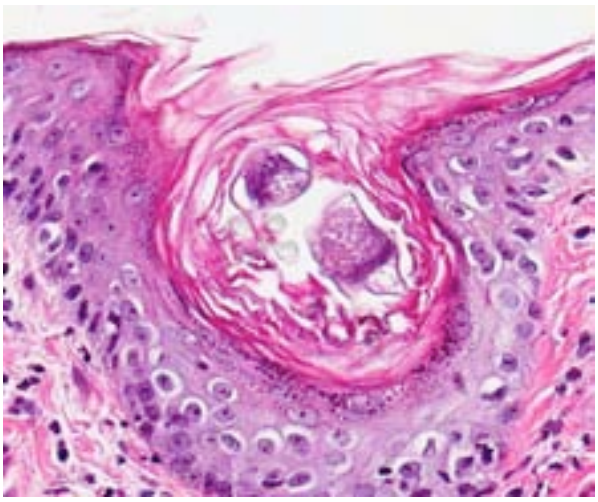

1-4. Haired skin, hamster: Epidermal pits and hair follicles contain cross-section of mites. (HE 400X)

euthanasia-to-necropsy interval of 13 hours. Throughout the body, adequate adipose stores are present. A focally extensive area of caudal abdominal skin, extending from the umbilicus to the perineal region and encompassing both the left and right inguinal areas, has an asymmetric, poorly haired, moist, red patch with a 0.1 cm in diameter paramedian ulcer and several small irregular brown crusts. No internal gross abnormalities are noted. Caudal abdominal skin is submitted.

Laboratory Results: Formalin-fixed, paraffin-embedded tissue was submitted for mycobacterial PCR, and the resulting sequence most closely matched that of *Mycobacterium marinum* and *M. ulcerans* (greater than 99% sequence identity with GenBank acc#AB026701 and CP000325).

Histopathologic Description: Abdominal skin: The dermis and panniculus are expanded by multifocal to coalescing nodular infiltrates of abundant histiocytes and neutrophils that form multifocal pyogranulomas with abundant central degenerative neutrophils and necrotic cellular debris surrounded by a thick rim of epithelioid macrophages. Low numbers of gram-positive, acid-fast bacilli are present in scattered histiocytes. The overlying epithelium is multifocally, irregularly hyperplastic with multifocal intracellular edema, frequent neutrophil and lymphocyte transmigration which frequently disrupts the basal layer, few intraepidermal neutrophil aggregates, and mild orthokeratotic hyperkeratosis. (The original pinna biopsy submission from the male hamster has similar histological findings.)

Contributor's Morphologic Diagnosis: Haired skin: Marked, multifocal to coalescing pyogranulomatous dermatitis and panniculitis with intralesional acid -fast bacilli (mycobacteriosis).

Contributor's Comment: Mycobacteriosis in mammals typically occurs via contamination of skin wounds or traumatic inoculation and rarely via inhalation.[6] Direct contact with environmental inhabitants generally results in local disease, but can pose a greater risk to immunocompromised individuals. *M. marinum* is ubiquitous in fresh, brackish, and salt water, and causes disease in fish and humans ("fish tank granulomas" or "swimming pool granulomas"). Human infection typically results from direct inoculation into skin abrasions while handling fish or tank water, leading to slow growing nodules at the site of inoculation and local lymphadenopathy.[3] *M. ulcerans* is the causative agent of Buruli ulcer, the third most common mycobacterial disease in humans. Epidemiologic factors are not completely understood, as the disease is most common in dry periods in wetlands of tropical or subtropical regions.[6] The toxin mycolactone is believed to cause the characteristic ulcerative and necrotic cutaneous and subcutaneous lesions.[2] *M. ulcerans* is a rare cause of atypical mycobacteriosis in cats, causing ulcerative and nodular skin lesions.[7] Koalas and possums in Australia are naturally infected with

M. ulcerans.[5] Recently it has been proposed that small mammals may serve as a reservoir for *M. ulcerans*.[1]

The source of mycobacterial infection in the museum hamsters was not identified, although there are numerous aquatic displays at the museum. Despite the zoonotic potential, no human cases of infection were reported.

JPC Diagnosis: 1. Haired skin and subcutis: Dermatitis, pyogranulomatous, multifocal to coalescing, moderate, with edema and rare intrahistiocytic acid-fast bacilli.
2. Haired skin, epidermis: Hyperplasia, multifocal, mild to moderate with mild orthokeratotic hyperkeratosis, intracorneal pustules and occasional acarid parasites.

Conference Comment: *Mycobacterium ulcerans* and *M. marinum* are closely related, slow growing, opportunistic pathogens most notable for causing skin disease in humans[8] (see WSC 2013-14 conference 2, case 2 for a summary of the mycobacterial classification system). Aquatic *Acanthamoeba* sp. has been implicated as a natural host of *M. marinum* and *M. ulcerans*, and may play an important role in disease transmission;[9] however, in this case there is no indication that the affected hamsters were housed near the museum's aquatic displays.

In addition to the striking dermal lesions in this hamster, attributed to infection with *M. marinum/ ulcerans*, there are rare intrafollicular and intracorneal segments of arthropods, up to 40 µm in diameter and 200 µm in length, with a thin, eosinophilic, chitinous exoskeleton, short jointed appendages, a hemocele, striated muscle, and digestive and reproductive tracts. These arthropods are associated with epidermal hyperplasia, orthokeratosis, and occasional intracorneal pustules. The differential diagnosis includes *Demodex* sp. and *Notoedres* sp. *Demodex criceti* and *D. aurati* infestation is common in many hamster colonies; however, these mites exhibit low pathogenicity and rarely cause clinical signs. *Notoedres notoedres*, a mite that burrows into the stratum corneum, is less common, although it can be enzootic in some hamster colonies. Males typically have a higher parasite load than females, and factors such as advanced age or stress from handling may predispose skin lesions in animals with no previous clinical signs.[4]

Contributing Institution: North Carolina State University, College of Veterinary Medicine
Department of Population Health and Pathobiology
1060 William Moore Drive, Raleigh, North Carolina 27607
http://www.cvm.ncsu.edu/dphp/path/anatomicpath.htmlhttp://www.cvm.ncsu.edu/dphp/path/anatomicpath_eduinfo.html#resprogram

References:

1. Durnez L, Suykerbuyk P, Nicolas V, Barriere P, Verheyen E, Johnson CR, et al. Terrestrial small mammals as reservoirs of *Mycobacterium ulcerans* in Benin. *Appl Environ Microbiol*. 2010;76(13):4574-4577.
2. George KM, Pascopella, L, Welty DM, Small PL. A *Mycobacterium ulcerans* toxin, mycolactone, causes apoptosis in guinea pig ulcers and tissue culture cells. *Infec. Immun*. 2000;68(2):877-883.
3. Iowa State Animal Disease Fact Sheet: Mycobacteriosis. 2007. www.cfsph.iastate.edu/DiseaseInfo/factsheets.php
4. Percy DH, Barthold SW. Hamster. In: *Pathology of Laboratory Rodents and Rabbits*. 3rd ed. Ames, IA: Blackwell Publishing; 2007:193-194.
5. Portaels F, Chemlal K, Elsen P, Johnson PDR, Hayman JAA, Hibble J, et al. *Mycobacterium ulcerans* in wild animals. *Rev Sci Tech*. 2001;20(1):252-264.
6. Portaels F. *Mycobacterial diseases of the skin*. 1995:207.
7. Songer JG, et al. *Veterinary Microbiology: Bacterial and Fungal Agents of Animal Disease*. St. Louis, MO: Elsevier Saunders; 2004:95.
8. Wayne LG, Sramek HA. Agents of newly recognized or infrequently encountered mycobacterial diseases. *Clin Microbiol Rev*. 1992;5(21):1-25.
9. Wilson MD, Boakye DA, Mosi L, Asiedu K. In the case of transmission of *Mycobacterium ulcerans* in buruli ulcer disease *Acanthamoeba* species stand accused. *Ghana Med J*. 2011;45(1): 31-34.

CASE II: AFIP1 Pfizer (JPC 4001270).

Signalment: 4.5- month-old male New Zealand white rabbit (*Oryctolagus cuniculus*).

History: Several rabbits presented with anorexia and loose feces.

Gross Pathology: Necropsy of one of the rabbits revealed that the stomach was distended with food and the remainder of the gastrointestinal tract contained loose digesta. Based on the necropsy findings and clinical observations, enteropathy was diagnosed and routine histology sections were processed.

Electron microscopy: Intestine: The image consists of portions of four enterocytes, identified by the presence of numerous normal and swollen microvilli. Some of the microvillar border is replaced by randomly arranged, oval to elongate, approximately 0.8 to 1.0 µm diameter, encapsulated bacilli. The bacilli are located outside the cell membrane on the apical surface of enterocyte where they create an indentation (cup and/or pedestal) where they abut the cell surface. At the attachment site, the apical portion of affected enterocytes is thickened by a homogeneous band of lightly electron dense material that disrupts the terminal web. In the swollen microvilli, the actin cystoskeleton is not recognizable. Both nucleated cells present in the image exhibit mild hydropic changes in the apical cytoplasm, indicative of degeneration.

Histopathologic Description: Multiple sections of large intestine are examined and all contain similar lesions. Along the apical surface of enterocytes, there are myriad, often adherent, short (approximately 1 x 2 µm), plump bacilli. The epithelium is often disorganized and crowded containing irregularly shaped enterocytes with slightly basophilic cytoplasm and prominent nuclei (regenerative epithelia) admixed with scattered necrotic epithelial cells. Occasionally, crypts are dilated with heterophils and necrotic cellular debris (crypt abscesses) and lined by flattened, frequently hyperplastic cells. The mucosa is variably edematous and contains moderate numbers of heterophils infiltrating the lamina propria.

Bacteria attached to the apical surface of enterocytes are gram-negative bacilli.

Other findings include renal tubular necrosis and regeneration, hepatic and myocardial necrosis with mineralization, focal heterophilic subpleural pneumonia, and tracheitis.

Contributor's Morphologic Diagnosis: Cecum, Colon: Typhlocolitis, erosive and heterophilic, mild, diffuse, subacute, with myriad attaching gram-negative bacilli.

Contributor's Comment: Attaching and effacing *Escherichia coli* (AEEC) is a prominent enteric pathogen in rabbits, and is a major cause of disease in commercial farms and occasionally

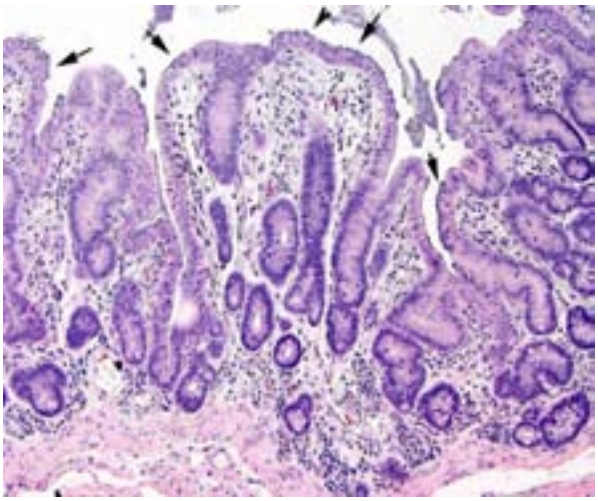

2-1. Colon, rabbit: Edema markedly expands the colonic lamina propria, separating glands. Even at low magnification, the apical brush border of colonic epithelium is prominently basophilic. (HE 80X)

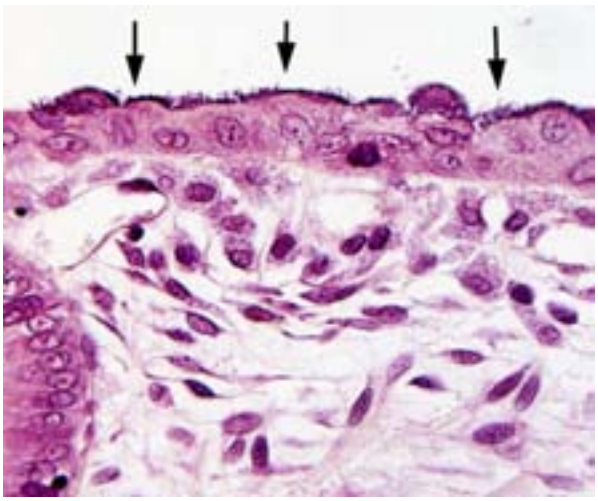

2-2. Colon, rabbit: The microvillar border of the colonic epithelium, both on the luminal surface and within glands is segmentally lined by large numbers of robust gram-negative rods, consistent with attaching and effacing E. coli infection. (Brown-Hopps 400X)

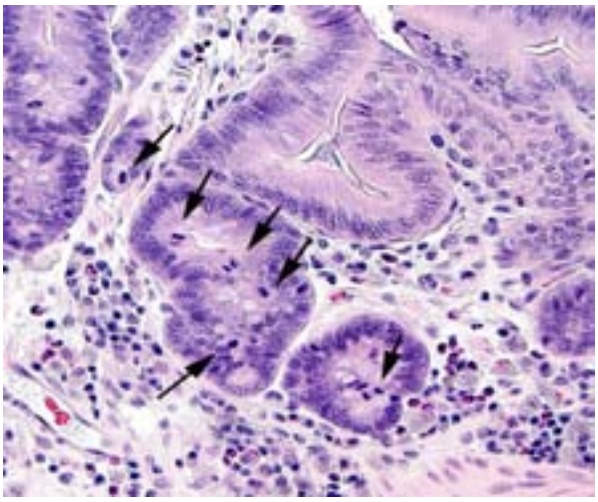

2-3. Colon, rabbit: Mitotic figures are numerous with glands (arrows). (HE 400X)

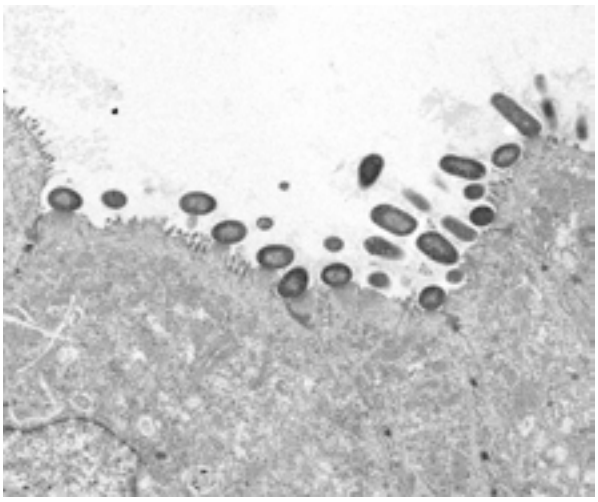

2-4. Colon, rabbit: Ultrastructurally, E coli attach to the microvillar border with formation of characteristic "cups and pedestals". (Photo courtesy of: Pfizer Inc., Global Research and Development, Groton/New London Laboratories, Eastern Point Road MS 8274-1330, Groton, CT., www.pfizer.com)

in research facilities.[9] Age, history, clinical signs, gross and microscopic findings are useful criteria in the diagnosis. Characterization of the isolate is recommended to determine whether the strain is likely to be a primary pathogen.[9] Mortality varies from very low to very high, and when dealing with low pathogenic strains, the infection can be controlled with hygiene and antibiotic treatments. In the case of highly pathogenic strains, most antibiotics fail and the whole rabbit stock must be killed and replaced.[7] The definitive method for the determination of AEEC lesions is the observation of the characteristic ultrastructural appearance of the lesion, which consists of bacteria attached to the apical surface of enterocytes and goblet cells, with swelling and effacement of microvilli and disruption of the actin cytoskeleton, followed by epithelial desquamation, villous atrophy and malabsorption.[5-7,11] Isolates of enteropathogenic *Escherichia coli* (EPEC) can be subdivided into strains affecting suckling rabbits and those affecting weanlings. In suckling rabbits, the infection is associated with yellowish watery diarrhea in animals ranging from 7 to 12 days old. Lesions are usually found throughout the small and large intestine, accompanied by mucosal ulcerations and hemorrhages. The serotype O109:H2 appears to be restricted to suckling rabbits and causes minimal disease in weaned animals.[8,9]

In weaned rabbits, bacterial attachment occurs in the ileum, cecum and colon. Weanling rabbits are typically affected at 4-6 weeks of age; diarrhea occurs approximately six days after infection and the gross findings include watery intestinal contents, serosal ecchymosis, edema of the intestinal walls and mesenteric lymphadenomegaly. Microscopically, bacteria adhere to enterocytes and have a typical bacillary appearance. Colonized cells appear degenerate and many are hyperchromatic, rounded-up and/or pyknotic, with frequent mucosal erosions and detachment. At low magnification, this confers a "cobblestone" appearance to the mucosal surface. The inflammatory component of the lesion is variable, ranging from mild edema to focal polymorphonuclear infiltrates infiltrating the lamina propria.[9,11] Serotypes frequently found in weaned rabbits are O15:H-, O26:H11, O103:H2 and O109:H2.[8,9]

Initial attachment of the bacteria is non-intimate and restricted to the follicle-associated epithelium of Peyer's patches in the ileum, hence the differences of strain causing disease in suckling and weanlings rabbits. It has been proposed that the resistance of suckling rabbits to weanling-associated strains is due to the fact that Peyer's patches do not develop before two weeks of age.[3]

Primary non-intimate adhesion is critical for the virulence of rabbit strains of EPEC, and is accomplished by a variety of adhesins, often targeted at the follicle associated epithelium of the ileal Peyer's patches, similar to the process

observed in humans.[10] Rabbit AEEC rarely produce enterotoxin or Verotoxin and in contrast to other host species, the presence of *eae* gene in the rabbit is closely associated with diarrheal disease.[2]

The attaching-effacing lesion is due to an interesting mechanism, which is well studied *in vitro* using enteropathogenic *E. coli* (EPEC) O127:H6. This mechanism consists of four stages, responsible for the pathologic and ultrastructural findings (reviewed by Wales et al, 2005).[11] Briefly, the first stage is initial non-intimate attachment. EPEC secreted proteins (Esp) Esp-A, -B and -D are exported via a type III secretion system into the host eukaryotic cell. Esp-B and -D, in addition, may create a pore forming structure in the cell membrane, and these elements form a channel for the introduction of bacterial macromolecules in the host cytoplasm. During this stage, there is translocation of the translocated-intimin-receptor protein (Tir) into the host cell. During the second stage, there is signal transduction leading to cytoskeletal reorganization and microvillus effacement. At the site of intimate attachment, there is considerable cytoskeletal reorganization, with depolarization of actin, formation of F-actin and accumulation of α-actinin, myosin light chain, talin and ezrin; all of these changes are associated with effacement of microvilli and disruption of the intestinal barrier function of enterocytes. During this second stage, Tir is inserted in host cell membrane. The third stage is known as intimate attachment. In the third stage, Tir focuses filamentous actin, forming a "pedestal." Intimin, encoded by the enterocyte attaching and effacing gene (*eae*), is a surface-exposed outer membrane protein. Intimin binds Tir, and this binding is indispensable for the development of AE lesions. The fourth stage is invasion. Intracytoplasmic bacteria have been observed in vacuoles and free in the cytoplasm of the host cell, and rarely in the lamina propria. In the rabbit AEEC is not considered to be enteroinvasive.[9]

In conclusion, even in absence of bacteriologic culture, the diagnosis of this case was possible based on the histopathological and electron microscopy findings. Culture and serotyping of the bacteria, plus histopathology, are the preferred methods of diagnosis. No other cases were identified in the colony after this event.

JPC Diagnosis: Colon: Colitis, heterophilic and proliferative, diffuse, mild, with edema and numerous enterocyte surface-associated Gram negative bacilli.

Conference Comment: Histochemical staining with Brown & Hopps stain reveals numerous gram-negative bacilli adhered to the large intestinal mucosa. This, in combination with the characteristic electron microscopy findings previously described, supports the contributor's diagnosis of enteropathogenic *Escherichia coli*.

Escherichia coli is a gram-negative, non-spore-forming bacillus. Non-virulent strains are often part of the normal intestinal flora, while virulent strains are capable of causing multiple disease syndromes in humans and animals via assorted combinations of virulence factors.[1,4] Specific serotypes of *E. coli* (e.g., O157:H7) are named based on the presence of the following antigens:[4]

- O-antigen (somatic): located on the lipopolysaccharide molecule
- K-antigen (capsular): outermost structural component composed of carbohydrates
- H-antigen (flagellar): composed of flagellin protein
- F-antigen (fimbrae or pili): adhesins which project from the bacterial cell wall

Enteric disease is a common manifestation of colibacillosis. The pathology of enteropathogenic, or attaching and effacing (AEEC) *E. coli* is described in detail by the contributor. In addition to rabbits, this form of colibacillosis can cause diarrhea in pigs, dogs and humans. Some strains of enterohemorrhagic *E. coli* (EHEC), also known as Shiga toxin-producing or verotoxin-producing *E. coli*, are attaching and effacing as well. This subset produces cytotoxins that are structurally similar to the Shiga toxins generated by *Shigella dysenteriae*, which bind the host cell glycolipid receptor globotriaosylceramide (Gb3), causing inhibition of protein synthesis with subsequent necrosis. Shiga toxins primarily affect intestinal epithelium and vascular endothelium, due to the presence of Gb3 receptors in these tissues. Enterohemorrhagic strains of *E. coli*, such asserotype O157:H7, are most notorious as a cause of human foodborne illness; however, they

are also associated with erosive fibrinohemorrhagic enterocolitis in calves under four weeks old. In dogs, EHEC has occasionally been linked with dysentery and, in greyhounds, a hemolytic uremic syndrome with cutaneous edema and ulceration known as cutaneous and renal glomerular vasculopathy. Furthermore, edema disease in weaned pigs is caused by enteric colonization with Shiga toxin-producing *E. coli*, mediated by F18ab fimbriae. This syndrome is characterized by central nervous system signs or sudden death due to vasculitis and edema. It is often associated with outbreaks of post-weaning *E. coli* enteritis (EHEC) and only occasionally produces diarrhea. Typically, edema disease results in a classical enterotoxemia without significant gross or microscopic lesions.[1]

Enterotoxigenic *E. coli* (ETEC) is a common cause of neonatal diarrhea in calves and piglets less than four days old. Among its most important virulence factors is its ability to colonize the intestine and produce enterotoxin. Fimbriae (also known as pili), composed of pilin, project from the bacterial cell wall, and attach to enterocyte surface receptors. Fimbrial adhesins are antigenically distinct and somewhat species-specific; immunohistochemical stains can thus be helpful in reaching a definitive diagnosis. Enterotoxins produced by ETEC include heat-labile toxin and heat-stable toxin. Heat-labile toxin is composed of two subunits, known as LTI and LTII. LTI resembles cholera toxin, while LTII utilizes an adenylate cyclase pathway (i.e., cAMP) to initiate irreversible intestinal secretion of electrolytes and water, leading to secretory diarrhea. The heat-stable toxin STa causes inhibition of Na/Cl co-transport and water absorption via an increase in cyclic guanosine monophosphate (cGMP), while STb (primarily associated with ETEC in pigs) promotes secretion by stimulating production of prostaglandin E_2 and 5-hydroxytrypamine. Although ETEC results in severe osmotic diarrhea, dehydration, and potentially death, this syndrome serves as another example of a classical enterotoxemia with minimal gross and microscopic lesions.[1]

Some strains of *E. coli* are able to invade intestinal enterocytes, eventually disseminating throughout the body and resulting in septicemic colibacillosis. These enteroinvasive strains are best described in humans; however, invasive strains of *E. coli* also affect fowl, resulting in myriad clinical syndromes including septicemia and enteric disease.[4] Other strains of *E. coli* induce systemic infection by avoiding host defense mechanisms, especially in young, compromised animals such as neonates subjected to failure of passive transfer of immunity, or those with concurrent, debilitating disease. Several important virulence factors of potentially septicemic *E. coli* strains, such as the capsule, outer membrane proteins, toxins, or fimbriae, are encoded on bacterial colicin V plasmids. When these bacteria die they often release endotoxin from lipopolysaccharide on the outer membrane, leading to the clinical signs and gross and microscopic lesions associated with endotoxic shock.[1]

Contributing Institution: Pfizer Inc.
Global Research and Development
Groton/New London Laboratories
Eastern Point Road MS 8274-1330
Groton, CT.
Phone: 860-441-4498
www.pfizer.com

References:

1. Baker DC, Barker IK, Brown. The alimentary system. In: Maxie MG, ed. *Jubb, Kennedy and Palmer's Pathology of Domestic Animals*. Vol. 2. 5th ed. Philadelphia, PA: Elsevier Saunders; 2007:183-193.
2. Blanco JE, Blanco M, Blanco J, Mora A, Balaguer L, Mourino M, Juarez A, et al. O serogroups, biotypes and eae genes in Escherichia coli strains isolated from diarrheic and healthy rabbits. *J Clin Microbiol*. 1996;34:3101-3107.
3. Heczko U, Abe A, Finlay BB. In vivo interaction of rabbit enteropathogenic *Escherichia coli* O103 with its host: electron microscopic and histopathologic study. *Microbes Infect*. 2000;2:5-16.
4. Hirsh DC. Family *Enterobacteriaceae*. In: Hirsh DC, Zee YC, eds. *Veterinary Microbiology*. Malden, MA: Blackwell Science; 1999:69-74.
5. Moon HW, Whipp SC, Argenzio RA, Levine MM, Giannella RA. Attaching and effacing activities of rabbit and human enteropathogenic *Escherichia coli* in pig and rabbit intestines. *Infect Immun*. 1983;41:1340-1351.
6. Peeters JE, Charlier GJ, Raeymaekers R. Scanning and transmission electron microscopy of attaching effacing *Escherichia coli* in weanling rabbits. *Vet Pathol*. 1985;22:54-59.

7. Peeters JE, Geeroms R, Ørskov F. Biotype, serotype, and pathogenicity of attaching and effacing enteropathogenic *Escherichia coli* strains isolated from diarrheic commercial rabbits. *Infect Immun*. 1988;56:1442-1448.
8. Peeters JE, Pohl P, Okerman L, Devriese LA. Pathogenic properties of *Escherichia coli* strains isolated from diarrheic commercial rabbits. *J Clin Microbiol*. 1984;20:34-39.
9. Percy DH, Barthold SW. *Pathology of laboratory rodents and rabbits*. 3rd ed. Ames, IA: Blackwell Publishing; 2007:273-274.
10. Phillips AD, Frankel G. Intimin-mediated tissue specificity in enteropathogenic *Escherichia coli* interaction with human intestinal organs in culture. *J Infect Dis*. 2000;181:1496-1500.
11. Wales AD, Woodward MJ, Pearson GR. Attaching-effacing bacteria in animals. *J Comp Path*. 2005;132:1-26.

CASE III: 13-V212 (JPC 4032443).

Signalment: 14-month-old female mouse αβ crystallin/HSPB2 knockout, C57Bl6 background (*Mus musculus*).

History: Genetically engineered mouse involved in ocular research relating to lens proteins. Three of three cagemates present with similar clinical signs, including hunched posture, rough haircoat, and poor body condition (body condition score 2/5). Marked kyphosis noted in all three mice. No improvement with supportive care over two days.

Gross Pathology: Reduced subcutaneous, peritoneal, and reproductive fat deposits. Marked kyphosis with prominent dorsal deviation of the mid-thoracic spine. No other gross abnormalities detected.

Laboratory Results: Splenic culture: No aerobic or anaerobic growth.

Histopathologic Description: On decalcified cross sectional views of the head, there is a focal, marked loss of the normal muscle architecture of the posterior tongue characterized by a large central region of myofiber loss and replacement by white fat. Diffusely throughout the remainder of the tongue, there is moderate myofiber size variation, myofiber pallor and cytoplasmic vacuolation, and myofiber loss and replacement by perimyseal white fat and endomysial fibrous connective tissue. Moderate multifocal myofibers have uneven cellular staining with central strongly eosinophilic homogenous material (hyaline degeneration of the sarcoplasm). There is mild, multifocal lymphocytic and histiocytic inflammation. Other muscles of the head show less pronounced changes, although mild hyaline degeneration of the sarcoplasm, central nuclei,

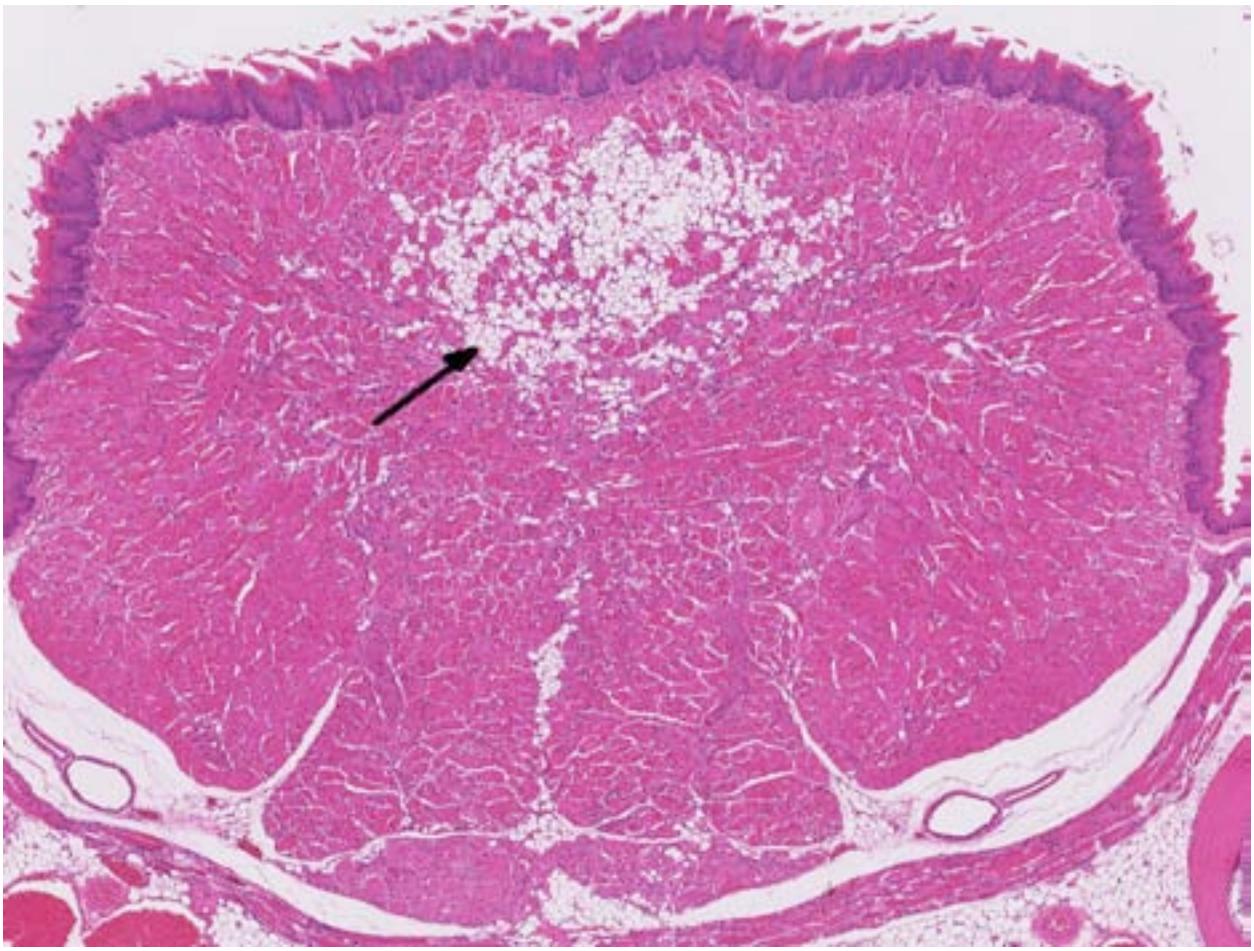

3-1. Tongue, αβ crystallin/HSPB2 knockout c57Bl6 mouse: Skeletal muscle of the tongue exhibits uneven staining characteristics, and is focally replaced by adipose tissue. (HE 40X)

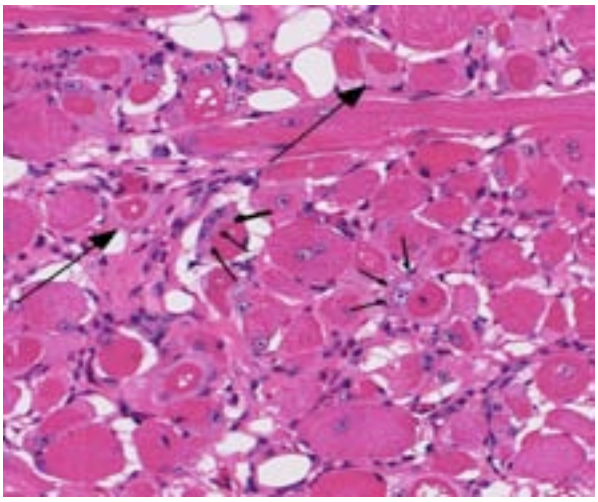

3-2. Tongue, αB crystallin/HSPB2 knockout c57Bl6 mouse: Myofibers exhibit vacuolation and central hyaline myodegeneration (arrows). Hypertrophic satellite nuclei (arrowheads) as well as nuclei located within myofibers indicate attempts at regeneration. (HE 270X)

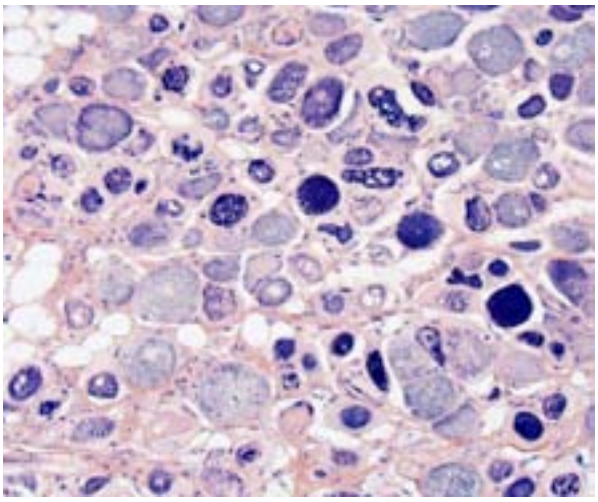

3-3. Tongue, α B crystallin/HSPB2 knockout c57Bl6 mouse: Phosphotungstic acid hematoxylin (PTAH) stain demonstrates the extent of myofibrillar degeneration in affected myocytes. (PTAH 360X)

myofiber size variation, and perimyseal fibrosis are present in the muscles ventral to the bulla, the lateral muscles of the head, and the muscles of the hyoid apparatus.

There are moderate artifacts of processing and decalcification in the sections. Bilaterally, the lens is rotated, shrunken, fragmented, and there is artifactual retinal separation. Multifocal moderate speckles in the lens are due to contraction. One lens has mild focal ballooning and swelling of the peripheral lens fibers consistent with early cataractous change. The other lens has mild multifocal granular debris (liquefaction) and scattered Morgagnian globules containing eosinophilic material (aggregates of lens crystallins).

Contributor's Morphologic Diagnosis: Tongue: Moderate, multifocal to coalescing chronic myopathy with myodegeneration, fibrous and fatty connective tissue replacement, and hyaline degeneration of the sarcoplasm.

Contributor's Comment: The αβ-crystallin knockout mouse is a genetically engineered model with a targeted deletion of the αβ-crystallin gene (and the nearby HSPB2 gene), created initially on a 129Sv background.[1] It has been proposed that αβ -crystallin functions as a molecular chaperone for intermediate filament proteins.[3] Alpha β-crystallin and HSPB2 are stress -inducible heat shock proteins, and αβ-crystallin is expressed predominantly in the lens but also in tissues such as cardiac and skeletal muscle.[1] These mice are viable and fertile and at approximately 40 weeks of age, they begin to develop skeletal muscle atrophy, kyphosis, osteoarthritis, and weight loss.[1] Myopathic changes in the tongue and axial musculature in αβ-crystallin knockout mice which appear similar to inherited myofibrillar myopathies seen in humans have been reported.[1,2] Many human patients with dominant negative αβ-crystallin mutations have an adult onset of the disease.[5,6] Axial muscles in the mice were examined and showed similar myopathic changes with marked fatty replacement and endomysial fibrosis and minimal associated inflammation. A predilection for tongue and truncal muscles has been previously reported in αB crystallinopathy; this predilection is thought to be secondary to increased expression of αβ-crystallin in type I muscle fibers which are more abundant in axial musculature.[2] Trichrome staining was performed and highlights the perimyseal collagen deposition in this case. Additionally, mild to moderate cardiomyopathy (characterized by cardiomyocyte hyaline and vacuolar degeneration, variable fiber size, and interstitial fibrosis with mononuclear inflammation) was identified in all three mice examined in this case, which has not been previously reported in αβ -crystallin knockout mice. Cardiomyopathy in human patients with αβ-crystallin mutations is rarely reported. The presence of cardiomyopathy in the mice we

examined may be related to genotype, background strain (increasing influence of C57BL6), or may represent an unrelated typical aging change in these mice. There are mild cataractous lens changes; however, significant artifact is present as these tissues were formalin fixed. Complete ocular phenotyping would require proper fixation and sectioning of the eyes.

JPC Diagnosis: 1. Skeletal muscle, tongue: Degeneration, necrosis and regeneration, focally extensive, marked, with fibrosis and fat infiltration.
2. Middle ear: Otitis media, suppurative, minimal.
3. Nasal cavity: Rhinitis, suppurative, minimal.

Conference Comment: As stated by the contributor, α β-crystallin is expressed primarily within the lens, as well as skeletal and cardiac muscle, where it is important for normal structure and function. Humans with αβ-crystallin mutations frequently present with cataracts, in addition to abnormal myofiber structure with subsequent myopathy.[1,5] The αB-crystallin knockout mouse was developed to study this rare human condition. In this case, lesions are confined to the tongue, while adjacent skeletal muscle appears relatively unaffected. Histochemical staining with Masson's Trichrome highlights moderate collagen deposition surrounding degenerate lingual myofibers, while PTAH outlines the well-defined, deep blue-purple striations of myofibers in the adjacent, normal skeletal muscle. This is a significant contrast to degenerate muscle fibers within the tongue, which often lack striations and exhibit patchy, irregular uptake of PTAH.

In addition to the key histological features discussed above, the moderator noted the presence of rare accumulations of a homogenous, eosinophilic substance within the interstitium of the anterioventral nasal septum. Although participants were unable to demonstrate this material during conference, deposition of amyloid-like material within the nasal septum is a documented background finding commonly reported in aging mice. Its composition remains unidentified, however PAS positivity and a lack of birefringence with polarized light after Congo red staining suggests that the substance is not amyloid.[4]

Contributing Institution: University of Washington
Department of Comparative Medicine
http://depts.washington.edu/compmed/

References:

1. Brady JP, Garland DL, Green DE, et al. aB-Crystallin in lens development and muscle integrity: a gene knockout approach. *IOVS*. 2001;42:2924-2934.
2. Del Bigio MR, Chudley AE, Sarnat HB, et al. Infantile muscular dystrophy in Canadian aboriginals is an aB-Crystallinopathy. *Ann Neurol*. 2011;69:866-871.
3. Djabali K, de Nechaud B, Landon F, et al. AlphaB-crystallin interacts with intermediate filaments in response to stress. *J Cell Sci*. 1997;110: 2759-2769.
4. Haines DC, Chattopadhyay S, Ward JM. Pathology of aging B6;129 mice. *Toxicol Pathol*. 2001;29(6):653-661.
5. Selcen D, Engel AG. Myofibrillar myopathy caused by novel dominant negative alpha B-crystallin mutations. *Ann Neurol*. 2003;54:804-10.
6. Vicart P, Caron A, Guicheney P, et al. A missense mutation in the alphaB-crystallin chaperone gene causes a desmin-related myopathy. *Nat Gen*. 1998;20:92-95.

CASE IV: 12-0122-7 (JPC 4035410).

Signalment: 10-week-old female Swiss-Webster ICR/CD-1 (Institute of Cancer Research/ Caesarean-Derived from ICR stock) mouse (*Mus musculus*).

History: This mouse presented with an acute onset of intermittent rolling to the left separated by brief periods of lateral recumbency. The animal's body weight/body condition score and coat were within normal limits and the mouse appeared to otherwise be in good health. After a brief period of observation, during which a video of the rolling behavior was recorded, humane euthanasia was elected and a necropsy was performed. The gross necropsy findings were unremarkable and selected tissues were submitted for histopathology.

Gross Pathology: No significant gross lesions were seen.

Histopathologic Description: Extending from the caudal mesencephalon to the medulla oblongata there is unilateral, sharply-demarcated pallor and rarefaction of the neuropil with variable, mild to marked, multifocal vacuolization (malacia), neuronal cell loss and necrosis, capillary congestion, and mild, multifocal hemorrhage. This lesion is ventral and lateral in the caudal-most portions of the mesencephalon but unilateral and diffuse in the more caudal portions of the brainstem including the pons and medulla oblongata (involving trigeminal nerve sensory nucleus and motor fiber tracts, vestibulocochlear nuclei, and facial nerve motor nuclei and fiber tracts).

Contributor's Morphologic Diagnosis: Caudal mesencephalon to the medulla oblongata: Severe, subacute, unilateral encephalomalacia with neuronal cell necrosis and loss, and mild multifocal hemorrhage and edema.

Contributor's Comment: Our differential diagnoses in this mouse included otitis media and/ or interna (bacterial: *Mycoplasma pulmonis, Pasteurella pneumotropica, Pseudomonas aeruginosa, Streptococcus* sp. or viral: reovirus) or, despite the young age of this mouse, a CNS tumor involving the brainstem. Although no occlusion was identified in the intracranial vertebral artery or its branches in this mouse, the histopathologic lesions in the brainstem are consistent with subacute, unilateral brainstem

4-1. Brainstem, Swiss-Webster ICR/CD-1 mouse: There is a focally extensive and unilateral area of encephalomalacia extending from the pons to the caudal brainstem (arrows). (HE 0.63X)

infarction. The vestibular clinical signs (intermittent rolling to one side) are secondary to severe, unilateral ischemia affecting the pontine or vestibulocochlear nuclei, resulting in central vestibular disease. There were no lesions in the outer, middle, or inner ears in this mouse.

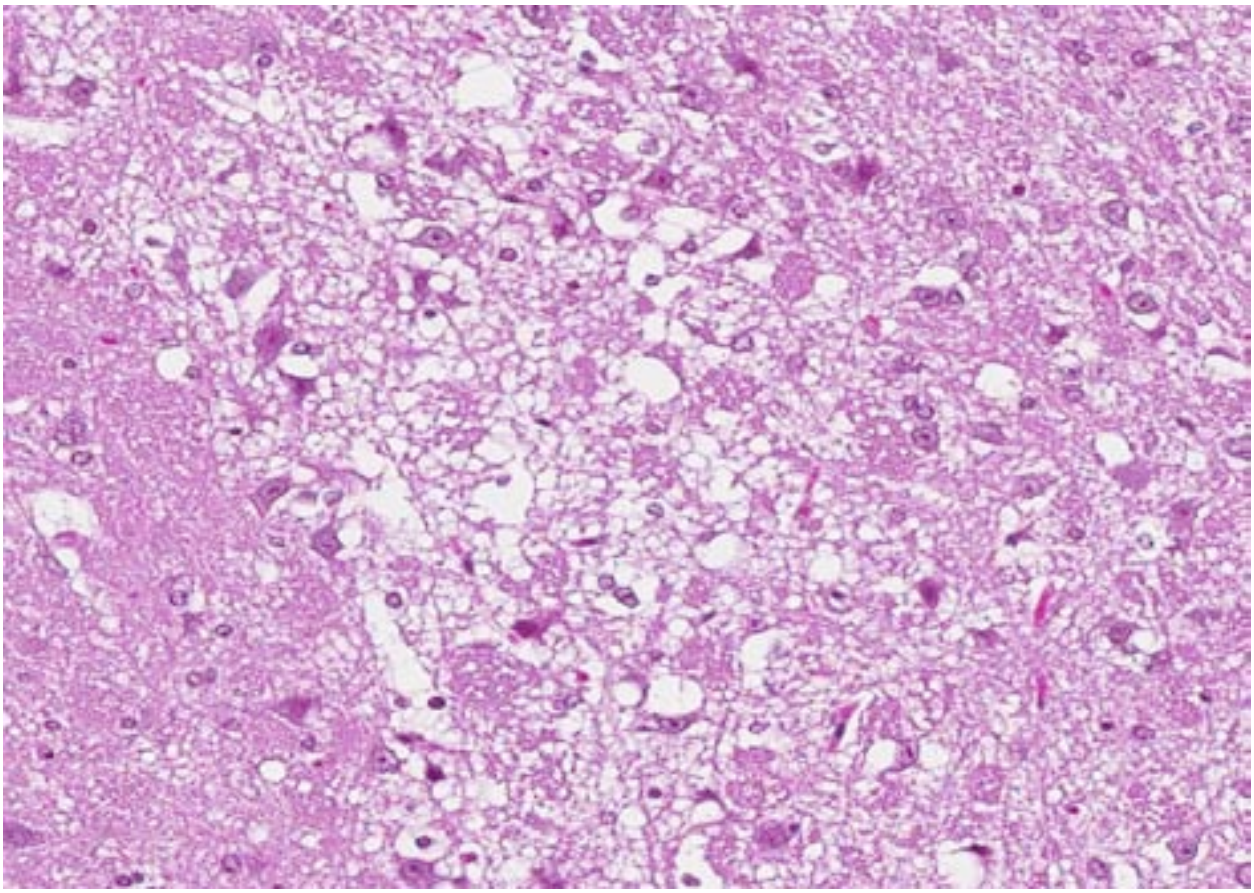

4-2. Brainstem, Swiss-Webster ICR/CD-1 mouse: The encephalomalacia is characterized by severe neuropil edema. (HE 100X)

This lesion has been previously reported by Southard and Brayton in Swiss ICR/CD-1 mice as "spontaneous vestibular syndrome" and "spontaneous unilateral brainstem infarction in Swiss mice."[11] Spontaneous vestibular syndrome in this outbred mouse stock is thought to be secondary to occlusion or dissection of the extracranial or intracranial vertebral artery and/or its branches.

The paired extracranial vertebral arteries arise from the subclavian artery, or rarely, directly from the aortic arch. The largest branch of the intracranial vertebral artery supplies the dorsal medulla and cerebellum and is termed the posterior inferior cerebellar artery (PICA). At the base of medulla oblongata the two intracranial vertebral arteries merge at the midline to form the basilar artery which then branches to form the posterior cerebral arteries and the posterior communicating arteries comprising the Circle of Willis.[1-3]

The clinical and histopathologic features of this syndrome in Swiss ICR/CD-1 mice have been compared by Southard and Brayton to a constellation of clinical signs seen secondary to occlusion or dissection of the intracranial vertebral artery or posterior inferior cerebellar artery in humans termed Wallenberg syndrome or lateral medullary syndrome.[9,10,12] However, these Swiss mice do not share the most common risk factors associated with stroke in humans, including hypertension, diabetes mellitus, smoking, and hyperlipemia leading to atherosclerosis[1,6,8] (in humans this constellation of clinical signs is sometimes also attributed to neoplasia involving the brainstem[12]). Currently, the underlying etiology in these Swiss mice, such as an underlying congenital intravertebral artery

stenosis, is not known and deserves further investigation.

Vertebral artery occlusions leading to medullary infarction in humans are associated with both gender and race predilections. Intracranial vertebral artery occlusions or dissections are more common in women and people of African and Asian descent, while extracranial vertebral artery occlusions or dissections are more common in white males.[1] Medullary infarctions are further classified as lateral medullary infarctions (LMI, Wallenberg, or Wallenberg's syndrome) and medial medullary infarctions (MMI or Dejerine syndrome).[4,5,7] The major symptoms associated with LMI include sensory disturbances affecting the face, dysarthria, vertigo, Horner's syndrome, cerebellar ataxia, and decreased pharyngeal reflexes. The major symptoms associated with MMI include motor weakness and sensory disturbances of the extremities, however, the clinical signs of LMI and MMI commonly overlap depending on the areas and extent of the brainstem affected.[4,5] It is not surprising that the vascular supply to the medial and lateral medulla differs (and sometimes varies). As mentioned above, the lateral medulla receives its arterial supply from the intracranial vertebral artery and PICA, while the upper and lower medial medulla receives arterial blood from the anteromedial medullary arteries. These arise from the intracranial vertebral artery in the upper medulla and from the anterior spinal artery in the lower medulla.[5] The reported prevalence of medullary infarctions in humans varies widely and is continually changing owing to the development and widespread use of magnetic resonance imaging as a diagnostic tool, which has improved anatomic localization of the lesions. The incidence of spontaneous medullary infarction in Swiss ICR/CD-1 mouse is not known.

JPC Diagnosis: Brainstem: Necrosis, unilateral, focally extensive, with edema.

Conference Comment: The contributor provides an excellent summary of unilateral brainstem infarction, a spontaneous condition rarely described in young Swiss mice. The histological lesions in this case are consistent with an early infarct, however, thrombi are not detected within examined sections, so the etiology cannot be confirmed. Examination of serial step sections of the head and neck may be helpful in definitively determining the underlying cause of these lesions. Many thrombi dissolve or break down and the affected area is reperfused, which causes additional damage, so the absence of thrombi does not necessarily indicate that they were not the inciting cause of the necrosis.

Contributing Institution: Integrated Research Facility
Division of Clinical Research NIAID, NIH
8200 Research Plaza
Frederick, MD 21702

References:

1. Caplan L, Wityk R, Pazdera L, Chang HM, Pessin M, Dewitt L. New England Medical Center Posterior Circulation Stroke Registry II. Vascular lesions. *J Clin Neurol*. 2005;1:31-49.
2. Caplan LR. The intracranial vertebral artery: a neglected species. The Johann Jacob Wepfer Award 2012. *Cerebrovasc Dis*. 2012;34:20-30.
3. Cloud GC, Markus HS. Diagnosis and management of vertebral artery stenosis. *QJM*. 2003;96:27-54.
4. Fukuoka T, Takeda H, Dembo T, Nagoya H, Kato Y, Deguchi I, et al. Clinical review of 37 patients with medullary infarction. *J Stroke Cerebrovasc Dis*. 2012;21:594-599.
5. Kameda W, Kawanami T, Kurita K, Daimon M, Kayama T, Hosoya T, et al. Lateral and medial medullary infarction: a comparative analysis of 214 patients. *Stroke*. 2004;35:694-699.
6. Lantelme P, Rohrwasser A, Gociman B, Hillas E, Cheng T, Petty G, et al. Effects of dietary sodium and genetic background on angiotensinogen and Renin in mouse. *Hypertension*. 2002;39:1007-1014.
7. Lee MJ, Park YG, Kim SJ, Lee JJ, Bang OY, Kim JS. Characteristics of stroke mechanisms in patients with medullary infarction. *Eur J Neurol*. 2012;19:1433-1439.
8. Lemini C, Jaimez R, Franco Y. Gender and inter-species influence on coagulation tests of rats and mice. *Thromb Res*. 2007;120:415-419.
9. Razak A, Clark D, Farooq MU, Kassab MY. Wallenberg's syndrome with extradural-extracranial origin of the posterior inferior cerebellar artery. *Neurol Sci*. 2011;32:711-713.
10. Sameshima T, Morita A, Yamaoka Y, Ichikawa Y. Ipsilateral sensorimotor deficits in lateral medullary infarction: a case report. *J Stroke Cerebrovasc Dis*. 2012.

11. Southard T, Brayton CF. Spontaneous unilateral brainstem infarction in Swiss mice. *Vet Pathol*. 2011;48:726-729.
12. van den Bergh P, Dom R. Wallenberg's syndrome caused by a craniopharyngioma "en plaque". *J Neurol*. 1983;229:61-64.

Joint Pathology Center
Veterinary Pathology Services

WEDNESDAY SLIDE CONFERENCE 2013-2014

Conference 13

29 January 2014

CASE I: AVC C3670-13 (JPC 4032590).

Signalment: 10-year-old male castrated Shetland Sheepdog (*Canis familiaris*).

History: This dog was diagnosed with dermatomyositis as a puppy; it had footpad lesions characterized by hyperkeratosis, erythema, scaling and crusting. The dog was treated first with novalexin and then prednisone; he did well for 10-12 days and then stopped eating. Most recently, the dog developed diarrhea, non-regenerative anemia and glucosuria. An abdominal ultrasound revealed a severe and diffuse mottled appearance of the liver with a honeycomb pattern. Liver aspirates were taken for cytology assessment and the footpads were biopsied. The animal continued to deteriorate and was euthanized at the owner's request. The veterinarian obtained permission to perform a postmortem examination. The liver was diffusely nodular; the rest of the abdominal viscera were unremarkable. Samples of liver and skin were submitted for histopathology.

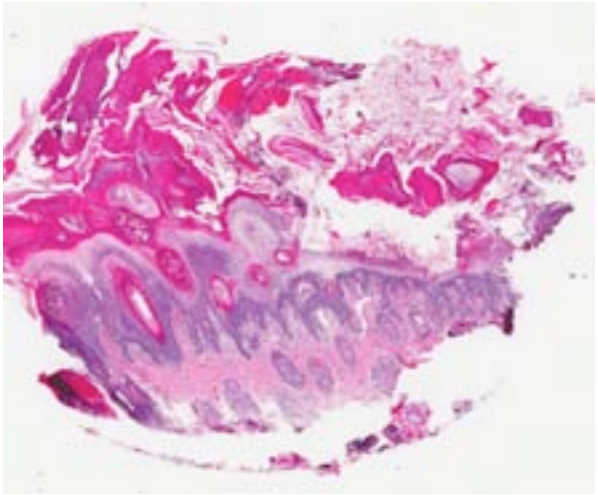

1-1. Haired skin, dog: This section of skin is covered by a thick parakeratotic serocellular crust (extending down into hair follicles), with marked acanthosis and hyperplasia of basal epithelium. (HE 0.63X)

Gross Pathology: Two punch skin biopsies (0.7 cm in greatest diameter) with ulcerated surfaces and two fragments of liver (3.5 cm and 2.5 cm in their largest dimension) were submitted for histopathology. The liver samples had a nodular, irregular, capsular surface.

Laboratory Results:

Parameter	Value	Reference Interval
Albumin	23 G/L	24-55
ALP	1632 U/L	20-150

ALT	442 U/L	10-118
Glucose	9.2 mmol/L	3.3-6.1
WBC	19.1 x 10^3/ mm^3	6.0-17.0
segmented	94%	
lymphocytes	3%	
monocytes	2%	
bands	1%	
RBC	4.12 x 10^6/ mm^3	5.50-8.50
urine glucose	3+	

Liver cytology performed approximately one week before euthanasia revealed cholestasis, low numbers of attenuated and rarefied hepatocytes and possible neutrophilic inflammation.

Histopathologic Description: Two samples taken from the edges of the metatarsal pad and including the adjacent haired skin are examined. The epidermis is markedly, irregularly acanthotic and covered with many layers of parakeratotic keratin admixed with multifocal dense aggregates of necrotic cell debris and hemorrhage. There are foci of erosion with multiple foci of epidermal neutrophilic and lymphocytic infiltration. Keratinocytes in the stratum spinosum are

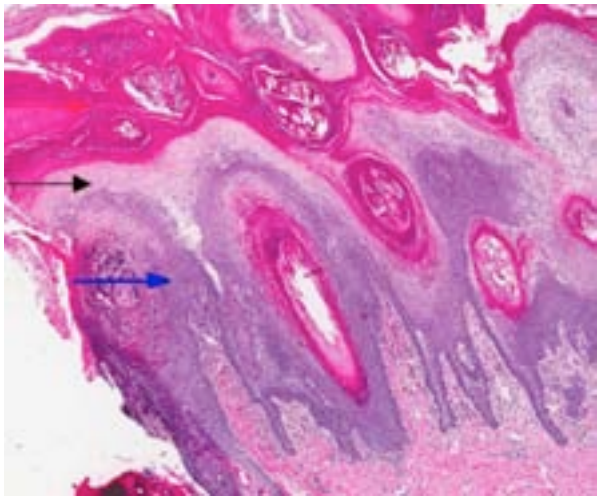

1-2. Haired skin, dog: Superficial necrolytic dermatitis exhibits what is known as the "red, white and blue sign", with superficial hyperkeratosis (red arrow), marked spongiosis of the stratum spinosum (black arrow), and marked hyperplasia of the basal layer (blue arrow). (HE 42X)

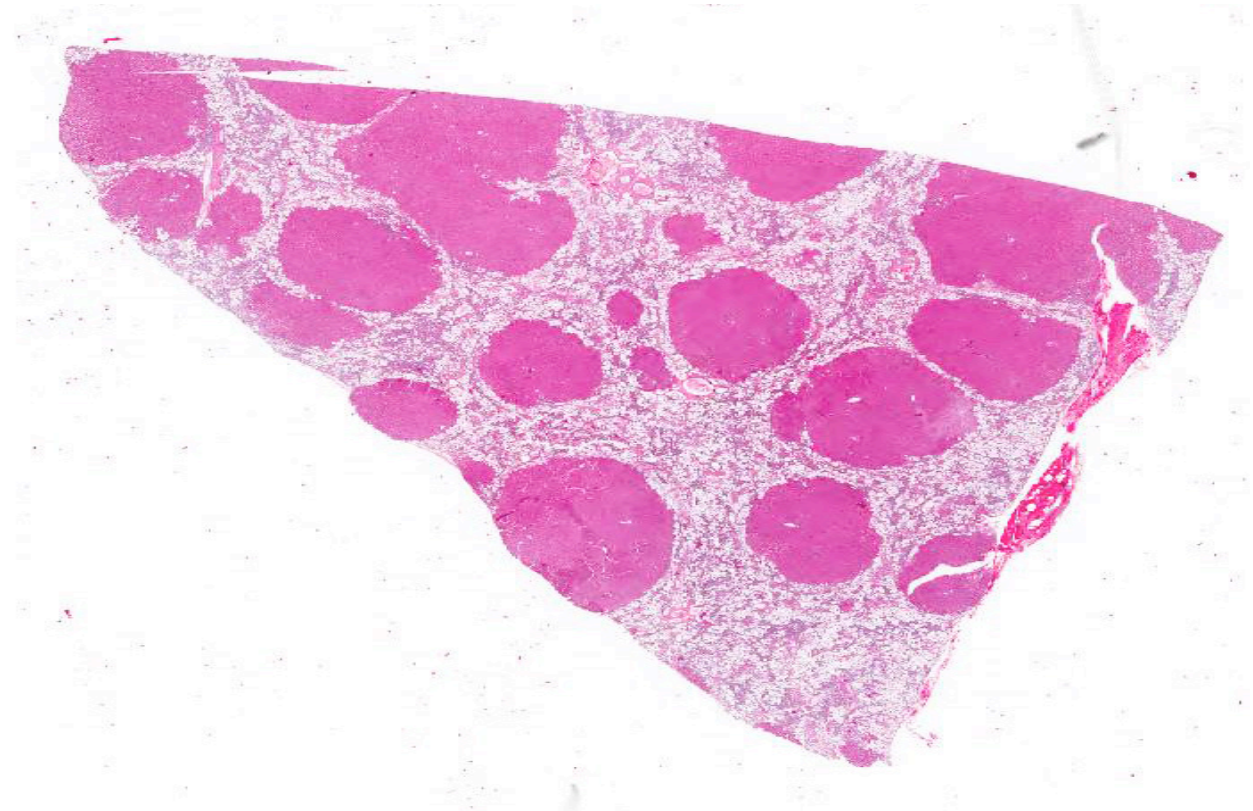

1-3. Liver, dog: This section of liver contains numerous regenerative nodules of hepatocytes, which are easily seen against the pallor of remaining glycogen-distended hepatocytes. (HE 0.63X)

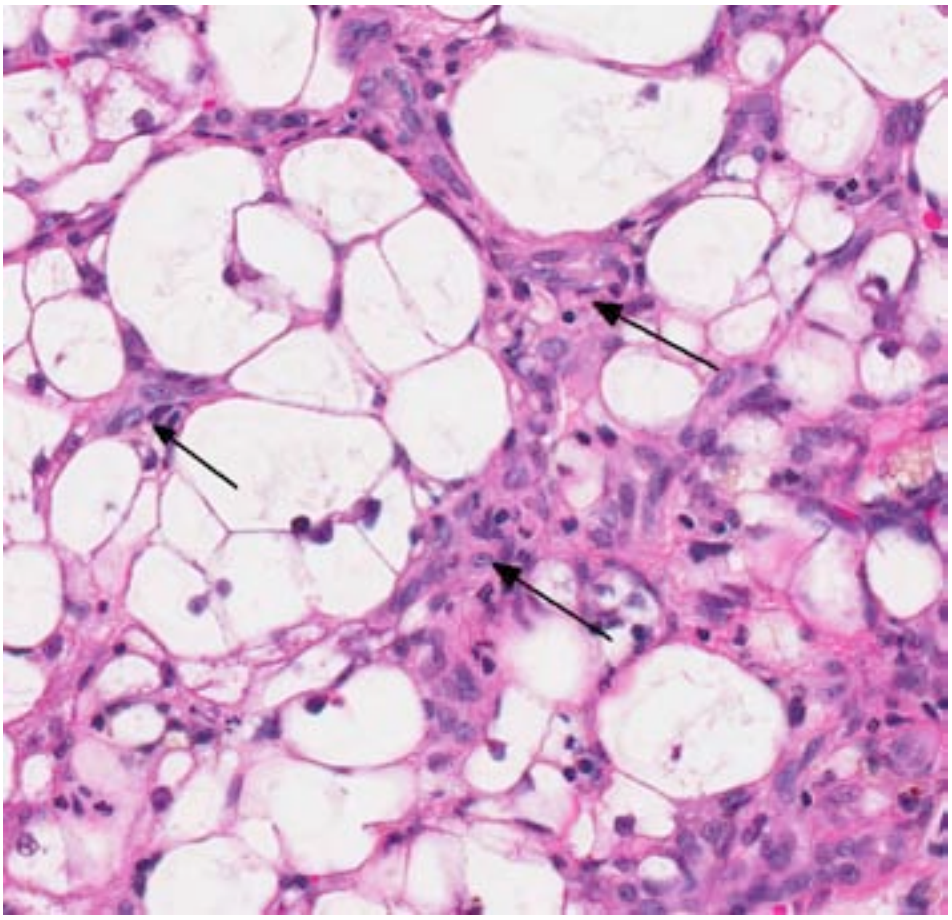

1-4. Liver, dog: Hepatocytes are swollen up to 5 times normal with numerous coalescing clear vacuoles (glycogen) surrounded by pale pink cytoplasmic strands ("spider cells"). Throughout the section there is marked ductular reaction (arrows). (HE 400X)

markedly vacuolated, swollen and pale (intracellular edema) with plump nuclei. The stratum basale is markedly hyperplastic with numerous mitotic figures and increased nuclear to cytoplasmic ratio (in general, giving the epidermis a "red, white and blue" layered appearance). Occasional apoptotic bodies and migrating leukocytes are noted within the epidermis. Numerous bacterial colonies and 7 x 2 micron, PAS positive, budding yeast (consistent with *Malassezia* sp.) are present within the surface keratin (not present in all slides). Multiple hair follicles are dilated and filled with fragmented keratin. Perifollicular, periadnexal and perivascular infiltrates of lymphocytes, plasma cells, macrophages and neutrophils, often associated with fibrous tissue, are present within the dermis. In rare instances, the infiltrates appear to invade the dermoepidermal junction. Gram staining of bacterial colonies reveals gram positive cocci and gram negative rods.

The liver sections show extensive, interconnecting areas of parenchymal collapse and hepatocellular vacuolation, usually surrounding and isolating variably sized nodules of hepatocytes (nodular regeneration). The vacuolated hepatocytes are often markedly enlarged with large amounts of clear to occasionally granular cytoplasm and peripheralized dense nuclei. The areas of vacuolar change also contain multifocal clusters of bile ducts and scant bundles of fibrous tissue. Small collections of band and segmented neutrophils (consistent with extramedullary myelopoiesis) and small numbers of plasma cells and lipid-laden macrophages infiltrate the portal spaces in these areas. Small aggregates of pigment (ceroid and/or iron)-laden macrophages are often seen within the nodules of parenchymal cells (pigment granulomas); scant neutrophils and plasma cells also infiltrate these nodules.

Contributor's Morphologic Diagnosis: 1. Haired skin, bilateral, metatarsal areas: Laminar epidermal edema, degeneration and necrosis, severe, with marked basal cell hyperplasia, parakeratotic hyperkeratosis (ie. superficial necrolytic dermatitis), and pustules/neutrophilic crusts containing bacterial colonies and budding yeast (*Malassezia* sp.).
2. Liver: Hepatocellular vacuolar change (vacuolar hepatopathy), severe, diffuse, with parenchymal collapse, moderate bile duct proliferation and nodular regeneration.

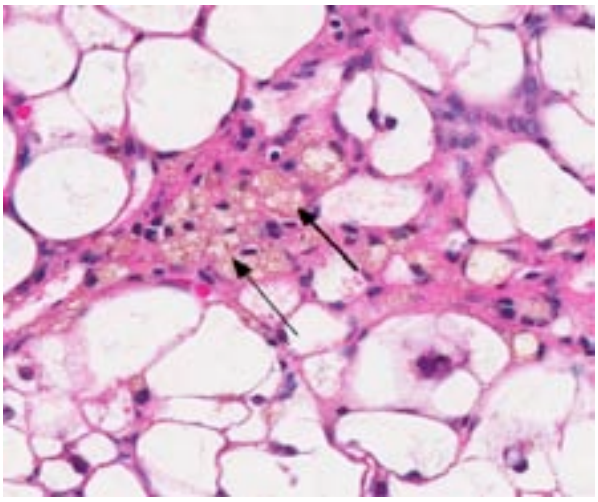

1-5. Liver, dog: Scattered throughout the section are aggregates of macrophages contain lipid and lipofuscin, resulting from rupture of hepatocytes (lipogranulomas). (HE 400X)

Contributor's Comment: The histomorphologic appearance of the skin and liver samples are consistent with hepatocutaneous syndrome (also called superficial necrolytic dermatitis, metabolic epidermal necrosis, and necrolytic erythema) with secondary pyoderma and cutaneous yeast infection.

Hepatocutaneous syndrome is a rare necrotizing skin disorder of dogs that is most often associated with metabolic hepatic disease (often idiopathic vacuolar hepatopathy),[2,8] although it has also been described in diabetes mellitus, glucagon-secreting tumors (glucagonomas)[2-4,9] and prolonged phenobarbital administration.[5] It is thought that hepatic dysfunction may result in hypoaminoacidema, preventing essential amino acids from reaching the skin, leading to nutritional deprivation and subsequent necrosis. The proposed pathogenesis involves increased hepatic catabolism of amino acids (from increased gluconeogenesis),[2,7] elevated glucagon levels (due to decreased hepatic metabolism or glucagon–secreting tumors), or disturbance of zinc metabolism (possibly a result of malabsorption).[4,9] A report of superficial necrolytic dermatitis (SND) in dogs receiving phenobarbital suggested that drug induction of hepatic microsomal enzymes may result in excessive utilization of amino acids by the liver leading to deficiency.[5]

Affected animals typically develop alopecia, erythema, crusting, exudation, and ulceration of the skin. The lesions are generally distributed over the ventral aspect of the abdomen, mucocutaneous junctions, ears, periorbital region, and distal portions of the extremities. Probably the most common clinical dermatologic lesion is hyperkeratosis and deep fissuring of the footpads. Secondary skin infections with bacteria, yeasts, and dermatophytes are common. Pruritus and signs of pain are often apparent.[2-4,9] Anorexia, weight loss and lethargy may also be present.[3,4,9] Circulating liver enzyme activities are frequently high and plasma amino acid concentrations are severely low.[2,7] Results of a study of 36 dogs with histologically confirmed SND indicated that older small-breed dogs (including Shetland Sheepdogs) were primarily affected. The median age was 10 years, and 27 (75%) dogs were male.[7] Superficial necrolytic dermatitis has also been reported in cats[4] and captive black rhinoceroses.[6]

In skin sections, the histopathologic finding of parakeratosis with crusting, hydropic degeneration of keratinocytes in the stratum spinosum, and hyperplasia of the basal cell layer, imparts the characteristic red, white, and blue appearance (referred to by some as the "French flag") that is diagnostic for the disease.[2] Livers of dogs with hepatocutaneous syndrome are grossly nodular. Histologically, there is severe vacuolation of hepatocytes, with parenchymal collapse and condensation of the reticulin fiber network accompanied by nodular regeneration.[8] This combination of liver features has been confused with hepatic cirrhosis by many authors. Ultrasonographic evaluation of the liver of affected dogs reveals an almost pathognomonic "honeycomb" pattern or Swiss cheese-like appearance consisting of a hyperechoic network surrounding hypoechoic areas of parenchyma.[2,3] The underlying cause of these hepatic changes is often undetermined; however, they have been suggested to support an underlying metabolic, hormonal, or toxic cause.[3] The cause for the hepatopathy in this dog was not determined.

Hepatocutaneous syndrome in dogs often has a poor prognosis, and survival times are often less than one year. Treatment generally includes parenteral and oral administration of amino acids, zinc, and essential fatty acids.[7] If the disease is caused by a glucagon-secreting pancreatic neoplasm, surgical removal of the neoplasm can lead to resolution of skin lesions.[2]

Differential diagnosis for canine SND includes other parakeratotic diseases such as zinc-

responsive dermatosis and generic dog food-associated dermatosis. Clinical differential diagnoses include chronic erythema multiforme of older dogs, drug eruption, pemphigus foliaceous and systemic lupus erythematosus. Most of these can be ruled out by appropriate clinical history, physical examination, clinical laboratory, and histopathologic findings.[2]

JPC Diagnosis: 1. Liver: Hepatocellular vacuolar degeneration, diffuse, marked with hepatocellular loss, nodular regeneration and ductular reaction.
2. Haired skin: Epidermal edema, degeneration, and necrosis, superficial, diffuse, marked, with basal cell hyperplasia, parakeratotic hyperkeratosis, and subacute dermatitis.

Conference Comment: We thank the contributor for providing this excellent example and thorough analysis of the entity. Some conference participants reported difficulty in distinguishing regenerative hepatic nodules from islands of pre-existing, normal hepatic parenchyma. Following an animated discussion regarding hepatic histopathology, participants eventually agreed that hepatocytes within regenerative areas tend to be larger than those in the surrounding parenchyma and nodules are often delineated by variable amounts of fibrosis.[10] Additionally, while foci of hepatic regeneration may contain rudimentary portal tracts and terminal venules, hepatic cords are usually more than two cells thick with reduced sinusoidal space, resulting in a somewhat disorganized nodule that may compress adjacent tissue.[1,9]

The distinctive gross and histological appearance of nodular regeneration occurs as a result of its contrast with adjacent expanses of parenchymal atrophy and loss, which typically occur due to reduced blood flow and bile drainage. Macro/micronodular hepatic regeneration is classically associated with cirrhosis, where bridging fibrosis is also a characteristic lesion; however, the liver in this case is striking in its relative lack of fibrosis. Instead, foci of regeneration are bound by extensive areas of parenchymal collapse, hepatocellular vacuolation and bile ductular proliferation, which is a consistent finding in superficial necrolytic dermatitis.[9]
Participants further noted the prominent hepatocellular vacuolar degeneration within submitted sections of liver, which prompted a focused exploration of the distinction between hydropic, glycogen and lipid-type vacuolar degeneration. Hydropic degeneration often follows hypoxic incidents, toxic/metabolic insults or cholestasis, while intracellular accumulation of lipid is a response to physiologic or pathologic increases in lipid mobilization or derangements in lipid metabolism. Hepatocellular glycogen accumulation, otherwise known as steroid-induced hepatopathy or hepatic glycogenosis, is typically induced by exogenous or endogenous corticosteroids. Histologically, lipid-type vacuolar degeneration produces hepatocytes with discrete globules which may coalesce into a single large vacuole that peripheralizes the nucleus, while glycogen or hydropic-type vacuolar degeneration causes significant cell swelling with indistinct vacuolar boundaries and fine, feathery cytoplasm. In severe cases of glycogenosis, nuclei and organelles may be displaced to the periphery of the cell, which complicates differentiation from lipid-vacuoles.[9] In this situation, histochemical stains may be helpful; glycogen stains strongly with PAS, while lipid stains with oil-red-O.

Contributing Institution: Atlantic Veterinary College
University of Prince Edward Island
http://home.upei.ca/

References:
1. Brunt EM, Neuschwander-Tetri BA, Burt AD. Fatty liver disease: alcoholic and non-alcoholic. In: Burt AD, Portmann BC, Ferrell LD, eds. *MacSween's Pathology of the Liver*. 6th ed. Philadelphia, PA: Elsevier Limited; 2012:313-315.
2. Gross TL, Ihrke PJ, Walder EJ, Affolter VK. *Skin Diseases of the Dog and Cat*. 2nd ed. Ames, Iowa: Blackwell Publishing; 2005:86-91.
3. Jacobson LS, Kirberger RM, Nesbit JW. Hepatic ultrasonography and pathological findings in dogs with hepatocutaneous syndrome: new concepts. *J Vet Intern Med*. 1995;9(6): 399-404.
4. Kimmel SE, Christiansen W, Byrne KP. Clinicopathological, ultrasonographic, and histopathologic findings of superficial necrolytic dermatitis with hepatopathy in a cat. *J Am Anim Hosp Assoc*. 2003;39:23-27.
5. March PA, Hillier A, Weisbrode SE, Mattoon JS, Johnson SE, DiBartola SP, et al. Superficial

necrolytic dermatitis in 11 dogs with history of phenobarbital administration (1995-2002). *J Vet Intern Med*. 2004;18:65-74.
6. Munson L, Koehler JW, Wilkinson JE, Miller RE. Vesicular and ulcerative dermatopathy resembling superficial necrolytic dermatitis in captive black rhinoceroses (*Diceros bicornis*). *Vet Pathol*. 1998;35:31-42.
7. Outerbridge CA, Marks SL, Rogers QR. Plasma amino acid concentrations in 36 dogs with histologically confirmed superficial necrolytic dermatitis. *Vet Dermatol*. 2002;13:177-186.
8. Stalker MJ, Hayes MA. Liver and biliary system. In: Maxie MG, ed. *Jubb, Kennedy, and Palmer's Pathology of Domestic Animals*. 5th ed. Vol. 2. St. Louis, MO: Elsevier Limited; 2007:297-388.
9. Turek MM. Cutaneous paraneoplastic syndromes in dogs and cats: a review of the literature. *Vet Dermatol*. 2003;14(6):279-296.
10. Wanless IR, Huang WY. Vascular disorders. In: Burt AD, Portmann BC, Ferrell LD, eds. *MacSween's Pathology of the Liver*. 6th ed. Philadelphia, PA: Elsevier Limited; 2012:627-629.

CASE II: 4378 (JPC 4006293).

Signalment: 5-year-old female spayed Shih Tzu (*Canis lupus familiaris*).

History: The animal presented with lethargy and decreased appetite of 5 days duration. No additional information was provided.

Laboratory Results:

Parameter	Value	Reference Interval
HCT	21.9 % ↓	35.0-57.0 %
RBC	3.1 x 10^6/µL ↓	4.95-7.87 x 10^6/µL
HgB	8.2 g/dL ↓	11.9-18.9 g/dL
MCV	79.4 fl	69-80 fl
MCHC	31.5 g/dL ↓	32.0-36.3 g/dL
WBC	62.1 x 10^3/µL ↑	5.5-13.9 x 10^3/µL
Segs	46.6 x 10^3/µL ↑	2.9-12.0 x 10^3/µL
Bands	9.9 x 10^3/µL↑	0.0-0.45 x 10^3/µL
Lymphocytes	1.2 x 10^3/µL	0.4-2.9 x 10^3/µL
Monocytess	4.3 x 10^3/µL ↑	0.1-1.4 x 10^3/µL
Eosinophils	0 x 10^3/µL	0.0-1.3 x 10^3/µL
nRBC	17 (per 100 WBC)	
Reticulocytes	9.4%	
Absolute retics	291 x 10^3/µL	
PLT	185 x 10^3/µL	235-694 x 10^3/µL

Histopathologic Description: Peripheral blood smear, erythron: The red blood cell mass is decreased, consistent with anemia. There is abundant evidence for regeneration, with numerous polychromatophils and many nucleated red blood cells, primarily metarubricytes, with fewer rubricytes. There is moderate to marked anisocytosis, likely due to the presence of large numbers of spherocytes. Occasional schistocytes and a few red blood cells containing Howell Jolly bodies are observed.

Leukon: There is a moderate to marked leukocytosis, characterized by a neutrophilia with a left shift (including bands and metamyelocytes) and a monocytosis. There is evidence for toxic change in the neutrophils, particularly the early stages, based on the presence of Döhle bodies and intracytoplasmic granules.

Thrombon: The platelet mass appears adequate.

Contributor's Morphologic Diagnosis: 1. Strongly regenerative anemia with evidence for probable immune-mediated destruction.
2. Inflammatory leukogram ("leukemoid" response).
3. Adequate platelet mass.

Overall Interpretation: Immune mediated hemolytic anemia (IMHA) with secondary leukemoid response.

Contributor's Comment: Immune-mediated hemolytic anemia is a disease condition that occurs when erythrocytes or their precursors in the bone marrow are destroyed via a type II hypersensitivity reaction. Initially immunoglobulin attaches to the red blood cell membrane and this can either 1) activate the classical pathway of complement resulting in the formation of membrane attack complexes and subsequent intravascular hemolysis or 2) interact with Fc and complement receptors on phagocytic cells in the liver and spleen, resulting in extravascular hemolysis. IMHA can be primary (with no known underlying cause) or secondary (due to the presence of antibody specific for infectious agents, drugs, or vaccine components). Many argue that only primary IMHA truly results from an autoimmune reaction and therefore should be termed autoimmune hemolytic anemia (AIHA).[2]

Numerous breed predispositions have been discovered for development of primary IMHA, including Cocker Spaniels, Old English Sheepdogs, Border Collies, Poodles, Irish Setters, and Miniature Schnauzers. One study suggests an association between disease development and the genetic structure of the major histocompatibility complex.[4] The average age of onset is 6-8 years and, although there is no clear gender

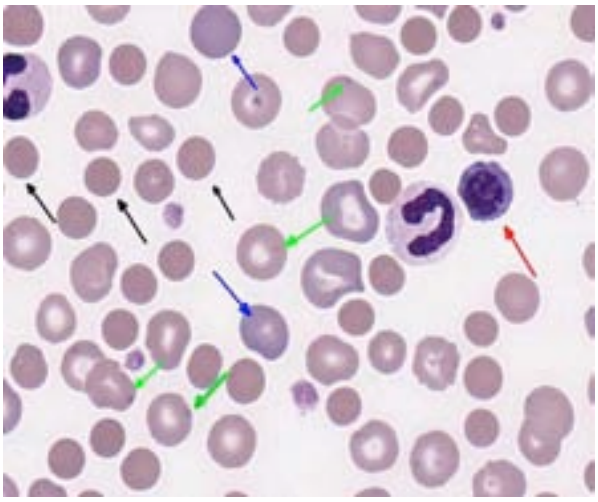

2-1. Peripheral blood smear, dog: Several characteristic findings of autoimmune hemolytic anemia – polychromasia (blue arrows), spherocytes (black arrows), a metarubricyte (red arrow), and Howell-Jolly bodies (green arrows). (Wright's 1000X)

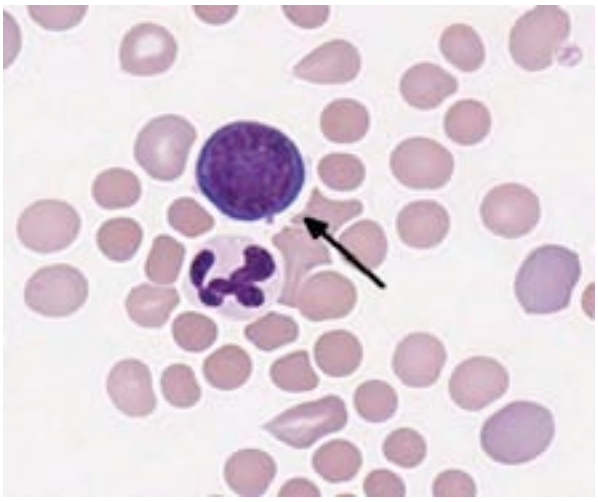

2-2. Peripheral blood smear, dog: Circulating rubricyte. (Wright's 1000X)

predisposition, it can be precipitated by the stress of heat or whelping.[2]

Affected animals can present with either chronic disease with nonspecific signs that have been present for days to weeks or they can present with acute illness, with severe signs of illness that have developed in one to two days. The chronic form is most commonly associated with extravascular hemolysis, while animals with acute disease typically exhibit signs secondary to intravascular hemolysis (e.g., icterus, hemoglobinemia, and hemoglobinuria).[2]

Diagnosis of IMHA begins with the examination of an EDTA anticoagulated blood sample for autoagglutination. This can be done both grossly and with a saline dilution. Microscopic examination of the blood smear typically shows a decreased red cell mass, usually with marked regeneration. The presence of abundant spherocytes is strongly suggestive for IMHA, although not pathognomonic, as these can be seen with other conditions, including zinc toxicity, DIC, and hemangiosarcoma.[3] A pronounced neutrophilia with a left shift is often seen in affected animals and is thought to be due to the effect of pro-inflammatory cytokines (e.g., IL-1, IL-6, and TNF-α), which are produced by activated macrophages. Tissue necrosis due to secondary thromboembolic disease may also play a role.[8] A Coombs' test using species specific serum that recognizes patient IgM, IgG, and complement C3 can be of value in further characterizing the underlying mechanism.

Recent studies have evaluated the outcome of dogs with IMHA.[5,7,10] Around 50% of affected animals die during initial hospitalization, with much worse outcome for patients with the acute versus the chronic form of the disease. The presence of gross autoagglutination, a profound neutrophilia with a left shift, and concurrent thrombocytopenia have been associated with worse prognosis. The average survival time of those patients surviving the initial insult is just over one year. However, approximately 25% of patients have good long-term survival with appropriate immunosuppressive therapy.[10]

The patient in this case presented with the chronic form of the disease. While there was no gross or microscopic evidence for autoagglutination, examination of her peripheral blood revealed many of the "classic" features for immune-mediated disease, including abundant spherocytes and a strongly inflammatory leukogram. The presence of schistocytes and the absence of evidence for intravascular hemolysis is suggestive for antibodies to Fc receptors that are removed by splenic and hepatic macrophages, as schistocytes are often seen circulating secondary to membrane phagocytosis by activated macrophages.[6] To date, this patient has responded well to immunosuppressive therapy.

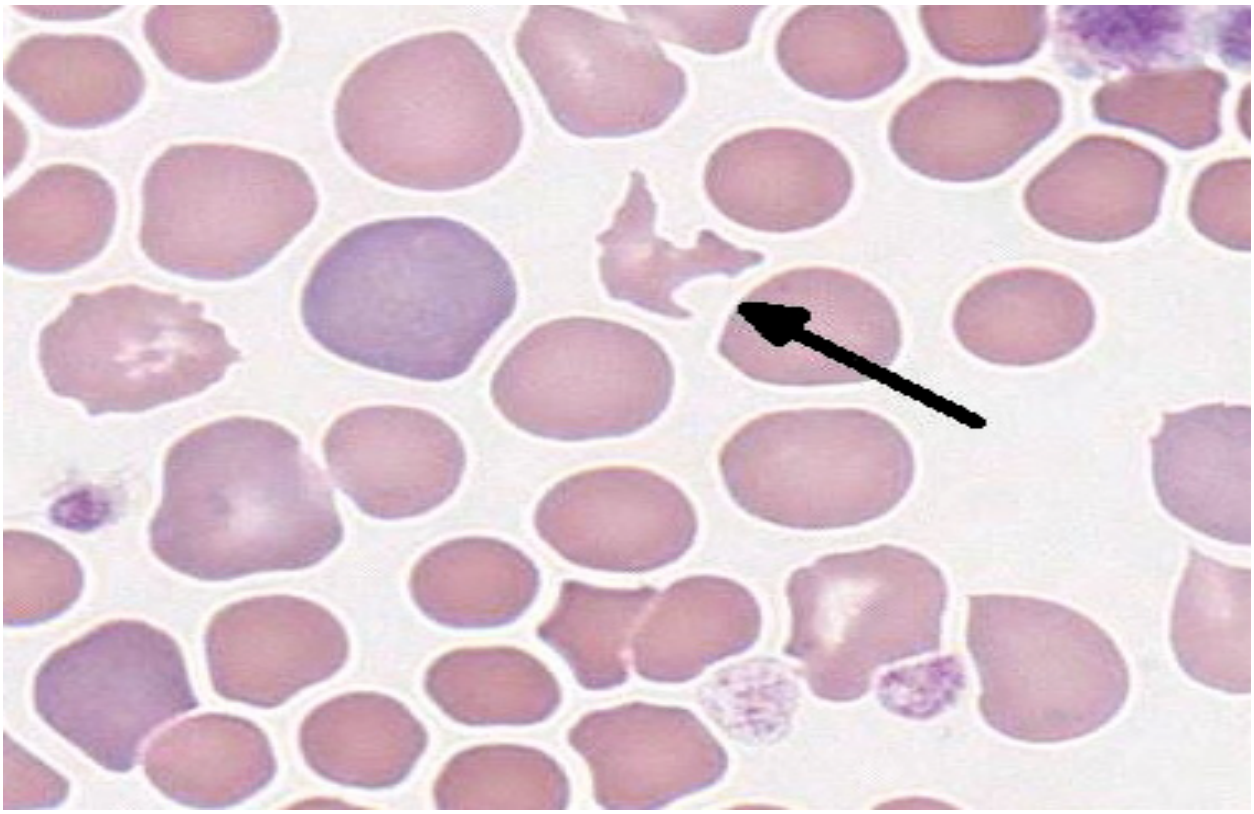

2-3. Peripheral blood smear, dog: Schistocyte. (Wright's 1000X)

JPC Diagnosis: 1. Peripheral blood smear, erythron: Severe regenerative anemia with spherocytosis, schistocytosis and metarubricytosis, consistent with hemolysis.
2. Peripheral blood smear, leukon: Inflammatory leukogram with significant left shift and toxic neutrophil change.

Conference Comment: The moderator led a detailed analysis of the clinicopathological findings in this case, which include reduced red blood cell mass with prominent anisocytosis, polychromasia, reticulocytosis, metarubricytosis and spherocytosis on the peripheral blood smear, in combination with decreased HCT, hemoglobin and MCHC, high normal MCV and reticulocytosis on the CBC. Mean corpuscular hemoglobin concentration (MCHC), the most accurate RBC index, is used to categorize anemia as normochormic or hypochromic. The most common cause of decreased MCHC is reticulocytosis; however, iron deficiency and lead toxicosis can cause hypochromic anemia as well. Hyperchromasia is not a true finding as erythrocytes do not overproduce hemoglobin; elevations in MCHC are typically secondary to erythrocyte hemolysis or Oxyglobin® administration. Increased erythrocyte mean corpuscular volume (MCV) is another laboratory finding associated with regenerative anemia; in this dog, MCV was at the high end of the reference range. Reticulocytosis is the most common cause of macrocytosis (i.e., elevated MCV), but other causes include folate (B9) or cobalamin (B12) deficiency and feline FeLV infection, as well as several congenital conditions in various species. Additionally, greyhounds normally have a higher MCV due to their shorter red blood cell lifespan. Erythrocyte agglutination can cause a false increase in MCV. Spherocytes are globoid erythrocytes with a lack of central pallor and decreased membrane surface area. In animals, they are strongly associated with immune-mediated hemolytic anemia (IMHA), and form when portions of the erythrocyte membrane bound with autoantibody are phagocytosed by macrophages.[1] Overall, the laboratory findings discussed above indicate a strongly regenerative anemia and support a diagnosis of IMHA.

Interestingly, avian species mount the most intense regenerative erythrocyte response,

followed (in decreasing order) by dogs, cats, cows and horses. The presence of nucleated erythrocytes on a stained blood smear is classified as an appropriate response in animals with a strongly regenerative anemia or increased erythropoiesis; in these cases nucleated red blood cells are accompanied by reticulocytosis. Additionally, moderate numbers of nucleated red blood cells are normal in the peripheral blood of healthy piglets, and of course all erythrocytes in birds and reptiles are nucleated. On the other hand, metarubricytosis associated with iron, lead and copper toxicosis; hemangiosarcoma; leukemia; bone marrow disease; intervertebral disc disease; hereditary macrocytosis of poodles; endotoxemia; and FeLV is considered an inappropriate response.[1]

The most common causes of regenerative anemia are hemolysis and blood loss. Reticulocytosis is generally more severe with hemolysis, because iron from hemolyzed erythrocytes is more readily available for erythropoeisis than storage forms of iron, which must be mobilized when there is external loss of erythrocytes. Hemolysis is further classified as extra- or intravascular. Extravascular hemolysis, which is much more common, results from phagocytosis or lysis of erythrocytes within the spleen or liver, whereas intravascular hemolysis is erythrocyte destruction within the circulation. Schistocytes, or fragmented red blood cells, often indicate a microangiopathic hemolytic anemia (MAHA) and intravascular hemolysis[1]; however, as noted by the contributor, they may result from membrane phagocytosis, as is likely in this case. Serum chemistry and urinalysis results (not provided in this case) can also be helpful in distinguishing extravascular from intravascular hemolysis; hyperbilirubinemia is typically associated with extravascular hemolysis, whereas hemoglobinemia and bilirubinuria occur subsequent to intravascular hemolysis.

As noted by the contributor, the severe neutrophilia with a left shift and toxic change in neutrophils present in this case is common in IMHA. Four manifestations of toxic change in canine neutrophils are cytoplasmic basophilia, vacuolation, Döhle bodies and toxic granulation.[9]

In conclusion, this case illustrates several distinctive clinicopathological findings that permit the diagnosis of IMHA, and underscores the importance of performing a manual differential count on all blood smears. Some conference participants detected a lymphopenia based upon their manual differential counts, despite a count within the reference interval on the automated CBC. Participants speculated on possible explanations for this discrepancy, including the possibility that nucleated erythrocytes were erroneously categorized as lymphocytes on the automated counter.

Contributing Institution: University of Georgia
http://www.vet.uga.edu/vpp/

References:

1. Brockus CW. Erythrocytes. In: Latimer KS, ed. *Duncan and Prasse's Veterinary Laboratory Clinical Pathology.* 5th ed. Ames, IA: Wiley Blackwell; 2011:3-41.
2. Day MJ. Immune-mediated anemias in the dog. In: Weiss DJ, Wardrop KJ, eds. *Schalm's Veterinary Hematology*. 6th ed. Ames, IA: Blackwell Publishing; 2010:216-225.
3. Harvey JW. Erythrocytes. In: *Atlas of Veterinary Hematology*. Philadephia, PA: Saunders; 2001:31-32.
4. Kennedy LJ, Barnes A, Ollier WER, Day MJ. Association of a common dog leucocyte antigen class II haplotype with canine primary immune-mediated haemolytic anaemia. *Tissue Antigens*. 2006;68:502-508.
5. Piek CJ, Junius G, Dekker A, Schrauwen E, Slappendel RJ, Teske E. Idiopathic immune-mediated hemolytic anemia. Treatment outcome and prognostic factors in 149 dogs. *J Vet Intern Med*. 2008;22:366-373.
6. Rebar AH, Lewis HB, DeNicola NB, Halliwell WH, Boon GD. Red cell fragmentation in the dog: an editorial review. *Vet Pathol*. 1981;18:415-426.
7. Reimer ME, Troy GC, Warnick LD. Immune mediated hemolytic anemia: 70 cases (1988-1996). *J Am Anim Hosp Assoc*. 1999;35:384-391.
8. Scott-Moncrieff, Treadwell NG, McCullough SM, Brooks MB. Hemostatic abnormalities in dogs with primary immune-mediated hemolytic anemia. *J Am Anim Hosp Assoc*. 2001;37: 220-227.
9. Webb JL, Latimer KS. Leukocytes. In: Latimer KS, ed. *Duncan and Prasse's Veterinary*

Laboratory Clinical Pathology. 5th ed. Ames, IA: Wiley Blackwell; 2011:45-80.
10. Weinkle TK, Center SA, Randolph JF, Warner KL, Barr SC, Erb HN. Evaluation of prognostic factors, survival rates, and treatment protocols for immune-mediated hemolytic anemias in dogs: 151 cases (1993-2002). *J Am Vet Med Assoc*. 2005;226:1869-1880.

CASE III: 17796-12 (JPC 4032251).

Signalment: 8-day-old female alpaca (*Vicugna paco*).

History: The cria presented with an abrupt onset of recumbency and illness. Clinically she was lethargic, febrile and has an elevated cardiac and respiratory rate. It was later revealed that she was being fed a powdered goat colostrum supplement.

Gross Pathology: A mildly autolyzed cria weighed 8.4 kg and was in thin body condition. She was mildly autolyzed. Mild, watery subcutaneous edema fluid was present in the fascia outside the ventral thorax. The abdominal cavity contained 300mL watery. Transparent, pale yellow fluid and an additional 30 ml similar fluid was present in the thorax. The lungs were mottled bilaterally, but floated in formalin. The left atrioventricular valve leaflets were diffusely opaque white. The kidneys were paler than expected and several milliliters of edema fluid surrounded each kidney. The abomasal mucosa was an intensely dark red.

Laboratory Results:

Test	**6 days of age**	**7 days of age**	**Normal values in llamas (Merck Veterinary Manual)**
Glucose	160	ND	90-140 mg/dL
Urea nitrogen	180 mmol/L	183	13-32 mg/dL
Creatine	10.5	10.8	1.5-2.9 mg/dL
Sodium	147	149	134-150 mmol/L
Potassium	8.5	9.0	4.3-5.6 mEq/L
Chloride	110	112	106-118mEq/L
Albumin	1.7	2.0	2.6-4.7 mg/dL
Total protein	3.3	ND	5.6-7.3 mg/dL
Calcium	13.1	13.1	2.0-2.6
Phosphorus	13.4	14.6	4.4-8.5
AST	141	ND	10-280 IU/L
GGT	17	ND	5-29 U/L
CK	65	ND	10-200 IU/L

Histopathologic Description: In both kidneys, glomeruli are diffusely replaced by hard, readily fractured, intensely basophilic granular to homogeneous material consistent with mineral. The nuclei of mesangial cells can occasionally be made out in this material. Cortical tubular basement membranes are also frequently affected, occasionally along with basophilic stippling of tubular epithelial cells. In other parts of the nephron, tubular epithelial cells contain protein-rich casts or cytoplasmic hyaline droplets.

Additional mineralized areas were found in elastic arteries near the heart, trachea, compartment 3, spleen and adrenal.

Contributor's Morphologic Diagnosis: Kidney: Metastatic calcification, renal glomeruli and tubules, severe.

Contributor's Comment: Rickets is an important nutritional metabolic disease of young animals, attributed to deficiencies of vitamin D, calcium, phosphorus, or combinations of those elements. In camelids, low serum phosphorus may be associated with vitamin D insufficiency. Vitamin D bioavailability is considered low in these species.[6] The submitter estimated that the cria was fed supplement 3 times a day for a total of 6 days. If she fed one dose/ feeding, that would be a total of 49,500 IU total Vitamin D or

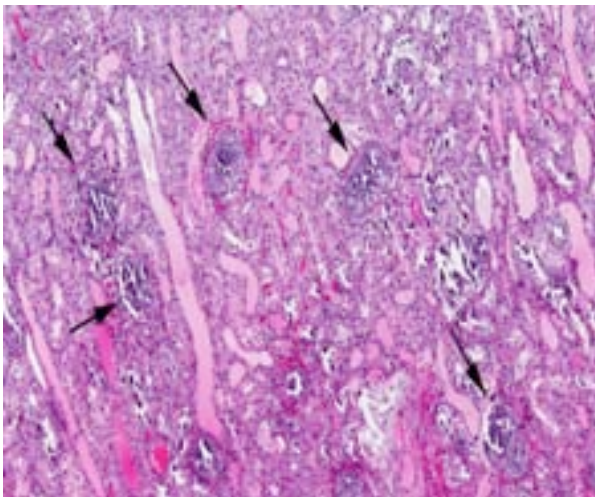

3-1. Kidney, cria: There is diffuse global mineralization of glomeruli (arrows). (HE 84X)

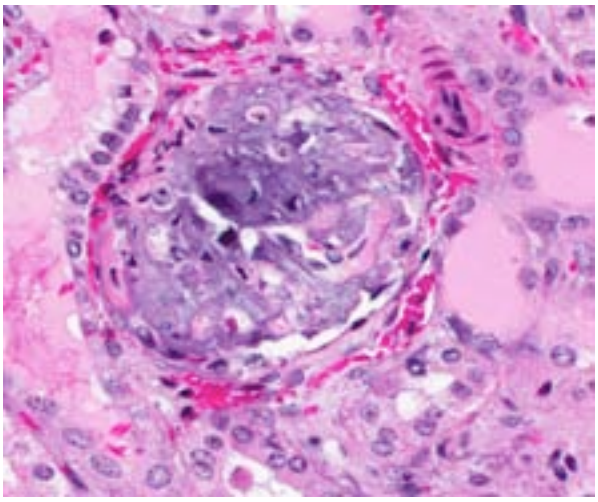

3-2. Kidney, cria: There is diffuse mineralization of basement membranes and mesangium, with pyknosis of mesangial and endothelial cells. Basement membranes are also markedly thickened. (HE 260X)

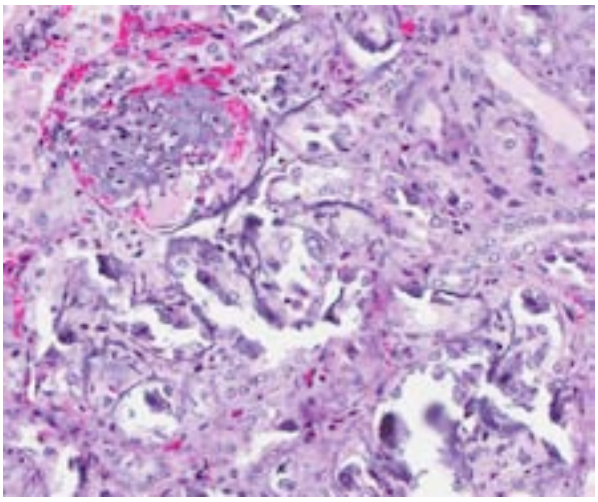

3-3. Kidney, cria: Adjacent to a mineralized, largely necrotic glomerulus, the basement membranes and epithelial cells are likewise mineralized (and the epithelium is necrotic). (HE 230X)

1,375 IU/kg/day (297,000 total IU or 8250 IU/kg).

Rickets is considered a common clinical problem in camelids and is particularly frequent in crias born in September to March period particularly in the high latitudes of the northern and southern hemispheres. Prolonged inclement weather and conditions of reduced sunlight can be contributory to vitamin D deficiency under these conditions.[4] This animal was born in late August. Thus many owners supplement.

This cria was given a goat colostrum supplement fortified with vitamin D due to the owner's concern that rickets was a possibility.[3] This supplement has been reported as a cause of hypervitaminosis D in alpaca crias previously. Among the signs found in other over-supplemented goats are hypercalcemia, hyperphosphatemia and renal dysfunction as seen in this case.

Metastatic calcification occurs in otherwise normal tissue due to hypercalcemia secondary to some disturbance in calcium metabolism. Entry of large amounts of calcium into cells results in its precipitation in organelles. Common causes are renal, vitamin D intoxication [commonly affects aorta, atrial and left ventricular endocarcium, lungs], elevated PTH or PTH-related protein, and neoplastic destruction of bone.[7] Common target tissues are gastric mucosa, kidney, lung, systemic arteries and pulmonary veins. Many of these cells lose acid and therefore have an alkaline internal compartment predisposing to deposition of mineral salts.

Calciferol and D3 localize in nucleus as do other steroids, turning on genes for increased calcium transport. In addition to being found in young animals due to vitamin overdose, as in this instance, pets ingesting "Rampage" rodent poison have similar lesions.

JPC Diagnosis: Kidney, glomeruli and tubules: Mineralization, diffuse, severe, with marked intratubular protein casts.

Conference Comment: The contributor provides an illustrative case of vitamin D-induced metastatic mineralization in the kidney of a cria, pairing it with a succinct synopsis of the entity. In conference, participants further explored the pathogenesis of this condition. As noted by the contributor, the renal mineralization in this case is an example of metastatic calcification, which is typically associated with hypercalcemia and/or hyperphosphatemia. In dogs, metastatic mineralization occurs if the calcium-phosphate solubility product, expressed in mg/dL, persistently exceeds 70. Conversely, dystrophic calcification occurs in normocalcemic animals in association with tissue damage, while calcinosis cutis is an example of idiopathic ectopic mineralization.[5]

Common causes of hypercalcemia include hyperparathyroidism, hypoadrenocorticism, acidosis, renal disease (in horses and some dog

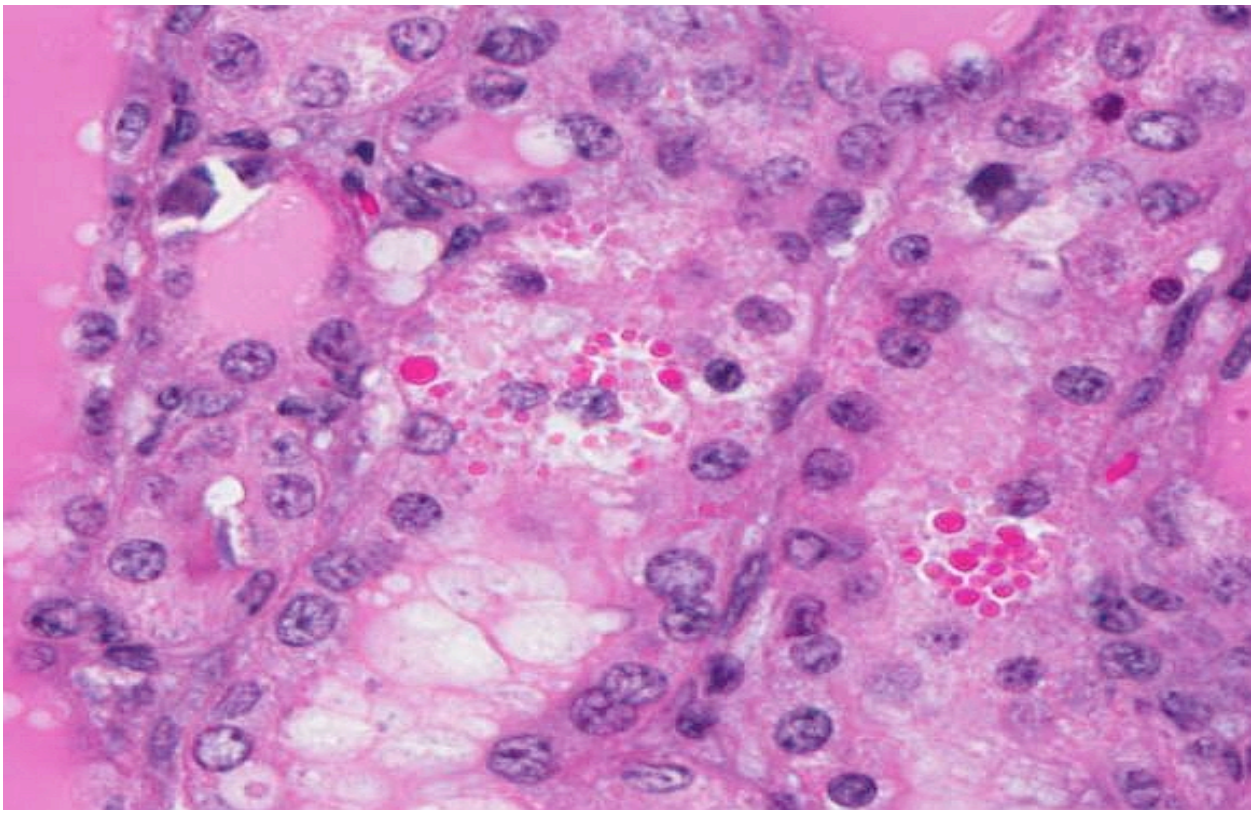

3-4. Kidney, cria: Multifocally, degenerate proximal tubular epithelium occasionally contains large brightly eosinophilic intracytoplasmic hyaline protein droplets. (HE 340X)

breeds), vitamin D toxicity, prolonged immobilization, osteolytic lesions, neoplasia (lymphoma, canine adenocarcinoma of the anal sac apocrine glands, plasma cell myeloma, some carcinomas), thiazide diuretics and granulomatous inflammation. Hyperproteinemia and hemoconcentration will also falsely elevate serum calcium.[2] Common causes of hyperphosphatemia include hemolysis, nutritional 2° hyperparathyroidism, hyperthyroidism, hypervitaminosis D, osteolytic bone lesions, hypoadrenocorticism, renal failure (in most species except for horses), hypoparathyroidism, tumor lysis and administration of phosphate-containing fluids or enemas. Relatively high phosphorus is normal in young animals.[2] In this case, serum chemistry revealed both hypercalcemia and hyperphosphatemia, narrowing the differential diagnosis down to hypervitaminosis D, osteolysis or hypoadrenocorticism. The history of repeated vitamin D supplementation supports a diagnosis of renal mineralization secondary to vitamin D toxicity. The marked azotemia is secondary to renal failure, while hyperkalemia is attributed to renal failure or acidosis.

Although excessive dietary supplementation of vitamin D is the most frequent cause, ingestion of cholecalciferol-containing rodenticides or plants containing vitamin D glycosides (*Cestrum dirunum, Solanum malacoxylon*, *Trisetum flavescens* and *Medicago sativa*) have also been implicated in cases of vitamin D toxicity.[5] Vitamin D maintains plasma levels of calcium and phosphorus by acting on the small intestine, bone, and kidneys. Specifically, it promotes active uptake and transcellular transport of calcium by increasing calbindin synthesis; it stimulates renal calcium absorption in distal tubules; and it stimulates mobilization of calcium and phosphorus from bones. The latter occurs upon binding of osteoblast RANKL (receptor activator for NF-kB ligand) to preosteoclast RANK, which induces differentiation into mature osteoclasts and initiates bone resorption via secretion of HCl and proteases such as cathepsin K. Additionally, vitamin D contributes directly to mineralization of epiphyseal cartilage and osteoid matrix by stimulating osteoblasts to synthesize the calcium-binding protein osteocalcin, which is involved in mineralization of these matrices.[1]

Vitamin D is obtained directly from dietary sources or synthesized endogenously from a precursor (7-dehydrocholesterol) that is present in the skin. Irradiation of 7-dehydrocholesterol with ultraviolet light induces the formation of cholecalciferol (vitamin D3). The precursor in plants is ergosterol, which is converted to vitamin D2 by ultraviolet light and then converted to vitamin D3 in the body.[1] Inactive cholecalciferol (vitamin D3) binds to plasma α1-globulin and is transported to the liver. There, it is converted by hepatic 25-hydroxylases to 25-hydroxy-cholecalciferol (25-OH-D). Finally, renal α1-hydroxylase converts 25-OH-D to active 1,25-dihydroxycholecalciferol. Regulation of renal vitamin D production occurs through three major mechanisms. Hypocalcemia upregulates parathyroid hormone production, which induces activation of α1-hydroxylase and thus increases 1,25-dihydroxycholecalciferol production. Hypophosphatemia directly activates of α1-hydroxylase, resulting in a similar increase in 1,25-dihydroxycholecalciferol production. Conversely, increased levels of 1,25-dihydroxycholecalciferol provoke negative feedback inhibition of α1-hydroxylase.[1] New world monkeys are entirely dependent upon dietary sources of vitamin D since it cannot be synthesized in their skin and, as noted by the contributor, vitamin D availability is considered low in camelids, a condition which is exacerbated during the winter at high latitudes when ultraviolet radiation is decreased.[1]

Contributing Institution: Veterinary Medical Diagnostic Laboratory
University of Missouri
http://vmdl.missouri.edu/

References:

1. Dittmer KE, Thompson KG. Vitamin D Metabolism and rickets in domestic animals: a review. *Vet Pathol*. 2011:48(2):389-409.
2. Ferguson DC, Hoenig M. Endocrine system. In: Latimer KS, ed. *Duncan and Prasse's Veterinary Laboratory Clinical Pathology.* 5th ed. Ames, IA: Wiley Blackwell; 2011:295-304.
3. Gerspach C, Bateman S, Sherding R, et al. Acute renal failure and anuria associated with vitamin D intoxication in two alpaca (*Vicugna paco*) cria. *J Vet Intern Med*. 2010;24:423-429.
4. McClanahan SL, Wilson JH, Anderson KL. What is your diagnosis? *J Amer Vet Med Assoc*. 2006; 229(4):499-500.
5. Thompson K. Bones and joints. In: Maxie MG, ed. *Jubb, Kennedy, and Palmer's Pathology of Domestic Animals*, 5th ed. Vol. 1. St. Louis, MO: Elsevier Limited; 2007:10-11, 58-59.
6. Van Suan RJ. Nutritional diseases of llamas and alpacas. *Vet Clin North Am Food Anim Pract*. 2009;25(3):797-810.
7. Zachary JF, McGavin MD, eds. *Pathologic Basis of Veterinary Disease*. 5th ed. St. Louis MO: Elsevier Mosby; 2012:40.

CASE IV: 33786/2-26 (JPC 4006472).

Signalment: 14-year-old male Holsteiner horse (*Equus caballus*).

History: The animal presented with a 10-day history of severe and rapid weight loss with anorexia, weakness, malaise, intermittent bilateral epistaxis and ascites. On physical exam, there was pallor of mucous membranes, splenomegaly and mild fever. On the labial, nasal, sublingual pharyngeal and anal mucosae there were numerous multifocal to coalescing, irregularly round, yellow to gray, plaque-like lesions ranging from 3 to 15 mm in diameter, with a thin hemorrhagic halo. After three days of corticosteroid and antibiotic therapy the horse became recumbent and the owner elected euthanasia.

Gross Pathology: On gross necropsy the following findings were noted:

- Severe, diffuse splenomegaly
- Severe, diffuse hepatomegaly; liver appeared yellow to pink in color with rounded margins
- Multifocal white, 2 cm to 4 cm, well demarcated, 1 mm thick plaque-like lesions on pulmonary and diaphragmatic pleura
- Numerous irregularly round, yellow to grey, 0.5 to 1.5 cm, plaque-like lesions on the mucosa of the lip, oral cavity, esophagus, small intestine and large intestine
- Severe distention of large intestine with liquid contents
- Plaque-like lesions were also evident on respiratory mucosa of the nasal cavity, larynx, trachea and bronchi
- Marked (up to 5 L) serosanguinous effusion in the abdomen
- Marked (up to 500 mL) serosanguinous effusion in the thorax
- Replacement of femoral bone marrow by a proliferative lesion

Laboratory Results:

Special stains:

- Giemsa: no cytoplasmic granules were evident in neoplastic cells.
- Toluidine blue: no cytoplasmic metachromatic granules were evident in neoplastic cells

Immunohistochemistry:

- Myeloperoxidase (M3/38 antibody clone from Cedarlanes): at least 20% of neoplastic cells in the liver and bone marrow were strongly positive.

4-1. Oral mucosa, horse: On the labial mucosa, numerous multifocal to coalescing irregularly round, yellow to gray, plaque-like lesions with a thin hemorrhagic halo were evident. (Photo courtesy of: Department of Public Health, Comparative Pathology and Veterinary Hygiene – Faculty of Veterinary Medicine – University of Padova - Viale dell'Università, 16 - Agripolis - Legnaro - 35020 - PADOVA – ITALY. http://www.veterinaria.unipd.it)

4-2. Liver, horse: The liver was mottled yellow-pink to gray and was markedly enlarged with rounded margins. (Photo courtesy of: Department of Public Health, Comparative Pathology and Veterinary Hygiene – Faculty of Veterinary Medicine – University of Padova - Viale dell'Università, 16 - Agripolis - Legnaro - 35020 - PADOVA – ITALY. http://www.veterinaria.unipd.it)

4-3. Femur, horse: Within the marrow of the diaphysis, there is a focal proliferative lesion which effaces both marrow and trabecular bone. (Photo courtesy of: Department of Public Health, Comparative Pathology and Veterinary Hygiene – Faculty of Veterinary Medicine – University of Padova - Viale dell'Università, 16 - Agripolis - Legnaro - 35020 - PADOVA – ITALY. http://www.veterinaria.unipd.it)

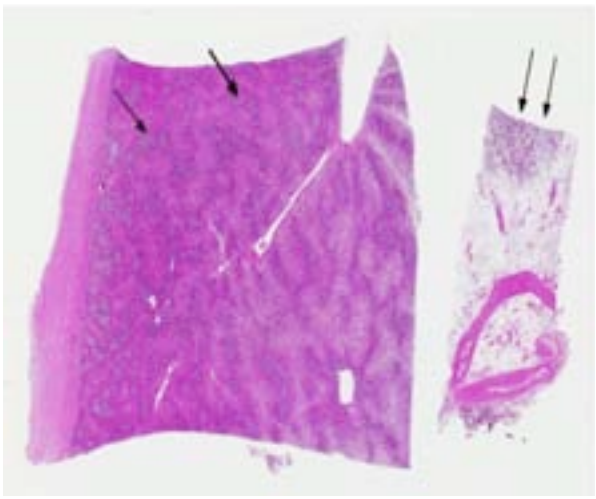

4-4. Liver and bone marrow, horse: Both organs are infiltrated by neoplasms composed of round cells (arrows). (HE 0.63X)

- Lysozyme: at least 40% of neoplastic cells in liver and bone marrow were positive.
- CD79 and CD5: neoplastic cells in liver and bone marrow were negative. Occasional CD79 positive lymphocytes were associated with the neoplastic population.

Histopathologic Description: Liver: Severely and diffuse expanding the portal areas, diffusely infiltrating and effacing the periportal hepatic parenchyma, and diffusely within the sinusoids and centrilobular veins there is a neoplastic population composed of round cells with distinct cell borders, ranging from 20 to 25 µm in size. Up to 70% of the neoplastic cells have a moderate amount of cytoplasm, an irregularly round to oval, occasionally indented 15 to 20 µm nucleus, with clumped or marginated chromatin and an occasional prominent nucleolus (blasts). Up to 10% of the cells are more condensed, with an eccentrically located, and round to kidney-shaped nucleus and numerous eosinophilic cytoplasmic granules. Approximately 15% of the cells are well differentiated eosinophils and there are scattered lymphocytes. There are up to 3 mitotic figures per HPF. There is marked dissociation of hepatocytes in the periportal areas with occasional fragmentation of hepatocytes (necrosis). The centrilobular hepatocytes are characterized by severe cytoplasmic vacuolar degeneration. The capsule is diffusely and severely thickened by collagen deposition and fibroblast hyperplasia (fibrosis). Within the lumen of the vessels in the capsule occasional neoplastic cells are evident.

Bone marrow: Bone marrow is effaced by the same neoplastic population described in the liver and there is an absence of erythroid precursors and megakaryocytes (myelophthisis). Blast cells compose up to 80% of neoplastic cells.

Spleen (tissue not submitted): A similar neoplastic population markedly expands the red pulp, filling the sinuses, expanding the splenic cords and multifocally replacing splenic trabeculae. There is diffuse atrophy of the white pulp.

Small intestine (tissue not submitted): The neoplastic cells multifocally infiltrate the mucosa and submucosa, forming flattened nodular lesions. The mucosal epithelium is severely and diffusely necrotic.

Lung (tissue not submitted): Neoplastic cells diffusely expand the alveolar walls and are present within the vessels.

Cytology: Imprint with blood coagulum show numerous irregularly round, 20 to 25 µ m neoplastic cells, characterized by moderate amount of blue cytoplasm and a round, often indented 15 to 20 µm nucleus, with clumped chromatin and an occasionally distinct nucleolus.

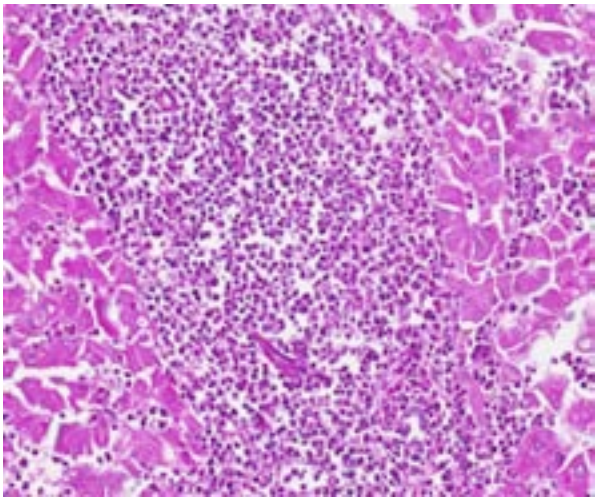

4-5. Liver, horse: Within the liver, the neoplasm effaces portal areas and extends into the adjacent hepatic plates. (HE 228X)

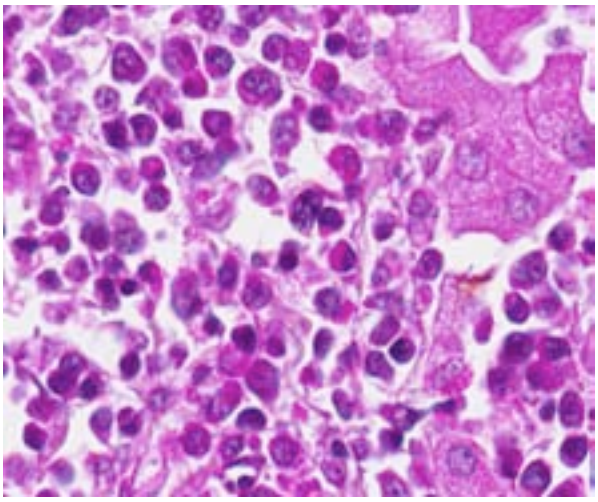

4-6. Liver, horse: Neoplastic round cells have distinct cell borders, round nuclei, and numerous brightly eosinophilic cytoplasmic granules. (HE 400X)

Contributor's Morphologic Diagnosis: Liver and bone marrow: Acute myeloid leukemia, *Equus caballus*, horse.

Contributor's Comment: Leukemia is a neoplasia of one or more cell lines of the bone marrow with distorted proliferation and development of leukocytes and their precursors.[3] Although more common in other domestic animal species, leukemia is also reported in horses. It is typically classified according to the affected cells (myeloproliferative or lymphoproliferative disorders), evolution of clinical signs (acute or chronic) and the presence or lack of abnormal cells in peripheral blood (leukemic, subleukemic and aleukemic leukemia).[3,4]

The most common lymphoproliferative disorders in horses are lymphoid leukemia, plasma cell or multiple myeloma and lymphoma.[3] Lymphoma is the most common hematopoietic neoplasia in horses and usually involves lymphoid organs, without leukemia, although bone marrow may be affected after metastasis.[3]

The following outline summarizes the classification scheme of acute myeloid leukemia according to World Health Organization (WHO) criteria:

AML M0: Acute myeloid leukemia/ undifferentiated leukemia

- Greater than or equal to 90% of myeloid cells are blasts
- Less than or equal to 5% of blasts in circulating blood stain with myeloperoxidase
- No Auer rods are seen

AML M1: Acute myeloid leukemia without maturation

- There is a predominance of blasts in circulating blood and bone marrow with less than 10% having cytoplasmic granulation
- At least 5% of the malignant blast population stains with Sudan Black and myeloperoxidase
- Reported in young mature dogs and cats, with increased frequency in males
- Swine are occasionally affected; rarely other domestic animal species
- In humans, at least 3% of bone marrow blasts label with myeloperoxidase
- Auer rods may be present

AML M2: Acute myeloid leukemia with maturation

- Approximately 30–80% of the myeloid cells are blasts, with at least 10% of neoplastic cells showing maturation (promyelocytes or beyond)
- At least 50% stain with myeloperoxidase
- May have Auer rods

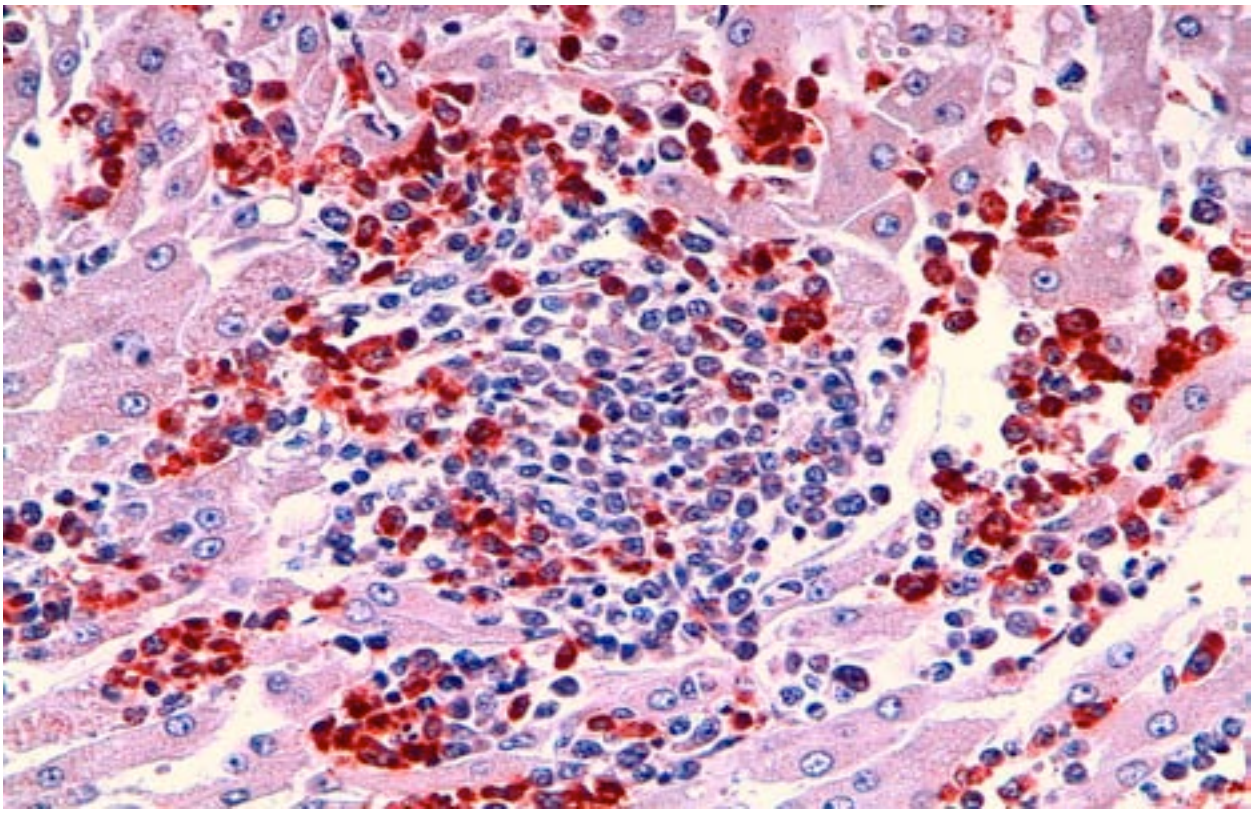

4-7. Liver, horse: Neoplastic cells multifocally exhibit strong cytoplasmic immunoreactivity for lysozyme. (400X) (Photo courtesy of: Department of Public Health, Comparative Pathology and Veterinary Hygiene – Faculty of Veterinary Medicine – University of Padova - Viale dell'Università, 16 - Agripolis - Legnaro - 35020 - PADOVA – ITALY. http://www.veterinaria.unipd.it)

AML M3: Acute promyelocytic leukemia

- There is a predominance of promyelocytes in both in the circulating blood and bone marrow
- There is strong cytochemical staining for myeloperoxidase
- Rare disease of young mature animals
- Commonly recognized in dogs, cats and swine

AML M4: Acute myelomonocytic leukemia

- Both granulocytic and monocytoid differentiation occurs
- Rare disease recognized in dogs, cat, horses
- At least 20% of both tumor cell lines stain for the neutrophil series or for the monocytic series
- At least 20% of blast cells in blood or marrow and at least 20% of the bone marrow cells must be of the monocytic lineage to distinguish M2 from M4

AML M5: Acute monocytic leukemia

M5a: poorly differentiated

- At least 20% blast cells in blood or bone marrow
- Poorly differentiated cells (blasts), monoblasts predominate
- In contrast to M4 less than 20% of cells stain with myeloperoxidase

M5b: well differentiated

- At least 20% blast cells in blood or bone marrow
- Promonocytes predominate
- In contrast to M4 less than 20% of cells stain with myeloperoxidase

AML M6: Erythroleukemia

M6a

- More than 50% of the bone marrow is composed of red blood cell precursors

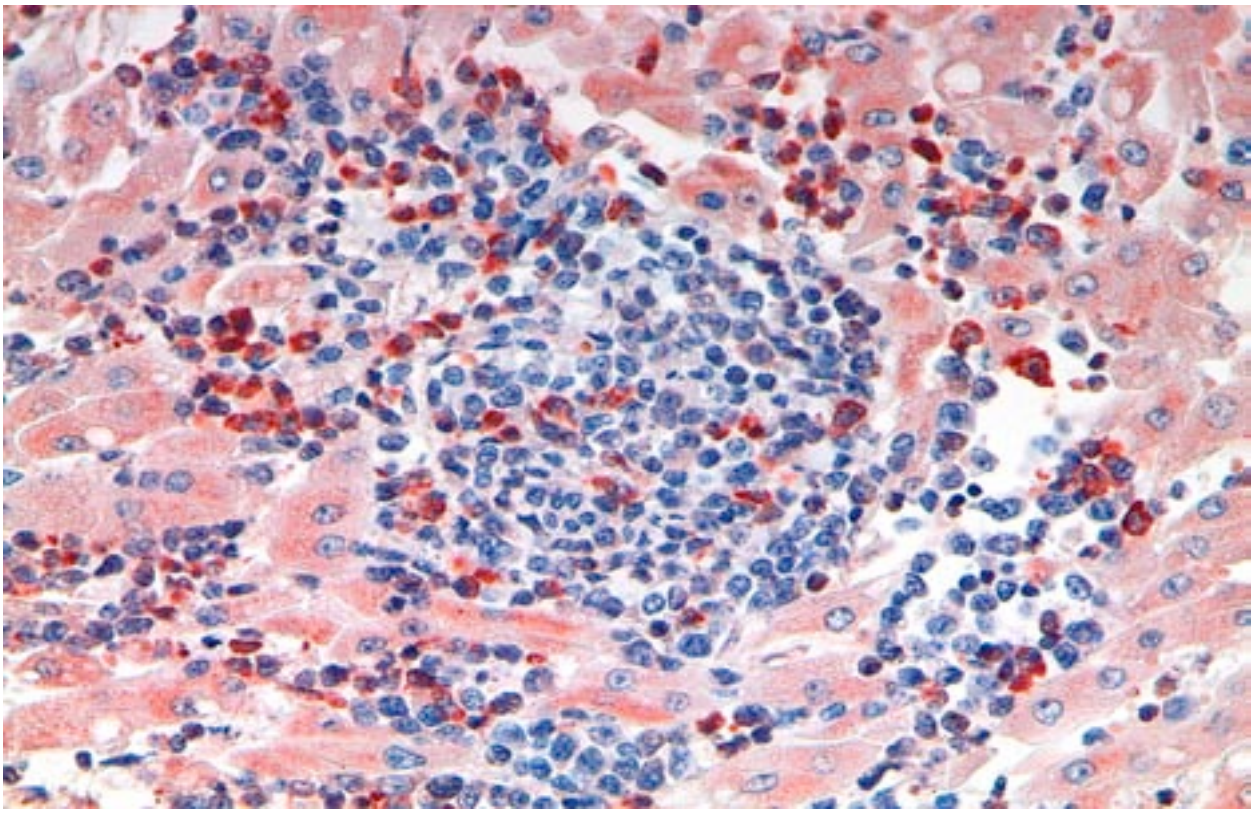

4-8. Liver, horse: Neoplastic cells multifocally exhibit strong cytoplasmic immunoreactivity for myeloperoxidase. (400X) (Photo courtesy of: Department of Public Health, Comparative Pathology and Veterinary Hygiene – Faculty of Veterinary Medicine – University of Padova - Viale dell'Università, 16 - Agripolis - Legnaro - 35020 - PADOVA – ITALY. http://www.veterinaria.unipd.it)

- More than 20% of the non-erythroid cells are myeloblasts

M6b

- Up to 80% of the bone marrow is composed of red blood cell precursors
- Less than 20% of the non-erythroid cells are myeloblasts

AML M7: Megakaryoblastic leukemia

- Rare disease, mainly in dogs
- Greater than or equal to 20% blasts in circulating blood or bone marrow and at least 50% of the marrow cells must be of megakaryocytic lineage
- Circulating blasts with abnormal megakaryocytes and fibrosis in the marrow
- Immunoreactivity for CD41, CD42 and CD61

In the present case, no lymphoadenomegaly or splenic nodules were evident at necropsy. Histopathologic evaluation of the lung, spleen, small and large intestine, esophagus, oral mucosa and nasal mucosa (slides not submitted) revealed a similar neoplastic population to the one in the liver and bone marrow.

Impression smears from the intracardiac coagulum demonstrated the presence of numerous neoplastic cells consistent with myeloblasts/ monoblasts.

Immunohistochemical staining of the neoplastic cells in liver and bone marrow for CD3 was negative. Occasional lymphocytes admixed with the neoplastic population were positive for CD79. Almost 25% of the neoplastic cells in the liver were positive for myeoloperoxidase and almost 40% were positive for lysozyme.

Based on the immunohistochemical results, a lymphocytic origin of the neoplastic cells can be ruled out. No laboratory tests for the evaluation of alpha napthyl acetate esterase activity or naphthol AS-D-chloroacetate esterase activity were available to assess the proportion of neoplastic cells with monocytic origin. Severe, diffuse infiltration of neoplastic cells in portal

areas of the liver is not reported in AML-M2 but is characteristic of AML-M4.

Two different types of acute myeloid leukemia must be considered as differential diagnosis: acute myeloid leukemia with eosinophilic differentiation (AML-M2) and acute myelomonocytic leukemia (AML-M4).

JPC Diagnosis: Bone marrow; liver: Acute myeloid leukemia, with eosinophilic differentiation.

Conference Comment: The contributor provides a comprehensive review of the WHO classification of leukemia, and the notes on differentiating various subtypes of acute myeloid leukemia are especially relevant. In conference, there was some difficulty in the histological identification of sections of bone marrow, however once the tissue type was confirmed, participants explored the immunohistochemical staining characteristics of this case. Myeloperoxidase (MPO) is a lysosomal enzyme found in myeloblasts, immature myeloid cells and the primary granules of mature neutrophils (see 2013-2014 WSC 10, case 3). Approximately 25% of the neoplastic cells were MPO positive, supporting myeloid origin. Additionally, 40% of neoplastic cells were positive for lysozyme, suggesting monocytic origin. Staining for alpha napthyl acetate esterase activity or naphthol AS-D-chloroacetate esterase may have been helpful in confirming monocytic origin;[2] however, due to lack of availability of these stains, we are unable to reach a definitive diagnosis and concur with the contributor's differential diagnosis of AML-M2 and AML-M4.

In addition to the microscopic lesions described by the contributor, some participants noted scattered cytosegrosomes and occasional intracytoplasmic or extracellular blue to purple granular material. Histochemical staining with Von Kossa identified the granular material as mineral; however, we are unsure of the origin or clinical significance of this material.

Contributing Institution: Department of Public Health, Comparative Pathology and Veterinary Hygiene, Faculty of Veterinary Medicine , University of Padova
Viale dell'Università, 16 Agripolis
Legnaro 35020 Padova, Italy
www.veterinaria.unipd.it

References:

1. Forbes G, Feary DJ, Savage CJ, Nath L, Church S, Lording P. Acute myeloid leukaemia (M6B: pure acute erythroid leukaemia) in a Thoroughbred foal. *Aust Vet J*. 2001;89(7): 269-272.
2. McManus P. Classification of myeloid neoplasms: a comparative review. *Vet Clin Pathol*. 2005;34(3):189–212.
3. Munox A, Riber C, Trigo P, Castejon F. Hematopoietic neoplasia in horses: myeloproliferative and lymphoproliferative disorders. *J Equine Sci*. 2009;20(4):59-72.
4. Newlands MC, Cole D. Monocytic leukemia in a horse. *Can Vet J*. 1995;36:765-766.
5. Valli VEO. Hematopoietic system. In: Maxie MG, ed. *Jubb, Kennedy, and Palmer's Pathology of Domestic Animals*. 5th ed. Vol. 3. St. Louis, MO: Elsevier Limited; 2007:107-324.

Joint Pathology Center
Veterinary Pathology Services

WEDNESDAY SLIDE CONFERENCE 2013-2014

Conference 14

5 February 2014

CASE I: 120657-05 (JPC 4032267).

Signalment: Adult male cynomolgus macaque (*Macaca fascicularis*).

History: This monkey was procured from a national laboratory animal supplier and was part of a study to characterize infectivity and disease progression of monkeypox virus. Before virus challenge, there were no significant clinical signs noted. This monkey received an aerosolized dose of 1,608 plaque-forming units (PFU) of monkeypox virus, survived to the end of the study, and was euthanized at day 29 postinfection (PI). Clinical changes were evident by day 4. PI and key abnormalities included increases in body temperature, lymphadenopathy, and relatively mild cutaneous pox lesions. All noted abnormalities are attributable to the monkeypox infection and are typical of aerosol monkeypox

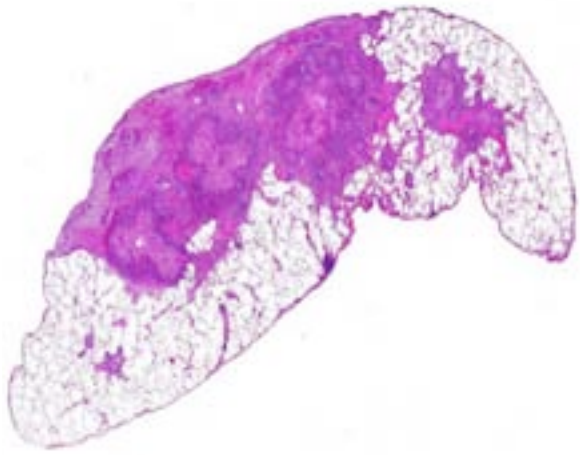

1-1. Lung, cynomolgus macaque: Approximately 50% of the section is effaced by multifocal to coalescing foci of pyogranulomatous inflammation. (HE 0.63X)

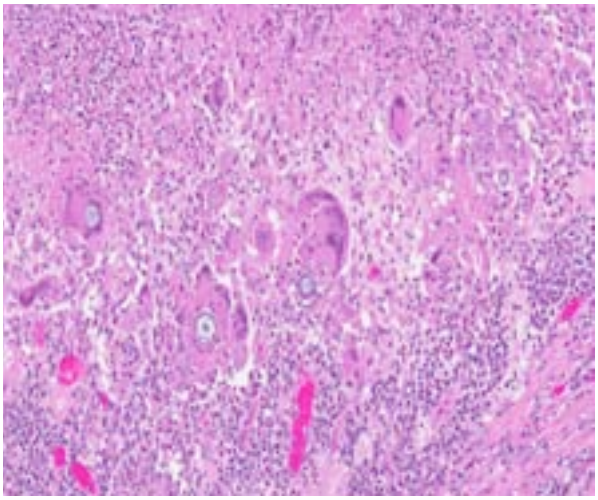

1-2. Lung, cynomolgus macaque: Inflammation is centered on numerous intra-and extracellular fungal sporangia ranging from 40-80 µm in diameter. Numerous foreign body and Langhans-type giant cell macrophages are present within the inflammatory foci. (HE 150X)

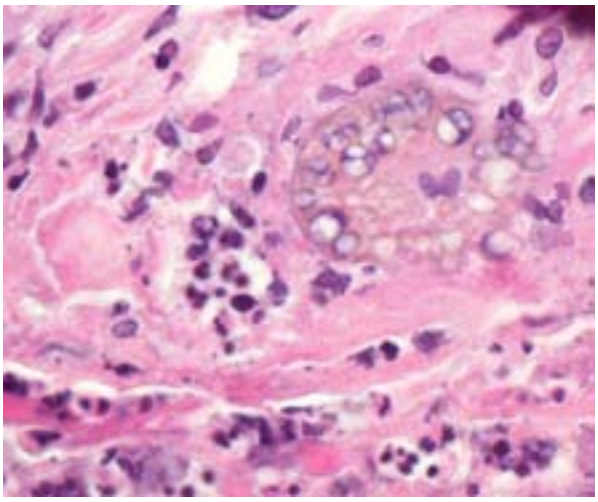

1-3. Lung, cynomolgus macaque: Mature sporangia rupture within the lesion, releasing endospores. (HE 400X) (Photo courtesy of: Pathology Division, USAMRIID, Building 1425, Fort Detrick, MD 21702 http://www.usamriid.army.mil/)

exposure.[11] No clinical respiratory signs were noted before or after viral challenge. This macaque was sourced from China and was quarantined in Texas before being transported to the contributing institute in Maryland.

Gross Pathology: Few faintly visible resolving pox lesions which consisted of 1 to 2 mm whitish/brown discolored spots were present on the skin of the axillary and inguinal areas. The lung lobes on the left side were diffusely very firm, while the right lobes contained few 5-10 mm pale firm foci affecting 10% of the apical and diaphragmatic lobes. All examined lymph nodes showed mild enlargement, and the spleen had marked enlargement with rounded edges and prominent white pulp on cut surface.

Laboratory Results: Hematology and clinical chemistry were performed before aerosol challenge and every 48 h after aerosol challenge; all results were unremarkable.

All tissues were evaluated with immunohistochemistry for orthropoxvirus antigen and all tissues were immunonegative suggesting either viral clearance (consistent with this animal's survival) or that the amount of antigen is too low for detection by immunohistochemistry.

Histopathologic Description: In 30% of the lung section are multifocal areas of granulomatous inflammation that obscure pulmonary architecture, fill the alveoli and bronchiolar lumina, and are composed of numerous multinucleate giant cells, admixed with lymphocytes, plasma cells, histiocytes, and viable and degenerate neutrophils and eosinophils. The bronchioles and alveoli are often dilated and filled with inflammatory cells, cellular debris, edema, and moderate numbers of fungal spherules that are 25-30 microns in diameter with a 2-3 micron wall. The spherules rarely undergo endosporulation and are filled with endospores that are 2-5 microns in diameter. The spherules are often contained within the cytoplasm of the multinucleate giant cells or are degenerate. There is hyperplasia of the epithelium lining the bronchioles with piling up and crowding of nuclei. Multifocally the alveoli are lined by plump cuboidal pneumocytes (type 2 pneumocyte hyperplasia). Multifocally there are peribronchiolar aggregates of histiocytes that contain a dark brown refractile material (anthracosilicosis).

The periodic acid-Schiff (PAS) reaction revealed that each of the spherules had a PAS positive wall.

Similar granulomatous inflammation and fungal spherules are present within the tracheobronchial and mediastinal lymph nodes (not submitted).

Contributor's Morphologic Diagnosis: Lung: Pneumonia, pyogranulomatous, chronic-active, multifocal, marked with large numbers of multinucleate giant cells, epithelial hyperplasia, and moderate numbers of fungal spores consistent with *Coccidioides* sp.

Contributor's Comment: This is a case of coccidioidomycosis based on morphology of the spherules and character of the gross and histologic lesions. Electron microscopy was performed on the lung tissue for characterization of the fungal spores. Mature and immature spherules were identified. The spherules measured approximately 15-20 microns in diameter. Mature spherules contained endospores and immature spherules lacked endospores and contained a 1 micron-thick electron dense wall. These findings support the diagnosis of coccidioidomycosis.

Coccidioidomycosis is a fungal disease found only in the Western Hemisphere in semi-arid regions known as the Lower Sonoran Life Zone. This zone within the United States encompasses

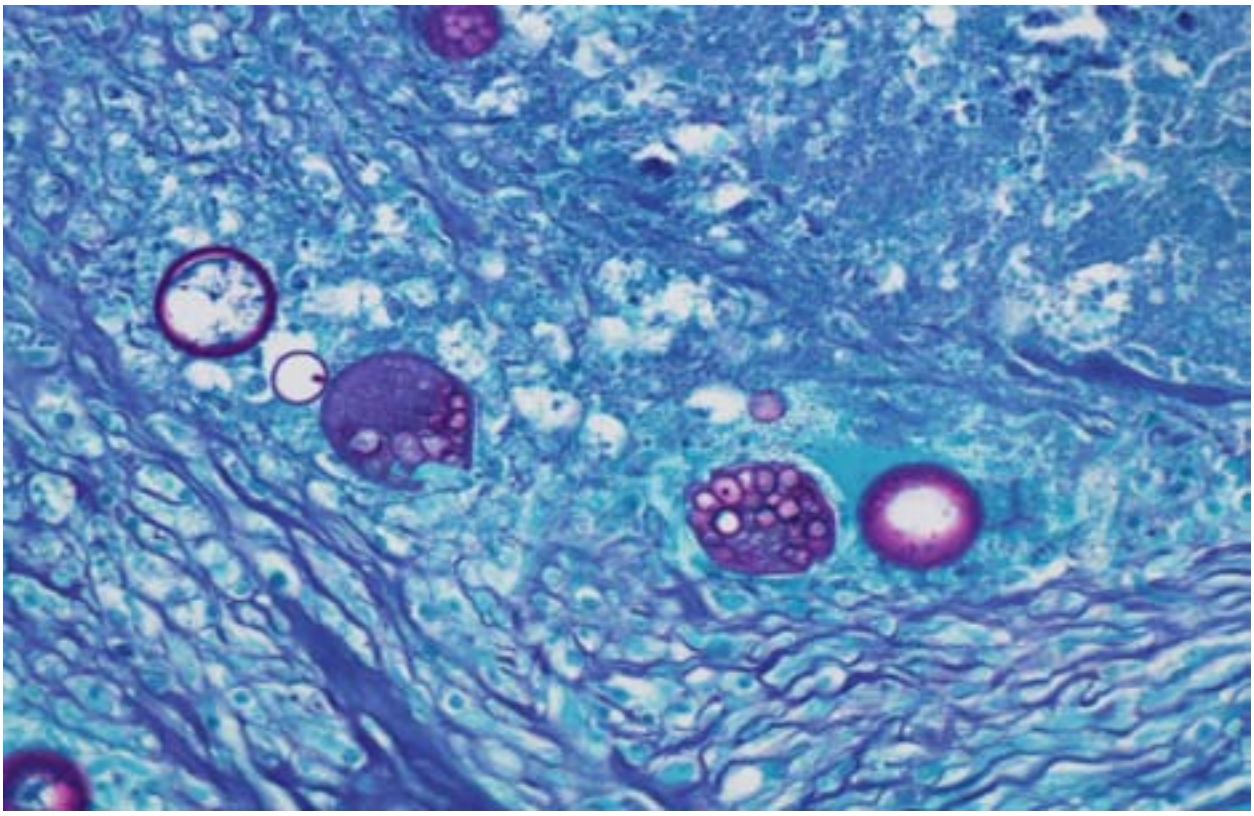

1-4. Lung, cynomolgus macaque: Staining with periodic-acid Schiff stains highlight the positive cell-wall and endospores. (PAS 400X) (Photo courtesy of: Pathology Division, USAMRIID, Building 1425, Fort Detrick, MD 21702 http://www.usamriid.army.mil/)

the southern parts of Texas, Arizona, New Mexico and much of central and southern California.[12,15] Endemic regions outside of the United States include semiarid regions of Mexico, especially northern Mexico, as well as smaller endemic foci within Central and South America.[15] It is caused by a geophilic dimorphic fungus of which two nearly identical species are recognized, *Coccidioides immitis* and *Coccidioides posadasii*. *C. posadasii* was recently proposed as a new species based on genetic and phenotypic analysis,[12] and is generically known as the non-California species with a geographically unique distribution. *C. immitis* is restricted to the endemic areas of California while *C. posadasii* is found outside of California.[15] In this case, *Coccidioides posadasii* is the most likely etiologic agent based on the travel history of this primate.

Infection with *Coccidioides* sp. occurs primarily via inhalation of arthroconidia (also called arthrospores) that are aerosolized when the soil is disturbed by wind or human activities. After inhalation, the arthroconidia enlarge and become spherules that eventually undergo endosporulation. After endosporulation, the spherules rupture releasing hundreds of endospores into the surrounding tissue. These released endospores also mature into new spherules, and the cycle continues until host control is achieved.[14]

Coccidioides spp. appear capable of infecting all mammals and at least some reptiles, but it has not been reported in avian species. The disease has been reported in several species of primates including lemurs, chimpanzees, gorillas, macaques, and baboons,[1-4,16,19,21] and many of these reports describe disseminated disease. As a group, primates appear particularly susceptible.[21]

In dogs, the majority of infections are limited to the lungs and associated hilar lymph nodes. In 20% of recognized infections in dogs and 50% of infections in cats there is dissemination to other sites. In dogs, the most common sites of dissemination are the bones, joints, and lymph nodes, while in cats, the skin is the most common site of dissemination.[14] The sites of dissemination in non-human primates seems to follow a similar pattern as dogs and sites reported in the literature include the eye, bone, and esophagus.[2,4,5,16,18]

Pulmonary and disseminated histopathologic lesions consist of pyogranulomas or granulomas. There are frequently aggregates of intermixed neutrophils resulting from the initial reaction to the endospores released from matures spherules. The lesion forms a granuloma or pyogranuloma as it matures, and is composed of the common components of a granulomatous reaction including giant cells.[6]

In this case, there were no clinical signs that were attributed to coccidioidomycosis despite the extensive granulomatous inflammation in the examined sections. This finding of a subclinical infection is not surprising provided that serologic surveillance studies have shown that asymptomatic infections represent a high percentage of infections in humans and other animals. In a survey of dogs in Arizona, 70% of dogs with seropositivity were subclinically infected and exhibited no sign of disease.[20] Converse and Reed showed that 100% of naturally exposed monkeys developed subclinical infections after being contained in outdoor housing in a river basin for a year in an endemic region (Tucson, Arizona). None of these monkeys exhibited clinical signs of disease, but all were positive by a coccidiodin skin test and complement fixation test; while 40% of the exposed monkeys had histological lesions.[10] A survey of nonhuman primates housed outdoors at the California Primate Research Center in 1977-78 showed that four out of 119 (3%) primates were seropositive; the seropositive cases were attributed to a dust storm that affected the area because there were no positive cases when they were surveyed before the dust storm.[1] In humans, approximately 60 percent of infected persons are asymptomatic; the remainder can develop manifestations that range from mild to moderate influenza-like illness to pneumonia. Overall, less than 5 percent of infected persons have progressive pulmonary infection or extrapulmonary dissemination of the disease.[17]

Additionally in humans, coccidioidal pneumonia may be associated with erythema nodosum, especially in females.[17] Erythema nodosum is characterized by panniculitis of the lower extremities, especially over the shins, and is due to an immunologic response to a variety of causes. A similar condition has not been described in the reports of coccidioidomycosis in animals.

We can only speculate on the source of infection in this case, but this monkey most likely inhaled dust-borne arthrospores when it was in Texas; this would mean that the fungus is *C. posadasii*. Research by Converse and Reed showed that infection can be established after aerosol exposure of rhesus macaques to as few as 10 arthrospores.[10]

In the last decade, the number of reported cases in humans has increased, but the reason for this increase is uncertain. A multitude of contributing factors have been identified and include increased population in the endemic area, climactic change (drought and increasing temperatures in southwestern United States), dust storms, soil disturbance caused by increased construction activity, growing numbers of persons who are immunocompromised or have other risk factors for severe disease, and immigration of previously unexposed persons from areas where coccidioidomycosis is not endemic.[7,8]

Antemortem diagnosis of coccidiomycosis in animals is primarily done with serology and uses the same reagents and controls as for serodiagnosis of humans. There is overlap of seropositivity with clinical disease and subclinical disease in dogs, but seropositivity appears to correlate well with clinically important disease in cats.[14]

Morphology of the *Coccidioides* spherules in histological sections is fairly unique. Other fungal organisms with similar but distinguishable morphology include *Emmonsia* spp., *Blastomyces dermatitidis*, and *Rhinosporidium seeberi*. The major distinguishing factor of coccidial spherules is the formation of thick walled endospores within the coccidioidal spherule as it matures. *Blastomyces dermatitidis* does not form endospores but forms broad-based buds and is smaller than mature coccidial spherules. *Rhinosporidium seeberi* forms endospores that have thin walls. In addition, rhinosporidial sporangia are much larger than coccidioidal spherules. *Emmonsia* spp. have the closest morphology but do not form thick-walled endospores, but rather form fruiting bodies that line the interior of the wall and form a honeycomb pattern which are much less distinct than those of *Coccidioides* spp. Additionally, *Emmonsia* spp. adiaspore walls are thicker than *Coccidioides* sp.[6] Fungal culture, immunohistochemistry (IHC), polymerase chain reaction (PCR), and in situ

hybridization (ISH) are other methods to provide an unequivocal diagnosis. Fungal cultures must be treated with precaution because the infectious arthroconidia may develop after incubation at room temperature.[14]

Research was conducted under an IACUC approved protocol in compliance with the Animal Welfare Act, PHS Policy, and other federal statutes and regulations relating to animals and experiments involving animals. The facility where this research was conducted is accredited by the Association for Assessment and Accreditation of Laboratory Animal Care, International and adheres to principles stated in the Guide for the Care and Use of Laboratory Animals, National Research Council, 2011.

The research described herein was sponsored by the Office of Biodefense Research Affairs (OBRA)/ National Institute of Allergy and Infectious Diseases (NIAID) with interagency agreement (A120-B.11) between USAMRIID and NIAID.

Opinions, interpretations, conclusions, and recommendations are those of the author and are not necessarily endorsed by the U.S. Army.

JPC Diagnosis: Lung: Pneumonia, pyogranulomatous, chronic-active, multifocal to coalescing, marked, with type II pneumocyte hyperplasia and intrahistiocytic endosporulating yeasts.

Conference Comment: The contributor provides an excellent review of coccidiomycosis in domestic and non-domestic species. Conference participants further explored the pathogenesis of this condition with a brief discussion of TH1 type cell mediated immunity (see WSC 2013-2014 conference 2 case 2). In addition to abundant pyogranulomatous inflammation, generally centered upon airways, there are discrete foci of perivascular inflammation, which are attributed to the migration of inflammatory cells from the circulation into infected tissue that occurs as part of the leukocyte adhesion cascade (see WSC 2013-2014 conference 6, case 2). The multifocal, marked type II pneuomocyte hyperplasia noted by the contributor is confirmed by immunohistochemical staining with TTF1, which, besides staining thyroid follicular cells, also stains the nuclei of type II pneumocytes and Clara cells.[11] Electron microscopy can also assist in identifying type II pneumocyte hyperplasia, as these cells typically contain characteristic lamellar inclusions.[9]

Contributing Institution: Pathology Division
USAMRIID
Building 1425
Fort Detrick, MD 21702
http://www.usamriid.army.mil/

References:

1. Beaman L, Holmberg C, Henrickson R, Osburn B. The incidence of coccidioidomycosis among nonhuman primates housed outdoors at the California Primate Research Center. *J Med Primatol.* 1980;9(4):254-261.
2. Bellini S, Hubbard GB, Kaufman L. Spontaneous fatal coccidioidomycosis in a native-born hybrid baboon (Papio cynocephalus anubis/ Papio cynocephalus cynocephalus). *Lab Anim Sci.* Oct 1991;41(5):509-511.
3. Breznock AW, Henrickson RV, Silverman S, Schwartz LW. Coccidioidomycosis in a rhesus monkey. *J Am Vet Med Assoc.* 1975;167(7): 657-661.
4. Burton M, Morton RJ, Ramsay E, Stair EL. Coccidioidomycosis in a ring-tailed lemur. *J Am Vet Med Assoc.* 1986;189(9):1209-1211.
5. Castleman WL, Anderson J, Holmberg CA. Posterior paralysis and spinal osteomyelitis in a rhesus monkey with coccidioidomycosis. *J Am Vet Med Assoc.*1980;177(9):933-934.
6. Caswell JL, Williams KJ. Respiratory system. In: Maxie MG, ed. *Jubb, Kennedy, and Palmer's Pathology of Domestic Animals.* Vol 2. 5th ed. Philadelphia, PA: Elsievier; 2007:644-645.
7. Centers for Disease Control and Prevention. Increase in Coccidioidomycosis - California, 2000-2007. *MMWR Morb Mortal Wkly Rep.* 2009;58(5):105-109.
8. Centers for Disease Control and Prevention. Increase in reported coccidioidomycosis - United States, 1998-2011. *MMWR Morb Mortal Wkly Rep.* 2013;62:217-221.
9. Cheville NF. *Ultrastructural Pathology: The Comparative Cellular Basis of Disease*. 2nd ed. Ames, IA: Wiley-Blackwell; 2009:720-722.
10. Converse JL, Reed RE. Experimental epidemiology of coccidioidomycosis. *Bacteriol Rev.*1966;30(3):678-695.
11. Dabbs DJ. *Diagnostic Immunohistochemistry*. 3rd ed. Philadelphia, PA: Saunders Elsevier; 2010:227.

12. Fisher MC, Koenig GL, White TJ, Taylor JW. Molecular and phenotypic description of Coccidioides posadasii sp. nov., previously recognized as the non-California population of Coccidioides immitis. *Mycologia.* 2002;94(1): 73-84.
13. Goff AJ, Chapman J, Foster C, et al. A novel respiratory model of infection with monkeypox virus in cynomolgus macaques. *J Virol.* 2011;85(10):4898-4909.
14. Graupmann-Kuzma A, Valentine BA, Shubitz LF, Dial SM, Watrous B, Tornquist SJ. Coccidioidomycosis in dogs and cats: a review. *J Am Anim Hosp Assoc.* 2008;44(5):226-235.
15. Hector RF, Laniado-Laborin R. Coccidioidomycosis--a fungal disease of the Americas. *PLoS Med.* 2005;2(1):e2.
16. Johnson JH, Wolf AM, Edwards JF, et al. Disseminated coccidioidomycosis in a mandrill baboon (Mandrillus sphinx): a case report. *J Zoo Wildl Med.*1998;29(2):208-213.
17. Kirkland TN, Fierer J. Coccidioidomycosis: a reemerging infectious disease. *Emerg Infect Dis.* 1996;2(3):192-199.
18. Pappagianis D, Vanderlip J, May B. Coccidioidomycosis naturally acquired by a monkey, Cercocebus atys, in Davis, California. *Sabouraudia.*1973;11(1):52-55.
19. Rosenberg DP, Gleiser CA, Carey KD. Spinal coccidioidomycosis in a baboon. *J Am Vet Med Assoc.*1984;185(11):1379-1381.
20. Shubitz LE, Butkiewicz CD, Dial SM, Lindan CP. Incidence of coccidioides infection among dogs residing in a region in which the organism is endemic. *J Am Vet Med Assoc.* 2005;226(11): 1846-1850.
21. Shubitz LF. Comparative aspects of coccidioidomycosis in animals and humans. *Ann N Y Acad Sci.* 2007;1111:395-403.

CASE II: SN 11-1511 (JPC 4007165).

Signalment: 2 to 3-year-old male cynomolgus macaque (*Macaca fascicularis).*

History: This monkey was part of a study investigating candidate renal biomarkers. It received seven daily IV doses of two potential renal toxicants, everninomicin (30 mg/kg) and gentamicin (10 mg/kg). The study included pre- and post-dose monitoring of serum and urine chemistry with necropsy and histologic examination. Examined tissues included adrenal glands, kidneys, testes, heart, liver, skeletal muscle and urinary bladder at the end of a one week dosing period. Gentamicin is an aminoglycoside antibiotic for the treatment of gram negative bacterial infection that can induce proximal tubular necrosis.[2,5] Everninomicin is an experimental oligosaccharide antibiotic that has a renal toxicity profile that is similar to gentamicin.[3]

Laboratory Results: Serum and urine chemistry were tested twice prior to dosing (6 and 1 day prior to dosing) and 3 times during the week of dosing (post-dose days 3, 6 and 8). Values for the five time points are below. Standard units of measure and abbreviations were used unless otherwise noted. NS = not significant.

Clinical Chemistry:

Parameter	Values
BUN	125, 118, 101, 123, 89
CREA	125, 118, 101, 123, 90
ALT	125, 118, 101, 123, 91
AST	125, 118, 101, 123, 92
AP	125, 118, 101, 123, 93
GGT	125, 118, 101, 123, 94
T BILI	125, 118, 101, 123, 95
TP	125, 118, 101, 123, 96
ALB	125, 118, 101, 123, 97
GLOB	125, 118, 101, 123, 98
A/G Ratio	125, 118, 101, 123, 99
CHOL	125, 118, 101, 123, 100
TRIG	41, 31, 41, 41, 50
Ca	9.7, 9.7, 10.1, 10.0, 9.2
PHOS	6.8, 6.2, 6.9, 4.3, 4.6
Na	141, 143, 142, 141, 137
K	4.4, 4.3, 4.5, 3.4, 3.1
Cl	107, 107, 106, 110, 111

Urinalysis:

Parameter	Values
pH	8.5, 8.5, 8., 8.5, 7.5
Protein	neg, neg, neg, trace, 3+
Glucose	neg, 1+, 2+, NS, NS
Ketones	1+, neg, neg, trace, 2+
Bilirubin	neg, neg, neg, neg, neg
Blood	neg, neg, 1+, neg, neg
Specific Gravity	1.019, 1.018, 1.018, 1.015, 1.017
CREA	103.6, 104.3, 87.6, 52.0, 67.1
N-acetyl glucosaminidase (NAG)	7.7, 7.2, 23.3, 28.0, 30.4
Microalbumin	NS, NS, 7.2, 103.6, 143.3
Total urine volume (ml/ day)	71.0, 65.0, 81.0, 127.0

Gross Pathology: None.

Histopathologic Description: There were everninomicin- and gentamicin-related kidney histologic changes that correlated with serum and urine chemistry changes. There were minimal casts, mild regeneration and marked degeneration. Degeneration was characterized by proximal tubule epithelial cell swelling, cytoplasmic hyaline droplets, epithelial sloughing and epithelial cell necrosis. Regeneration included tubule epithelial cell cytoplasmic basophilia, crowding and slight increases in mitotic figures. There was also tubular dilatation with occasional scattered mononuclear cell accumulations in interstitium adjacent to degeneration or regeneration in some but not all sections.

Contributor's Morphologic Diagnosis: Kidney: Subacute diffuse renal proximal tubular degeneration and necrosis with regeneration.

Contributor's Comment: Aminoglycosides cause acute renal failure by accumulating in proximal tubular epithelial cells where they damage mitochondria, ribosomes, and other intracellular components.[3] Proximal tubules resorb sodium, chloride, calcium, glucose, amino acids from glomerular ultrafiltrate.[3,8] Insufficient resorption following loss of proximal tubular epithelium can cause hyperkalemia, sodium alterations, hyperphosphatemia, azotemia, acid-base disturbances, enzymuria, cylinduria oliguria, isosthenuria and/or anuria.[3] A concise yet comprehensive review of renal physiology and antibiotic-induced renal failure can be found at http://www.vet.uga.edu/VPP/clerk/Matthews/index.php.[6]

JPC Diagnosis: Kidney, proximal convoluted tubules: Degeneration, necrosis and regeneration, diffuse, marked, with numerous cytoplasmic protein droplets.

Conference Comment: The primary function of the renal glomerulus is blood filtration, while the proximal convoluted tubules are predominantly involved with absorption; in fact, sixty percent of all reabsorption of the filtered solute occurs in the proximal tubules. They are responsible for

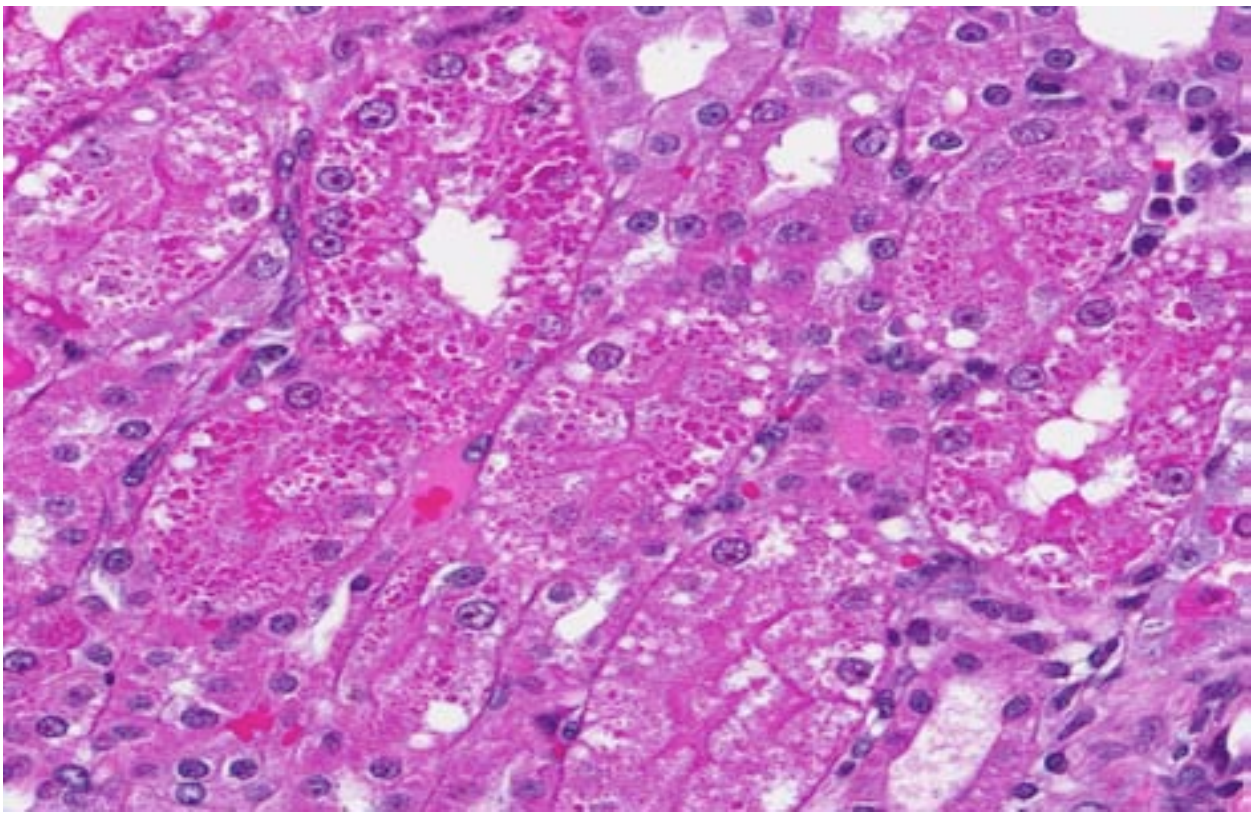

2-1. Kidney, cynomolgus macaque: A characteristic finding in cases of aminoglycoside toxicity is degeneration of tubular epithelium with formation of brightly eosinophilic hyaline droplets. The droplets represent concentric multilaminated phospholipid membrane whorls in the phagolysosome (myeloid bodies). (HE 288X)

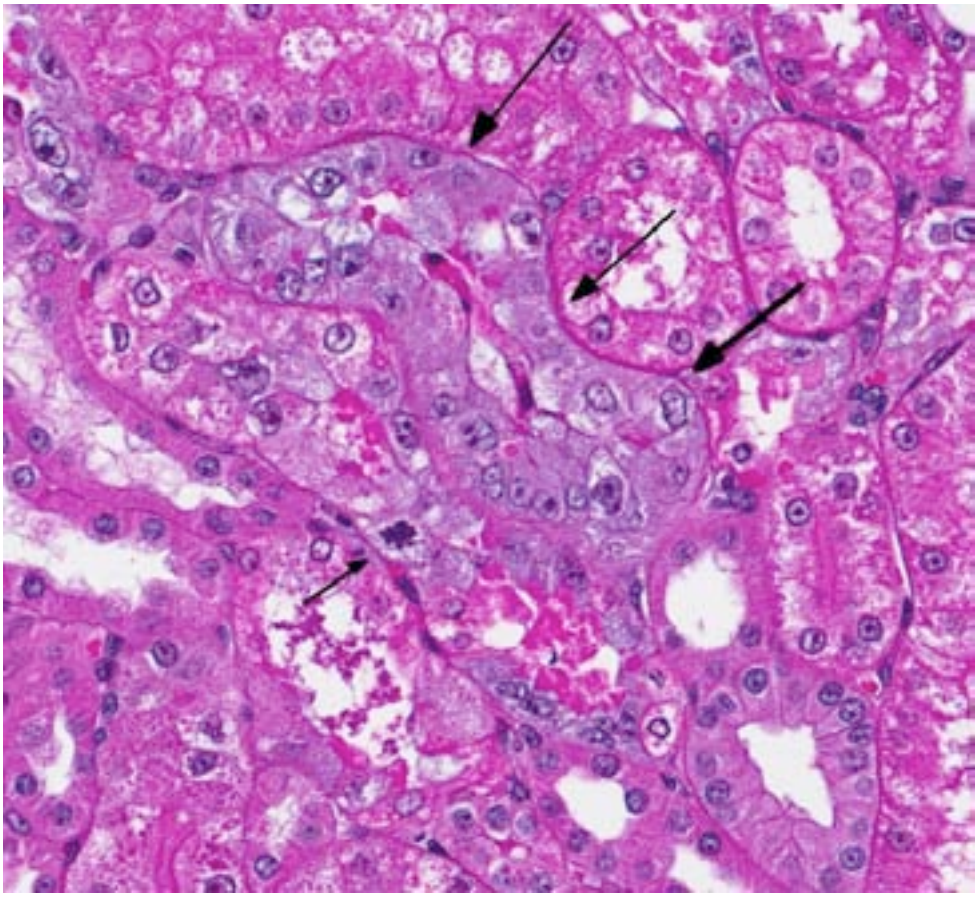

2-2. Kidney, cynomolgus macaque: Regenerative changes within proximal tubular epithelium (large arrows) include cytoplasmic basophilia, vesicular nuclei with prominent nucleoli, and mitotic figures (arrow). (HE 288X)

reabsorbing water, glucose, sodium, chloride, amino acids and calcium from glomerular ultrafiltrate; thus damage can result in the clinicopathologic findings enumerated above.[3] There are two main types of acute tubular necrosis: nephrotoxic and ischemic. Antimicrobials such as aminoglycosides (considered obligate nephrotoxins), heavy metals, chemotherapeutic agents and other nephrotoxins damage the tubular epithelium while sparing the basement membrane.[6] In contrast, renal ischemia is usually a consequence of hypotension; it is characterized histologically by tubular epithelial necrosis or apoptosis with disruption of the basement membrane.[6] In this case, the presence of an intact tubular basement membrane may be demonstrated with the periodic acid-Schiff stain, supporting a toxic etiology rather than an ischemic insult.

Considerable discussion surrounded the pathogenesis of aminoglycoside nephrotoxicity in animals. Common aminoglycosides employed in veterinary medicine (in decreasing order of nephrotoxicity) include neomycin, kanamycin, gentamicin, streptomycin, tobramycin and amikacin. Foals are particularly susceptible to aminoglycoside-induced nephrotoxicosis, while in cats, this class of drugs has been associated with ototoxicity as well as nephrotoxicity. Aminoglycosides typically accumulate within proximal tubular epithelial cell lysosomes and damage is thought to be dose-dependent. They induce tubular damage via a number of ways: destruction of the sodium-potassium pump with subsequent oncotic necrosis; inhibition of phospholipase with accumulation of lysomosmes filled with cellular membranes ("myeloid bodies") impairment of mitochondrial respiration and cation transport; inhibition of protein synthesis; and loss of the epithelial brush border.[4,6,7]

In addition to the histological features described by the contributor, some conference participants noted that epithelial cells lining medullary collecting tubules are occasionally multinucleated, bulging into the tubular lumen. This is considered to be an incidental finding in cynomolgus macaques that is thought to be either a normal anatomic variation in this species or at best, a minor finding of little pathological significance.[1]

Contributing Institution: www.merck.com

References:

1. Chamanza R, Marxfeld HA, Blanco AI, Naylor SW, Bradley AE. Incidences and range of spontaneous findings in control cynomolgus monkeys (*Macaca fascicularis*) used in toxicity studies. *Toxicol Pathol*. 2010;38(4):642-657.

2. Davis JW , Goodsaid FM, Bral CM, et al. Quantitative gene expression analysis in a nonhuman primate model of antibiotic-induced nephrotoxicity. *Toxicol Appl Pharmacol*. 2004;200(1):16-26.

3. DiBartola SP. Urinary system. In: Ettinger SJ, Feldman EC, eds. *Textbook of Veterinary Internal Medicine*. Vol. 2. 7th ed. St. Louis, Missouri: Elsevier-Saunders; 2010:1976-1979.

4. Hottendorf GH, Williams PD. Aminoglycoside nephrotoxicity. *Toxicol Pathol*. 1986;14(1):66-72.

5. Matthews C, Camus M, LeRoy B. Antibiotics and Acute Renal Failure. http://www.vet.uga.edu/VPP/clerk/Matthews/index.php

6. Maxie MG, Newman SJ. Urinary system. In: Maxie MG, ed. *Jubb, Kennedy, and Palmer's Pathology of Domestic Animals*. Vol 2. 5th ed. Philadelphia, PA: Elsievier; 2007:466-470.

7. Mingeot-Leclercq MP, Tulkens PM. Aminoglycosides: Nephrotoxicity. *Antimicrob Agents Chemother*. 1999;43(5):1003-1012.

8. Plumb DC. *Plumb's Veterinary Drug Handbook*. 5th ed. Blackwell Publishing; 2005:206-209; 864-867.

CASE III: PO-507/13 (JPC 4035680).

Signalment: 3-year-old female mixed breed pig (*Sus scrofa domesticus*).

History: The animal was slaughtered in an officially inspected abattoir in Catalonia (Spain).

Gross Pathology: Two prominent exophytic, multinodular, cauliflower shaped masses of 4 and 5 cm in diameter were noticed in the inner side of the thoracic cavity arising from the rib surface. The masses had a smooth surface and were attached with a broad sessile base to the costal body of the ribs. The masses were solid, had a hard consistency and at cross section had bluish to white areas. During the inspection, no other abnormalities were observed in the carcass or in the internal organs of the animal.

Histopathologic Description: Rib, transverse section: There is an exophytic, broad based, multinodular, well demarcated, expansive, and non-encapsulated neoplastic proliferation arising from the rib poriosteum. Every nodule is lined by fibrovascular stroma of variable thickness (perichondria). Neoplastic cells are well-differentiated chondrocytes enmeshed within an abundant hyalinized amphophilic extracellular matrix. They are arranged from the periphery to the center in well-defined layers mimicking growth plate endochondral ossification. The outer layer is made up of multiple small groups of chondrocytes with high nucleus/cytoplasm ratio (resting layer). Secondly, there is a thicker layer constituted by larger chondrocytes forming columns (proliferative layer), and a deeper layer where chondrocytes undergo hypertrophy (hypertrophic layer). Underneath the hypertrophic layer, the cartilage matrix is replaced by hyaline, eosinophilic osteoid matrix (calcification layer) and subsequently, there is loss and replacement of the chondrocytes by osteocytes. This is partially lined by osteoclasts and rows of plump osteoblasts. In the center of the nodule, several septa of mature trabecular bone are seen. Amongst the septa, bone marrow with a heterogeneous population of hematopoietic precursors and scattered adipocytes are present.

Contributor's Morphologic Diagnosis: Rib osteochondroma.

Contributor's Comment: An osteochondroma is a benign, cartilage-capped tumor arising from the surface of bones formed by endochondral ossification. Osteochondromas may occur in two forms: solitary or multiple.[2,5] This condition is usually recognized as an incidental finding during routine controls, radiographic examination or at necropsy. Occasionally, clinical signs might occur and are due to compression or distortion of adjacent structures. Osteochondromatosis is infrequently reported in humans, horses, dogs, a macaque and cats.[2,3,6] In the present case, considered differential diagnoses included chondroma and chondrosarcoma. Histologically, chondroma consists of irregular lobules of hyaline

3-1. Rib, pig: Two prominent exophytic, multinodular, cauliflower shaped masses of 4 and 5 cm in diameter were noticed in the inner side of the thoracic cavity arising from the rib surface. (Photo courtesy of: Servei de Diagnostic de Patologia Veterinaria, Facultat de Veterinaria, Bellaterra (Barcelona), 08193 SPAIN)

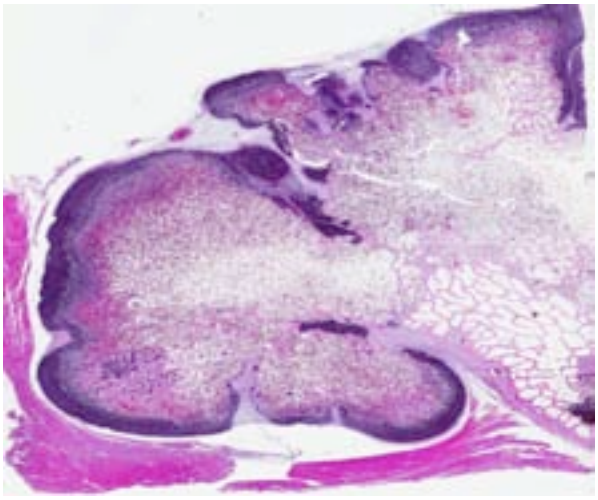

3-2. Rib, pig: A multilobular fungating bony mass covered by hyaline cartilage arises from the periosteum of the rib and communicates with the medullary cavity of the rib. (HE 0.63X)

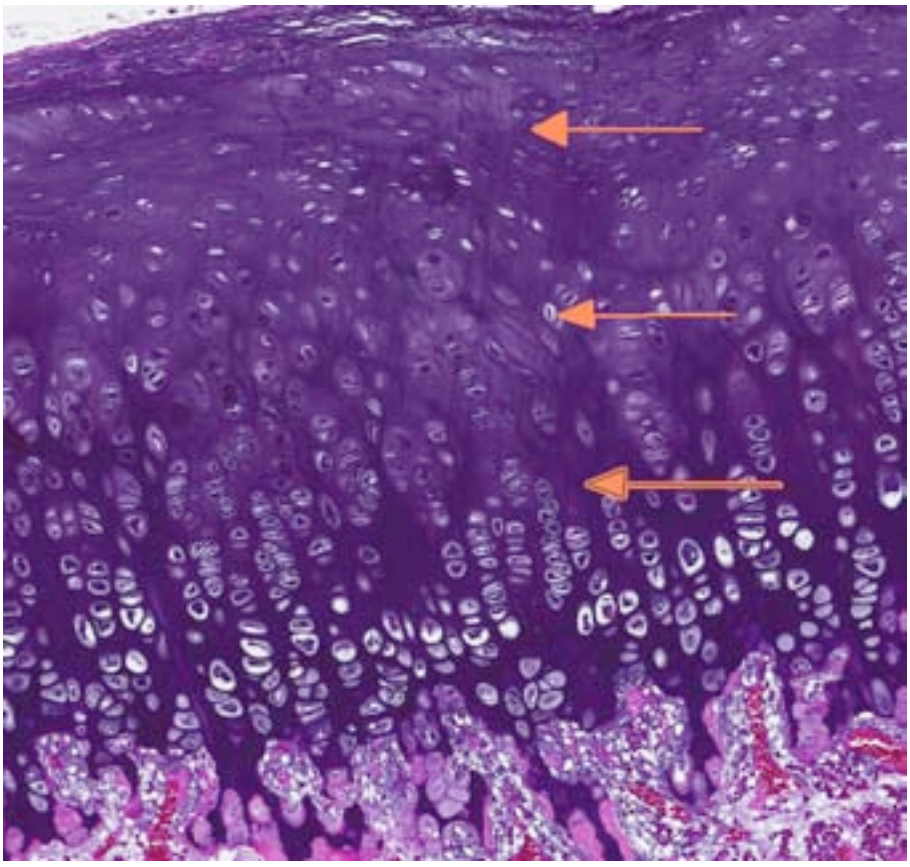

3-3. Rib, pig: The hyaline cartilage is arranged in a zonal fashion similar to physeal cartilage – the resting zone (top arrow), zone of proliferation (middle arrow), and hypertrophic zone (bottom arrow). (HE 60X)

cartilage which may also show foci of endochondral ossification and mineralization.[7,8] However, chondroma misses the growth plate-like organization of the cartilaginous matrix that characterizes osteochondroma. Malignant transformation of osteochondroma to chondrosarcoma has occasionally been described in older dogs and humans. Histologically osteochondroma can be very difficult to differentiate from low grade chondrosarcoma, which may show few indications of malignancy and may closely resemble benign tumors of cartilage.

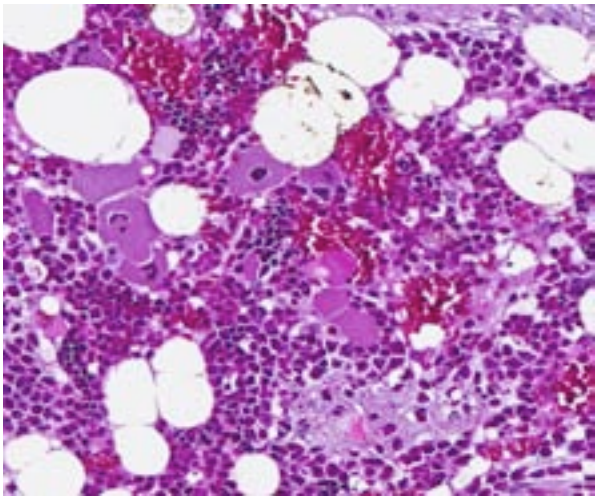

3-4. Rib, pig: Marrow spaces within the bony masses are filled with trilinear erythropoietic marrow. (HE 400X)

JPC Diagnosis: Rib: Osteochondromas (multiple cartilaginous exostoses).

Conference Comment: Osteochondroma are typically continuous with the marrow cavity of the underlying bone, a feature which is helpful in differentiation from other proliferative or neoplastic bone lesions.[8] This lesion is relatively uncommon in swine, however it occurs fairly frequently in dogs and horses, where it is inherited in an autosomal dominant pattern and typically arises from scapula, ribs, vertebrae, and pelvis of young animals.[1] Although the underlying genetic defect in these species is unknown, it likely involves the perichondrial ring. Since enlargement ceases at the time of physeal closure, and the cartilage cap is eventually replaced by bone in an orderly fashion, there is some debate regarding its classification; many do not consider osteochondroma to be a true neoplasm, but rather a skeletal dysplasia.[8] As a result, the terminology associated with osteochondromas can be somewhat confusing. Osteochondromatosis is also known as multiple osteochondromas, multiple hereditary exostoses, multiple cartilaginous exostoses, multiple osteochondromatosis, diaphyseal aclasis, and hereditary chondrodysplasia.[4]

In contrast, feline osteochondromatosis occurs in older animals and primarily affects intramembranous flat bones, while long bones are

seldom affected. The lesion does not generally communicate with the marrow cavity of the underlying bone. Cells may appear somewhat atypical and pleomorphic, and growth tends to be progressive, with the potential for malignant transformation and metastasis. Thus feline osteochondromatosis is more consistent with a true neoplasm and has a more guarded prognosis. Inheritance does not appear to play a role in the pathogenesis; instead, viral particles resembling feline leukemia virus (FeLV) have been demonstrated within the proliferating cells of the hyaline cartilage cap in these tumors.[1]

Contributing Institution: Serve de Diagnostic de Patologia Veterinària
Facultat de Veterinària
Bellaterra (Barcelona), Spain 08193

References:

1. De Brot S, Grau-Roma L, Vidal E, Segales J. Occurence of osteochondromatosis (multiple cartilaginous exostoses) in a domestic pig (*Sus scrofa domesticus*). *J Vet Diagn Invest*. 2013;25(5):599-602.
2. Franch J, Font J, Ramis A, et al. Multiple cartilaginous exostosis in a Golden Retriever cross-bred puppy. Clinical, radiographic and backscattered scanning microscopy findings. *Vet Comp Orthop Traumatol*. 2005;18:189-193.
3. Matthews KA, Strait K, Connor-Stroud F, Courtney CL. Osteochondromatosis in a Rhesus Macaque (*Macaca mulatta*). *Comp Med*. 2012;62:149-152.
4. Ranade SA, Pacchiana PD. What is your diagnosis? Osteochondromatosis. *J Am Vet Med Assoc*. 2011;238(10):1243-1244.
5. Romeo S, Hogendoorn PC, Dei Tos AP. Benign cartilaginous tumors of bone: from morphology to somatic and germ-line genetics. *Adv Anat Pathol*. 2009;16:307-315.
6. Saglik Y, Altay M, Unal VS, et al. Manifestations and management of osteochondromas: a retrospective análisis of 382 patients. *Acta Orthop Belg*. 2006;72:748-755.
7. Thompson KG, Pool RR. Tumors of bone. In: Meuten DJ, ed. *Tumors of Domestic Animals*. 4th ed. Ames, Iowa: Iowa State Press; 2002:245-317.
8. Thompson KG. Bones and joints. In: Maxie MG, ed. *Jubb, Kennedy, and Palmer's Pathology of Domestic Animals*. 5th ed. Vol. 1. St. Louis, MO: Elsevier Limited; 2007:118-124.

CASE IV: 13-6408 (JPC 4033119).

Signalment: One of twin male and female lambs stillborn at term from a white, mixed breed ewe (*Ovis aries*).

History: Twin stillborn lambs were received from a property in New York state housing 65 adult sheep purchased in November 2011. They began lambing in December 2012 and of the 22 lambs dropped by 14 ewes between December and early January, 12 were stillborn, some of which had deformities of the spine and limbs. Ten were born healthy and one was born deformed but alive. There were no clinical signs reported in the ewes.

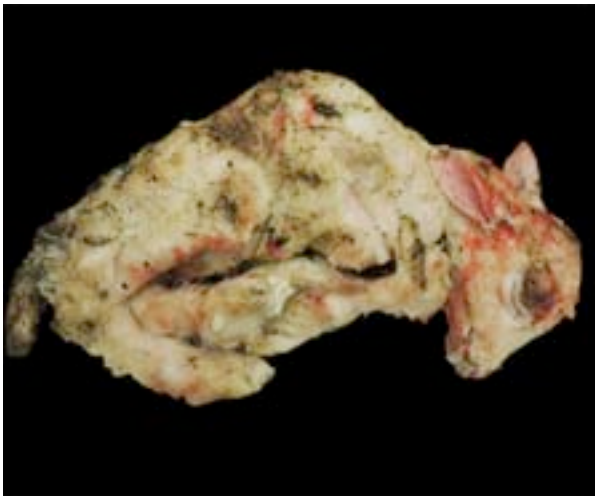

4-1. Top, fetus A exhibits arthrogryposis, bottom, Fetus B demonstrates kyphosis as well as arthrogryposis. (Photo courtesy of: Cornell University College of Veterinary Medicine, Department of Biomedical Sciences, S2-121 Schurman Hall, Ithaca, NY 14850 http://www.vet.cornell.edu/biosci/pathology/services.cfm)

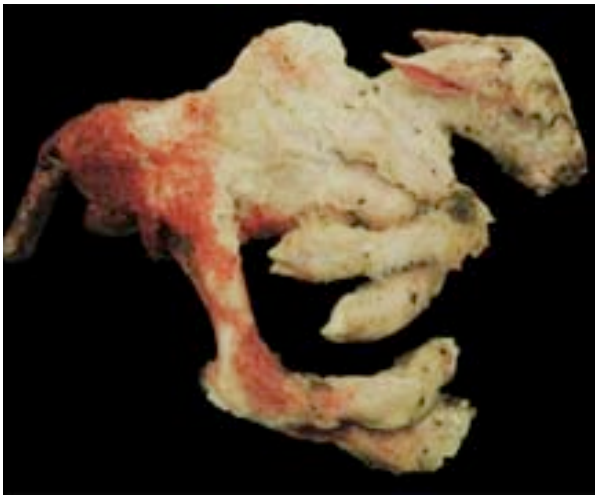

Gross Pathology: In one lamb, there was contraction of the elbow, stifle, carpal and tarsal joints (arthrogryposis). There was moderate lateral and dorsal deviation of the thoracic spine (scoliosis and kyphosis, respectively) and the sternum was curved dorsally. In the skull, the right orbit was located more rostroventally compared to the left orbit and there was deviation of the mandible to the right of the maxilla. The calvarium contained a thin membrane of cerebral cortex surrounding abundant clear, lightly red, thin fluid (hydranencephaly). The brainstem and hippocampi were small and the cerebellum absent. In the other lamb, there was arthrogryposis with contraction of the elbow and carpal joints and extension of the stifle and tarsal joints. There was severe scoliosis and kyphosis of the thoracic spine and the sternum was curved ventrally. The brain was fluctuant with marked dilation of the lateral ventricles (hydrocephalus) and cerebellar hypoplasia.

Laboratory Results: Virus neutralization testing (NVSL, Iowa) was performed in 7 ewes and 1 live affected lamb: 6 ewes, including the ewe of the fetuses examined, and the affected lamb were positive for Cache Valley virus and all were negative for Schmallenberg virus. Serum neutralization testing for Bovine Virus Diarrhea virus was negative. Polymerase chain reaction (PCR) testing for Bunyavirus and Schmallenberg virus and virus isolation in the two lambs were negative.

Histopathologic Description: Throughout the section, myocytes are small, thin, individualized and rounded. There is an absence of cross-striations and increased cytoplasmic basophilia. Diffusely, there is moderate expansion of the endomysium and perimysium with loosely arranged fibromyxomatous extracellular matrix material and edema. Scattered bundles of less affected muscle fibers composed of smaller myofibers with decreased sarcoplasm and peripheral and occasional central nuclei. Multifocally, there is parenchymal replacement by adipocytes and few small areas of hemorrhage.

Contributor's Morphologic Diagnosis: Skeletal muscle: Severe, diffuse myofiber hypoplasia and atrophy with fatty replacement.

Contributor's Comment: Cache Valley Virus (CVV) belongs to the family Bunyaviridae, genus

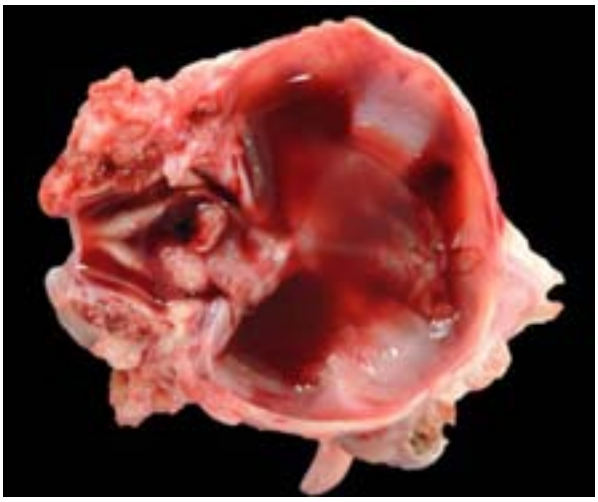

4-2. Fetus B demonstrates numerous neural defects within the cranium, with hydranencephaly being the most severe. (Photo courtesy of: Cornell University College of Veterinary Medicine, Department of Biomedical Sciences, S2-121 Schurman Hall, Ithaca, NY 14850 http://www.vet.cornell.edu/biosci/pathology/services.cfm)

4-3. Fetus B exhibits severe craniofacial abnormalities. (Photo courtesy of: Cornell University College of Veterinary Medicine, Department of Biomedical Sciences, S2-121 Schurman Hall, Ithaca, NY 14850 http://www.vet.cornell.edu/biosci/pathology/services.cfm)

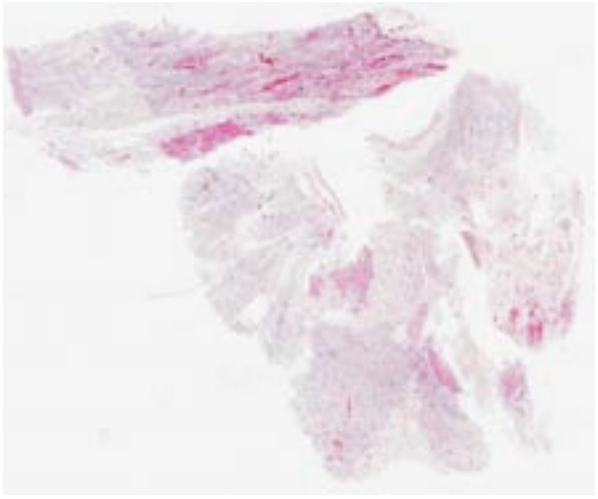

4-4. Stillborn lamb, skeletal muscle: Longitudinal (upper left) and transverse (lower right) sections of skeletal muscle show minimal development of skeletal muscle fibers, with marked infiltration by adipose tissue, as well as marked edema. (HE 0.63X)

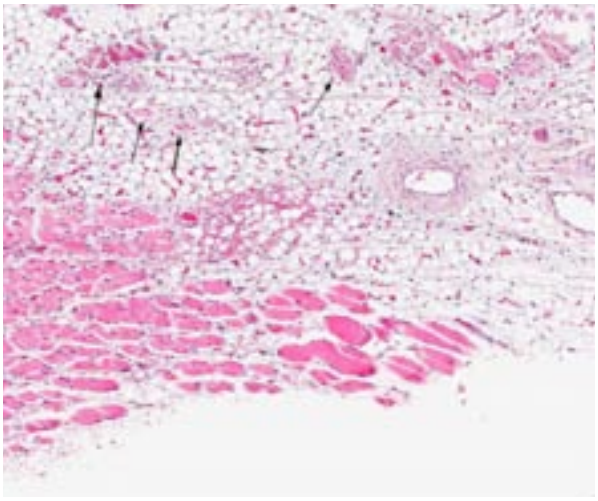

4-5. Stillborn lamb, skeletal muscle: Longitudinal section demonstrates normal skeletal muscle at lower right, hypoplastic skeletal muscle (arrows) scattered amongst abundant fatty tissue. (HE 128X)

Orthobunyavirus, serogroup Bunyamwera, and is transmitted by arthropod vectors (arbovirus) to mammalian hosts. CVV is endemic to North America with a wide geographic distribution and was first isolated from *Culiseta inornata* mosquitoes collected in Cache Valley, Utah, in 1956. Other vectors for CVV include *Aedes* spp., *Anopheles* spp. and *Aedeomyia* spp. mosquitoes and *Culicoides* spp. biting midges. CVV is known to infect a wide range of mammals, including sheep, cattle, horses, white-tailed deer, cottontail rabbits and, rarely, humans. The lifecycle of CVV is poorly studied and the primary mammalian amplifying host is unknown. A potential primary host is the white-tailed deer, when experimentally infected develops a transient viremia lasting 1-3 days in naïve animals or less in previously exposed animals.[1] However, experimental infection of cottontail rabbits revealed a similar duration of viremia which was insufficient to infect mosquito vectors.[2] CVV is known to be present in the area of this farm[6] but malformed lambs are rare as local farmers breed at times which coincide with low numbers of flying insects.

The clinical signs of CVV infection in adults are generally subclinical causing only a transient

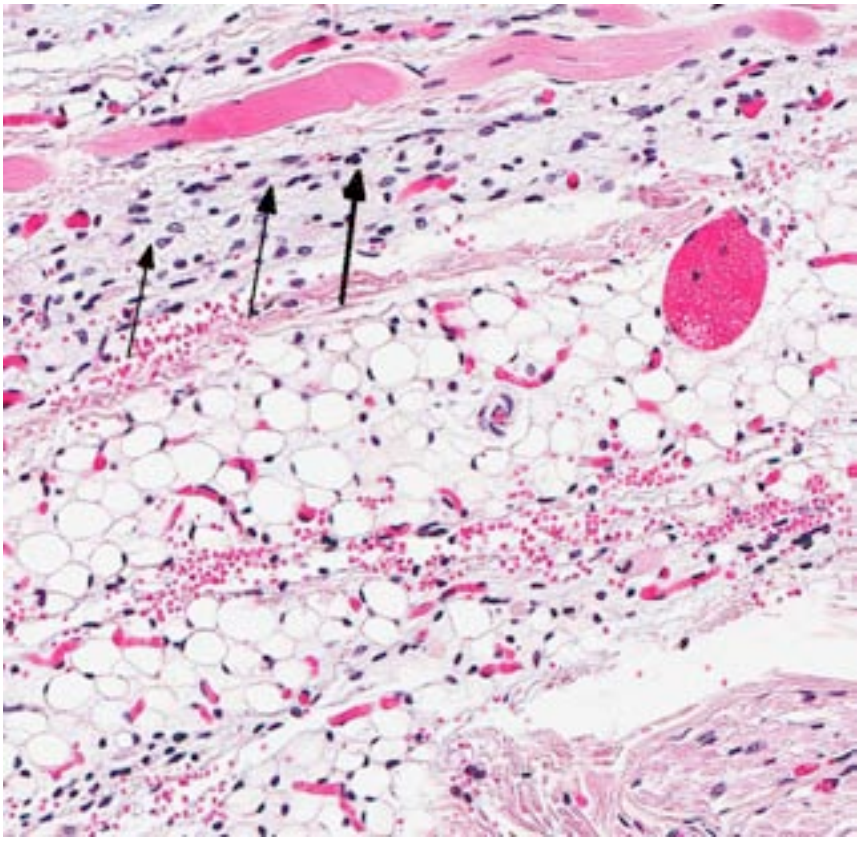

4-6. Stillborn lamb, skeletal muscle: In some areas, severely hypoplastic myofibers have a diameter equal or even less than a satellite cell nucleus. (HE 200X)

febrile response. In sheep, CVV is a well-recognized cause of congenital malformations and early fetal loss. Infection of ewes between 27 to 50 days of gestation results in congenital abnormalities including arthrogryposis, torticollis, hydranencephaly, hydrocephalus, porencephaly, microencephaly, cerebral and cerebellar hypoplasia, micromelia, anasarca and oligohydroamnios; mummification, reabsorption and dead embryos without deformities are also seen.[4] Infection at 28–36 days gives rise to central nervous system and musculoskeletal defects while infection at 37–42 days gives rise to musculoskeletal deformities only. Histological changes in addition to the muscular changes presented in this case include areas of necrosis and loss of paraventricular neuropil in the brain together with a reduction in the number of motor neurons.

CVV can be diagnosed on the basis of suggestive fetal malformations, histopathological changes, the demonstration maternal and neonatal antibodies and the presence of virus in pools of resident mosquitoes and viremic adults. At birth, CVV generally cannot be isolated aborted fetuses. Experimentally in sheep, CVV could be isolated from the allantoic fluid at less than 70 days of gestation but was not recovered from the allantoic fluid of fetuses after 76 days gestation.[4] Virus neutralization and ELISA testing are available for serological testing while PCR and virus isolation are available for virus detection.

JPC Diagnosis: Skeletal muscle and adipose tissue: Myofiber hypoplasia, diffuse, severe, with fatty infiltration.

Conference Comment: Histochemical staining with PTAH demonstrates the shrunken, irregular nature of fetal myocytes and highlights the multifocal loss of cross striations. The edema in the submitted tissue sections incited some debate among conference participants; several considered this a normal finding in fetal tissue and speculated that ongoing vasculogenesis may play a role, while others attributed the edema in the perimuscular connective tissue to a diminished intensity of skeletal muscle contraction secondary to myocyte hypoplasia. Since muscle contraction normally helps transport fluid from the interstitium into local lymphatics, skeletal muscle hypoplasia could theoretically contribute to widespread edema. Ultimately, participants concluded that both of these factors likely contributed to the edema.

Plant toxins and teratogenic viruses, including those belonging to the genera *Orthobunyavirus, Pestivirus* and *Orbivirus*, are often associated with congenital fetal malformations of the musculoskeletal and central nervous systems in ruminants. The most common cause of arthrogryposis, whether due to teratogenic plants or viruses, is denervation.[7] Ingestion of wild lupins (*Lupinus caudatus, sericeus*, or *formosus*) by pregnant cows may result in "crooked calf disease," which is characterized by fetal

musculoskeletal malformations such as arthrogryposis, torticollis, scoliosis, kyphosis, brachygnathia superior or palatoschisis. Similarly, maternal ingestion of *Veratrum californicum* can cause arthrogryposis or cyclopia in neonatal ruminants, and *Nicotiana* spp. (tobacco), jimsonweed and wild black cherry have also been associated with arthrogryposis; however, these plant toxins are not generally linked with hydranencephaly or cerebellar hypoplasia.[7]

Cache Valley, Akbane, Schmallenberg and Aino viruses belong to the genus *Orthobunyavirus* and are known for causing outbreaks of arthrogryposis, hydranencephaly and occasionally cerebellar hypoplasia in calves and lambs (see WSC 2012-2013, conference 22, case 3, table 1). Cache Valley virus is more common in sheep, while Akbane and Aino viruses primarily affect cattle. Fetal infection of calves and lambs with bovine virus diarrhea virus or border disease virus (pestiviruses) often results in cerebellar hypoplasia, or, less commonly, hydranencephaly, porencephaly, hydrocephalus or ocular abnormalities. Likewise, classical swine fever virus (also a pestivirus) infection can cause mummification, arthrogryposis and cerebellar hypoplasia in piglets. Infection with bluetongue virus (orbivirus) causes hydranencephaly and porencephaly in lambs and occasionally calves; however, arthrogryposis is not a characteristic lesion. Wesselsbron virus (flavivirus) is associated with mummification, hydranencephaly, arthrogryposis, porencephaly and cerebellar hypoplasia in lambs and calves.[3,7]

Virus-induced teratogenic effects are far less common in small domestic animals and laboratory species than in livestock. One exception is feline parvovirus which causes cerebellar hypoplasia in kittens due to selective necrosis of the external granular cell layer. Less commonly, canine parvovirus and Kilham rat virus (also a parvovirus) can also result in cerebellar hypoplasia in neonatal dogs and rats, respectively.[3,5]

Contributing Institution: Department of Biomedical Sciences
College of Veterinary Medicine
Cornell University
240 Farrier Rd
Ithaca, NY 14853
http://www.vet.cornell.edu/biosci/pathology/services.cfm

References:

1. Blackmore CG, Grimstad PR. Evaluation of the eastern cottontail *Sylvilagus floridanus* as an amplifying vertebrate host for Cache Valley virus (Bunyaviridae) in Indiana. *J Wildl Dis*. 2008;44(1):188-192.
2. Blackmore CGM, Grimstad PR. Cache Valley and Potosi viruses (Bunyaviridae) in white-tailed deer (*Odocoileus virginianus*): experimental infections and antibody prevalence in natural populations. *Am J Trop Med Hyg*. 1998;59(5): 704-709.
3. Maxie MG, Youssef S. Nervous system. In: Maxie MG, ed. *Jubb, Kennedy, and Palmer's Pathology of Domestic Animals*. 5th ed. Vol. 1. St. Louis, MO: Elsevier Limited; 2007:304-322.
4. OIE. 2008. Chapter 2.9.1 - Bunyaviral diseases of animals (excluding Rift Valley fever). Manual of Diagnostic Tests and Vaccines for Terrestrial Animals 2012. Accessed: 25/02/2013. URL: http://www.oie.int/fileadmin/Home/eng/Health_standards/tahm/2.09.01_BUNYAVIRAL_DISEASES.pdf http://www.oie.int/fileadmin/Home/eng/Health_standards/tahm/2.09.01_BUNYAVIRAL_DISEASES.pdf
5. Percy DH, Barthold SW. *Pathology of Laboratory Rodents and Rabbits*. 3rd ed. Ames, IA: Blackwell Publishing; 2007;127-129.
6. Sahu, SP, Pedersen, DD, Ridpath, HD, Ostlund, EN, Schmitt, BJ, Alstad, DA. Serological survey of cattle in the northeastern and north central United States, Virginia, Alaska, and Hawaii for antibodies to Cache Valley and antigenically related viruses (Bunyamwera serogroup viruses). *Am J Trop Med Hyg*. 2002;67(1):119-122.
7. Thompson KG. Bones and joints. In: Maxie MG, ed. *Jubb, Kennedy, and Palmer's Pathology of Domestic Animals*. Vol. 1. 5th ed. St. Louis, MO: Elsevier Limited; 2007:60-62, 204-206.

Joint Pathology Center
Veterinary Pathology Services

WEDNESDAY SLIDE CONFERENCE 2013-2014

Conference 15

12 February 2014

CASE I: T2319/13 (JPC 4035545).

Signalment: Juvenile male castrated domestic shorthair cat (*Felis catus*).

History: A juvenile stray cat was found in neglected condition in the spring of 2012. The animal had diarrhea and an ulcerative stomatitis as well as many endoparasites and a marked ectoparasitosis (fleas and mites). Serological testing revealed an infection with feline lentivirus (FIV virus). Kept in an animal shelter, the condition of the cat improved with still occasional episodes of stomatitis. In summer 2012, a pedunculated mass on a forepaw was removed surgically. In spring 2013, the cat showed severe facial dermatitis, otitis, and the mass at the paw had recurred. Suspecting a malignant neoplasm, the tumor tissue, including the claw, was resected and submitted for histopathological examination.

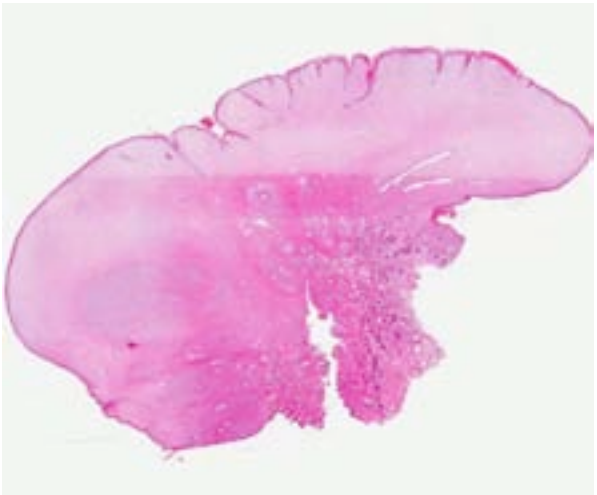

1-1. Footpad, cat: A polypoid mesenchymal neoplasm arises from the haired skin and pawpad. (HE 0.63X)

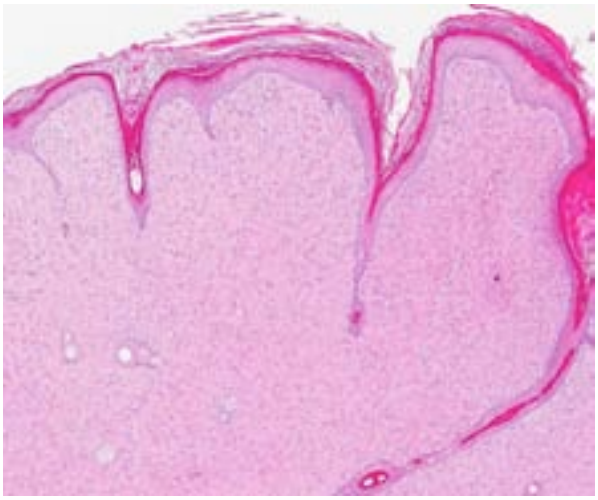

1-2. Footpad, cat: The moderately cellular neoplasm is composed of spindle cells arranged in vague bundles. The overlying epithelium is moderately hyperplastic and forms deep rete ridges. There is mild orthokeratotic hyperkeratosis overlying the neoplasm. (HE 38X)

Gross Pathology: A 2.5 x 2 x 1.5 cm mass close to a claw, partially covered by skin, was submitted. The mass had an irregular cauliflower-like surface. The consistency was firm and the color on the cut surface was grey-white throughout.

Laboratory Results: Detection of papillomaviral DNA (PCR): positive
[Institute of Hygiene and Infectious Diseases of Animals, Justus Liebig University Giessen]
Detection of FeSarPV (PCR): positive
[Institute of Virology, Justus Liebig University Giessen]

Histopathologic Description: Skin, claw: Protruding from the superficial dermis and elevating the overlying epidermis, there is a moderately cellular, well-demarcated, lobular and pedunculated, expansively growing, unencapsulated neoplasm composed of spindle cells arranged haphazardly in interweaving bundles and streams within moderate amounts of collagen and sparse vessels. Neoplastic cells are spindle shaped, have indistinct cell borders, and a moderate amount of fine fibrillar, pale eosinophilic cytoplasm. Nuclei are oval to elongated with finely stippled, occasionally vesicular chromatin and a single, variably distinct nucleolus. Mitotic rate is very low (<1 per 10 high power fields). Cells show mild anisocytosis and anisokaryosis. Occasionally, neoplastic cells are arranged perpendicular to the dermal-epidermal interface. Interspersed within the spindle cells, there are moderate numbers of well-differentiated mast cells (3-4 per high power field). The overlying epidermis is hyperplastic with occasional papillary projections, acanthosis and spongiosis, elongated, thin, often branching rete ridges, and moderate orthokeratotic and parakeratotic hyperkeratosis.

Contributor's Morphologic Diagnosis: Skin and claw: Feline sarcoid, feline, *(Felis domesticus*).

Contributor's Comment: Feline sarcoids are also known as feline fibropapillomas. They most often occur in young male cats at various sites of the skin (e.g. pinna, lip, nose, digits, tail, gingiva). They can be ulcerated and cats can harbor one or several of these tumors. Recurrence often occurs; metastasis has not yet been described.[3,4,5] Feline sarcoids share many similarities with sarcoids in equine species regarding their etiology, clinical outcome, morphology, and prognosis.[3,4,10]

Different papillomaviruses are suspected to be responsible for feline sarcoids. The feline sarcoid associated papillomavirus (FeSarPV) is similar to BPV-1, OvPV-1 and BPV-2. The genome of FeSarPV shows high homology with the genome of papillomaviruses of different ruminants.[22] Some of these papillomaviruses are classified as members of the genus *Deltapapillomavirus*. In contrast, the host specific papillomaviruses of cats, causing papillomatous plaques and real papillomas, are members of the genus *Lambdapapillomavirus*.[9] Infection of horses or cats by ruminant papillomaviruses is therefore regarded as cross-species papillomavirus infection.

For a recent classification of animal papillomaviruses, see Rector and van Ranst, 2013.[16]

Sarcoids are also described in lions. A possible mode of infection of large felids may be the consumption of bovine carcasses that had not been skinned.[15,17]

Viral papillomas caused by feline papillomavirus (FdPV-1) are rarely found in domestic cats.[22] These lesions are most likely associated with different forms of immunodeficiency in stray cats often in association with FIV infection.[2,11] Feline papillomatous plaques, often caused by FdPV-2[8], sometimes undergo malignant transformation to squamous cell carcinoma (SCC).[4,8,19] In one report, Human papillomavirus type 9 was identified using molecular biology.[13]

Predisposing factors of feline sarcoids are the behavior of rural cats. Contact with ruminants is occasionally mentioned. Numerous cases of sarcoids are reported from areas with dairy industry (e.g. New Zealand, Minnesota).[3,5,12,18] However, many interspecies contacts or modes of virus transmission are possible. A recent study demonstrated detection of feline sarcoid PV genome sequences within different bovine skin samples.[12]

Additional factors that favor the development of sarcoids in cats are in discussion, for example, trauma.[6] Interestingly, as in the presented case, FIV infection is reported in cases of feline

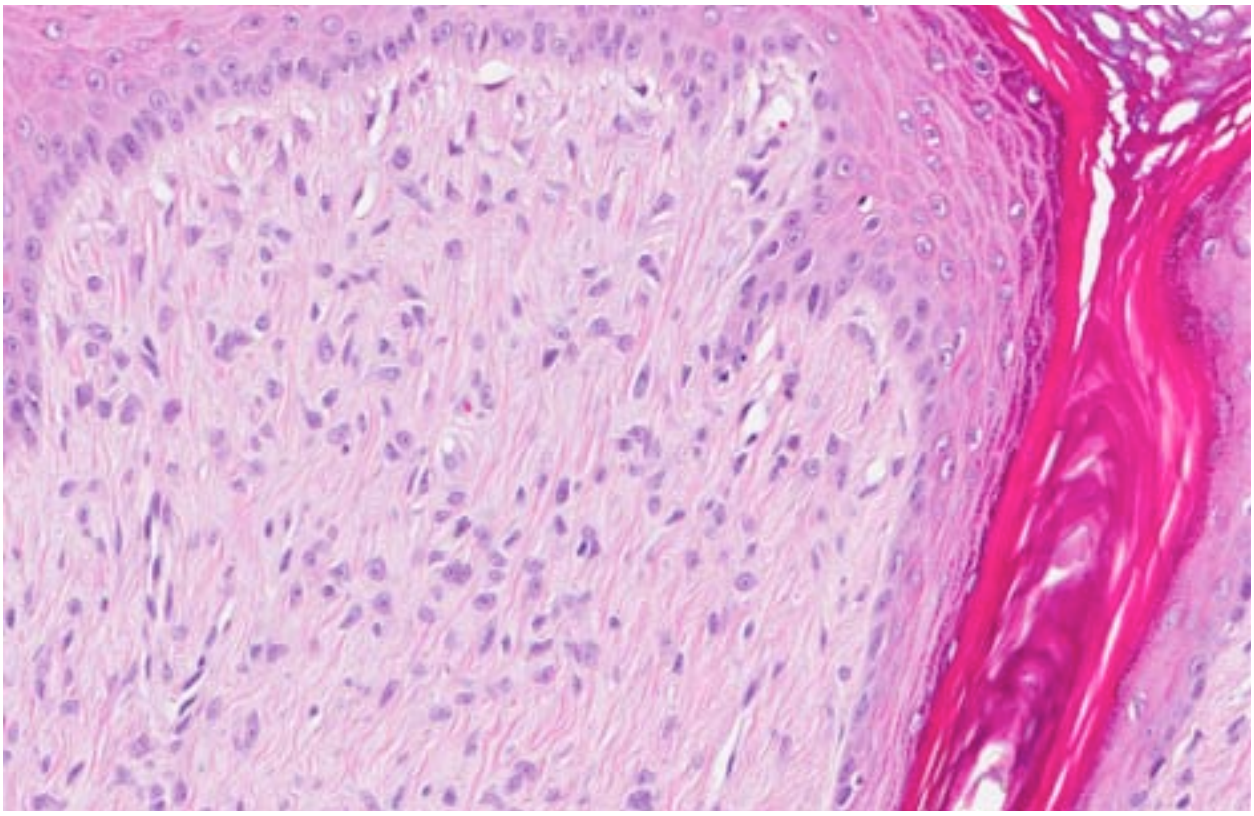

1-3. Footpad, cat: Neoplastic spindle cells are spindled to stellate with a small amount of eosinophilic cytoplasm on a moderately dense fibrous stroma. Rarely, spindle cells are oriented perpendicularly to the epidermis. (HE 260X)

sarcoids[21] and can play a role in the pathogenesis of the disease.

Tumors most often occur in young male cats. They are solitary or multiple skin nodules that measure up to 2 cm and they can be pedunculated or ulcerated. Predilection sites are the skin at the ears, lips, tail or paws. Their consistency is firm.[3,4,18]

Histomorphology of feline sarcoids is identical to equine sarcoids. Characteristically they show proliferating fibroblasts covered by hyperplastic epidermis.[18] Differentials are fibrosarcoma, histiocytic sarcoma, other spindle cell sarcomas, peripheral nerve sheath tumor and amelanotic melanoma.[3,4]

Feline sarcoids often show local recurrence after surgery. Often, relapses show a marked increase in growth rate.[4]

The presented case shares most of the characteristics described for that entity. Three months after surgery, the health status of the cat was good, and there were no signs of tumor recurrence.

JPC Diagnosis: Haired skin and footpad: Feline fibropapilloma (sarcoid).

Conference Comment: Papillomavirus (PV) belongs to the family *Papillomaviridae* (formerly *Papovaviridae*); it is a non-enveloped, icosahedral virus with double stranded DNA that is resistant to high temperatures, low pH, lipid solvents and detergents. Infection occurs via direct/indirect contact with entry through cutaneous abrasions, and virus replication is intimately linked to the growth and differentiation of epidermal and mucosal squamous epithelial cells. Papillomaviruses are divided into 16 genera (*Alpha, Beta, Gamma, Delta, Epsilon, Zeta, Eta, Theta, Iota, Kappa, Lambda, Mupa, Nupa, Xipa, Omikron and Pipapapillomvirus*) on the basis of DNA sequence/genome, host range and biological properties. The most important genera in veterinary medicine include the following:[7,10]

- *Alpha* (α): Oncogenic "high risk" mucosal types that cause benign mucosal/ cutaneous lesions

- *Beta* (β): Cutaneous PVs that rarely cause lesions without immunosuppression
- *Delta* (δ): Cause benign fibropapillomas in ungulates; unique ability to infect multiple species (e.g. Bovine papillomavirus (BPV)-1 and -2 affects both cattle and horses)
- *Epsilon* (ε): BPV-5 and -8; cause both fibropapillomas and true papillomas
- *Lambda* (λ): Associated with skin lesions in the dog and cat; *Felis domesticus* PV1 (FdPV-1) and canine oral PV (COPV)
- *Xipa* (ζ): Bovine papillomaviruses (BPV)-3, -4, -6, -9 and -10; restricted to cattle and cause true, cutaneous squamous papillomas

Papillomaviruses are usually host specific, with a strong tropism for cutaneous and mucosal squamous epithelium, where they typically induce the formation of benign squamous papillomas or fibropapillomas. These tumors tend to spontaneously regress as a result of cell-mediated immunity; however, some PVs can undergo malignant transformation, leading to locally aggressive tumors such as equine sarcoids, or invasive squamous cell carcinomas (ISCC).[3,7,10]

In horses, infection with BPV-1 and -2 in areas subjected to trauma may induce the formation of a fibropapilloma, also known as equine sarcoid, which is grossly and histologically similar to the neoplasm described in this case.[3,10] The most important proteins expressed by equine sarcoids are BPV major transforming protein E5, BPV E6 protein and BPV E7 protein. BPV E5 binds the β-receptor of PDGF (PDGFβ-r) and activates kinases, such as cyclin A-cdk2, MAP, JNK, PI3 and c-Src, thus interfering with cell-cycle control and signal transduction cascades and ultimately promoting fibroblast growth as well as loss of contact inhibition. E5 also downregulates MHC1 expression, which allows infected cells to evade immunosurveillance. BPV E6 protein binds a calcium-binding protein (ERC-55/E6BP), a transcriptional co-activator (CBP/p300), a focal adhesion protein (paxillin), and the adaptor complex AP-1, which is important in control of cell proliferation and differentiation. Overall, these interactions lead to disruption of the cytoskeleton and cell–cell/cell–matrix interactions, ultimately contributing to uncontrolled cellular proliferation. This is in contrast to Human papillomavirus (HPV) E6 protein, which acts by stimulating degradation of p53.[1,14] Furthermore, there is some evidence to suggest that co-expression of BPV E5 and E7 is necessary for neoplastic transformation in horses. In human mucosal alpha-PVs (e.g. HPV-16, -17), E7 binds and inactivates the tumor suppressor Rb, promoting cell cycling.[10] In addition to equine sarcoids induced by BPV-1 and -2, *Equus caballus* papillomavirus-2 (EcPV-2) has recently been identified in equine genital papillomas, in situ carcinomas (ISC) and ISCCs.[6]

In cats, FdPV-1 and -2 infection, in combination with solar-induced p53 mutation and papillomavirus-induced inhibition of keratinocyte apoptosis, may lead to uncontrolled cell proliferation, progressing to Bowenoid in situ carcinoma (BISC) and, less commonly, SCC. Additionally, as noted by the contributor, papillomavirus DNA has been localized to proliferating fibroblasts suggesting an association between feline fibropapillomas (sarcoids) and PV.[10] As in cats, cutaneous PV infections in dogs can generate viral plaques that may subsequently progress to ISC or ISCC; pugs, miniature schnauzers and immunosuppressed dogs are predisposed. Although Canine oral papillomavirus (COPV) infection is not associated with cutaneous neoplasia, vaccination with a live COPV vaccine may result in cutaneous ISCC.[10]

There are currently ten different papillomaviruses described in cattle.[14,20] BPV-1 and BPV-2 cause fibropapillomas, while BPVs-3, -4, -6, -9 and -10 are epitheliotropic and induce true cutaneous squamous papillomas. BPV-5 and BPV-8 appear to have a dual pathology, causing both fibropapillomas and cutaneous squamous papillomas. Bracken fern (*Pteridium aquilinum*) contains immunosuppressants and a number of mutagens; in cattle that have ingested bracken fern, BPV-4-induced alimentary papillomas may progress to SCC, while transforming protein E5 associated with BPV-2 or -4 may synergize with ptaquiloside to produce bladder cancer.[14] See table 1 for a summary of select papillomaviruses and their affects on various species.

Table 1: Select papillomaviruses in domestic animal species.[3,6,7,10,14,20]

Species	Skin lesion	Papilloma virus	Type
Cat	Feline viral plaque progressing to BISC +/- ISCC	FdPV-1, -2	λ(1)
Cat	SCC	FdPV-2	novel
Cat	Feline sarcoid (feline cutaneous fibropapilloma)	FeSarPV BPV-1,-2	novel δ
Dog	Canine pigmented viral plaque progressing to ISC and SCC	CfPV-3, -4	novel
Dog	Endophytic papilloma and SCC in immunosuppressed dogs	CfPV-2	novel
Dog	Oral papilloma and vaccine-induced cutaneous SCC	COPV	λ
Horse	Equine sarcoid (equine cutaneous fibropapilloma)	BPV-1, -2	δ
Horse	Equine penile papillomas, ISC & SCC	EcPV2	
Ox	Cutaneous fibropapilloma	BPV-1,-2	δ
Ox	Both fibropapillomas and squamous papilloma	BPV-5,-8	Epsilon(ε)
Ox	Cutaneous squamous papilloma	BPV-3, -6, -9, -10	Xi (ξ)
Ox	Squamous papilloma of alimentary tract & urinary bladder	BPV-4	Xi (ξ)
Ox	Co-carcinogen with bracken fern (ptaquiloside) to induce urinary bladder neoplasms	BPV-2	δ
Bull (young)	Papilloma/fibropapilloma of glans penis	BPV-1	δ
Ox	Squamous papilloma	BPV-7	novel
Cotton-tail rabbit	Cutaneous SCC	CRPV	Kappa (κ)
Western barred bandicoot	Cutaneous papillomatosis & SCC (digits, lips)	BPCV-1	novel
Egyptian fruit bat	Basosquamous carcinoma	RaPV-1	novel
Natal multimammate mouse	Keratoacanthoma and SCC	MnPV	Iota (ι)
European harvest mouse	Sebaceous carcinoma	MmPV	Pi (π)

Contributing Institution: Institut fuer Veterinaer-Pathologie, Justus-Liebig-Universitaet Giessen
Frankfurter Str. 96, 35392 Giessen, Germany
http://www.uni-giessen.de/cms/fbz/fb10/institute_klinikum/institute/pathologie

References:

1. Chambers G, Ellsmore VA, O'Brien PM, Reid SWJ, Love S, Campo MS, et al. Association of bovine papillomavirus with the equine sarcoid. *J Gen Virol*. 2003;84:1055-1062.
2. Egberink HF, Berrocal A, Bax HA, van den Ingh TS, Walter JH, Horzinek MC. Papillomavirus associated skin lesions in a cat seropositive for feline immunodeficiency virus. *Vet Microbiol.* 1992;31:117-125.
3. Ginn PE, Mansell JEKL, Rakich PM. Skin and appendages. In: Maxie MG, ed. *Jubb, Kennedy, and Palmer's Pathology of Domestic Animals*. 5th ed. Vol 1. Philadelphia, PA: Elsevier Limited; 2007:553-781.
4. Gross TL, Ihrke PJ, Walder EJ, Affolter VK. *Skin diseases of the dog and cat: clinical and histopathologic diagnosis*. 2nd ed. Oxford, UK: Blackwell Science Ltd; 2005:567-589, 730-731.
5. Hanna PE, Dunn D. Cutaneous fibropapilloma in a cat (feline sarcoid). *Can Vet J*. 2003;44:601-602.
6. Lange CE, Tobler K, Lehner A, et al. EcPV2 DNA in equine papillomas and in situ and invasive squamous cell carcinomas supports papillomavirus etiology. *Vet Pathol*. 2012;50:686-692.
7. MacLachlan NJ, Dubovi EJ. *Fenner's Veterinary Virology*. 4th ed. London, UK: Academic Press; 2011:213-221.
8. Munday JS, Peters-Kennedy J. Consistent detection of *Felis domesticus* papillomavirus 2 DNA sequences within feline viral plaques. *J Vet Diagn Invest*. 2010;22:946-949.
9. Munday JS, Knight CG, Howe L. The same papillomavirus is present in feline sarcoids from North America and New Zealand but not in any non-sarcoid feline samples. *J Vet Diagn Invest*. 2010;22:97-100.
10. Munday JS, Kiupel M. Papillomavirus-associated cutaneous neoplasia in mammals. *Vet Pathol*. 2010;47:254-264.
11. Munday JS, Witham AI. Frequent detection of papillomavirus DNA in clinically normal skin of cats infected and noninfected with feline immunodeficiency virus. *Vet Dermatol*. 2010;21:307-310.

12. Munday JS, Knight CG. Amplification of feline sarcoid-associated papillomavirus DNA sequences from bovine skin. *Vet Dermatol*. 2010;21:341-344.
13. Munday JS, Hanlon EM, Howe L, Squires RA, French AF. Feline cutaneous viral papilloma associated with human papillomavirus type 9. *Vet Pathol*. 2007;44:924-927.
14. Nasir L, Saveria Campo M. Bovine papillomaviruses: their role in the aetiology of cutaneous tumours of bovids and equids. *Vet Dermatol.* 2008;19(5):243-254.
15. Orbell GM, Young S, Munday JS. Cutaneous sarcoids in captive African lions associated with feline sarcoid-associated papillomavirus infection. *Vet Pathol*. 2011;48:1176-1179.
16. Rector A, Van Ranst M. Animal papillomaviruses. *Virology*. 2013 (in press).
Schulman FY, Krafft AE, Janczewski T, Mikaelian I, Irwin J, Hassinger K. Cutaneous fibropapilloma in a mountain lion (Felis concolor). *J Zoo Wildl Med*. 2003;34:179-183.
17. Schulman FY, Krafft AE, Janczewski T. Feline cutaneous fibropapillomas: clinicopathologic findings and association with papillomavirus infection. *Vet Pathol*. 2001;38:291-296.
18. Schwittlick U, Bock P, Lapp S, Henneicke K, Wohlsein P. [Feline papillomavirus infection in a cat with Bowen-like disease and cutaneous squamous cell carcinoma]. *Schweiz Arch Tierheilkd*. 2011;153:573-577.
19. Silvestre O, Borzacchiello G, Nava D, et. al. Bovine papillomavirus type 1 DNA and E5 oncoprotein expression in water buffalo fibropapillomas. *Vet Pathol.* 2009;46:636-641.
20. Sundberg JP, Van Ranst M, Montali R, Homer BL, Miller WH, Rowland PH, et al. Feline papillomas and papillomaviruses. *Vet Pathol*. 2000;37:1-10.
21. Teifke JP, Kidney BA, Löhr CV, Yager JA. Detection of papillomavirus-DNA in mesenchymal tumour cells and not in the hyperplastic epithelium of feline sarcoids. *Vet Dermatol*. 2003;14:47-56.

CASE II: 10058-12 (JPC 4018119).

Signalment: Six-month-old male castrated German short-haired pointer dog, (*Canis familaris*).

History: Three punch biopsies were submitted from a patient with a 4 month history of alopecia and scaling. The submitting veterinarian reported initial presentation was on the nose and above the eyes. It progressed to the ears and ventrum. Therapy consisting of dermatologic shampoos gave mild relief of clinical signs. Little response was noted with omega-3 fatty acids nor with vitamin E. There was a recent development of pruritus.

Gross Pathology: None.

Histopathologic Description: In sections of haired skin examined, there are multiple changes of the dermal epithelium and follicular epithelium as well as the superficial dermis. Changes in the dermal epithelium include moderate orthokeratotic hyperkeratosis with colonization with rare bacterial cocci. Basilar hydropic degeneration (Civatte body formation) is present in the stratum basal, mural follicular epithelium and less commonly in the stratum spinosum. Moderate numbers of the cells of the stratum basale exhibit apoptosis. Few exocytic lymphocytes are seen within the epidermis. A focal area of separation of the epidermis from the underlying dermis is noted (dermoepidermal clefting-not present in all sections). One section has a mild lichenoid infiltrate of lymphocytes. Follicular changes include similar changes as seen in the epidermis as well as ectasia of the follicles due to mild hyperkeratosis. The dermis is characterized by mild superficial edema, moderate multifocal pigmentary incontinence, and very mildly increased numbers of lymphocytes. Formal hair is frequently present in all stages including anagen. Sebaceous glands are unaffected by inflammatory changes.

Contributor's Morphologic Diagnosis: Mild, diffuse, subacute to chronic, lymphocytic and apoptotic basilar epidermitis and folliculitis.

Contributor's Comment: The lesions present, the breed of the patient, and the age are all

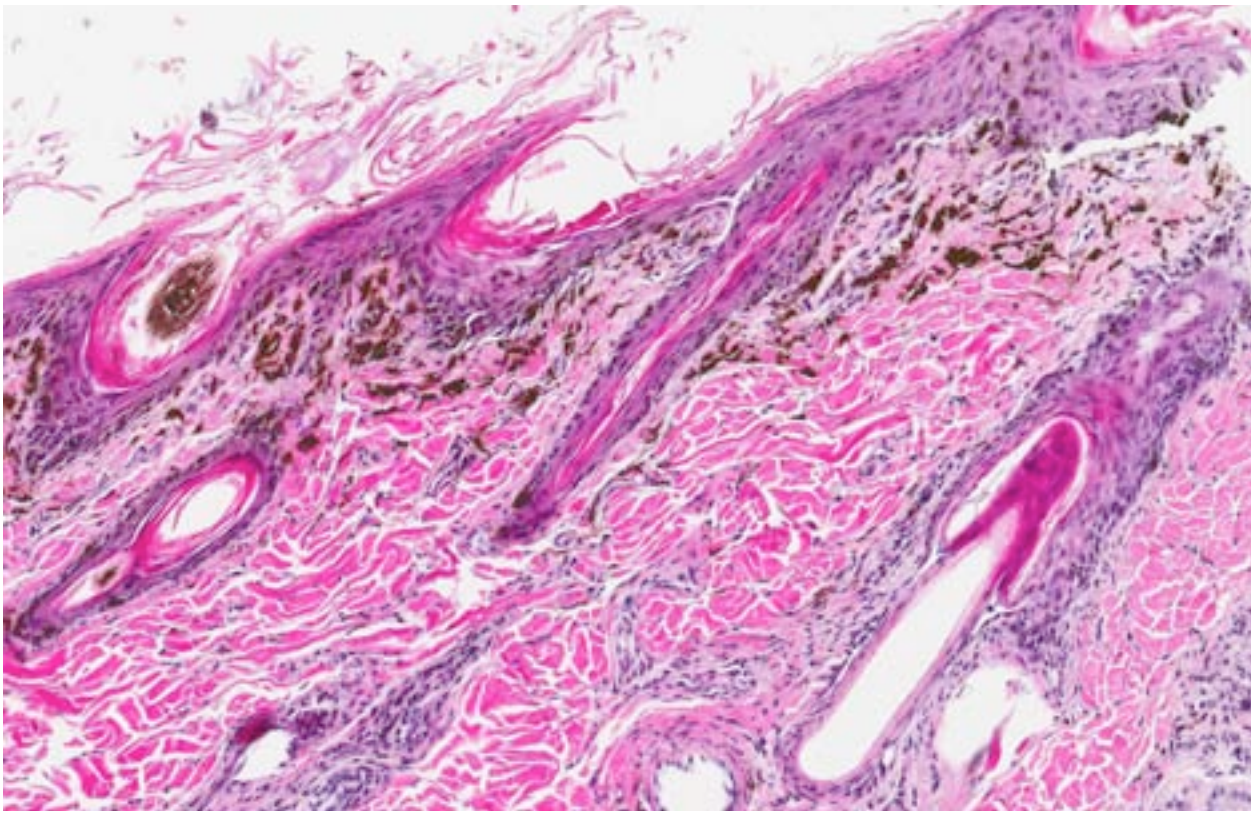

2-1. Skin, German Shorthaired Pointer: This section of skin demonstrates remarkable pigmentary incontinence, and the dermal-epidermal junction is indistinct ("smudgy"). This lack of clarity is a common, but slightly subjective finding associated with interface dermatitis. (HE 200X)

consistent with a diagnosis of exfoliative cutaneous lupus erythematosus of the German shorthaired pointer. This is an autosomal recessive subclassification of lupus erythematosus.[4]

This disease was first reported in 1992 under the name of "Hereditary lupoid dermatosis of the German Shorthaired Pointer."[3] In a relatively recent study, 17 patients were evaluated. The lesion distribution among the sexes was approximately 2:1 (female:male).[1] Young dogs were affected with a mean of 10 months of age (1.8-48 months). Prominent clinical findings in the study were initially scaling (100%), alopecia (76%), crusting with or without ulceration (52%), generalized lymphadenopathy (32%), follicular casts (28%), mild pruritus (28%), and intermittent pyrexia (12%). Lesion distribution early in the course of the disease was reported at the muzzle, pinnae, and the dorsal trunk. The distribution progressed to the limbs and ventral trunk with 52% of the dogs displaying generalized disease.

Clinical pathologic changes included lymphopenia (3/17), hyperglobulinemia (4/17), mild thrombocytopenia (4/17), and lack of antinuclear antibodies in all 17 patients.[1,5] Bryden et al additionally reported anemia.

Histologic findings reported parallel the microscopic findings in our case. They include a moderate to marked lymphocytic interface dermatitis, diffuse hyperkeratosis, basal keratinocyte vacuolation and individual necrosis, exocytosis of lymphocytes into the epithelium, with the interface dermatitis and hyperkeratosis being the most common findings.[1,5]

Primarily CD3 + lymphocytes were identified in the inflammatory infiltrate in the deep epidermis, superficial dermis, hair follicular infundibula, and surrounding sweat glands.[3] In greater than half of the dogs examined, indirect immunofluorescence detected the presence of IgG specific to the follicular basement membranes and specific against sebaceous glands.[1]

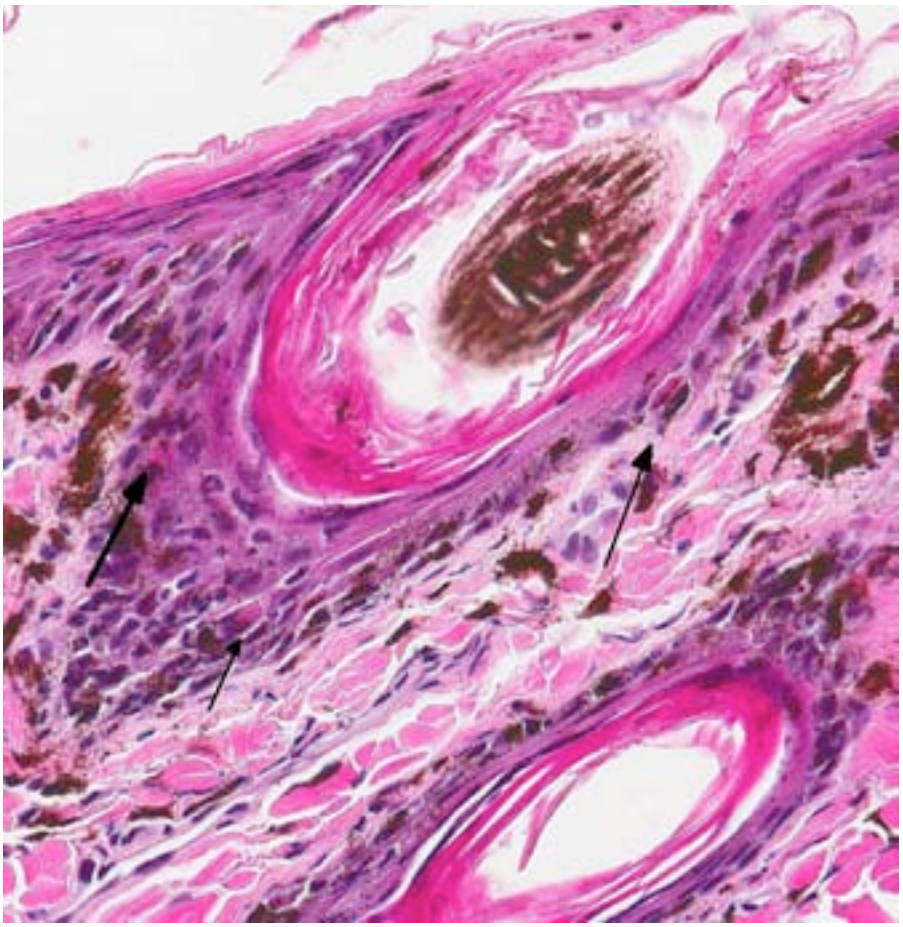

2-2. Skin, German Shorthaired Pointer: The basal epithelium contains several apoptotic basal cells ("Civatte bodies"). (HE 400X)

Some patients receiving immunomodulatory therapy additionally had generalized demodicosis.[5] Noncutaneous findings consisted of peripheral lymphadenopathy, colitis, eosinophilic and lymphoplasmacytic enteritis.

A recent study evaluating the genetic heritability of this disease showed an autosomal recessive pattern of inheritance due to singular nucleotide polymorphism of an as-of-yet unidentified gene on chromosome 18.[8]

Histologic differential diagnoses include sebaceous adenitis, lupus-

like drug reactions, lupus erythematosus and erythema multiforme.[4] Sebaceous adenititis can be differentiated from the above condition by a lack of an interface dermatitis. Lupus-like drug reactions are reported commonly to otic preparations placed topically and may have a similar histologic appearance. Other forms of lupus erythematosus can be differentiated by the breed and age of the patient and decreased instensity of an inflammatory infiltrate when compared to discoid lupus erythematosis. Erythema multiforme has a similar distribution, is more ulcerative than exfoliative, has a mixed lymphocytic and histiocytic interface dermatitis, may have apoptosis in all levels of the epidermis, and generally occurs in animals greater than one year of age.[4]

JPC Diagnosis: Haired skin: Dermatitis, interface, cell-poor, diffuse, mild, with basal epithelial degeneration and necrosis, pigmentary incontinence and loss of sebaceous glands.

Conference Comment: The contributor provides a complete review of exfoliative cutaneous lupus erythematosus of the German shorthaired pointer, and in a well-constructed description of the microscopic findings, mentions that sebaceous glands are generally spared; however, conference participants observed that they appear decreased in number. The moderator pointed out that while loss of sebaceous glands is not a finding specific for this condition, it is consistent with interface dermatitis, because as inflammation progresses along the epidermis and follicular infundibula, the normal organization of adnexal structures is disrupted. Additionally, as noted by the contributor, a recent study detected the presence of IgG antibody against sebaceous glands in many of these cases.

Lupus erythematosus occurs in two distinct forms in animals: Systemic lupus erythematous (SLE), which affects multiple tissues, occasionally including the skin; and cutaneous or discoid lupus erythematous (CLE/DLE), in which lesions are localized to the skin. There is some controversy over the designation of DLE; some pathologists prefer the term "generalized chronic cutaneous lupus."[2] Exfoliative cutaneous lupus erythematosus (ECLE) of the German shorthaired pointer is a unique form of CLE.[5]

In addition to humans, systemic lupus erythematosus (SLE) is recognized in mice, non-human primates and various domestic animals. SLE is characterized by the loss of B- and T-cell tolerance to self-antigens, resulting in polysystemic inflammation.[6] Patients with SLE produce autoantibodies against a range of nuclear and cytoplasmic components of the cell, including histones, double-stranded DNA, nonhistone proteins bound to RNA, and nucleolar antigens.[2] Autoantibodies and self-antigen complexes deposit within glomeruli, blood vessels, skin and joints, inciting a type III hypersensitivity reaction. To a lesser extent, tissue damage is induced by antibodies directed toward self-antigen on erythrocytes, leukocytes and thrombocytes initiating a type II hypersensitivity reaction, or cell-mediated immunity (type IV hypersensitivity).[7] As a result of all of these variables, SLE generates a wide spectrum of clinical presentations and is often referred to as "the great imposter." Affected patients may exhibit a combination of renal disease (glomerulonephritis, interstitial nephritis, vasculitis, and proteinuria), polyarthritis, skin lesions, hematologic disorders, respiratory, or neurologic dysfunction.[6]

Although the definitive cause of SLE remains unknown, numerous endogenous (genetic, hormonal, metabolic, immunologic) and exogenous (drugs, ultraviolet light, infectious agents) factors have been implicated in its pathogenesis.[7] In NZB/W mice, one of the most common strains used in models of SLE, multiple genes have been shown to contribute to the development of SLE, including major histocompatibility complex (MHC) and several non-MHC genes. Recent research has also shown that SLE patients often have hypomethylated DNA, which may lead to an anti–MHC class II response and apoptosis of MHC class II antigen presenting cells. In addition to loss of phagocytic cells, genetic deficiencies of complement components may lead to decreased clearance of apoptotic debris and circulating immune complexes, which is another predisposing factor for SLE.[6] Sex hormones, nutrition and both humoral (via autoantibodies) and cell-mediated immunologic factors also contribute to SLE. In dogs, abnormalities in cellular immunity result in lymphopenia characterized by a high CD4+:CD8+ ratio. In normal dogs this ratio is less than 2, while it may reach as high as 6 in dogs with SLE.

Additionally, cutaneous disease in affected dogs is exacerbated by ultraviolet light, which may be related to tissue damage and inflammation resulting in elaboration of IL-1, IL-1, IL-2, IL-6, and TNF-b and further damage to the epidermis.[2,7] Alternatively, UV radiation may render DNA immunogenic.[7] Interestingly, ECLE in German shorthaired pointers occurs/progresses without the influence of ultraviolet light.[5] In humans, drugs such as hydralizine, procainamide and D-penicillamine are also associated with SLE, while in animals, drug exposure is a suspected trigger, but specific drugs have not been implicated.[7]

In domestic animals, lupoid skin disorders, such as CLE, are most frequently seen in the dog, often localized to the nose. "Lupus-specific" histopathological features include hyperkeratosis, epidermal atrophy, basal cell vacuolar degeneration or necrosis ("Civatte bodies"), basement membrane thickening, mononuclear cell infiltration at the dermoepidermal interface and subepidermal cleft formation. Gross lesions range from alopecia to ulcerative dermatitis.[2,5] On the other hand, skin disorders associated with SLE are non-specific and may not display the lupus specific findings enumerated above.[5]

Contributing Institution: Veterinary Diagnostic Center
University of Nebraska-Lincoln
Lincoln, NE
nvdls.unl.edu

References:

1. Bryden SL, White SD, Dunston SM, et al. Clinical, histopathological and immunological characteristics of exfoliative cutaneous lupus erythematosus in 25 German short-haired pointers. *Vet Dermatol*. 2005;16:239–252.
2. Ginn PE, Mansell JEKL, Rakich PM. Skin and appendages. In: Maxie MG, ed. *Jubb, Kennedy, and Palmer's Pathology of Domestic Animals*. Vol 1. 5th ed. Philadelphia, PA: Elsevier; 2007:652-655.
3. Gross TL, Ihrke PJ, Walder EJ. Hereditary lupoid dermatosis of the German shorthaired pointer. In: *Veterinary Dermatopathology: a Macroscopic and Microscopic Evaluation of Canine and Feline Skin Diseases*. St Louis, MO: Mosby Year Book; 1992:26–28.
4. Gross TL, Ihrke PJ, Walder EJ, Affolter VK. *Skin Diseases of the Dog and Cat: Clinical and Histopathologic Diagnosis*. 2nd ed. Ames, IA: Blackwell Science; 2005:59-68.
5. Mauldin EA, Morris DO, Brown DC, Casal ML. Exfoliative cutaneous lupus erythematosus in German shorthaired pointer dogs: disease development, progression and evaluation of three immunomodulatory drugs (ciclosporin, hydroxychloroquine, and adalimumab) in a controlled environment. *Vet Dermatol*. 2010;21(4):373–382.
6. Rottman JB, Willis CR. Mouse models of systemic lupus erythematosus reveal a complex pathogenesis. *Vet Pathol*. 2010;47:664-676.
7. Snyder PW. Diseases of immunity. In: McGavin MD, Zachary JF, eds. *Pathologic Basis of Veterinary Disease*. 5th ed. St. Louis, MO: Mosby Elsevier; 2012:275-278.
8. Wang P, Zangerl B, Werner P, Mauldin EA, Casal ML. Familial lupus erythematosus (CLE) in the German shorthaired pointer maps to CFA18, a canine orthologue to human CLE. *Immunogenetics*. 2011;63(4):197-207.

CASE III: 6069-12 (JPC 4018118).

Signalment: 4-year-old female spayed domestic short hair cat, (Felis domesticus).

History and Gross Pathology: A 4-year-old spayed female domestic short-haired cat presented with weight loss of 3.5 lbs over the past several months. The cat lived indoors and had no major previous health problems, but recently the owners felt the cat had appeared agitated and possibly painful. On presentation the cat weighed 7.5 lbs and appeared quiet, alert, and responsive although was easily stressed and began to pant. Physical examination was unremarkable with the exception of a fractured tooth and a tooth with an enamel defect. A CBC with manual differential count was performed and the cat had a mature neutrophilic, lymphocytic, and monocytic leukocytosis. A chemistry panel revealed an elevated GGT and slightly elevated sodium. A urinary tract infection was noted on urinalysis. Heartworm testing, FeLV, and FIV were negative and total T4 was normal. The referring veterinarian recommended radiographs, ultrasound, and screening for a variety of infectious diseases, which the owner declined at the time. The cat was sent home on clindamycin 25 mg capsules, for treatment of the urinary tract infection, with the option for adding buprenorphine and high calorie diets with appetite stimulants. The cat returned to the clinic 6 weeks later for euthanasia due to further decline. While restraining the cat for euthanasia the cat was unruly and appeared to be in pain. After euthanasia a technician went to move the cat by its scruff, and the skin over the dorsal thorax tore forming a large flap. A section of skin and liver was collected and submitted for histological evaluation.

3-1. Haired skin, cat: After euthanasia a technician went to move the cat by its scruff, and the skin over the dorsal thorax tore forming a large flap. (Photo courtesy of: Veterinary Diagnostic Center, University of Nebraska-Lincoln, Lincoln, NE nvdls.unl.edu)

Laboratory Results:

CBC

Parameter	Value	Reference Range/ Units
RBC	7.5	6.54-12.20 M/ µL
HCT	37.1	30.3-52.3%
HGB	11.4	9.8-16.2 g/dL
MCV	49.5	35.9-53.1 fL
MCH	15.2	11.8-17.3 pg
MCHC	30.7	28.1-35.8 g/dL
RDW	20.9	15-27%
% Retic	0	%
Retic	2.3	3-50 K/µL
WBC	38.22	2.87-17.02 K/ µL
%Neu	53.8	%
%Lym	37.2	%
%Mono	7	%
%Eos	2	%
Neu	20.53	1.15-10.29 K/ µL
Lym	14.23	0.92-6.88 K/µL
Mono	2.69	0.02-0.67 K/µL
Eos	0.77	0.17-1.57 K/µL
Plt	116	151-600 K/µL
FeLV	negative	

FIV	negative	
Heartworm	negative	

Chemistry

GLU	120	74-159 mg/dL
BUN	31	15-36 mg/dL
CREA	1.4	0.8-2.4 mg/dl
BUN/CREA	22	
PHOS	5.9	3.1-7.5 mg/dL
Ca	9.9	7.8-11.3 mg/dL
TP	7.5	5.7-8.9 g/dL
ALB	3.4	2.2-4.0 g/dL
Glob	4.1	2.8-5.1 g/dL
Alb/Glob	0.8	
ALT	<10	12-130 U/L
ALKP	<10	14-111
GGT	4	0-1 U/L
TBIL	0.6	0.0-0.9 mg/dL
CHOL	97	65-225 mg/dL
AMYL	487	500-1500 U/L
LIPA	998	100-1400
Na	169	150-165 mmol/L
K	5.6	3.5-5.8 mmol/L
Na/K	30	
Cl	125	112-129 mmol/L
Osm Calc	342	mmol/kg
TT4	0.8	µg/dL

Urinalysis (collected off counter)

Color	bright yellow
Appearance	clear
SpGr (refractometer)	>1.050

Test strip

Urobilinogen	normal
Glucose	negative
Ketone	negative
Bilirubin	negative
Protein	100 mg/dl
Nitrite	negative
Leukocytes	3+
Blood	negative
pH	6.5 on strip, 7.4 on meter
Specific gravity	1.02

Sediment

WBC	1-2/hpf
RBC	rare
Epithelial cells	occasional squamous
Casts	Waxy (one seen)
Crystals	triple phosphate 1-2+
Bacteria	cocci 2+

Histopathologic Description: Skin: Two sections of haired skin are examined. The sections consist of epidermis and dermis, with normal appearing hair follicles. The epidermis is thin and ranges from 1-2 cell layers thick, and has diffuse mild orthokeratotic hyperkeratosis. The dermis is severely atrophied and there is loss of a majority of the dermal collagen. The remnant collagen is loosely packed and interspersed with small to moderate numbers of lymphocytes, plasma cells and mast cells. The erector pili muscles within the specimen are prominent.

Liver: The cytoplasm of nearly all of the hepatocytes is expanded by several small, distinct, clear cytoplasmic vacuoles (lipid). The swollen hepatocytes have compression of the associated

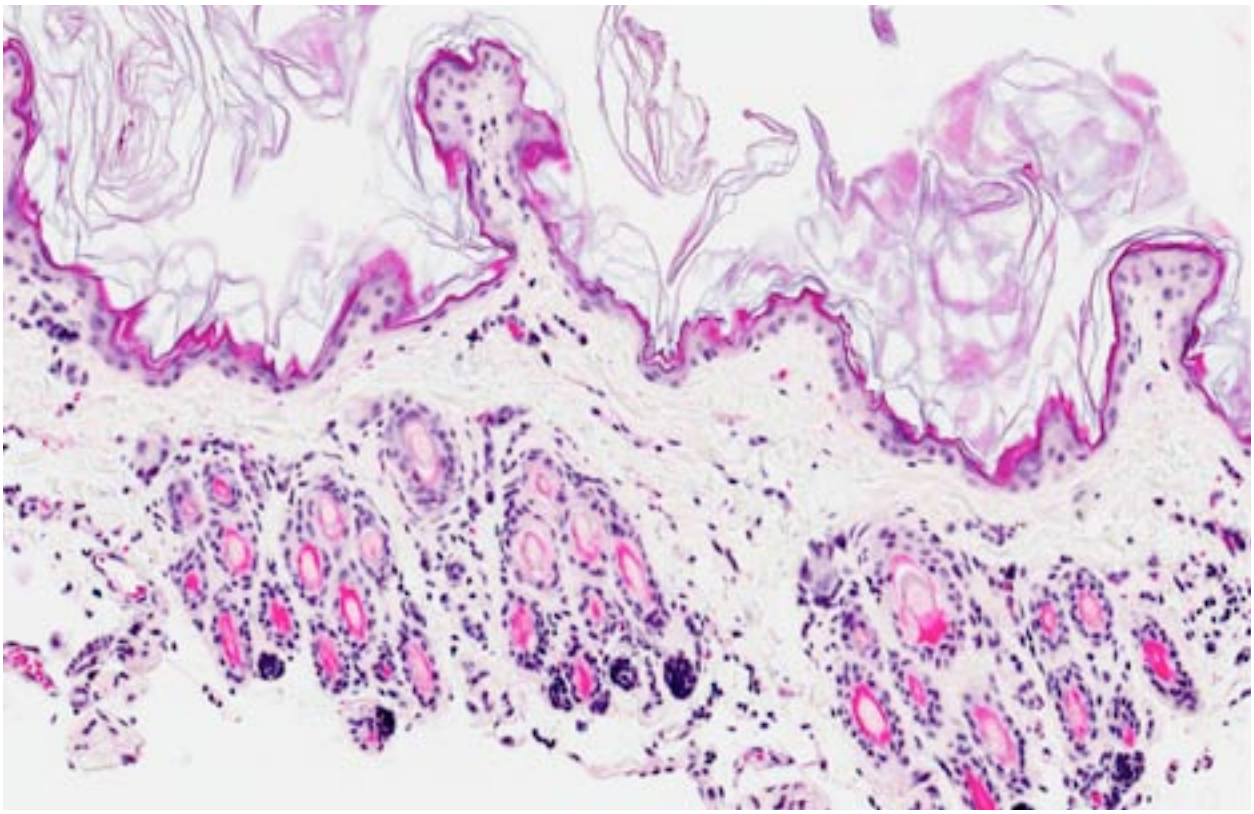

3-2. Haired skin, cat. The epithelium is atrophied at 1-2 layers thick, and dermal collagen is markedly diminished. Hair follicles, although diffusely telogenic, and within normal limits. (HE 200X)

sinusoids. Moderate numbers of hepatocytes, often within the periacinar region have intracytoplasmic green-brown pigment (hemosiderin).

Contributor's Morphologic Diagnosis: 1. Dermal atrophy, diffuse, chronic, severe.
2. Hepatic lipidosis, diffuse chronic, moderate to severe.

Contributor's Comment: Acquired skin fragility syndrome has long been recognized in the cat.[2] The gross and histologic lesions are consistent with the condition feline skin fragility syndrome (FSFS). The pathogenesis of the syndrome is unknown; however, it is typically associated with a hyperglucocorticoidism, diabetes mellitus, or excessive use of progestational compounds.[4] It has been seen in conjunction with severe liver disease, including hepatic lipidosis.[4,8] This cat did have hepatic lipidosis. However, it is unknown whether this was a primary condition or secondary to some other systemic illness that resulted in anorexia as has been reported previously.[8]

Ehlers-Danlos syndrome was considered to be one of the differential diagnoses by the submitting veterinarian. Ehlers-Danlos syndrome was ruled out due to the severe dermal atrophy, being more consistent with acquired skin fragility syndrome. Dermis is of normal thickness and lacks attenuation of dermal collagen seen in Ehlers-Danlos syndrome.[2,5] Another case of dermal atrophy in a cat reports the occurrence after treatment of the cat with phenytoin, but no mechanism was established.[1] It is important to note, phenytoin is metabolized in the liver. Not all cases of FSFS are related to endocrine or hepatic disease. There is a report of fragile skin due to cutaneous histoplasmosis.[7] In that case, the epidermis was attenuated and there was dermal edema. Fibrinoid necrosis of blood vessels in the subcutis with granulomatous inflammation was reported.

Skin fragility cases have been reported associated with a variety of concurrent diseases. However, the mechanism for this syndrome has yet to be determined. Clinical cases of FSFS should be an indication of concurrent disease and further evaluation of cases should be performed.

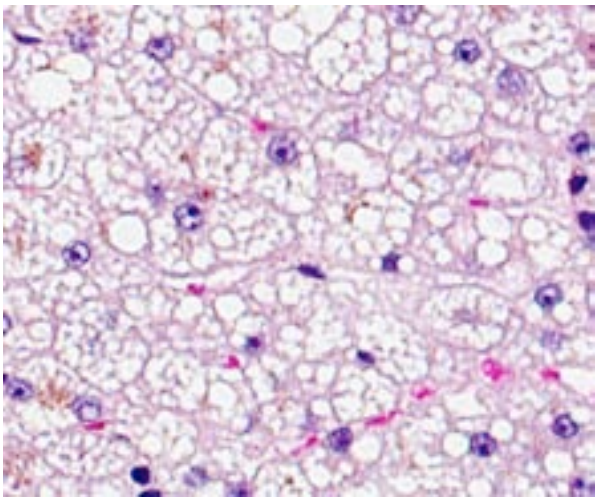

3-3. Liver: Diffusely, hepatocytes are expanded by numerous lipid droplets, consistent with hepatic lipidosis. (HE 400X).

JPC Diagnosis: 1. Haired skin: Epidermal, dermal, and follicular atrophy, diffuse, severe.
2. Liver, hepatocytes: Lipidosis, diffuse, severe.

Conference Comment: As there was some difficulty in distinguishing glycogen from lipid type hepatocellular vacuolar change, initial conference discussion focused on the histological differences between these two processes. In general, lipid-type vacuolar degeneration produces hepatocytes with discrete globules which may coalesce into a single large vacuole that peripheralizes the nucleus, while glycogen-type vacuolar degeneration causes significant cell swelling with indistinct vacuolar boundaries and fine, feathery cytoplasm (see WSC 2013-2014 conference 13, case 1 for a more detailed summary as well as an example of glycogen-type change). Unlike dogs, steroid hepatopathy is uncommon in cats, even those with hyperadrenocorticism. Additionally, cats suffering from hepatic lipidosis typically exhibit micro- or macrovesicular hepatocellular vacuolation, rather than a single large vacuole that peripheralizes the nucleus.[6] Thus in this case, hepatic lipidosis is a more likely diagnosis than glycogen-type hepatocellular degeneration. There was also some debate regarding the origin of the golden-brown granular material noted multifocally within Kupffer cells. Initially, some participants speculated that this was bile pigment, lipofuscin or ceroid, but histochemical staining for iron identifies the material as hemosiderin. The significance of the iron is not evident in this case.

Conference participants went on to discuss the differential diagnosis for the histological skin lesions. Ehlers-Danlos syndrome is reported (albeit rarely) in cats, and results in hyperextensible skin; however, severe, diffuse attenuation of dermal collagen is not a characteristic feature. Additionally, acquired feline skin fragility syndrome (FSFS) typically presents in middle aged to older cats, while Ehlers-Danlos occurs in young animals.[4] Electron microscopy (not performed in this case) is also a useful tool in diagnosis of Ehlers-Danlos syndrome, which classically demonstrates enlarged, fragmented collagen fibrils.[3] Similarly, ultrastructural studies in cats with FSFS reveal disorganized, tangled, variably sized collagen fibrils, although fibrils are not generally fractured.[4] Paraneoplastic alopecia secondary to pancreatic/biliary carcinoma was also suggested as a possible rule-out. While this condition is associated with follicular atrophy, the dermis is unaffected and epidermal hyperplasia, rather than atrophy, is the most frequent microscopic characteristic; furthermore, the footpads are often involved and skin fragility is not reported, which aids in differentiating this condition from FSFS.[9]

Contributing Institution: Veterinary Diagnostic Center
University of Nebraska-Lincoln
Lincoln, NE
nvdls.unl.edu

References:

1. Barthold SW, Kaplan BJ, Schwartz A. Reversible dermal atrophy in a cat treated with phenytoin. *Vet Pathol.* 1980;17:469-476.
2. Butler WF. Fragility of skin in a cat. *Rsch Vet Sci*. 1975;19:213-216.
3. Cheville NF. Ultrastructural Pathology: The Comparative Cellular Basis of Disease. 2nd ed. Ames, IA: Wiley-Blackwell; 2009;300.
4. Gross TL, Ihrke PJ, Walder EJ, Affolter VK. *Skin Diseases of the Dog and Cat: Clinical and Histopathologic Diagnosis*. 2nd ed. Blackwell Science Ltd, Oxford, UK, 2005:389-391.
5. Patterson DF, Minor RR. Hereditary fragility and hyperextensibility of the skin of cats. A defect in collagen fibrillogenesis. *Lab Invest*. 1977;37:170-179.
6. Stalker MJ, Hayes MA. Liver and biliary system. In: Maxie MG, ed. *Jubb, Kennedy, and Palmer's Pathology of Domestic Animals*. Vol 2.

5th ed. Philadelphia, PA: Elsevier Limited; 2007:310-315.
7. Tamulevicus AM, Harkin K, Janardhan K, Debey BM. Disseminated histoplasmosis accompanied by cutaneous fragility in a cat. *J Am Anim Hosp Assoc*. 2011;47:e36-41.
8. Trotman TK, Mauldin E, Hoffmann V, Del Piero F, Hess RS. Skin fragility syndrome in a cat with feline infectious peritonitis and hepatic lipidosis. *Vet Dermatol*. 2007;18:365-369.
9. Turek MM. Cutaneous paraneoplastic syndromes n dogs and cats: a review of the literature. *Vet Dermatol.* 2003;14:279-296.

CASE IV: 2011905671 (JPC 4018075).

Signalment: Age unknown castrated male mongrel dog, (*Canis familiaris*).

History: A solitary subcutaneous mass was surgically excised from the perianal region.

Gross Pathology: The mass was approximately 6 mm in diameter with a red surface. The cut surface (after fixation) was smooth, firm and white.

Histopathologic Description: The well-circumscribed dermal/subcutaneous mass is adjacent to several islands of normal perianal glands. The mass is composed of round cells arranged in cords, nests and sheets on a fibrous stroma. Neoplastic cells often separate and surround pre-existing perianal glands. Neoplastic cells are round, with a centrally placed round to oval nucleus, indistinct nucleoli, and a small amount of eosinophilic to clear cytoplasm. Histochemical staining with periodic acid-Schiff (PAS) and silver impregnation stain demonstrates that neoplastic cells are often surrounded by a prominent basement membrane that resembles "chicken-wire."

Immunohistochemically, neoplastic cells are diffusely, strongly positive for vimentin, multifocally, weakly positive for desmin, and negative for alpha-smooth muscle actin, calponin, cytokeratins (AE1/AE3, 7, 14, CAM5.2 and CK-MNF), chromogranin A, synaptophysin, PGP9.5, NSE, CD31, Factor VIII, melan-A, PNL2, S-100, MHC Class II, Iba-1and CD18. The cytoplasmic border of each neoplastic cell is strongly positive for type IV collagen.

Contributor's Morphologic Diagnosis: Perianal region; glomus tumor.

Contributor's Comment: Glomus tumors are rare, benign neoplasms in humans and animals, which originate from the glomus cells that compose the glomus body, an arterioveneous anastomosis. Glomus tumors typically occur in areas that reflect the normal anatomic location of the glomus body; most tumors occur in the subungual region of the fingers.[10] In humans, these tumors are occasionally reported in various other locations, including the precoccygeal area, head, neck, bone, nerve, stomach, colon, nasal cavity and trachea.[1,3,5,10] Human glomus tumors are classified, based on the proportion of glomus cells, vascular structures and smooth-muscle components, into three subtypes: the classical glomus tumor (solid type), glomangioma (angiomatous type), and glomangiomyoma (myxoid type).[5,10] The classical (solid) is type most common and accounts for approximately 75 percent human glomus tumors.[10]

Glomus tumors are rare in animals, though there are a few case reports in dogs and cats.[2,3,8,9] Similarly to humans, most tumors in dogs and cats arise on the lower extremities and the digit.[2,3,8,9]

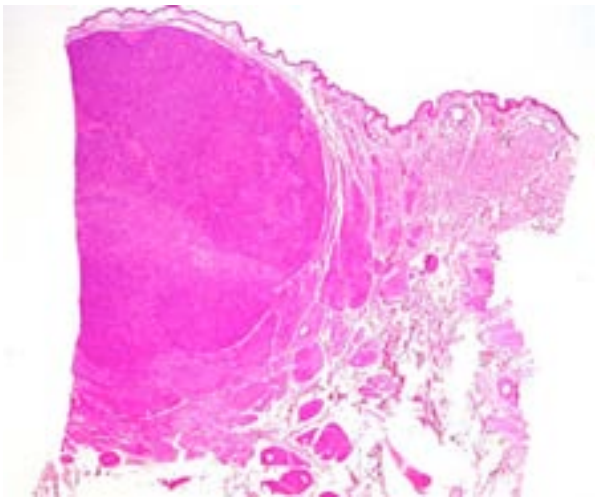

4-1. There is a nodular neoplasm within the dermis which infiltrates and replaces perianal glands. (Photo courtesy of: Department of Pathology, Faculty of Pharmaceutical Science, Setsunan University,45-1 Nagaotohge-cho, Hirakata, Osaka 573-0101, JAPAN)

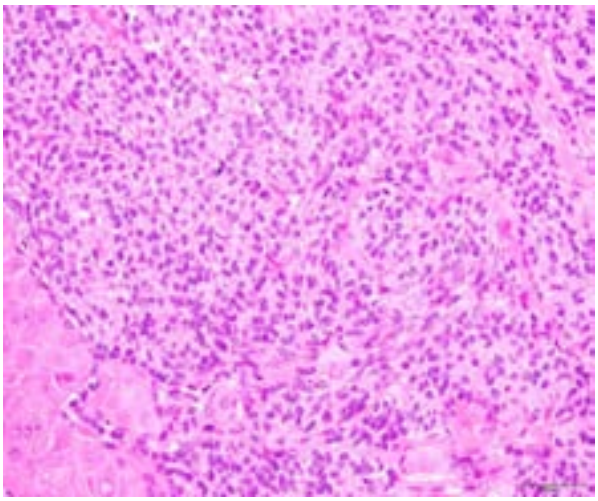

4-2. Neoplastic cells are arranged in nest and packets and have numerous discrete cytoplasmic vacuoles. (HE 400X) (Photo courtesy of: Department of Pathology, Faculty of Pharmaceutical Science, Setsunan University,45-1 Nagaotohge-cho, Hirakata, Osaka 573-0101, JAPAN)

Although glomangioma has been reported n a cow and a dog,[4,7] most glomus tumors in animals are most consistent with the classical glomus tumor (solid type) in humans.[2,3,8,9] Histopathologically, glomus tumors are composed of small round cells with round nucleus and eosinophilic cytoplasm, arranged in sheets, nests, cords, ribbons or duct like structures.[2,3,8-10] Nests and individual tumor cells are surrounded by a basement membrane.[1,9,10] Variably sized vascular structures are present within the neoplasm, and tumor cells often palisade along vessel walls.[1-3,6-8,10] Immunohistochemically, nearly all glomus tumors express vimentin and alpha-smooth muscle actin. Desmin is variably expressed.[1-3,8-10] The basement membrances surrounding neoplastic cells typically express type IV collagen and laminin.[1,10]

All glomus tumors reported in dogs and cats demonstrate palisading of tumor cells along vessel walls, as well as positive immunoreactivity for vimentin and alpha-smooth muscle actin.[2,3,8,9] Although the present case does not display all of these features, the morphological and immunohistochemical characteristics are most consistent with a glomus tumor. In particular, the basement membrane around each tumor cell is strongly suggestive of a glomus tumor. Glomus tumors in humans and animals must be distinguished from epithelial tumors (such as trichoblastoma), canine hemangiopericytoma, synovial sarcoma and epithelial leiomyoma.[2,3,8-10] In this case, all of these tumors were ruled out based on the histopathological and immunohistochemical features of the neoplastic cells.

JPC Diagnosis: Haired skin, perianal region: Glomus tumor.

Conference Comment: The glomus is a convoluted segment of arteriovenous shunt, composed of an afferent arteriole and an efferent venule with multiple communications, enveloped by collagenous tissue. Blood flow in these shunts is controlled by the glomus body, which (in humans) is typically found in the dermis of the fingertips and is involved in regulating body temperature.[7,11] Glomus tumors arise from modified smooth muscle cells of the glomus body.[1] In veterinary medicine, glomus tumors are most frequently described in dogs, but have also been reported in cats, horses, non-human primates and a cow.[1,6,7] This tumor typically arises on the distal extremities; however three of the four reported equine glomus tumors occurred on the head or neck. Nevertheless, more cases must be examined in order to determine whether there is a true predilection for this site in horses.[1] Interestingly, the single bovine case report describes multiple glomus tumors of the urinary bladder, associated with bovine papillomavirus type 2 (BPV-2) infection.[7] Malignant glomus tumors in humans are defined by being larger than 2 cm with a deep location (below the muscular fascia), having marked nuclear atypia, having more than five mitoses per 50 high-power fields, or having atypical mitotic figures.[1] Due to the small number of identified cases in animals, there are no firmly established criteria of malignancy, although there are rare reports of aggressive, biological behavior.

This case is challenging, in that it demonstrates some, but not all of the classic histomorphologic and immunohistochemical features of a glomus tumor. After extensive debate within conference and consultation with pathologists from the Join Pathology Center soft tissue subspecialty, we are unable to definitively diagnose a glomus tumor; however we concur with the contributor's conclusion that the microscopic and staining characteristics are most consistent with this entity.

Contributing Institution: Department of Pathology
Faculty of Pharmaceutical Science
Setsunan University
45-1 Nagaotohge-cho, Hirakata
Osaka 573-0101, JAPAN
ozaki@pharm.setsunan.ac.jp

References:

1. Burns RE, Pesavento PA, McElliott VR, Ortega J, Affolter VK. Glomus tumours in the skin and subcutis of three horses. *Vet Dermatol*. 2011;22:225-231.
2. Dagli ML, Oloris SC, Xavier JG, dos Santos CF, Faustino M, Oliveira CM, Sinhorini IL, Guerra JL. Glomus tumour in the digit of a dog. *J Comp Pathol*. 2003;128:199-202.
3. Furuya Y, Uchida K, Tateyama S. A case of glomus tumor in a dog. *J Vet Med Sci*. 2006;68:1339-1341.
4. Galofaro V, Rapisarda G, Ferrara G, Iannelli N. Glomangioma in the prepuce of a dog. *Reprod Domest Anim*. 2006;41:568-570.

5. Rosai J. *Rosai and Ackerman's Surgical Pathology*. Vol. 2. 9th ed. St Louis MO: Mosby; 2004:2288-2290.
6. Park CH, Kozima D, Tsuzuki N, Ishi Y, Oyamada T. Malignant glomus tumour in a German shepherd dog. *Vet Dermatol*. 2009;20:127-130.
7. Roperto S, Borzacchiello G, Brun R, Perillo A, Russo V, Urraro C, et al. Multiple glomus tumors of the urinary bladder in a cow associated with bovine papillomavirus type 2 (BPV-2) infection. *Vet Pathol.* 2008;45:39-42.
8. Shinya K, Uchida K, Nomura K, Ozaki K, Narama I, Umemura T. Glomus tumor in a dog. *J Vet Med Sci.* 1997;59:949-950.
9. Uchida K, Yamaguchi R, Tateyama S. Glomus tumor in the digit of a cat. *Vet Pathol*. 2002;39:590-592.
10. Weiss SW, Goldblum JR. *Enzinger and Weiss's Soft Tissue Tumors*. 5th ed. St. Louis, MO: Mosby; 2008:751-754.
11. Young B, Lowe JS, Stevens A, Heath JW, eds. *Wheater's Functional Histology: A Text and Colour Atlas*. 5th ed. Philadelphia, PA: Elsevier Limite; 2006:183.

Joint Pathology Center
Veterinary Pathology Services

WEDNESDAY SLIDE CONFERENCE 2013-2014

Conference 16

19 February 2014

CASE I: 11-V62 (JPC 4001100).

Signalment: 1.5-year-old genetically-modified mouse (*Mus musculus*). Strain is mdx -/- on C57Bl6/J background.

History: Animal was reported for hind limb paralysis/paresis, with slow to absent withdrawal reflexes. The left side was more severely affected than the right side. The animal had also been on oral sildenafil (Viagra; dose and duration not given) and had been anesthetized for an echocardiogram the week before coming to necropsy. The mouse was submitted for necropsy and though the investigative group collected most tissues, the carcass with a peritoneal mass was submitted to the Veterinary Diagnostic Lab for histology.

1-1. Vertebral column, epaxial musculature, and overlying haired skin, mouse: The epaxial musculature is effaced by a mesenchymal neoplasm which infiltrates the spinal canal and elevates the overlying haired skin. (HE 0.63X)

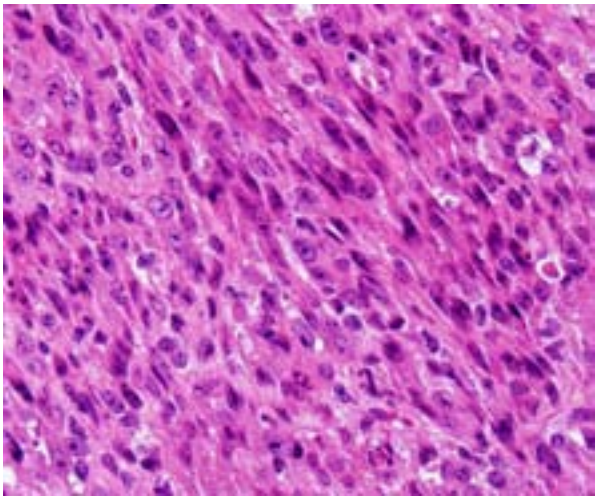

1-2. Vertebral column, epaxial musculature, and overlying haired skin, mouse: Neoplastic cells are arranged in broad streams and spindle shaped with large nuclei. Mitotic figures are common. (HE 320X)

Gross Pathology: The gross necropsy was not performed by the Veterinary Diagnostic Lab. Veterinary Services reported that an older adult mouse, well-groomed and in good body condition (adequate fat stores), was euthanized by the investigative group with an overdose of isoflurane. In the abdominal cavity, a pale tan soft tissue mass was found adhered bilaterally in the region of the lumbosacral spine, appearing to fuse with the spine.

Peritoneal cavity: Lumbosacral soft tissue mass.

Histopathologic Description: Lumbosacral spine mass: In a section of body wall with overlying haired skin, lumbar muscle and spinal cord, is a very large (~1 cm diameter at widest point), densely cellular, unencapsulated tumor. It is invasive, infiltrating through lumbar musculature, lymph node, and into the spinal canal. The tumor cells vary in shape, ranging from small round cells with scant cytoplasm to spindle-shaped cells. Occasional mitotic figures are seen. The cells form densely packed bundles and streams, arranged in medium-sized alveolar-type structures. Cell borders are indistinct and there is marked anisocytosis and anisokaryosis. "Strap" cells appear as a single elongated nucleus or series of nuclei lined up across a band of elongated cytoplasm. "Paddle" cells are hypereosinophilic cells that appear to sit on a stalk and occupy a cleared space and are particularly evident where the tumor borders and infiltrates skeletal muscle. The tumor effaces one side of the spinal canal, displacing the cord laterally and causing compression of the spinal nerve, which shows some axon loss, vacuolization, and smaller caliber fibers compared to the contralateral nerve. The spinal cord neuropil shows some mild gliosis and neuronal cell death on the affected side.

Contributor's Morphologic Diagnosis: Lumbar musculature: Rhabdomyosarcoma with invasion into the spinal canal and spinal cord compression.

Spinal cord: Compressive unilateral leukomalacic myelitis, white matter degeneration and regeneration, and spinal ganglia neuritis, chronic-active.

Contributor's Comment: Duchenne's muscular dystrophy (DMD) in humans is due to defective or absent dystrophin, a protein integral to structural stability of myofibers. Dystrophin is a large protein (427 kDa) on the inner face of the sarcolemma that binds with cytoskeletal f-actin and the transmembrane protein beta-dystroglycan as part of a complex, multimolecular unit that mediates signaling between the intracellular cytoskeleton and the extracellular matrix. Duchenne's muscular dystrophy is the most common lethal inherited disorder of children (1/3500 newborn males).[11] The disease shows X-linked recessive inheritance. There are no signs at birth. As affected children age, they develop weakness, hyperlordosis with wide-based gait, and hypertrophy of weak muscles. The disease follows a progressive course, with eventual reduced muscle contractility, bladder/bowel dysfunction, and death due to respiratory failure. Two cases of rhabdomyosarcoma in DMD patients has been reported, one alveolar and one embryonal,[1] though the incidence does not appear to exceed that of the general population.[3] There are no therapies currently available, though stem cells and viral gene therapy show some promise.[10]

The most effective model for characterizing the structure and function of dystrophin and possible therapeutic interventions for DMD is the *mdx* mouse.[1] The official nomenclature of *mdx* mice is C57BL/10Scsn-*Dmd*^{mdx}/J. A point mutation in exon 23 of the x-linked dystrophin gene (dmd) creates a nonsense mutation that converts cytosine to thymine. This substitution replaces a glutamine codon with a termination codon, causing abnormal production, and/or reduced stability of truncated gene products. In *mdx* mice, skeletal muscle has normal histologic features until about 3 weeks of age.[4] It then undergoes progressive degeneration and necrosis; small caliber fibers with central nuclei can be observed as part of the regenerative response.[4] In mice, the mutated dystrophin gene does not manifest with severe muscular dystrophy, as it does in humans, due to compensatory responses by utrophin. It does however have a somewhat shortened lifespan,[1] though not as dramatic as in humans. In mice with both utrophin and dystrophin knocked out, there is more severe disease and premature death.

In our facility and others,[1] *mdx* mice show a tendency toward developing spontaneous rhabodmyosarcomas. They can occur on the distal limb or the trunk, as in this case. There is no limb predilection.[1] Rhabdomyosarcoma is a

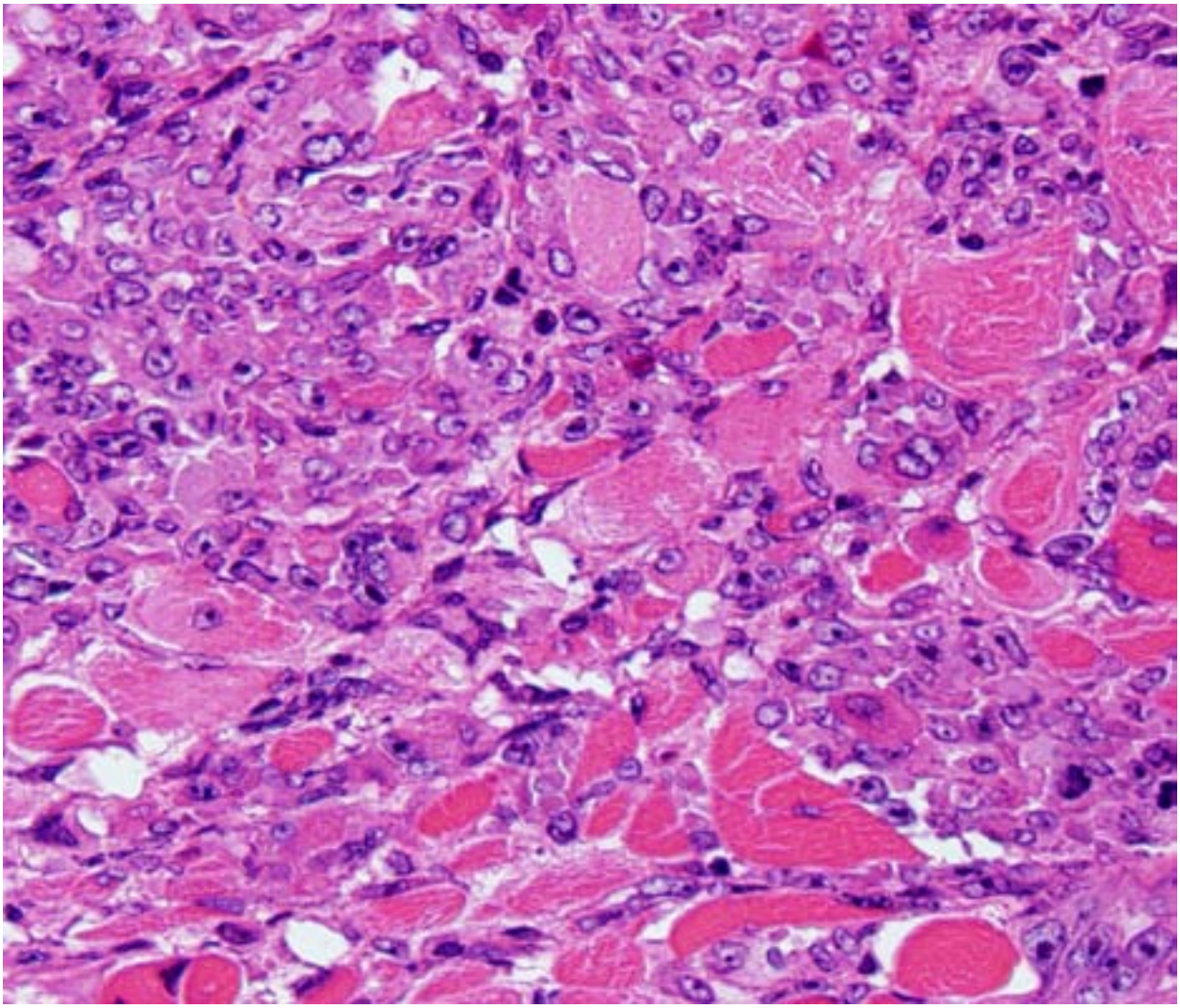

1-3. Vertebral column, epaxial musculature, and overlying haired skin, mouse: At the edge of the neoplasm, neoplastic cells surround, separate, and replace remaining skeletal muscle. (HE 320X)

malignant tumor of striated muscle that is, in veterinary medicine, divided into four major histologic categories: embryonal, botryoid, alveolar, and pleiomorphic {Mueuten, 2002 #129}. Diagnostic features of rhabdomyosarcoma include elongate "strap" cells, "racket" cells, as well as cross striations which can be highlighted with phosphotungstic acid-hematoxylin stain (PTAH).[5] These tumors can also be labeled with myosin, actin, desmin, vimentin, BB creatine kinase, NCAM, IFG-II and TGF-Beta.[5] Rhabdomyosarcoma in mice has been shown to express the myogenic differentiation factors myogenin, MyoD, and the muscle intermediate filament protein desmin.[3] It is speculated that *mdx* mice are predisposed because of the lifelong continuous myofiber degeneration and regeneration, which is associated with continuous and massive activation and proliferation of satellite cells (muscle progenitor cells), increasing the chance of developing random and spontaneous mutations.[2] Inactivation of p53 is a primary event in *mdx* rhabodmyosarcoma.[3]

Other animal models of DMD include dogs, cats, zebrafish, and *C. elegans*.[2] In dogs, there is an X-linked muscular dystrophy in several breeds, including golden retrievers, Rottweilers, German short-haired pointers, and beagles. The manifestation in golden retriever is most closely homologous model of DMD. In this breed, the disease results from a single base pair change in the 3' consensus splice site of intron 6, which leads to skipping of exon 7 and a misaligned reading frame in exon 8 that causes a premature stop codon.[11] The myocardium is more severely

affected in the golden retriever than in other animal models, though this feature of the disease course makes it much closer to the manifestation in humans.[11] Cats have a hypertrophic feline muscular dystrophy that has limited similarity to DMD. In cats, the disease is due to a 200 kb deletion of the dystrophin gene, which causes a hypertrophic muscular dystrophy.[11] Affected cats typically have elevated creatine kinase in the blood by 4-5 weeks of age, before apparent muscle involvement, which can be seen at 10-14 weeks.[11] Affected cats die of esophageal compression by a hypertrophic diaphragm, or of the inability to drink due to glossal hypertrophy.[11] Zebrafish and *C. elegans* express a dystrophin homologue that is used for gene analysis and drug discovery. There are no primate models of DMD.[11]

JPC Diagnosis: 1. Vertebral body and epaxial musculature: Rhabdomyosarcoma.
2. Spinal cord: Leukomalacia, focally extensive, moderate.

Conference Comment: The contributor provides a thorough overview of rhabdomyosarcoma in this transgenic mouse model, as well as summarizing various animal models of DMD (see table 1). Readers may also wish to review the conference proceedings for WSC 2012-2013, conference 16, case 3 for a general discussion of rhabdomyosarcoma. As expected, neoplastic cells in this case expressed strong, multifocal positive cytoplasmic immunoreactivity for desmin, while histochemical staining with PTAH demonstrated rare islands of neoplastic cells with cross striations.

Table 1: Animal models of muscular dystrophy.[2,6,7-9,11]

Model	Species	Defect	Other
X-linked muscular dystrophy (mdx; Duchenne's-like)	mdx mouse	X-linked dystrophin defect	No muscle wasting due to compensatory responses by utrophin
Human classical congenital muscular dystrophy	dy+/dy+ mouse	Autosomal recessive laminin alpha 2 (merosin) deficient	Loss of myelin in ventral nerve roots
X-linked muscular dystrophy (xmd; Duchenne's-like)	Dog	X-linked dystrophin defect	Best characterized in golden retriever; myocardium more severely affected than other muscles
Hypertrophic feline muscular dystrophy	Cat	X-linked dystrophin defect	Protruding tongue, bunny-hopping gait; malignant hyperthermia-like syndrome
Hereditary muscular dystrophy	Chicken	Autosomal dominant defect in Ubiquitin ligase gene (WWP1)	Superficial pectoralis (large breast muscle); affects type II muscle fibers
Ovine muscular dystrophy	Merino sheep	Autosomal recessive	Australia
Muscular dystrophy	Meuse-Rhine-Yssl cattle (Netherlands); rarely in Holstein-Friesians	Probably autosomal recessive	Usually affects diaphragm

Contributing Institution: University of Washington
Department of Comparative Medicine
http://depts.washington.edu/compmed/index.html

References:

1. Chamberlain JS, Metzger J, Reyes M, Townsend D, Faulkner JA. Dystrophin-deficient mdx mice display a reduced life span and are susceptible to spontaneous rhabdomyosarcoma. *FASEB J*. 2007;21:2195-2204.
2. Collins CA, Morgan JE. Duchenne's muscular dystrophy: animal models used to investigate pathogenesis and develop therapeutic strategies. *Int J Exp Pathol*. 2003;84:165-172.
3. Fernandez K, Serinagaoglu Y, Hammond S, Martin LT, Martin PT. Mice lacking dystrophin or alpha sarcoglycan spontaneously develop embryonal rhabdomyosarcoma with cancer-associated p53 mutations and alternatively spliced or mutant Mdm2 transcripts. *Am J Pathol*. 2010;176:416-434.

4. The Jackson Laboratory, JAX mice database-C57BL/10ScSn-*Dmd*^{mdx}/J. http://jaxmice.jax.org/strain/001801.html.
5. Maronpot RR. *Pathology of the Mouse: Reference and Atlas*. Vienna, IL: Cache River Press; 1999:637-642.
6. Matsumoto H, Maruse H, Inaba Y, et al. The ubiquitin ligase gene (WWP1) is responsible for the chicken muscular dystrophy. *FEBS lett*. 2008;582(15):2212-2218.
7. Nakamura N. Dystrophy of the diaphragmatic muscles in Holstein-Friesian steers. *J Vet Med Sci*. 1996;58(1):79-80.
8. van Lunteren E, Moyer M, Leahy P. Gene expression profiling of diaphragm muscle in alpha2-laminin (merosin)-deficient dy/dy dystrophic mice. *Physiol Genomics*. 2006;25(1): 85-95.
9. van Vleet JF, Valentine BA. Muscle and tendon. In: Maxie MG, ed. *Jubb, Kennedy, and Palmer's Pathology of Domestic Animals*. Vol 1. 5th ed. Philadelphia, PA: Elsevier Limited; 2007:210-216.
10. Wang Z, Chamberlain JS, Tapscott SJ, Storb R. Gene therapy in large animal models of muscular dystrophy. *ILAR J*. 2009;50:187-198.
11. Willmann R, Possekel S, Dubach-Powell J, Meier T, Ruegg MA. Mammalian animal models for Duchenne muscular dystrophy. *Neuromuscul Disord*. 2009;19: 241-249.

CASE II: 161 2A (JPC 4003041).

Signalment: Adult male crested-wood partridge, (*Rollulus rouloul*).

History: This bird was found dead on the floor of its enclosure. It had recently been the target of increased conspecific aggression.

Gross Pathology: The skull was crushed with loss of overlying skin and soft tissues. The dorsal aspects of the cerebral hemispheres and cerebellum were exposed, lacerated and hemorrhagic. Fragments of brain tissue were embedded in bone at the fracture sites.

Histopathologic Description: Lungs: Throughout the section, pulmonary arterioles are diffusely congested and filled by variably sized, fragmented sections of neuropil sparsely populated by neurons, supportive glial cells and capillaries (gray matter) while others contain sections of white matter, portions of the molecular layer and granular layer separated by large multipolar Purkinje cells (cerebellum). In some sections there is a focal aggregate of macrophages, multinucleated ciant cells and fewer lymphocytes and plasma cells that surround a central area of necrosis (granuloma). There are multifocal aggregates of macrophages that contain both fine black pigmented (carbon) and slightly larger, crystalline-like birefringent particulate debris associated with the parabronchi (anthracosis).

Contributor's Morphologic Diagnosis: Lungs:
1) Brain tissue emboli, pulmonary arterioles, multifocal, peracute, moderate to severe with arteriolar congestion.
2) Pneumonia, granulomatous, multifocal, chronic, mild (not present in all sections).
3) Anthracosis, parabronchial, chronic, multifocal, mild.

Contributor's Comment: This crested wood partridge died from severe head trauma that resulted in fracture of the skull and disruption of the dorsal venous sinus and subjacent cerebrum and cerebellum. This severe trauma resulted in embolization of fragments of brain tissue that are visible throughout the pulmonary arterioles. The small granuloma present in one of the lungs was fungal in origin. Anthracosis is an exceedingly common finding in animals that inhabit densely populated urban environments. In this case, fungal pneumonia and anthracosis were mild and incidental to the death of this bird.

Cerebral tissue pulmonary embolization (CTPE) is a possible sequel to severe penetrating or closed head trauma. CTPE is most commonly associated with high impact blunt force trauma (i.e. automobile collision) in adults and instrument-assisted delivery in neonates.[4,5] Though a rare occurrence, post-traumatic pulmonary emboli can cause significant mortality (up to 43%) in the absence of prophylactic treatment.[6] Massive CTPE is detectable at autopsy and is associated with disruption of the large dorsal cerebral venous sinus in addition to brain injury. Microscopic brain emboli, however, have been identified in

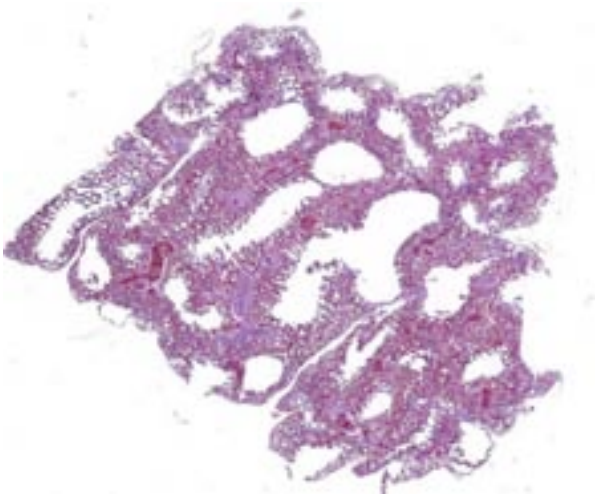

2-1. Lung, partridge: Several pulmonary arterioles contain eosinophilic material. (HE 0.63)

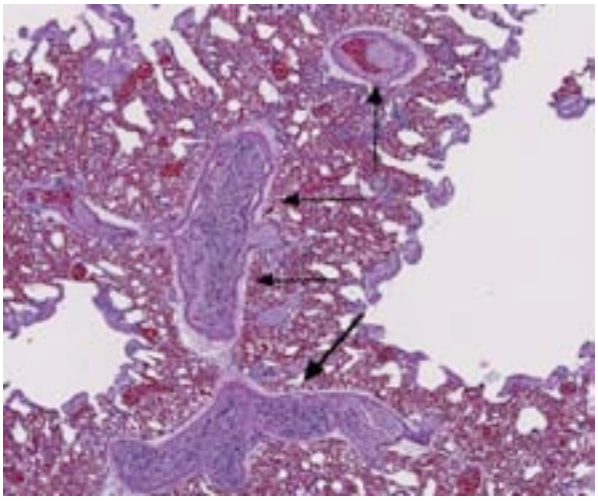

2-2. Lung, partridge: Higher magnification demonstrates neural tissue occluding several pulmonary arteries (arrows). (HE 34X)

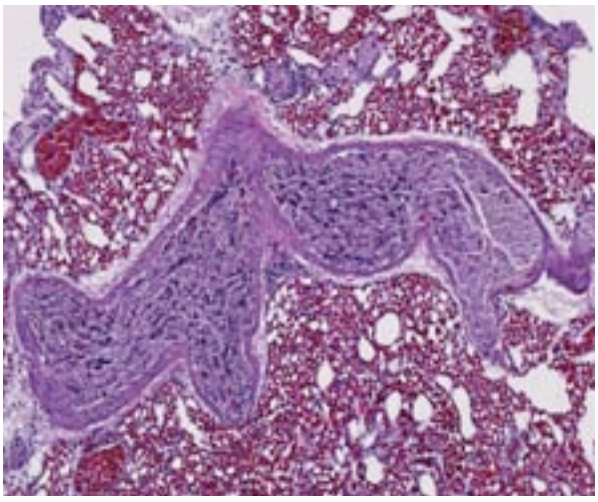

2-3. Lung, partridge: Cerebral grey matter occludes a pulmonary arteriole. (HE 116X)

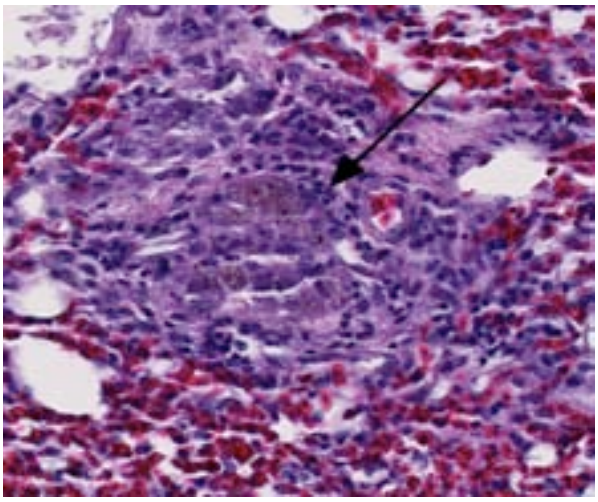

2-4. Lung, partridge: Adjacent to airways, granulomas surround black anthracotic pigment. (HE 248X)

pulmonary arterioles and systemic veins in cases with intact dura, suggesting embolic entry through smaller cerebral and meningeal veins.[8]

The behavior, physiology and anatomy of flighted birds may increase the likelihood of CTPE in avian species compared to terrestrial animals. Behaviorally, flighted birds are prone to severe brain trauma due to in-flight speed and prevalent collision injuries. Physiologically, avian veins, unlike mammalian veins, are compliance vessels, and they actively dilate during flight to increase cardiac output.[9] A larger venous diameter permits embolization of larger tissue fragments to the lungs. Anatomically, the avian brain and spinal cord are surrounded by a series of contiguous venous sinuses including the dorsal cerebral, occipital and vertebral sinuses and the ventral sinus cavernosus. These sinuses drain blood to the heart via the jugular or vertebral veins.[10] These extensive, superficial structures are prone to rupture with severe, closed or penetrating head trauma, presenting direct venous access to injured neural tissue.

This case illustrates dissemination of central nervous system (CNS) tissue to the venous system after head trauma. Consumption of meat products contaminated with CNS tissue from cattle with bovine spongiform encephalopathy is considered to be a significant route of transmission for mutant proteinase-resistant protein (PrP^{sc}), the proposed etiologic agent of variant Creutzfeldt–Jakob disease (vCJD) in humans.[2,7] Air-injection penetrating captive bolt stunning prior to terminal exsanguination has been identified as a major risk factor in CNS contamination of meat products. This method allows dislodged CNS tissue to disseminate through the bloodstream during the brief period of sustained cardiac function, followed by contamination of skeletal muscle with jugular exsanguination. For this reason, this method of cattle slaughter is currently banned in the United States and the European Union.[1]

JPC Diagnosis: 1. Lung, pulmonary arteries: Neural emboli, multiple.
2. Lung: Granulomas, parabronchiolar, multiple, with anthracosis.

Conference Comment: The contributor provides an outstanding review of cerebral tissue pulmonary embolization. Both cerebral and cerebellar tissue was identified in emboli. This particular case has significant slide variation; in several sections the neural emboli are not as striking; however, immunohistochemical staining with GFAP confirms the presence of cerebrum or cerebellum within numerous pulmonary arterioles.

Conference participants conducted an abbreviated discussion of the anatomy and physiology of the normal avian lung. The avian mesobronchus (similar to the mammalian bronchus) is an airway lined with ciliated respiratory epithelium that has hyaline cartilage and smooth muscle within its walls; it has no direct function in gas exchange. The mesobronchus gives rise to the recurrent secondary bronchi, which are analagous to

mammalian bronchioles and contain smooth muscle, but no cartilage within their walls. These further divide into tertiary bronchi (parabronchi) with walls that are "scalloped" by bay-like air vesicles, where gas exchange takes place. Air vesicles are composed of simple squamous epithelium with an underlying supporting connective tissue. Air passes through numerous air capillaries in the wall of each air vesicle; these are adjacent to the blood capillaries, an arrangement that results in the establishment of a countercurrent flow. Unlike mammalian ventilation, in which a part of the ventilator volume is "stale" air, and mammalian structure with its numerous blind alleys and abundant dead space, the avian lung is a continuous flow system. Thus, avian lungs are much more efficient than mammalian, which is not surprising, considering the high demand of flight muscles for oxygenation.[3]

Participants closed with a brief summary of other reported causes of pulmonary emboli, including trophoblastic emboli (especially in guinea pigs), fibrocartilaginous emboli, neoplastic cells (especially lymphocytes in mice with tumor lysis syndrome), bone marrow elements (subsequent to injury/fracture), and allantoic fluid (in humans).

Contributing Institution: Wildlife Conservation Society
Global Health Program - Pathology and Disease Investigation
2300 Southern Blvd
Bronx, NY 10460
www.wcs.org

References:

1. Bowling MB, Belk KE, Nightingale KK, Goodridge LD, Scanga JA, Sofos JN, et al. Central nervous system tissue in meat products: an evaluation of risk, prevention strategies, and testing procedures. *Adv Food Nutr Res*. 2007;53:39-64.
2. Brown P, Will RG, Bradley R, Asher DM, Detwiler L. Bovine spongiform encephalopathy and variant Cruetzfeldt-Jakob disease: background, evolution and current concerns. *Emerg Infect Dis*. 2001;7:6-16.
3. Caceci T. Virginia-Maryland Regional College of Veterinary Medicine, Blacksburg, VA. VM8054 Veterinary Histology website. Respiratory System II: Avians. http://www.vetmed.vt.edu/education/Curriculum/VM8054/Labs/Lab26/lab26.htm. Accessed February 22, 2014.
4. Cox P, Silvestri E, Lazda E, Nash R, Jeffrey I, Ostojic N et al. Embolism of brain tissue in intrapartum and early neonatal deaths: report of 9 cases. *Pediatr Dev Pathol*. 2009;12:464-468.
5. Echeverria RF, Baitello AL, Pereira de Godoy JM, Espada PC, Morioka RY. Prevalence of death due to pulmonary embolism after trauma. *Lung Indi*a. 2010;27:72-74.
6. Geerts WH, Code KI, Jay RM, Chen E, Szalai JP. A prospective study of venous thromboembolism after major trauma. *N Engl J Med*. 1994;331:1601–1606.
7. Jones M, Peden AH, Prowse CV, Gröner A, Manson JC, Turner ML, et al. In vitro amplification and detection of variant Creutzfeldt–Jakob disease PrPSc. *J Pathol*. 2007;213:21-26.
8. Morentin B, Biritxinaga B. Massive pulmonary embolization by cerebral tissue after head trauma in an adult male. *Am J Forensic Med Pathol*. 2006;27:268-270.
9. Smith FM, West NH, Jones DR. The Cardiovascular system. In: Whittow GC, ed. *Sturkie's Avian Physiology*. 5th ed. San Diego, CA: Academic Press; 2000:174.
10. West NH, Langille BL, Jones DR. Cardiovascular system. In: King AS, McLelland J, eds. *Form and Function in Birds*. Vol. 2. San Francisco, CA: Academic Press; 1981:278-283.

CASE III: JPC WSC #2 (JPC 4025665).

Signalment: 13-week-old male Sprague-Dawley CD/IGS rat, (*Rattus norvegicus*).

History: Rats were necropsied 24 hours following two daily oral gavage doses of a test article.

Gross Pathology: There were no notable gross observations.

Histopathologic Description: Many seminiferous tubule profiles, both early-stage and late-stage, have abnormal features including Sertoli cell vacuolation and germ cell degeneration, disorganization and depletion. Features of germ cell degeneration/necrosis include individual necrotic/apoptotic cells (especially spermatocytes); round spermatids with condensed and marginated nuclear chromatin and sometimes with excessive lightly basophilic granular cytoplasm or forming multinucleated giant cell syncytia. Some late-stage tubules have elongated spermatids with wavy, bent, or folded heads.

Contributor's Morphologic Diagnosis: Testis, seminiferous tubule: Germ cell degeneration/ necrosis and Sertoli cell vacuolation, acute, diffuse, marked.

Contributor's Comment: The case provides an example of testicular injury 48 hours following treatment with 1,3-dinitrobenzene (1,3-DNB), a chemical intermediate formed during manufacture of many chemical compounds and a robust testicular toxicant in rodents.[3] Testicular toxicity is thought to be mediated by a reactive intermediate, 3-Nitrosonitrobenzene, formed during the reduction of 1,3-DNB to nitroaniline.[1,3] The Sertoli cell is thought to be the primary target cell of toxicity since ultrastructural changes in Sertoli cells have been shown to precede germ cell changes.[3] Sertoli cell vacuolation followed by degeneration of pachytene spermatocytes occur within the first 12 to 24 hours after administration of toxic doses and are reported to initially affect selected late stage tubules preferentially.[3,4] In the submitted case, 48 hours following exposure to the toxin, damage is more widespread across stages of the spermatogenic cycle and includes changes to early-stage as well as late-stage tubules. Tubular atrophy is a common sequel to the acute degenerative changes resulting from a single oral toxic dose of 1,3-DNB and may become apparent within about three weeks, though tubular regeneration and recovery may occur.[4]

The severity of testicular damage induced by 1,3-DNB increases with age in rodents, and the proportion of early-stage tubules exhibiting

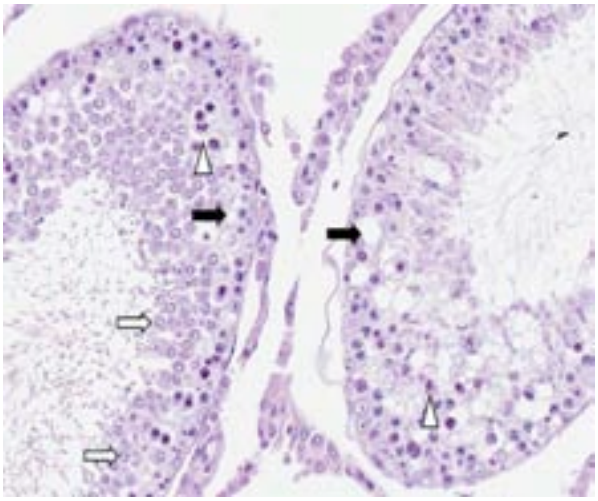

3-1. Testis, rat: Early (left) and late (right) stage tubule exhibiting Sertoli cell vacuolation (black arrow), spermatocyte necrosis (white arrowhead), and round spermatid marginated chromatin (white arrow). Disorganization and loss of germ cells is evident in both tubules but particularly in the late-stage tubule. (Photo courtesy of: Eli Lilly and Company, Department of Pathology and Toxicology, Indianapolis, IN 46285 www.lilly.com)

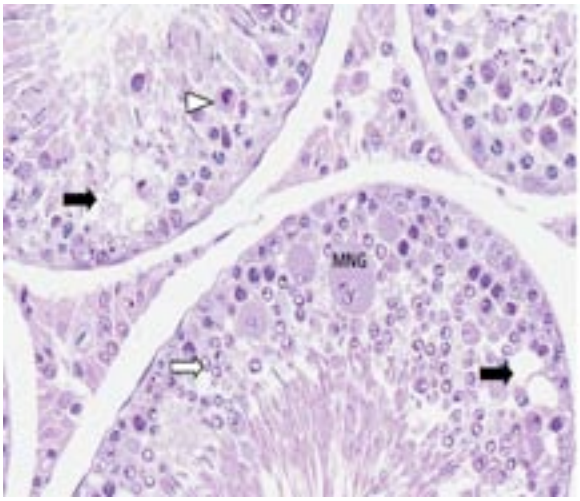

3-2. Testis, rat: Early stage tubule (bottom) and late-stage tubule (upper left). Multinucleated giant cell round spermatids (MNG), Sertoli cell vacuolation (black arrow), spermatocyte necrosis (white arrowhead), and round spermatid marginated chromatin (white arrow). Disorganization and loss of germ cells is evident in both tubules but particularly in the late-stage tubule. (Photo courtesy of: Eli Lilly and Company, Department of Pathology and Toxicology, Indianapolis, IN 46285 www.lilly.com)

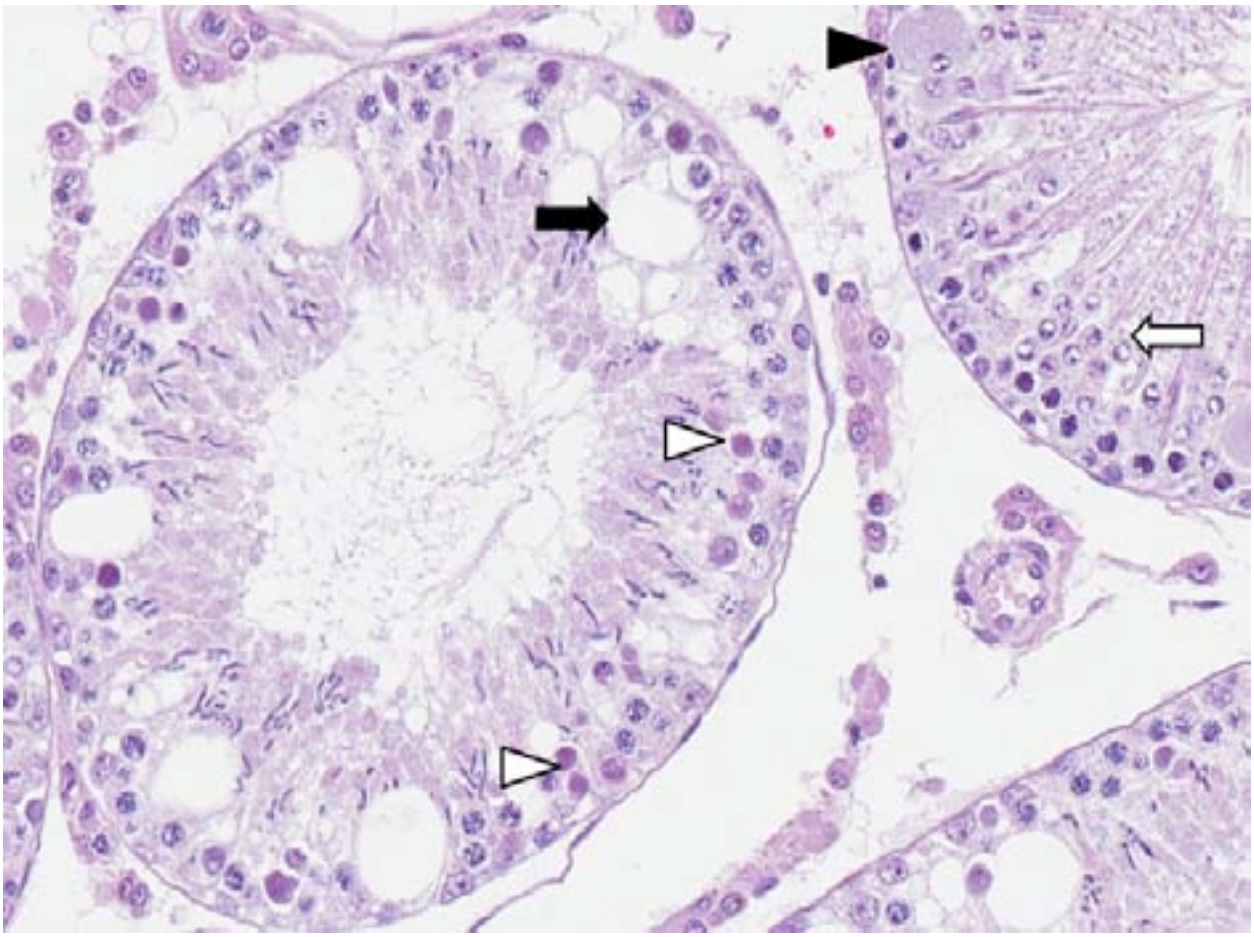

3-3. Testis, rat: Late (left) and early (right) stage tubules. Sertoli cell vacuolation (black arrow), necrotic spermatocytes (white arrowhead), giant cell round spermatid (black arrowhead), round spermatid marginated chromatin (white arrow). Many elongated spermatids in the late-stage tubule have misshapen (wavy or bent) heads. (Photo courtesy of: Eli Lilly and Company, Department of Pathology and Toxicology, Indianapolis, IN 46285 www.lilly.com)

significant injury was shown to be notably higher in 120 day-old compared to 75 day-old rats.[1] Differences in susceptibility to testicular toxicity are thought to be related to differences in rates of hepatic clearance and intratesticular metabolism.[1] Methemoglobinemia, anemia, and liver injury are features of 1,3-DNB toxicity in humans; a literature search did not identify citations confirming that testicular injury is recognized in humans.

JPC Diagnosis: Testicle, seminiferous tubules: Degeneration, multifocal, moderate, with Sertoli cell vacuolation, spermatocyte degeneration and necrosis and multinucleate spermatid formation.

Conference Comment: Spermatogenesis results from a complex interaction between various hormones, germ cells, Sertoli cells and interstitial (Leydig) cells. Luteinizing hormone (LH) released from the pituitary gland binds LH receptors on Leydig cells, inducing the production of testosterone, which binds to receptors on Sertoli cells (and possibly germ cells). Testosterone has also been shown to inhibit germ cell apoptosis, a normal method of regulating the cell population. Follicle-stimulating hormone (FSH) from the pituitary gland directly stimulates Sertoli cells (and possibly germ cells), while inhibin, produced by Sertoli cells, is a negative feedback mechanism that inhibits FSH production. During spermatogenesis, germ cells pass through spermatogonia, spermatocyte and spermatid stages.[2] In the rat, spermatogenesis is divided into 19 stages.[5] Spermiation is the active release of spermatozoa by Sertoli cells into the lumen. Sertoli cells, the support cells of the seminiferous tubule, maintain tubular epithelial integrity, phagocytose apoptotic germ cells, secrete fluid and proteins, regulate

spermatogenesis, metabolize steroids, provide nutrients to germ cells, and mediate hormonal effects on the germ cells. Furthermore, occluding junctions of Sertoli cells form an important part of the blood-testis barrier.[2] Thus, damage to Sertoli cells can also result in degenerative changes in the germ cell line, as demonstrated in this case.

The moderator additionally offered several recommendations for performing testicular and epididymal evaluation in the rat, including: a) using Bouin's or Modified Davidson's solution for fixation; histochemical staining with PAS-Hematoxylin to highlight the acrosome (this does not work in dogs); and performing a "stage-aware" assessment of seminiferous tubules using species-specific spermatogenesis chart.

Contributing Institution: Eli Lilly and Company
Department of Pathology and Toxicology
Indianapolis, IN 46285
www.lilly.com

References:

1. Brown CD, Forman CL, McEuen SF, Miller MG. Metabolism and testicular toxicity of 1,3-dinitrobenzene in rats of different ages. *Fundam Appli Toxicol*. 1994;23:439-446.
2. Foster RA, Ladds PW. Male genital system. In: Maxie MG, ed. *Jubb, Kennedy, and Palmer's Pathology of Domestic Animals*. Vol. 3. 5th ed. Philadelphia, PA: Elsevier Limited; 2007:566-567.
3. Foster PMD, Sheard CM, Lloyd SC. 1,3-Dinitrobenzene: a Sertoli Cell toxicant? In: Stefanini M, Conti M, Geremia R, Ziparo E, eds. *Molecular and Cellular Endocrinology of the Testis*. New York, NY: Elsevier Science Publishers; 1986:281-288.
4. Hess RA, Linder RE, Strader LF, Perreault SD. Acute effects and long-term sequelae of 1,3-dinitrobenzene on male reproduction in the rat I. Quantitative and qualitative histopathology of the testis. *J Androl*. 1988;9:327-342.
5. Russell LD, Ettlin RA, Sinha Hikim AP, Clegg ED. *Histological and Histopathological Evaluation of the Testis*. Clearwater, FL: Cache River Press; 1990:65.

CASE IV: A543/405/223-13 (JPC 4035678).

Signalment: 3-week-old broiler chicken, (*Gallus gallus domesticus*).

History: There was a sudden onset of mortality affecting 10% of the flock. Sick birds adopted a crouching position with ruffled feathers and died within 48 hours.

Gross Pathology: At necropsy, diffuse yellowish-pale, friable and swollen livers are seen. Multiple petechiae beneath the capsule are present in some livers.

Histopathologic Description: There is a disruption of the hepatic parenchyma due to the presence of multifocal to coalescing randomly distributed foci of degenerated hepatocytes. These hepatocytes are swollen with hypereosinophilic and highly vacuolated cytoplasm, and a pyknotic nucleus with karyorrhexis and/or karyolysis. Associated with these foci and randomly scattered throughout the parenchyma are hepatocytes with marked karyomegaly, chromatin condensation at the nuclear membrane and large basophilic intranuclear inclusion bodies. There is a moderate lymphoplasmacytic and heterophilic inflammatory infiltrate in the periportal areas. Diffuse cytoplasmic vacuolation is observed within remaining hepatocytes. Occasionally, there is focal widening and infiltration of sinusoids with lymphocytes, heterophils and histiocytes.

Contributor's Morphologic Diagnosis: Liver: Acute, severe, multifocal to coalescing necrotizing hepatitis with intranuclear inclusion bodies in hepatocytes.

Contributor's Comment: Inclusion body hepatitis (IBH) is a viral disease produced by a member of the family *Adenoviridae*, genus *Aviadenovirus*,[1] which was first described in chickens by Helmboldt and Frazier in 1963.[3] IBH is a ubiquitous disease in commercial and farm birds,[1] although recently infection has also been

4-1. Liver, broiler chicken: At necropsy, the liver is swollen, yellow, and friable. (Photo courtesy of: Servei de Diagnostic de Patologia Veterinaria, Facultat de Veterinaria, Bellaterra (Barcelona), 08193 SPAIN)

demonstrated in wild and exotic birds, producing the same characteristic hepatic lesions.[5]

The liver is the primary organ affected.[1] The infection produces a multifocal necrotizing hepatitis with intranuclear inclusion bodies in the hepatocytes.[1,6] Within the literature, the description of these intranuclear inclusion bodies is variable; inclusions have been described as large and eosinophilic or basophilic, or irregularly shaped, but they always replace/peripherally displace chromatin, and produce significant karyomegaly.[1]

JPC Diagnosis: Liver: Hepatitis, necrotizing, diffuse, severe, with numerous hepatocellular intranuclear viral inclusions.

Conference Comment: Although tissue sections are somewhat poorly preserved, the characteristic microscopic features, including the presence of viral inclusions with corresponding karyomegaly and peripheralization of chromatin, are nicely demonstrated in this case. Furthermore, the image of the affected liver submitted by the contributor provides an excellent example of the gross findings classically associated with IBH in chickens.

Members of the family *Adenoviridae* are non-enveloped, icosahedral, dsDNA viruses composed of four genera: *Aviadenovirus* (infects birds), *Mastadenovirus* (infects mammals), *Atadenovirus* (infects birds, mammals and reptiles) and *Siadenovirus* (infects birds, amphibians, reptiles); there is also a proposed fifth genus that includes adenoviruses of fish, such as white sturgeon adenovirus. Adenoviruses characteristically produce viral inclusion bodies within the host cell nucleus, where replication occurs.[4] Readers are urged to review WSC 2009-2010, Conference 9, case 3 for additional details regarding general characteristics of adenoviruses. See table 1 for a summary of select adenoviruses significant in veterinary medicine.

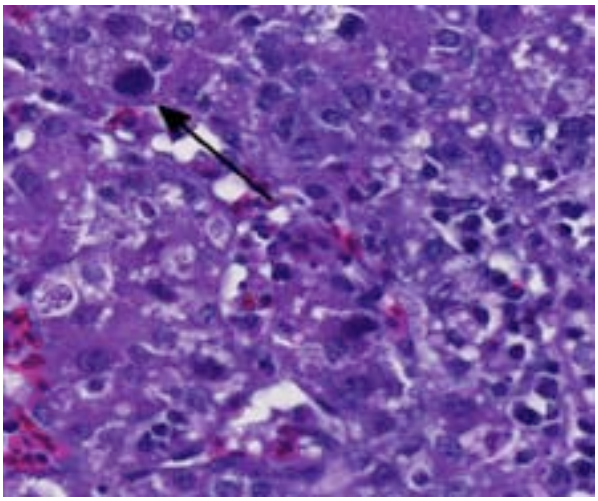

4-2. Liver, broiler chicken: At the edges of necrotic areas, hepatocellular nuclei are often expanded by a large basophilic adenoviral inclusion. Degenerating hepatocytes contain numerous cytoplasmic lipid droplets. (HE 360X)

Important aviadenoviruses (subgroup I) include inclusion body hepatitis virus, quail bronchitis virus and hydropericardium syndrome virus. Turkey adenovirus 3, the causative agent of hemorrhagic enteritis in turkeys, marble spleen disease in pheasants and avian adenovirus splenomegaly in broilers, is a siadenovirus (subgroup II), while egg drop syndrome virus is a member of the genus *Atadenovirus* (subgroup III).[1] The pathogenesis of subgroup I avian adenoviruses is less defined than that of subgroups II and III; however, in general, both vertical and horizontal (especially fecal-oral) transmission are thought to be important in all aviadenoviruses. As noted by the contributor, IBH virus primarily targets hepatocytes, but pancreatic lesions are reported as well. Infection tends to occur in 3-7 week old broiler chickens (although it has been reported in birds as young as 7 days and as old as 20 weeks) resulting in up to 30% mortality. It often occurs as a secondary infection in immunodeficient birds with other diseases, predominantly infectious bursal disease (birnavirus, serotype 1) and chicken infectious anemia (circovirus). Outbreaks of IBH with similar gross and histological lesions have also been reported in columbiformes, psittacines and raptors.[1]

The recently identified falcon adenovirus, which is distantly related to fowl adenovirus types 1 and 4 (see WSC 2007-2008, Conference 23, case 3) rarely causes necrotizing hepatitis and splenitis with characteristic intranuclear viral inclusions; stress related to shipping or breeding is a likely predisposing factor for clinical disease.[2] Quail bronchitis virus, caused by avian adenovirus 1, is a worldwide disease of both captive and wild bobwhite quail; birds present with respiratory distress, nasal discharge, coughing, sneezing, conjunctivitis and, occasionally in older birds,

diarrhea. Mortality approaches 100% in the young, but falls below 25% in those older than 4 weeks. Microscopic findings include tracheitis, air sacculitis and enteritis, with characteristic intranuclear viral inclusions. Infection with fowl adenovirus type 4 is believed to be the cause of hydropericardium syndrome virus (Angara disease), which is found in the Middle East as well as South America; particularly severe manifestations are also associated with immunosuppression. Lesions include pericardial effusion, pulmonary edema, hepatomegaly and renomegaly; mortality can range from 20-80%; and affected broilers are usually 3-5 weeks old.[4]

Egg drop syndrome, an atadenovirus (subgroup III) recognized in chickens, ducks and geese results in the production of soft-shelled or shell-less eggs. It is suspected that the virus originated in ducks and was passed to chickens via contaminated Marek's disease vaccine produced with duck embryo fibroblasts; spread within flocks occurs through contaminated eggs, droppings and fomites. Egg drop syndrome has worldwide distribution except the United States and Canada. The siadenovirus (subgroup II), turkey adenovirus 3, produces splenomegaly, hemorrhagic enteritis and immunosuppression with secondary opportunistic infections in turkeys older than 4 weeks. A serologically identical virus also causes marble spleen disease in pheasants and splenomegaly in chickens. Microscopic lesions are similar in all species and include splenic reticuloendothelial hyperplasia with intranuclear viral inclusions and fibrinonecrotic, hemorrhagic enteritis. There is a vaccine available.[4]

Table 1: Select adenoviruses in veterinary species.[1,4]

Species	Name	Comment
Dogs	Canine adenovirus 1 Canine adenovirus 2 (mastadenovirus)	- Infectious canine hepatitis - Infectious canine tracheobronchitis
Horses	Equine adenovirus 1 & 2 (mastadenovirus)	- Asymptomatic or mild respiratory disease in immunocompetent hosts - Bronchopneumonia/ systemic disease in Arabian foals with SCID
Cattle	Bovine adenovirus (mastadenovirus and atadenovirus)	- 10 serotypes - Asymptomatic or mild respiratory disease - Occasionally pneumonia, enteritis, keratoconjunctivitis in calves
Swine	Porcine adenovirus (mastadenovirus)	- 4 serotypes - Asymptomatic or mild respiratory disease/ enteritis; rarely encephalitis
Sheep	Ovine adenovirus (mastadenovirus and atadenovirus)	- 7 serotypes - Asymptomatic or mild respiratory disease - Occasionally severe respiratory/enteric disease in lambs
Goats	Caprine adenovirus (mastadenovirus and atadenovirus)	- 2 serotypes - Asymptomatic or mild respiratory disease
Deer	Cervine adenovirus (Odocoileus adenovirus 1; atadenovirus)	- Vasculitis, hemorrhage, pulmonary edema
Rabbits	Adenovirus 1 (mastadenovirus)	- Diarrhea
Mice	Murine adenovirus 1 & 2 (mastadenovirus)	- Murine adenovirus 1: experimental infections - Murine adenovirus 2: enterotropic; causes runting in neonates
Guinea pigs	Guinea pig adenovirus (mastadenovirus)	- Usually asymptomatic; rarely pneumonia with high mortality, low morbidity
Chickens	Fowl adenovirus (aviadenovirus, atadenovirus and siadenovirus)	- 12 serotypes of aviadenovirus (inclusion body hepatitis, hydropericardium syndrome) - 1 serotype of atadenovirus (egg drop syndrome) - 1 serotype of siadenovirus (adenovirus-associated splenomegaly)

Turkeys	Turkey adenovirus 1-3 (siadenovirus and aviadenovirus)	- turkey adenovirus 3, siadenovirus (hemorrhagic enteritis, egg drop syndrome) - turkey adenovirus 1 & 2, aviadenovirus (depressed egg production)
Quail	Avian adenovirus 1 (aviadenovirus)	- 1 serotype, aviadenovirus (bronchitis)
Pheasants	- serologically indistinguishable from Turkey adenovirus 3 (siadenovirus)	- Siadenovirus (marble spleen disease)
Ducks	Duck adenovirus 1 & 2 (atadenovirus and aviadenovirus)	- 1: atadenovirus (asymptomatic or drop in egg production) - 2: aviadenovirus (rare hepatitis)

Contributing Institution: Servei de Diagnostic de Patologi Veterinària
Facultat de Veterinària
Bellaterra (Barcelona), 08193 Spain

References:

1. Adair BM, Fitzgerald SD. Group I adenovirus infections. In: *Diseases of Poultry*. 12th ed. Ames, IA: Iowa State Press; 2008:252-266.
2. Dean J, Latimer KS, Oaks JL, Schrenzel M, Redig PT, Wünschmann A. Falcon adenovirus infection in breeding Taita falcons (*Falco fasciinucha*). *J Vet Diagn Invest*. 2006;18:282-286.
3. Hollell J, McDonald DW, Christian RG. Inclusion body hepatitis in chickens. *Can Vet J*. 1970;11:99-101.
4. MacLachlan NJ, Dubovi EJ. *Fenner's Veterinary Virology*. 4th ed. London, UK: Academic Press; 2011:203-212.
5. Ramis A, Marlasca MJ, Majo N, Ferrer L. Inclusion body hepatitis (IBH) in a group of Eclectus parrots (*Eclectus roratus*). *Avian Pathol*. 1992;21(1):165-169.
6. Randall CJ, Reece RL. *Color Atlas of Avian Histopathology*. Mosby-Wolfe, Times Mirror International Publishers Limited; 1996:95-96.

Joint Pathology Center
Veterinary Pathology Services

WEDNESDAY SLIDE CONFERENCE 2013-2014

Conference 17

26 February 2014

CASE I: 48772-A (JPC 4033980).

Signalment: 1-year-old intact male Romney sheep (*Ovis aries*).

1-1. Heart, sheep: The incised myocardium contained several sharply demarcated, irregular-shaped 2-3 cm diameter foci which varied from pale tan to grey/green, and often had a red margin. (Photo courtesy of: IVABS, Massey University, Palmerston North, New Zealand http://www.massey.ac.nz)

History: This sheep was one of several rams purchased 10 days earlier from the sale yards for a research trial. The animals had been transported for approximately 2 hours by truck to the sale yards and had been drenched with an anthelmintic on two occasions during the 10 days since purchase. This animal was found dead in its paddock without showing any previous signs of illness. The vaccination history was unknown.

Gross Pathology: The ram was in good physical condition but was relatively small for its age, weighing 36.5kg. Although the abdomen was distended and blood-stained froth was exuding from the nostrils, there was little evidence of post-mortem decomposition at the time of examination. The lungs were diffusely red and edematous and contained multiple 2-3 mm dark red foci. The thoracic cavity contained approximately 1.5 liters of red fluid. Clear, yellow fluid was also present in the pericardial sac and the epicardial surface of the heart was almost completely covered by a thick, loosely adherent sheet of fibrin. On cut surface, the myocardium contained several sharply demarcated, irregular 2-3 cm diameter foci which varied from pale tan to grey/green, and often had a red margin. One focus involved the interventricular septum and extended to the

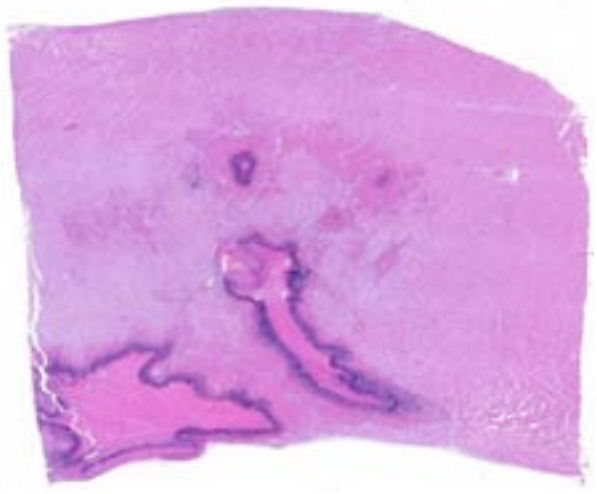

1-2. Heart, sheep: The myocardium contains several extensive areas of coagulative necrosis outlined by a dark blue band of cellular debris. (HE 0.63X)

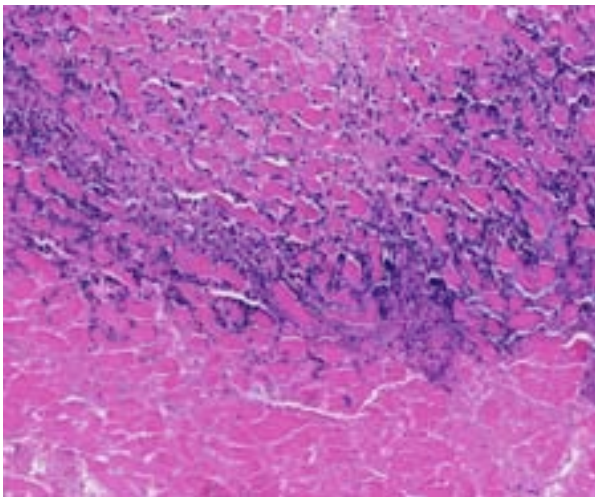

1-3. Heart, sheep: At higher magnification, areas of coagulative necrosis (lower left) are surrounded by a band of degenerate neutrophils and abundant cellular debris which surrounds and separates adjacent degenerating myofibers. (HE 200X)

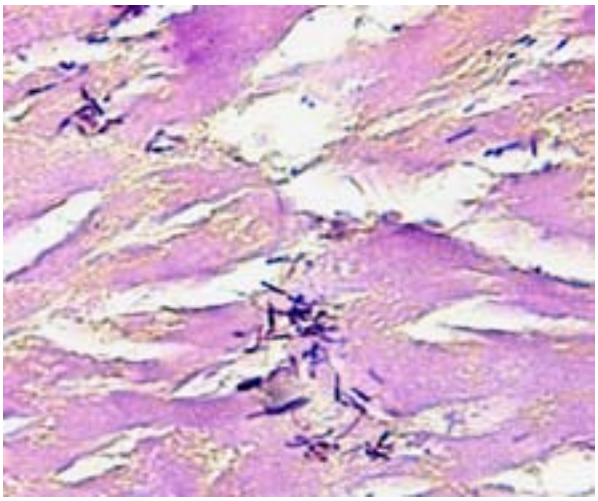

1-4. Heart, sheep: Moderate numbers of robust bacilli are scattered throughout the areas of coagulative necrosis. (Brown and Brenn 400X)

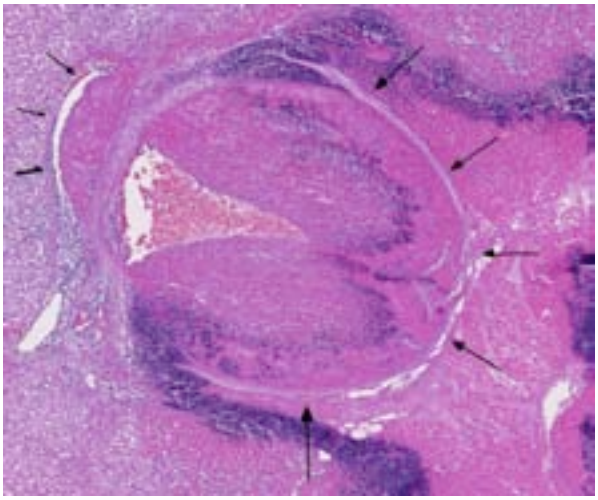

1-5. Heart, sheep: One area of necrosis incorporates a partially thrombosed arteriole (large arrows), and a smaller thrombosed vein (smaller arrows). (HE 160X)

luminal surface of the right ventricle, where it was covered by a fibrin thrombus.

Histopathologic Description: The focal lesions observed grossly in the heart consisted of acute coagulation necrosis surrounded by a thick layer of degenerate neutrophils. Within the necrotic areas, the interstitium was expanded with fibrinous exudate and many interstitial blood vessels and lymphatics contained fibrin thrombi. Large numbers of long, rod-shaped, gram-positive bacteria were present in necrotic areas, particularly near the margins. In surrounding areas of myocardium there was variable acute necrosis of myocardial fibers, neutrophilic interstitial infiltration and edema. The epicardium in some areas was markedly thickened with a layer of fibrin and moderate to large numbers of neutrophils. Necrotic foci that extended to the endocardial surface were covered with a layer of fibrin containing degenerate neutrophils.

Immunohistochemistry for *C. chauvoei*, *C. septicum*, *C. novyi* and *C. sordelli* performed at CAHFSL, San Bernardino (courtesy of Dr. F. Uzal) revealed organisms reacting positively for both *C. chauvoei* and *C. septicum*.

In the lungs, there was diffuse congestion of alveolar capillaries and proteinaceous alveolar

Table 1: Select clostridial diseases in veterinary species.[1,4,5]

Name	Species
C. perfringens type:	
A (α toxin)	• Enterocolitis in many species: ○ Foals, piglets, lambs, calves ○ Necrotic enteritis- chickens ○ Hemorrhagic canine gastroenteritis ○ Hemorrhagic bowel syndrome- dairy cattle • Yellow lamb disease- IV hemolysis (rare) • Gas gangrene- humans and animals
B (α, β, ε toxins)	• Enterocolitis in Europe, South Africa, Middle East ○ Lamb dysentery; similar condition in neonatal calves
C (α, β toxins)	• Enterocolitis in many species: ○ "Struck" in adult sheep in the UK; similar condition in goats and feedlot cattle ○ Necrohemorrhagic enteritis- lambs, calves, piglets, foals
D (α, ε toxins)	• Enterocolitis: ○ overeating disease/pulpy kidney- sheep, goats, cattle • Focal symmetric encephalomalacia- sheep and (rarely) goats
E (α, ι toxins)	• Enterotoxemia- calves, lambs, guinea pigs, rabbits
C. haemolyticum	• Bovine bacillary hemoglobinuria ("redwater") 2º to fluke migration
C. septicum	• Necrohemorrhagic abomasitis ("braxy") • Malignant edema • Postparturient vulvovagnitis and metritis in dairy cattle
C. novyi	• Hepatic necrosis ("black disease") 2º to fluke migration • Wound infections
C. chauvoei	• Necrotizing myositis ("blackleg") in cattle and sheep
C. colinum	• Ulcerative enteritis- "quail disease" in gallinaceous birds
C. spiroforme	• Spontaneous or antibiotic-induced enterotoxemia in rabbits and rodents
C. difficile	• Spontaneous or antibiotic-induced enterocolitis in hamsters, rabbits, guinea pigs, dogs, swine and horses
C. piliforme	• Necrotizing enteritis/colitis, hepatitis, myocarditis in many species (Tyzzer's disease) • Obligate intracellular, gram-negative
C. carnis, C. histolyticum	• Wound infections in many species
C. tetani	• Tetanus- muscle spasms, stiff gait, rigid posture, trismus (lockjaw)
C. botulinum	• Botulism- flaccid paralysis→ respiratory paralysis

oedema. There was also multifocal intra-alveolar haemorrhage and fibrinous exudation. Moderate numbers of neutrophils were present in the interstitium and in many alveoli.

Contributor's Morphologic Diagnosis: 1. Acute multifocal necrotising myocarditis.
2. Acute diffuse fibrinous epicarditis

Contributor's Comment: Clostridial myocarditis is a rare disease of sheep. To our knowledge, it has only been reported once previously (in Australia)[2] and is probably analogous to the myocardial form of "blackleg" in cattle, which is caused by *Clostridium chauvoei.*[3] No lesions were present in skeletal muscles of the ram, supporting primary myocardial involvement. The myocardial lesions were characterized by a greater neutrophilic response than would be expected in clostridial myositis involving skeletal muscles. This was also a feature of lambs and calves in previous reports of clostridial myocarditis.[2,3] An unexpected finding in this case was the presence of both *C. chauvoei* and *C. septicum* in the myocardial lesions, suggesting that latent spores of both organisms were present in the myocardium.

In published reports of clostridial myocarditis in lambs and calves, potential risk factors included lush pasture growth following a period of high rainfall, and stress associated with yarding and management procedures. Both factors existed in the present case. It is possible that the stress involved in recent transport and yarding for drenching caused focal catecholamine-induced myocardial necrosis, allowing germination of latent clostridial spores. Vaccination with a 5 in 1 clostridial vaccine would have been expected to prevent the disease, suggesting that this ram had not been vaccinated.

JPC Diagnosis: Heart: Myocarditis, necrotizing, multifocal to coalescing, moderate with large colonies of bacilli, necrotizing arteritis and thrombosis.

Conference Comment: There is moderate slide variation in this case; some sections contain a large arteriole adjacent to a focus of myocardial necrosis which is 80-90% occluded by an organizing fibrin thrombus, while in other sections, necrotizing arteritis and fibrin thrombi

are limited to smaller coronary vessels within the endocardium. The presence of these fibrin thrombi supports the interpretation of the well demarcated areas of necrosis as infarcts. Additionally, most sections of myocardium contain rare protozoal cysts packed with numerous bradyzoites (*Sacrocystis* sp.), without evidence of associated inflammation; infection with *Sarcocystis* sp. is a common, incidental finding in the skeletal and cardiac muscle of ruminants.[4] Histochemical staining with a Giemsa as well as a Gram stain highlighted the presence of numerous gram-positive bacilli with multifocal subterminal spores, a characteristic feature of *Clostridium* sp.

Members of the genus *Clostridium* are spore forming, gram-positive, anaerobic bacilli, whose spores are ubiquitous in soil, highly resistant to environmental changes and disinfectants, and able to persist in the environment for many years. Germination of spores, which are often ingested by ruminants during grazing, requires specific conditions, including low oxygen levels and an alkaline pH; necrotic lesions and penetrating wounds provide appropriate conditions for growth of clostridial spores. Clostridia typically produce disease via production of exotoxins which cause widespread necrosis with edema and extensive gas formation.[1,4,5] See table 1 for an abbreviated list of *Clostridium* sp. important in veterinary medicine.

Contributing Institution: IVABS
Massey University
Palmerston North, New Zealand
http://www.massey.ac.nz

References:

1. Brown CC, Baker DC, Barker IK. Alimentary system. In: Maxie MG, ed. *Jubb, Kennedy and Palmer's Pathology of Domestic Animals*. Vol. 2. 5th ed. Philadelphia, PA: Elsevier; 2007:213-222.
2. Glastonbury JRW, Searson JE, Links IJ, Tuckett LM. Clostridial myocarditis in lambs. *Australian Veterinary Journal*. 1988;65:208-209.
3. Uzal FA, Paramidani M, Assis R, Morris W, Miyakawa MF. Outbreak of clostridial myocarditis in calves. *Vet Rec.* 2003;152:134-136.
4. Van Vleet JF, Valentine BA. Muscle and tendon. In: Maxie MG, ed. *Jubb, Kennedy and Palmer's Pathology of Domestic Animals*. Vol. 1. 5th ed. Philadelphia, PA: Elsevier; 2007:259-267.
5. Zachary JF, McGavin MD, eds. *Pathologic Basis of Veterinary Disease*. 5th ed. St. Louis, MO: Elsevier; 2012:175-175, 192-196, 377-379, 866, 891-898.

CASE II: AFIP-WSC H8674 39 (JPC 3165179).

Signalment: 18-year-old female Indian origin rhesus macaque, (*Macaca mulatta*).

History: Female with 7-week-old infant sedated (ketamine) for routine blood work developed seizures, high heart rate, pale mucous membranes, fixed pupils, euthanized.

Gross Pathology: Minimal pitting edema in the subcutaneous tissues; ~ 300 ml straw colored fluid within the abdominal cavity; ~ 350 ml straw colored fluid within the thoracic cavity with collapsed lung lobes and the diaphragm bulging into the abdominal cavity.

Histopathologic Description: A multifocal to diffuse inflammatory process is evident within the myocardium. There are large numbers of lymphocytes, plasma cells, macrophages and smaller areas of neutrophil infiltration. Many cardiomyocytes contain protozoal organisms consistent with amastigotes of *Trypanosoma cruzi*. The cardiomyocytes containing amastigotes have lost sarcomeres and are undergoing degeneration.

Contributor's Morphologic Diagnosis: Heart, diffuse, marked, chronic active inflammation, myocardium with intracellular protozoal organisms consistent with *Trypanosoma cruzi*.

Contributor's Comment: *Trypanosoma cruzi,* the etiologic agent of Chagas disease, is endemic within portions of the southern United States, including Texas and the colony where this case occurred.[4-7] Nonhuman primates housed outdoors within areas endemic for this parasite should be monitored with increased vigilance for contact

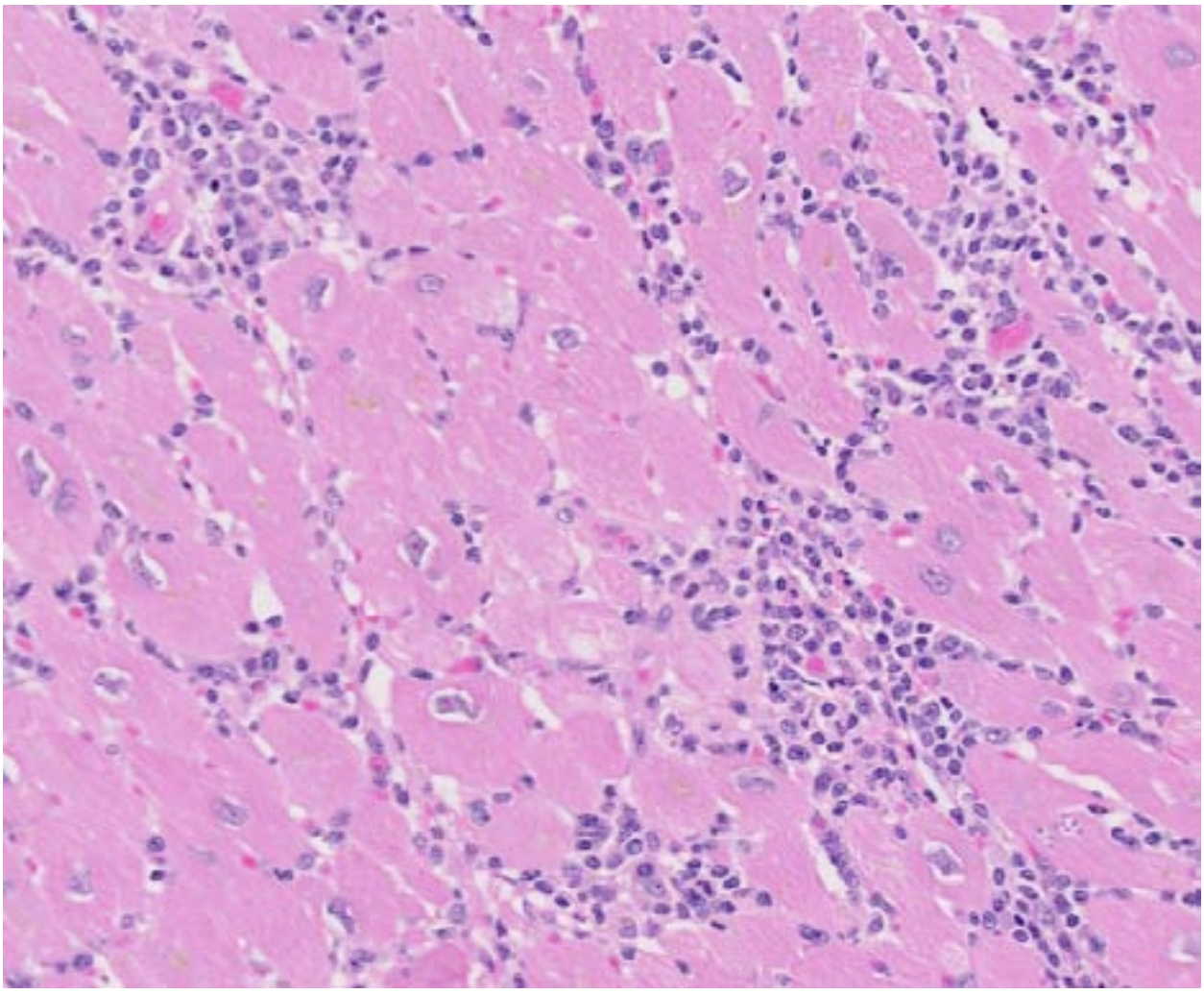

2-1. Heart, rhesus monkey: Diffusely, numerous lymphocytes, plasma cells, and fewer histiocytes surround and separate cardiomyocytes. (HE 180X)

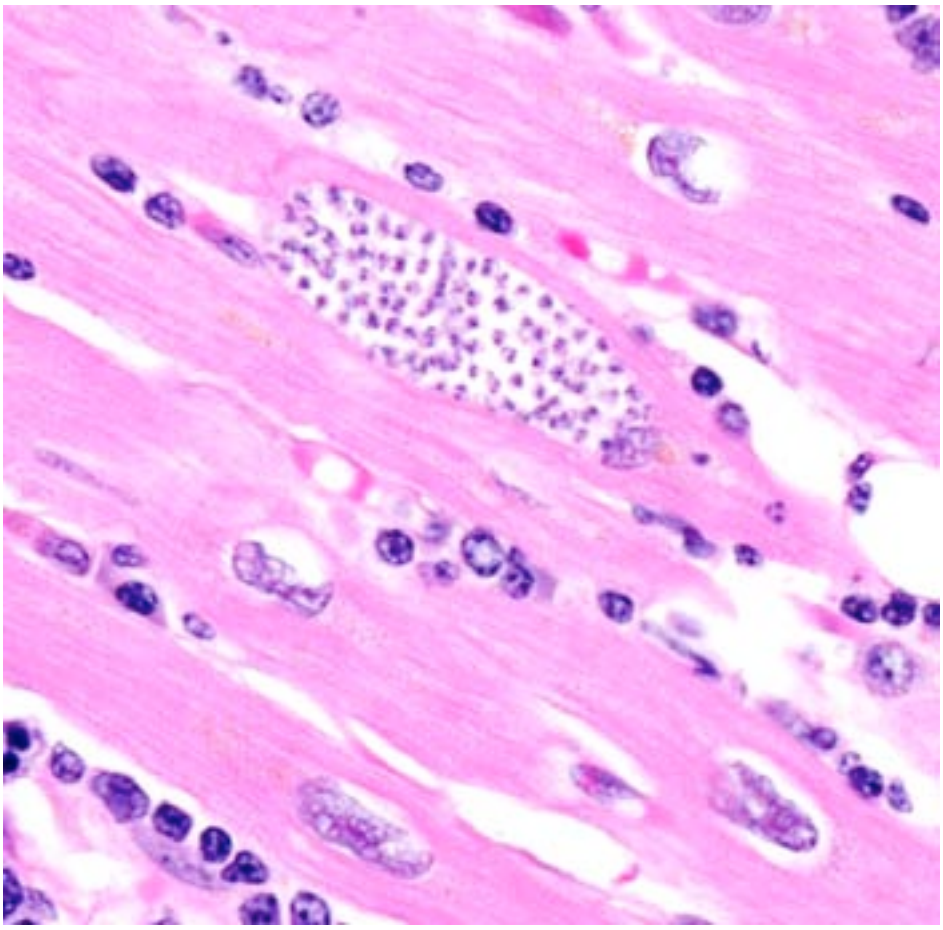

2-2. Heart, rhesus monkey: Occasional cardiomyocytes contain numerous 2-3 µ m amastigotes within their cytoplasm. The surrounding cardiomyocytes contain small amounts of perinuclear lipofuscin. (HE 400X)

with both vectors (triatomine beetles such as the kissing bug, assassin bug, reduviid beetle)[4-6] and reservoir hosts (sylvatic small mammals such as rodents and opossums).[6] It has been postulated that the alert nature of rhesus macaques makes feeding by triatomine beetles unlikely.[6]

A review of the database of pathologic lesions diagnosed within our colony over the last thirty years revealed no other cases of severe trypanosomiasis, and even mild cases were rare. Pest control procedures are well established and vigilantly enforced; no increased incidence of pests (either rodents or triatomine beetles) was noted before or since the identification of this case. In May of 2005 a survey of sixty apparently normal animals from this colony revealed a single animal with a positive culture. Serendipitously, the animal presented in this case was included in that study and had a negative culture at that time. This case is considered unusual, due to the high number of leishmanial forms of *Trypanosoma cruzi* organisms that are present within pseudocysts in individual cardiomyocytes as well as the abundant inflammatory reaction. At locations where pseudocysts have ruptured a suppurative inflammatory reaction is observed; however, the primary inflammatory population within this lesion is mononuclear, composed primarily of lymphocytes, macrophages and plasma cells. The affected animal was in late pregnancy when she presented for annual physical examination. During routine sedation, the animal became cyanotic and when emergency drugs failed to elicit any positive response the animal was euthanized. Potential immune suppression associated with pregnancy or mildly advanced age may have resulted in the development of this protozoal infection; alternatively, a concentrated mucocutaneous exposure secondary to ingestion of the vector may have led to this disease.[5,6]

JPC Diagnosis: Heart: Myocarditis, necrotizing, lymphoplasmacytic and histiocytic, subacute, diffuse, severe with numerous intramyocytic amastigotes.

Conference Comment: Trypanosomes are hemoflagellate protozoans that typically cause cardiac disease; *Trypanosoma cruzi* is the major etiologic agent of American trypanosomiasis, while *T. brucei* and *T. congolense* (among others) cause African trypanosomiasis. Humans, as well as numerous domestic and wild mammalian species within the Western Hemisphere, are susceptible to *T. cruzi*, although disease is most

common in South and Central America. As noted by the contributor, transmission is typically associated with intermediate arthropod vectors, particularly *Triatoma* sp. (i.e., Reduviidae, or the "kissing bug"); stercorarian transmission occurs when feces from an infected bug contaminates the bite wound or nearby abrasions.

T. cruzi occurs in three morphologic forms. Epimastigotes are found within the arthropod vector, while the extracellular trypomastigote (blood form) and intracellular amastigote (tissue form) occur within the mammalian host. The amastigote contains a large round nucleus and a rod-like kinetoplast similar to that of *Leishmania* sp.[7,8] Leishmanial and trypanosomal amastigotes are anecdotally described as having rod-shaped kinetoplasts oriented perpendicular and parallel to the long axis of the oval nucleus, respectively; however, most current references simply describe a juxtanuclear kinetoplast composed of DNA and representative of the mitochondrial genome,[3] which led conference participants to conclude that kinetoplast orientation relative to the nucleus is not an accurate or reliable method for distinguishing *Trypanosoma* sp. from *Leishmania* sp. Readers may refer to WSC 2011-2012, Conference 18, case 1 for further discussion of *Trypanosoma cruzi*.

African trypanosomiasis, or sleeping sickness, also occurs in humans and a variety of animal species. It is transmitted through the saliva of the tsetse fly (*Glossina* sp.). Unlike *T. cruzi*, African trypanosomes are capable of continuous antigenic variation of their outer glycoprotein coat in order to evade the host immune response. They also produce sialidases, which hydrolyze host cell membrane sialic acid and facilitate invasion. In addition to myocarditis, ocular involvement, anemia, thrombocytopenia and even disseminated intravascular coagulation have been reported in association with African trypanosomiasis.[8]

In this case, anesthesia likely led to decompensation of existing cardiac disease. There is multifocal cardiomyocyte hypertrophy, characterized by fiber thickening and change of the nuclei from spindle/cigar shaped to "box car" like (rectangular). Additionally, cardiomyocytes often contain aggregates of golden-brown granular pigment, interpreted as lipofuscin, which represents intralysosomal accumulation of cellular debris (i.e., residual bodies).[9] There is also mild slide variation, with varying degrees of myocardial fibrosis (demonstrated with a Masson's trichrome stain) depending on the section; however, fibrosis is a common background finding in macaque hearts[2] and may not be a direct result of the trypanosome infection. Conference participants briefly discussed the differential diagnosis for the gross and histological findings, including leishmaniasis, toxoplasmosis, sarcocystosis, encephalitozoonosis and African histoplasmosis. Histochemical staining with giemsa highlights the presence of moderate numbers of intracellular cardiomyocyte protozoal amastigotes with a rod-like kinetoplast, consistent with trypanosomiasis or leishmaniasis. It can be difficult to differentiate *Trypanosoma* spp. from *Leishmania* spp.; however, the kinetoplast of *T. cruzi* is typically larger, and leishmanial amastigotes tend to concentrate in the phagocytic cells of the skin, mouth, nose and throat, or in the macrophages of the reticuloendothelial system, which are all uncommon sites for *T. cruzi*.[1] Based on the species, its geographic location and the anatomic location of the lesions, trypanosomiasis is the most likely diagnosis; however, since additional diagnostic testing, such as PCR, culture or serology was not performed, leishmaniasis cannot be completely ruled out.

Contributing Institution: The University of Texas MD Anderson Cancer Center
Michale E. Keeling Center for Comparative Medicine and Research
http://www.mdanderson.org/education-and-research/departments-programs-and-labs/programs-centers-institutes/michale-e-keeling-center-for-comparative-medicine-and-research/index.html

References:

1. Binford CH, Connor DH, eds. *Pathology of Tropical and Extraordinary Diseases: An Atlas*, Vol. 1. Washington, DC: United States Government Printing; 1976:45.
2. Chamanza R, Marxfeld HA, Blanco AI, Naylor SW, Bradley AE. Incidences and range of spontaneous findings in control cynomolgus monkeys (*Macaca fascicularis*) used in toxicity studies. *Toxicol Pathol*. 2010;38:642-657.
3. Cheville NF. *Ultrastructural Pathology: The Comparative Cellular Basis of Disease.* 2nd ed. Ames, IA: Wiley-Blackwell; 2009:529-536.

4. Cicmanec JL, Neva FA, McClure HM, Loeb, WF. Accidental infection of laboratory-reared *Macaca mulatta* with *Trypanosoma cruzi*. In: *Laboratory Animal Science*. 1974;24(5):783-787.
5. Gleiser CA, Yaeger RG, Ghidoni JJ. *Trypanosoma cruzi* infection in a colony-born baboon. *J Vet Med Assoc* 1986;189(9):1225-1226.
6. Kasa TJ, Lathrop GD, Dupuy HJ, Bonney CH, Toft JD. An endemic focus of *Trypanosoma cruzi* infection in a subhuman research colony. *J Vet Med Assoc*. 1977;171(9):850-854.
7. Kunz E, Matz-Rensing K, Stolte N, Hamilton PB, Kaup FJ. Reactivation of a *Trypanosoma cruzi* infection in a rhesus monkey (*Macaca mulatta*) experimentally infected with SIV. *Vet Pathol*. 2002;39:721-725.
8. Snowden KF, Kjos SA. Trypanosomiasis. In: Greene CE, ed. *Infectious Diseases of the Dog and Cat*. 4th ed. St. Louis, MO: Elsevier Saunders; 2012:722-734.
9. Zachary JF, McGavin MD, eds. *Pathologic Basis of Veterinary Disease*. 5th ed. St. Louis, MO: Elsevier; 2012:551-555.

CASE III: 12-17590 (JPC 4034294).

Signalment: 6-year-old female polled Hereford cow (*Bos taurus*).

History: Cow is in good body condition on native pasture. She was seen to have an elevated respiratory rate and standing in water. After walking, she had muscle fasciculations in her left hind leg. She then died.

Gross Pathology: Both kidneys exhibit multiple abscesses ranging from 2-10 mm diameter containing greenish caseous material. The right kidney is small and fibrotic. The liver is mildly swollen with a pale khaki coloration on cut surface and is friable. There is ulceration in the distal esophagus. The pericardial surface of the right ventricle contains mild petechiation.

Laboratory Results: Culture (routine): Kidney- moderate pure growth of *Corynebacterium renale*.

Sensitivity:

Sulphafurazole	Sensitive
Trimethoprim	Resistant
Tetracycline	Sensitive
Erythromycin	Sensitive
Penicillin	Resistant
Novobiocin	Sensitive

Hematology:

Parameter	**Value**	**Reference Range/ Units**
RBC	7.06	5.00-8.00 x 10^{12}/ L
PCV	38	23-44 %
HGB	14.6	8.0-15.0 g/dL
MCV	54	44-62 fL
MCH	21 H	14-20 pg
MCHC	38 H	30-35 g/dL
WBC	3.8 L	4.0-12.0 x 10^9 /L
BANDS	0.00	0.00-0.12 x 10^9 /L
NEUT	0.95	0.60-4.00 x 10^9 /L
LYMPH	2.58	2.50-7.50 x 10^9 /L
MONO	0.27	0.03-0.84 x 10^9 / L
EOS	0.00	0.00-2.40 x 10^9 /L
BASO	0.00	0.00-0.20 x 10^9/L
NUCL.RBC	3	/100 WBC

Platelet clumping observed; platelets appear adequate on blood film; Anisocytosis (+); Rouleaux

Biochemistry:

BUN	98.9 H	2.1-10.7 mmol/L
CREA	2550 H	0-186 umol/L
BUN/CREA	0.04	0.00-0.07
PHOS	3.45 H	0.80-2.80 mmol/L
Ca	2.60	2.00-2.75 mmol/L
TP	105.9 H	60.0-85.0 g/L
ALB	36.0	25.0-38.0 g/L
Glob	69.9 H	30.0-45.0 g/L
Alb/Glob	0.5 L	0.7-1.1
AST	998 H	0-120 U/L
GLDH	19	0-30 U/L
GGT	14	0-35 U/L
TBIL	4.0	0.0-24.0 umol/L
CK	3215 H	0-300 U/L
MG	1.05	0.74-1.44 mmol/L
BHB	0.10	0.00-0.80 mmol/L
PROT-RTS	130 H	65-85 g/L
FIBRIN	19 H	3-7 g/L
PR/FI	6 L	15-100

Histopathologic Description: Extending from the renal papilla into the medulla and effacing the normal architecture is irregular, focally extensive necrosis characterized by cellular and nuclear debris. The tubules are ectatic, serpentine and variably lined by vacuolated, attenuated to swollen epithelial cells (degeneration), hypereosinophilic epithelial cells with pyknotic nuclei (necrosis) or hypertrophic crowded epithelial cells with plump vesicular nuclei (regeneration). Tubule lumina often contain deeply eosinophilic proteinaceous material, moderate numbers of degenerate neutrophils and cellular debris. Large numbers of tubules are expanded by anisotropic, refractile, birefringent, pale yellow crystals containing radiating spokes (oxalate crystals) and occasional clusters of coccobacilli. There is moderate expansion of the interstitium with multifocal infiltrates of lymphocytes and plasma cells, mature fibrosis and multifocal loss of tubules and glomeruli. Within necrotic foci are discrete colonies of coccobacili.

Special Stain: Gram-positive coccobacilli noted within necrotic foci.

Contributor's Morphologic Diagnosis: Kidney: Pyelonephritis, suppurative, diffuse,

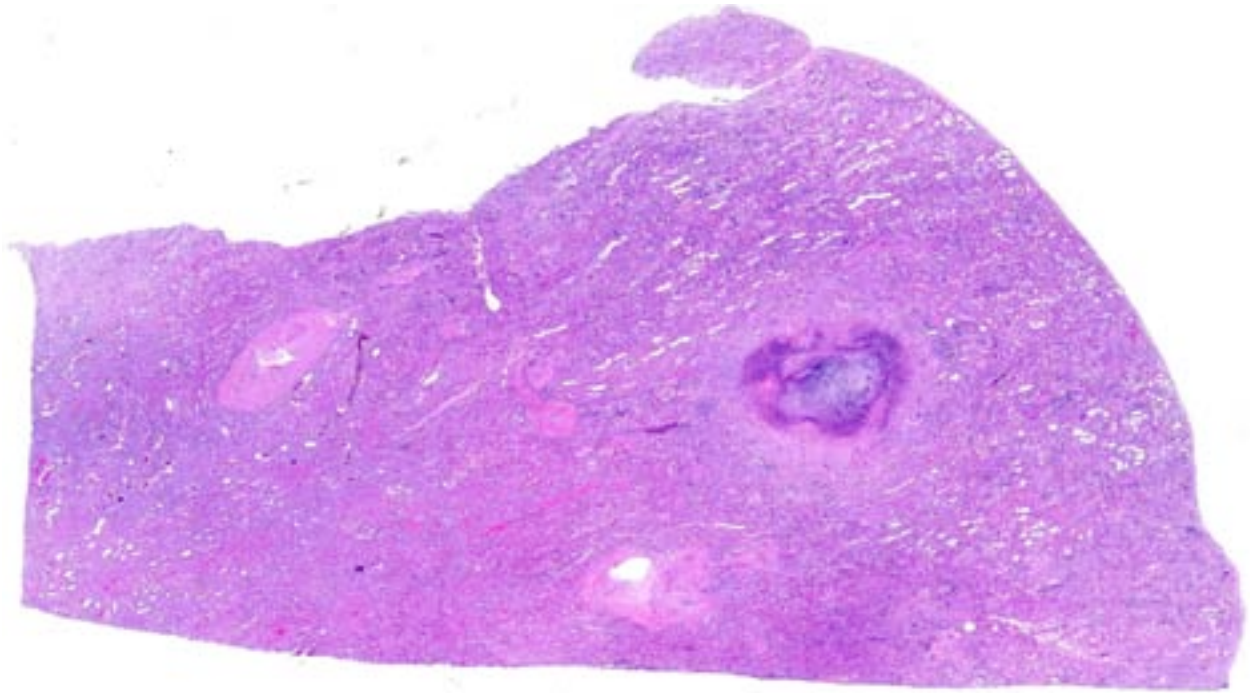

3-1. Kidney, ox: The section of kidney is diffusely and moderately hypercellular. The center of the cortex contains a focal abscess which is outlined by degenerate neutrophils and cellular debris. (HE 0.63X)

severe with tubular ectasia, proteinosis and scant coccobacilli.
Kidney: Nephrosis, multifocal, moderate with tubular necrosis, degeneration and regeneration, interstitial fibrosis, and numerous intratubular oxalate crystals.

Contributor's Comment: This case is a classic example of two diseases that occur commonly in cattle; however, what makes this case interesting is that they are occurring concurrently.

The clinical pathology results support the gross and histological findings of severe renal disease, hepatic necrosis (histopathological finding, slide not included), and a significant inflammatory process (elevated immunoglobulins and fibrinogen). The leukogram shows a mild leukopenia, which in this case is likely to be due consumption of leukocytes as part of the inflammatory response. Rouleaux formation is a common finding in hyperglobulinemic or hyperfibrinogenemic states.[7]

Pyelonephritis is an inflammation of the renal pelvis and renal parenchyma, usually resulting from an ascending infection from the lower urinary tract.[3]

In cattle, *Corynebacterium renale* is a common cause of pyelonephritis.[2] In a survey of clinically affected animals, *C. renale* was the most common bacteria isolated[1] and in a slaughterhouse survey of cattle with gross kidney lesions, it was the third most predominant organism isolated.[6] It is a facultative commensal organism that is commonly isolated from the urinary tracts of healthy cattle.[1]

Other common causes of pyelonephritis in cattle include:[6,1]

- *E.coli*
- *Truperella pyogenes (*formerly *Arcanobacter pyogenes)*
- *Corynebacterium cystitides*
- *Corynebacterium pilosum*
- *Streptococcus* spp.
- *Enterococcus faecalis*

Acute pyelonephritis characteristically begins with necrosis and inflammation of the renal crest in an irregular pattern that, as the disease progresses, results in chronic changes where mononuclear cells replace neutrophils and fibrosis eventually predominates. Chronic pyelonephritis occurs more commonly in cattle than acute disease, with acute pyelonephritis often an incidental finding at post mortem.[3]

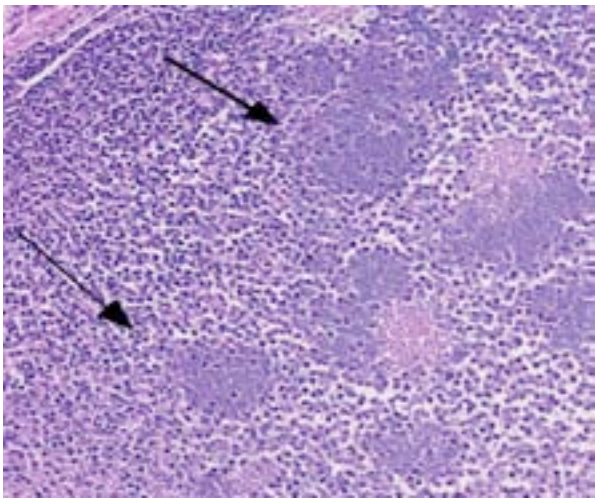

3-2. Kidney, ox: Even at moderate magnification, large colonies of bacilli are visualized within the center of the abscess. (HE 100X)

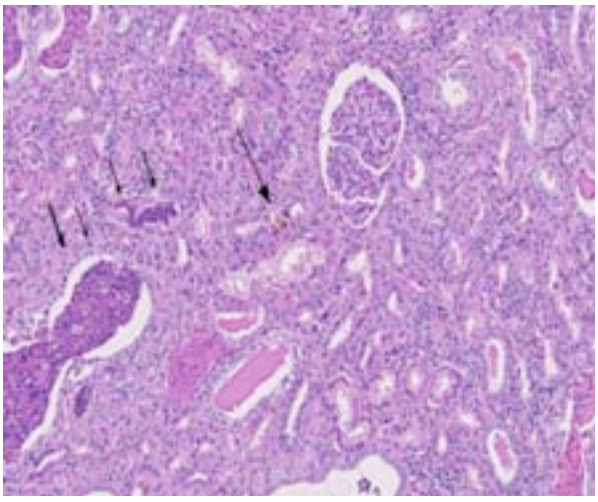

3-3. Kidney, ox: Throughout the cortex, tubules are ectatic, and contain variable amounts of protein, degenerate neutrophils, and necrotic epithelial cells (small arrows). Scattered throughout the cortex, there are low numbers of fan-shaped, birefringent oxalate crystals within tubular lumina. (HE 320X)

Vesicoureteral reflux is the most significant mechanism for transporting bacteria from the bladder to the kidney with refluxed urine occasionally being transported to the urinary space of the glomeruli.[3] Bacteria can spread hematogenously to the kidney, but this is a less common mode.

Within the kidney, the medullary region is the most susceptible to infection. This is due to its:

- Relative hypoxia (due to the low haematocrit in the vasa recta)
- Hypertonicity (depressed the phagocytic activity of leukocytes)
- High ammonia concentration (which interferes with the activation of complement).[3]

Several virulence factors make *C. renale* a significant pathogen for cattle. These include:

- Urea hydrolysis, which converts urea to ammonia. Ammonia initiates the inflammatory process and causes suppression of antibacterial defenses through complement inactivation.
- Pilli mediated attachment to the urothelium, which allows for persistence within the lower urinary tract in alkalotic urine. Cattle normally have alkalotic urine due to their herbivorous diet.[8]

Oxalate nephrosis can also be a common finding in ruminants which may manifest as acute or chronic renal disease, abortion or hypocalcaemia without renal damage.[5]

In ruminants, oxalate nephrosis is commonly caused by grazing plants high in soluble oxalate, typically those with greater than 2-2.5% soluble oxalate in dry matter. Many plants of this type contain greater than 10% soluble oxalate. Oxalate is higher in young plants with actively growing leaves. Soils high in nitrogen will also boost the concentration of oxalates.[4] It has been reported that annual deaths in sheep flocks grazing soursob (*Oxalis pes-caprae*) in Australia have had mortalities of 1%, although up to 25% of a flock may be affected.[5]

Naive or hungry cattle are more likely to suffer from oxalate toxicosis. Most oxalate containing plants are not readily eaten under normal grazing conditions and ruminal flora is not adapted to metabolize oxalates.[4]

Oxalate toxicosis occurs by calcium binding of the ingested soluble oxalates in the rumen, blood vessels liver and kidneys and leads to hypocalcaemia and oxalate crystal formation in the nephrons and blood vessels.[5]

The mechanism of injury in the kidney is from both mechanical obstruction of the nephrons and the cytotoxic effects of oxalate metabolites in the renal epithelium.[3]

Plants that are known to cause oxalate nephrosis in Australia and US include:

Scientific Name	Common Name
Halogeton glomerulatus	Halogeton, Barillia
Chenopodium spp.	Fat hen
Sarcobatus vermiculatus	Grease wood
Rumex spp.	Sorrel, dock
Mesembryanthemum spp.	Ice plants
Tetragonia tetragonioides	New Zealand spinach
Trianthema spp.	Black pig weed, Red spinach
Amaranthoretroflexus	Red root amaranth
Beta vulgaris	Beet
Rheum x cultorum	Rhubarb
*Oxalis pes-caprae**	Soursob
Portulaca oleracea *	Pigweed
Acetocella vulgaris	Sheep Sorrel
Atriplex muelleri	Salt Bush
Emex Australia	Spiney emex
Pennisetum ciliare	Buffel grass
*Seratia sphacelata**	Seratia
Acetosa vesicara	Ruby dock
Brassica spp.	

*Denotes common causes of oxalate poisoning in Australia.[5]

Other substances that are known to cause oxalate nephrosis include:

- Fungi (in feedstuffs)
  - *Aspergillus niger*
  - *Aspergillus flavis*
  - Some *Penicillium* spp.
- Ethylene glycol
- Primary hyperoxaluria- a rare genetic disorder that affects Beefmaster cattle
- Pyridoxine (vitamin B6) deficiency
- Excess ascorbic acid (vitamin C)reported in humans and a goat[3]

Although commonly reported, hypocalcaemia associated with oxalate nephrosis is not often seen at out laboratory.

JPC Diagnosis: 1. Kidney: Pyelonephritis, suppurative and necrotizing, chronic, diffuse, severe with large colonies of bacilli.
2. Kidney, tubules: Oxalate crystals, multiple.

Conference Comment: The contributor provides an excellent, thorough review of both pyelonephritis caused by *C. renale* infection and oxalate nephrosis. Microscopically, there are low to moderate numbers of intratubular calcium oxalate crystals with rare foci of minimal granulomatous response; however, these mild histopathologic features in combination with the serum biochemistry results (specifically the lack of hypocalcemia), led conference participants to conclude that oxalate toxicosis did not contribute significantly to the pathogenesis in this case. There was also some debate regarding the composition of the deeply basophilic material often present within necrotic renal tubules. Although most participants initially identified this substance as mineral, the moderator suggested instead that it is composed of aggregates of DNA secondary to widespread necrosis, pointing out its similarity to the microscopic appearance of material seen in acute tumor lysis syndrome, a condition seen in mice. As noted by the contributor, the clinical pathology findings are consistent with severe pyelonephritis due *C. renale*; however, the significant elevations in CK and AST could also result from hemolysis. Additionally, there is some slide variation; not all sections contain renal pelvis and in those that do, medullary tubules are often widely separated by fibrosis (demonstrated with Masson's trichrome). A brief discussion ensued regarding the severity of the medullary fibrosis in this case, with the moderator suggesting that this was within normal limits for ruminants.

Contributing Institution: State Diagnostic Veterinary Laboratory
Elizabeth Macarthur Agricultural Institute.
Wodbridge Rd, Menangle NSW 2568, Australia
http://www.dpi.nsw.gov.au/research/centres/emai

References:

1. Braun U, Nuss K, Wehbrink D, et al. Clinical and ultrasonographic findings, diagnosis and treatment of pyelonephritis in 17 cows. *The Veterinary Journal.* 2008;175:240-248.
2. Jones TC, Hunt RD, King NW. *Veterinary Pathology*. 6th ed. Baltimore, MD: Williams & Wilkins; 1997:1126-1131.
3. Maxie MG, Newman SJ. Urinary system. In: Maxie MG, ed. *Jubb, Kennedy and Palmer's Pathology of Domestic Animals*. Vol. 2. 5th ed. Philadelphia, PA: Elviser Saunders; 2007:470-494.
4. McKenzie RA. *Australia's Poisonous Plants, Fungi and Cyanobacteria: A Guide to Species of Medical and Veterinary Importance*. Collingwood, Victoria: CSRIO Publishing; 2012:45-46.

5. McKenzie RA. Plant toxicology. In: *Toxicology for Australian Veterinarians.* 1st ed. Brisbane, Queensland; Ross A. McKenzie; 2002:28-36.
6. Rosenbaum A, Guard CL, Njaa BL, et al. Slaughterhouse survey of pyelonephritis in dairy cows. *Vet Rec.* 2005;157:652-655.
7. Stockham SL, Scott MA. *Fundamentals of Veterinary Clinical Pathology.* 2nd ed. Ames, IA: Blackwell Publishing LTD; 2008:393-396, 415-440, 677-681.
8. Takai S, Yanagawa R, Kitamura Y. pH-dependant adhesion of piliated *Corynebacterium renale* to bovine bladder epithelial cells. *Infection and Immunity.* 1980;28(3):669-674.

CASE IV: 0386/10 (JPC 4032715).

Signalment: 20-month-old female landrace goat, (*Capra aegagrus hircus)*.

History: This animal was used for teaching physiology to veterinary students at the Swedish University of Agricultural Sciences. The other goats in the herd were all healthy without respiratory symptoms. The goat had been showing signs of dyspnea for 1.5 weeks and was treated with penicillin without improvement. The animal was anorectic, with a temperature of 39.5°C and started to become dehydrated. The goat was euthanized due to increasing dyspnea.

Gross Pathology: The lungs were pale, enlarged and firm. Cut surfaces showed multiple to diffuse solid, poorly circumscribed, pale areas. Regional lymph nodes (mediastinal and tracheo-bronchial) were severely enlarged and pale with well-defined cortex and medulla structures.

The liver had pale severely fibrotic bile ducts, diffusely. Bilateral mild hyperemia of carpal joints was noted as well as mild meningeal hyperemia.

Laboratory Results: An ELISA with antibodies against CAEV (caprine arthritis-encephalitis virus) was performed on a suspension of lung tissue, post mortem. This test was positive for presence of these antibodies.

Histopathologic Description: The lung displays frequent diffuse eosinophilic homogenous fluid and debris in most of the alveolar spaces and bronchiole lumina. The homogenous fluid also contains a small amount of nuclear debris and degenerating granulocytes. The alveolar septal walls are markedly widened due to multiple foci of necrotic debris and moderate diffuse to multifocal infiltration of lymphocytes. There are also moderate multifocal to diffuse, infiltrates of eosinophils within alveolar and bronchiolar septal walls, and perivascularly adjacent to bronchi. A few follicular accumulations of lymphocytes are present in the septal walls.

There is severe type II pneumocyte hyperplasia and hypertrophy, characterized by typical cuboidal cells outlining the septal walls.

Bronchioli are often difficult to separate from alveoli, since the bronchiolar epithelium is hyperplastic and sometimes necrotic. Bronchiolar lumina are also filled with an eosinophilic exudate and nuclear debris, with degenerating eosinophils. The bronchiolar walls show moderate hypertrophy of the smooth muscles.

The interstitial fibrous tissue septa exhibit mild to moderate diffuse infiltration of eosinophils, dilated blood vessels and moderate edema.

There is diffuse mild subpleural edema.

Occasionally within alveoli there are transverse and longitudinal sections of nematode larvae admixed with eosinophilic debris. In some sections rare adult lung worms are present in alveolar lumina. The distinctive pointed tail that is characteristic of a *Protostrongylidae* was not identified; however, only a single transversely cut adult was seen.

In addition, there is eosinophilic and granulomatous lymphadenitis of the mediastinal and tracheobronchial lymph nodes, as well as lymphohistiocytic (subependymal) encephalitis and meningitis.

Contributor's Morphologic Diagnosis: Lung: Pneumonia, interstitial, chronic, lymphocytic, severe, diffuse with intra-alveolar eosinophilic fluid and hyperplasia of pneumocytes type II and smooth muscles.

Lung: Pneumonia, interstitial, eosinophilic, moderate, multifocal with few intralesional larvae and adults of small lung worm, (family *Protostrongylidae*).

Etiology: CAEV (caprine arthritis-encephalitis virus).

Contributor's Comment: CAEV (caprine arthritis-encephalitis virus) is a *lentivirus* of the family *Retroviridae*, a member of the small ruminant lentiviruses (SRLVs). CAEV causes arthritis in adult goats, neurologic disease in younger animals and pneumonia that can occur concurrently with arthritis and encephalitis.

The disease is characterized by dyspnea, and the respiratory form is closely related to a small

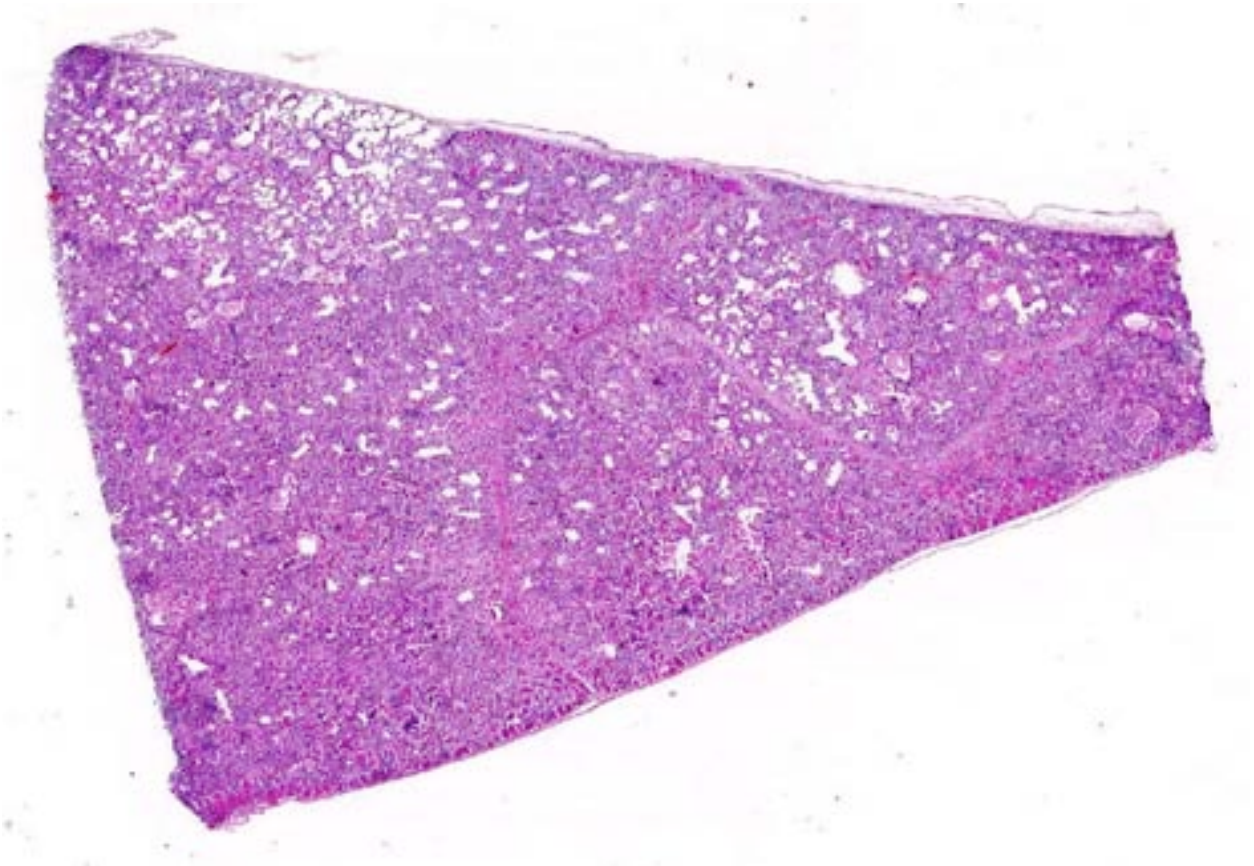

4-1. Lung, goat: The section of lung is diffusely hypercellular with marked thickening of alveolar septa. (HE 0.63X)

ruminant *lentivirus* infection in sheep called maedi, meaning dyspnea in Icelandic. CAEV and maedi-visna virus have also been found as co-infections in naturally infected goats.[4]

The SRLVs cause chronic multi-systemic inflammatory disease and mammary gland epithelium is often infected. Transmission to young animals is through milk (colostrum) via the intestine, or, less commonly, horizontally via the respiratory tract. Transmission from infected domestic goats through milk to Rocky Mountain goats has recently been described,[3] and in these cases a direct transmission between animals also was reported.

The natural infection of the SRLVs is with virus or virus-infected cells through the mucous membranes such as respiratory or intestinal tracts. The tropism of SRLVs is primarily the monocytes/macrophages and dendritic cells. Infected dendritic cells migrate to lymph nodes and transmit the virus to macrophages. The macrophages are then responsible for systemic infection. Persistent infection can be established in bone marrow cells, and infected monocytes continue the transmission of infection to mainly lung, mammary gland, CNS and joints. The immune activation to the viral antigen causes an inflammatory response with mononuclear cells such as lymphocytes, macrophages and plasma cells, which gives the virus access to more macrophages, continuing the inflammation, hence the multi-systemic disease of SRLVs is immunopathogenic (for review see Blacklaws).[1]

The most common tissues involved in SRLV infection are lung, CNS, mammary gland and joint. Other organs such as kidney, liver and heart can also be involved.

The time between infection and clinical disease is dependent on the strain and amount of the virus as well as the genetic background of the host.

CAEV is characterized by chronic interstitial pneumonia with infiltration of lymphocytes into alveolar septa which are lined by a layer of

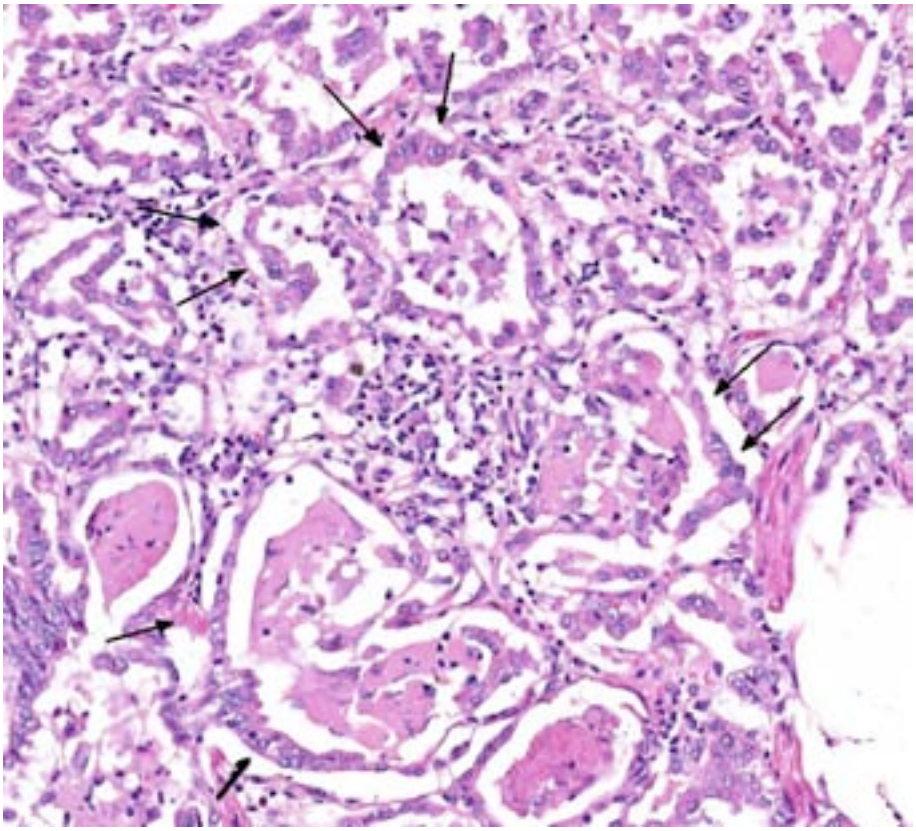

4-2. Lung, goat: Alveolar septa are thickened by collagen, marked type II pneumocytes hyperplasia (arrows), and small aggregates of lymphocytes with fewer histiocytes and plasma cells. (HE 200X)

hyperplastic cuboidal type II pneumocytes, and accumulation of eosinophilic fluid within alveoli.

The exudative form of the acute phase is followed by regenerative lesions characterized mainly by hyperplasia as well as hypertrophy of the type II pneumocytes.

The differential diagnosis for interstitial pneumonia is extensive;[2] however, the typical type II reaction together with accumulation of eosinophilic fluid within alveoli and diffuse infiltration of lymphocytes is typical for CAEV infection. This pneumonia, together with multisystemic involvement including arthritis and encephalitis, further strengthens the diagnosis, which was confirmed by immunological testing.

Muellerius capillaris is a common small (12 -24 mm adults) lungworm of goats and sheep. Infection with this nematode is often characterized by nodular inflammation with eosinophils and giant cells; however, the inflammation depends on the amount of larvae/ adults present in the alveoli. Eggs are rapidly hatched and first-stage larvae are found in alveolar spaces. These are coughed up, swallowed and eventually found in the feces. Intermediate hosts are snails and slugs and the life cycle of the nematode is completed when the goat digests the intermediate host. The larvae will migrate via lymphatics to the lungs and adults can be seen in the alveolar spaces.

Subpleural nodules are a characteristic finding in heavy worm infections, but this was not seen in the present case.

Another member of the family *Protostrongylidae* is *Protostrongylus rufescens*, which measure 16-35 mm. These small lung worms have a similar life cycle to *Muelleris capillaris* and also cause inflammation in the lungs with pulmonary nodules.

The few larvae/adults found in the present case could not be classified on histological slides as *Muellerius* or *Protostrongylus*.

The clinical symptoms and severity of the inflammatory reaction depend on the number of invading worms, the stage of the larvae and the immune status of the animal. The severity of the pneumonia in this case does not correlate with the animal's low parasite burden; thus CAEV infection is a much more likely diagnosis.

JPC Diagnosis: 1. Lung: Pneumonia, interstitial, lymphohistiocytic, chronic, diffuse, severe, with marked type II pneumocyte hyperplasia and alveolar proteinosis.
2. Lung, alveoli: Trichostrongyle larvae, multiple.

Conference Comment: This case is an excellent example of a classic entity, and the contributor provides a thorough review of the disease

pathogenesis, clinical signs and gross and microscopic lesions. Readers are urged to review WSC 2011-2012, Conference 7, case 2 for further discussion of CAEV.

Contributing Institution: Department of BVF, Division of Pathology, Pharmacology & Toxicology, SLU (Swedish University of Agricultural Sciences)
Box 7028, SE-750 07 Uppsala, Sweden
http://www.bvf.slu.se/

References:

1. Blacklaws BA. Small ruminant lentiviruses: immunopathogenesis of visna-maedi and caprine arthritis and encephalitis virus. *Comparative Immunology, Microbiology and Infectious Diseases.* 2012;35:259-269.
2. Panciera JR, Confer AW. Pathogenesis and pathology of bovine pneumonia. *Vet Clin Food Anim*. 2010;26:191-214.
3. Patton MK, Bildfell RJ, Anderson Ml, et al. Fatal caprine arthritis encephalitis virus-like infection in 4 Rocky Mountain goats (*Oreamnos americanus*). *J Vet Diagnostic*. 2012;24(2): 392-396.
4. Pisoni G, Bertonei G, Puricelli M, et al. Demonstration of coinfection with recombination by caprine arthritis-encephalitis virus and maedi-visna virus in naturally infected goats. *J Virol.* 2007;81(10):4948-4955.

Joint Pathology Center
Veterinary Pathology Services

WEDNESDAY SLIDE CONFERENCE 2013-2014

Conference 18

12 March 2014

CASE I: N13-46 (JPC 4032911).

Signalment: 13-year-old Bay Warmblood mare (*Equus caballus*).

History: Since December 2012 the horse has had fever and increased respiratory rate. The horse started being treated by Baytril and Naxcel, but did not improve. At this time, the animal was presented to Tufts University Cummings School of Veterinary Medicine. Transtracheal aspirate (TTA) fluid was cultured, but no pathogen was found. Thoracic radiographs show that the lung has a diffuse, severe, interstitial, and nodular pattern. The TTA fluid was positive for equine herpesvirus 5 by PCR test. The biopsy of lung tissue reveals fibrotic changes. Later, the mare developed laminitis and was humanely euthanized.

Gross Pathology: All lung lobes contain multifocal to coalescing, firm, white to tan, variably-sized, slightly-raised nodules, ranging from 0.5 cm x 0.3 cm x 15 cm to 15 cm x 9 cm x 7 cm. The cut surface of the nodules is tan and firm. Lung parenchyma between the nodules is dark red and markedly congested. The tracheobrochial lymph nodes are enlarged ranging from 5 cm x 3 cm x 2.5cm to 9 cm x 4 cm x 3 cm. The midsagittal section of hoof of both forelimbs revealed the dorsal surface of third phalanx is widely separated (up to 0.5 cm) from the epidermal laminae of the inner surface of hoof wall with ventral rotation of the tip of the third phalanx. The space between them is filled with tan-white firm tissue.

Laboratory Results: Transtracheal aspirate (TTA)

1. PCR test: Equine herpesvirus 5 positive
2. Bacterial culture: Negative

Histopathologic Description: In a multifocal to regionally extensive area, the alveolar septa are variably thickened up to 3 times by fibrous connective tissue composed of well differentiated to plump fibroblasts admixed with moderate to high numbers of foamy macrophages, neutrophils, lymphocytes, plasma cells, and necrotic cellular and karyorrhectic debris. The alveoli are lined by plump cuboidal cells (type II pneumocyte hyperplasia) and filled with moderate to marked numbers of giant foamy macrophages, intact and degenerate neutrophils, and necrotic epithelial cell debris with karyorrhexis and karyolysis. Occasionally, macrophages contain up to 5 µm diameter eosinophilic to amphophilic intranuclear inclusion bodies that marginate chromatin.

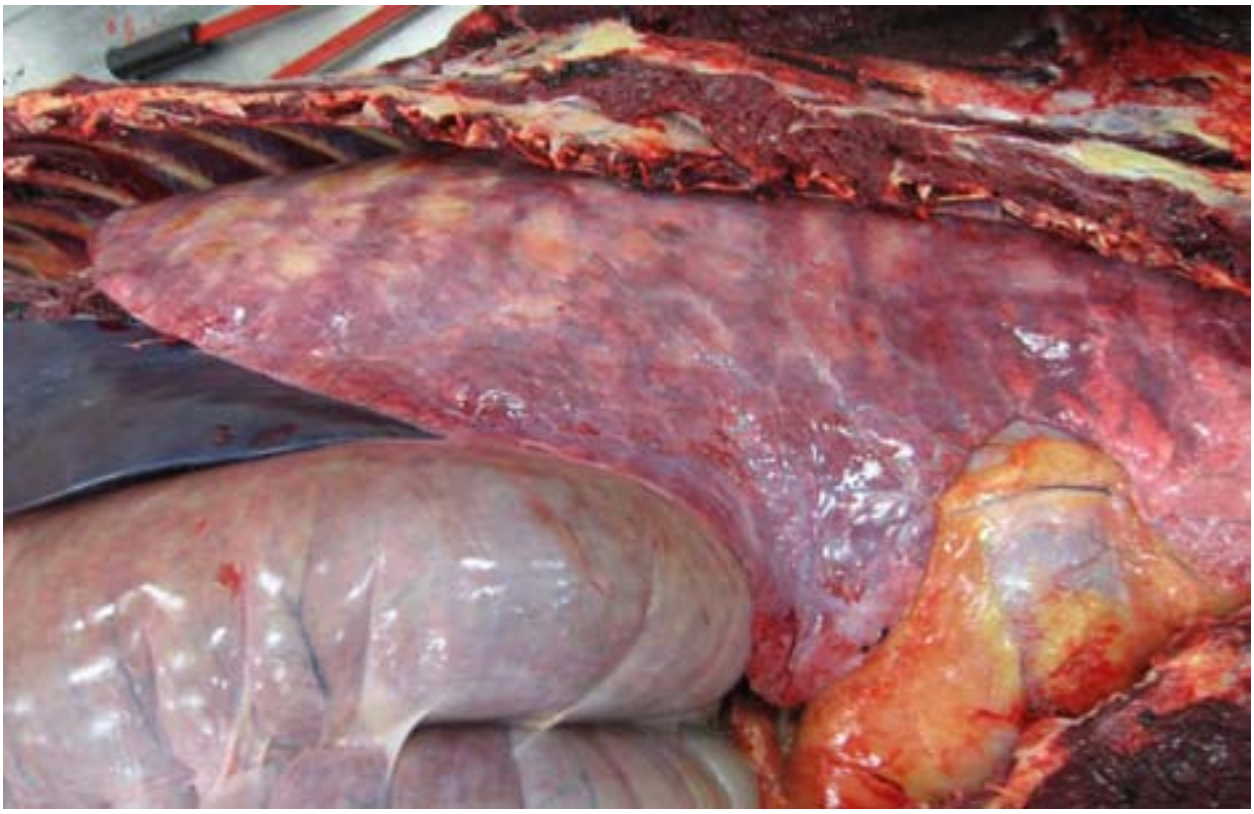

1-1. Lung, horse: All lung lobes contain multifocal to coalescing, firm, white to tan, variably-sized, slightly-raised nodules. (Photo courtesy of: Section of Pathology, Department of Biomedical Science, Tufts Cummings School of Veterinary Medicine http://vet.tufts.edu/dbs/pathology.html

Bronchi and bronchioles within the affected areas contain a minimal to mild amount of cellular and karyorrhectic debris sometimes with few degenerate neutrophils. Occasionally, bronchi have mild epithelial hyperplasia. Multifocally, there is moderate perivascular, peribronchial and peribronchiolar fibrosis admixed with moderate number of macrophages, lymphocytes, plasma cells, and few neutrophils. Multifocally, the adjacent relatively normal lung parenchyma has mild amounts of eosinophilic, homogenous, acellular material in the alveoli and the interstitia is diffusely thickened by increased clear spaces (edema).

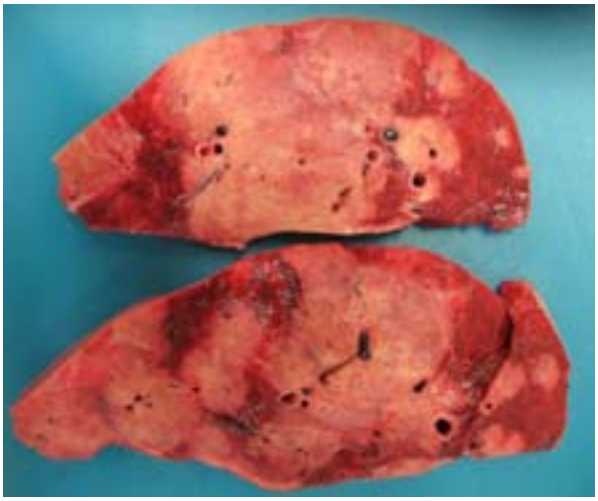

1-2. Lung, horse: The cut surface of the nodules is tan and firm. Lung parenchyma between the nodules is dark red and markedly congested. (Photo courtesy of: Section of Pathology, Department of Biomedical Science, Tufts Cummings School of Veterinary Medicine http://vet.tufts.edu/dbs/pathology.html

Contributor's Morphologic Diagnosis: Multifocal to regionally extensive moderate pulmonary fibrosis and bronchointerstital pneumonia with intrahistiocytic intranuclear viral inclusion bodies consistent with equine multinodular pulmonary fibrosis.

Contributor's Comment: Equine multinodular pulmonary fibrosis (EMPF) is a recently reported fibrotic interstitial lung disease in adult horses.[5] No breed or sex predilection was determined. The mean age of affected horses was 13 years. The common clinical presentations are weight loss, pyrexia, and tachypnea.[5,6] Thoracic radiographs often demonstrate an interstitial to nodular pulmonary pattern. Grossly, there are two

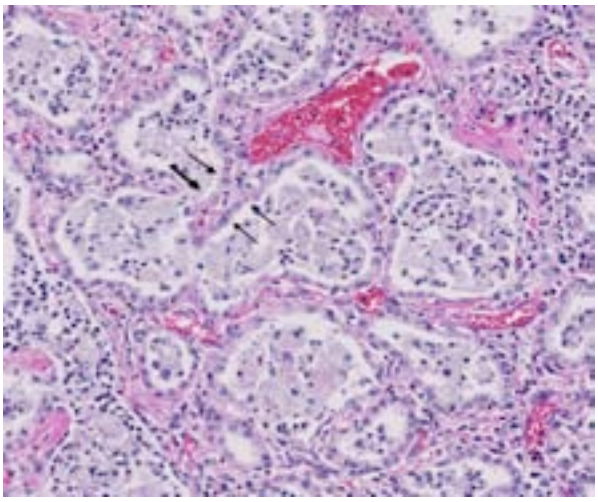

1-3. Lung, horse: Alveolar septa are markedly expanded by fibrous connective tissue and lined by type II pneumocytes (arrows). (HE 168X)

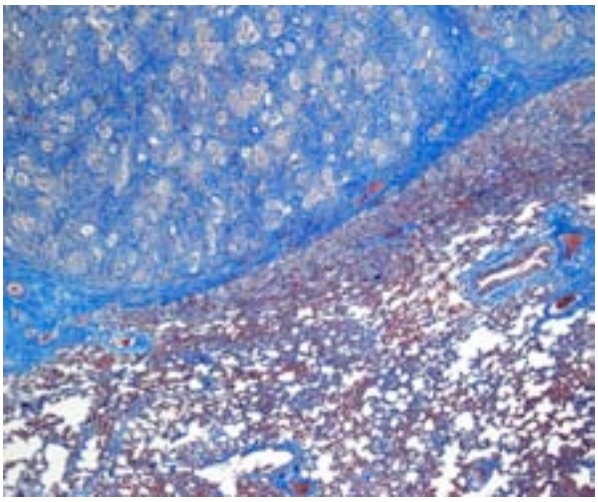

1-4. Lung, horse: A Masson's trichrome stain demonstrates the amount of fibrous connective expanding alveolar septa. (Masson's trichrome 4X)

major manifestations. The more common lesions are numerous pale tan-white, coalescing, firm nodules, involving all lung lobes. Sometimes, the lesions form masses, which makes it difficult in differentiating from neoplasia. The borders are discrete where they meet unaffected lung. The less common one often only demonstrates multiple discrete nodules separated by grossly normal lung.[5] Histopathologically, there is often marked multifocal and regionally extensive interstitial and alveolar septa fibrosis with often preservation of cuboidal epithelial cells (type II pneumocytes) forming alveolar-like structures. The lumen of the structures is often filled with mild to moderate number of intact and degenerate neutrophils, macrophages and cellular and karyorrhectic debris. Dark eosinophilic intranuclear viral inclusion bodies may be seen in the foamy macrophages.[4-6]

Equine herpesvirus 5 (EHV-5), a gamma herpesvirus, is consistently detected in the lung tissue of affected horses.[1,4-6] And, compared to other tissues, lung has a remarkably higher viral load than in other organs, especially within the pulmonary fibrotic lesions. These evidences support the high correlation between EHV-5 and EMPF.[4] Interestingly, equine herpesvirus 2 and asinine herpesvirus 5 (AHV5), another two types of gammaherpes viruses, may also be detected in the lesions.[1,4] Although these gammaherpes viruses are detected in the lesions, the pathogenic roles of them are currently still unclear.

JPC Diagnosis: Lung: Pneumonia, interstitial, necrotizing and fibrosing, focally extensive, severe, with marked type II pneumocyte hyperplasia, neutrophilic and histiocytic alveolitis, and rare intrahistiocytic viral intranuclear inclusion bodies.

Conference Comment: Conference participants observed that pleural arteries are often quite prominent, with hypertrophied smooth muscle within the tunica media and abundant collagen; this is likely an indication of severe pulmonary hypertension secondary to diffuse fibrosis. The differential diagnosis for the gross and histopathological lesions in this case includes silicate pneumoconiosis, which generally exhibits variable amounts of granulomatous inflammation in association with pulmonary interstitial fibrosis;[5] idiopathic pulmonary fibrosis, which more commonly affects foals than adults and is attributed to diffuse alveolar damage;[1,5] paraquat/diquat toxicosis, which, although rare, also causes fulminant pulmonary fibrosis;[2] and exercise-induced pulmonary hemorrhage, which has large areas of pulmonary fibrosis admixed with numerous hemosiderophages.[2] Participants also noted that the fibrosis in this case did not appear as nodular as normally described in cases of EMPF; this led to the suggestion of equine herpes virus (EHV)-1, which is most notorious as a cause of abortion in horses, but may also cause respiratory disease and encephalomyelitis, or EHV-4 (equine rhinopneumonitis virus) as possible etiologies.[3]

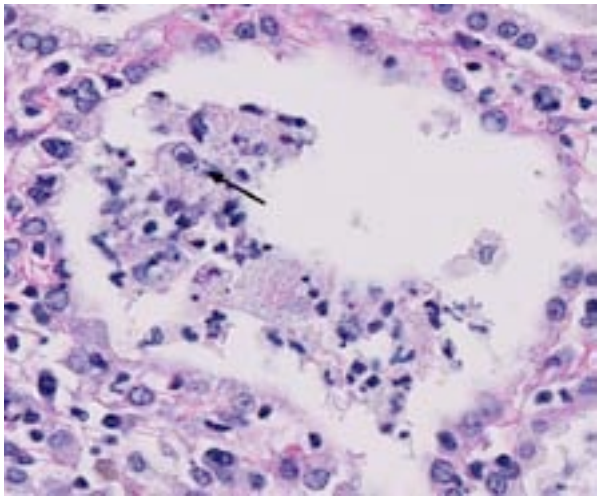

1-5. Lung, horse: Rarely, alveolar macrophages contain a single, intranuclear viral inclusion body. (HE 400X)

In conference, the moderator led a detailed review of the immune response as it relates to this case, touching upon various general pathology concepts such as the components of innate immunity (see WSC 2013-2014 conference 3, case 1 for an abridged examination of toll-like receptors), the cellular and humoral arms of the adaptive immune response, the MHC molecule, and potential paths of differentiation for T-helper cells (see WSC 2013-2014 conference 2, case 2 for a review of T_H1 versus T_H2 reactions). Additionally, participants briefly discussed an interstitial pneumonia of donkeys which has been reported in association with asinine herpesvirus. This disease differs from EMPF in that it is a diffuse inflammatory disease with syncytial cell formation without viral inclusions; interstitial fibrosis is considered a secondary component.[5]

Contributing Institution: Section of Pathology
Department of Biomedical Science
Tufts Cummings School of Veterinary Medicine

References:

1. Back H, Kendall A, Grandón R, et al. Equine multinodular pulmonary fibrosis in association with asinine herpesvirus type 5 and equine herpesvirus type 5: a case report. *Acta Vet Scand*. 2012;54:57.
2. Caswell JL, Williams KJ. Respiratory system. In: Maxie MG, ed. *Jubb, Kennedy and Palmer's Pathology of Domestic Animals*. Vol 2. 5th ed. Philadelphia, PA: Elsevier; 2007:549, 574-575.
3. MacLachlan NJ, Dubovi EJ. *Fenner's Veterinary Virology*. 4th ed. London, UK: Academic Press; 2011:188-190.
4. Marenzoni ML, Passamonti F, Lepri E, et al. Quantification of Equid herpesvirus 5 DNA in clinical and necropsy specimens collected from a horse with equine multinodular pulmonary fibrosis. *J Vet Diagn Invest*. 2011;23(4):802-806.
5. Williams KJ, Maes R, Del Piero F, et al. Equine multinodular pulmonary fibrosis: a newly recognized herpesvirus- associated fibrotic lung disease. *Vet Pathol*. 2007;44:849–862.
6. Wong DM, Belgrave RL, Williams KJ, et al. Multinodular pulmonary fibrosis in five horses. *J Am Vet Med Assoc*. 2008;232:898–905.

CASE II: KAHDL 8398 (JPC 4035597).

Signalment: 7-year-old gelded male mixed breed pony, (*Equus ferus caballus*).

History: The horse was a seven-year-old mixed breed gelded pony kept in a grassy pasture and fed a diet of hay and grain. Two weeks prior to euthanasia, the horse was in the proximity of strong winds and tornados which leveled several buildings on the adjacent property. For approximately 5-7 days after the storm, the pony avoided its pasture-mate (another horse) and human contact. During this time, he avoided being touched on the left and seemed lethargic. Thereafter he returned to normal behavior but two days prior to euthanasia he was unable to eat and held his head at the water trough without seeming to drink much. He progressively developed a generalized weakness and had difficulty standing. He avoided contact with his head (i.e., became "head-shy") and started to have intermittent trembling of his lips and mouth. The owners tried rinsing his mouth with salt water and thoroughly examined the oral cavity (by touch). Given the progression of clinical signs and poor prognosis, owners elected euthanasia.

Gross Pathology: A seven-year-old gelded mixed breed horse with a body condition score of 2 out of 5 and mild to moderate autolysis (16 hour post-mortem interval) was received for necropsy and rabies testing. On oral exam there were moderate lingual points on the mandibular cheek teeth and buccal points on the maxillary check teeth. The spleen had an approximately 12-15 cm long laceration of the parietal surface opposite the stomach and extending transversely over the middle of the organ. The laceration site had organizing blood clots (red but with visible surrounding contraction and pallor (fibrosis)). Numerous 2-8 mm brown red nodules were scattered throughout the omentum in the area of the ruptured spleen. The cervical spinal cord had a focal area of hemorrhage and swelling at approximately the level of C1-C2.

2-1. Spinal cord, horse: There is a focal area of hemorrhage unilaterally within the dorsal horn. (HE 0.63X)

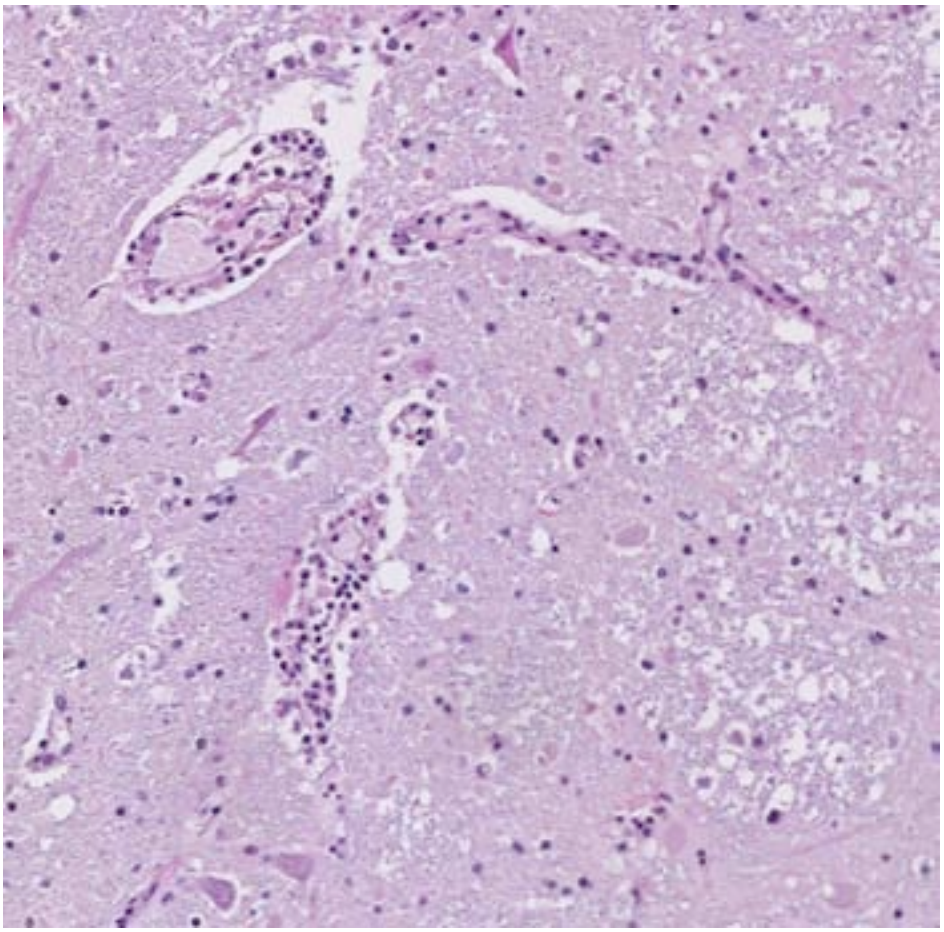

2-2. Spinal cord, horse: Blood vessel walls and surrounding parenchyma are expanded by edema and are surrounded and rarely infiltrated by moderate numbers of lymphocytes and plasma cells. Rabies inclusions were not seen in this individual. (HE 140X)

Laboratory Results: Rabies virus fluorescent antibody was positive for rabies. Speciation of the virus was interpreted as the North Central United States and California skunk rabies.

Histopathologic Description: The section of spinal cord has multifocal perivascular cuffing by 2-4 layers of mononuclear cells dominated by lymphocytes with fewer histiocytes and occasional plasma cells. Most vessels are lined by plump endothelial cells and a focus of vessels near the tip of a dorsal funiculus is surrounded by amorphous eosinophilic material (high-protein edema fluid or an autolyzed area of hemorrhage). Axon sheaths in this area frequently contain macrophages (axonophagia) or dilated nerve processes (spheroids). Within the gray matter, neurons frequently have loss of nissl substance and nuclear material (chromatolysis) and there are multifocal small aggregates of glial cells (Babe's nodules).

Contributor's Morphologic Diagnosis: Diffuse non-suppurative and hemorrhagic vasocentric encephalomyelitis with neuronolysis with focal myelomalacia and hemorrhage.

Contributor's Comment: This case was challenging clinically because of the seemingly waxing and waning history. Nevertheless, the referring veterinarian had some concern about rabies at the time of submission. The lesion on the spleen and the history immediately after the local tornado activity are thought to represent the effects of blunt trauma from an airborne projectile. It was not until the three days preceding euthanasia that the horse was thought to be showing signs attributable to rabies.

Antemortem diagnosis of rabies remains problematic, but the disease should be considered in horses whenever there are rapidly progressing and/or diffuse neurologic signs. Differentials for rabies include hepatoencephalopathy, Eastern equine encephalitis, herpesviral encephalomyelopathy, protozoal encephalomyelitis, nigropallidal encephalomalacia, botulism, lead poisoning, cauda equine neuritis, meningitis, space-occupying masses, CNS trauma, or esophageal obstruction.[4]

Equine rabies can also be challenging to diagnose on necropsy. Numerous cases of disease confined to the spinal cord in horses have been reported making it advisable to include spinal cord in routine rabies testing in horses.[1] Horses are also

unique in that their lesions often are associated with significant hemorrhage making it a consideration for focal spinal lesions associated with hemorrhage. Finally, as is demonstrated in this case, greater than half of the rabies cases in horses do not have identifiable Negri bodies.[2]

JPC Diagnosis: Spinal cord, gray matter: Neuronal degeneration, multifocal, moderate, with mild gliosis and lymphoplasmacytic meningitis.

Conference Comment: Although the contributor identified multifocal small nodules of glial cells, known as Babe's nodules,[4] most conference participants did not appreciate this feature. The anatomic location as well as the subtle microscopic findings and lack of Negri bodies in this case engendered some difficulty in arriving at a diagnosis of rabies; many participants suspected an alternate viral etiology, such as Eastern equine encephalitis (alphavirus) or West Nile virus (flavivirus).

Rabies virus is an enveloped RNA virus of the family *Rhabdoviridae* and the genus *Lyssavirus*; it causes meningoencephalomyelitis, ganglionitis and parotid adenitis, is almost invariably fatal, and is capable of affecting any mammalian species. Following infection with the virus, herbivores, unlike carnivores, are typically dead-end hosts. Reservoir hosts may vary temporally and regionally; among the most common are foxes, skunks, raccoons, feral dogs, wolves, jackals and mongoose. Fructivorous, insectivorous and vampire bats are also capable of transmitting rabies virus. Rabies viral neurotropism is due to a viral coat protein known as rabies virus glycoprotein (RVG), which binds several neural tissue receptors, including neuronal cell adhesion molecule (NCAM) and the p75 neurotrophin receptor (p75NTR). Virus inoculation typically occurs through contaminated saliva entering bite wounds inflicted by rabid animals. Initial viral replication occurs in myocytes adjacent to the bite wound, with subsequent invasion of the local neuromuscular junction and, eventually, the CNS and paravertebral ganglia via axoplasmic flow. Following viral replication in the CNS, there is centrifugal spread to salivary glands, nasal mucosa and adrenal glands.[3,4]

Three clinical manifestations of rabies are described: dumb, furious, and paralytic forms. The two most common clinical signs in affected mammals are progressive paralysis and aberrant behavioral patterns. In addition, horses in particular can have clinical signs associated with spinal cord injury, such as pelvic limb lameness, proprioceptive defects, ataxia, paralysis, and colic. Other reported species-specific features of the clinical progression of rabies include the following: cattle commonly exhibit excessive salivation and vocalization, swine are often found dead with no preceding clinical signs, sheep display passive behavior and dogs appear agitated or anxious. There are typically no gross lesions, although in horses infection may be associated with spinal cord hemorrhage. Historically, intracytoplasmic viral inclusions (i.e., Negri bodies) occur in the Purkinje cells of the cerebellum in herbivores and in neurons of the hippocampus in carnivores. In most mammalian species, Negri bodies are identified in 70% to 85% of affected animals; however, in horses this figure falls to 30% to 50%.[3,4] As an example of equine rabies with lesions limited to the spinal cord, without demonstrable Negri bodies, this case illustrates the potential variability of gross and histopathologic findings associated with rabies virus infection.

Contributing Institution: Kord Animal Health Diagnostic Lab
Ellington Agricultural Center
Porter Building
436 Hogan Road
Nashville, TN 37220
http://www.tn.gov/agriculture/regulatory/kord.shtml

References:

1. Boone A, Susta L, Rech R, et al. Pathology in practice. *J Am Vet Med Assoc*. 2010;237(3): 277-279.
2. Green S, Smith L, Vernau W, et al. Rabies in horses: 21 cases (1970-1990). *J Am Vet Med Assoc*. 1992;200:1133-1137.
3. Maxie MG, Youssef S. Nervous system. In: Maxie MG, ed. *Jubb, Kennedy and Palmer's Pathology of Domestic Animals*. Vol 1. 5th ed. Philadelphia, PA: Elsevier; 2007:413-416.
4. Reed S, Bayly W, Sellon D, eds. *Equine Internal Medicine*. St. Louis, Missouri: Saunders; 2004:644-646.

CASE III: 12-258-13 (JPC 4032444).

Signalment: 36-year-old male chimpanzee, (*Pan troglodytes*).

History: The chimpanzee was found dead. There was no history of prior illness, other than a single episode of vomiting several days prior to death.

Gross Pathology: The intact heart is moderately, diffusely enlarged and weighs 497.3 grams. The heart:BW ratio is 0.68 (normal 0.54 - 0.60). There are multifocal streaks of pale, firm fibrosis, predominantly within the left ventricular free wall, interventricular septum, and apex of the heart. The right ventricle appears mildly dilated. Additionally, there is a focal discrete, white, firm 2 cm diameter multicystic nodule within the superficial to mid cortex of the right kidney.

Histopathologic Description: There is moderate to severe, multifocal to coalescing myocardial fiber degeneration, characterized by myocardiocyte pallor and loss of cross striations. There is multifocal, moderate cardiac myofiber disorganization and separation and replacement of myofibers by pale pink, predominantly mature fibrous connective tissue (fibrosis) and adipose tissue. There is significant fibrosis at the base of the mitral valve. The cardiac myocardial fiber nuclei are frequently moderately enlarged, basophilic, and bizarre. Minimal, light brown intracytoplasmic granular pigment (lipofuscin) is present in scattered myocytes. Rare, minimal to mild atherosclerotic changes are seen in random coronary arterioles, characterized by few mural macrophages, foamy cells and eosinophilic matrix material. There is multifocal mild lymphocytic and lesser histiocytic inflammation within the areas of fibrosis or surrounding degenerate myofibers and within the epicardial connective tissue.

Contributor's Morphologic Diagnosis: Heart: Moderate to severe, multifocal to coalescing, chronic myocardial degeneration and fibrosis with mild multifocal chronic myocarditis.

Contributor's Comment: Cardiomyopathy was first reported in the chimpanzee in 1984, and the initial case report describes a 26-year-old male chimpanzee with history of heart murmur progressing to weight loss, heart failure, and coma

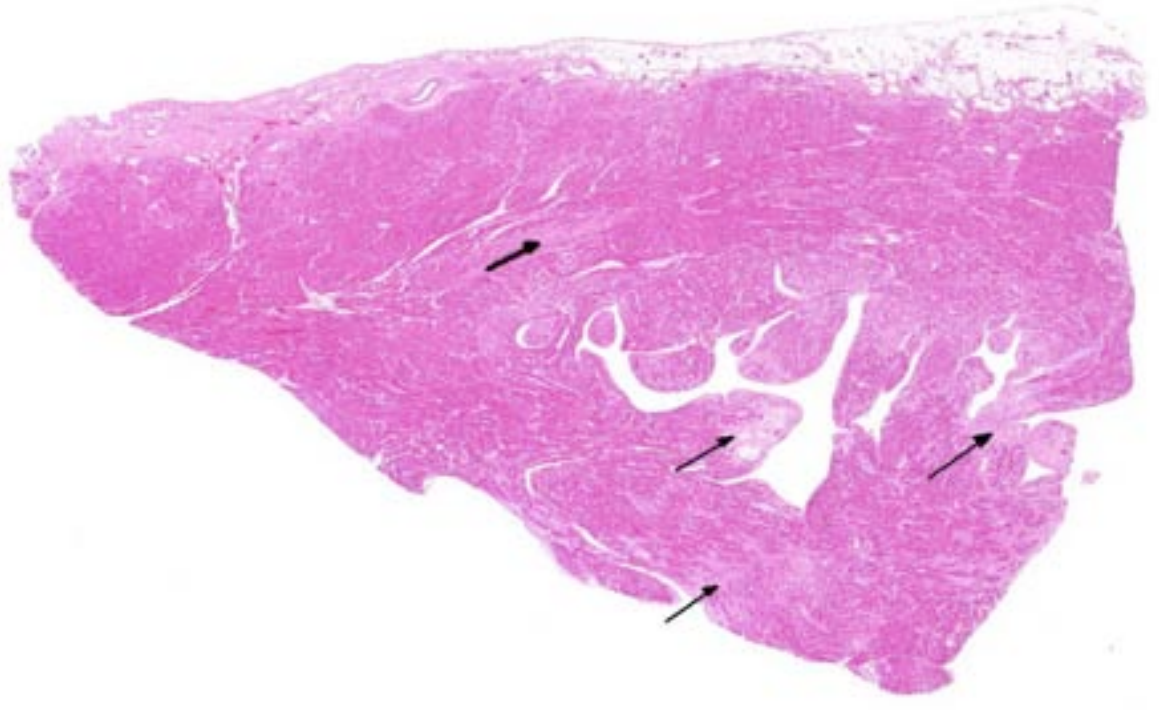

3-1. Heart, chimpanzee: Throughout the myocardium, there are numerous areas of myofiber loss and replacement by fibrous connective tissue (arrows). (HE 0.63X)

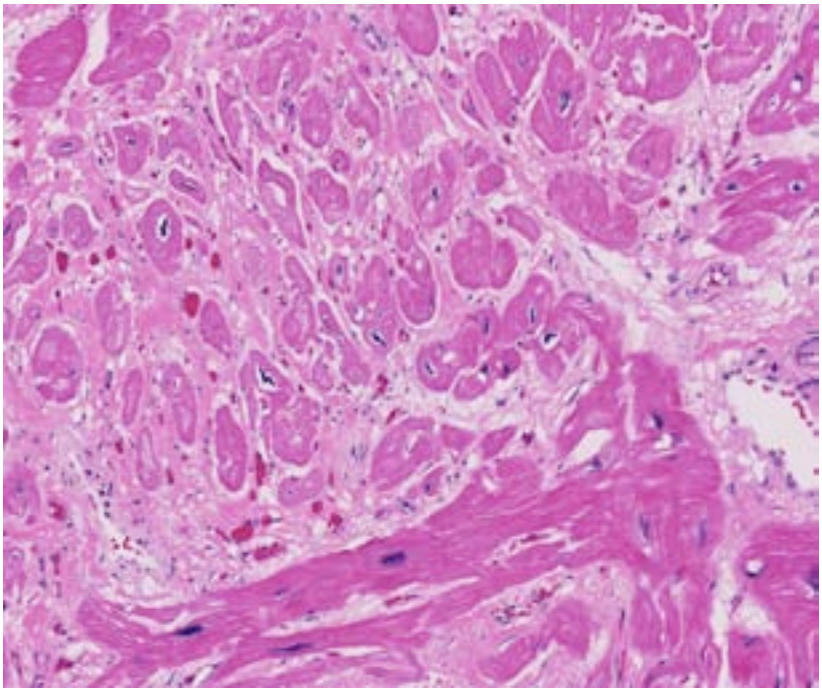

3-2. Heart, chimpanzee: Within areas of fibrosis, remaining myofibers are often atrophic and contain enlarged basophilic nuclei. (HE 116X)

over a 10 month period.[2] Gross lesions in this case included dilated cardiomyopathy, pericardial effusion, cerebral infarct, and hepatomegaly, and cardiac histopathology showed myocardial fibrosis and coronary atherosclerosis.[2] Subsequently, interstitial myocardial fibrosis has emerged as a major cause of heart disease and sudden death in chimpanzees, and in most cases there are no associated lesions of atherosclerosis.[3] Sudden death is thought to be secondary to conduction abnormalities and arrhythmias. A 2009 study of 87 adult chimpanzees found a 68% prevalence of heart disease and a 52% prevalence of idiopathic cardiomyopathy, with heart disease the primary cause of death.[5] In another study, interstitial myocardial fibrosis was identified as the most common cause of sudden death in chimpanzees, and was present in 92% cases of sudden cardiac death and 81% cases of all sudden death.[5] In humans, myocardial fibrosis occurs secondary to systemic hypertension, myocarditis, cardiomyopathy, or as response to myocardial injury, and can be a replacement (scarring) response to injury such as myocardial infarction or reactive and triggered by external stimuli such as pressure or volume overload.[5] In great apes, myocardial fibrosis with atrophy and hypertrophy of cardiac myocytes occurs with minimal or no inflammation and often no apparent cause or associated disease.[5] Potential biomarkers for myocardial fibrosis in chimpanzees have been investigated, and brain natriuretic protein and cardiac troponin I were elevated in cases of cardiovascular disease in one report.[1] In this study, neither a lipid panel including cholesterol, LDL, and triglycerides nor hsCRP, one of the best biomarkers for indicating ischemic disease in man, were useful in the diagnosis of heart disease in chimpanzees.[1]

JPC Diagnosis: Heart: Fibrosis, multifocal, moderate, with myofiber degeneration, atrophy and loss.

Conference Comment: The contributor provides an excellent overview of cardiomyopathy in great apes; the microscopic lesions in this case are consistent with this well-documented condition. Interestingly, myocyte degeneration and fibrosis appear most severe in the subendocardial and subepicardial tissue, while sparing the rest of the myocardium; the clinical significance of this finding is unknown. Additionally, moderate numbers of Anitschkow cells, also known as caterpillar cells due to their wavy nuclei, are present within affected areas of myocardium. These are thought to be macrophages or attempts at myofiber regeneration and are found in the myocardium in certain disease states.[4] Other striking features include widespread cardiomyocyte hypertrophy, characterized by fiber thickening and a change in nuclear morphology from spindle/cigar shaped to a “box car” like (rectangular) silhouette (see WSC 2013-2014, case conference 17, case 2), as well as frequently enlarged, bizarre cardiomyocyte nuclei. Conference participants speculated that these nuclear changes may represent abortive attempts at regeneration.

Contributing Institution: University of Washington
Department of Comparative Medicine (http://depts.washington.edu/compmed/)
Washington National Primate Research Center (www.wanprc.org/)

References:

1. Ely JJ, Zavaskis T, Lammey ML, et al. Association of brain-type natriuretic protein and cardiac troponin I with incipient cardiovascular disease in chimpanzees (*Pan troglodytes*). *Comp Med*. 2011;61:163-169.
2. Hansen JF, Alford PL, Keeling ME. Diffuse myocardial fibrosis and congestive heart failure in an adult male chimpanzee. *Vet Path*. 1984;21:529-531.
3. Lammey ML, Baskin GB, Gigliotto AP, et al. Interstitial myocardial fibrosis in a captive chimpanzee (*Pan troglodytes*) population. *Comp Med*. 2008;58:389-394.
4. Maxie MG, Robinson WF. Cardiovascular system. In: Maxie MG, ed. *Jubb, Kennedy and Palmer's Pathology of Domestic Animals*. Vol 3. 5th ed. Philadelphia, PA: Elsevier; 2007:35.
5. Seiler BM, Dick EJ, Guardado-Mendoza R, et al. Spontaneous heart disease in the adult chimpanzee (*Pan troglodytes*). *J Med Primatol*. 2009;38:51-58.

CASE IV: 46184-1 (JPC 4001561).

Signalment: 8-month-old female sheep, (*Ovis aries*).

History: The lamb had been growing well until 4 weeks earlier when it was noticed to have edematous ears and was lying in the shade during the day. Over the following 4 weeks the lamb progressively lost weight and skin sloughed from around the eyes, the dorsal aspect of both ears, and on the face. The owner elected euthanasia on humane grounds because the lamb had not shown any signs of improvement and was constantly rubbing its face and ears.

Gross Pathology: On post-mortem examination, adipose tissue throughout the carcass was pale yellow. The liver was normal in shape, but slightly firm and had a bronze discoloration. No other gross abnormalities were apparent.

Histopathologic Description: Throughout the section, portal triads are variably expanded by increased numbers of bile ductules and loose fibrous connective tissue infiltrated with moderate numbers of lymphocytes and plasma cells. Many large and medium-sized bile ductules are lined by dysplastic epithelial cells and surrounded by an edematous adventitia containing capillaries and reactive fibroblasts. Some large ducts have been either completely replaced by edematous granulation tissue or are represented by a markedly attenuated lumen. Occasional large blood vessels in portal regions have segmental thickening of their wall adjacent to damaged bile ducts. Scattered aggregates of neutrophils and occasional foci of fibrosis are present in the parenchyma but hepatocytes are unaffected.

Contributor's Morphologic Diagnosis: Subacute lymphocytic/plasmacytic cholangitis with periductular edema, replacement fibrosis and recanalization.

Contributor's Comment: These hepatic lesions are typical of those caused by exposure to sporidesmin, a toxin produced by the fungus *Pithomyces chartarum.* This fungus grows readily on dead plant material in ryegrass pastures and spores containing sporidesmin can reach high levels during periods of warm, moist weather, as often occurs during the fall. Sporidesmin toxicity is an important cause of production loss, ill thrift and sometimes death in ruminants and camelids in the North Island of New Zealand. The disease is also reported in southern Australia and South Africa. The disease is characterized by hepatogenous photosensitivity and is commonly known in New Zealand as facial eczema.

Large and medium-sized intrahepatic and extrahepatic bile ducts are the primary target of the toxin and may become attenuated or completely occluded in severe cases. The changes in these ducts is virtually pathognomonic for sporidesmin toxicity,[3,4,6] the portal fibrosis and biliary ductular hyperplasia representing non-

4-1. Haired skin, sheep: This 8-month old female lamb progressively lost weight, and skin sloughed from around the eyes, the dorsal aspect of both ears and on the face. (Photo courtesy of: Institute of Veterinary, Animal, and Biomedical Sciences, Massey University, Tennant Drive, Palmerston North, New Zealand)

4-2. Liver, sheep: The liver was normal in shape, but was slightly firm and had a bronze discoloration. (Photo courtesy of: Institute of Veterinary, Animal, and Biomedical Sciences, Massey University, Tennant Drive, Palmerston North, New Zealand)

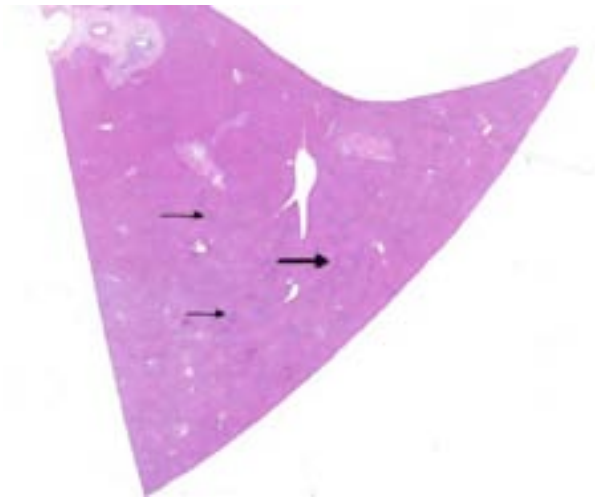

4-3. Liver, sheep: Within the section, the adventitia of bile ducts is edematous, and portal triads are prominent due to their hypercellularity (arrows). (HE 0.63X)

specific secondary changes following blockage of larger ducts.

Although lesions occur throughout the liver, the left (ventral) lobe is affected more severely than the right lobe. In chronic cases, especially those where animals are exposed to sublethal doses over more than one year, the left lobe may be markedly atrophic and exist only as a fibrous remnant, sometimes containing small remnants of hyperplastic hepatocytes. In such cases, the right lobe is typically hypertrophic and the liver is rounded in shape.

Subacute sporidesmin toxicity is characterized by a marked increase in the serum activity of GGT (often well above 1000 IU/L), which remains elevated for several months following exposure to the toxin.

JPC Diagnosis: Liver: Biliary hyperplasia, diffuse, marked, with reactive dysplasia, moderate portal and bridging fibrosis and mild lymphoplasmacytic portal hepatitis.

Conference Comment: Although conference participants were not provided with gross necropsy findings or the clinical history of facial eczema, most suspected a toxic etiology based upon the presence of portal and bridging fibrosis. Moreover, the prominent biliary hyperplasia led many participants to consider toxins that target the biliary epithelium, specifically the mycotoxin sporidesmin; however, the differential diagnosis for these lesions must also include phomopsin, *Lantana*, aflatoxin and pyrrolizidine alkaloid hepatotoxicity, as well as the South African condition known as geeldikkop.

Phomopsin is a mycotoxin produced by the saprophytic fungus *Phomopsis leptostromiformis*, which commonly infects lupines; it is a potent microtubule inhibitor that results in mitotic arrest during metaphase. Thus, in addition to biliary hyperplasia and hepatic fibrosis, this condition is characterized microscopically by the presence of numerous bizarre mitoses. Phomopsin toxicosis is also associated with hepatogenous photosensitivity.[1,5] Toxic pentacyclic triterpenes (especially Lantadene A, B, and C) from the shrub *Lantana camara* induce hepatic cholestasis, icterus and hepatogenous photosensitization in ruminants, primarily cattle. *Lantana* hepatotoxicosis is distinguished histologically by megalocytosis, bile accumulation and bile duct proliferation.[5] Saponins of the South African plant *Tribulus terrestris* (alone or in combination with sporidesmin) are likely responsible for geeldikkop ("yellow bighead") in sheep, which is characterized by hepatocyte vacuolation and Kupffer cell hyperplasia in acute toxicosis, and the presence of crystalline material within bile ducts in chronic intoxication.[5]

Aflatoxicosis and pyrrolizidine alkaloid toxicity are less commonly associated with photosensitivity in sheep and are considered less likely causes in this case. Of the numerous types

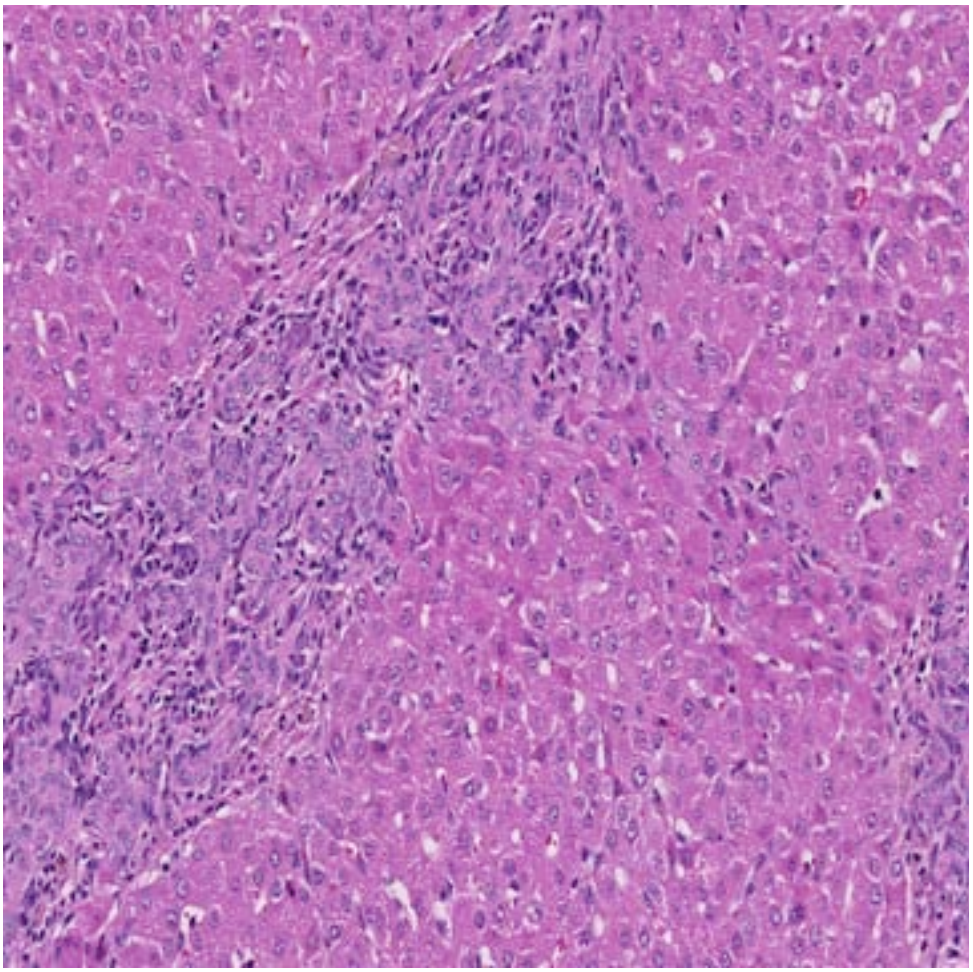

4-4. Liver, sheep: Portal triads are expanded by marked biliary reduplication, and mild fibrosis which often breaches the limiting plate and bridges to adjacent portal areas. (HE 118X)

of aflatoxin reported, the most common is aflatoxin B1, which is typically produced by *Aspergillus* sp. Following metabolism by hepatic cytochrome p450 enzymes, in species that lack adequate glutathione-s-transferase, toxic metabolites cause multiple carcinogenic, toxic and teratogenic effects. In the liver, histological features include hepatocellular necrosis in acute cases, and hepatic fibrosis, hepatocellular megalocytosis and biliary hyperplasia in more chronic cases. Pyrrolizidine alkaloids from *Senecio, Crotalaria* and *Heliotropium* sp. are metabolized via hepatic cytochrome p450 enzymes into dehydropyrrolizidine (DHP) derivatives, which cause similar hepatic lesions to those described for aflatoxicosis. Sheep are thought to be relatively resistant to both aflatoxin and pyrrolizidine alkaloid toxicity; cattle, horses, farmed deer, and pigs are most susceptible.[1,5]

Photosensitization is generally classified into three broad categories: types 1, 2 and 3 (see included table). Type 1, or primary photosensitization occurs following ingestion of preformed photodynamic toxins, such as hypericin in St. John's Wort, fagopyrin in buckwheat, and certain drugs, including phenothiazine and tetracycline. Type 2 photosensitization is due to congenital enzyme deficiencies resulting in endogenous pigment accumulation. Bovine congenital hematopoietic porphyria results from deficient levels of uroporphyrinogen III cosynthetase, a key enzyme in heme biosynthesis. Porphyrins subsequently accumulate in dentin and bone, causing the teeth and bone to appear pink and fluoresce upon exposure to ultraviolet radiation. Porphyrins also accumulate in the skin, where they cause necrosis, likely via induction of reactive oxygen species or xanthine oxidase. Affected cattle are anemic, and the accumulated pigments are excreted in the urine, which appears brown. Bovine erythropoietic protoporphyria, on the other hand, is an autosomal recessive condition in Limousin cattle caused by a defect in ferrochelatase, which allows accumulation of protoporphyrin IX in the blood and tissue. This disease is characterized solely by the presence of photodermatitis. There is no anemia, and the teeth, bones and urine are not discolored. Facial eczema, as demonstrated in this case, is associated with type 3, or hepatogenous, photosensitization. This is the most common form. It occurs in conjunction with primary hepatocellular damage

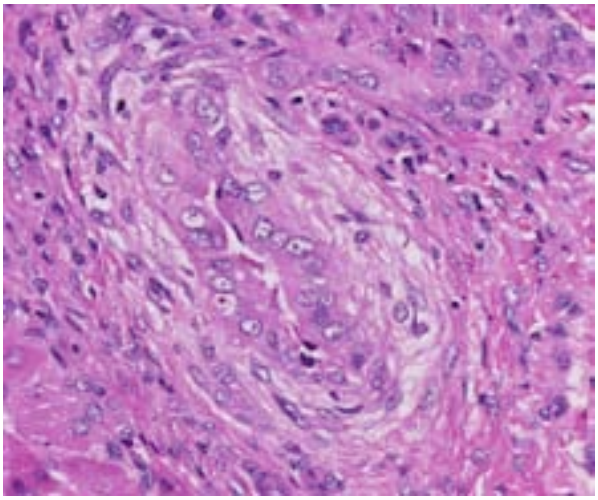

4-5. Liver, sheep: Bile ducts are lined by dysplastic epithelium, which exhibits markedly enlarged anisokaryotic nuclei and multinucleated cells. (HE 288X)

(or, less commonly, bile duct obstruction) and is due to impaired hepatic excretion of the potent photodynamic agent, phylloerythrin. Phylloerythrin is a breakdown product of chlorophyll, formed by microbes in the gastrointestinal tract and transported via portal circulation; hepatocytes normally take up phylloerythrin and excrete it into bile. In animals on a chlorophyll-rich diet and generalized hepatic damage, phylloerythrin builds up in various tissues, including the skin. The distribution of the photodermatitis is similar in all types of photosensitization; it is generally confined to sparsely-haired, lightly pigmented, sunlight exposed areas of the skin.[2]

Table: Categories of photosensitization.[2]

Type	Causes
Type 1: Primary	Ingestion of preformed **photodynamic toxins** in plants and drugs: • St. John's Wort (hypericin) • Buckwheat (fagopyrin) • Phenothiazine
Type 2	Congenital **enzyme deficiencies** resulting in endogenous pigment accumulation: • Uroporphyrinogen III cosynthetase deficiency (bovine congenital hematopoietic porphyria) • Ferrochelatase deficiency (bovine erythropoietic protoporphyria)
Type 3: Hepatogenous	Build-up of **phylloerythrin** due to generalized hepatocellular damage or bile duct obstruction

Contributing Institution: Institute of Veterinary, Animal and Biomedical Sciences
Massey University
Tennant Drive, Palmerston North, New Zealand

References:

1. Gelberg HB. Alimentary system and the peritoneum, omentum, mesentery and peritoneal cavity. In: Zachary JF, McGavin MD, eds. *Pathologic Basis of Veterinary Disease*. 5th ed. St. Louis, MO: Elsevier; 2012:439-442.
2. Ginn PE, Mansell JE, Rakich PM. Skin and appendages. In: Maxie MG, ed. *Jubb, Kennedy and Palmer's Pathology of Domestic Animals*. Vol 1. 5th ed. Philadelphia, PA: Elsevier; 2007:623-626.
3. Mortimer PH, Stanbridge TA. Changes in biliary secretion following sporidesmin poisoning in sheep. *Journal of Comparative Pathology*. 1969;79:267-275.
4. Smith BL, Embling PP. Facial eczema in goats: the toxicity of sporidesmin in goats and its pathology. *New Zealand Veterinary Journal*. 1991;39:18-22.
5. Stalker MJ, Hayes MA. Liver and biliary system. In: Maxie MG, ed. *Jubb, Kennedy and Palmer's Pathology of Domestic Animals*. Vol 2. 5th ed. Philadelphia, PA: Elsevier; 2007:368-381.
6. Thompson KG, Jones DH, Sutherland RJ, Camp BJ, Bowers DE. Sporidesmin toxicity in rabbits: biochemical and morphological changes. *Journal of Comparative Pathology*. 1983;93:319-329.

Joint Pathology Center
Veterinary Pathology Services

WEDNESDAY SLIDE CONFERENCE 2013-2014

Conference 19

19 March 2014

CASE I: No label (JPC 4004355).

Signalment: 1-year-old intact female Sprague-Dawley rat, (*Rattus norvegicus*).

History: A one-year-old intact female experimentally naïve Sprague-Dawley rat (NTac:SD) used as a soiled bedding sentinel was noted to have buphthalmia of the right eye and had multiple foci of white tissue within the anterior chamber, in addition to a Y-shaped band of tissue (2mm in diameter) present within the posterior chamber. The vasculature surrounding the pupil was prominent and the anterior chamber was cloudy. Apart from the ocular lesion, the animal appeared to be in good health. The animal

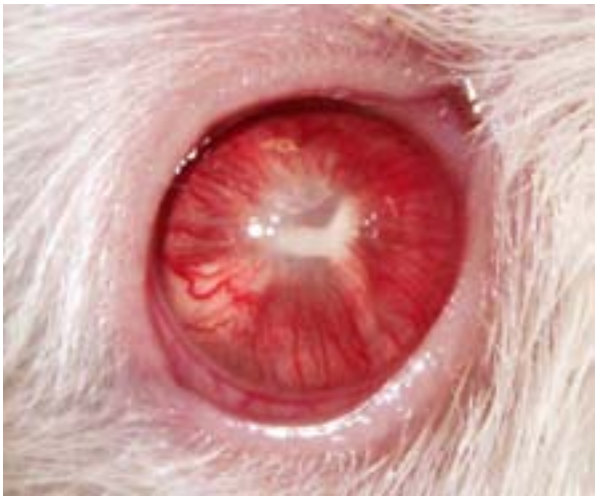

1-1. Eye, SD rat: The right eye was bupthalmic and had multiple foci of white tissue within the anterior chamber in addition to a Y-shaped band of tissue (2mm in diameter) present within the posterior chamber. The vasculature surrounding the pupil was prominent and the anterior chamber was cloudy. (Photo courtesy of: Laboratory of Comparative Pathology, Memorial Sloan Kettering Cancer Center, 1275 York Av Box 270, New York, NY 10065)

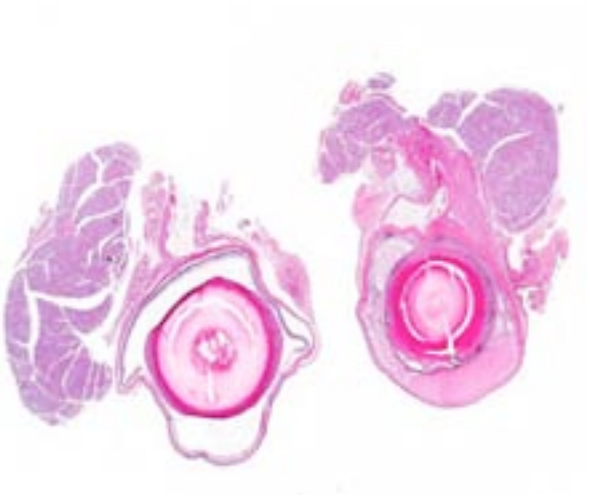

1-2. Eye, SD rat: The affected eye on right shows a marked protein effusion filling the anterior chamber as well as a posterior synechia and mineralization subjacent to the lens capsule. Normal eye at left for comparison. (HE 0.63X)

was monitored and the lesion showed no signs of progression. The animal was later euthanized for routine sentinel testing.

Gross Pathology: Gross lesions were observed in the right eye, as described in the history. No other gross changes were observed on complete necropsy.

Histopathologic Description: Right eye: The lens is misshapen and has a wrinkled capsule. Multifocally extensive areas of loss of sub-capsular lenticular fibers (both on anterior and posterior surfaces) and replacement by mineralized debris are evident. Lenticular epithelium is hyperplastic and there is migration of epithelium to the posterior lens surface. Several lenticular epithelial cells are spindle-shaped (fibrous metaplasia).

Multifocal adhesions between the lens and posterior surface of the iris (posterior synechiae) are present. Extensive fibrovascular membranes are present and are adhered to the ciliary body, posterior lens capsule, and choroid (cyclitic membranes). The retina shows full thickness atrophy. The iris shows mild vascular congestion. The iris, ciliary body and choroid are thickened by fibroplasia and an inflammatory infiltrate composed of numerous lymphocytes, and moderate numbers of plasma cells, eosinophils, neutrophils and hemosiderin-laden macrophages, with multifocal formation of lymphocytic aggregates in the choroid. Remnant spaces in the posterior chamber that are bordered by cyclitic membranes are filled with eosinophilic homogenous proteinaceous fluid.

The anterior chamber is filled with eosinophilic homogenous proteinaceous fluid (plasmoid aqueous).

Left eye (section not provided): Within normal limits.

Contributor's Morphologic Diagnosis: Right eye:
1. Marked panuveitis, lymphocytic, with posterior synechiae and cyclitic membranes, chronic.
2. Hypermature cataract, subcapsular, chronic.
3. Retina: Marked retinal atrophy, chronic.

Contributor's Comment: Histopathological changes in the right eye are consistent with advanced cataract, and other changes within the eye suggest phacolysis (lens protein leakage) leading to secondary uveitis (phacolytic uveitis). The pathogenesis is suspected to be leakage of lenticular protein from the lens (even with intact lens capsule) leading to uveal inflammation. Predominant lymphocytic uveitis present in this case is also consistent with phacolysis leading to secondary uveitis. The Y-shaped macroscopic appearance of the aforementioned cataract is similar to the congenital sutural cataract that occurs along the suture lines of the lens in humans and may also be observed as a late change in advanced cataracts of other etiologies. Although

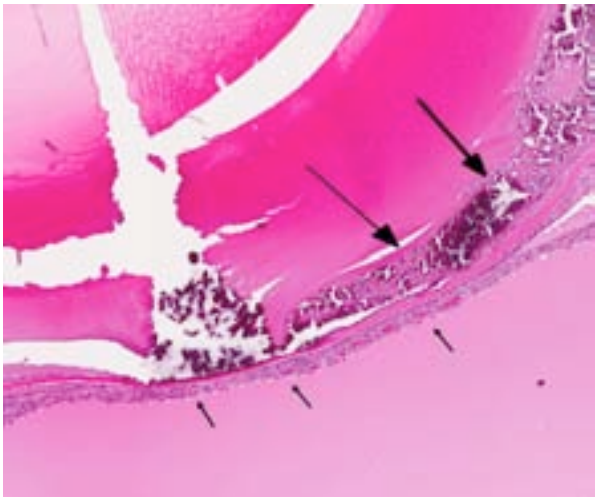

1-3. Eye, SD rat: Higher magnification of the adherence of the iris to the lens capsule (posterior synechia) (small arrows) as well as loss of subcapsular lens fibers with replacement by mineralized debris. (Large arrows). (HE 41X)

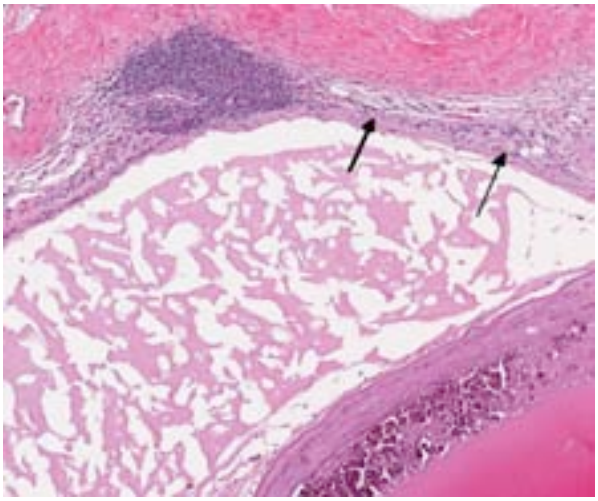

1-4. Eye, SD rat: The lens is in direct apposition to the retina at right. At left, the vitreous is markedly diminished and there is severe full thickness retinal atrophy (arrows). Underneath the wrinkled lens capsule, there is fibrous metaplasia of lens fibers adjacent to areas of mineralization.

suture lines are present in both anterior and posterior lens capsules, it is the posterior capsular suture lines that manifest a characteristic Y-shape grossly when cataract forms along its margins. Some forms of non-congenital mature cataracts can progress along suture lines.

Cataracts are commonly associated with aging in various strains, including Sprague-Dawley (SD) rats. No sex predilection for the development of cataracts has been reported in the literature. Capsular cataracts, specifically posterior sub-capsular cataracts, are noted with increasing incidence starting at week 57 of age in SD rats (Week 57- 2.7%, Week 83- 8.5% and Week 110-13.4%).[1] Diffuse opacification of the lens along the posterior suture lines has also been reported in this strain.[1] Anterior cortical striations that can eventually progress to senile cataracts are commonly seen in SD rats between 83 and 110 weeks.[1] It is interesting to note that this case has hypermature cataract in both anterior and posterior subcapsular regions. It is difficult to ascertain the region where the cataract first started. However, based on the reported age-based incidence, it is speculated that the posterior subcapsular region is the first site of cataract formation. It is also possible that both anterior and posterior regions co-evolved the cataractous change independently of one another.

Approximately 3-4% of Sprague-Dawley rats have minor lens lesions comprised of foci of swollen or degenerate lens fibers starting as early as 19-20 days of gestation and these may represent early changes that may eventually lead to cataract.[2] Glaucoma has been described as a complication of advanced cataracts in rats, and the proposed pathogenesis was lens-induced uveitis.[3]

JPC Diagnosis: Eye: Uveitis, lymphoplasmacytic, chronic, diffuse, severe, with cataract formation, drainage angle occlusion, and posterior synechiae.

Conference Comment: Cataract is the most common lens disorder in any domestic species; it can be distinguished microscopically from fixation/sectioning artifact by (in order of occurrence) detection of Morgagnian globules (eosinophilic globules of denatured lens protein), bladder cells (large, foamy nucleated cells that may represent abortive epithelial attempts at new lens fiber formation), lens epithelial hyperplasia and/or posterior migration of lens epithelium (occasionally followed by fibrous metaplasia), and mineralization. Hypermature cataracts often exhibit residual nuclei within lakes of proteinaceous fluid, surrounded by a wrinkled capsule. Cataracts can be inherited (i.e. familial cataracts in dogs) or secondary to anatomic anterior segment anomalies; formation may also be induced by a variety of stimuli, including solar (or other) irradiation, cold, increased intraocular pressure, toxins, nutritional derangements, local inflammation and direct trauma. Most cataracts encountered within veterinary medicine are classified as inherited, post-inflammatory or idiopathic; however, cataract formation due to canine diabetes, galactose accumulation in kangaroos and wallabies raised on cow's milk, arginine deficiency in puppies, wolf cubs, or kittens on milk replacer, dietary deficiencies (in sulfur-containing amino acids, zinc or vitamin C) or solar irradiation in farmed fish and administration of the aminoglycoside hygromycin B in sows, have also been described, although the pathogenesis of these examples is not necessarily fully elucidated.[4] Additionally, as noted by the contributor, cataract formation is a common age-related change in several strains of rats.

In this case, we concur with the contributor's comprehensive histological description as well as the proposed pathogenesis. The formation of age-induced cataracts likely resulted in lens protein leakage (phacolysis), with subsequent phacolytic uveitis, occlusion of the drainage angle, increased intraocular pressure, glaucoma and eventually, full thickness retinal atrophy.

Contributing Institution: Laboratory of Comparative Pathology
MSKCC
1275 York Av Box 270
New York, NY 10065

References:

1. Taradach C, Regnier B, Perraud J. Eye lesions in Sprague-Dawley rats: type and incidence in relation to age. *Lab Anim*. 1981;15(3):285-287.
2. Taradach C, Greaves P. Spontaneous eye lesions in laboratory animals: incidence in relation to age. *Crit Rev Toxicol*. 1984;12(2): 121-147.
3. Wegener A, Kaegler M, Stinn W. Frequency and nature of spontaneous age-related eye lesions

observed in a 2-year inhalation toxicity study in rats. *Ophthalmic Res*. 2002; 4:281-287.
4. Wilcock BP. Eye and ear. In: Maxie MG, ed. *Jubb, Kennedy and Palmer's Pathology of Domestic Animals*. Vol 1. 5th ed. Philadelphia, PA: Elsevier; 2007:494-497.

CASE II: E3236/07 (JPC 3164800).

Signalment: 8-year-old neutered male Cairn terrier, (*Canis familiaris*).

History: Surgical extirpation of the bulbus, further clinical data not available.

Gross Pathology: None.

Histopathologic Description: Replacing, infiltrating and expanding the optic nerve disc and proximal parts of the optic nerve origin is a moderately circumscribed, densely cellular neoplasm extending bilaterally into the choroid and the retrobulbar adipose tissue. The mass is separated by a thin fibrovascular stroma into nests of closely packed predominantly epithelioid cells or spindle to polygonal cells arranged in loosely interlacing streams and whorls. In areas extending into the choroid variable numbers of melanin-containing cells are intermingled in the stroma. Neoplastic cells have variably distinct borders with varying amounts of eosinophilic cytoplasm, oval to spindle-shaped and occasionally vesicular nuclei with finely stippled chromatin and predominantly one distinct nucleolus. Epithelioid cells forming small nests often show abundant eosinophilic cytoplasm and eccentric nuclei. Mitotic rate is less than one mitotic figure per high power field. Multifocally, especially in extrabulbar parts of the mass are foci of myxoid, cartilaginous or osseous metaplasia. Multifocally, mainly perivascularly, there are few lymphocytes, plasma cells, neutrophils and intermingled with some pigment (hemosiderin) laden macrophages.

Additionally, segments of the retina adjacent to the tumor are mildly atrophic.

Contributor's Morphologic Diagnosis: Eye, optic nerve: Meningioma, optic nerve type, canine.

Contributor's Comment: In dogs and cats, meningiomas are the most common primary tumor arising in the nervous system.[7] In the dog they occur more commonly in the brain than in the spinal cord.[4,7] Those arising in the brain are often localized over the convexities, attached to the falx or the tentorium cerebelli or inside the ventricular system. Rarely they occur retrobulbarly.[3,7] In general intracranial meningiomas are slow growing, discrete, expansile neoplasms and malignant behavior or extracranial metastases are only rarely reported.[1,6] Due to the embryonic origin of the meninges from both mesoderm and neural crest, they can undergo mesenchymal and epithelial differentiation and show highly variable morphological patterns.[7] The current World Health Organization (WHO)

2-1. Eye, dog: A cross section of the globe shows an infiltrative neoplasm expanding the optic nerve, and expanding laterally underneath the detached retina, and protruding into the posterior chamber (arrows). (HE 0.63X)

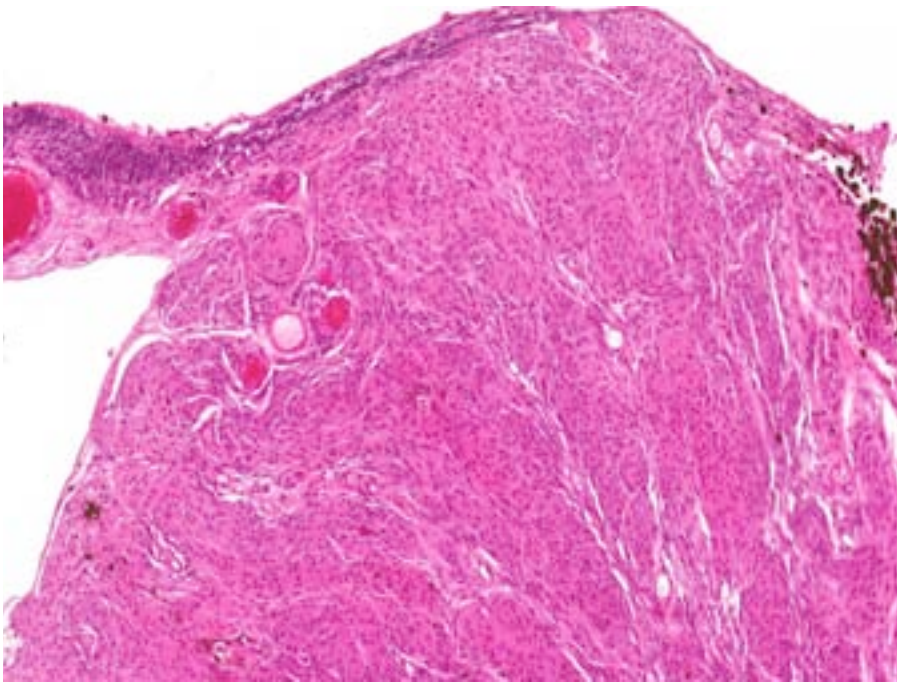

2-2. Eye, dog: Underneath the detached atrophic retina, neoplastic cells are arranged in discrete bundles and whorls characteristic of meningioma. There are aggregates of melanin containing cells, likely from the infiltrated choroid. (HE 140X)

classification of tumors of the nervous system in domestic animals[2] describes nine histological patterns: meningothelial, fibrous (fibrobroblastic), transitional (mixed), psammomatous, angiomatous, papillary, granular cell, myxoid and anaplastic (malignant). Montoliu et al. reviewed 30 cases of meningiomas and divided into transitional, meningothelial, psammomatous, anaplastic, fibroblastic, angioblastic, papillary, microcystic and those types arising from the optic nerve.[5] The latter were characterized predominantly by meningothelial or transitional patterns and contained multiple areas of myxoid, cartilaginous and osseous metaplasia. Because of this distinctive morphology they suggested to include optic nerve meningiomas into the classification as a separate entity. The case presented here qualifies for this type due to localization and histological appearance.

Immunohistochemically, most of the cases stain positive for vimentin, less often also for cytokeratin, pointing to a more mesenchymal and less epithelial differentiation. Expression of S-100 protein and neuron-specific enolase (NSE) is inconstant and rarely a predominant feature.[5]

JPC Diagnosis: Eye, optic nerve: Meningioma with acute neural retinal detachment.

Conference Comment: The contributor provides an excellent summary of canine intra- and

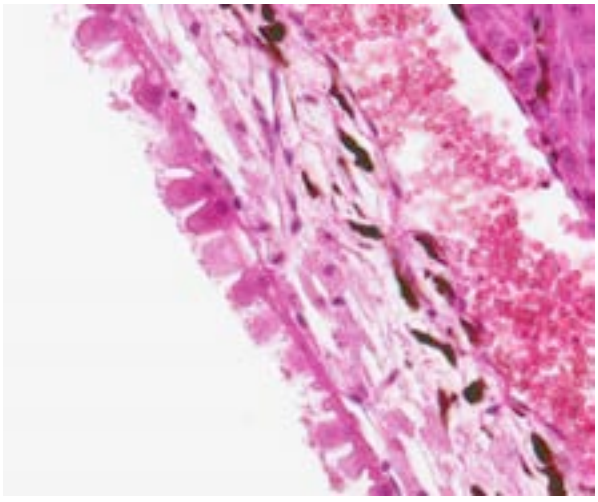

2-3. Eye, dog: The retinal pigmented epithelial cells are markedly hyperplastic ("tombstoned"), indicating that the retinal detachment occurred prior to sectioning. (HE 256X)

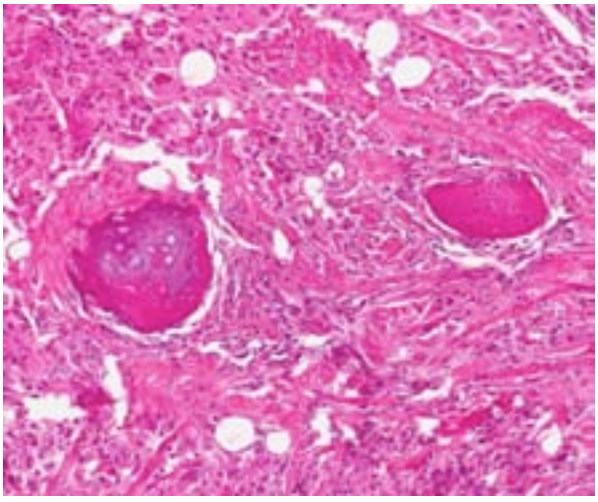

2-4. Eye, dog: Scattered foci of metaplastic bone are present within the neoplasm. (HE 180X)

extracranial meningioma. In addition to the distinct neoplastic features described above, participants observed a striking separation of the retinal pigment epithelium (RPE) from the photoreceptors (i.e., neural retina) with diffuse, marked hypertrophy ("tombstoning") and multifocal cystic degeneration of the RPE, as well as pockets of proteinaceous fluid and few neutrophils within the subneural retinal space. There is also mild retinal atrophy, as noted by the contributor. These histopathological findings support an additional diagnosis of neural retinal detachment, which refers specifically to a separation between the neural retina and the RPE. Neural retinal detachment was likely secondary to locally infiltrative neoplastic cells cleaving photoreceptors from their interdigitations with the RPE. Conversely, artifactual retinal separation is a common sequela of formalin fixation, and is distinguished from pathologic retinal detachment by the absence of RPE hypertrophy and absence of fluid and/or inflammatory cells in the subneural retinal space.[8,9]

Contributing Institution: Department of Veterinary Pathology
Freie Universitaet
Berlin, Germany
http://www.vetmed.fu-berlin.de/einrichtungen/institute/we12/index.html

References:

1. Dugan SJ, Schwarz PD, Roberts SM, Ching SV. Primary optic-nerve meningioma and pulmonary metastasis in a dog. *Journal of the American Animal Hospital Association*. 1993;29:11-16.
2. Koestner A, Bilzer T, Fatzer R, Schulman FY, Summers BA, van Winkle TJ. *World Health Organization: Histological Classification of Tumors of the Nervous System of Domestic Animals*. Washington, DC: Armed Forces Institute of Pathology; 1999.
3. Mauldin EA, Deehr AJ, Hertzke D, Dubielzig RR. Canine orbital meningiomas: a review of 22 cases. *Vet Ophthalmol*. 2000;3:11-16.
4. Meuten DJ. *Tumors in Domestic Animals*. 4th ed. Ames, IA: Iowa State University Press; 2002:717-723, 753.
5. Montoliu P, Anor S, Vidal E, Pumarola M. Histological and immunohistochemical study of 30 cases of canine meningioma. *J Comp Pathol*. 2006;135:200-207.
6. Schulman FY, Ribas JL, Carpenter JL, Sisson AF, LeCouteur RA. Intracranial meningioma with pulmonary metastasis in three dogs. *Vet Pathol*. 1992;29:196-202.
7. Summers BA, Cummings JF, de Lahunta A. *Veterinary neuropathology*. St. Louis, MO: Mosby; 1995:355-362.
8. Wilcock BP. Eye and ear. In: Maxie MG, ed. *Jubb, Kennedy and Palmer's Pathology of Domestic Animals*. Vol 1. 5th ed. Philadelphia, PA: Elsevier; 2007:518.
9. Yanoff M, Sassani JW, eds. *Ocular Pathology*. 6th ed. London, UK: Mosby Elsevier; 2009:395, 462-463.

CASE III: UW case 1 (JPC 4032969).

Signalment: 17-year-old male neutered domestic shorthaired cat, (*Felis catus).*

History: The cat presented with a 1-year history of severe conjunctivitis and corneal ulceration with secondary corneal sequestrum formation. Clinically, a collapsed anterior chamber, symblepharon, blepharospasm and protrusion of the third eyelid were observed. Additionally, the cat had chronic corneal disease that was considered a sequel to poorly managed feline herpes virus-related keratoconjunctivitis when it was young. Due to a poor prognosis, the eye was enucleated and sent to the Comparative Ocular Pathology Laboratory of Wisconsin (COPLOW) at the University of Wisconsin-Madison.

Gross Pathology: There is diffuse white to tan opacification and thickening of the peripheral cornea and limbus extending concentrically towards the axial cornea. The most axial cornea surface is depressed and ulcerated, presenting moderate brown discoloration at the periphery and center of the ulceration. On cut section the corneal profile, limbus, equatorial sclera, episclera, and ciliary body stroma are expanded by a white, firm and irregular tissue. The anterior surface of the iris is thickened and irregular. The posterior aspect of the globe is grossly normal.

Laboratory Results: Mildly increased intraocular pressure (25mmHg) and positive fluorescein stain in the central cornea.

Histopathologic Description: There is a poorly delineated, highly infiltrative and highly cellular neoplastic tissue infiltrating, expanding and partially replacing the superior and inferior limbus, extending approximately 8 mm into the peripheral cornea, affecting the superficial 2/3 of the stroma. The neoplastic tissue also infiltrates the conjunctival substantia propria, equatorial sclera and episclera, ciliary body stroma, base of the iris and trabecular meshwork causing complete collapse of the iridocorneal angle. A second, distinctive pattern of infiltration is present with the neoplastic cells carpeting the anterior and posterior iris surfaces, the surface of the ciliary body *plicae,* trabecular meshwork beams, and the ulcerated corneal surface, mimicking the corneal epithelium. Neoplastic cells are arranged in cords and nests, sometimes forming anastomosing trabeculae, and are supported by abundant fibrovascular stroma (desmoplastic reaction). Multifocally there is keratinization and sloughing of the neoplastic cells in the center of neoplastic nests. Neoplastic cells present moderate amounts of eosinophilic cytoplasm with variably distinct cell borders, oval nuclei with coarsely stippled chromatin and usually one large central magenta nucleolus. There are 32 mitotic figures in 10 hpf. Cellular pleomorphism is marked with multiple karyomegalic cells and atypical mitotic figures.

3-1. Eye, cat, sagittal section: There is diffuse thickening of the peripheral cornea and limbus and axial corneal ulceration and brown discoloration. (Photo courtesy of: Department of Pathobiological Sciences, School of Veterinary Medicine, University of Wisconsin-Madison, http://www.vetmed.wisc.edu)

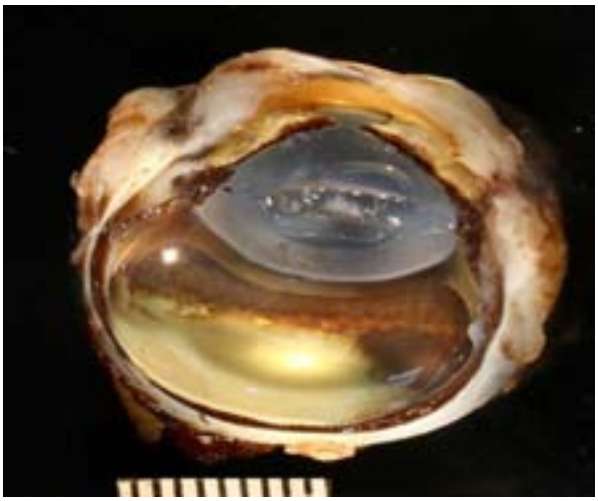

3-2. Eye, cat, sagittal section: Neoplastic tissue infiltrates the corneal, limbus, equatorial sclera and episclera, ciliary body stroma and iris surface. The posterior aspect of the globe is grossly normal. (Photo courtesy of: Department of Pathobiological Sciences, School of Veterinary Medicine, University of Wisconsin-Madison, http:// www.vetmed.wisc.edu)

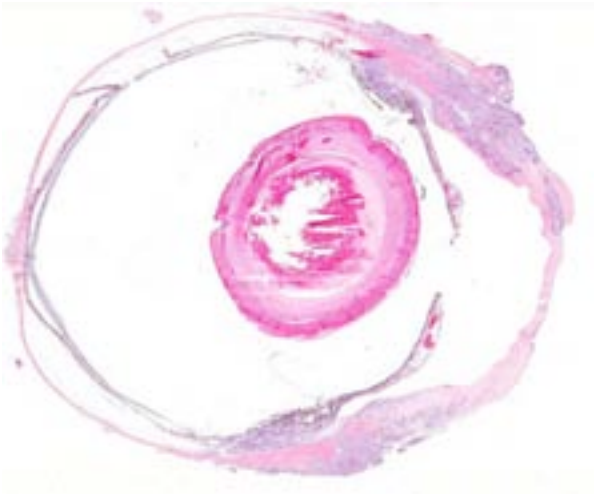

3-3. Eye, cat: The corneal limbus, sclera, uviea, and ciliary body are markedly expanded by an infiltrative neoplasm. (HE 0.63X)

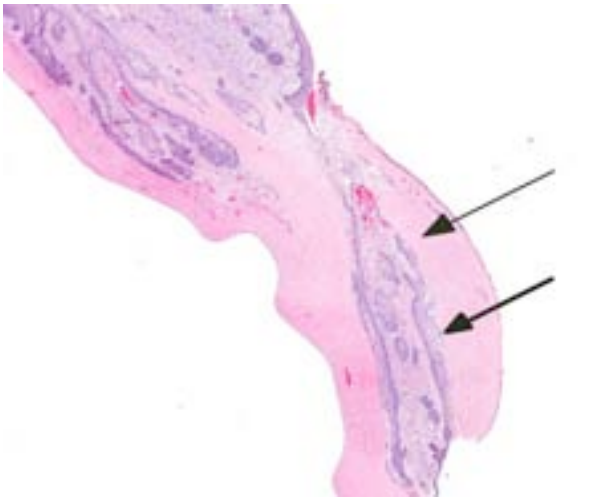

3-4. Eye, cat: Neoplastic cells infiltrate a corneal fissure (arrows). (HE 14X)

Neoplastic cells are also seen infiltrating and completely filling and expanding multiple vascular profiles in the equatorial sclera, ciliary body and iris stroma, and peripheral and peri-papillary choroid. There is diffuse corneal ulceration and marked loss of axial corneal stroma (facet lesion). The peripheral corneal stroma presents focally extensive areas of liquefaction of the corneal lamellae (collagenolysis) with accumulation of fine nuclear debris. There is moderate vascularization of the deep corneal stroma and moderate infiltration of neutrophils. There are diminished numbers of ganglion cells in the inner retina.

Contributor's Morphologic Diagnosis: 1. Eye, Metastatic carcinoma.
2. Cornea, severe and diffuse ulcerative and collagenolytic keratitis with axial facet lesion formation.
3. Retina, Marked and diffuse ganglion cell layer atrophy.

Contributor's Comment: Metastases to the eye are less frequently diagnosed than primary ocular tumors.[1,2,3,4] Despite this, the rich vascularization of the uveal tissue and the immune privilege associated with the intraocular environment favor the globe as a site for metastatic disease.[2] Ocular metastases have been diagnosed in cats with many forms of malignant neoplasia. Pulmonary carcinoma, squamous cell carcinoma of undetermined origin, mammary adenocarcinoma and fibrosarcoma are the most commonly reported.[1,3] There are 4,542 cases of feline ocular neoplasia in the COPLOW collection database. Of those, 580 are metastatic tumors (12%), 423 of which are lymphoma (72%). The remaining 157 metastatic, non-lymphoma cases are described in Table 1.

Table 1. Cases of feline metastatic tumor to the eye on the COPLOW database

	Cases	%
Feline ocular tumors (total)	4542	
Feline metastatic tumors to the eye	580	12% of total cases
1. Lymphomas	423	72% of metastatic cases
1. Non-lymphoma	157	28% of metastatic cases
a. Undifferentiated neoplasia	5	3.1% of non-lymphomas
a. Sarcoma	25	15.9% of non-lymphomas
a. Carcinoma	127	81% of non-lymphomas
- Undifferentiated carcinoma	74	58.2% of carcinomas
- Pulmonary carcinoma	24	18.8% of carcinomas
- Squamous cell carcinoma	24	18.8% of carcinomas
- Mammary carcinoma	3	2.3% of carcinomas
- Anal sac adenocarcinoma	1	0.7% of carcinomas
- Uterine carcinoma	1	0.7% of carcinomas

3-5. Eye, cat: Neoplastic cells carpet the ulcerated corneal surface and multifocally infiltrate the superficial corneal stroma (arrow). (HE 100X) (Photo courtesy of: Department of Pathobiological Sciences, School of Veterinary Medicine, University of Wisconsin-Madison, http://www.vetmed.wisc.edu)

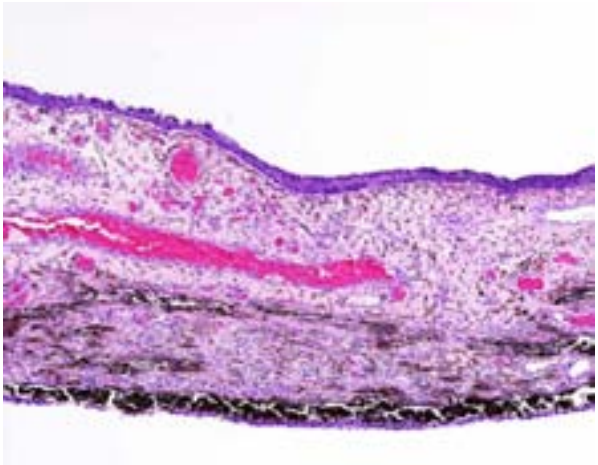

3-6. Eye, cat: Neoplastic cells carpet the anterior and posterior iris surface. (HE 100X) (Photo courtesy of: Department of Pathobiological Sciences, School of Veterinary Medicine, University of Wisconsin-Madison, http://www.vetmed.wisc.edu)

Common morphologic features of metastatic neoplasia in cat eyes include[1]:

1. Uni- or bilateral uveal metastases.
2. A tendency to affect the choroid more often than the anterior uvea.
3. When the anterior uvea is affected, neoplastic cells line or carpet the surfaces of the iris and ciliary body.
4. Extensive and widespread invasion of blood vessels.
5. A pattern of choroidal infarction with characteristic, wedge-shaped areas of tapetal discoloration and profound vascular attenuation visible on funduscopy.
6. Orbital involvement may accompany involvement of the posterior segment of the globe.

The present case shows most of the previously described common morphologic features of metastatic neoplasia. Of those features, the lining of ocular surfaces and the marked vascular invasion – especially of the choroidal vessels – are the most salient. Interestingly, the neoplastic cells also produce an unusual pattern of carpeting by proliferating over the ulcerated corneal surface, mimicking the corneal epithelium. The absence of the native corneal epithelium and subsequent exposure of the corneal stroma might have facilitated/stimulated neoplastic cells to proliferate in that pattern.

The neoplastic tissue presents classic epithelial morphology with multiple areas developing keratinization of the inner cellular layers. This feature points towards a squamous cell carcinoma, but other undifferentiated carcinomas with squamous metaplasia cannot be ruled out.

Other possible differential diagnoses include pulmonary carcinomas, primary corneo-conjunctival squamous cell carcinomas and mammary carcinomas. Metastatic pulmonary carcinomas tend to form acinar/glandular structures on the uveal tissue and/or present ciliated epithelium carpeting the ocular surfaces. Primary ocular squamous cell carcinomas in cats can invade the intraocular structures, especially the anterior chamber and uvea, but they seldom infiltrate vessels and the posterior aspect of the globe.[4] Metastatic mammary carcinoma is a remote possibility since the cat in this case is male and neutered.

The decrease number of ganglion cells in the retina confirms the clinical diagnosis of secondary glaucoma. In cats, the main histologic feature of glaucoma is loss of ganglion cells without progressive degeneration of the outer retina, as seen in dogs.[1] The majority of glaucomas in cats are secondary to other ocular diseases, most notably chronic lymphoplasmacytic anterior uveitis, systemic hypertension-related intraocular hemorrhages, and intraocular neoplasia.[1,2]

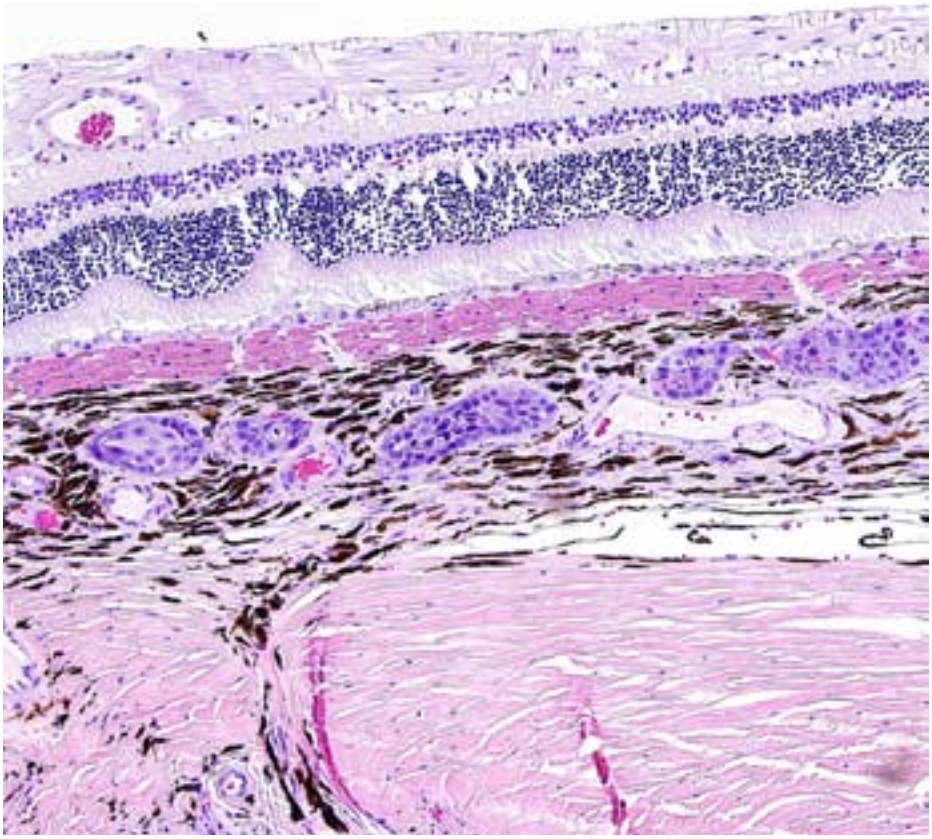

3-7. Eye, cat: Neoplastic cells infiltrate and expand peri-papillary choroidal vessels. (HE 100X) (Photo courtesy of: Department of Pathobiological Sciences, School of Veterinary Medicine, University of Wisconsin-Madison, http://www.vetmed.wisc.edu)

The patient in the present case was lost to follow-up before the identification of a primary tumor.

JPC Diagnosis: Eye, globe: Carcinoma, poorly differentiated with drainage angle occlusion, retinal atrophy, multifocal detachment, ulcerative keratitis with axial facet lesion formation and numerous tumor emboli.

Conference Comment: We thank the contributor for providing this unique, interesting case as well as a comprehensive review of primary and metastatic ocular tumors in cats. The notes on salient histopathology findings in primary versus metastatic ocular tumors are especially relevant. Prior to the conference, the moderator led a particularly informative discussion encompassing normal ocular anatomy and physiology, touching upon the concept (also noted by the contributor) that the abundant uveal vascularization and associated immune privilege of ocular tissue provide a favorable environment for tumor metastasis; however, the moderator pointed out that these conditions are also advantageous for the development of primary ocular tumors. So, while this neoplasm admittedly exhibits similar morphologic features to those described above for metastatic ocular tumors, the moderator suggests that definitive differentiation from a primary tumor is quite difficult, and likely requires identification of the initial tumor at another anatomic location.

Many conference participants tentatively identified this tumor as squamous cell carcinoma (SCC). Ocular involvement of SCC is most common in cattle and horses, but has also been reported in cats and dogs. In all domestic species, SCC involving the ocular surface appears to have a preference for the limbus (corneoscleral junction) which is the transition zone between the corneal and conjunctival epithelial cell populations. The limbus is home to the local stem cell population; stem cells have a high proliferative capacity, are susceptible to the accumulation of oncogenic mutations, and are thought to be the source of many neoplasms. Corneolimbal SCC refers specifically to a neoplasm originating at the limbus with extension into the cornea (as opposed to originating from the corneal epithelium itself).[4] This neoplasm manifests several histologic features suggestive of corneolimbal SCC: neoplastic cells are most numerous in the sclera, ciliary body and limbus, there is fairly prominent intracellular bridging with moderate desmoplasia and there is scattered infiltration of neutrophils; however, participants did not appreciate significant dyskeratosis or formation of keratin pearls, so we are unable to definitively diagnose ocular SCC. The contributor provides a brief, but thorough differential diagnosis for the gross and microscopic lesions in this case.

Contributing Institution: Department of Pathobiological Sciences
School of Veterinary Medicine
University of Wisconsin-Madison
http://www.vetmed.wisc.edu

References:

1. Dubielzig RR, Ketring KL, McLellan GJ, et al. *Veterinary Ocular Pathology: a Comparative Review*. London: Elsevier; 2010.
2. Grahn BH, Peiffer RL. Fundamentals of veterinary ophthalmic pathology. In: Gelatt KN, ed. *Veterinary Ophthalmology*. 4th ed. Victoria: Blackwell Publishing, 2007:411-502.
3. Wilcock BP. The eye and ear. In: Maxie MG, ed. *Jubb, Kennedy and Palmer's Pathology of Domestic Animals*. Vol 1. 5th ed. Philadelphia: Elsevier; 2007:459–552.
4. Scurell EJ, Lewin G, Solomons M, et al. Corneolimbal squamous cell carcinoma with intraocular invasion in two cats. *Vet Ophthalmol*. 2013 Feb 20. doi: 10.1111/vop.12036. [Epub ahead of print]

CASE IV: Case 1 N092-2012 (JPC 4035683).

Signalment: 1-year-old intact domestic shorthair cat, (*Felis catus*).

History: A recently rescued approximately 1-year-old stray, intact DSH cat, weighing 3.2 kg was presented to the Ross University Veterinary Teaching Hospital (RU-VTH) for routine physical examination and vaccination. A 1 cm smooth, firm to hard, unilateral, non-painful mass was detected on the right mid-mandible. Multifocal areas of ulceration were present on the buccal surface of the gums along the molar portion of the body of the mandible. Despite antibiotic therapy the cat's overall physical condition deteriorated and two months later it was brought back to the RU-VTH for evaluation. The mass was fast growing, reaching 6 cm in its largest dimension. The cat was euthanized due to poor body condition and progression of the lesion despite therapy.

Gross Pathology: Abnormal findings were confined to the right mandible and the regional lymph nodes. The mandible was brittle and could be sliced with the necropsy knife. The right lower gingival mucosa was diffusely red, firm and swollen. The swelling extended to the right sublingual inter-mandibular space. The right submandibular and parotid lymph nodes were markedly enlarged (up to 2 cm in the largest dimension), firm and wet.

Laboratory Results: A core bone marrow biopsy was used for culture and incubated at 37°C in aerobic and anaerobic conditions. Microscopically the cultured organisms were characterized as Gram positive, acid fast negative, filamentous bacteria. Molecular testing of the isolates by amplification and sequencing of the 16S rRNA gene identified the isolates as *Nocardia cyriacigeorgica*.

Histopathologic Description: Mandibular mass: Routine H&E sections from the core biopsy revealed focal new bone formation around areas of osteolysis and inflammatory cell infiltration surrounding large, irregularly-shaped, faintly basophilic clusters of filamentous bacteria rimed by fine eosinophilic amorphous material (Splendore-Hoeppli phenomenon). Bacterial colonies were surrounded by neutrophils, lesser numbers of plasma cells, macrophages, and occasional multinucleated giant cells and fibroblasts at the outermost layer. Anastomosing trabeculae of newly deposited woven bone (bone proliferation) were seen around inflammatory foci.

4-1. Mandible, cat: A 1 cm smooth, hard unilateral mass was present on the right mid-mandible of a 1-year-old cat. (Photo courtesy of: Department of Biomedical Sciences, Ross University School of Veterinary Medicine, St. Kitts, West Indies www.rossu.edu)

Contributor's Morphologic Diagnosis: Chronic multifocal pyogranulomatous osteomyelitis with intralesional filamentous bacteria.

Contributor's Comment: Mandibular osteomyelitis, also known as "lumpy jaw" in ruminants and other domestic and wild animal species, is uncommon in domestic cats. It is a condition characterized by pyogranulomatous inflammation resulting in bone destruction and remodeling. Lumpy jaw in hoofed animals is believed to occur secondary to oral infection, poor drainage, coarse forage ingestion, dental eruptions and oral abrasions. Common bacterial etiologies for lumpy jaw are *Actinomyces*

bovis in ruminants and *Fusobacterium necrophorum* in kangaroos.[1] Nocardia spp. are aerobic actinomycetes ubiquitous in soil and water, and are known to cause opportunistic infections in terrestrial and marine mammal species.[4] The severe pyogranulomatous mandibular osteomyelitis diagnosed in this cat was the result of infection with a recently described Nocardia species, *Nocardia cyriacigeorgica*. In recent years, *Nocardia* species identification and taxonomy has greatly improved with the availability of molecular methods such as 16S rRNA and hsp65 gene sequence analysis. *Nocardia cyriacigeorgica* is an actinomycete which, since its first description in 2001, has been reported as a causative agent of human disease in Europe, Asia, Canada and the USA.[5] While *Nocardia cyriacigeorgica* infection has not been described in domestic species, it has been reported in a captive beluga whale,[4] and is currently regarded as an emergent pathogen in people.[3] To our knowledge this is the first report of *N. cyriacigeorgica*-induced mandibular osteomyelitis in a cat. Interestingly, gross and microscopic

4-2. Mandible, cat: A dorsoventral view of the right mandibular mass. (Photo courtesy of: Department of Biomedical Sciences, Ross University School of Veterinary Medicine, St. Kitts, West Indies www.rossu.edu)

4-3. Mandible, cat: A core biopsy of the mandibular mass both loss of cortical bone adjacent to periosteal new bone growth (top) and multifocal areas of hypercellularity scattered through the cancellous bone. (HE 0.63X)

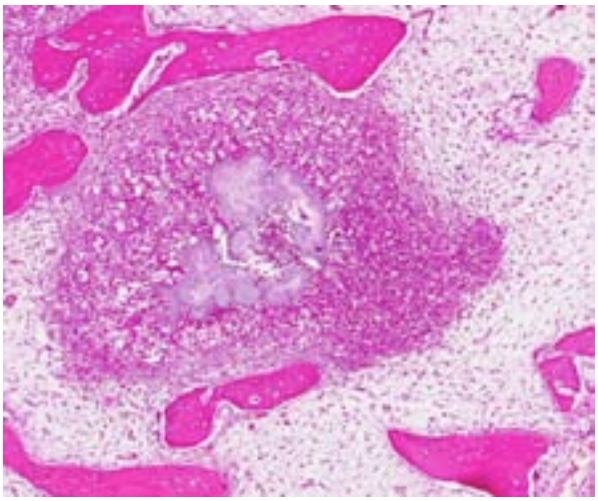

4-4. Mandible, cat: Areas of hypercellular within the medulla correspond to pyogranulomas centered on foci of Splendore-Hoeppli material. (HE 48X)

findings of the mandibular lesions caused by this potentially zoonotic bacterium closely resemble those of mandibular actinomycosis (lumpy jaw) in cattle.

JPC Diagnosis: Bone: Osteomyelitis and cellulitis, pyogranulomatous, multifocal to coalescing, marked, with large colonies of filamentous bacteria.

Conference Comment: This case is interesting in that *Nocardia* spp. is not generally classified as a large colony forming bacterium in tissue; *Yersinia* spp., *Actinomyces* spp., *Actinobacillus* spp., *Corynebacterium* spp., *Staphylcoccus* spp. and *Streptococcus* spp. (see WSC 2013-14, conference 1, case 3) are the most common bacteria that form large colonies in tissues in veterinary species. The main etiologic rule-out for the gross and histopathologic findings is *Actinomyces* spp., a gram-positive, non-acid fast filamentous bacteria commonly associated with cutaneous infection secondary to bite wounds and penetrating injuries from grass awns or other foreign bodies. The gross lesions of actinomycosis and nocardiosis are typically identical (cellulitis, abscesses, draining tracts, osteomyelitis), and although it is a more common feature of actinomycosis, both conditions can produce "sulfur granules" (grains composed of necrotic debris, aggregates of bacteria and Splendore-Hoeppli material). Both bacteria are gram-positive, while *Nocardia* spp. is often, but not always, acid fast; if negative, it cannot be differentiated microscopically from *Actinomyces* spp.[2] In this case, filamentous bacteria were both gram-positive and acid-fast; these histochemical staining characteristics, along with the culture results reported by the contributor, support a diagnosis of nocardiosis.

Contributing Institution: Department of Biomedical Sciences
Ross University School of Veterinary Medicine, St. Kitts, West Indies
www.rossu.edu

References:

1. Brookins MD, Rajeev S, Thornhill TD, Kreinheder K, Miller DL. Mandibular and maxillary osteomyelitis and myositis in a captive herd of red kangaroos (*Macropus rufus*). *J Vet Diagn Invest*. 2008;20:846-849.
2. Ginn PE, Mansell JEKL, Rakich PM. Skin and appendages. In: Maxie MG, ed. *Jubb, Kennedy and Palmer's Pathology of Domestic Animals*. Vol.1. 5th ed. Philadelphia: Elsevier; 2007:686-687.
3. Schlaberg R, Huard RC, Della-Latta P. Pathogen in the United States *Nocardia cyriacigeorgica*, an emerging pathogen in the United States. *J Clin Microbiol.* 2008;46:265-273.
4. St. Leger JA, Begeman L, Fleetwood M, et al. Comparative pathology of nocardiosis in marine mammals. *Vet Pathol.* 2009;46:299-308.
5. Yassin AF, Raieny FA, Steiner U. *Nocardia cyriacigeorgici* sp. nov. *Int J Syst Evol Microbiol*. 2001;51:1419-1423.

Joint Pathology Center
Veterinary Pathology Services

WEDNESDAY SLIDE CONFERENCE 2013-2014

Conference 20

26 March 2014

CASE I: Case 1 (JPC 3167249).

Signalment: Mature adult male cynomolgus macaque, (*Macaca fascicularis*).

History: This animal was treated with Cyclosporine A for 30-days before being euthanized and necropsied due to decreased activity, food consumption, and body weight.

Gross Pathology: Both kidneys were brown and the heart contained a small focus of epi/ myocardial hemorrhage.

Laboratory Results: Only hematology parameters were evaluated. There was a regenerative macrocytic microchromic anemia, and schistocytes were noted upon microscopic examination of the blood smear.

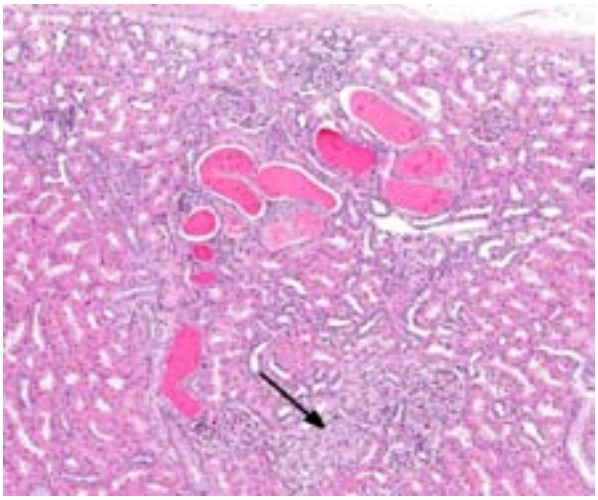

1-1. Kidney, cynomolgus macaque: Segments of the kidney are hypercellular with enlarged glomeruli, ectatic tubules with protein casts, and markedly enlarged arterioles (arrow). (HE 60X)

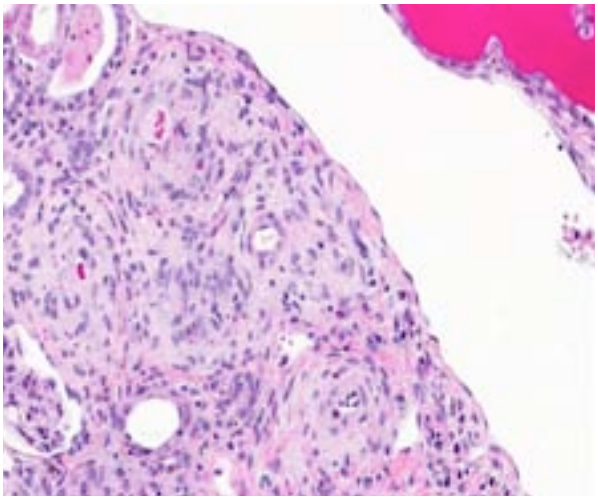

1-2. Kidney, cynomolgus macaque: Renal arterioles are tortuous and markedly expanded by disorganized hyperplastic smooth muscle cells, extracellular protein and extruded erythrocytes. (HE 250X)

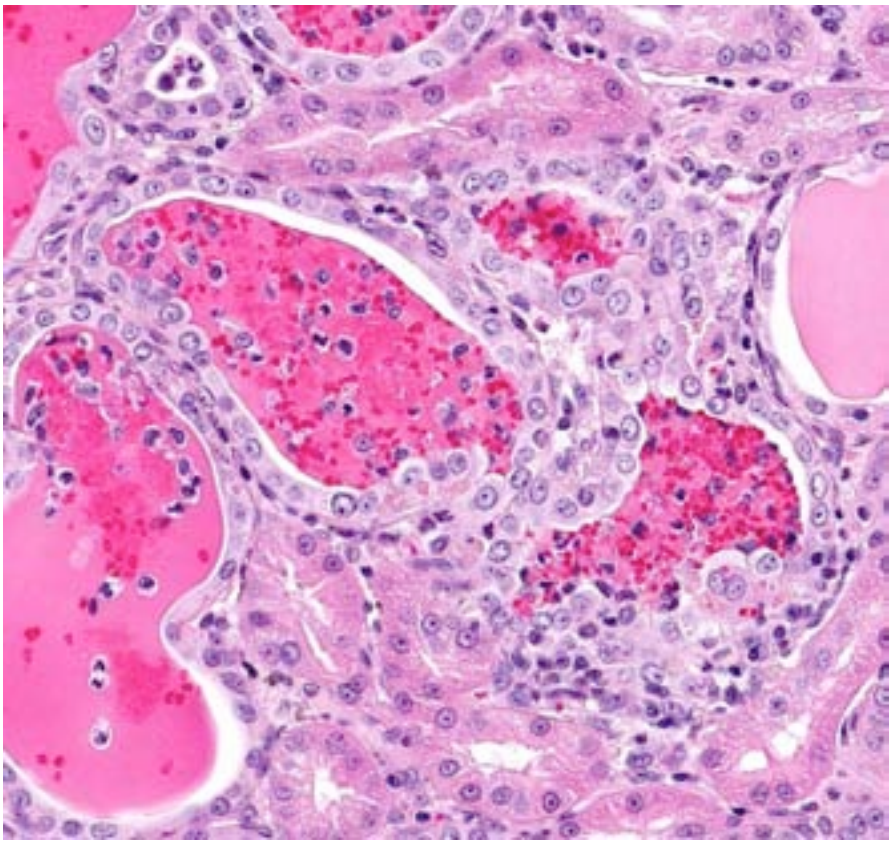

1-3. Kidney, cynomolgus macaque: Multifocally, tubules are ectatic, contain protein and cellular casts, and are lined by basophilic cuboidal epithelial cells with large nuclei (regenerative tubules). (HE 360X)

Histopathologic Description: There is minor variation between slides, but all slides contain the following main histopathologic features: Numerous arterioles in the interstitium of the cortex and corticomedullary junction have marked mural expansion by amphophilic myxomatous material and hypertrophy of medial smooth muscle cells, which are rarely necrotic, and less often contain infiltrating fibroblasts and extravasated red blood cells. Affected vessels have lumina which are reduced in diameter to completely occluded, are sometimes lined by hypertrophied endothelial cells, and rarely contain fibrin. Other vasculature sometimes contains circulating erythroid precursor cells. Cortical tubules adjacent to affected vessels are occasionally effaced, but more often are lined by epithelial cells with large vesicular nuclei and lightly basophilic cytoplasm (regenerative cells). Cortical tubules are sometimes dilated and contain either protein casts, casts comprised of fragmented red blood cells, and/or a small amount of necrotic debris. Scattered medullary tubules also contain protein casts. Scattered glomeruli are mildly hypercellular with thickened capillary basement membranes, and contain occasional adhesions (synechiae) to Bowman's capsule and/or hypertrophy of parietal cells. There are a few foci in which the cortical interstitium is minimally expanded by fibrous connective tissue and small numbers of lymphocytes and plasma cells.

Contributor's Morphologic Diagnosis:
Kidney:
1. Marked multifocal arteriopathy
2. Moderate multifocal subacute renal cortical tubular degeneration and regeneration with tubular dilation and casts
3. Mild multifocal membranoproliferative glomerulopathy
4. Minimal multifocal chronic interstitial nephritis

Contributor's Comment: The renal lesions[3,4,5,7] and hemolytic anemia[2,3] are consistent with cyclosporine or other calcineurin inhibitor (tacrolimus) toxicity in primates. Most of the literature pertaining to calcineurin inhibitor toxicity refers to humans, but there are reports of such in tacrolimus treated rhesus monkeys[3] and streptozotocin-diabetic cyclosporine treated cynomolgus monkeys.[7]

A recent review paper on calcineurin inhibitor nephrotoxicity in humans describes the chronic morphologic features as nodular hyaline material deposition in the tunica media of afferent arterioles, tubular atrophy, interstitial fibrosis, and glomerular sclerosis, with the hallmark feature being the arteriolar lesion.[5] It has been speculated that the non-vascular renal changes, which are said to have a "stripe-like" distribution, are due, at least in part, to ischemia resulting from the renal arteriolar changes.[4,5] Similarly, the arteriolar changes are also thought to be responsible for the associated hemolytic anemia because they result

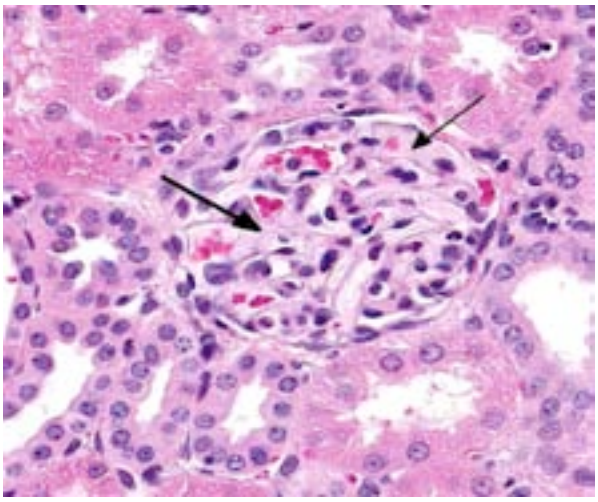

1-4. Kidney, cynomolgus macaque: Glomeruli are enlarged and contain increased amounts of eosinophilic protein surrounding glomerular capillaries (membranous glomerulonephritis). (HE 320X)

in mechanical damage and eventual intravascular hemolysis of red blood cells.[2]

This case was complicated by the fact that this animal also had a mononuclear meningitis, suggestive of a viral etiology (although no viral inclusion bodies were noted microscopically) secondary to cyclosporine-induced immunosuppression. Primary differentials for meningoencephalitis include simian virus 40 (SV-40), which can also cause interstitial nephritis,[6] and herpesviral infection, specifically cytomegalovirus (CMV).[1]

Immunohistochemistry on affected areas of brain was attempted and was negative for SV-40, but CMV antibodies were not reactive against macaque CMV.

JPC Diagnosis: 1. Kidney, arterioles: Arteritis, proliferative, diffuse, moderate.
2. Kidney, tubules: Degeneration and necrosis, multifocal, mild with tubular ectasia and protein casts.
3. Kidney: Glomerulonephritis, membranous, diffuse, moderate.

Conference Comment: Cyclosporine and tacrolimus are often used in conjunction with human kidney transplants in an attempt to prevent chronic allograft rejection. The immunosuppressive properties associated with these drugs result from inhibition of calcineurin (a calcium- and calmodulin-dependent phosphatase protein), with subsequent reduction in the transcription of T-cell-dependent lymphokines, such as interleukin-2 (IL-2), interferon-γ (IFN-γ, tumor necrosis factor-α (TNF-α), and granulocyte macrophage colony-stimulating factor (GM-CSF); these are regulated through calcineurin-dependent dephosphorylation of NFAT. The selective immunosuppressive properties of calcineurin inhibitors (CNIs) are attributed to the localization of NFAT predominantly within T-lymphocytes; however, long-term administration may result in toxic changes, specifically nephrotoxicity.[8-10]

Acute CNI nephrotoxicity results from vasoconstriction of the afferent arteriole due to increased levels of vasoconstrictors (such as endothelin, thromboxane and activation of the renin-angiotensin system) and decreased quantities of vasodilators (such as prostaglandin-E2, prostacyclin, and nitric oxide). This dose-dependent and reversible arteriolar vasoconstriction results in reduced renal blood flow, reduced glomerular filtration, increased renal vascular resistance and tubular dysfunction.[8] Chronic CNI nephrotoxicity is also associated with impairment of renal function and is likely mediated by several different growth factors and cytokines, including transforming growth factor beta (TGFβ), platelet derived growth factor (PDGF), fibroblast growth factor (FGF) and TNF-α. CNIs have been shown to produce various side effects in addition to nephrotoxicity, including diabetes, neurological dysfunction, hemolytic anemia, hemolytic uremic syndrome, hypertension and hypercholesterolemia.[2,9,10]

Although there is significant tubular degeneration/regeneration as well as mild glomerulonephritis and glomerulosclerosis, conference participants agree that the most striking lesions in this interesting case are the occlusive arteriolar changes, consisting of disruption of the internal elastic membrane, proliferation, hypertrophy, hyalinosis and fibrosis within the tunica intima/media and significant narrowing of affected lumina. Similar changes are reported in association with chronic allograft nephropathy (characterized by progressive and irreversible deterioration of renal function with interstitial fibrosis, tubular atrophy, arteriolar hyalinosis, and glomerulosclerosis) and systemic hypertension.[8] In addition to the microscopic lesions described above, which are consistent with cyclosporine nephrotoxicity, there is evidence of

microangiopathic hemolytic anemia, supported by the finding of regenerative anemia on the CBC and the detection of schistocytes, which are fragmented erythrocytes suggestive of shearing of erythrocyte membranes, on the peripheral blood smear. Microangiopathic hemolytic anemia is another well-described sequela to administration of CNIs,[2,9] presumably secondary to erythrocyte damage from the turbulence that results from vasoconstriction and occlusion of renal arterioles. Although further clinical-pathologic data is not available, hemoglobinemia and hemoglobinuria, as well as hyperbilirubinemia, are also expected findings in cases of microangiopathic anemia.[11]

Contributing Institution: Pfizer Inc. Global Research and Development
Eastern Point Rd.
Groton, CT 06340
http://www.pfizer.com

References:

1. Baskin, GB. Disseminated cytomegalovirus infection in immunodeficient rhesus monkeys. *Am J Pathol*. 1987;129(2):345-352.
2. Danesi R, Del Tacca M. Hematologic toxicity of immunosuppressive treatment. *Transplantation Proceedings*. 2004;36:703-704.
3. Kindt MV, Kemp R, Allen HL, Jensen RD, Patrick DH. Tacrolimus toxicity in rhesus monkey: model for clinical side effects. *Transplantation Proceedings*. 1999;31:3393-3396.
4. Myers BD, Newton L. Cyclosporine-induced chronic nephropathy: an obliterative microvascular renal injury. *Journal of American Society of Nephrology*. 1991;2:S45-S52.
5. Naesens M, Kuypers DRJ, Sarwal M. Calcineurin inhibitor nephrotoxicity. *Clinical Journal American Society Nephrology*. 2009;4:481-508.
6. Simon MA, Ilyinshii PO, Baskin GB, Knight HY, Pauley DR, Lackner AA. Association of simian virus 40 with a central nervous system lesion different from progressive multifocal leukoencephalopathy in macaques with AIDS. *Am J Pathol*. 1999;154(2):437-446.
7. Wijkstrom M, Kirchhof N, Graham M, Ingulli E, Colvin RB, Christians U, et al. Cyclosporine toxicity in immunosuppressed streptozocin-diabetic nonhuman primates. *Toxicology*. 2005;207:117-127.
8. Issa N, Kukla A, Ibrahim HN. Calcineurin inhibitor nephrotoxicity: a review and perspective of the evidence. *Am J Nephrol*. 2013;37(6): 602-612.
9. Fellstrom B. Cyclosporine nephrotoxicity. *Transplant Proc*. 2004;36(2 Suppl):220S-223S.
10. Busauschina A, Schnuelle P, van der Woude FJ. Cyclosporine nephrotoxicity. *Transplant Proc*. 2004;36(2 Suppl):229S-233S.
11. Brockus CW. Erythrocytes. In: Latimer KS, ed. *Duncan and Prasse's Veterinary Laboratory Medicine Clinical Pathology*. 5th ed. Ames, IA: Wiley-Blackwell, 2011:30-35.

CASE II: 13-226/227 (JPC 4033976).

Signalment: Two age-unknown (post-weaning) female and castrated male Norwegian Landrace pigs, (*Sus scrofa domesticus*).

History: Two pigs were received for necropsy from a farm with diarrhea among weaned pigs.

Gross Pathology: The nutritional status of both pigs was slightly below normal. Feces in the large bowel of both pigs had looser consistency than normal, but the cecum and colon were otherwise normal macroscopically. One of the pigs had slightly enlarged mesenteric lymph nodes.

Laboratory Results: From colons of both pigs a mixed bacterial growth with *Brachyspira sp.* was cultured and from both pigs the *Brachyspira sp.* were identified as *Brachyspira pilosicoli.*

Histopathologic Description: Histologic findings were similar in colon and cecum from one pig (13/226) and colon from the other pig (13/227). Surface epithelium was multifocally attenuated, and variably covered by numerous bacteria. Numerous crypts contained abundant bacteria with a morphology consistent with spirochetes. Number of goblet cells in crypt epithelium varied from few to moderate, but was generally decreased. Some crypts contained abundant neutrophils (crypt abscesses), and some crypts were lined by flattened attenuated epithelial cells. The lamina propria contained a moderate increase in lymphocytes and macrophages and few neutrophils.

In the deeper parts of some crypts (moderate numbers in the colon of pig 13/226, and few in the cecum from pig 13/226 and colon from pig 13/227) there were luminal pyriform to crescent-shaped organisms, approximately 5 x 7 µm in size, with a faint nucleus and eosinophilic cytoplasm (consistent with trichomonads).

In a few sections there were also a few ciliated large protozoa (*Balantidium coli*) on the surface of the mucosa (incidental finding).

Contributor's Morphologic Diagnosis: Cecum and colon: Typhlocolitis, catarrhal, diffuse, mild with moderate numbers of crypt abscesses, high numbers of intracryptal spirochetes and moderate numbers of intracryptal trichomonads and few surface ciliated large protozoa.

Contributor's Comment: Two members of the genus *Brachyspira* may cause colitis in swine: the strongly hemolytic *Brachyspira hyodysenteriae* which is the cause of swine dysentery, and the weakly hemolytic *B. pilosicoli* which is the cause of porcine intestinal spirochetosis.[1,3] *B. pilosicoli* has a wide host range, is capable of infecting a

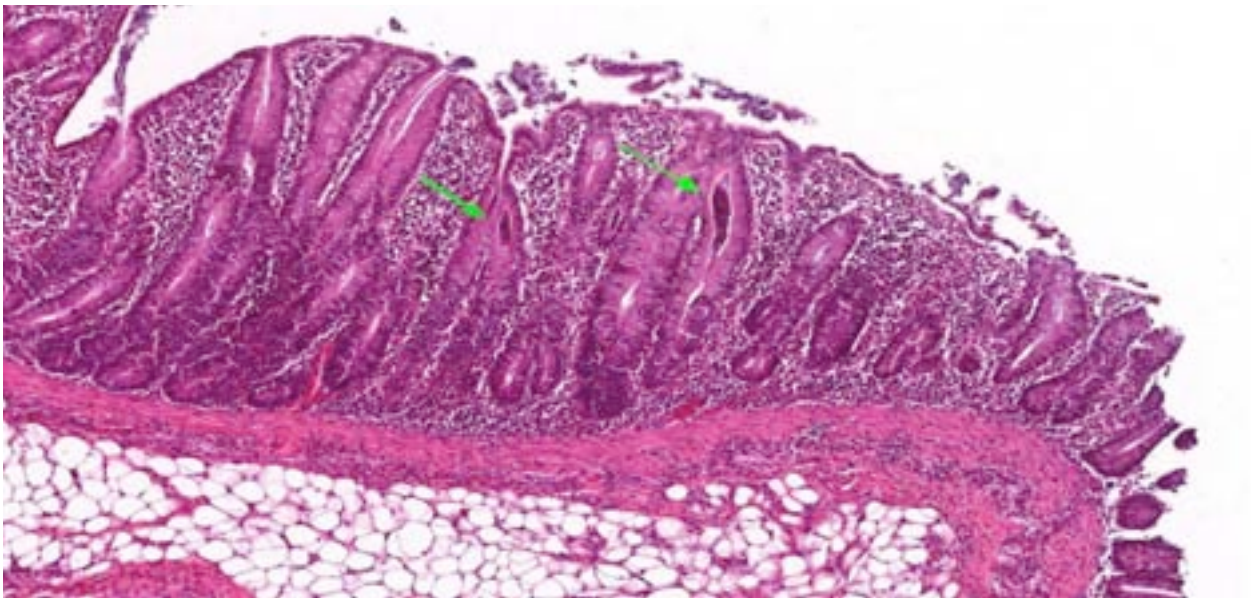

2-1. Colon, pig: The lamina propria is markedly expanded by numerous inflammatory cells including neutrophils and lymphocytes, and there are occasional crypt abscesses. (HE 160X)

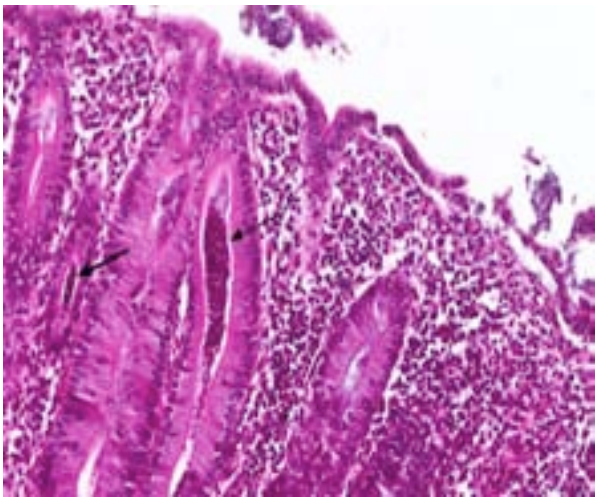

2-2. Colon, pig: Higher magnification of Fig 2-1 with dilated glands (arrows) filled with neutrophils, degenerate epithelial cells, and occasional trichomonads. (HE 240X)

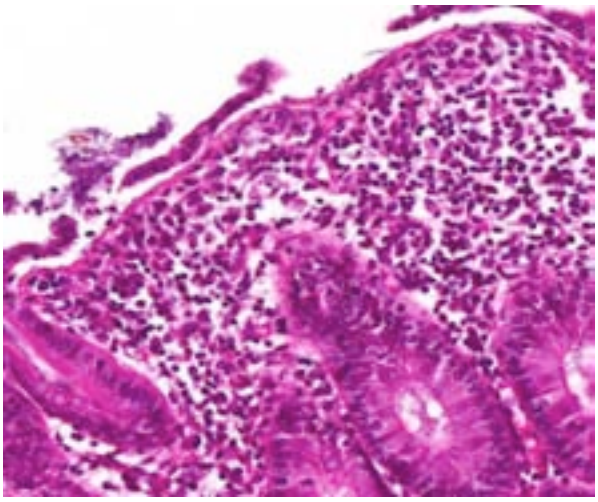

2-3. Colon, pig: The overlying epithelium is multifocally infiltrated by inflammatory cells, often detached, and multifocally covered by mats of robust bacilli. (HE 400X)

number of animal species, both mammals and birds, and may also be zoonotic.[1] Other weakly hemolytic members of the *Brachyspira* genus that may be isolated from swine, *B. innocens, B. intermedia* and *B. murdochii*, have not been shown to cause disease in experimentally infected conventional pigs and are considered to be nonpathogenic commensals in pigs.[3] While swine dysentery is a highly infectious disease of mainly weaned pigs characterized by a large bowel diarrhea with mucus, blood, or fibrin in the feces, porcine intestinal spirochetosis is typically a milder disease characterized by transient watery to mucoid diarrhea without blood,[1] as was seen in these two pigs. The histologic findings are focal erosions, slight edema, crypt abscesses, mild infiltrate of mononuclear cells in lamina propria and the spirochetes may be found attached to surface epithelium, inside dilated crypts, invading through tight junctions between colonic enterocytes, within goblet cells, and within the lamina propria.[3,4]

The protozoal organisms located in colonic crypts were interpreted as trichomonads. *Tritrichomonas suis* is considered to be an apathogenic commensal in pigs that may colonize nasal cavity and intestines of pigs. This species has been found to be identical in sequence to *T. foetus*,[2,7] a venereally transmitted pathogen that affects cattle; however, other trichomonads may also be identified in fecal samples from pigs, such as *Tetratrichomonas buttreyi,*[6] *Trichomitus rotunda* and others unrelated to previously described trichomonads.[5]

JPC Diagnosis: Colon: Colitis, necrotizing, subacute, diffuse, moderate, with marked crypt hyperplasia.

Conference Comment: Conference participants conducted a brief discussion of the differential diagnosis for the clinical, gross and histological findings in this case, including *Brachyspira hyodysenteriae, Lawsonia intracellularis, Salmonella* spp., *Clostridium* spp., *Escherichia coli*, *Trichuris suis*, coronavirus and rotavirus. As noted by the contributor, *B. hyodystenteriae* is strongly beta-hemolytic and highly infectious, causing severe hemorrhagic diarrhea and fibrinonecrotic pseudomembranous colitis in affected swine. Although virulence factors are poorly defined, both *B. dysenteriae* and *B. pilosicoli* are thought to be chemotactically attracted to intestinal mucin and tend to be intimately associated with the intestinal mucus layer. *Lawsonia intracellularis*, on the other hand, is an obligate intracellular gram-negative bacterium that colonizes enterocytes in the ileum and colon, resulting in proliferative to necrotizing enteritis/colitis. *Salmonella* spp. are important enteric pathogens of swine. *S. typhimurium* causes acute/chronic enterocolitis in feeder pigs; it has also been associated with necrotizing proctitis and subsequent rectal stricture. The major clinical manifestation of *S. cholerasuis* is septicemia with secondary endothelial damage. Common microscopic findings include interstitial pneumonia, multiple foci of hepatic necrosis ("paratyphoid nodules"), renal cortical microhemorrhages ("turkey egg" kidney),

polyarthritis or polysynovitis, meningoencephalomyelitis and enterocolitis, often with colonic "button ulcers."[1]

C. perfringens type C is associated with outbreaks of necrohemorrhagic enteritis in suckling piglets, while *C. difficile* is recognized as a cause of fibrinous typhlocolitis and mesocolonic edema in neonatal piglets (see WSC 2013-2014, conference 17, case 1 for a more detailed discussion of *Clostridium* spp.). Enterotoxigenic *E. coli* (ETEC) causes profuse watery diarrhea in neonatal piglets via heat-labile (LTI and LTII) and heat-stable (STa and STb) enterotoxins (see WSC 2013-2014, conference 12, case 2 for a more detailed discussion of *E. coli*); however, histological changes are typically minimal. Enteropathogenic (attaching and effacing) *E. coli* is a less frequently reported cause of diarrhea in swine, and, although an uncommon manifestation, enteritis has also been associated with some strains of enterohemorrhagic, Shiga-like toxin producing *E. coli*, the cause of porcine edema disease. The whipworm *Trichuris suis* inhabits the cecum and colon of swine, where it embeds in the surface epithelium; severe infections may lead to mucohemorrhagic typhlocolitis.[1]

There are two coronaviruses associated with porcine diarrhea. Transmissible gastroenteritis (TGE) is a highly contagious disease that is most severe in piglets younger than 10 days of age, characterized by high morbidity with vomiting and profuse diarrhea. The causative agent, a group 1 porcine coronavirus, destroys intestinal villar epithelial cells, resulting in marked villar atrophy and diarrhea secondary to malabsorption. Porcine epidemic diarrhea (PED) virus is another group 1 coronavirus that causes similar, though less severe signs in older pigs. The PED virus is endemic in many Asian countries, and has been present in Europe since the early 1970s; however, until recently (i.e., May 2013), it was not present in the United States, and its emergence has caused epidemic disease with important economic implications for the American pork industry. Rotavirus is enzootic in many swine herds and causes villar atrophy with ensuing diarrhea in both suckling and weaned pigs, although it is generally less severe than TGE. Finally, porcine adenoviral inclusions have been identified within small intestinal enterocytes in both asymptomatic pigs and those presenting with watery diarrhea; however, the significance of this finding remains controversial, and adenoviral infection is not yet recognized as a significant cause of enteric disease in swine.[1]

In this case, histochemical staining with Warthin-Starry highlights numerous argyrophilic spirochetes adhered to the enteric mucosa, supporting a diagnosis of colonic spirochetosis, while the culture results as reported by the contributor definitively identify the etiologic agent as *Brachyspira pilosicoli*.

Contributing Institution: Norwegian School of Veterinary Science
Institute of Basic Science and Aquatic Medicine
PO box 8146 Dep.
0033 Oslo
Norway
www.nvh.no

References:

1. Brown CC, Baker DC, Barker IK. Alimentary system. In: Maxie MG, ed. *Jubb, Kennedy and Palmer's Pathology of Domestic Animals*. Vol. 2. 5th ed. Philadelphia, PA: Elsevier; 2007:3-296.
2. Frey CF, Muller N. Tritrichomonas-systematics of an enigmatic genus. *Mol Cell Probes*. 2012;26:132-136.
3. Hampson DJ, Duhamel GE. Porcine colonic spirochetosis / intestinal spirochetosis. In: Straw BE, Zimmerman JJ, D'Allaire S, Taylor DJ, eds. *Diseases of swine*. Oxford, UK: Blackwell Publishing; 2006:755-783.
4. Jensen TK, Moller K, Boye M, Leser TD, Jorsal SE. Scanning electron microscopy and fluorescent in situ hybridization of experimental *Brachyspira* (*Serpulina*) *pilosicoli* infection in growing pigs. *Vet Pathol*. 2000;37:22-32.
5. Mostegl MM, Richter B, Nedorost N, Lang C, Maderner A, Dinhopl N, et al. First evidence of previously undescribed trichomonad species in the intestine of pigs? *Vet Parasitol*. 2012;185:86-90.
6. Rivera WL, Lupisan AJ, Baking JM. Ultrastructural study of a tetratrichomonad isolated from pig fecal samples. *Parasitol Res*. 2008;103:1311-1316.
7. Tachezy J, Tachezy R, Hampl V, Sedinova M, Vanacova S, Vrlik M, et al. Pathogen *Tritrichomonas foetus* (Riedmuller, 1928) and pig commensal *Tritrichomonas suis* (Gruby & Delafond, 1843) belong to the same species. *J Eukaryot Microbiol*. 2002;49:154-163.

CASE III: AFIP Case 2 (JPC 3165069).

Signalment: 3-year old male Boer goat, (*Capra hircus*).

History: Per referring veterinarian: This goat presented with a severe anemia due to parasitism (9% hematocrit), and a fresh, whole blood transfusion was administered. Four hours after transfusion, the goat developed an increased respiratory rate and open-mouthed breathing. Treatments with anti-inflammatory drugs, anti-bacterial drugs, and thoracocentesis for hydrothorax did not ameliorate clinical signs, and the goat died three hours later.

Gross Pathology: Within the thoracic cavity are approximately 700 ml of clear, watery, yellow fluid. Lungs are diffusely rubbery and mottled red and tan with few foci of atelectasis. The pericardial sac contains approximately 70 ml of fibrinous exudate.

The mediastinal lymph nodes are expanded by abundant amounts of caseous material. Scattered throughout the liver and spleen are dozens of variably-sized abscesses. The kidneys are slightly tan to grey, and the subcapsular surface is slightly granular and mottled with pinpoint, tan foci.

Laboratory Results: *Corynebacterium pseudotuberculosis* was cultured from the hepatic and splenic abscesses. Fecal floatation revealed a trichostongyle egg count of 3,400.

Histopathologic Description: On histology, the majority of hepatic tissue is replaced by multifocal, large abscesses that compress hepatic parenchyma and distort hepatic lobules. Abscesses are composed of large central aggregates of necrotic cellular debris infiltrated by many neutrophils and surrounded by a thick fibrous capsule consisting of well-organized fibroblasts admixed with lymphocytes and occasional bile ducts. In the surrounding hepatic tissue, portal triads are markedly expanded by proliferative bile ducts, admixed with large aggregates of amyloid and many lymphocytes, plasma cells, and macrophages.

Within the spleen are numerous large abscesses, and surrounding periarteriolar lymphoid aggregates are large aggregates of amyloid. Amyloid distends glomerular tufts. Histochemical staining with Congo red confirms the presence of amyloid as congophilic material that is birefringent and apple green on polarization.

Histologic examination of the lungs revealed an acute, neutrophilic interstitial pneumonia.

Contributor's Morphologic Diagnosis: Liver: Severe, multifocal, chronic hepatic abscesses with marked portal fibrosis, biliary hyperplasia, and portal amyloidosis.

Contributor's Comment: Multiple abscesses in the liver, spleen, and lymph nodes were due to

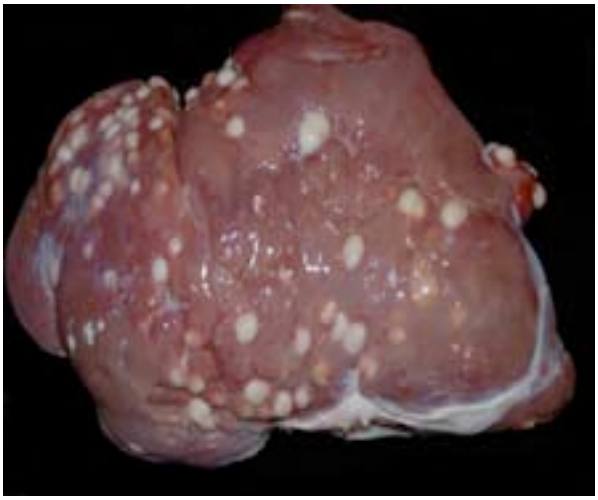

3-1. Liver, Boer goat: Variably sized abscesses are distributed randomly throughout all lobes of the liver. (Photo courtesy of: Oklahoma State University Department of Veterinary Pathobiology, Room 250 McElroy Hall, Stillwater, OK 74078 www.cvm.okstate.edu)

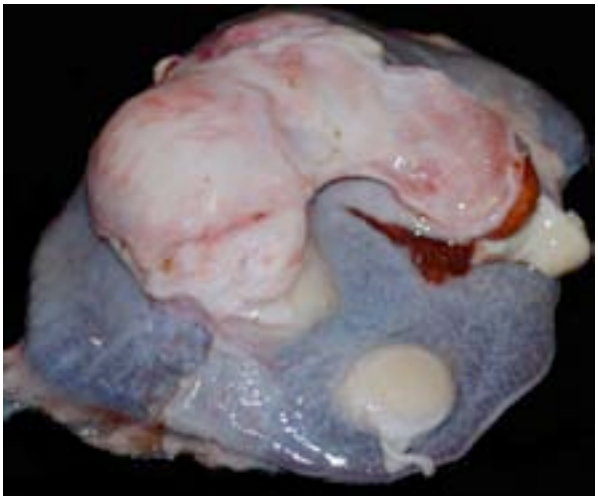

3-2. Spleen, Boer goat: Variably sized abscesses are distributed randomly throughout the spleen. (Photo courtesy of: Oklahoma State University Department of Veterinary Pathobiology, Room 250 McElroy Hall, Stillwater, OK 74078 www.cvm.okstate.edu)

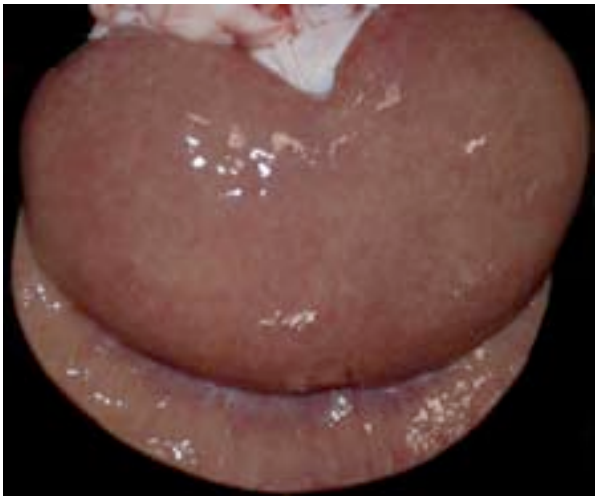

3-3. Kidney, Boer goat: The kidneys are slightly enlarged and a mottle tan-grey color with numerous pinpoint tan foci. (Photo courtesy of: Oklahoma State University Department of Veterinary Pathobiology, Room 250 McElroy Hall, Stillwater, OK 74078 www.cvm.okstate.edu)

infection with *Corynebacterium pseudotuberculosis*. As a result of chronic inflammatory disease, the goat developed secondary systemic amyloidosis. Death was attributed to the acute pneumonia, possibly due to a transfusion reaction.

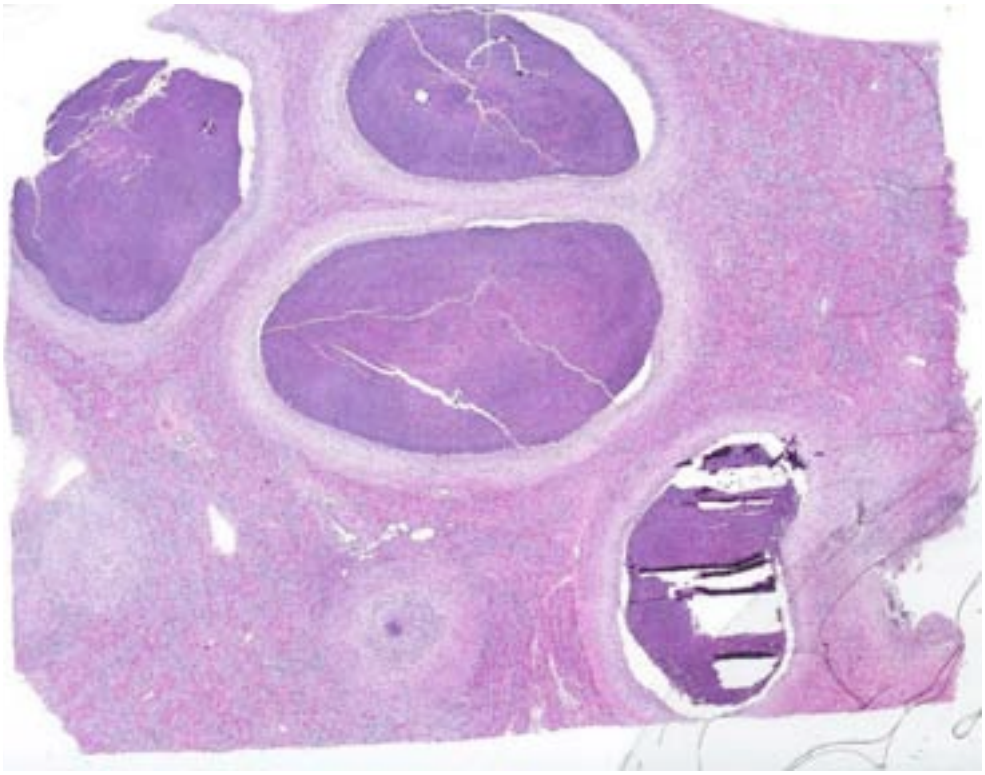

3-4. Liver, Boer goat: The section contains multiple discrete abscesses measuring up to a centimeter in diameter. (HE 14X)

Corynebacterium pseudotuberculosis is a gram-positive, pleomorphic, facultative, anaerobic bacillus that commonly causes disease in several domestic species, including goats, sheep, cattle, and horses. In small ruminants, *C. pesudotuberculosis* is a common cause of lymphadenitis (caseous lymphadenitis), and it may cause pectoral muscle abscesses in horses (pigeon fever) and ulcerative lymphangitis in cattle. In addition, *C. pseudotuberculosis* may cause subcutaneous abscesses, splenic abscesses, embolic nephritis, and orchitis.[6] As in this case, C. *pseudotuberculosis* infection is occasionally associated with systemic amyloidosis in small ruminants.[4,7]

Systemic amyloidosis refers to the deposition of amyloid in multiple organs, as opposed to localized amyloidosis, where amyloid is deposited in a single organ. Systemic amyloidosis may result from an immunocyte dyscrasia (primary systemic amyloidosis) or from chronic inflammation (secondary systemic amyloidosis). Amyloid deposited in secondary systemic amyloidosis is composed of AA (amyloid-associated) protein that forms β-pleated sheets. AA protein is derived from serum amyloid-associated (SAA) protein which is produced by the liver as an acute phase reaction to inflammation.[6]

In small ruminants, secondary systemic amyloidosis has been reported to most commonly result from pneumonia,[5,7] though it may also occur in association with nephritis,[5] polyarthritis, urolithaisis, and mastitis.[7] Typically, small ruminants with secondary systemic amyloidosis may have deposits of amyloid in the kidneys, spleen,

liver, lymph nodes, gastrointestinal tract, adrenal gland, and vascular tunica media.[2,7]

As in this case, renal glomeruli may be more effected than the renal medulla, and amyloid may form aggregates surrounding splenic periarteriolar lymphoid aggregates.[7] In contrast to this case, hepatic amyloidosis in small ruminants, is more commonly associated with expansion of the sinusoids rather than the portal triads.[4,7]

JPC Diagnosis: Liver: Abscesses, multiple, with marked hepatocellular fibrosis, hepatocellular atrophy and loss, biliary hyperplasia, and amyloid formation.

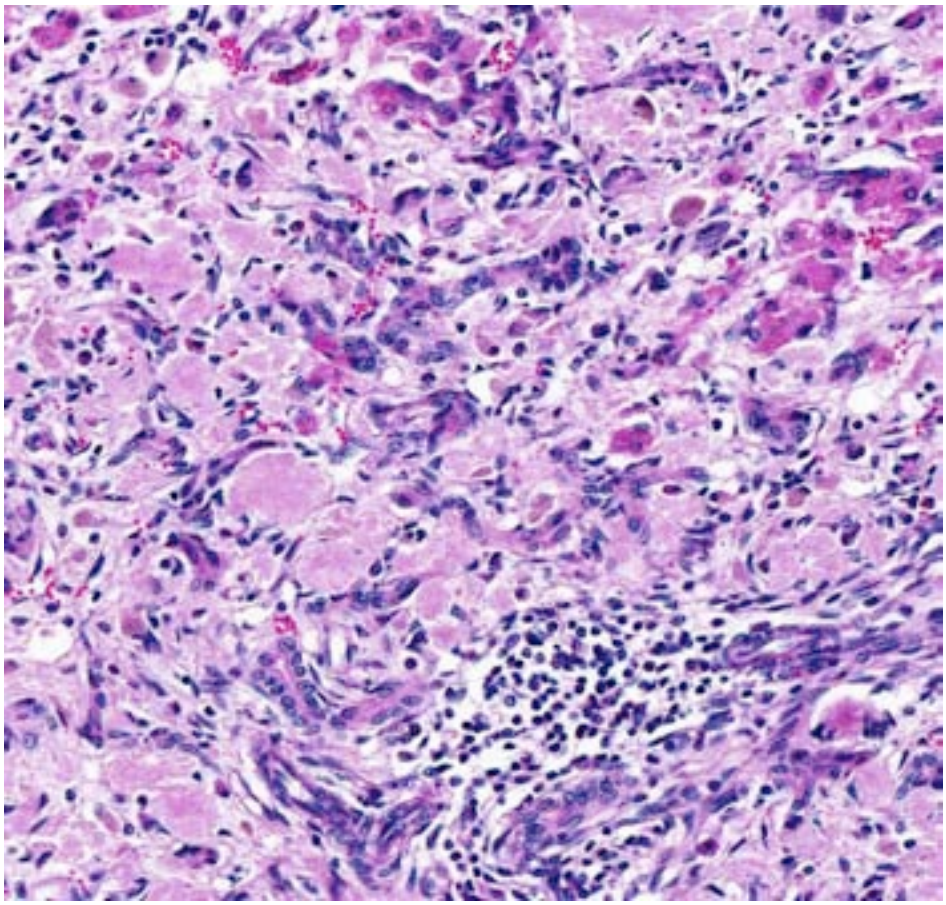

3-5. Liver, Boer goat: Throughout the remaining liver, hepatic sinusoids and portal triads are expanded by abundant amyloid which compresses adjacent hepatocytes. There is marked ductular reaction. (HE 220X)

Conference Comment: There is some slide variation in this case, and several conference participants described multiple hepatic abscesses while others identified the lesions as pyogranulomas. Participants further noted numerous small, duct-like structures composed of cuboidal cells within the hepatic parenchyma, which prompted a focused exploration of the distinction between bile duct hyperplasia and ductular reaction. Although the liver maintains the ability to "regenerate" via a tightly controlled process of compensatory hyperplasia, some types of damage, such as toxic injury and massive hepatic necrosis, may render hepatocytes unable to multiply. Instead, there is proliferation of progenitor cells (oval cells), which often form vague, poorly-differentiated ductular structures that are connected to individual canals of Hering and eventually differentiate into hepatocytes or cholangiocytes. This phenomenon, known as ductular reaction, occurs within the hepatic parenchyma.[3] Conversely, bile ductular hyperplasia and proliferation (as seen in cases of bile duct obstruction) are characterized by piling up of epithelium, micropapillary projections, and/or luminal enlargement or distortion, while tortuous bile ducts manifest histopathologically as increased ductular profiles; these changes are generally confined to portal tracts.[8]

Based on the microscopic findings in this case, *Fusobacterium necrophorum* was suggested as a possible etiologic agent. Hepatic necrobacillosis in ruminants typically occurs when this opportunistic, gram-negative bacterium enters portal circulation as a sequela to toxic rumenitis.[6] Gram-negative septicemia, due to agents such as *E. coli* or *Salmonella* spp., could also result in hepatic abscessation. In this case, a Masson's trichrome and a Gram stain reveal thick connective tissue capsules surrounding multiple abscesses containing numerous gram-positive bacilli. This, in combination with the culture results as reported by the contributor, identifies *C. pseudotuberculosis* as the underlying cause.

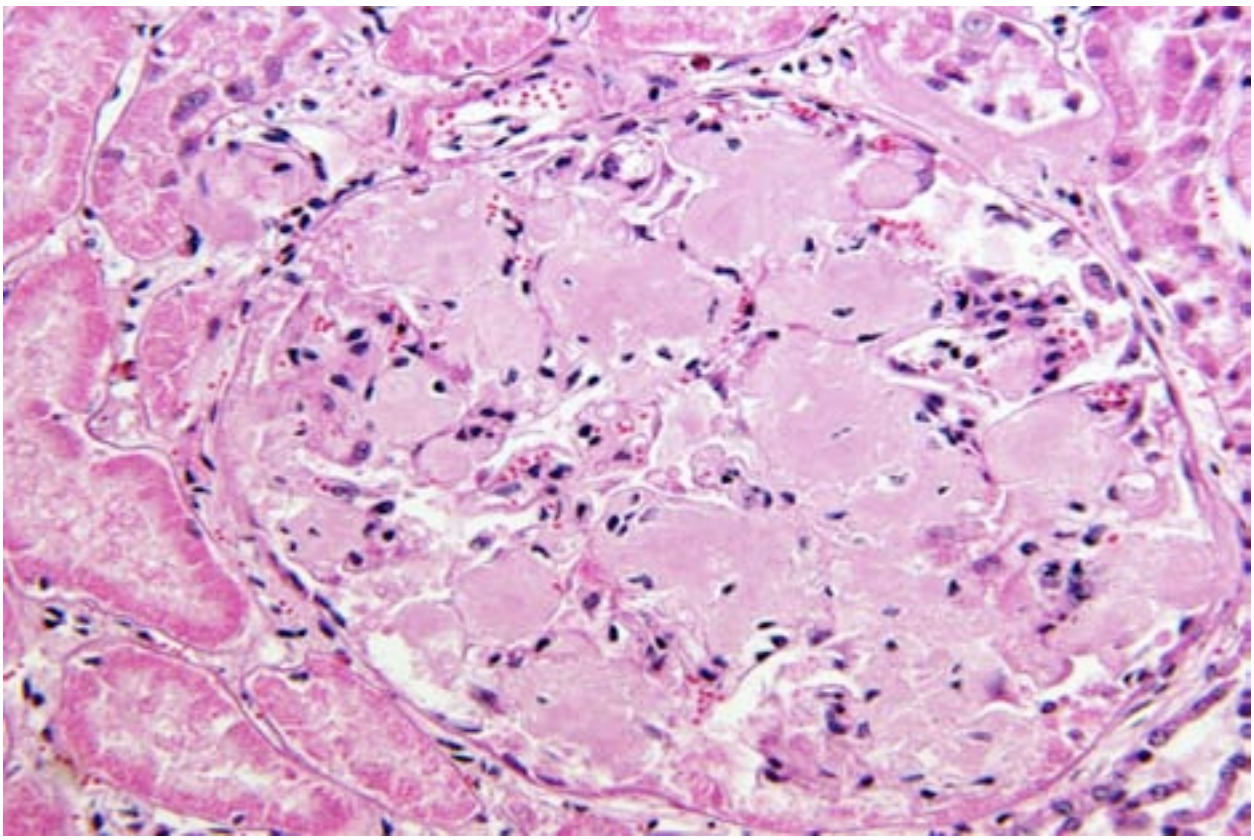

3-6. Kidney, Boer goat: Glomerular tufts are markedly expanded by amyloid. (HE 400X) (Photo courtesy of: Oklahoma State University Department of Veterinary Pathobiology, Room 250 McElroy Hall, Stillwater, OK 74078 www.cvm.okstate.edu)

The contributor provides an excellent summary of both *Corynebacterium pseudotuberculosis* (which is a potential zoonosis) and systemic amyloidosis in ruminants. Although *C. pseudotuberculosis* is relatively poorly characterized, some virulence determinants include the following: the leukotoxic phospholipase D exoprotein (PLD) contributes to the destruction of caprine macrophages during infection; the fagABC operon and the fagD gene play a role in virulence and are involved in iron acquisition; the high cell wall concentration of lipids aids in resistance to enzymatic digestion, allowing the bacterium to persist as a facultative intracellular parasite; and CP40, an immunogenic protein that exhibits proteolytic activity as a serine protease.[9] Additionally, recent studies have demonstrated that serum concentrations of haptoglobin (Hp), serum amyloid A and α1 acid glycoprotein are increased in experimental models of ovine caseous lymphadenitis due to *C. pseudotuberculosis*, which may predispose affected animals to systemic amyloidosis.[1] Readers are urged to review WSC 2013-2014, conference 6, case 4 for a more detailed discussion of amyloidosis.

Contributing Institution: Oklahoma State University
Department of Veterinary Pathobiology
Room 250 McElroy Hall
Stillwater, OK 74078

References:

1. Bastos BL, Loureiro D, Raynal JT, et al. Association between haptoglobin and IgM levels and the clinical progression of caseous lymphadenitis in sheep. *BMC Vet Res*. 2013;9(1): 254-262.
2. Biescas E, Jiron W, Climent S, Fernandez A, Perez M, Weiss DT, et al. AA amyloidosis induced in sheep principally affects the gastrointestinal tract. *J Comp Pathol*. 2009;140:238-246.
3. Crawford JM, Burt AD. Anatomy, pathophysiology and basic mechanisms of disease. Burt AD, Portmann BC, Ferrell LD, eds. *MacSween's Pathology of the Liver*. 6th ed. London, UK: Churchill Livingstone Elesvier; 2012:45-48.

4. Farnsworth GA, Miller S. An unusual morphologic form of hepatic amyloidosis in a goat. *Vet Pathol*. 1985;22:184-186.
5. Kingston RS, Shih MS, Snyder SP. Secondary amyloidosis in Dall's sheep. *J Wildl Dis*. 1982;18:381-383.
6. McGavin MD, Zachary JF, eds. *Pathologic Basis of Veterinary Disease*. 5th ed. St. Louis, MO: Mosby Elsevier; 2012:36-38, 182-189, 284-288, 429-432, 627-628, 758-764, 1031-1032, 1141-1142.
7. Mensua C, Carrasco L, Bautista MJ, Biescas E, Fernandez A, Murphy CL, et al. Pathology of AA amyloidosis in domestic sheep and goats. *Vet Pathol*. 2003;40:71-80.
8. Nakanuma Y, Zen Y, Portmann BC. Diseases of the bile ducts. Burt AD, Portmann BC, Ferrell LD, eds. *MacSween's Pathology of the Liver*. 6th ed. London, UK: Churchill Livingstone Elesvier; 2012:495-497.
9. Pinto AC, de Sá PH, Ramos RT, et al. Differential transcriptional profile of *Corynebacterium pseudotuberculosis* in response to abiotic stresses. *BMC Genomics*. 2014;15:1-14.

CASE IV: NEPRC Case 2 (JPC 3163069).

Signalment: 5-year-old male intact rhesus macaque, (*Macaca mulatta*).

History: This monkey was inoculated with SIVmac251 and was started on combined anti retroviral treatment (CART) 2 months following inoculation. CD 8 depletion was performed on days 6, 8, and 12 post infection.

Gross Pathology: The animal was in thin body condition and alopecia was present over the neck and back. The lungs were mottled, firm and partially collapsed with the left more affected than the right. The small intestine was multifocally thickened.

Histopathologic Description: Lung: Within the lung parenchyma, there are multifocal to coalescing areas (50 % of total area) of inflammation composed of a mixed population of foamy macrophages, histiocytes, multi-nucleated giant cells, and few numbers of neutrophils, lymphocytes, and plasma cells. Interspersed with these areas of inflammation is marked type II pneumocyte hyperplasia that often protrudes into and obscures affected alveolar lumina. Additionally, alveoli frequently contain foamy macrophages that are admixed with proteinaceous fluid (edema). The multinucleate cells are abundant in many areas and often contain up to 25 irregularly spaced nuclei. Often interspersed with the areas of inflammation are aggregates of non-degenerate neutrophils and macrophages in which the macrophages often are cytomegalic with marked karyomegaly and intranuclear eosinophilic inclusion bodies that measure 15-25 µm in diameter and are surrounded by a clear halo. Within large airways are occasional plugs of mucus, degenerate cellular debris, and scattered degenerate neutrophils. The pleura is multifocally thickened by fibrosis in several areas.

Contributor's Morphologic Diagnosis: Lung: Multifocal to coalescing severe chronic neutrophilic and histiocytic interstitial pneumonia with giant cells and intranuclear cytomegalovirus inclusions.

Contributor's Comment: Simian acquired immunodeficiency syndrome (SAIDS) is characterized by chronic persistent infection with simian immunodeficiency virus (SIV) along with high viremia, low CD4 titer as well as low anti-SIV antibodies that results in opportunistic infections.[14] These opportunistic infections include cytomegalovirus (CMV), *Pneumocystis*, *Mycobacterium* and adenoviral infections.[1]

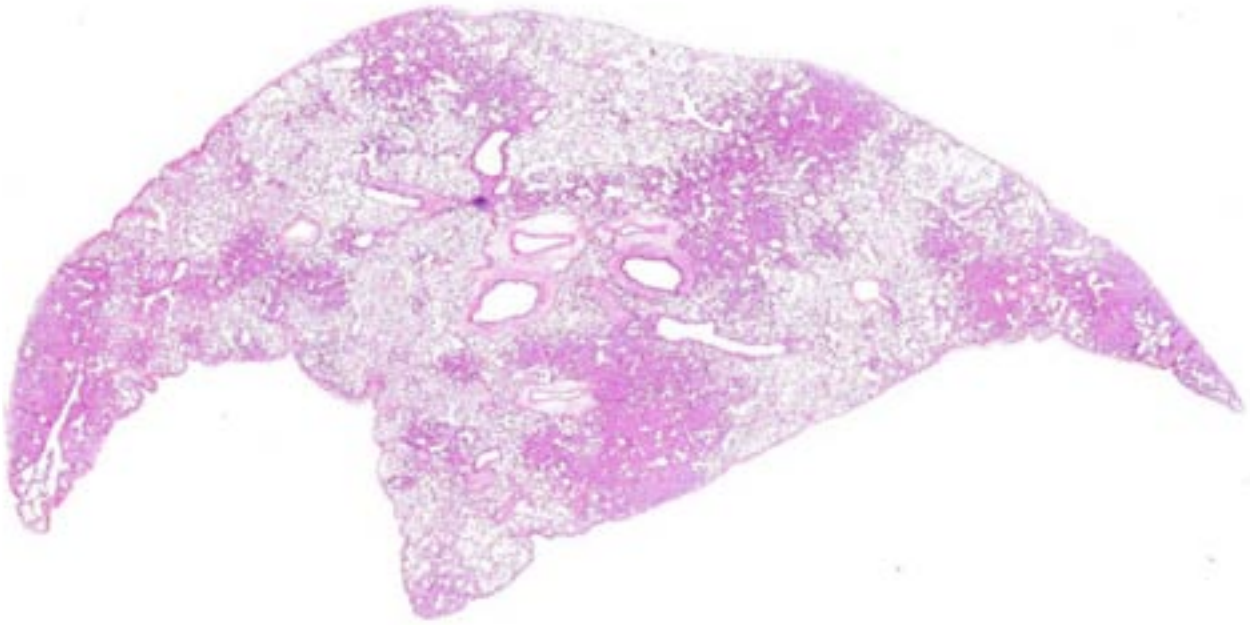

4-1. Lung, rhesus macaque: Approximately 50% of the lung exhibits patchy consolidation. (HE 0.63X)

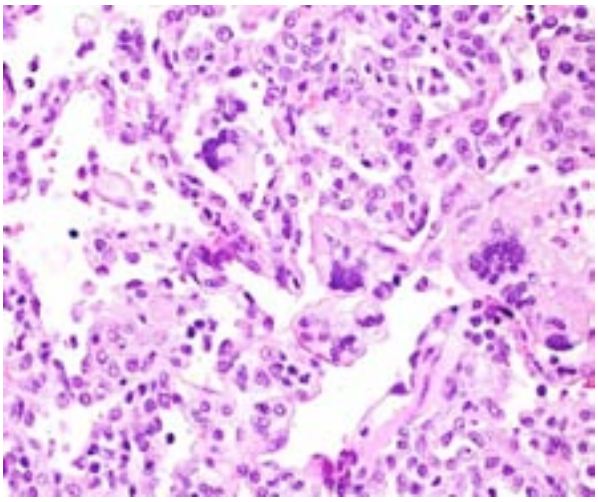

4-2. Lung, rhesus macaque: Within consolidated areas, alveolar septa are expanded by hyperplastic type II pneumocytes, macrophages, edema, and alveoli contain numerous foamy macrophages, multinucleated viral syncytia, and fewer neutrophils. (HE 400X) (Photo courtesy of: New England Primate Research Center, Harvard Medical School, One Pine Hill Dr., Southborough, MA 01772 http://www.hms.harvard.edu/nerprc)

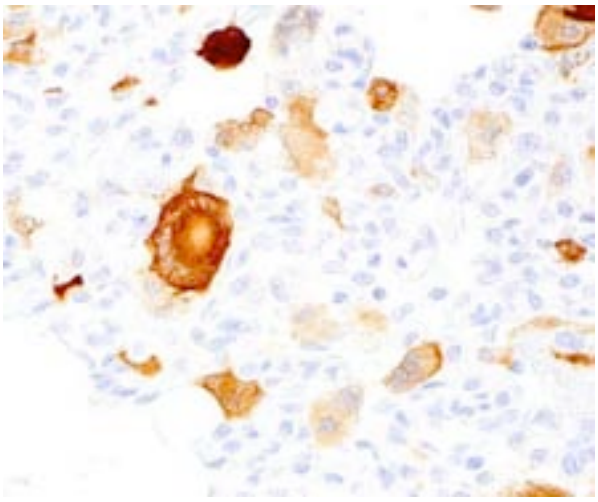

4-3. Lung, rhesus macaque: Giant cell macrophages are immunopositive for simian immunodeficiency viral antigen. (400X) (Photo courtesy of: New England Primate Research Center, Harvard Medical School, One Pine Hill Dr., Southborough, MA 01772 http://www.hms.harvard.edu/nerprc)

SIV belongs to genus lentivirus under the family *Retroviridae*. Retrovirus virions are enveloped, 80-100 nm in diameter, and have a unique three-layered structure. Innermost is the genome nucleoprotein complex, which includes about 30 molecules of reverse transcriptase, and has helical symmetry. This structure is enclosed within an icosahedral capsid, about 60 nm in diameter, which in turn is surrounded by a host cell membrane-derived envelope from which glycoprotein peplomers project. The genome is diploid, consisting of an inverted dimer of two molecules of linear positive-sense, single stranded RNA; each monomer is 7-11 kb in size and has a 3'-polyadenylated tail and a 5'-cap; the retrovirus genome is organized into 9 ORFs producing 15 proteins. SIV infection causes a spectrum of virally-induced lesions that include enteropathy, lymphocytic interstitial pneumonitis, giant cell pneumonia/lymphadenitis, and SIV encephalitis.

Giant cell pneumonia is characterized by multinucleated giant cells that are frequently found in terminal cases of SAIDS.[3] Formation of multinucleated giant cells is not completely defined but requires a myriad of factors including 1) infection with SIV, 2) cytokine elaboration from the multinucleated giant cells, and 3) macrophage infiltration.[2]

Cytomegalovirus (CMV) virions are enveloped, about 150 nm in diameter, and contain an icosahedral nucleocapsid about 100 nm in diameter. The genome consists of a single linear molecule of double-stranded DNA, 125-235 kbp in size. CMV belongs to the *Betaherpesvirinae* subfamily of *Herpesviridae,* under the order *Herpesvirales*. There are number of cytomegalovirus isolated from non-primates that include Cercopithecine herpesvirus 5 (CeHV-5) in African green monkeys, Cercopithecine herpesvirus 8 (CeHV-8) in rhesus monkeys, Human herpesvirus 5 (HHV-5) in humans, as well as Pongine herpesvirus in chimpanzees, Aotine herpesvirus 1 & Aotine herpesvirus 3 in owl monkeys. Betaherpesviruses replicate more slowly than alphaherpesviruses and often produce greatly enlarged cells, hence the designation cytomegalovirus.[16] Cytomegaloviruses infect the salivary glands, liver, spleen, lungs, eyes, and other organs, in which they produce characteristically enlarged cells with intranuclear inclusions and are typically accompanied by neutrophilic infiltrates.

Another common opportunistic lung infection in immunocompromised rhesus macaques is *Pneumocystis*. *Pneumocystis* pneumonia (PCP) is one of the most common opportunistic diseases in SAIDS.[1,2] Characteristic pathologic features of PCP include infiltration of inflammatory cells in the lung interstitium, thickened alveolar septa by hyperplastic type II pneumocytes, and foamy exudates in the alveoli. Some of these features

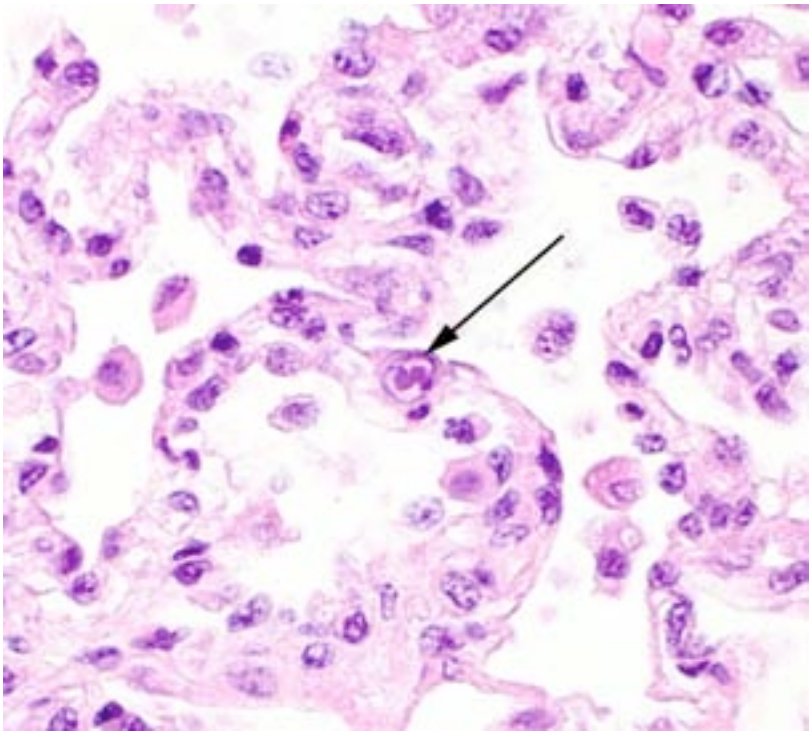

4-4. Lung, rhesus macaque: Within consolidated areas, occasional pneumocytes are karyomegalic and the nucleus contains a single enlarged eosinophilic cytomegaloviral inclusion. (400X) (Photo courtesy of: New England Primate Research Center, Harvard Medical School, One Pine Hill Dr., Southborough, MA 01772 http://www.hms.harvard.edu/nerprc)

were present in the submitted case; however, immunohistochemistry for *Pneumocystis* was negative in this case. Since *Pneumocystis* has a morphology similar to protozoa, it was initially considered as such; however, it is now classified as a fungus because the composition and structure of its cell wall [12,15] and nucleotide sequences are more similar to those of fungi than to those of protozoa.[6,13] Although *Pneumocystis* organisms are found in many different species of mammals, they are strictly species specific.[7] Some of the more common organisms include: *Pneumocystis jirovecii* (human), *P. wakefieldii* (rat), *P. murina* (mouse), and *P. carinii* (rhesus macaque).[5] In immunocompetent humans and animals, alveolar macrophages (AMs) protect the hosts against *Pneumocystis* infection by actively removing this extracellular organism from the alveoli. However, AMs from Pneumocystis infected animals are defective in phagocytosis,[4,9] and the number of AMs in humans and animals with PCP is reduced. These two defects impair innate immunity against *Pneumocystis* infection. The defect in phagocytosis is correlated to down regulation of mannose receptor on the macrophages.[8] The reduction in alveolar macrophage (AM) number is mainly due to increased rate of apoptosis[10] that is triggered by increased levels of intracellular polyamines[11] which could be due to either increased de novo synthesis and uptake of exogenous polyamines. Very little is known about the defect in phagocytosis during PCP.

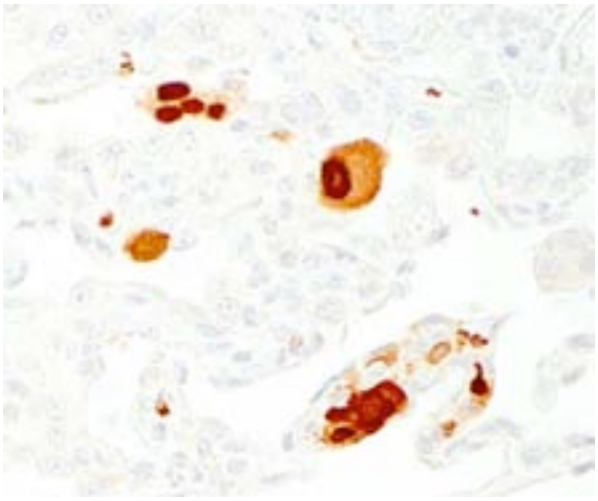

4-5. Lung, rhesus macaque: Pneumocytes are rarely immunopositive for cytomegalovirus antigen. (400X) (Photo courtesy of: New England Primate Research Center, Harvard Medical School, One Pine Hill Dr., Southborough, MA 01772 http://www.hms.harvard.edu/nerprc)

JPC Diagnosis: 1. Lung: Pneumonia, interstitial, histiocytic, with numerous viral syncytial giant cells.
2. Lung, alveolar macrophages: Intranuclear viral inclusions, rare.

Conference Comment: We thank the contributor for providing this excellent example and thorough analysis of two important entities in non-human primates. As noted by the contributor and demonstrated in this case, giant-cell pneumonia is a pathognomonic condition associated with SIV infection, while secondary infection with CMV produces significantly enlarged cells with characteristic intranuclear inclusion bodies. Although neutrophilic infiltrates typically accompany CMV infection, they are not a prominent feature in this case. The moderator also pointed out several opportunistic infections

(in addition to cytomegalovirus, *Pneumocystis* spp. mycobacteriosis, and adenovirus) associated with SIV infection in non-human primates, including *Cryptosporidium* spp., *Shigella* spp., *Campylobacter* spp. and Epstein-Barr virus.

Contributing Institution: New England Primate Research Center
Harvard Medical School
One Pine Hill Dr.
Southborough, MA 01772
http://www.hms.harvard.edu/nerprc

References:

1. Apetrei C, Robertson DL, Marx PA. The history of SIVS and AIDS: epidemiology, phylogeny and biology of isolates from naturally SIV infected non-human primates (NHP) in Africa. *Front Biosci*. 2004;9:225-254.
2. Baskar P, Narayan O, McClure HM, Hildreth JE. Simian immunodeficiency virus SIVsmmPBj 1.9 induces multinucleated giant cell formation in human peripheral blood monocytes. *AIDS Res Hum Retroviruses*. 1994;10:73-80.
3. Baskin GB, Murphey-Corb M, Martin LN, Soike KF, Hu FS, Kuebler D. Lentivirus-induced pulmonary lesions in rhesus monkeys (*Macaca mulatta*) infected with simian immunodeficiency virus. *Vet Pathol*. 1991;28:506-513.
4. Chen W, Mills JW, Harmsen AG. Development and resolution of *Pneumocystis carinii* pneumonia in severe combined immunodeficient mice: a morphological study of host inflammatory responses. *Int J Exp Pathol*. 1992;73:709-720.
5. Durand-Joly I, Wakefield AE, Palmer RJ, Denis CM, Creusy C, Fleurisse L, et al. Ultrastructural and molecular characterization of *Pneumocystis carinii* isolated from a rhesus monkey (*Macaca mulatta*). *Med Mycol*. 2000;38:61-72.
6. Edman JC, Kovacs JA, Masur H, Santi DV, Elwood HJ, Sogin ML. Ribosomal RNA sequence shows *Pneumocystis carinii* to be a member of the fungi. *Nature*. 1988;334:519-522.
7. Gigliotti F, Harmsen AG, Haidaris CG, Haidaris PJ. *Pneumocystis carinii* is not universally transmissible between mammalian species. *Infect Immun*. 1993;61:2886-2890.
8. Koziel H, Eichbaum Q, Kruskal BA, Pinkston P, Rogers RA, Armstrong MY, et al. Reduced binding and phagocytosis of *Pneumocystis carinii* by alveolar macrophages from persons infected with HIV-1 correlates with mannose receptor downregulation. *J Clin Invest*. 1998;102:1332-1344.
9. Lanken PN, Minda M, Pietra GG, Fishman AP. Alveolar response to experimental Pneumocystis carinii pneumonia in the rat. *Am J Pathol*. 1980;99:561-588.
10. Lasbury ME, Durant PJ, Ray CA, Tschang D, Schwendener R, Lee CH. Suppression of alveolar macrophage apoptosis prolongs survival of rats and mice with pneumocystis pneumonia. *J Immunol*. 2006;176:6443-6453.
11. Lasbury ME, Merali S, Durant PJ, Tschang D, Ray CA, Lee CH. Polyamine-mediated apoptosis of alveolar macrophages during Pneumocystis pneumonia. *J Biol Chem*. 2007;282:11009-11020.
12. Matsumoto Y, Matsuda S, Tegoshi T. Yeast glucan in the cyst wall of *Pneumocystis carinii*. *J Protozool*. 1989;36:21S-22S.
13. Pixley FJ, Wakefield AE, Banerji S, Hopkin JM. Mitochondrial gene sequences show fungal homology for *Pneumocystis carinii*. *Mol Microbiol*. 1991;5:1347-1351.
14. Silvestri G. AIDS pathogenesis: a tale of two monkeys. *J Med Primatol*. 2008;37 Suppl 2: 6-12.
15. Walker AN, Garner RE, Horst MN. Immunocytochemical detection of chitin in *Pneumocystis carinii*. *Infect Immun*. 1990;58:412-415.
16. Yue Y, Barry PA. Rhesus cytomegalovirus a nonhuman primate model for the study of human cytomegalovirus. *Adv Virus Res*. 2008;72:207-226.

Joint Pathology Center
Veterinary Pathology Services

WEDNESDAY SLIDE CONFERENCE 2013-2014

Conference 21

2 April 2014

CASE I: JHU 63507 (JPC 4019896).

Signalment: Adult age unknown male eastern box turtle, (*Terrapene carolina carolina*).

History: A colony of 27 box turtles has been maintained at the Maryland Zoo in Baltimore for many years without major disease issues. In 2011, 2 of the turtles were found dead and considered to be too autolyzed for necropsy submission. At that time, clinical findings in many of the other turtles included lethargy, inappetence, plaques on the tongue, soft palate, and cloaca. Remaining turtles were triaged, separated based on severity of clinical signs, and treated with antimicrobials, gavage feeding, and additional supportive care. Some turtles were euthanized due to lethargy, severe oral and cloacal

1-1. Oral cavity, box turtle: The tongue, soft palate and hard palate are covered in multifocal to coalescing fibrinonecrotic plaques. (Photo courtesy of: The Department of Molecular and Comparative Pathobiology, Johns Hopkins University, School of Medicine, 733 N. Broadway St., Suite 811 Baltimore, MD 21205)

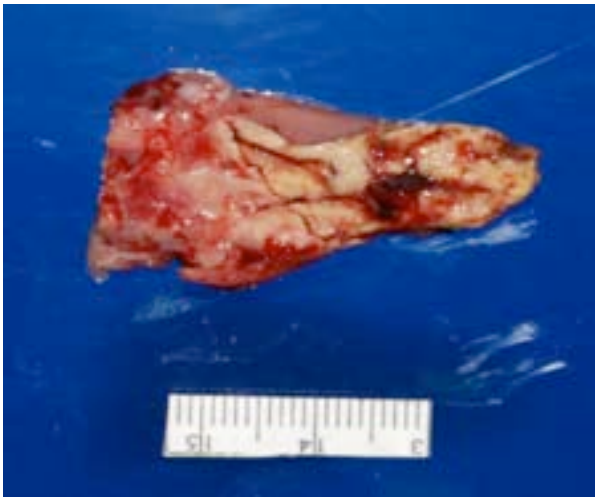

1-2. Tongue, box turtle: The tongue is covered by a fibrinonecrotic membrane. (Photo courtesy of: The Department of Molecular and Comparative Pathobiology, Johns Hopkins University, School of Medicine, 733 N. Broadway St., Suite 811 Baltimore, MD 21205. http://www.hopkinsmedicine.org/mcp/index.html)

plaques, and overall clinical decline. Over six weeks a total of 13 box turtles died or were euthanized. This turtle was placed in the severely affected group when triaged and did not respond to supportive therapy. It was found dead three days after triage and was submitted to the Johns Hopkins Department of Molecular and Comparative Pathobiology for evaluation.

Gross Pathology: Gross findings included severe multifocal to coalescing fibrinonecrotic plaques within the oral cavity including the tongue and soft palate and the hard palate. Mucosal plaques into the proximal half of the esophagus and mild multifocal mucosal plaques were present in the cloaca. The stomach had intralumenal non-adherent fibrinonecrotic debris, and 1-6mm ulcerated mucosal nodules with adherent superficial fibrinonecrotic material. The turtle was in poor to fair body condition with scant perivisceral fat.

Laboratory Results: PCR positive for ranavirus; sequencing result in other individuals: *frog virus 3*, PCR negative for herpesvirus.

1-3. Cross-section of skull, box turtle: The hard palate is multifocally covered by a serocellular crust (arrows). (HE 0.63X)

Histopathologic Description: Decalcified transverse section of the head, including oral cavity. The hard palate has multifocal to coalescing regions of mucosal loss with replacement by abundant fibrin, necrotic debris, and mixed heterophilic and lymphocytic infiltrates (including degenerate heterophils), with an overlying pseudomembranous crust consisting of sloughed epithelial cells, necrotic heterophils, fibrin, and bacterial colonies. At some edges of ulcerated areas, remnant squamous mucosa has ballooning degeneration, scattered intraepithelial heterophils and lymphocytes, intraepithelial edema, and occasional intracorneal foci of heterophilic and lymphocytic inflammatory cells. The submucosa contains multifocal perivascular lymphocytic and histiocytic infiltrates.

The lacrimal gland has multifocal mild interstitial lymphocytic inflammation with necrosis.

Contributor's Morphologic Diagnosis: 1. Oral cavity (hard palate): Stomatitis, heterophilic and lymphohistiocytic, ulcerative, fibrinonecrotic, multifocal to coalescing, subacute, severe, with moderate submucosal lymphohistiocytic perivasculitis, superficial pseudomembrane formation, and superficial bacteria.
2. Lacrimal gland: Adenitis, lymphocytic, necrotizing, multifocal to coalescing, moderate.

Contributor's Comment: The submitted case was one of 13 adult captive eastern box turtles from a zoological exhibit that all died over a span of several weeks. In addition to the severe stomatitis, microscopic findings included ulcerative and fibrinonecrotic glossitis, esophagitis, gastritis, cloacitis with pseudomembrane formation, and fibrinoid degeneration of vessel walls in the spleen,

subacute interstitial nephritis, subacute periportal hepatitis, lymphocytic enterocolitis, and lymphocytic perivasculitis in several organs. Inclusion bodies were not definitively identified in most cases and were rare in the lung and liver of one case. Incidental findings in several turtles included nodular gastritis with mixed necrotizing inflammation and intralesional nematode larvae. Primary differentials were ranavirus, herpesvirus, and septicemia.

Antemortem oropharyngeal samples were collected from many turtles and submitted for PCR detection. Ranavirus was confirmed in 8 of the 10 tested turtles submitted for necropsy, including all of the turtles with oral plaques similar to the submitted case. In two turtles, PCR was followed by DNA sequencing, identifying the ranavirus frog virus 3 in both cases. Herpesvirus was confirmed in 4 of the 10 tested turtles. Tissue from this turtle was negative for herpesvirus. Several bacterial agents were detected in oropharyngeal and blood samples from other ranavirus-positive turtles in this population, highlighting the potential role of secondary bacterial pathogens as factors contributing to inflammation, sepsis, and death of ranavirus-infected turtles.

Ranavirus currently is classified as a genus in the *Iridoviridae* family. Iridoviruses are large (120-200nm), icosahedral, double stranded DNA viruses that replicate in the cytoplasm. Ranavirus infections are important causes of disease in fish[9] and amphibians.[4] The ranavirus frog virus 3 has been reported with increasing frequency as a significant cause of mortality in several reptile species.[5] Environmental stressors, naïve or suppressed immunity, or introduction of novel strains may play a role in outbreaks that emerge in wild and captive reptiles. Amphibians and reptiles have been suggested as important reservoirs for ranaviruses that may cause economically and ecologically important disease in finfish.

Typical presentations of ranavirus infection in turtles includes cervical edema, palpebral edema, rhinitis, and stomatitis-glossitis.[5] A series of cases of ranavirus in captive eastern box turtles in North Carolina[1] describes clinical signs that also included cutaneous abscesses, oral erosions and abscesses, and respiratory distress. Other studies that include several species of turtles and tortoises describe similar signs as well as yellow-white oral plaques.[6,7] In these studies, histopathology revealed fibrinoid vasculitis of skin, mucous membranes, lungs, and liver, multifocal hepatic necrosis, multicentric fibrin thrombi, fibrinous

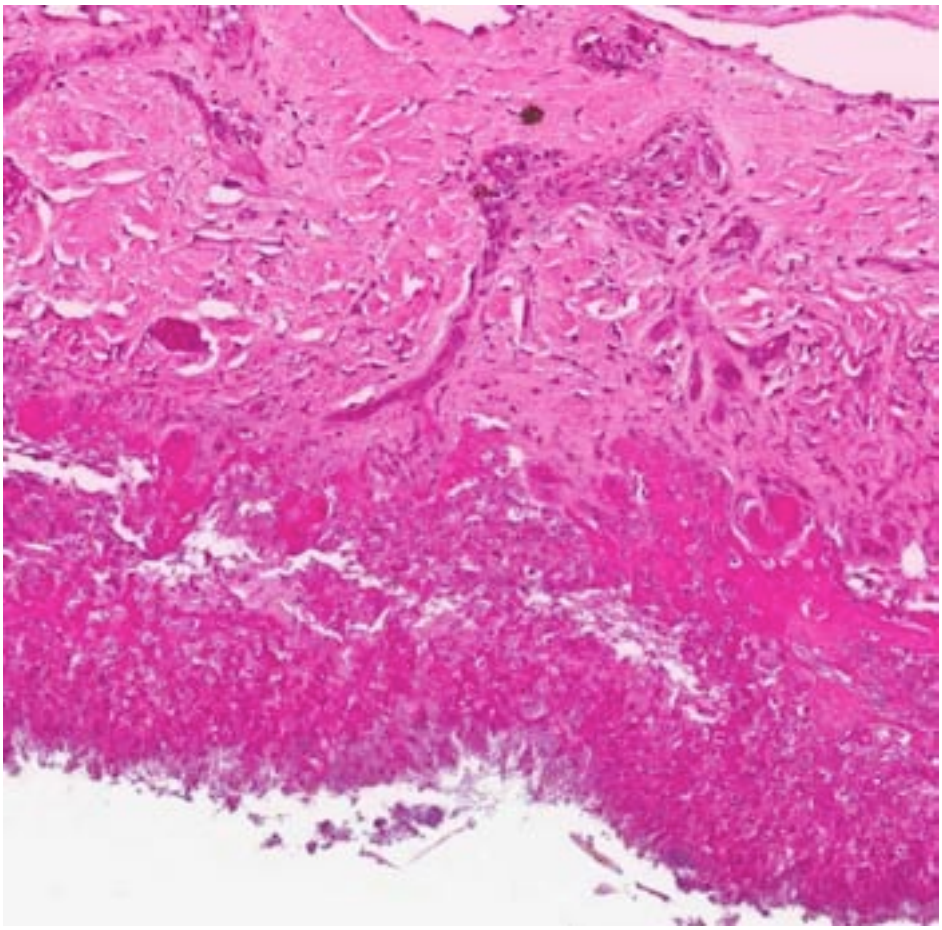

1-4. Oral cavity, hard palate, box turtle: There is full thickness necrosis of the mucosa overlying the hard palate, which is replaced with a serocellular crust. (HE 104X)

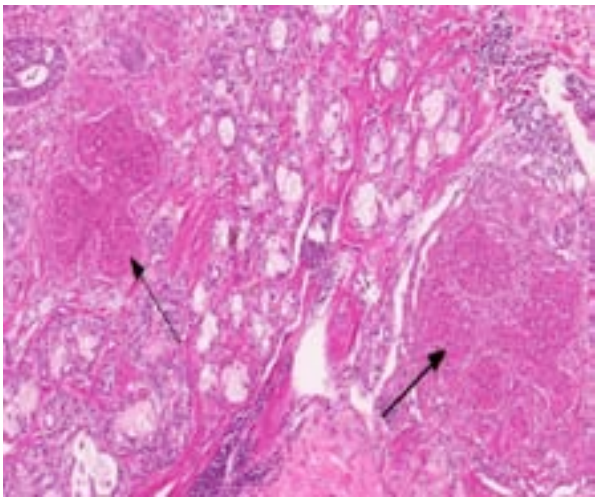

1-5. Lacrimal gland, box turtle: The gland contains multiple well-defined areas of lytic necrosis. (HE 84X)

and necrotizing splenitis, and necrotizing stomatitis and esophagitis. While basophilic intracytoplasmic inclusion bodies have been reported in ranavirus infections,[5] often they are not observed, even with ranavirus infection confirmed by PCR, electron microscopy, or virus isolation.[3,6]

JPC Diagnosis: 1. Oral cavity (hard palate): Stomatitis, necrotizing, focally extensive, severe. 2. Lacrimal gland: Dacryoadenitis, necrotizing, multifocal, moderate.

Conference Comment: Due to mild slide variation, the degree of lacrimal gland necrosis and inflammation within submitted sections varies; however, most conference participants appreciated some degree of necrotizing dacryoadenitis. The moderator concurred with this observation, but points out that reptiles and birds tend to have relatively high numbers of plasma cells within the normal lacrimal gland, so dacryoadenitis must be diagnosed with caution in these species. In addition to the differential diagnosis addressed by the contributor, including herpesvirus, bacterial septicemia and ranavirus, participants briefly discussed fungal infection (*Candida* spp.) and poxvirus as rule-outs for fibrinonecrotic stomatitis with pseudomembrane formation. These conditions can generally be differentiated histologically. Herpesvirus results in characteristic intranuclear viral inclusions, and poxvirus, while rarely reported in turtles, produces large intracytoplasmic inclusions.[1] Candidiasis can be distinguished microscopically by the presence of budding yeast, pseudohyphae and true hyphae.[2] In this case, viral inclusions were not identified and ranavirus was confirmed by PCR.

The contributor does an outstanding job of covering all the salient features of ranavirus infection in reptiles. Ranavirus, specifically frog virus 3, was initially associated with widespread disease epizootics in amphibians. Affected tadpoles (who are particularly vulnerable to infection) and frogs typically present with cutaneous hemorrhage/ulceration or disseminated disease with multiorgan necrosis. Subclinical infections are common in frogs; the kidneys and macrophage populations are considered the primary sites of virus persistence.[7] Both adult and larval salamanders are susceptible to a ranavirus known as Ambystoma tigrinum virus, which results in splenic, hepatic, renal and gastrointestinal necrosis, sloughing of the skin, and discharge of inflammatory exudate from the vent. Interestingly, ambient temperature appears to play a significant role in disease pathogenesis, as high mortality is observed in those salamanders infected at 18^{o}C, while those infected at 26^{o}C tend to survive.[8] Ranavirus infection in fish populations was first reported in Australian redfin perch and rainbow trout in the 1980's; it has since been implicated in multiple disease episodes in both farmed and wild freshwater fish worldwide. Fingerlings and juveniles are most susceptible, and disease is characterized by severe necrosis in the liver, pancreas and renal/splenic hematopoietic cells. In addition to these tissues, Santee-Cooper virus, a ranavirus in wild largemouth bass, also causes enlargement and inflammation of the swim bladder, resulting in moribund fish that tend to float to the surface. As in amphibians, ranavirus infections in fish can be subclinical.[8] Furthermore, inter-species transmission between amphibians and fish has been demonstrated, implicating both species as potential reservoirs for the virus.[8] Ranavirus is such a significant problem in both fish and amphibians that it meets the criteria for listing by the World Organization for Animal Health (OIE).[1]

Contributing Institution: The Department of Molecular and Comparative Pathobiology
Johns Hopkins University, School of Medicine
733 N. Broadway St., Suite 811
Baltimore, MD 21205
http://www.hopkinsmedicine.org/mcp/index.html

References:

1. Ariel E. Viruses in reptiles. *Vet Res*. 2011;42(1): 100-112.
2. Brown CC, Baker DC, Barker IK. Alimentary system. In: Maxie MG, ed. *Jubb, Kennedy and Palmer's Pathology of Domestic Animals*. Vol 2. 5th ed. Philadelphia, PA: Elsevier Limited; 2007:230.
3. De Voe R, Geissler K, Elmore S, Rotstein D, Lewbart G, Guy J. Ranavirus-associated morbidity and mortality in a group of captive eastern box turtles (*Terrapene carolina carolina*). *J Zoo Wildl Med:* official publication of the American Association of Zoo Veterinarians. 2004;35:534-543.
4. Gray MJ, Miller DL, Hoverman JT. Ecology and pathology of amphibian ranaviruses. *Dis Aquat Org*. 2009;87:243-266.
5. Jacobson ER. *Infectious Diseases and Pathology of Reptiles: Color Atlas and Text*. Boca Raton, FL: CRC/Taylor & Francis; 2007:288, 404-406, 440.
6. Johnson AJ, Pessier AP, Jacobson ER. Experimental transmission and induction of ranaviral disease in Western Ornate box turtles (*Terrapene ornata ornata*) and red-eared sliders (*Trachemys scripta elegans*). *Vet Pathol*. 2007;44:285-297.
7. Johnson AJ, Pessier AP, Wellehan JF, Childress A, Norton TM, Stedman NL, et al. Ranavirus infection of free-ranging and captive box turtles and tortoises in the United States. *J Wildl Dis*. 2008;44:851-863.
8. MacLachlan NJ, Dubovi EJ, eds. *Fenner's Veterinary Virology*. 4th ed. London, UK: Academic Press; 2011:172-175.
9. Whittington RJ, Becker JA, Dennis MM. Iridovirus infections in finfish - critical review with emphasis on ranaviruses. *J Fish Dis*. 2010;33:95-122.

CASE II: R13/337 (JPC 4035417).

Signalment: Adult male garter snake, (*Thamnophis sirtalis parietalis*).

History: Recurring skin masses after surgical excision.

Gross Pathology: Located caudo-dorsally on the body there were two skin masses measuring 2 x 1 x 1cm and 0.5 x 0.5 x 0.5 cm in size, covered by crusts. The masses were orange and firm and the larger mass infiltrated the underlying muscle. Located on the ventral side of the body there were two smaller nodules. The kidneys and liver were moderately enlarged and both organs showed multifocal to coalescing, poorly demarcated and infiltrative growing orange nodules of 0.1 x 0.1 x 0.1cm up to 2 x 2 x 2 cm size. The coelomic cavity and hemipenis were also infiltrated by small multifocal orange masses.

2-1. Skin, garter snake: Multiple orange-colored firm infiltrative nodules are present within the skin and extend into the underlying musculature. (Photo courtesy of: Institute of Animal Pathology, University of Berne, Länggassstrasse 122, Postfach 8466 CH-3001 Bern, Switzerland http://www.itpa.vetsuisse.unibe.ch/content/index_eng.html)

Histopathologic Description: Liver: 90 - 95% of the tissue is replaced by a poorly demarcated, non encapsulated, infiltrative, multilobulated and densely cellular mass with small groups of remaining hepatocytes. Neoplastic cells are closely packed, supported by scant amount of fibrovascular stroma and arranged in anastomosing cords, islands and sheets. The neoplastic cells are polygonal to spindleoid, 15 to 30 µm in size with indistinct cell borders and have a high amount of granular eosinophilic cytoplasm and often contain birefringent olive-green to golden-brown granular pigment within the cytoplasm. Nuclei are round to oval to irregular with finely stippled chromatin and have up to three prominent nucleoli. Many cells contain up to five oval to irregular nuclei or have a huge nucleus (megakaryosis). Anisocytosis and anisokaryosis are high and there is anaplasia of neoplastic cells. In 10 HPF there are nine mitotic figures, some of which are bizarre. There are multifocal randomly distributed areas of necrosis, characterized by hypereosinophilia of the cytoplasm, pyknotic nuclei, karyolysis and karyorhexis mixed with hemorrhage. Multifocally there are small groups and cords of remaining hepatocytes often showing hypereosinophilic, vacuolated and pyknotic nuclei (degeneration).

Contributor's Morphologic Diagnosis: Liver: Iridophoroma, malignant, metastatic, garter snake (*Thamnophis sirtalis parietalis*), reptile.

Contributor's Comment: Fish, amphibians and reptiles contain pigment cells in their skin that are called dermochromatophores.[1] These cells are derived from the neural crest and are characterized by the pigment they contain within their cytoplasm.[1] There are four types of dermochromatophores: melanophores, which contain melanin pigment, iridophores containing purines (colorless pigment), xanthophores containing carotenoids (yellow pigments) and erythrophores containing carotenoids and pteridines (red pigments).[1] Chromatophoromas are tumors arising from the cutaneous pigment cells that have been rarely reported[2,3] and are subclassified into three types

2-2. Liver, garter snake: The liver is moderately enlarged and contain multifocal to coalescing, poorly demarcated and infiltrative orange nodules of ranging up to 2cm in diameter. (Photo courtesy of: Institute of Animal Pathology, University of Berne, Länggassstrasse 122, Postfach 8466 CH-3001 Bern, Switzerland http://www.itpa.vetsuisse.unibe.ch/content/index_eng.html)

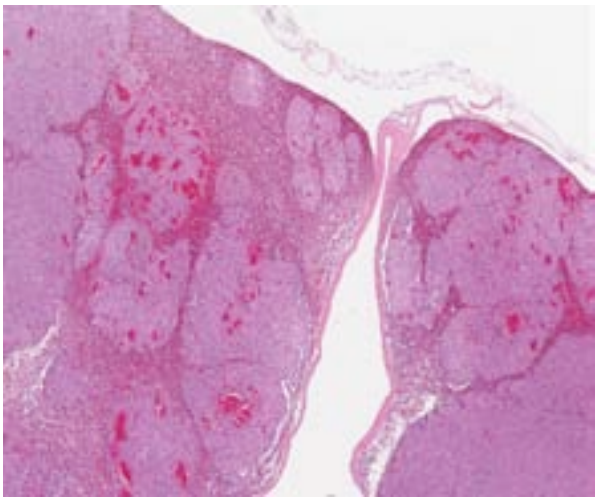

2-3. Liver, garter snake: 95% of the section is replaced by numerous nodules of an infiltrative, moderate cellular neoplasm. (HE 0.63X)

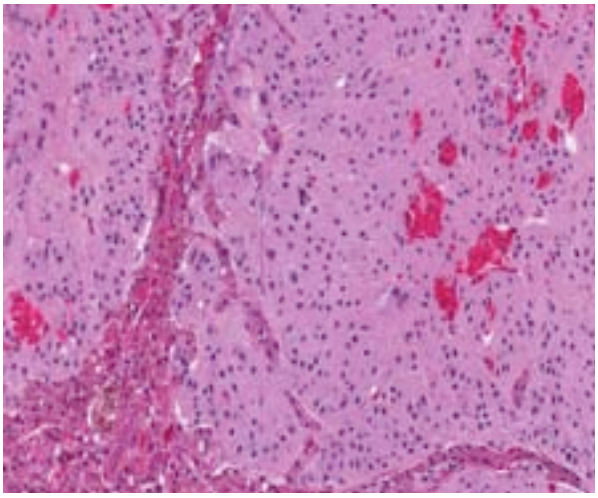

2-4. Liver, garter snake: Neoplastic iridophores are arranged in nests and packets, with a large amount of granular basophilic cytoplasm and hyperchromatic nuclei. There is marked anisokaryosis and occasional multinucleated cells. (HE 160X)

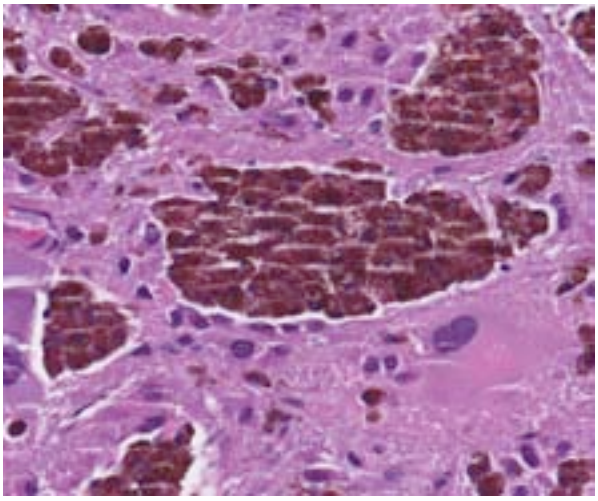

2-5. Liver, garter snake: Scattered throughout the neoplasm are islands of well-differentiated iridophores which contain greenish black bifrefringent granules. (HE 256X)

(melanophoromas or melanomas, xanthophoromas and iridophoromas) by the type of pigment they contain.[1,2] Chromatophoromas with combined features of all cell types have also been described.[4] The occurrence of these tumors in reptiles is higher than assumed and metastases are common.[1]

Iridophoromas occur as intraepidermal white masses and metastases have been observed in several organs.[2] Diagnosis of an iridophoroma is based on birefringent anisotropic granules within the neoplastic cells, distinguishing the iridophoroma from a melanophoroma and xanthophoroma. Based on the olive-green to golden-brown birefringent pigment within neoplastic cells we diagnosed a chromatophoroma of the subtype iridophoroma. Both benign and malignant iridophoromas have been reported in snakes, lizards, and fish.[1-3] Malignancy criteria of chromatophoromas in reptiles encompass the presence of intravascular (lymphatic/blood vessel) neoplastic cells, visceral metastasis, high pleomorphism and the presence of mitotic figures.[2]

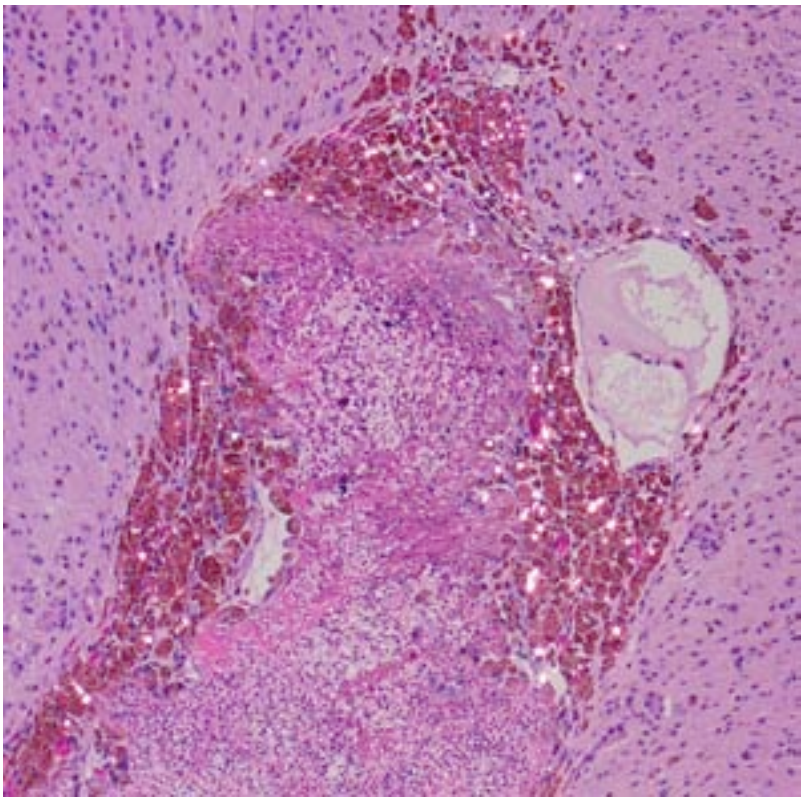

2-6. Liver, garter snake: The granules of well-differentiated iridophores are birefringent under polarized light. (Photo courtesy of: Institute of Animal Pathology, University of Berne, Länggassstrasse 122, Postfach 8466 CH-3001 Bern, Switzerland http://www.itpa.vetsuisse.unibe.ch/content/index_eng.html)

Both Melan-A and S-100 protein can be detected by immunohistochemistry in iridophoromas.[2]

JPC Diagnosis: Liver: Iridophoroma.

Conference Comment: The contributor provides an excellent summary of chromatophores and chromatophoromas in non-mammalian species. Chromatophores are contractile pigment cells that originate from embryonic neural crest cells and migrate to numerous tissues. Intracellular aggregation and dispersion of pigment granules engenders an ability to display rapid color changes in the skin, which can be important in camouflage, mating, and protection in many non-mammalian species.[4] Based on the presence of birefringent material within neoplastic iridophores, conference participants on the whole concurred with the diagnosis of iridophoroma; however, there was also a lively debate concerning the histogenesis of a collection of morphologically distinct cells within the neoplasm. These cells appear slightly more individualized and polygonal, with atypical nuclear morphology and abundant dark-brown to occasionally greenish intracellular pigment that is not as birefringent. Although a consensus was not reached, discussion centered upon whether these cells represent a unique clonal variant of the more spindled neoplastic cell population, or perhaps, as some participants suggested, these are simply aggregates of melanomacrophages, which are a normal component of many reptile and amphibian livers, trapped within the neoplasm.

Contributing Institution:
Institute of Animal Pathology, University of Berne
Länggassstrasse 122, Postfach 8466
CH-3001 Bern, Switzerland
http://www.itpa.vetsuisse.unibe.ch/content/index_eng.html

References:

1. Okihiro MS. Chromatophoromas in two species of Hawaiian butterflyfish, *Chaetodon multicinctus and C. miliaris*. *Vet Pathol*. 1988;25:422-431.
2. Heckers KO, Aupperle H, Schmidt V, Pees M. Melanophoromas and iridophoromas in reptiles. *J. Comp. Path.* 2012;146:258-268.
3. Suedmeyer K, Bryan JN, Johnson G, Freeman A. Diagnosis and clinical management of multiple chromatophoromas in an eastern yellowbelly racer (*Coluber constrictor flaviventris*). *J Zoo Wildl Med*. 2007;38(1):127-130.
4. AFIP Wednesday Slide Conference 29, 3 May 2000, Case I e S-49-98 (AFIP 2681629) http://www.askjpc.org/wsco/wsc/wsc99/99wsc29.htm

CASE III: 55819 (JPC 4032565).

Signalment: 1-month-old male Cape buffalo, (*Syncerus caffer caffer*).

History: The calf was part of a small herd in a large field enclosure at a zoological park. It was noted to be depressed and slow for 5 days and was briefly caught for examination, collection of blood and fecal samples for diagnostic testing, and empirical treatment with a non-steroidal anti-inflammatory drug, antibiotics and an anthelmintic. The calf was found dead the next day.

Gross Pathology: The calf was 42 kg and had adequate adipose stores. In both kidneys, the renal papillae were streaked with pale yellow, finely granular material. Similar material was also present in variable amounts in calices and pelvices as sand-like to 2-3 mm diameter, rough, irregular, friable stones. The urinary bladder was distended with thin, cloudy, off-white urine.

Laboratory Results:

Serum Chemistry	Value	Reference Range	Units
Albumin	3.7	2.8-3.8	g/dL
Total Protein	7.7	6.7-8.8	g/dL
Globulin	4.0	3.3-6.3	g/dL
BUN	**148**	10-23	mg/dL
Creatinine	**10.3**	0.7-1.2	mg/dL
Cholesterol	310	157-393	mg/dL
Glucose	246	41-74	mg/dL
Calcium	6.7	9.1-11.3	mg/dL
Phosphorus	**14.8**	5.1-8.7	mg/dL
Chloride	132	93-100	mEq/L
Potassium	5.6	4.1-5.5	mEq/L
Sodium	157	136-148	mEq/L
Alk Phos	225	23-96	U/L
ALT	11	15-43	U/L
Total Bilirubin	0.4	0.0-0.2	mg/dL

CBC	Value	Reference Range	Units
HCT	31	24-38	%
WBC	19.4	5.3-14.9	K/uL
Neutrophils	16498	2200-8073	per ul
Lymphocytes	2328	1431-8694	per ul
Monocytes	582	0-774	per ul
Eosinophils	0		per ul
Basophils	0		per ul
Platelets	1692		K/ul

Kidney stone analysis (Minnesota Urolith Center): 100% xanthine

Histopathologic Description: Kidney: The calices are dilated and contain abundant irregular, rounded, lamellated, basophilic concretions (nephroliths), which are partially composed of and mixed with refractile, birefringent, brown to green crystalline material. These concretions and crystals are mixed with neutrophils and cellular debris and multifocally disrupt the renal papillae and urothelium of the calices, which is variably attenuated or hyperplastic. Throughout the section, tubules are frequently dilated and contain pale eosinophilic hyaline casts, coarse granular eosinophilic debris, sloughed necrotic epithelial cells, neutrophils, or lamellated concretions of amphophilic, wispy, radiating, predominantly non-birefringent material similar to that in the calices. The tubular epithelium is often attenuated, necrotic or disrupted by the embedded concretions, which are sometimes covered with a layer of epithelium. There is multifocal mild fibrosis in the interstitium, and glomeruli are diffusely subjectively small.

Contributor's Morphologic Diagnosis: Kidneys: Severe diffuse chronic nephrolithiasis with myriad intra-tubular and intra-calices calculi and crystals, tubular ectasia, hyaline and cellular casts, interstitial fibrosis, hypoplastic glomeruli and mild neutrophilic pyelonephritis.

Contributor's Comment: This case is typical of xanthine urolithiasis, though this condition has not previously been reported in Cape buffalo. Small stones in the kidneys were composed of 100% xanthine by quantitative stone analysis. Accumulation of xanthine crystals and stones in renal tubules and calices results in obstruction, progressive tubular damage, and eventually renal failure. Xanthine urolithiasis is very rare in animals but has been described in Japanese Black calves, a Galician Blond beef calf, sheep, certain breeds of dogs (e.g. Cavalier King Charles Spaniels, Dachshunds), and cats.[1,3,6,7] The disease in this buffalo calf was very similar to cases of xanthine nephrolithiasis in domestic cattle, in which calves present between 1 and 6 months of age with renal failure.[1,4] The variably-sized, yellow to brown stones can be present in the kidneys, ureters, and bladder and are radiolucent. Diagnosis is based on stone analysis. In this case,

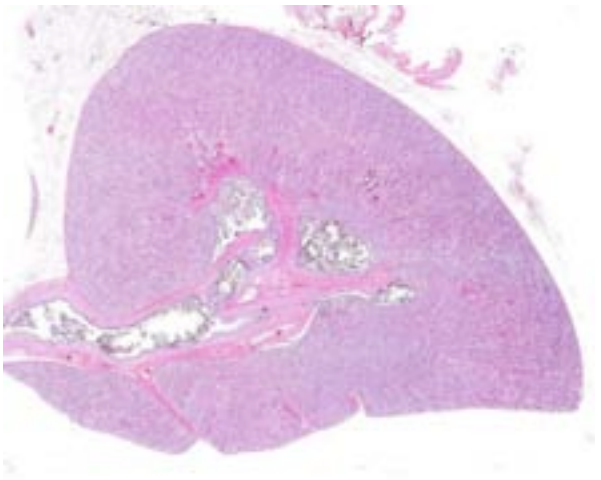

3-1. Kidney, Cape buffalo calf: The calyx is markedly expanded by lamellated birefringent mineralized concretions. (HE 0.63X)

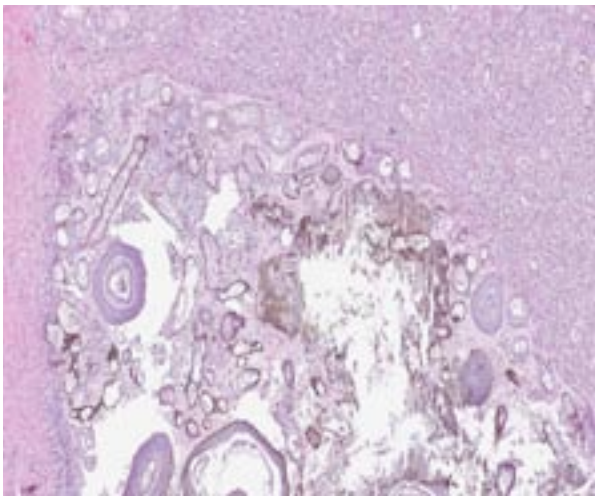

3-2. Kidney, Cape buffalo calf: Crystals are birefringent and amphophilic and range from 30- 250 µm in diameter. Occasionally crystals are outlined by highly birefingent greenish black pigment. They are admixed with moderate numbers of degenerate neutrophils and cell debris. (HE 88X)

other supporting findings included myriad small, spiculate crystals on examination of urine sediment and failure of the renal concretions to stain with von Kossa and Alizarin Red in histologic sections.

Xanthine is a metabolite of purines normally converted to uric acid by xanthine oxidase. Xanthinuria and xanthine urolithiasis result from loss of function of this enzyme, which can be the result of a primary enzyme defect inherited as an autosomal recessive condition or from secondary inhibition of enzyme function.[3,7] Cases of the secondary form are most often caused by treatment with allopurinol, an inhibitor of xanthine oxidase, and are thus most commonly seen in Dalmatian dogs treated for urate urolithiasis.[2,3] Dietary deficiency of molybdenum, a component of an essential cofactor of xanthine oxidase, was thought to account for xanthine urolithiasis in sheep.[3] The Cape buffalo calf in this report had not been treated with allopurinol and had normal levels of molybdenum on postmortem analysis of liver. It is therefore thought to have had a primary (hereditary) form of the disease, similar to cases in domestic cattle.[1,4,8] A half-sibling of this calf (same sire, different dam) had previously died at 2 months of age with nearly identical lesions, although stone analysis was not performed in that case. Four prior calves from the same dam and sire were unaffected. Characterization of the hypothesized genetic defect in this group of Cape buffalo has not yet been attempted.

JPC Diagnosis: Kidney: Nephrolithiasis, intracalyceal and intratubular, moderate to severe, with mild suppurative pyelonephritis, tubular proteinosis and tubular necrosis.

Conference Comment: Urolithiasis, a condition frequently encountered in domestic animal species, refers to the presence of calculi within urinary passages. Calculi can form in any part of the urinary system from the kidneys to the urethra. Due to the length and narrow diameter of the penile urethra, impaction secondary to urethral calculi is common in males, especially at the ischial arch, the sigmoid flexure in ruminants, the vermiform appendage in rams, and the proximal end of the os penis in dogs. Calculi are grossly visible concretions of precipitated mineral, urinary proteins and debris, while urethral plugs are composed of aggregates of "sandy sludge" with a higher proportion of organic material that tend to conform to the shape of the urinary cavity that they fill. Urolith formation is influenced by familial, congenital and pathophysiologic factors including urinary pH, relative dehydration, infection, anatomic abnormalities, foreign bodies (such as grass awns) and drug administration. The supersaturation of urine with stone-forming salts is an important precursor to urolith nucleation.[3] Crystal precipitation and aggregation also play a role in the development of urolithiasis, although crystalluria without calculus formation is a fairly common finding and the factors that promote/prevent the formation of uroliths are complicated and poorly understood. Horse urine,

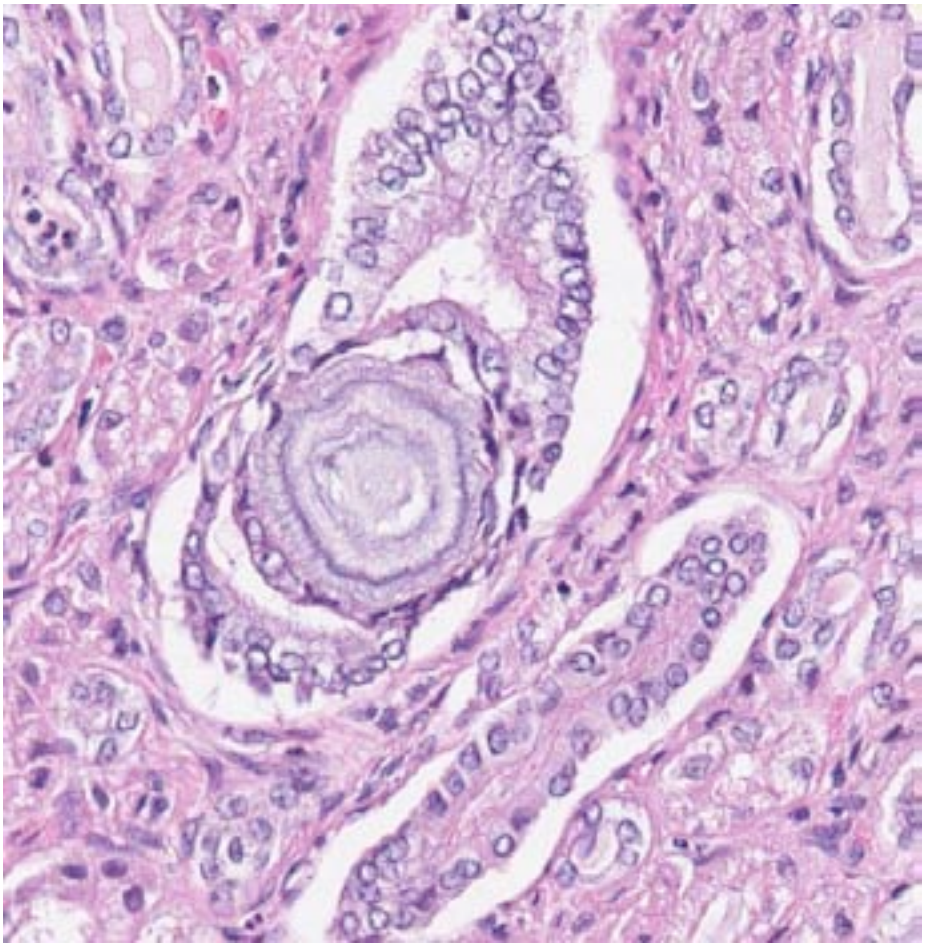

3-3. Kidney, Cape buffalo calf: Crystals are occasionally present within renal tubules. (HE 168X)

for instance, is normally supersaturated with calcium carbonate and crystalluria is a normal finding on equine urinalysis, yet horses rarely develop urinary calculi.[5]

The important types of urinary calculi in various species are listed in table 1; it is also worthwhile to remember that many uroliths are of mixed composition (although one mineral may predominate). Silica calculi are a significant cause of urinary tract obstruction in pastured ruminants and are occasionally seen in male dogs, especially German shepherds and old English sheepdogs or dogs receiving a ration high in plant-derived ingredients (i.e. corn gluten or rice/ soybean hulls). They are hard, white to dark brown, radiopaque and spherical/ovoid (in the urinary bladder) or angular/irregular (when in renal calyces) with a friable core.[3]

Struvite calculi are composed of magnesium ammonium phosphate hexahydrate; historically, they were inappropriately identified as "triple phosphate" calculi. Grossly, these radiopaque stones appear white to gray, chalky, smooth and easily fractured. They typically contain additional compounds such as calcium phosphate (which often forms a shell around the struvite), ammonium urate, oxalate or carbonate.[3] Struvites are most important in dogs, cats and ruminants where they are commonly associated with infection. Ureases produced by bacteria such as *Staphylococcus* spp. or *Proteus* spp. increase the urine pH, which decreases struvite solubility, thus favoring the formation of calculi. Miniature schnauzers appear predisposed, probably due to a familial susceptibility to urinary tract infections. Sterile struvite urolithiasis has been reported in a line of English cocker spaniels and beagles. The formation of struvite calculi within the urinary bladder of cats is one manifestation of an idiopathic condition known as feline lower urinary tract disease (FLUTD); Russian blues, Himalayans, Persians and castrated/spayed males and females are predisposed. Of note, struvite crystalluria is often seen in cats even without calculi; the reasons for this phenomenon are poorly understood. It should also be noted that amorphous urethral plugs containing Tamm-Horsfall mucoprotein, albumin, globulins, cellular debris and struvite crystals are a much more important cause of urethral obstruction in male cats, typically associated with concurrent urinary tract inflammation. Struvite calculi also occur in feedlot steers and sheep on a high grain ration. Much like cats, obstruction in ruminants is typically due to formation of a gritty sludge, rather than discrete calculi, while a high

phosphate diet predisposes sheep to struvite urolithiasis.[3,5]

Oxalate calculi tend to develop as large, solitary, white to yellow bladder stones covered with sharp spines. They are composed of calcium oxalate monohydrate or calcium oxalate dihydrate, and although the pathogenesis is poorly understood, it likely involves some combination of hypercalciuria and hyperoxaluria. The major causes of hypercalcemia/hypercalciuria are briefly discussed in WSC 2013-2014, conference 13, case 3. Oxalic acid may be ingested in some foods or synthesized from glyoxylic and ascorbic acid. The formation of calcium oxalate uroliths is inhibited by dietary magnesium, which forms soluble complexes with oxalate, and citrate, which forms a similar complex with calcium. Oxalate uroliths are the second most common type of calculi encountered in dogs and have been associated with hyperparathyroidism, hypercalcemia, hyperadrenocorticism and exogenous steroid administration. Male miniature schnauzers, bichon frises, lhasa apsos, Yorkshire terriers, shih tzus and miniature poodles are predisposed. The prevalence of oxalate urolithiasis is increasing in cats and is likely related to dietary factors, although the specifics are not clear. Since oxalate is metabolized in the rumen, oxalate calculi are not generally considered important in ruminants; however, they are reported in sheep grazing grain stubble, although the source of the oxalates in these cases remains unknown.[3,5]

Uric acid and urates are products of purine metabolism; calculi usually contain ammonium urate in combination with uric acid and phosphate. Uric acid/urate calculi are typically multiple, hard, laminated green-brown, radiodense spherical stones found within the urinary bladder. Urate stones are rarely reported in swine and cats but are most common in Dalmation dogs. In neonatal pigs in a negative energy balance, there is increased production of purine catabolites, which also predispose the formation of urate calculi. Urate urolithiasis in Dalmations results from an autosomal recessive defect in the hepatic uptake of uric acid, leading to its incomplete metabolism and accumulation. This defective transport system also inhibits tubular reabsorption of uric acid from the glomerular filtrate, resulting in urine that is supersaturated with urates.[3,5]

Xanthine is another purine metabolite, which, as noted by the contributor, is normally degraded via xanthine oxidase to uric acid. Xanthine stones are irregular, yellow to brown-red, laminated, friable and radiolucent.[3,5] This interesting case provides an excellent example of an uncommon condition (xanthine urolithiasis) in an unusual species. The contributor provides a thorough description of the gross pathology, histology, clinical-pathology and pathogenesis of xanthine urolithiasis in veterinary medicine.

Table 1. Composition of urinary calculi in select domestic animal species.[3]
* urinary calculi are uncommon in horses and rare in swine

Species	Common Types	Uncommon Types
Ox	Silica Struvite Carbonate	Xanthine
Sheep	Silica Struvite Oxalate "Clover stones" Carbonate	Xanthine
Dog	Struvite Oxalate Purines (urate, uric acid, xanthine)	Silica Cystine Calcium phosphate
Cat	Struvite Oxalate	Urate Cystine
Horse*	Carbonate	
Pig*		Urate (neonates)

Contributing Institution: Wildlife Disease Laboratories
Institute for Conservation Research, San Diego Zoo Global
http://www.sandiegozooglobal.org

References:
1. Hayashi M, Ide Y, Shoya S. Observation of xanthinuria and xanthine calculosis in beef calves. *Jap J Vet Sci*. 1979;41:505-510.
2. Ling GV, Ruby AL, Harrold DR, Johnson DL. Xanthine-containing urinary calculi in dogs given allopurinol. *J Am Vet Assoc*. 1991;198:1935-1940.
3. Maxie MG, Newman SJ. Urinary system. In: Maxie MG, ed. *Jubb, Kennedy and Palmer's*

Pathology of Domestic Animals. Vol 2. 5th ed. Edinburgh, UK: Elsevier Limited; 2007:508-514.
4. Miranda M, Rigueira L, Suarez ML, et al. Xanthine nephrolithiasis in a Galician blond beef calf. *J Vet Med Sci.* 2010;72(7);921-923.
5. Newman SJ. The urinary system. In: Zachary JF, McGavin MD, eds. *Pathologic Basis of Veterinary Disease*. 5th ed. St. Louis: Elsevier; 2012:643-645.
6. Tsuchida S, Kagi A, Koyama H, Tagawa M. Xanthine urolithiasis in a cat: a case report and evaluation of a candidate gene for xanthine dehydrogenase. *J Feline Med Surg*. 2007;9:503-508.
7. Van Zuilen CD, Nickel RF, van Dijk TH, Reijngoud D-J. Xanthinuria in a family of Cavalier King Charles spaniels. *Vet Quart.* 1997;19:172-174.
8. Watanabe T, Ihara N, Itoh T, Fujita T, Sugimoto Y. Deletion mutation in *Drosophila ma-l* homologous, putative molybdopterin cofactor sulfurase gene is associated with bovine xanthinuria type II. *J Biol Chem.* 2000;275(29); 21789-21792.

CASE IV: HE6491 (JPC 4033566).

Signalment: 2-year-old female green anaconda, (*Eunectes murinus*).

History: The snake was kept in a zoological garden and died suddenly.

Gross Pathology: The serosal surface of posterior half of small intestine was severely congested and the mucosal surface was diffusely covered with fibrinonecrotic exudate. The mucosa of large intestine had severe edema with mild fibrinous exudate on the surface.

Histopathologic Description: The normal structure of small intestine is largely lost but a portion of the lamina propria and tunica muscularis retains a normal lymphoid follicle. The lumen of small intestine is filled with fibrinonecrotic debris and the intestinal wall is diffusely and transmurally necrotic with moderate hemorrhage and edema. Smooth muscle fibers in the tunica muscularis are separated by edema and hemorrhage. Diffusely, macrophages and heterophils infiltrate the submucosa and extend to the serosal surface. Macrophages often contain hemosiderin and there are scattered multinucleated giant cells. Numerous amoebic trophozoites are admixed with multifocal aggregates of bacteria within the luminal necrotic debris. Amoebic trophozoites are also present within the submucosa and tunica muscularis; they are often vacuolated and rarely contain cellular debris. The trophozoites average 16 µm and range from 10 to 27 µm in diameter. They are positive for PAS stain. Cysts are also occasionally noted in and around the serosa. There is also multifocal vasculitis with thrombi and/or necrotic debris occluding the lumen. Serosal blood vessels are severely congested and occasionally contain amoebic trophozoites.

Contributor's Morphologic Diagnosis: Small intestine: Enteritis, fibrinonecrotizing, transmural, acute, diffuse, severe, with numerous amoebic trophozoites.

Contributor's Comment: Based on the species and histopathology as well as their size and morphology, amoebic trophozoites were tentatively identified as *Entamoeba sp.,* an obligate intracellular parasite with a direct life cycle.[4] *E. invadens* is one of the most significant protozoal parasites of reptiles, especially captive snakes and lizards.[2] *E. invadens* trophozoites range from 10 to 35 µm in diameter and the cysts range from 10 to 20 µm, with up to four nuclei.[6] Although the trophozoites and quadrinucleated cysts described above are morphologically indistinguishable from the primate amoeba, *E. histolytica*, *E. invadens* prefers a host or culture temperature of less than 31°C whereas *E. histolytica* evolves to thrive at 37°C.[2]

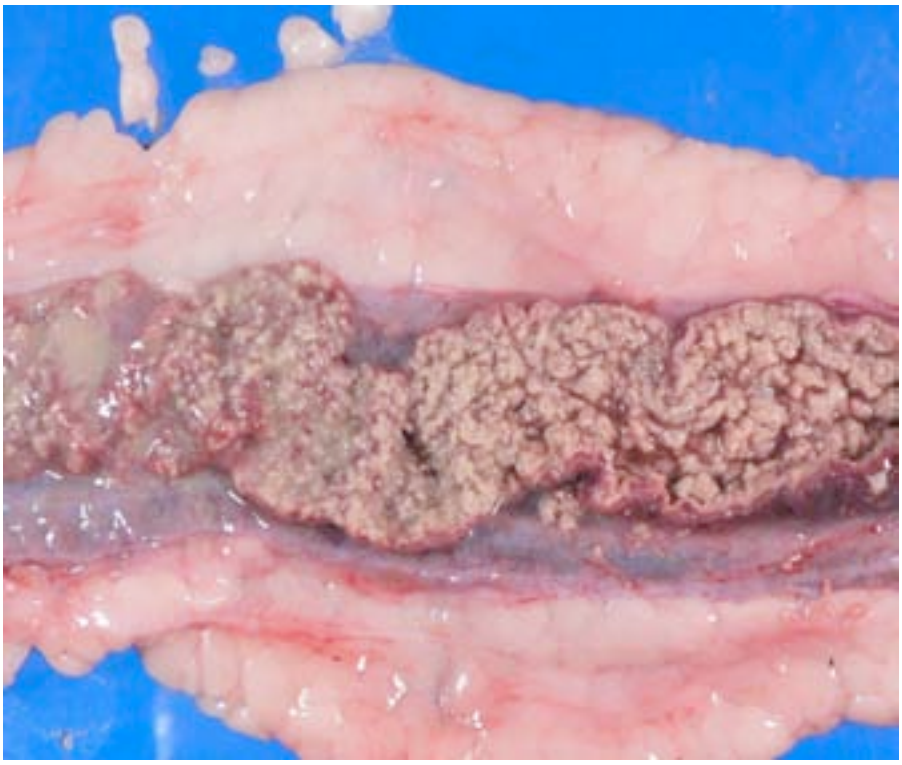

4-1. Ileum, green anaconda: The ileal mucosa is diffusely and circumferentially necrotic. (Photo courtesy of: Laboratory of Comparative Pathology, Graduate School of Veterinary Medicine, Hokkaido University, Sapporo 060-0818, Japan http://www.hokudai.ac.jp/veteri)

Herbivorous turtles are thought to serve as the

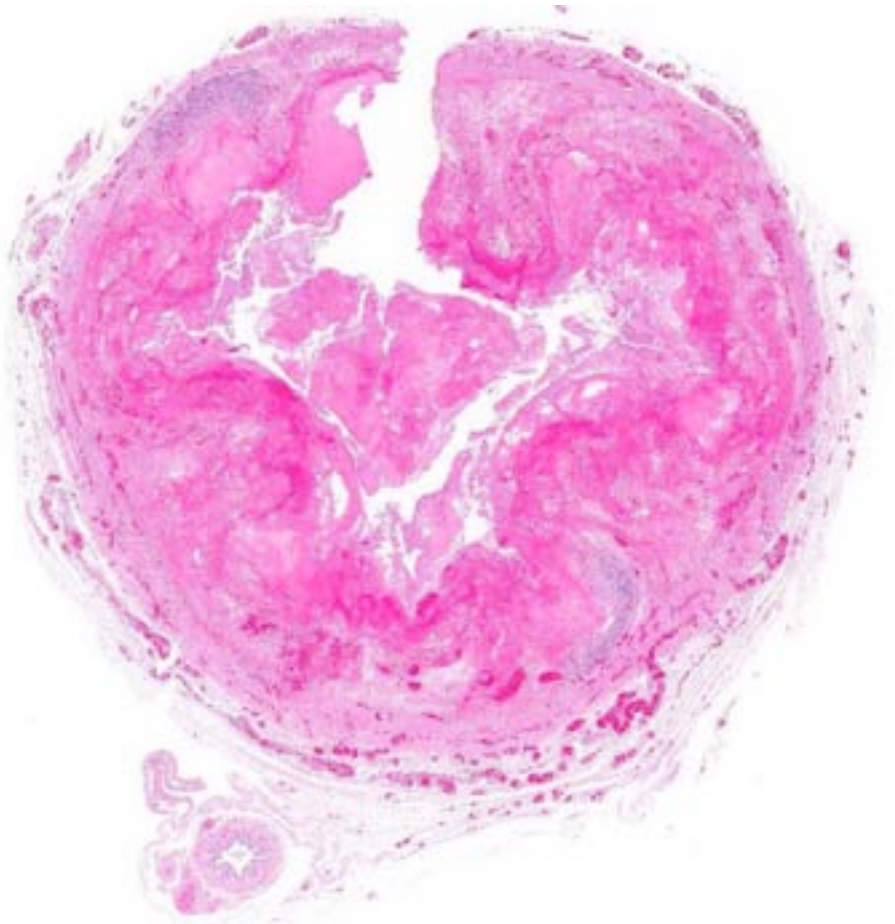

4-2. Intestine, green anaconda: There is diffuse circumferential and transmural necrosis of the intestine. (HE 0.63X)

natural host for *E. invadens*. In turtles, the parasite likely lives as a commensal symbiont without any pathogenicity.[2] While in the trophozoite state, these protozoa locomote and feed by forming pseudopodia. The resistant cyst stage is excreted in the feces. Following contamination of the water supply of snakes and lizards, the protozoa are ingested and induce a fulminating enteritis and hepatitis in these species. The clinical signs include regurgitation of undigested food and severe diarrhea, occasionally accompanied by blood- or bile-tinged green mucus, and/or remnants of intestinal mucosa.

The most characteristic microscopic lesion induced by *E. invadens* is severe intestinal erosion, ulceration and inflammation, often with formation of fibrinonecrotic pseudomembranes (diphtheritic enteritis).[2,6] Typically, the ileum and colon are the most severely affected intestinal segments and the affected gut wall is severely thickened. The protozoa invade blood vessels, spread systemically and induce necrosis and inflammation in various extra-intestinal tissues, especially the liver.

This anaconda has typical diphtheritic ileitis with numerous amoebic trophozoites and similar (though less severe) inflammation is observed in the large intestine. Although the protozoa often migrate in the sinusoids of liver and occasionally in the vessels of lung and kidney, there is no apparent damage to these organs in this case. We conferred with a veterinarian in the zoological garden in an attempt to elucidate the mechanism of infection in this case and were unable to reach a definitive conclusion; however, we suspect that the anaconda's water supply was contaminated by turtle feces.

Immunosuppression has been suggested as an important predisposing factor in snake *Entamoeba* infections. There is a recent report of diphtheritic colitis caused by an amphibian *Entamoeba* sp. in a Boa constrictor kept in a zoological garden.[6] Histopathological changes in this case were limited to the large intestine, implying that this *Entamoeba* may have a lower pathogenicity than *E. invadens*. As the snake suffered simultaneously from endoparasitism and inclusion body disease, the animal was suspected to be in an immunocompromised state. Our case also demonstrated moderate atrophy of lymphoid follicles in spleen, which may be a result of inadequate nutrition; however, the details are unclear.

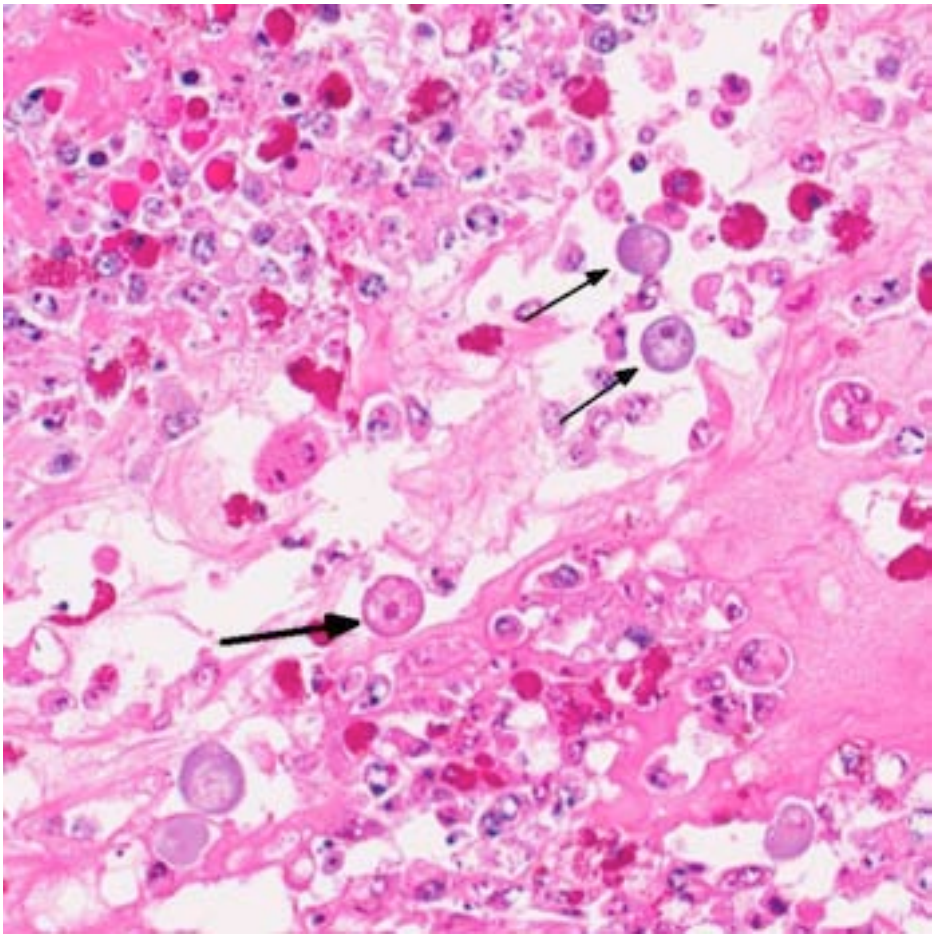

4-3. Intestine, green anaconda: Throughout the necrotic areas, numerous amoebic trohozoites (arrows) are admixed with numerous heterophils and abundant cellular debris. (HE 320X)

JPC Diagnosis: 1. Intestine: Enteritis, fibrinonecrotic, circumferential, diffuse, severe, with numerous amoebic trophozoites.
2. Mesenteric vessels: Vasculitis, necrotizing, multifocal, moderate.

Conference Comment: *Entamoeba* spp. is a protozoan parasite belonging to the phylum Sarcomastigophora, subphylum Sarcodina (Rhizopoda), order Amoebida, family Entamoebidae, genus *Entamoeba*.[3] Amoebae are normal, nonpathogenic inhabitants of the large bowel lumen in many species. Disease occurs upon invasion of the intestinal mucosa, and severity is influenced by diet, immune status, and the particular strain and virulence of the organism.[8] *E. invadens* and *E. histolytica* are two commonly important species in veterinary medicine, both of these amoebae have similar life cycles with two morphologically distinct stages. The labile trophozoite inhabits the host and is capable of locomotion, while the resistant quadrinucleate cyst form is protected by a cell wall and is able to survive under unfavorable environmental conditions. The cyst is infectious, and releases the motile trophozoite following ingestion by the host.[1,3] Virulence factors of *Entamoeba* spp. include 1) a Gal/GalNAc-specific lectin, which facilitates trophozoite adhesion to intestinal epithelial cells and may contribute to amoebic resistance to complement, 2) pore-forming polypeptides called amoebapores that insert a channel into the host cell membrane, leading to cell lysis, and 3) a family of cysteine proteases that function to break down the extracellular matrix, allowing amoebic tissue invasion.[1,5]

The contributor provides an excellent summary of *Entamoeba invadens* in reptiles. Chelonians and crocodilians are considered to be the natural hosts of *E. invadens* and may serve as a reservoir for infection in snakes and lizards in captivity. As noted by the contributor, transmission is typically feco-oral (probably related to contamination from turtle feces) and the most common presentation of invasive amoebiasis in reptiles is enteritis, often with subsequent hepatitis following hematogenous dissemination via the portal vein. After entering the mesenteric circulation, trophozoites may disseminate to other organs, although this is uncommon. There is a single report of amoebic myositis in a water monitor (*Varanus salvator*), presumably due to either hematogenous spread or direct invasion via skin wounds.[1]

Entamoeba histolytica is the etiologic agent of amoebic dysentery in humans, with an incidence of up to 500 million clinical cases per year,

including up to 100,000 fatalities.[5] *E. histolytica* is distributed worldwide among humans, but also occurs in a broad range of New and Old World monkeys and apes, and can be transmitted to dogs, cats, cattle and macropods; the pathogenesis is similar to *E. invadens*.[5,7,8] In Old World monkeys, amoebic dysentery typically induces necrotizing colitis, with occasional dissemination to the liver or (rarely) other tissues. Conversely, in certain species of leaf-eating monkeys, including colobus monkeys, silver leaf monkeys, douc langurs and proboscis monkeys, fibrinonecrotizing gastritis is the principle lesion associated with *E. histolytica*. It is thought that the normal neutral pH within these gastric compartments provides a favorable environment for excystation of ingested *E. histolytica*, followed by tissue invasion.[7] *E. histolytica* can be transmitted to dogs, cats and cattle, where it typically causes colitis;[3] gastric amoebiasis has been reported in a wallaby, a species with a complex, sacculated stomach adapted for fermentation that is similar to that of leaf-eating monkeys.[7]

In addition to severe fibrinonecrotic enteritis, conference participants found the multifocal necrotizing vasculitis and thrombosis within adjacent mesenteric vessels particularly striking. The etiology of this finding is unclear; discussion centered upon the possibility of direct damage from amoebic trophozoites versus the potential of a concomitant gram-negative septicemia (i.e. salmonellosis) with subsequent vasculitis.

Contributing Institution: Laboratory of Comparative Pathology
Graduate School of Veterinary Medicine, Hokkaido University
Sapporo 060-0818, Japan http://www.hokudai.ac.jp/veteri

References:

1. Chia MY, Jeng CR, Hsiao SH, Lee AH, Chen CY, Pang VF. *Entamoeba invadens* myositis in a common water monitor lizard (*Varanus salvator*). *Vet Pathol*. 2009;46(4):673-676.
2. Frye F. *Reptile Care: An Atlas of Diseases and Treatments*. Vol. I. Neptune City, NJ: T.F.H. Publications; 1991:278-285.
3. Gardiner CH, Fayer R, Dubey JP. *An Atlas of Protozoal Parasites in Animal Tissues*. 2nd ed. Washington, DC: Armed Forces Institute of Pathology; 1998:10-11.
4. Gelberg, HB. Alimentary system and the peritoneum, omentum, mesentery, and peritoneal cavity. In: Zachary JF, McGavin MD, eds. *Pathologic Basis of Veterinary Disease.* 5th ed. St. Louis: Elsevier; 2012:395.
5. Petri, WA Jr. Intestinal invasion by *Entamoeba histolytica. Subcell Biochem.* 2008;47:221-232.
6. Richter B, Kübber-Heiss A, Weissenböck H. Diphtheroid colitis in a Boa constrictor infected with amphibian *Entamoeba* sp. *Vet. Parasitol.* 2008;153:164-167.
7. Stedman NL, Munday JS, Esbeck R, Visvesvara GS. Gastric amebiasis due to *Entamoeba histolytica* in a Dama Wallaby (*Macropus eugenii*). *Vet Pathol*. 2003;40(3): 340-342.
8. Strait K, Else JG, Eberhard ML. Parasitic diseases of nonhuman primates. In: Abee CR, Mansfield K, Tardif S, Morris T, eds. *Nonhuman Primates in Biomedical Research: Diseases*. London, UK: Academic Press; 2012:206-208.

Joint Pathology Center
Veterinary Pathology Services

WEDNESDAY SLIDE CONFERENCE 2013-2014

Conference 22

09 April 2014

CASE I: 13-31218 (JPC 4033968).

Signalment: 4.5-year-old female spayed Yorkshire terrier, (*Canis familaris*).

History: A 4.5-year-old, spayed female Yorkshire terrier dog was referred to the University of Illinois Veterinary Teaching Hospital for neurologic evaluation. The animal had become blind and was circling to the right six months prior to presentation to the hospital. One week prior to presentation, the animal had become ataxic and unable to right itself after falling.

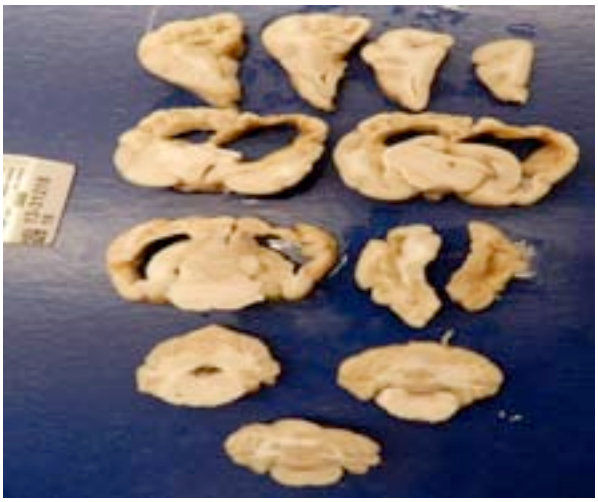

1-1. Cerebrum, dog: The ventricles are markedly dilated. There were multiple, 1 mm to 8 mm in diameter, gray to pink, depressed foci in the periventricular areas and within the cortical white matter and are associated with thinning of the cortical grey matter. (Photo courtesy of: Department of Pathobiology, College of Veterinary Medicine, University of Illinois Urbana-Champaign, 2001 S. Lincoln Ave., Urbana, IL 61801 http://vetmed.illinois.edu/path/)

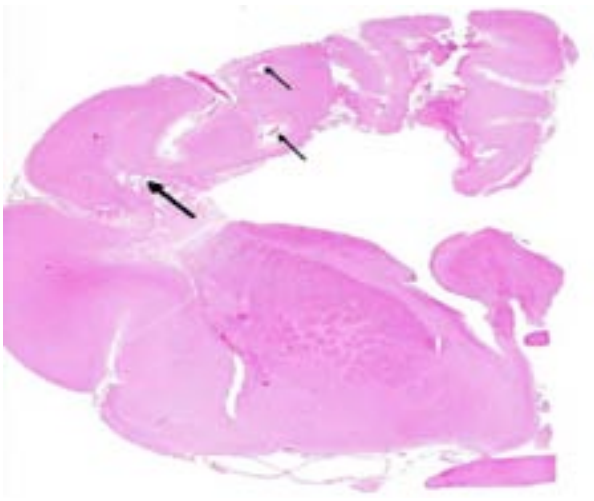

1-2. Cerebrum, dog: There are multiple areas of cavitation within the cortical white matter. (HE 0.63X)

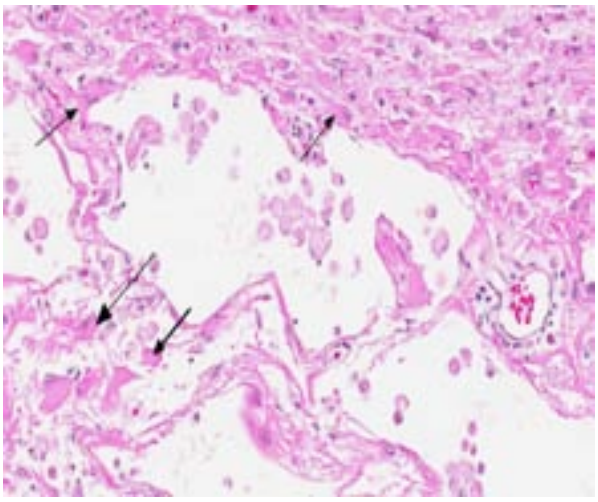

1-3. Cerebrum, dog: Cavitated areas contain few Gitter cells and are bounded by gemistocytic astrocytes. (arrows). (HE 140X)

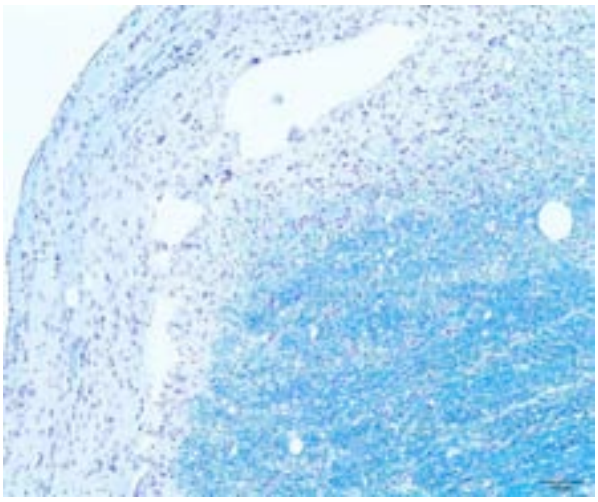

1-4. Cerebrum, dog: A Luxol fast blue stain for myelin shows the absence of myelin in cavitated areas. (Photo courtesy of: Department of Pathobiology, College of Veterinary Medicine, University of Illinois Urbana-Champaign, 2001 S. Lincoln Ave., Urbana, IL 61801 http://vetmed.illinois.edu/path/)

On initial neurologic examination, the animal had a left head turn and tilt, thoracolumbar kyphosis and extensor rigidity of the pelvic limbs. The animal was tetraplegic but could move all limbs when supported ventrally. The animal would alligator roll to the left when attempting to stand. Placing responses and hopping were absent in all four limbs. Muscle tone was increased in all four limbs, most markedly in the pelvic limbs. Spinal reflexes were increased in the pelvic limbs (with a crossed extensor). Menace response was absent in both eyes and there was a resting ventrolateral strabismus in the left eye. Pain could be elicited on palpation over the calvarium and cervical spine. Complete blood count, chemistry profile and preprandial and postprandial bile acids testing showed no significant abnormalities.

The animal's neurologic status improved somewhat after treatment with prednisone, and the animal was no longer painful. Two weeks after starting the steroid medication, a neurologic examination showed no change to the cranial nerve deficits and a continued head tilt and turn; however, the animal was able to walk again (with tetraparesis and tetrataxia). The animal continued to show improvement on steroids for six weeks but then began to show worsening neurologic symptoms. At final examination, the animal's demeanor was dull, and it was unable to stand with or without support. Proprioception was decreased to absent in all four limbs. In addition to previously observed cranial nerve symptoms, the animal now had mild anisocoria (left > right) and positional slow rotary nystagmus. The owner elected euthanasia.

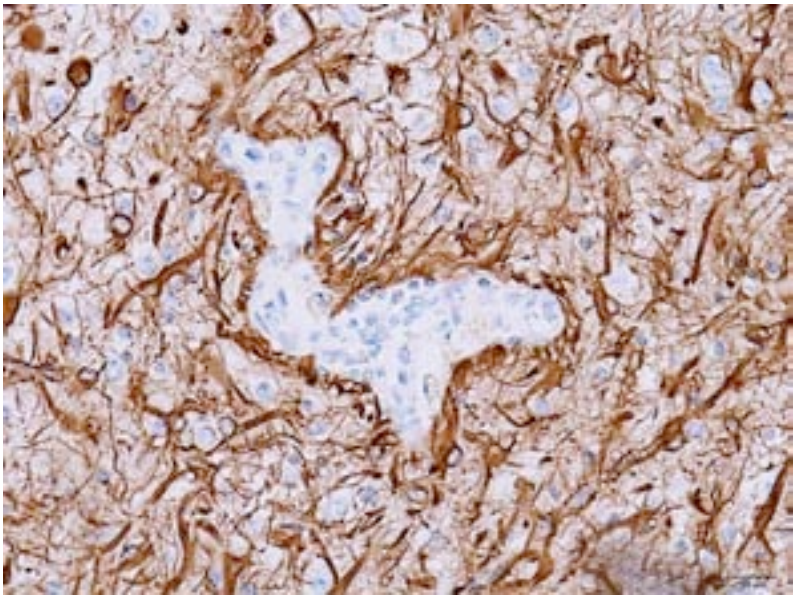

1-5. Cerebrum, dog: A glial fibrillary acidic protein (GFAP) stain highlights the numerous astrocytes and their processes in tissue bordering areas of cavitation. (Photo courtesy of: Department of Pathobiology, College of Veterinary Medicine, University of Illinois Urbana-Champaign, 2001 S. Lincoln Ave., Urbana, IL 61801 http://vetmed.illinois.edu/path/)

Gross Pathology: On necropsy, the

animal was in fair to poor nutritional condition, with mottled dark pink to red lungs (congestion), mild tonsillar atrophy, and moderate cardiomegaly. On opening of the calvarium, the right hemisphere of the brain was fluctuant. The exterior of the cerebral cortex was moderately to markedly thinned, and partially translucent. On coronal incision into the cerebral hemispheres, a large amount of clear, slightly yellow fluid was released from the markedly distended ventricles. There were multiple, 1 mm to 8 mm in diameter, gray to pink, depressed foci in the periventricular areas and within the cortical white matter. Extending from the frontal to the occipital cerebral cortex, these white matter lesions were irregular, bilateral but non-symmetrical, and often associated with thinning of the cortical grey matter. Lesions were more severe in the right hemisphere than the left. There was a focal, 1 mm in diameter cavitation in the left metencephalon. Other areas of the brain (i.e. cerebellum, retina, optic nerve) were not affected.

	Value	Reference Range	Units
HCT	55.8%	35-52%	
MCHC	31.3	32.0-36.0	g/dL
Eosinophils	$0.081x10^3$	0.1-1.0 $x10^3$	/μL

Laboratory Results:

CBC:

- Anisocytosis: 1+
- Polychromasia: rare

	Value	Reference Range	Units
Globulin	2.6	2.7-4.4	g/dL
Alb/Glob ratio	1.3	0.6-1.1	
ALT	93	8-65	U/L
Total T4	14.3	15.0-48.0	nmol/L
Bile acids (preprandial)	15.5	0.0-7.5	nmol/L
Bile acids (postprandial)	16.0	0.0-25.0	nmol/L

- Target cells: 4+

Chemistry:

Microbiology:

Aerobic culture:

- Brain: *Pasteurella multocida* – few
- Brain: Alpha strep non-Enterococcus – rare
- Brain: *Escherichia coli* - rare

Anaerobic culture:

- Brain: *Clostridium perfringens* - v. few
- Brain: *Prevotella* - few

Histopathologic Description: The cerebral white matter was severely affected by bilateral but asymmetric white matter degeneration. Loss of white matter ranged from 75% to nearly 100%, generally decreasing in a cranial to caudal direction through the cerebral hemispheres. Degeneration was characterized by loss of tissue substance with formation of pseudo-cysts delineated by numerous reactive astrocytes (gemistocytes) admixed with foamy macrophages (gitter cells) and few lymphocytes. The ventricles were markedly enlarged (compensatory hydrocephalus). Staining with GFAP for astrocytes revealed a marked gliosis throughout the affected areas. The Virchow-Robin space of occasional blood vessels was expanded by a mild infiltrate of lymphocytes, plasma cells, and occasional macrophages. The loss of white matter was verified by an almost complete lack of staining for myelin with Luxol fast blue within affected areas. In less severely affected white matter areas, like the corpus callosum, marked and abrupt areas of demyelination were often noted. Within the brain stem, similar multifocal loss of white matter was identified in the dorsal thalamus, geniculate area, and mesencephalon. One focal area of cavitation was noted in the metencephalon. The occasional neurons encountered within degenerate areas appeared unaffected. No histopathologic lesions were noted within gray matter adjacent to areas of white matter degeneration.

Contributor's Morphologic Diagnosis: Brain, cerebrum: Severe, necrotizing, leukoencephalitis with marked astrogliosis and compensatory hydrocephalus.

Contributor's Comment: Necrotizing leukoencephalitis of Yorkshire Terriers (NLE) is a rare, idiopathic, inflammatory disease of the central nervous system. It is characterized by infiltration by inflammatory cells into the white matter of the cerebrum and brainstem, with consequent widespread cavitation necrosis, demyelination, perivascular lymphoplasmacytic

cuffing and glial scarring. Active lesions are characterized by marked lymphohistiocytosis, glial activation, and infiltration by numerous gitter cells and gemistocytes. Quiescent, chronic lesions are characterized by marked cavitation, advanced gliosis, and a relative paucity of inflammatory and gitter cells.[11] Lymphoplasmacytic cuffing in the case under discussion was relatively mild, but in other reported cases of NLE, perivascular lymphoplasmacytic exudate has been marked and extensive.[4,7,11] NLE is relatively sparing of the cerebral cortex and meninges, and predominantly affects periventricular cerebral white matter, including the centrum semiovale, thalamocortical fibers, internal capsule and thalamus.[7]

NLE is commonly grouped with Necrotizing Meningoencephalitis (NME) or pug dog encephalitis[7] in veterinary literature. While breed predilection and lesion topography vary between the two diseases (NME affects gray and white matter primarily in the cerebral cortex, hippocampus and thalamus,[4] while NLE affects the cerebra and brainstem), the hallmark of both diseases is lymphoplasmacytic meningoencephalitis and bilateral, asymmetric, cerebral necrosis.[7] There is some debate as to whether these diseases are two distinct entities or one disease with a similar pathogenesis but histopathologic differences as a result of minor genetic differences between breeds, modifying genes and/or variations in antigenic exposures.[7]

NLE was first described in Yorkshire terriers in 1993,[9] and has since been diagnosed in French bulldogs as well.[6,8] It primarily affects young adult dogs, with a mean age of onset of 4.5 years (range, 4 months to 10 years old).[8] It appears to affect male and female dogs equally.[9] Clinical signs on initial presentation are referable to the location of the cerebral lesions, and commonly include visual deficits or blindness, depression, seizures, circling, ataxia and head tilt.[6] Conventional treatment is with immunosuppressive doses of glucocorticoids. Survival after diagnosis varies between 3 and 18 months[2] and the disease is invariably progressive and fatal.

The etiology of NLE is poorly understood. No infectious agents have ever been identified in association with NLE; PCR screening in dogs with histopathologic diagnoses of NLE and NME for the presence of degenerate herpesvirus, adenovirus, and canine parvovirus viral proteins have revealed no viral proteins,[1] and IHC staining for *Toxoplasma gondii* and *Neospora caninum* are routinely negative. However, negative PCR results for viruses does not rule out the possibility of a viral trigger for the disease via molecular mimicry, or the possibility that a pathogen is present at undetectable levels in the presence of a self-perpetuating immune response, a phenomenon that has been described for flavivirus infections.[7] Genetics may play a role in pathogenesis, as the disease is breed specific, and a strong familial inheritance pattern was detected in pugs with NME.[7] There is likely an immune-mediated component to NLE, as evidenced by the variable but generally positive response of the disease to treatment with glucocorticosteroids. In one case report of NLE, major infiltration of necrotic areas by cytotoxic T-lymphocytes, IgG producing plasma cells, macrophages and microglial cells was identified, suggesting a possible delayed T-cell immune response in the pathogenesis of the disease.[3] It is most likely that NLE is a multifactorial disorder caused by an as yet unknown combination of the factors above.

Diagnosis of NLE can be made on a combination of factors: age, breed affected, clinical signs that can be localized to the cerebra and brainstem, and a chronic, progressive course should all be considered when making a diagnosis. MRI imaging can be a very helpful diagnostic tool, and allows the diagnosis of NLE with a high degree of suspicion based on lesion localization, lesion appearance in different sequences and contrast enhancement.[11] Protein levels and cell counts in the CSF may also be increased in cases of NLE,[5,6] but this is a non-specific finding and should only be used in conjunction with the factors above in making a diagnosis.

JPC Diagnosis: Cerebrum, frontal cortex: Leukoencephalitis, necrotizing, multifocal, severe with hydrocephalus *ex vacuo* and numerous gemistocytic astrocytes.

Conference Comment: Small/toy breeds are susceptible to several potentially overlapping, idiopathic encephalitides which are poorly understood. Necrotizing leukoencephalitis (NLE) of the periventricular cerebral white matter (and brainstem) is described in Yorkshire terriers and occasionally French bulldogs and is discussed

comprehensively by the contributor. Necrotizing meningoencephalitis (NME) is a similar syndrome, known historically as "pug dog encephalitis," that is reported in various toy breeds including the pug, Maltese terrier, chihuahua, Yorkshire terrier, Pekingese, West Highland white terrier, Boston terrier, Japanese spitz, and miniature pinscher. In contrast to NLE, NME typically affects the leptomeninges, cerebral hemispheres and subcortical white matter, with loss of the anatomic demarcation between gray and white matter.[7] Granulomatous meningoencephalitis (GME) is a progressive, generally fatal neurologic disease of unknown origin that typically affects toy and terrier breeds; it is characterized by focal (mass-like) or disseminated perivascular accumulations of histiocytes, lymphocytes and plasma cells, primarily within the white matter of the brain, spinal cord and the optic nerve.[4,7] Due to considerable overlap in the clinical presentation of these conditions, some researchers suggest that the terminology meningoencephalitis of unknown etiology (MUE) may be preferable for an antemortem diagnosis of idiopathic meningoencephalitis without concurrent histopathology. Although the etiopathogeneses for these disorders remain elusive, immunosuppressive therapy is the mainstay of treatment, suggesting that an aberrant immune response directed against the CNS may play a role in the development of idiopathic canine meningoencephalitis.[7] A similar, fatal condition, known as Alaskan husky encephalopathy (AHE) affects young huskies, and is characterized by bilateral thalamic necrosis and cavitation. AHE is thought to be similar to Leigh syndrome, which is a group of diseases in humans attributed to mutations in either nuclear or mitochondrial DNA. A recent study found a mutation in the gene encoding a thiamine transporter protein (SLC19A3.1) plays a critical role in the pathogenesis of AHE.[10]

The microscopic lesions in this case, particularly their cavitating nature and specific location within the white matter, are most consistent with the condition known as necrotizing leukoencephalitis of Yorkshire terriers (NLE). Conference participants speculated that the mild perivascular and leptomeningeal inflammation was likely a reactive change secondary to marked necrosis and that the presence of hydrocephalus *ex vacuo* was probably due to the filling of the large pseudocysts with CSF.

Contributing Institution: Department of Pathobiology
College of Veterinary Medicine
University of Illinois Urbana-Champaign
2001 S. Lincoln Ave.
Urbana, IL 61801
http://vetmed.illinois.edu/path/

References:

1. Jung D, Kang B, Park C, Yoo J, Gu S, Jeon H, et al. A comparison of combination therapy (cyclosporine plus prednisolone) with sole prednisolone therapy in 7 dogs with necrotizing meningoencephalitis. *J Vet Med Sci*. 2007;69(12): 1303-1306.
2. Kuwamura M, Adachi T, Yamate J, Kotani T, Ohashi F, Summers B. Necrotising encephalitis in the Yorkshire terrier: a case report and literature review. *J Small Anim Prac*. 2002;43:459-463.
3. Lezmi S, Toussaint Y, Prata D, Lejeune T, Ferreira-Neves P, Rakotovao F, et al. Severe necrotizing encephalitis in a Yorkshire terrier: topographic and immunohistochemical study. *J Vet Med Assoc*. 2007;54:186-190.
4. Park E, Uchina K. Nakayama H. Comprehensive immunohistochemical studies on canine necrotizing meningoencephalitis (NME), necrotizing leukoencephalitis (NLE), and granulomatous meningoencephalitis (GME). *Vet Pathol*. 2012;49(4):682-692.
5. Schatzberg S, Haley N, Barr S, de LaHunta A, Sharp N. Polymerase chain reaction screening for DNA viruses in paraffin-embedded brains from dogs with necrotizing meningoencephalitis, necrotizing leukoencephalitis, and granulomatous meningoencephalitis. *J Vet Intern Med*. 2005;19:553-559.
6. Spitzbarth I, Schenk H, Tipold A, Beineke A. Immunohistochemical characterization of inflammatory and glial responses in a case of necrotizing leukoencephalitis in a French bulldog. *J Comp Path*. 2010;142:235-241.
7. Talarico L, Schatzberg S. Idiopathic granulomatous and necrotising inflammatory disorders of the canine central nervous system: a review and future perspectives. *J Small Anim Pract*. 2010;51:138-149.
8. Timmann D, Konar M, Howard J, Vandevelde M. Necrotizing encephalitis in a French bulldog. *J Small Anim Pract*. 2007;48:339-342.

9. Tipold A, Fatzer R, Jaggy A. Necrotizing encephalitis in Yorkshire terriers. *J Small Anim Pract*. 1993;34:623-628.
10. Vernae KM, Runstadler JA, Brown EA, et al. Genome-wide association analysis identifies a mutation in the thiamine transporter 2 (SLC19A3) gene associated with Alaskan husky encephalopathy. *PLOS One*. 2013;8(3):e57195.
11. von Praun F, Matisek K, Grevel V, Alef M, Flegel T. Magnetic resonance imaging and pathologic findings associated with necrotizing encephalitis in two Yorkshire terriers. *Veterinary Radiology & Ultrasound*. 2006;47(3):260-264.

CASE II: 13/326 (JPC 4033975).

Signalment: 3-year-old female domestic cat, (*Felis catus*).

History: The cat had three episodes of seizures with increasing severity during a period of one month. There was loss of proprioception and loss of vision after an episode with cluster attacks, but both proprioception and vision showed some improvement the following days. The cat was dehydrated at admission, but after rehydration the hematocrit was still very high (see below). The cat was euthanized. The differential diagnosis included encephalitis due to dry form of feline infectious peritonitis, *Toxoplasma*, neoplasia or polycythemia.

Gross Pathology: The cat was not macroscopically dehydrated (normal position of eyes in orbits). The heart was moderately rounded in shape and the right side was moderately dilated. Between the atria there was a persistent foramen ovale that measured 8 mm in diameter. The lungs were congested and edematous with moderate amounts of red colored mucus in the bronchi. In the stomach there was one nematode and in the small intestine there was one tapeworm. Colonic contents were moderately increased in amount and drier than normal. The renal cortices contained numerous petechiae on the cut surface. The texture of the cortex was normal. The size of the spleen was normal. Bone marrow was diffusely red. In formalin fixed brain there were bilateral mildly accentuated vascular structures on the cut surface of the hippocampus.

2-1. Hippocampus, cat: The neuronal population of the hippocampus is less prominent than normal. (HE 0.63X)

Laboratory Results:

Complete blood count:
RBC: 20.56 (5-10)
HGB: 239 (80-150)
HCT: 0.72 (0.24-0.45)
MCV: 35.1 (40-52)
RDW: 18.5 (13-17)
Lymphocytes: 0.2 (1.5-7.0)

Conclusion: marked erythrocytosis and marked lymphopenia

Histopathologic Description: In the brain there was bilateral and nearly diffuse neuronal necrosis in the hippocampus. The necrosis affected both the dentate gyrus and the pyramidal neurons. There were some segments with intact neurons in the dentate gyrus, but most neurons were necrotic with a shrunken hypereosinophilic appearance with a pyknotic or karyolytic nucleus. There were some mitotic figures probably representing proliferating glial cells. There was mild multifocal rarefaction and vacuolation of the neuropil and proliferation of vessels with hypertrophied endothelial cells. A similar but small focus of necrosis was detected in the pyriforme lobe. Otherwise, the brain was unremarkable, except for one vessel with perivascular infiltrates of

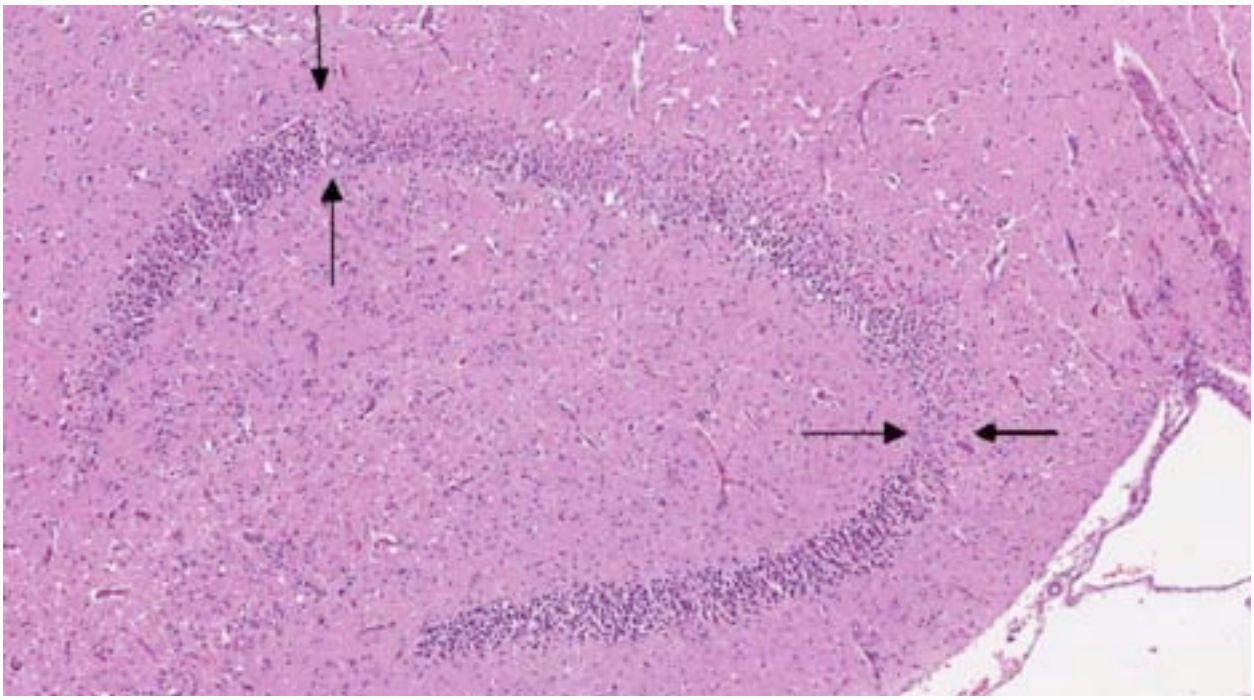

2-2. Hippocampus, cat: A segmental area of hypercellularity (between arrows) is present within the hippocampal neurons. There is also a prominent gliosis within the hippocampus as a whole. (HE 75X)

lymphocytes in the cerebral cortex laterally to the thalamus.

Other relevant histological findings: In the lungs there was severe congestion and edema. Pulmonary vessels were normal. There was moderate acute congestion in the liver. Although renal cortical petechiae were detected macroscopically, this could not be confirmed histologically, but the glomerular capillaries were engorged with blood. Cell density of bone marrow was moderately increased with mixed cell types but dominated by erythroid cells of mature stages.

Contributor's Morphologic Diagnosis: Brain, hippocampus: Neuronal necrosis, subtotal, bilateral, subacute.

Contributor's Comment: Feline hippocampal necrosis is a neurological disorder with unknown cause, characterized by generalized or complex-partial seizures of acute onset and rapid progression.[3] Fatzer et al described the findings in 38 domestic cats suffering from the disease.[3] Most cats were between 1-6 years old, and there was no breed or sex predisposition. The typical distribution of the lesions is severe involvement of the hippocampus with sparing of the remaining parts of the brain, except for the pyramidal lobes in some cases.[3,10] Histopathologic findings are acidophilic neuronal necrosis that may be diffuse in severe cases, gliosis, and proliferated vessels with hypertrophied endothelial cells.[3,10] The hippocampal lesions in this case were consistent with the findings described by Fatzer et al.[3] Some cases may have perivascular lymphohistiocytic infiltrates,[3] but this was only present around one vessel in this case and in a location not related to the necrotic lesions.

The polycythemia observed in this cat was interpreted to be an absolute polycythemia (primary or secondary) and not a relative polycythemia due to dehydration, since the cat presented with a high hematocrit (0.72) even after rehydration. The rare disease primary polycythemia (polycythemia vera) must be distinguished from secondary polycythemia which is more common. In primary polycythemia, the bone marrow has a very high cellularity with little remaining fat. Aspirated marrow has a synchronous trilineage hyperplasia with a myeloid:erythroid ratio of near 1.0.[9] This cat had had a moderately cellular bone marrow with a dominance of mature erythroid cells, possibly indicating a secondary polycythemia. Measurement of blood oxygen levels would be

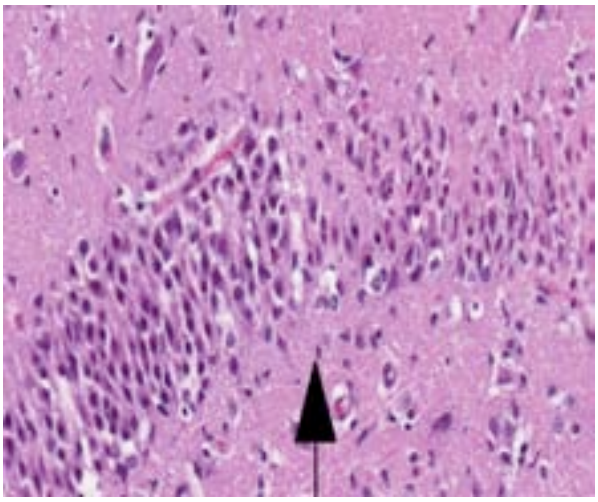

2-3. Hippocampus, cat: Higher magnification of Figure 2-2, demonstrating marked neuronal loss. In addition, many of the remaining neurons are shrunken, eosinophilic, and or pyknotic (degeneration and necrosis). (HE 160X)

helpful differentiating between primary and secondary polycythemia, but this was not performed in this case. A cause of secondary polycythemia is vascular anomalies causing anoxia. This cat had a persistent foramen ovale of 8 mm in diameter, a lesion usually not causing anoxia unless the blood flow through the atrial defect switches from left-right to right-left (Eisenmenger syndrome).[5] Pulmonary hypertension may be the result of heart malformations causing left to right shunting of blood and increased blood flow to the lungs.[1] Vascular lesions in the lungs due to pulmonary hypertension were not detected in this cat; neither acute lesions consisting of endothelial degeneration, fibrinoid necrosis and vasculitis, nor chronic lesions consisting of remodeling of pulmonary arterioles with thickening of the tunica intima and hypertrophy of the media were noted.[1] Interestingly, hypoxia due to patent foramen ovale in the absence of pulmonary hypertension is described in humans.[4] It is not clear to what degree the cardiac and hematological abnormalities contributed to the hippocampal necrosis in this cat. Of the 38 cats described by Fatzer et al, no similar hematological abnormalities were described; however, it is unclear whether hematological examinations were performed on all cats.

JPC Diagnosis: Cerebrum, hippocampus and piriform lobe: Neuronal necrosis, multifocal, subacute, with edema, gliosis and neovascularization.

Conference Comment: Conference participants briefly discussed the differential diagnosis for the histological findings, including ischemic encephalopathy, neuronal toxicity and rabies viral infection. Within the central nervous system, neurons and oligodendroglia are the most sensitive to ischemia, while blood vessels are more resistant and may survive in necrotic areas. In general, the grey matter is more sensitive to hypoxia than the white matter; specifically neurons of the hippocampus (especially the CA1 region) and the deeper laminae of the cerebral cortex, as well as Purkinje cells, are the most sensitive to ischemic necrosis.[6] Ischemic necrosis following fibrocartilagenous embolus (FCE) is a possible explanation for the lesions in this case; however, FCE is rare in cats, and when it occurs, it is asymmetric and typically affects the spinal cord, rather than the brain.[2] Feline ischemic encephalopathy (FIE) is quite similar to feline hippocampal necrosis, and has been associated with aberrant migration of *Cuterebra* spp. larvae. This condition is characterized by severe necrotizing lesions and infarction of areas of the cerebrum supplied by the middle cerebral artery, and thus often involves the hippocampus and piriform lobe; however, in contrast to feline hippocampal necrosis, which is bilateral and symmetric, the lesions in FIE are typically unilateral or asymmetric with spontaneous resolution and often partial to total recovery.[3,6]

Due to its use of glutamate (or possibly aspartate) as an excitatory neurotransmitter, the hippocampus is also particularly vulnerable to neuronal excitotoxicity, which may have played a role in the pathogenesis of this case. Glutamate is toxic to neurons and is normally cleared rapidly by glial cells. Conditions such as ischemia, hypoxia, seizures, and hypoglycemia promote a cascade of unregulated events including endogenous glutamate release, activation of glutamate receptors, decreased clearance of glutamate, and opening of voltage gated calcium channels, ultimately resulting in neuronal degeneration and necrosis; this is known as endogenous neuronal excitotoxicity.[6,8] A comparable neurotoxic condition has been described in marine mammals and seabirds in association with exposure to domoic acid (an analog of L-glutamate) following harmful algal blooms.[8]

In contrast to the microscopic lesions in this case, which are confined to the hippocampus, the lymphoplasmacytic perivascular cuffing, focal gliosis and neuronal intracytoplasmic viral inclusions (Negri bodies) commonly associated with rabies virus tend to be most severe from the pons to the hypothalamus and within the cervical spinal cord.[6] Nevertheless, definitive diagnosis of feline hippocampal necrosis in this case (versus rabies viral infection) was complicated for some participants by identification of scattered eosinophilic, intracytoplasmic "rabies-like" inclusions. The occurrence of intracytoplasmic neuronal inclusions indistinguishable from Negri bodies is a fairly common incidental finding in older dogs and cats which must be differentiated from true viral inclusions with laboratory diagnostics such as fluorescent antibody testing.[7]

Contributing Institution: Norwegian School of Veterinary Science
PO Box 8146 Dep.
0033 Oslo, Norway
www.nvh.no

References:

1. Caswell JL, Williams KJ. Respiratory system. In: Maxie MG, ed. *Jubb, Kennedy and Palmer's Pathology of Domestic Animals*. Vol 2. 5th ed. Philadelphia, PA: Elsevier Limited; 2007:523-654.
2. Coradini M, Johnstone I, Filippich LJ, Armit S. Suspected fibrocartilaginous embolism in a cat. *Aust Vet J*. 2005;83:550-551.
3. Fatzer R, Gandini G, Jaggy A, Doherr M, Vandevelde M. Necrosis of hippocampus and piriform lobe in 38 domestic cats with seizures: a retrospective study on clinical and pathologic findings. *J Vet Intern Med*. 2000;14:100-104.
4. Maraj R, Ahmed O, Fraifeld M, Jacobs LE, Yazdanfar S, Kotler MN. Hypoxia due to patent foramen ovale in the absence of pulmonary hypertension. *Tex Heart Inst J*. 1999;26:306-308.
5. Maxie MG, Robinson WF. Cardiovascular system. In: Maxie MG, ed. *Jubb, Kennedy and Palmer's Pathology of Domestic Animals*. Vol 3. 5th ed. Philadelphia, PA: Elsevier Limited; 2007:1-106.
6. Maxie MG, Youssef S. Nervous system. In: Maxie MG, ed. *Jubb, Kennedy and Palmer's Pathology of Domestic Animals*. Vol 1. 5th ed. Philadelphia, PA: Elsevier Limited; 2007:284-285, 336-337, 413-416.
7. Nietfeld JC, Rakich PM, Tyler DE, Bauer RW. Rabies-like inclusions in dogs. *J Vet Diagn Invest*. 1989;1(4):333-338.
8. Silvagni PA, Lowenstine LJ, Spraker T, Lipscomb TP, Gulland FM. Pathology of domoic acid toxicity in California sea lions (*Zalophus californianus*). *Vet Pathol*. 2005;42(2):184-191.
9. Valli VEO. Hematopoietic system. In: Maxie MG, ed. *Jubb, Kennedy and Palmer's Pathology of Domestic Animals*. Vol 3. 5th ed. Philadelphia, PA: Elsevier Limited; 2007:107-324.
10. Vandevelde M, Higgins RJ, Oevermann A. Metabolic-toxic diseases. In: *Veterinary Neuropathology: Essentials of Theory and Practice*. Chichester, UK: Wiley-Blackwell; 2012:106-128.

CASE III: AFIP Case 1 (JPC 4003089).

Signalment: 1-year-old intact male Argentinian Mastiff dog, (*Canis familaris*).

History: The dog had an approximately 1-week history of hindlimb ataxia. Upon referral to the Boren Veterinary Medical Teaching Hospital, CT imaging revealed a mass in the L1-L2 spinal cord. Dorsal laminectomy was performed, and the mass was considered non-resectable. The dog was euthanized.

Gross Pathology: Over the dorsal vertebral processes, centered on the thoracolumbar junction, is a 12 cm long incision that is closed with surgical staples. Subcutaneous tissue deep to the incision is dark red and contains large aggregates of friable, dark red material (clot, fibrin). The right dorsal pedicles and lamina of the lumbar vertebrae 1 and 2 are absent (surgical artifact), and the surrounding tissue is dark red. Dura overlying the mass is mostly intact with a single small defect (surgical artifact). At the level of L1-L2, the spinal cord is moderately enlarged and dark brown to red. Protruding from subdural space into the spinal cord is a 1 cm diameter, well-demarcated, soft, white mass. The tissue immediately surrounding the mass is markedly expanded by abundant dark red material (hemorrhage).

Histopathologic Description: Spinal cord, L1-L2: Expanding from within and beneath the dura and infiltrating the underlying spinal cord is a densely cellular, well-demarcated, partially encapsulated neoplasm. Neoplastic cells are of two distinct cell populations. One population forms tubules lined by cuboidal cells that have a small amount of eosinophilic cytoplasm and a single round nucleus with finely stippled chromatin. Surrounding the neoplastic tubules are sheets of polygonal blastemal cells that have minimal cytoplasm and a round, deeply basophilic nucleus with slight vesicular chromatin. The mitotic rate is high with 25 mitoses in 10 high-powered fields. Surrounding the neoplasm is abundant hemorrhage that extends cranially and caudally, obliterating large portions of the spinal cord and surrounding few remaining neurons. Scattered throughout the areas of hemorrhage are few small aggregate of neutrophils. Cranial and caudal to the mass, white matter tracts are markedly vacuolated with many spheroids.

Immunostaining of the mass demonstrates that neoplastic epithelial cells are immunoreactive on staining with cytokeratin and mesenchymal cells are immunoreactive on staining with vimentin. Neoplastic cells are not immunoreactive on staining with neuron specific enolase or glial fibrillary acidic protein.

Contributor's Morphologic Diagnosis: Spinal cord, L1-L2: Nephroblastoma.

3-1. Spinal cord, dog: A large mass disrupts the normal architecture of the spinal cord. (Photo courtesy of: Oklahoma State University, Department of Veterinary Pathobiology, Room 250 McElroy Hall, Stillwater, OK 74078 http://www.cvhs.okstate.edu)

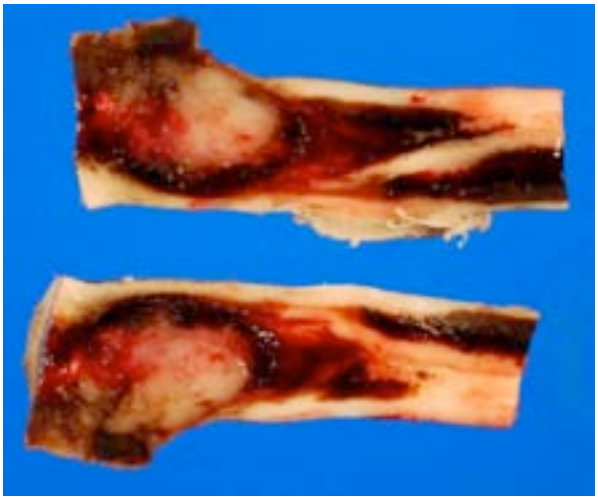

3-2. Spinal cord, dog: Cut surface of the spinal cord reveals a large, white mass with abundant surrounding hemorrhage. (Photo courtesy of: Oklahoma State University, Department of Veterinary Pathobiology, Room 250 McElroy Hall, Stillwater, OK 74078 http://www.cvhs.okstate.edu)

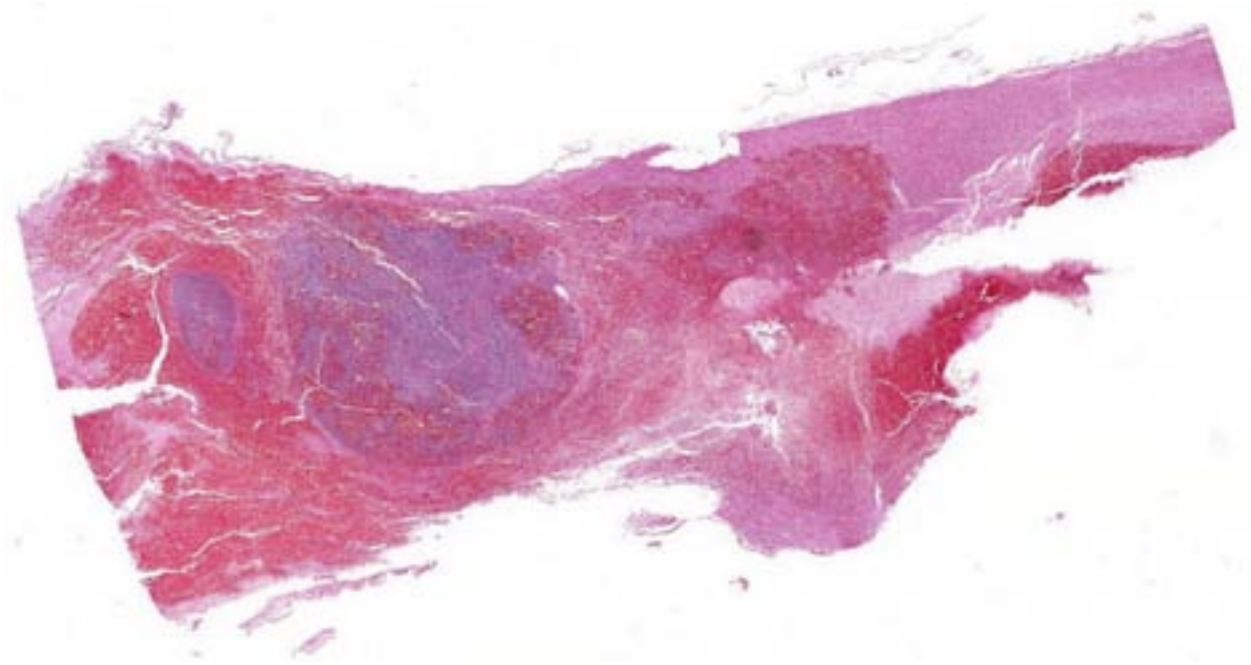

3-3. Spinal cord, dog: Section of neoplasm demonstrating the abundant hemorrhage associated with this neoplasm. (HE 0.63X)

Contributor's Comment: Spinal nephroblastomas are rare neoplasms that occur in young dogs, and German Shepherds may be over-represented.[2] These neoplasms typically arise at the thoracolumbar junction and are thought to arise from ectopic rests of embryonal renal tissue entrapped in the subdural space.[2] Metastasis is not typical[4] though possible intraspinal metastasis has been reported.[5] Affected animals typically present with hindlimb ataxia, paresis, and proprioceptive deficits.[4,5]

The classic histomorphology of spinal nephroblastoma is similar to that of renal nephroblastoma. Neoplastic cells form embryonic glomeruli, primitive tubules, and primitive acini, surrounded by a mesenchymal stroma.[2] Cytologic evaluation shows a characteristic triphasic pattern with mesenchymal cells, epithelial cells, and undifferentiated hyperchromatic cells.[1] The submitted neoplasm demonstrates characteristic primitive tubules,

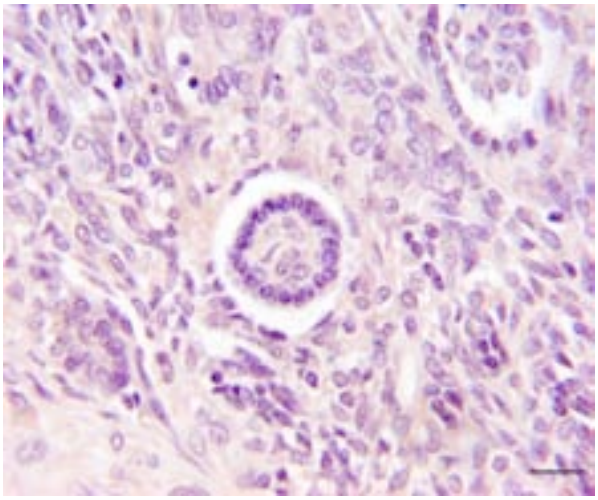

3-4. Spinal cord, dog: Scattered throughout the neoplasm are structures resembling embryonic glomeruli. (Photo courtesy of: Oklahoma State University, Department of Veterinary Pathobiology, Room 250 McElroy Hall, Stillwater, OK 7407 http://www.cvhs.okstate.edu)

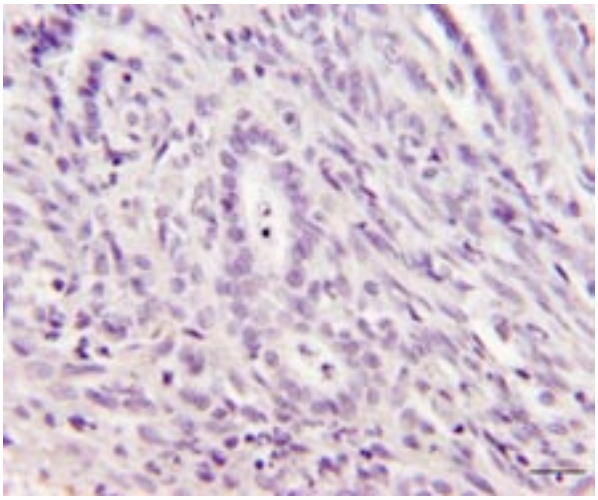

3-5. Spinal cord, dog: In other areas, neoplastic cells form primitive tubules. (Photo courtesy of: Oklahoma State University, Department of Veterinary Pathobiology, Room 250 McElroy Hall, Stillwater, OK 74078 http://www.cvhs.okstate.edu)

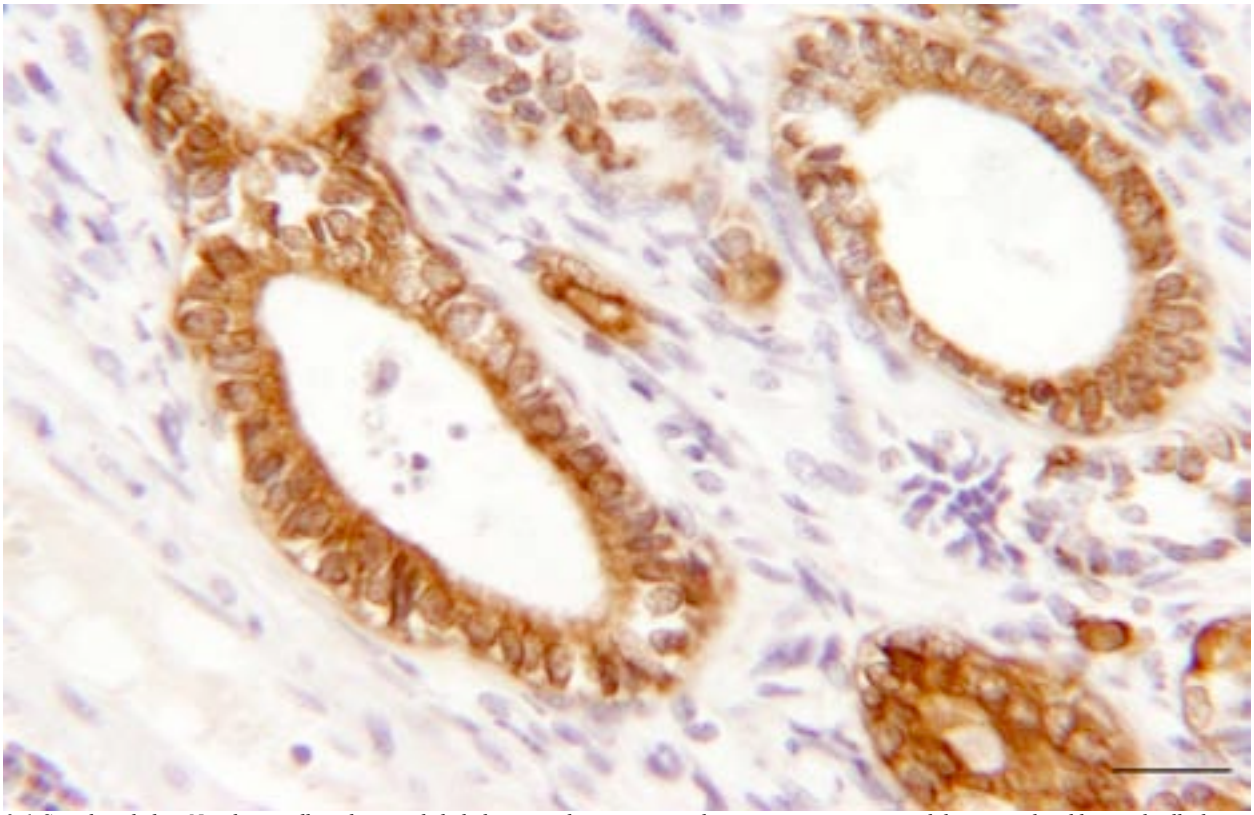

3-6. Spinal cord, dog: Neoplastic cells with an epithelial phenotype demonstrate cytokeratin immunopositivity, while surrounding blastemal cells do not. (Photo courtesy of: Oklahoma State University, Department of Veterinary Pathobiology, Room 250 McElroy Hall, Stillwater, OK 74078 http://www.cvhs.okstate.edu)

acini, and mesenchymal stroma, though it lacks classic embryonic glomeruloid structures.

Differential diagnoses include ependymoma, primitive neuroectodermal tumor, or poorly differentiated astrocytoma.[5] Immunohistochemistry can aid in establishing a definitive diagnosis. The epithelial cells within spinal nephroblastomas are immunopositive for cytokeratin, and the blastemal cells and stroma are immunopostive for vimentin.[2,5] The neoplastic cells are immunonegative for NSE, GFAP, neurofilament, or chromogranin.[2,5] In addition, these neoplasms may be immunopositive on staining with a nephroblastoma-specific marker, Wilm's tumor gene protein product (WT1).[3] Immunostaining of this neoplasm was consistent with spinal nephroblastoma; immunostaining for Wilm's tumor gene protein product was not performed.

JPC Diagnosis: Spinal cord: Nephroblastoma.

Conference Comment: Nephroblastoma, also known as Wilms' tumor, is an important human pediatric neoplasm. The term "blastoma" defines the neoplastic population as embryonic, rather than mature terminally differentiated cells; histologically, nephroblastoma recapitulates the embryologic development of the kidney.[1] The protein product of the Wilms' tumor suppressor gene-1 (WT-1) is a DNA binding protein important in normal renal development; inactivation of this gene likely prevents differentiation of primitive metanephric cells and is documented in some pediatric nephroblastomas.[3] A similar intradural extramedullary spinal cord neoplasm occurs between the tenth thoracic (T10) and second lumbar (L2) spinal cord segments in large breed dogs, typically less than three years old, and is thus referred to as thoracolumbar spinal tumor of young dogs.[5] Although the histogenesis of this tumor has not been firmly established, it is thought to originate from ectopic metanephric blastema trapped between the dura and the developing spinal cord.[5] The Wilms' tumor gene protein product, WT1, has been identified immunohistochemically in some of these "canine spinal cord nephroblastomas."[3] As noted by the

contributor, the microscopic features (a poorly differentiated blastemal component, mesenchymal stroma, and an epithelial component forming tubules and vague glomeruloid structures) and immunohistochemical staining characteristics (cytokeratin positive epithelial cells and vimentin positive blastemal and mesenchymal cells) in this case are consistent canine spinal cord nephroblastoma (or perhaps more accurately, thoracolumbar spinal tumor of young dogs); however, there is significant slide variation and tissue identification for some conference participants was difficult, as some sections did not contain any identifiable spinal cord.

Contributing Institution: Oklahoma State University
Department of Veterinary Pathobiology
Room 250 McElroy Hall
Stillwater, OK 74078
http://www.cvhs.okstate.edu

References:

1. De Lorenzi D, Baroni M, Mandara MT. A true "triphasic" pattern: thoracolumbar spinal tumor in a young dog. *Vet Clin Pathol*. 2007;36:200-203.
2. Meuten DJ. Tumours of the urinary system. In: Meuten DJ, ed. *Tumors in Domestic Animals*. Ames, IA: Iowa State Press; 2002:519-520.
3. Pearson GR, Gregory SP, Charles AK. Immunohistochemical demonstration of Wilms tumour gene product WT1 in a canine "neuroepithelioma" providing evidence for its classification as an extrarenal nephroblastoma. *J Comp Pathol*. 1997;116:321-327.
4. Summers BA, deLahunta A, McEntee M, Kuhajda FP. A novel intradural extramedullary spinal cord tumor in young dogs. *Acta Neuropathol*. 1988;75:402-410.
5. Terrell SP, Platt SR, Chrisman CL, Homer BL, de Lahunta A, Summers BA. Possible intraspinal metastasis of a canine spinal cord nephroblastoma. *Vet Pathol*. 2000;37:94-97.

CASE IV: NC-10-667-4 (JPC 3175517).

Signalment: 12-year-old spayed female beagle dog (*Canis familiaris*).

History: This beagle presented with a 2-year history of chronic pancreatitis and a 24-hour history of icterus. She had a 3/6 heart murmur, elevated liver enzymes, and elevated BUN/ creatinine. Abdominal ultrasound revealed pancreatitis, gastritis, enteritis, and lymphadenopathy. A moderate to severe, unstructured interstitial pattern was noted in the caudodorsal lungs on radiographs, especially in the hilar region, leading to a clinical differential diagnosis of pulmonary lymphoma or other hematogenous disease. An alveolar pattern was noted along the cranial margin of the right caudal lung lobe. Cytology of the liver showed few bile plugs, and was considered indicative of cholestasis. The dog was subsequently euthanized due suspected severe pancreatitis and a poor, long-term prognosis.

Gross Pathology: The body of a female beagle in good body condition (body condition score: 6/9) and in a state of mild autolysis was presented for necropsy. Icterus was evident in the sclera, mucous membranes, and shaved skin.

The ventral pylorus was adhered to the left ventral abdominal wall by bands of dense, tan fibrous tissue. The liver was firm with irregular, rounded margins and contained approximately 10-12, 0.2 cm to 3.5 cm diameter, fluid-filled cysts (suspect biliary cysts). The gall bladder was moderately enlarged and contained variably-sized clumps of dark green, inspissated bile. The pancreas was atrophied, pale, firm, and nodular. The mucosa of both the small and large intestines was moderately thickened and the jejunum was corrugated. The kidneys contained multiple cysts that were approximately 0.2 cm in diameter and contained clear fluid. These cysts were present throughout the parenchyma and along the capsular surface. Multiple pale, tan, round, 0.5 mm diameter foci were scattered regularly throughout the cortical tissue.

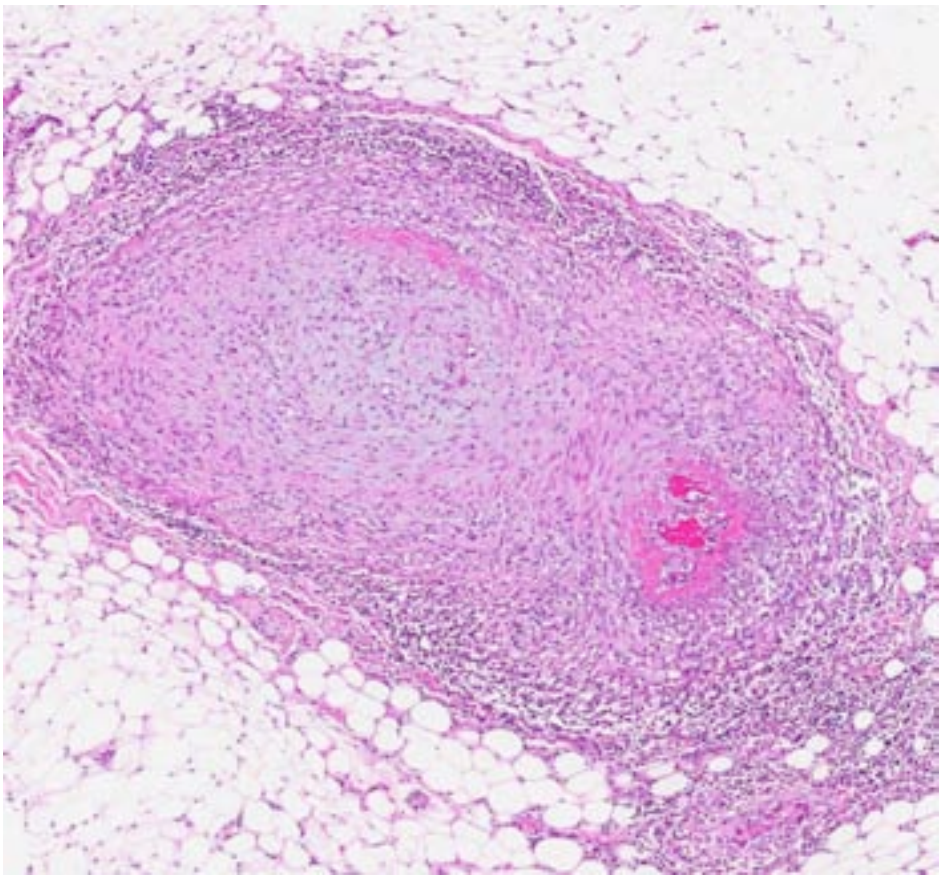

4-1. Mediastinum, dog: Arterioles are tortuous, with extrusion of bright red protein into the subintimal layers (fibrinoid necrosis). (HE 50X)

Five to ten milliliters of clear, serosanguineous fluid were in the pleural space. The lungs were markedly congested and oozed blood on cut surface. The heart was rounded and the septal leaflets of the mitral valve were moderately thickened by smooth, variably-sized nodules (nodular endocardiosis).

Laboratory Results: Anaerobic and aerobic bacterial cultures of the peritoneal fluid obtained in the clinic were negative.

Histopathologic Description: In multiple tissues, including the heart, kidney, liver, spleen,

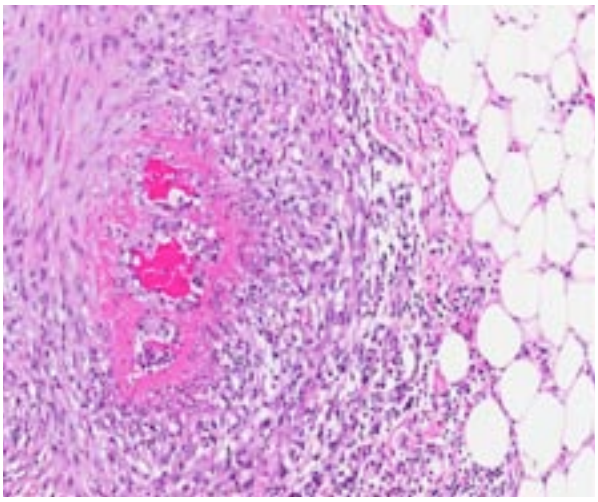

4-2. Mediastinum, dog: Higher magnification of Fig. 4.1. The arteriolar wall is infiltrated by large numbers of degenerate neutrophils and histiocytes, admixed with bright red protein and cellular debris. In addition, smooth muscle cells are variably hypertrophic and or necrotic, and admixed with numerous fibroblasts (fibrinoid necrosis). (HE 175X)

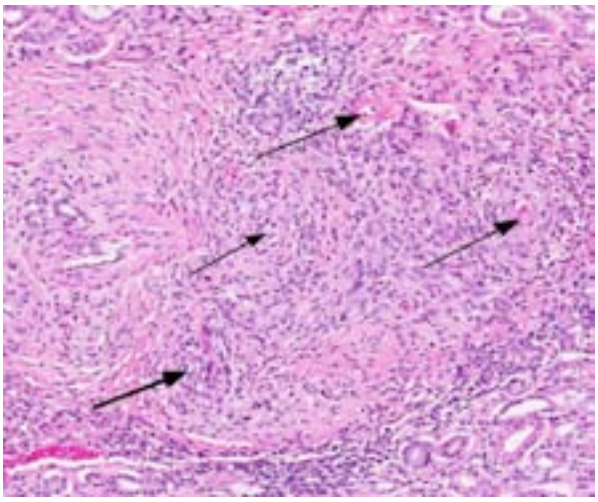

4-3. Kidney, dog: Similar proliferative lesions are present within small renal arterioles. (HE 150X)

pancreas, stomach, and intestine, the tunica media of medium to small arteries was variably inflamed and necrotic. Affected vessels had multifocal regions of smooth muscle hypertrophy, fibrosis, and luminal obstruction. In most medium-sized vessels, the wall was infiltrated and moderately to markedly expanded by neutrophils, lymphocytes, plasma cells, and occasional macrophages and eosinophils. The tunica media often contained several nodules composed of hypertrophied smooth myocytes and chronic, swirling fibrosis. In other vessels, the tunica media contained regions of fibrinoid degeneration characterized by brightly eosinophilic, amorphous material with admixed pyknotic nuclear debris, faded smooth muscle cells with karyolysis, and regions of brightly eosinophilic fibrin deposition. The necrosis spanned the internal elastic lamina, which was segmentally fragmented and lost, and also involved the intima. The intima was multifocally, moderately expanded by fibrosis. In occasional vessels, a portion of the lumen contained brightly eosinophilic fibrin, with occasional reorganization and recanalization. Mild numbers of red blood cells diapedesed into the adjacent tissues. Inflammatory infiltrates extended into the perivascular connective tissues with associated vacuolated, lightly eosinophilic edema fluid.

The walls of arteries throughout the kidney and perirenal fat were markedly expanded by hypertrophied smooth myocytes, fibrosis, and infiltrating neutrophils and lymphocytes, leading to the obstruction of the vascular lumens (as described above). Affected vessels were surrounded by moderate, streaming fibrosis. Moderate to marked interstitial lymphoplasmacytic infiltrates were scattered throughout the renal parenchyma. Bowman's capsule was moderately expanded in the majority of the glomeruli, as was the mesangium of several glomerular tufts. Glomerular tufts occasionally adhered to the capsule (synechia). Multifocally, the tubular epithelium was variably swollen, vacuolated or attenuated, and hypereosinophilic, suggestive of early epithelial degeneration. Occasional tubules were dilated and contained glassy, amorphous, lightly eosinophilic material. A few, scattered tubules were markedly dilated by a flocculent, eosinophilic material. In both kidneys, the connective tissues around the renal pelvises were moderately to markedly infiltrated by lymphocytes and plasma cells.

Within the heart, the coronary arteries and vessels in the pericardial fat were multifocally, markedly affected by the vascular changes described above. Multifocally, the myocardium was mildly infiltrated by mature fat. In one section of myocardium, the myofibers were mildly separated by a fine fibrous connective tissue.

The lobules within the pancreas were moderately to markedly separated by dense fibrosis, which occasionally invaded into the lobules, isolating

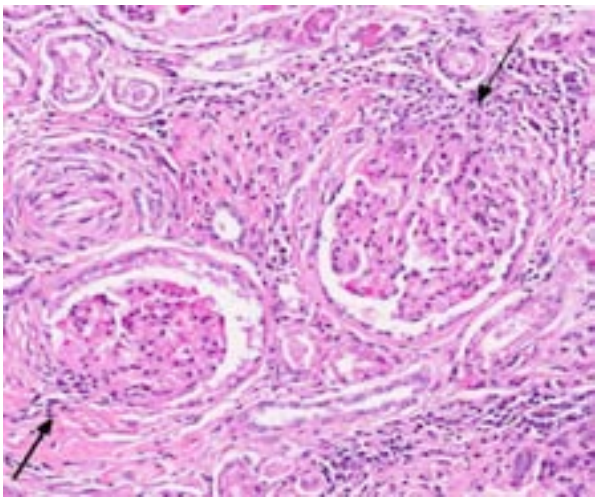

4-4. Kidney, dog: Basement membranes are markedly expanded and there is mild to moderate hypertrophy of parietal epithelium with periglomerular fibrosis (membranous glomerulonephritis). Afferent arterioles are sclerotic and inflamed. (HE 175X)

small islands of acini. Multifocal, mild aggregates of lymphocytes were apparent within the fibrosis. Multifocal vessels in the pancreatic parenchyma and the adjacent mesentery were effaced by the previously described inflammatory process (pancreas not submitted).

Contributor's Morphologic Diagnosis: Small to medium arteries: Multifocal, moderate to marked, neutrophilic, lymphoplasmacytic, and fibrinonecrotic to fibrosing polyarteritis.

Kidney:

1. Moderate, global, diffuse membranoproliferative glomerulopathy
2. Multifocal, moderate lymphoplasmacytic interstitial nephritis
3. Acute tubular degeneration and multifocal tubular proteinosis

Heart:

1. Mild, multifocal fatty infiltration
2. Focal, mild myocardial fibrosis

Pancreas (not submitted): Moderate, chronic-active, fibrosing pancreatitis

Contributor's Comment: This dog was diagnosed with a necrotizing polyarteritis that involved multiple organs, including the heart, kidney, spleen, stomach, intestine, liver, lung, lymph node, and pancreas. Interestingly, this animal showed no clinical signs that were directly related to vasculitis and the evenly-spaced, raised, pinpoint foci in the kidneys, the irregular margins of the liver, the chronic peritonitis, and the thickened intestines were the only apparent gross lesions that were interpreted to be associated with this disease process.

Vasculitis is defined as the invasion of vessel walls by inflammatory cells with associated vascular damage, which can include fibrin deposition, collagen degeneration, and necrosis.[5,6] In animals and humans, vasculitis can be categorized as immune-mediated, infectious, toxic, hemodynamic-mediated, or idiopathic.[1,4,5] Infectious causes of vasculitis in dogs include canine distemper virus, bacterial septicemia and endotoxemia, rickettsial organisms, mycotic infections, protozoal organisms, and rarely helminths.[5] In this patient, infectious causes were considered unlikely based on the lack of an organism seen histologically, the negative peritoneal culture, and the lack of any other histologic or gross features associated with an infectious organism.

Immune-mediated vasculitis is a differential diagnosis for the vascular changes in this dog, though such immune-mediated reactions are less common in dogs than in humans.[1,5] The main pathologic processes that can lead to immune-mediated vasculitis include antibody/antigen complex deposition secondary to an infection or a hypersensitivity response, anti-neutrophil cytoplasmic antibodies, or anti-endothelial cell antibiodies.[4] One type of vasculitis that is thought to be immune-mediated is polyarteritis nodosa. Polyarteritis nodosa is rarely described in dogs and is considered to be similar to idiopathic juvenile polyarteritis (discussed below). This condition is characterized by segmental, necrotizing vasculitis of small to medium sized arteries. Arterioles, capillaries, and venules are typically not involved, and glomerulonephritis is not present.[5] Type IV hypersensitivity-associated vasculitis is also an immune-mediated vasculitis that has also been described as affecting small vessels (though sparing muscular arteries) and is characterized by a non-necrotizing, mononuclear vasculitis.[1] Hypersensitivity vasculitides commonly occur in the skin, and have been associated with systemic lupus erythematosis in dogs.[3,5] Drug reactions occasionally cause type III hypersensitivities, which result from the deposition of antibody/antigen complexes within small vessels, leading to a necrotizing vasculitis.[5]

The skin was not examined histologically in this dog.

Toxic damage to the endothelium or to the vascular smooth muscle cells caused by medications has been reported to lead to a necrotizing vasculitis. This form of vasculitis affects small to medium arteries in multiple organs, and is characterized by transmural segmental fibrinoid necrosis and neutrophilic inflammation, which also affects surrounding tissues. Focal medial scarring and adventitial fibrosis has also been described.[1] Toxic vasculitis is difficult to differentiate from polyarteritis nodosa. Medications can also lead to vascular damage caused by excessive hemodynamic activity. For example, dogs have been reported to be sensitive to vasodilators and positive inotropes, and develop vascular lesions associated with their use. The acute histologic features of this lesion include segmental medial necrosis and hemorrhage of the coronary arteries. Chronic changes include smooth muscle hyperplasia of the intima and adventitial fibroplasia, and medial degeneration, necrosis, and variable inflammation.[1] There was no history of vasodilator or positive inotrope use in this dog.

In most cases of vasculitis in dogs, the cause is unknown. Some idiopathic vasculitides appear to occur more commonly in certain breeds. For example, several authors have described a juvenile polyarteritis in beagle dogs.[1,2,5,8,9] This syndrome occurred primarily in young beagle dogs (<40 months of age). These dogs developed sudden-onset fever, anorexia, and a hunched stance that waxed and waned. However, in one study, affected beagles did not show any clinical signs.[9] Histologically, acutely affected small to medium-sized muscular arteries were characterized by necrotizing vasculitis with occasional fibrinoid change and perivascular nodules predominately composed of neutrophils with multifocal accumulations of macrophages, lymphocytes and plasma cells. Affected organs included the extramural coronary arteries, cervical spinal cord, and the cranial mediastinum. Less commonly affected organs included thyroid glands, thymus, lymph nodes, stomach, small intestine, esophagus, urinary bladder, epididymis, gall bladder, lung, and diaphragm. Few dogs exhibit severe, diffuse, membranoproliferative glomerulonephritis.[8,9] Hemorrhage and necrosis were not associated with the vascular lesions in these studies.[1]

In this case of necrotizing polyarteritis, beagle pain syndrome was considered unlikely due to the age of the patient. Additionally, based on the histologic features described above, including the presence of necrotizing vasculitis in multiple organs, the minimal associated necrosis and hemorrhage, and the restriction of the lesions to the small and medium muscular arteries, type IV hypersensitivity reactions were considered less likely. These lesions typically spare muscular arteries, typically occur in the skin, and generally do not have associated fibrinoid necrosis. Vasculitis secondary to excessive hemodynamic activity was also unlikely, because these lesions are often restricted to coronary arteries, and are less likely to have associated inflammation. Interestingly, this dog had a history of chronic pancreatitis, which may have caused or at least contributed to the vasculitis and the glomerulopathy through the production of circulating antigen/ antibody complexes. As a result, a toxic vasculitis, an immune-mediated vasculitis, or an idiopathic vasculitis remain the most likely differentials for this patient.

JPC Diagnosis: 1. Kidney, heart and adjacent vessels: Arteritis, necrotizing and proliferative, chronic, diffuse, severe with fibrinoid change.
2. Kidney: Glomerulonephritis, membranoproliferative, diffuse, moderate, with multifocal tubular necrosis and lymphoplasmacytic interstitial nephritis.

Conference Comment: Although the specific etiopathogenesis is not clear, this case provides an excellent example of canine polyarteritis combined with other renal changes. The contributor provides a thorough summary of the histological findings, differential diagnosis and proposed pathogeneses associated with vasculitis in dogs. Conference participants discussed the differential diagnosis for this case, including immune-mediated vasculitis, which led to a brief review of mechanisms of immunologically mediated hypersensitivity reactions (see table 1).

Type I, or immediate type hypersensitivity reactions involve an initial sensitization phase to an allergen or parasite, as well as an effector phase upon secondary or prolonged initial

exposure, mediated by IgE antibody cross-linking, mast cell degranulation (resulting in release of vasoactive amines and other mediators) and, in late phase reactions, recruitment of inflammatory cells, especially eosinophils. Type I hypersensitivity is associated with anaphylaxis, and is characterized by increased vascular permeability (edema) and dilation (hypotension), smooth muscle contraction (bronchospasm), mucus production and inflammation. Interestingly, the guinea pig is the species most sensitive to the development of anaphylaxis.

Type II, or cytotoxic hypersensitivity reactions occur following the development of antibodies against cell surface antigens or receptors, with subsequent phagocytosis or lysis of the target cell by activated complement or Fc receptors, as well as recruitment of leukocytes. Due to the presence of numerous blood group surface antigens and a predilection for absorbing drugs and antigens associated with infectious agents or tumors, erythrocytes are particularly prone to this type of antibody-mediated hypersensitivity reaction (e.g. autoimmune hemolytic anemia and foal neonatal isoerythrolysis). Furthermore, antibodies directed against cell surface receptors can either activate or inhibit cell function. For instance, binding of antibody to the thyroid stimulating hormone (TSH) receptor activates thyroid follicular epithelial cells, resulting in hyperthyroidism, while antibody binding the acetylcholine neurotransmitter receptor at the neuromuscular junction inhibits cell function, resulting in myasthenia gravis.[7]

Type III hypersensitivity reactions, as noted by the contributor, can incite necrotizing vasculitis via formation and deposition of antigen-antibody complexes which lead to complement activation, recruitment of leukocytes, release of free radicals, proteolytic enzymes and other toxic molecules. In order for deposition of antigen-antibody complexes to occur, there must be a slight antigen excess with the formation of intermediate sized complexes; deposition tends to occur at sites where blood is filtered at high pressure, such as glomeruli, joints, small vessels, the heart, the skin, or the serosa. Examples include systemic lupus erythematosus, equine infectious anemia and acute glomerulonephritis.[9]

Type IV hypersensitivity reactions, also known as cell mediated or delayed-type, are mediated by

Table 1. Mechanisms of Immunologically Mediated Hypersensitivity Reactions.[7]

Type	Prototype Disorder	Immune Mechanisms	Pathologic Lesions
Type I (immediate) hypersensitivity	Anaphylaxis; allergies; bronchial asthma	Cross linking of IgE antibody, mast cell degranulation → release of vasoactive amines and other mediators; recruitment of inflammatory cells (late-phase reaction)	Vascular dilation, edema, smooth muscle contraction, mucus production, inflammation
Type II (antibody-mediated/ cytotoxic) hypersensitivity	Autoimmune hemolytic anemia; neonatal isoerythrolysis	Production of IgG, IgM → binds to antigen on target cell or tissue → phagocytosis or lysis of target cell by activated complement or Fc receptors; recruitment of leukocytes	Cell lysis; inflammation
Type III (immune complex-mediated) hypersensitivity	Systemic lupus erythematosus; glomerulonephritis; serum sickness; Arthus reaction	Deposition of antigen-antibody complexes → complement activation → recruitment of leukocytes → release of enzymes and other toxic molecules	Necrotizing vasculitis (fibrinoid necrosis); inflammation
Type IV (cell-mediated/ delayed-type) hypersensitivity	Contact dermatitis; transplant rejection; tuberculosis; Johne's disease	Activated T lymphocytes: 1. Release of cytokines and macrophage activation 2. T cell-mediated cytotoxicity	Perivascular cellular infiltrates; edema; cell destruction; granuloma formation

$CD4^+$ or $CD8^+$ T-lymphocytes (see WSC 2013-2014, conference 2, case 2 for a review of $CD4^+$ T-lymphocyte mediated hypersensitivity). CD8+ T-lymphocytes are activated by antigen expressed in the context of MHCI and are directly cytotoxic to target cells via granzyme A/perforin (which leads to caspase-independent apoptosis), granzyme B (leading to caspase-dependent apoptosis) or Fas:Fas ligand interactions (which induces extrinsic apoptosis). Tuberculosis, Johne's disease, allograft rejection and allergic contact dermatitis are all diseases associated with primary type IV hypersensitivity reactions.[7]

Contributing Institution: Molecular Pathology Unit
Laboratory of Cancer Biology and Genetics
Center for Cancer Research
National Cancer Institute
http://ccr.ncifcrf.gov/resources/molecular_pathology/

References:

1. Clemo FAS, Evering WE, Snyder PW, Albassam MA. Differentiating spontaneous from drug-induced vascular injury in the dog. *Toxicol Pathol*. 2003;31(Suppl.):25-31.
2. Hayes TJ, Roberts GK, Halliwell WH. An idiopathic febrile necrotizing arteritis syndrome in the dog: beagle pain syndrome. *Toxicol Pathol*. 1989;17(2):129-137.
3. Hoff E J, Vandevelde M. Case report: necrotizing vasculitis in the central nervous systems of two dogs. *Vet Pathol.* 1981;18:219.
4. Maxie MG, Robinson WF. Cardiovascular system. In: Maxie MG, ed. *Jubb, Kennedy and Palmer's Pathology of Domestic Animals*. Vol 3. 5th ed. Philadelphia, PA: Elsevier Limited; 2007:1-103.
5. Mitchell RN, Schoen FJ. Blood vessels. In: Kumar V, Abbas AK, Fausto N, Aster JC, eds. *Pathologic Basis of Disease*. 8th ed. Philadelphia, PA: Elsevier Saunders; 2010:487-528.
6. Nichols PR, Morris DO, Beale KM. A retrospective study of canine and feline cutaneous vasculitis. *Vet Dermatol*. 2001;12:255-264.
7. Snyder PW. Diseases of immunity. In: Zachary JF, McGavin MD, eds. *Pathologic Basis of Veterinary Disease.* 5th ed. St. Louis, MO: Elsevier; 2012:258-270.
8. Snyder PW, Kazacos EA, Scott-Moncrieff JC, et al. Pathologic features of naturally occurring juvenile polyarteritis in beagle dogs. *Vet Pathol.* 1995;32(4):337-345.
9. Son W. Idiopathic canine polyarteritis in control beagle dogs from toxicity studies. *J Vet Sci*. 2004;5(2):147-150.

Joint Pathology Center
Veterinary Pathology Services

WEDNESDAY SLIDE CONFERENCE 2013-2014

Conference 23

23 April 2014

CASE I: 10N-1078 (JPC 4002848).

Signalment: Adult gravid female koi, (*Cyprinus carpio koi*).

History: The adult female koi was submitted to UC Davis, VMTH Companion Avian and Exotic Animal Medicine and Surgery/Aquatic Animal Health service, dead on arrival from a non-commercial pond. Three other koi had died over the past 10-month period (August 2009 through May 2010), with similar clinical signs. The owner reported that this fish developed ulcerations on the dorsal head a few months ago and had been lethargic for the past three to four days. After being isolated from the pond, it

1-1. Skin, koi: There was an irregular, coalescing, well demarcated area of scale and skin loss with exposed underlying subcutis and muscles at the dorso-lateral trunk. The eroded areas were surrounded with hemorrhage. (Photo courtesy of: UC Davis School of Veterinary Medicine, Anatomic Pathology Department, One Shields Ave, Davis, CA 95616 http://www.vetmed.ucdavis.edu/pmi/)

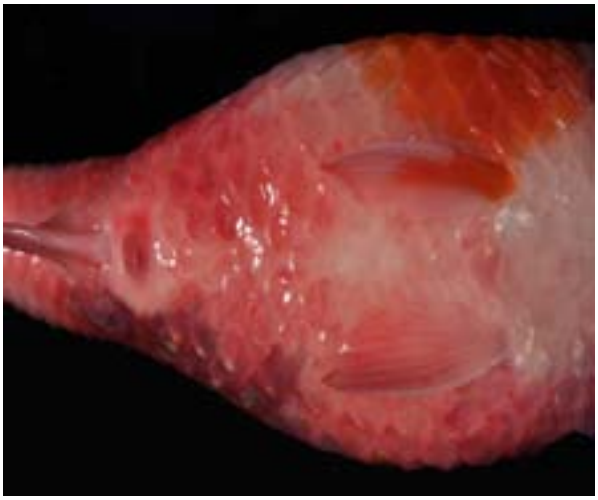

1-2. Skin around vent, koi: Diffusely throughout the body, clear fluid was exuding from the vesicles expanding the skin and elevating the scales producing a "pinecone" appearance. Pink discolorations of the skin as shown around the vent were due to petechiae and small congested vessels. (Photo courtesy of: UC Davis School of Veterinary Medicine, Anatomic Pathology Department, One Shields Ave, Davis, CA 95616 http://www.vetmed.ucdavis.edu/pmi/)

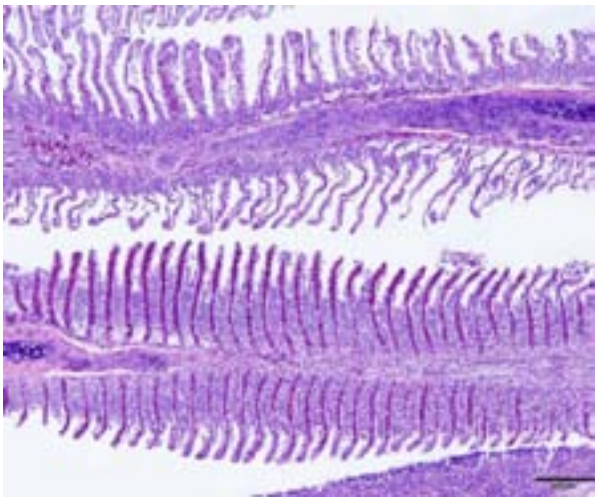

1-3. Gill, koi: Low power view demonstrates clubbing and fusion of the gill lamellae. Interstitial edema, necrosis and detachment of gill epithelium are also present. (HE 40X) (Photo courtesy of: UC Davis School of Veterinary Medicine, Anatomic Pathology Department, One Shields Ave, Davis, CA 95616 http://www.vetmed.ucdavis.edu/pmi/)

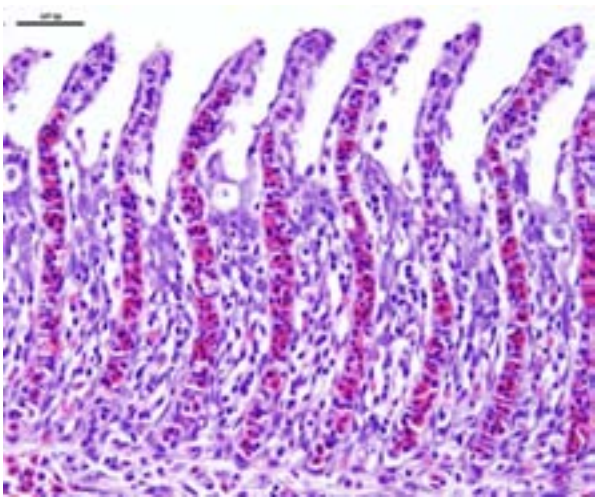

1-4. Gill, koi: Low power view demonstrates clubbing and fusion of the gill lamellae. Interstitial edema, necrosis and detachment of gill epithelium are also present. (HE 40X) (Photo courtesy of: UC Davis School of Veterinary Medicine, Anatomic Pathology Department, One Shields Ave, Davis, CA 95616 http://www.vetmed.ucdavis.edu/pmi/)

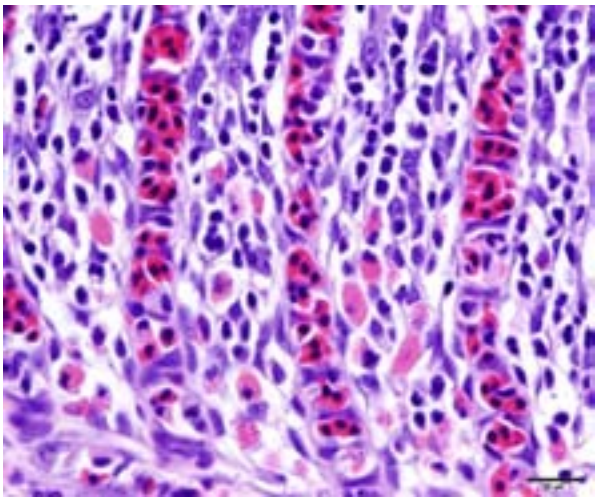

1-5. Gill, koi: Gill inflammation consists of mononuclear cells and granular leukocytes. (HE 400X) (Photo courtesy of: UC Davis School of Veterinary Medicine, Anatomic Pathology Department, One Shields Ave, Davis, CA 95616 http://www.vetmed.ucdavis.edu/pmi/)

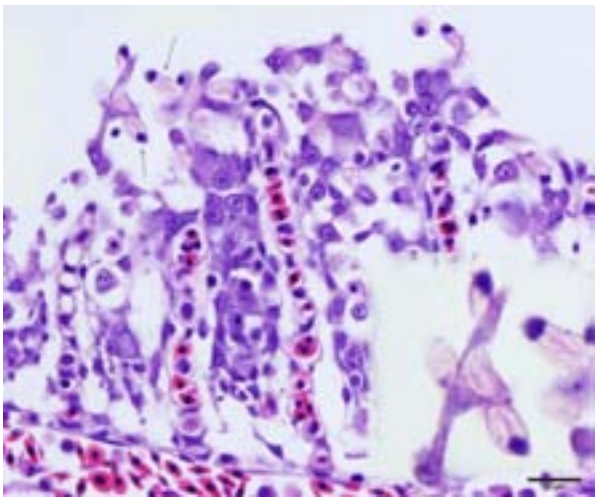

1-6. Gill, koi: High magnification of gill secondary lamellae demonstrates gill epithelium degeneration, necrosis and numerous rodlet cells. (HE 400X) (Photo courtesy of: UC Davis School of Veterinary Medicine, Anatomic Pathology Department, One Shields Ave, Davis, CA 95616 http://www.vetmed.ucdavis.edu/pmi/)

developed generalized edema. The other affected fish similarly developed ulcerations prior to death. The owner offered antibiotic-containing feed to the pond after the third fish died. The pond is a converted swimming pool also being used by waterfowl.

Upon clinical examination, ulceration on the lateral trunk and prominent edema of the gills were noted. Post mortem gill biopsy and skin scrapings were done using light microscopy immediately on arrival, and revealed gill flukes (*Dactylogyrus* sp.). Skin scraping did not reveal additional findings.

The fish was submitted for full necropsy to rule out viral, including koi herpes virus (KHV, Cyprinid herpesvirus 3), spring viremia of carp virus (SVCV), or bacterial infections. Fresh samples of gill and kidney were tested for KHV and carp edema virus (CEV). The molecular techniques used were PCR as described by Oyamatsu T. et al., for CEV and Taqman - PCR for KHV by Bercovier H. et al. A sample of

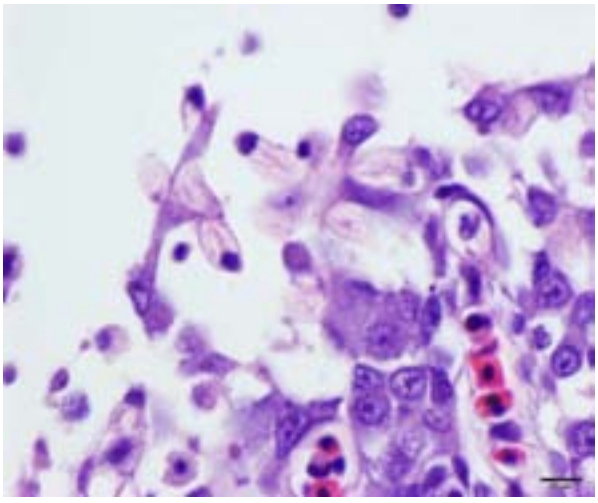

1-7. Gill, koi: Closer view of the rodlet cells. (HE 600X) (Photo courtesy of: UC Davis School of Veterinary Medicine, Anatomic Pathology Department, One Shields Ave, Davis, CA 95616 http://www.vetmed.ucdavis.edu/pmi/)

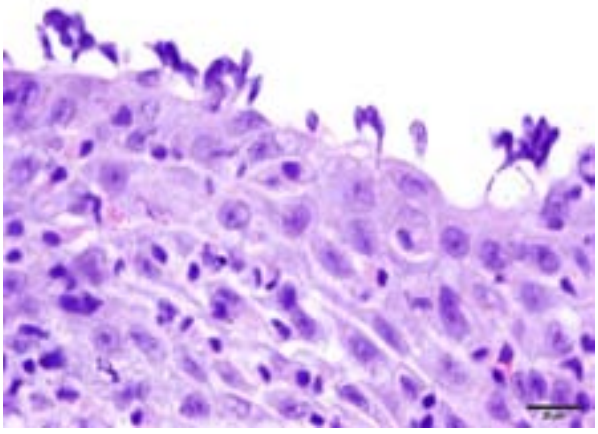

1-8. Skin, koi: Adjacent to the ulcerated regions, on the intact epidermal surface, there were thin pyriform protozoa attached by thin stalks (flagella), approximately 6x5 mm (similar in size to a red blood cell), consistent with Ichthyobodo sp., (formerly known as Costia sp). (HE 400X) (Photo courtesy of: UC Davis School of Veterinary Medicine, Anatomic Pathology Department, One Shields Ave, Davis, CA 95616 http://www.vetmed.ucdavis.edu/pmi/)

water from the pond was submitted for toxicological and other water quality analyses.

Gross Pathology: The submitted fish had irregular, coalescing, well demarcated areas of scale and skin loss with exposed underlying subcutis and muscles at the dorso-lateral trunk. The eroded areas were surrounded with hemorrhage. Diffusely, the scales fell out with little manipulation of the body. Clear fluid was exuding from the vesicles expanding the skin and elevating the scales producing a "pinecone" appearance. The skin on the head, around the vent, and diffusely throughout the body, had numerous pinpoint red discolorations (consistent with petechiation) and small vessel congestion. The mucosa of the upper palate of the mouth was diffusely swollen, partially occluding the pharyngeal region. The coelomic organs were intertwined and adhered to the parietal serosa with numerous thin fibrous attachments. The ovary, liver, spleen and kidneys were extremely friable. The gastrointestinal tract was surrounded with a large amount of adipose tissue.

Laboratory Results:

- Molecular analysis of the fresh tissues (gill, kidney) were positive for Carp Edema Virus (CEV) or "Koi Sleepy Disease," a pox - like virus, and negative for KHV.
- Toxicological analysis of the water did not demonstrate any elevated heavy metals except for copper, measuring 0.02ppm (reference at 0.01ppm).
- Elevated nitrite (0.085mg/L NO_2-N) and ammonia nitrogen (0.11mg/L NH_3-N) were detected using spectrophotometer.

Histopathologic Description: Gill: The secondary gill lamellae are partially fused due to marked, diffuse epithelial cell hyperplasia and hypertrophy, mixed interstitial inflammation and edema. The interstitium of the primary lamellae is also expanded with marked edema and contains mixed inflammation. The inflammation consists of abundant mononuclear cells, such as lymphocytes and macrophages, as well as eosinophilic granular cells. Thickened and distorted secondary lamellae are lined with plump, sometimes vacuolated epithelium that piles up into confluent sheets with admixed inflammation, particularly at the base of the filaments. The gill epithelial cells frequently have rounded margins, hypereosinophilic cytoplasm, and karyorrhectic, pyknotic or indistinct nuclei. Sloughed necrotic cells mix in with cellular debris and erythrocytes at the gill surface. There is rare multifocal rodlet cell hyperplasia throughout the affected regions. Rare gill arch arterioles contain fibrin thrombi. Multifocally in the gill and mucosal epithelium, smudged basophilic aggregates and sometimes eosinophilic material

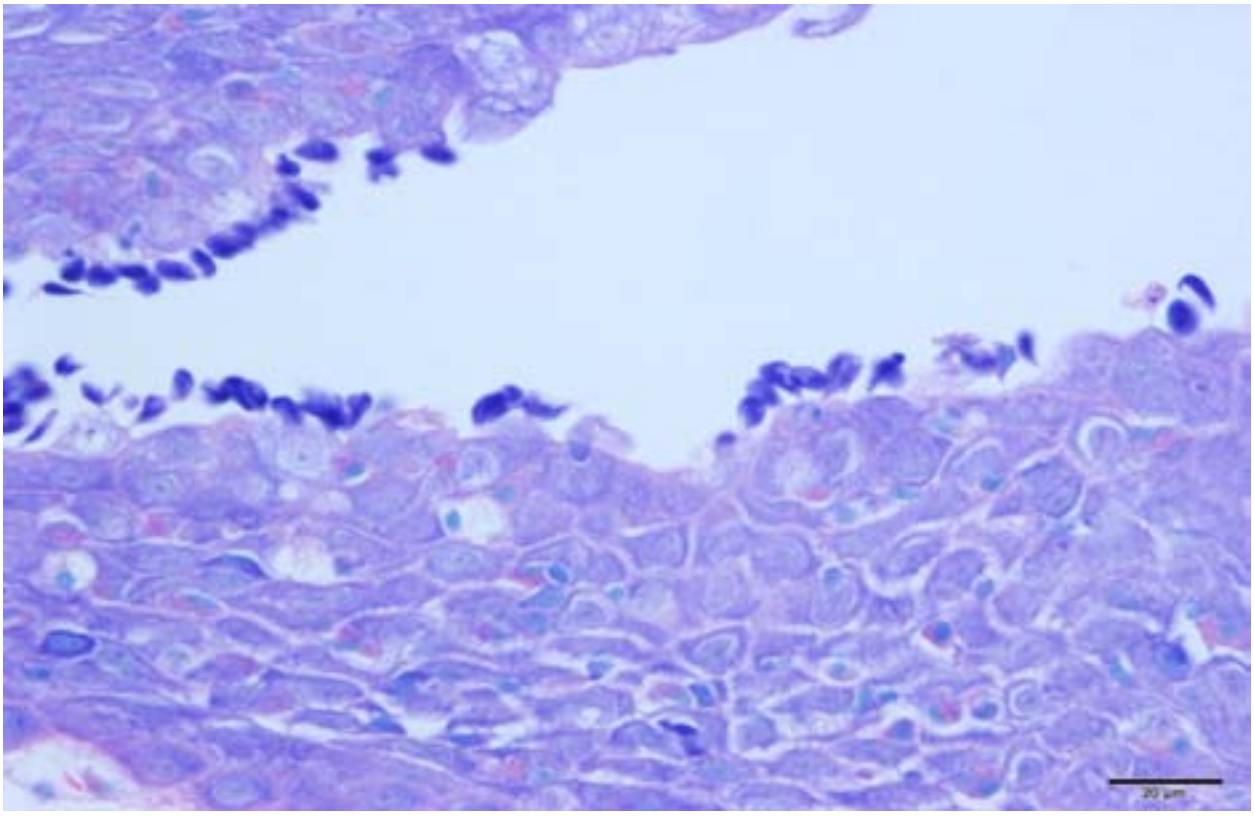

1-9. Skin, koi: Pyriform protozoa attached to the intact epidermal surface adjacent to the ulcer are highlighted with Giemsa. (Giemsa, 400X) (Photo courtesy of: UC Davis School of Veterinary Medicine, Anatomic Pathology Department, One Shields Ave, Davis, CA 95616 http:// www.vetmed.ucdavis.edu/pmi/)

disperses the chromatin (presumed cytoplasmic invagination, early chromatin changes in necrotic cells). Vessels throughout the gill are dilated.

Skin (slide not provided): Associated with superficial areas of ulceration are small, gram-negative bacterial aggregates (presumed *Aeromonas* sp.) mixed in with rare gram-positive larger rods. Adjacent to the ulcerated regions, on the intact epidermal surface, there were thin pyriform protozoa attached by thin stalks (flagella), approximately 6x5 µm (similar in size to a red blood cell), consistent with *Ichthyobodo* sp., (formerly known as *Costia* sp.). The scales are elevated above the dermis by clear spaces (edema). Skeletal muscles in the region of skin ulceration are inflamed and necrotic. The myocytes have fragmented, vacuolated or pale eosinophilic sarcoplasm with loss of distinct striations. Mononuclear inflammatory, often fragmented cells aggregate between myocytes, and along with erythrocytes spill onto the exposed surface.

Contributor's Morphologic Diagnosis: 1. Gill: Moderate diffuse subacute necrotizing branchitis with marked interstitial edema and multifocal branchial arteriole thrombosis (PCR positive for carp edema virus).
2. Integument, mid left dorso-lateral body wall: Severe multifocal subacute regionally extensive ulcerative and fibrinohemorrhagic dermatitis and necrotizing myositis with epidermal protozoal parasites (probable *Ichthyobodo* sp.).
3. Integument: Severe diffuse edema, petechiation, scale loss and lymphocytic and granulocytic dermatitis.

Contributor's Comment: Carp edema virus (CEV) is the causative agent of sleepy disease of koi (SDK) with devastating outbreaks in koi or ornamental variety of carp (*Cyprinus carpio koi,* also known as Japanese color carp). This disease occurs epizootically in the fall and spring in commercially cultured young fish. Occurrence of outbreaks is associated with mild water temperature ranges of 15 to 25 degrees Celsius. Affected fish are lethargic, found at the bottom/ surface of the tank or pond with sunken eyes and

skin erosions/ulcerations. The most distinct gross finding is diffuse edema, particularly affecting the gills. Microscopic findings include clubbing and swelling of gill filaments with interlamellar fusion, and hypertrophy, hyperplasia and necrosis of the gill epithelium. CEV, a pox – like virus, particles can be visualized with transmission electron microscopy in the infected gill epithelium.[6] Electron microscopy demonstrates cytoplasmic viral particles in the gill epithelium with immature virus measuring up to 450nm in diameter and mature, roughly oval, virions measuring about 400x413nm. Mature virions are decorated with surface globules and have a dense core enclosed by a prominent membrane.[6] Cytoplasmic inclusions characteristic of pox virus infections were not observed in the gills of this fish, neither they were described by T. Miyazaki et al. The CEV PCR assay can detect the virus in multiple different tissues from affected fish including skin, liver and kidney.[6]

In this case, the diagnosis of carp edema virus was made on the characteristic gross and histologic findings with confirmation by PCR. No virions were identified in gill tissue by electron microscopy; however, the tissue was not optimally preserved. Combination of CEV, protozoal, and bacterial infections may have played a role in the skin ulceration. The latter two could potentially be opportunistic pathogens infecting the compromised host.

Based on the history (mild water temperature, season, age of affected fish) and gross lesions (skin ulcerations and petechiae), differentials for this case would include KHV and SVC. The pronounced branchial edema distinguishes the CEV infection, grossly. As a brief review, KHV is characterized grossly by necrotizing branchitis and is a reportable disease of wild and cultured common carp. Histological findings include epithelial proliferation, fusion of the gill lamellae, and epithelial necrosis (cytopathic effect of the virus). Typical of KHV, there are intranuclear inclusions in many cell types, including but not limited to respiratory epithelial cells, macrophages, hematopoietic cells in the kidney, and cardiac myocytes. Electron microscopy demonstrates enveloped herpes virus with mature nucleocapsids measuring up to 117nm and mature enveloped nucleocapsids up to 180nm in the affected cells.[7] KHV virus can be isolated from multiple organs and confirmed with PCR and immunohistochemistry.[2,5] Spring viremia of carp virus (SVCV) from the family Rhabdoviridae, genus *Vesiculovirus,* is the causative agent of another reportable, contagious, fatal disease of farmed carp and related species. The virus causes petechial hemorrhages in the gill and skin, as well as internal hemorrhage in the kidneys, spleen and liver, and exophthalmia. SVCV targets the swim bladder, resulting in edema and inflammation, as well as ascites.[1,3] Skin ulceration can also be caused by parasitic infection such as *Ichthyobodo* sp. (formerly known as *Costia* sp.) that may also affect the gills.[4,9] The latter agent can be seen on scrapings from gills and skin lesions, and on histological examination. Koi ulcer disease (also known as summer ulcer disease and carp erythrodermatitis), associated with bacterial pathogens such as *Aeromonas* spp., can also present similarly.[4,9]

JPC Diagnosis: 1. Gill: Branchitis, proliferative, diffuse, severe, with marked epithelial hypertrophy and hyperplasia, lamellar fusion, arteriolar fibrin thrombi and mild goblet cell hyperplasia.
2. Oral mucosa: Stomatitis, proliferative and lymphocytic, diffuse, mild, with numerous intraepithelial intranuclear inclusions.

Conference Comment: The moderator began with a brief review of the normal anatomy, histology and physiology of the gill. The gill arch is a curved bony structure with double rows of paired primary lamellae (filaments). Each primary lamella, in turn, encompasses an array of perpendicularly oriented secondary lamellae. The entire gill arch is covered by epidermis; the epidermis overlying the origin of the primary lamellae is thicker and often contains numerous mucous cells, with a subepidermal array of lymphoid tissue. The primary lamellae are covered by a mucoid epidermis which may contain round, pale, eosinophilic, salt-secreting chloride cells (especially at the basal/proximal part of the lamellae). These chloride cells function in ionic transport and may also play a role in detoxification.[8]

Gas exchange occurs via countercurrent exchange at the surface of the secondary lamellae, which are lined by overlapping squamous epithelial cells, usually one layer thick, surrounding numerous capillaries that are supported by rows of pillar cells. Where the pillar cells encroach on

the basement membrane, they spread to coalesce with neighboring pillar cells to complete the lining of lamellar blood channels. Pillar cells contain contractile protein elements that resist distension and support the lamellar blood spaces. The surface of the lamellar epithelium gives rise to microvilli that aid in attachment of the epidermal (cuticular) mucus. This mucus, in addition to providing protection against abrasion and infection, is important in the exchange of gas, water and ions. The combined thickness of the cuticle, respiratory epithelium and flanges of the pillar cells (which is the total diffusion distance for gas exchange) ranges from 0.5 to 4 µm. Low to moderate numbers of goblet cells are scattered among lamellar squamous epithelial cells of both primary and secondary lamellae.[8]

Much like mammalian lungs, the gill epithelium is thin with a large surface area in order to maximize the exposure of gill capillaries to water. While this is an important factor for efficient gas exchange, it is a fairly ineffective physical barrier and results in increased branchial vulnerability to inflammation and infection. Gills also play an essential role in regulating the exchange of salt and water, as well as the excretion of the nitrogenous wastes (primarily ammonia). Thus, even minimal damage can result in significant osmoregulatory and respiratory difficulties.[8]

As noted by the contributor, the proliferative nature of these microscopic lesions is striking, with marked epithelial cell hypertrophy and hyperplasia leading to lamellar fusion; however, many conference participants also identified moderate numbers of fairly prominent, eosinophilic, intracytoplasmic inclusions within the epithelium of the (presumed) oral mucosa, which appear to peripheralize the chromatin. After scrupulous examination of H&E sections, and consideration of the laboratory results reported by the contributor (molecular analysis for koi herpes virus was negative), we are unable to elucidate the nature of these inclusions. There is also some slide variation - not all sections contain fibrin thrombi within arterioles of the gill arch, as reflected in the JPC morphologic diagnosis. Furthermore, the moderator observed that cartilage of the gill arch appears somewhat irregular and deformed, which may suggest a previous nutritional deficiency, but is probably unrelated to the current disease process.

Contributing Institution: UC Davis School of Veterinary Medicine
Anatomic Pathology Department
One Shields Ave
Davis, CA 95616
http://www.vetmed.ucdavis.edu/pmi/

References:

1. Ahne W, Bjorklund HV, Essbauer S, et al. Spring viremia of carp (SVC). *Dis of Aquat Org*. 2002;52:261–272.
2. Bercovier H, Fishman Y, Nahary R, et al. Cloning of the koi herpesvirus (KHV) gene encoding thymidine kinase and its use for a highly sensitive PCR based diagnosis. *BMC Microbiol*. 2005;5:13.
3. Dikkeboom AL, Radi C, Toohey-Kurth K, et al. First report of spring viremia of carp virus (SVCV) in wild common carp in North America. *Journal of Aquatic Animal Health*. 2004;16:169–178.
4. Ferguson HW. *Systemic Pathology of Fish*. 2nd ed. London, UK: Scotian Press; 2006:55, 72-73.
5. Ilouze M, Dishon A, Kotler M. Characterization of a novel virus causing a lethal disease in carp and koi. *Microbiology and Molecular Biology Reviews*. 2006;70:147–156.
6. Miyazaki T, Isshiki T, Katsuyuki H. Histopathological and electron microscopy studies on sleepy disease of koi (*Cyprinus carpio koi*) in Japan. *Dis of Aquat Org*. 2005;65:197–207.
7. Miyazaki T, Kuzuya Y, Yasumoto S, et al. Histopathological and ultrastructural features of koi herpesvirus (KHV)-infected carp *Cyprinus carpio*, and the morphology and morphogenesis of KHV. *Dis of Aquat Org*. 2008;80:1–11.
8. Mumford S, Heidel J, Smith C, Morrison J, MacConnell B, Blazer V. *Fish Histology and Histopathology*. US Fish and Wildlife Service, National Conservation Training Center. http://nctc.fws.gov/resources/course-resources/fish-histology/index.html. Accessed April 26, 2014.
9. Noga EJ. *Fish Disease*: *Diagnosis and Treatment*. St. Louis, MO: Wiley-Blackwell; 1996:108-110, 141-146.

CASE II: 10-5509 (JPC 4006285).

Signalment: Adult male zebrafish, (*Danio rerio*).

History: This fish was submitted as part of a breeding pair being screened for infection by *Pseudoloma neurophilia* prior to placing their bleached embryos on the system. Fish were processed by making a ventral midline incision to facilitate fixation and placing in Bouin's solution for 24 hours. The entire fish was then bisected parasagittally, and four levels were taken at 100 µm increments for histopathologic evaluation. Each level was stained with both H&E and Luna stain to screen for *Pseudoloma*.

Gross Pathology: None.

Histopathologic Description: Within the brainstem and spinal cord, few microsporidian xenomas are present that range in size from approximately 20-40 µm in diameter, and which contain aggregates of ovoid spores measuring approximately 5.5 x 2.5 µm. The spores are uninucleate and are segregated into sporophorous vesicles within the xenoma. A few developmental stages (sporoblasts) are also present within the xenomas. Additionally, several nerve roots contain individual spores, either free or within the cytoplasm of macrophages. Individual spores are best visualized on the Luna-stained section, in which they stain dark orange. The neuropil adjacent to the xenomas is free of an inflammatory response. A mild histiocytic response is present within the nerve roots in association with individual spores.

Contributor's Morphologic Diagnosis: 1. Brain, spinal cord: Microsporidian xenomas, few, morphology consistent with *Pseudoloma neurophilia.*
2. Nerve roots: Radiculoneuritis, histiocytic, multifocal, mild, with intralesional microsporidan spores (morphology consistent with *Pseudoloma neurophilia*).

Contributor's Comment: *Pseudoloma neurophilia* is a microsporidian parasite related to *Loma* and *Ichthysporidium*, which also infect fish and lead to the formation of xenomas within various tissues.[5] It is reported to be the most common pathogen in zebrafish facilities.[3] Mild infections (as was present in this case) may be associated with no clinical signs; however, heavily infected fish (which we have also encountered in our laboratory) often demonstrate significant weight loss (known as "skinny disease") and/or scoliosis. Fish with mild to moderate infections have been shown to exhibit poor growth and reproductive performance, particularly in the face of other environmental stressors.[7]

Xenomas, which may measure up to 200 µm in diameter, are composed of several aggregates of up to 16 uninucleate spores segregated within

2-1. Zebrafish, presentation: This individual presented with poor weight gain and scoliosis. (Photo courtesy of: Laboratory of Comparative Pathology, Memorial Sloan Kettering Cancer Center, New York, NY 10065 http://www.mskcc.org)

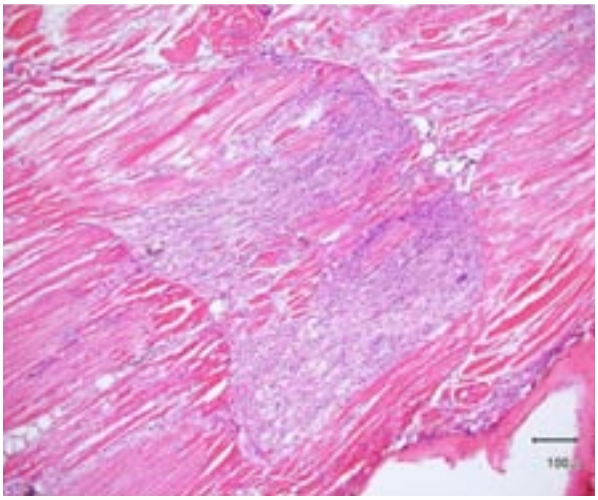

2-2. Zebrafish, skeletal muscle: Multifocally, skeletal muscle is infiltrated by large numbers of macrophages and exhibits moderate to severe myodegeneration and atrophy. (Photo courtesy of: Laboratory of Comparative Pathology, Memorial Sloan Kettering Cancer Center, New York, NY 10065 http://www.mskcc.org)

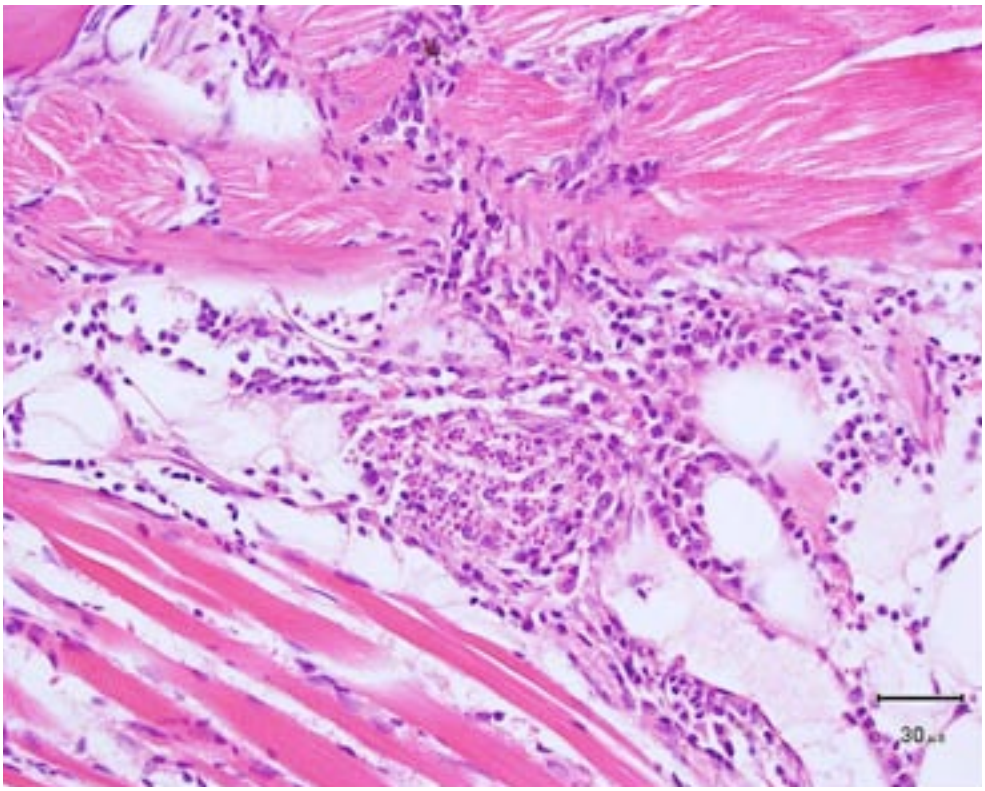

2-3. Zebrafish, skeletal muscle: Scattered throughout inflammatory foci are low numbers of myxosporidian cysts which, when rupture, are surrounded by numerous macrophages, which often contain phagocytosed spores. (HE 400X) (Photo courtesy of: Laboratory of Comparative Pathology, Memorial Sloan Kettering Cancer Center, New York, NY 10065 http://www.mskcc.org)

sporophorous vesicles. Spores are oval to pyriform and measure approximately 5.5 x 2.5 µm. Like other microsporidians, the spores contain a polar filament. In addition to mature spores, sporophorous vesicles contain a few developmental stages known as sporoblasts. Unlike many other microsporidia, developmental stages are in direct contact with the host cytoplasm, rather than within parasitophorous vacuoles, based on electron microscopic studies.[5]

As was the case in this fish, a few xenomas usually do not stimulate a significant inflammatory response; however, large numbers of xenomas and/or the presence of free spores within tissues may be associated with significant inflammation. In heavily infected fish, the inflammatory reaction may extend from the spinal cord meninges or nerve roots into the adjacent skeletal musculature, where it may be associated with massive chronic inflammation and myodegeneration, with relatively few organisms present (either within xenomas or free spores which undergo phagocytosis by macrophages).

Transmission is primarily through the ingestion of infective spores, either free in the water or within the tissues of cannibalized fish. Experimental transmission following exposure of fish to water contaminated with organisms derived from infected spinal cords resulted in infection as early as 8 weeks post-exposure, with 100% of exposed fish infected by week 20.[4] As its name implies, *P. neurophilia* has a tendency to infect the central nervous system (particularly the brainstem and spinal cord), as well as nerve roots. However, both xenomas and free spores have been identified in other tissues, particularly the ovary and developing follicles, leading to speculation that vertical transmission (or at least transmission via sexual products released during spawning) may occur. Because of this and the fact that routine chlorine bleaching does not appear to kill the infective spores,[1] techniques involving re-derivation of colonies by the screening of adult fish using histopathology and/or of a percentage of their offspring by PCR have been developed and are being used by some facilities (including ours) in order to create SPF lines.[3] In addition to being used to test adults and eggs, PCR may be used to test water filtrates, biofilms, and other samples.[8] Histopathologic diagnosis is greatly facilitated by the use of a Luna stain, which binds to chitin and stains spores bright orange.[6] Other histochemical stains, such as Gram, Fite's acid-fast, and Giemsa are variably effective in staining spores. Spores may also be visualized using fluorescent stains (Fungi-Fluor).[4] No treatment is currently available,[3] and infections persist following exposure, with no evidence for immune clearance by the host.[7]

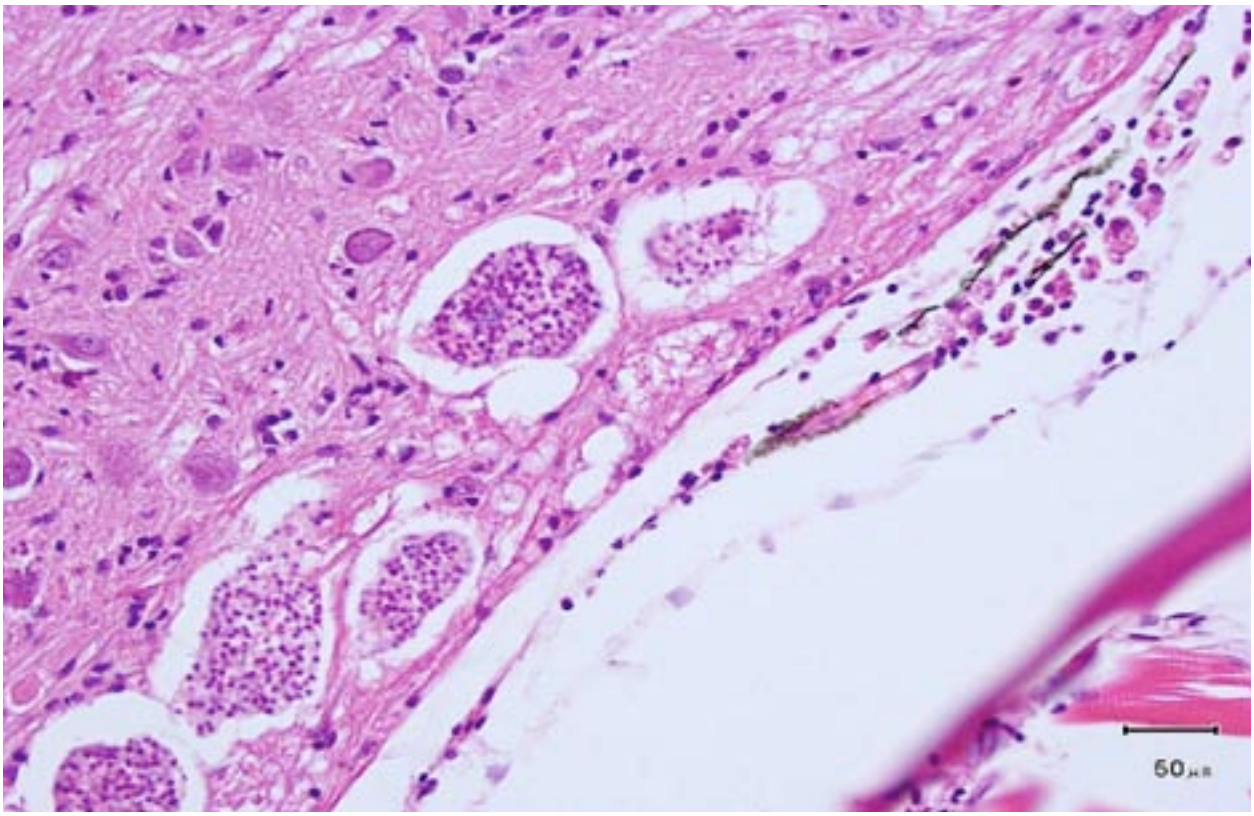

2-4. Zebrafish, spinal cord: Low to moderate numbers of intact xenomas are scattered throughout the spinal cord. (HE 400X) (Photo courtesy of: Laboratory of Comparative Pathology, Memorial Sloan Kettering Cancer Center, New York, NY 10065 http://www.mskcc.org)

JPC Diagnosis: 1. Brain: Microsporidial xenomas, multiple.
2. Spinal cord: Ganglioneuritis, histiocytic, multifocal, mild, with intracytoplasmic microsporidian spores.

Conference Comment: The contributor provides an excellent summary of *Pseudoloma neurophilia* infection in fish; readers are urged to review WSC 2013-2014, conference 4, case 3 for a detailed discussion of other microsporidian species encountered in veterinary medicine. Microsporidia are obligate intracellular, unicellular eukaryotes that are most closely related to fungi, specifically zygomycetes. They have one of the smallest known genomes and exist extracellularly only as small, thick-walled spores with a coiled polar filament. Developing spores can be packaged within a parasitophorous vacuole (e.g., *Encephalitozoon* spp.) or can remain within the cytoplasm (e.g., *Enterocytozoon bieneusi*, *Nosema* spp.).[2] Interestingly, the conference moderator notes that some microsporidia (including *P. neurophila*) appear birefringent under polarized light.

Contributing Institution: Laboratory of Comparative Pathology
Memorial Sloan Kettering Cancer Center
New York, NY 10065
http://www.mskcc.org

References:

1. Ferguson JA, Watral V, Schwindt AR, Kent ML. Spores of two fish microsporidia (*Pseudoloma neurophilia* and *Glugea anomala*) are highly resistant to chlorine. *Dis Aquat Org*. 2007;76:205-214.
2. Keeling PJ, McFadden GI. Origins of microsporidia. *Trends Microbiol*. 1998;6(1):19–23.
3. Kent ML, Buchner C, Watral VG, Sanders JL, LaDu J, Peterson TS, Tanguay RL. Development and maintenance of a specific pathogen-free (SPF) zebrafish research facility for *Pseudoloma neurophilia*. *Dis Aquat Org*. 2011;95:73-79.
4. Kent ML, Bishop-Stewart JK. Transmission and tissue distribution of *Pseudoloma neurophilia* (Microsporidia) of zebrafish, *Danio rerio* (Hamilton). *J Fish Dis*. 2003;26:423-426.
5. Matthews JL, Brown AMV, Larson K, Bishop-Stewart JK, Rogers P, Kent ML. *Pseudoloma*

neurophilia n. g., n. sp., a new microsporidian from the central nervous system of the zebrafish (*Danio rerio*). *J Eukaryot Microbiol*. 2001;48:227-233.
6. Peterson TS, Spitsbergen JM, Feist SW, Kent ML. Luna stain, an improved selective stain for detection of microsporidian spores in histologic sections. *Dis Aquat Org*. 2011;95:175-180.
7. Ramsay JM, Watral V, Schreck CB, Kent ML. *Pseudoloma neurophilia* infections in zebrafish *Danio Rerio*: effects of stress on survival, growth, and reproduction. *Dis Aquat Org*. 2009;88:69-84.
8. Whipps CM, Kent ML. Polymerase chain reaction detection of *Pseudoloma neurophilia*, a common microsporidian of zebrafish *(Danio rerio*) reared in research laboratories. *J Am Assoc Lab Ani Sci*. 2006;45:13-16.

CASE III: U-30918-12 (JPC 4032588).

Signalment: Mature adult unknown gender Atlantic Salmon, (*Salmo salar*).

History: These fish are from a research facility where they are held in 1500L tanks at approximately 12°C, pH of ~8, nitrogen gas saturation ~100 % and oxygen at 80 % saturation. Tissues were collected during end of study post-mortem examinations on extra salmon. The study duration was no greater than 24 months.

Gross Pathology: The right pseudobranch was swollen and mottled.

Histopathologic Description: Expanding and effacing the pseudobranch is a non-encapsulated, well demarcated, expansile, highly cellular mass composed of three haphazardly intermingled cellular populations embedded in small amounts of dense fibrous stroma. These cell populations consist of dense aggregates of basophilic blastemal cells, polygonal to cuboidal epithelial cells and islands of cartilage. Epithelial populations often consist of cuboidal cells which sometimes form structures resembling branchial lamellae. In other areas, dense cords and trabeculae of epithelial cells often are intermingled with numerous round cells with small dense, eccentrically located nuclei which are compressed against the cell margins by moderate amounts of pink, round cytoplasm (interpreted as mucous producing goblet cells). Blastemal cells are round to slightly spindloid, darkly basophilic and have sparse, poorly defined, cytoplasm, round to ovoid, dark nuclei with finely stippled chromatin and unapparent to small, nucleoli. Islands of cartilage are often surrounded by concentric layers of thin spindloid cells with scant, poorly defined, pale basophilic cytoplasm, fusiform, nuclei with finely stippled chromatin and unapparent nucleoli. The mitotic rate is 10 figures noted in ten randomly selected fields at high power objective (40x) with mitotic figures only observed within the epithelial populations. Multifocal aggregates of lymphocytes and granular leucocytes are present at the periphery of the mass.

Contributor's Morphologic Diagnosis: Pseudobranch: Branchioblastoma.

3-1. Pseudobranch, salmon: An 8mmx6mm well-demarcated expansile neoplasm expands the pseudobranch. (HE 0.63X)

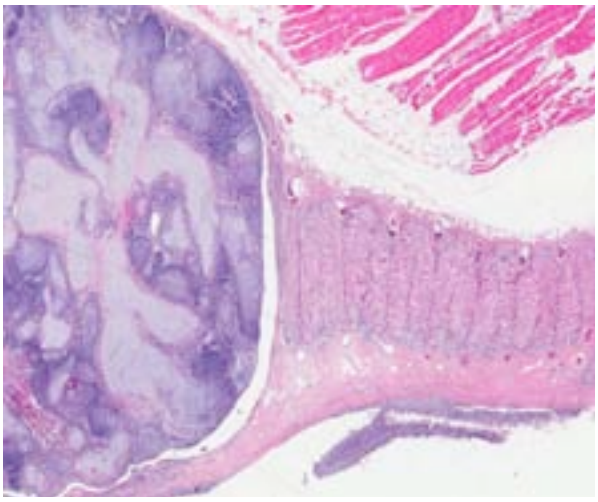

3-2. Pseudobranch, salmon: The neoplasm is composed of multiple lobules of small, densely packed blastemal cells separated by thick trabeculae of well-differentiated cartilage. These components are similar to those seen in the pseudobranch, but markedly disordered. (HE 14X)

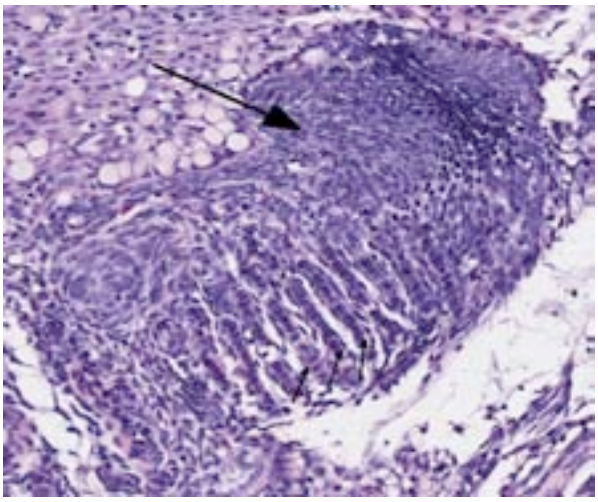

3-3. Pseudobranch, salmon: Densely packed polygonal to spindle blastemal cells (large arrow), occasionally are arranged into structures resembling secondary lamellae. (HE 164X)

Contributor's Comment: There is increasing interest in the use of fish as models for carcinogenicity studies as well as ecosystem monitors within the environment.[6,7] Neoplasms of the gill and pseudobranch are rare compared to other locations such as the skin or liver, but have been previously described in koi carp (*Cyprinus carpio*).[3] To the author's knowledge, it has not been previously reported in Atlantic salmon (*Salmo salar*).

Branchioblastoma is a tumor of embryologic blast-type cells with mesenchymal and epithelial components. It is histologically considered a benign tumor because it is expansile and often well demarcated. However, the mass can interfere with gaseous exchange in the gill with potentially fatal consequences. Affected fish may present with respiratory distress, an inability to close their mouth or multilobulated mass/masses appearing to originate from a gill arch or the pseudobranch.[3]

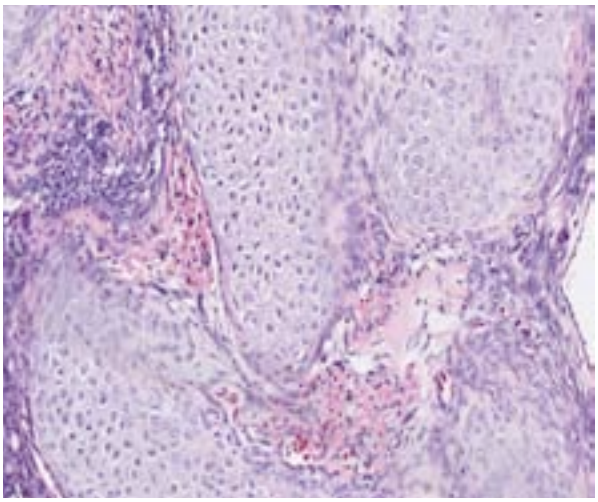

3-4. Pseudobranch, salmon: Scattered among cartilage trabeculae and nests of blastemal cells are large numbers of granulated leukocytes. (HE 220X)

Select differentials for a multilobular lesion in the region of the operculum, gill and oral cavity may include granulomatous or inflammatory lesions due to infection by bacteria (eg. *Mycobacterium* sp.), fungi (eg. *Banchiomyces*), microsporidia (eg. *Loma* sp.), myxozoa (eg. *Myxobolus* sp.), branchial trematodes, and iridovirus (eg. lymphocystis).

Neoplasia in fish is likely multifactorial and has previously been associated with exposure to carcinogens,[6] genetic causes,[5] and retrovirus infection.[1] No underlying cause was identified in this case.

JPC Diagnosis: Pseudobranch: Branchioblastoma.

Conference Comment: The pseudobranch is not found in all fish species, but where present it is a red, gill-like tissue attached to the internal surface of the operculum. It is composed of cartilage-supported parallel blood capillaries that create a counter-current system which likely functions to increase oxygen uptake. The pseudobranch has a direct vascular connection with the ocular choroid, which is composed of similar capillary

arrays alternating with rows of slender fibroblast-like cells; it may also play a role in the filling of the air bladder.[4]

In addition to branchioblastoma, which can arise from the gill or the pseudobranch and may be spontaneous or carcinogen-induced,[3] conference participants briefly discussed teratoma as a rule-out with similar histological features. Branchioblastoma, as noted by the contributor, is composed of embryologic blast-type cells with mesenchymal and epithelial components; similarly, teratomas are classically defined as having at least two of the three embryonic layers-endoderm, mesoderm, and ectoderm (see WSC 2013-2014, conference 8, case 2). Teratomas occur most frequently in the gonads; however, these tumors can also develop at extragonadal locations, usually along the midline.[2] They are rarely (if ever) reported in fish. The moderator points out that branchioblastoma and teratoma have analogous etiopathogeneses; however, the neoplastic cell types comprising branchioblastomas are appropriate to the anatomic location (i.e. this tumor appears to be attempting to form normal gill tissue in a relatively normal location), while teratomas tend to produce poorly differentiated, disorganized tissue that does not belong (i.e. foci of squamous epithelium, bone and tooth within the gonad). Based on these broad attributes, this neoplasm is most consistent with a branchioblastoma.

Contributing Institution: Department of Pathology/Microbiology
Atlantic Veterinary College
University of Prince Edward Island
550 University Avenue
Charlottetown, Prince Edward Island
C1A 4P3
http://avc.upei.ca/diagnosticservices

References:

1. Coffee L, Casey J, Bowser P. Pathology of tumors in fish associated with retroviruses: a review. *Vet Pathol*. 2013;50:390-403.
2. Foster RA. Male reproductive system. In: McGavin MD, Zachary JF, eds. *Pathologic Basis of Veterinary Disease*. 5th ed. St. Louis, MO: Elsevier; 2012:1142-1143.
3. Knüsel R. Brandes R, Lechleiter S, Schmidt-Posthaus H. Two independent cases of spontaneously occurring branchioblastomas in koi carp (*Cyprinus carpio*). *Vet Pathol*. 2007;44:237-239.
4. Mumford S, Heidel J, Smith C, Morrison J, MacConnell B, Blazer V. *Fish Histology and Histopathology*. US Fish and Wildlife Service, National Conservation Training Center. http://nctc.fws.gov/resources/course-resources/fish-histology/index.html. Accessed April 26, 2014.
5. Shin J, Padmanabhan A, de Groh E, Lee J-S, Haidar S, Dahlberg S, et al. Zebrafish neurofibromatosis type 1 genes have redundant functions in tumorigenesis and embryonic development. *Dis Model Mechan*. 2012;5:881-894.
6. Williams D, Bailey G, Reddy A, Hendricks J, Oganesian A, Orner G, et al. The rainbow trout (*Oncorhynchus mykiss*) tumor model: recent applications in low-dose exposures to tumor initiators and promoters. *Toxicol Pathol*. 2003;31:58-61.
7. Wirgin I, Waldman J. Altered gene expression and genetic damage in North American fish populations. *Mutation Res*. 1998;399:193-219.

CASE IV: 65066 (JPC 4032696).

Signalment: 20-year-old male white-lipped mud turtle, (*Kinosternon leucostomum*).

History: This turtle was from a large regional aquarium collection and presented to veterinary clinicians with coelomic distension and periocular swelling. Ultrasound examination confirmed coelomic effusion that was classified as a transudate following fluid analysis. Radiographs demonstrated diffuse, bilateral mineral opacities within the kidneys. Bloodwork showed a moderate anemia and severe elevation in uric acid. With a presumptive diagnosis of chronic renal failure in an elderly and fractious turtle, the animal was maintained on hospice care without further diagnostics. The turtle died 3.5 months after initial presentation.

Gross Pathology: Grossly, there was severe coelomic distention and subcutaneous edema of the neck and limbs. Both kidneys were diffusely off-white and hard, with no normal renal tissue apparent. The liver was friable and enlarged with rounded edges and multifocal green-tan mottling.

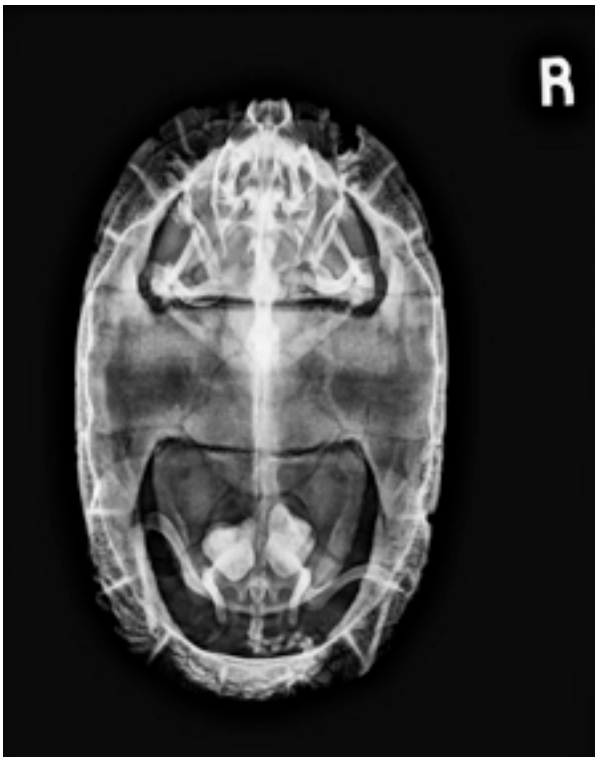

4-1. Radiograph, dorsoventral view, white-lipped mud turtle: The kidneys are outlined by diffuse bilateral mineral opacities. (Photo courtesy of: Johns Hopkins University School of Medicine, Dept. of Molecular and Comparative Pathobiology, http://www.hopkinsmedicine.org/mcp/)

Histopathologic Description: Approximately 80% of the renal parenchyma is replaced by anastomosing trabeculae of well-differentiated mature bone. The bone contains scattered osteocytes and the trabecular surface is lined by flattened to cuboidal osteoblasts and occasional multinucleated osteoclasts. In non-ossified parenchyma, there is moderate, multifocal expansion of the interstitium by increased clear space (edema) and loosely arranged, fusiform to stellate cells (fibroblasts), as well as scattered infiltrates of mixed inflammatory cells including lymphocytes, plasma cells, heterophils, and azurophils. Remaining renal tubules are frequently ectatic, and/or lined by variably enlarged epithelial cells with abundant indistinct cytoplasmic vacuolization (hydropic degeneration). Increased cytoplasmic basophilia and occasional mitotic figures are also observed among tubular epithelial cells, suggestive of tubular regeneration. Flocculent, lightly eosinophilic proteinaceous material is often present within tubular lumens along with rare cellular debris. Glomeruli are multifocally affected by mild segmental thickening of the mesangial matrix and capillaries by lightly eosinophilic material and mild hypercellularity (membranoproliferative glomerulonephritis).

Contributor's Morphologic Diagnosis: Kidneys, nephropathy, diffuse, chronic, severe, with marked osseous metaplasia, fibroplasia, tubular degeneration, mild membranoproliferative glomerulonephritis, mild lymphocytic and granulocytic interstitial nephritis.

Contributor's Comment: Osseous metaplasia (ectopic ossification), the formation of non-neoplastic bone in soft tissues, has been reported to occur in numerous extra-skeletal organ systems and in the setting of many, clinically disparate disease processes. The ectopic osseous matrix can be mineralized and is typically associated with osteocytes, osteoclasts, osteoblasts, and, in some cases, hematopoietic cells and adipocytes. It is frequently encountered in veterinary medicine as an incidental lesion in the pulmonary connective tissue of dogs and cattle and in the canine dura mater (ossifying pachymeningitis). Ectopic ossification has also been reported in a

4-2. Radiograph, lateral view, white-lipped mud turtle: The kidneys are outlined by diffuse bilateral mineral opacities. (Photo courtesy of: Johns Hopkins University School of Medicine, Dept. of Molecular and Comparative Pathobiology http://www.hopkinsmedicine.org/mcp/)

spectrum of human and animal neoplasms, notably in canine mammary tumors, where it is a common feature.[1] For reasons that are not entirely clear, non-mammalian species empirically are more prone to developing osseous metaplasia than mammals.

Ectopic bone either arises from embryonic cell rests or by differentiation of adult, pluripotent mesenchymal cells into osteoblasts (osseous metaplasia).[2] Osseous metaplasia can occur anywhere uncommitted mesenchymal cells reside, including skeletal muscle, perivascular tissue, and connective tissue or sites of tissue regeneration and repair. It requires the influence of local osteogenic signals in an environment conducive to bone production.[3] Chronic ischemia, trauma, persistent hematoma, chronic inflammation, neoplasia, hypercalcemia, and hypervitaminosis D are among the factors known to stimulate osseous

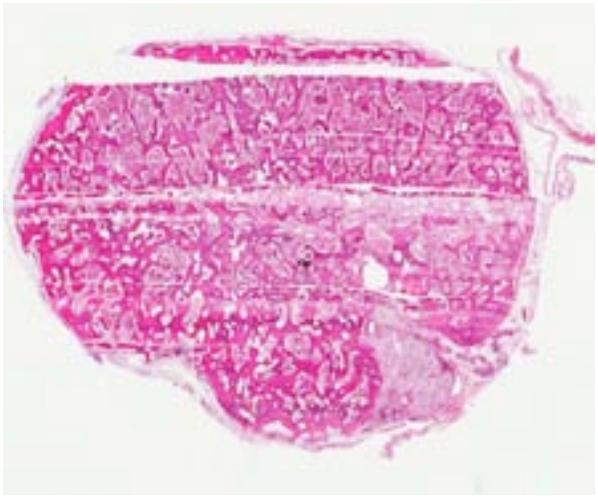

4-3. Kidney and adrenal gland, white-lipped mud turtle: The kidneys are largely replaced by trabeculae of lamellar bone. (HE 0.63X)

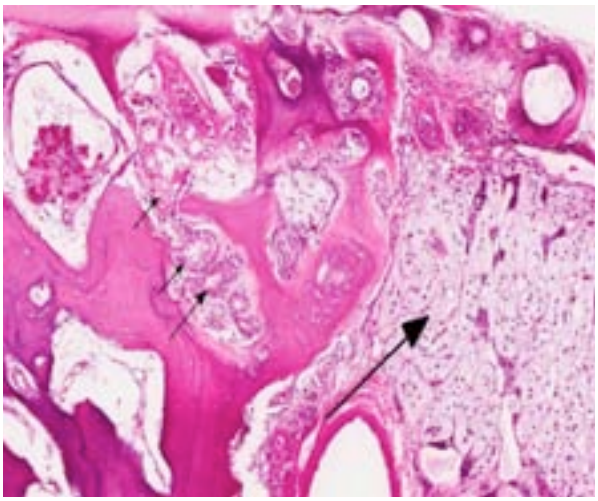

4-4. Kidney and adrenal gland, white-lipped mud turtle: The kidneys are largely replaced by trabeculae of lamellar bone. Glomeruli, tubules (small arrows) and adrenal gland are encased within bony trabeculae. (HE 130X)

metaplasia.[4,5] While the pathophysiologic mechanisms leading to bone formation is not completely understood, paracrine signaling leading to the expression of bone morphogenetic proteins (BMPs) is likely a common key factor.[3] Most BMPs are members of the TGF beta superfamily and are critical signaling agents in normal development and differentiation and in the formation of new bone during fracture healing.[6] BMP expression has been demonstrated to play a role in neoplastic processes associated with ectopic bone formation, as well as experimental models of chronic inflammation.[7] In addition to non-committed mesenchymal cells, vascular endothelial cells[8] and pericytes[9] have also been implicated as potential cells of origin for osseous metaplasia. Interestingly, inactivating germline mutations of the α-subunit of the stimulatory G protein gene leads to subcutaneous and sometimes deeper ectopic bone formation in humans (Albright hereditary osteodystrophy) and in mice.[10] Osseous metaplasia is also seen in association with dystrophic cardiac and pulmonary mineralization in particular strains of mice where early events involve abnormal cellular calcium, mitochondrial alterations, and myocyte injury in the absence of elevation of serum calcium.[12,13]

While pathologic mineralization within the kidney is a not an uncommon finding in cases of chronic renal disease, the presence of abundant, trabecular bone in the renal parenchyma of this turtle is remarkable. Reports of spontaneous osseous metaplasia in the kidney are rare in the human medical literature and even rarer in the veterinary medical literature. In humans, ossified tissue in the kidney is associated with chronic interstitial nephritis, chronic ischemia, pyelonephritis, and papillary necrosis, and it is an uncommon nidus for renal calculus formation.[5,11] Contributing factors for renal osseous metaplasia observed in this turtle likely included chronic inflammatory stimulation and possibly calcium/phosphorous imbalance secondary to chronic renal dysfunction.

JPC Diagnosis: 1. Kidney: Osseous metaplasia, diffuse, severe, with renal tubular degeneration and necrosis.
2. Kidney: Nephritis, interstitial, lymphoplasmacytic, diffuse, moderate.

Conference Comment: We thank the contributor for providing such a thorough summary of osseous metaplasia in veterinary species, and we concur with the proposed explanation that a combination of mineral imbalance due to chronic renal dysfunction (supported by the clinical pathology results and radiographs) and chronic inflammatory stimulation likely contributed to the striking pathologic findings observed in this case. Conference participants briefly considered osteoma as a rule out; however, this benign tumor is generally attached to the periosteum and should not result in the incorporation of renal glomeruli/tubules within bony trabeculae. Additionally, the moderator observed that some tissue sections contain portions of adrenal gland adjacent to the renal hilus, which is a normal anatomic location in some turtle species. Conference participants also noted that the large collecting duct within the hilus appears to contain numerous spermatozoa.

Contributing Institution: Johns Hopkins University School of Medicine
Dept. of Molecular and Comparative Pathobiology
http://www.hopkinsmedicine.org/mcp/

References:

1. Thompson K. Bones and joints. In: Maxie MG, ed. *Jubb, Kennedy, and Palmer's Pathology of Domestic Animals*. Vol. 1. 5th ed. Philadelphia, PA: Saunders Elsevier, 2007:1-184.
2. Myers R, McGavin M, Zachary J. Cellular adaptations, injury, and death: morphologic, biochemical, and genetic basis. In: Zachary JF, McGavin MD, eds. *Pathologic Basis of Veterinary Disease*. 5th ed. St. Louis, MO: Elsevier; 2012:2-59.
3. McCarthy EF, Sundaram M. Heterotopic ossification: a review. *Skeletal Radiol*. 2005;34:609–619.
4. Landim FM, Tavares JM, de Melo Braga DN, da Silva JE, Bastos Filho JBB, Feitosa RGF. Vaginal osseous metaplasia. *Arch Gynecol Obstet*. 2009;279:381–384.
5. Bataille S, Daniel L, Legris T, Vacher-Coponat H, Purgus R, Berland Y, Moal V. Osseous metaplasia in a kidney allograft. *Nephrol Dial Transplant*. 2010;25:3796–3798.
6. Wozney JM, Rosen V. Bone morphogenetic protein and bone morphogenetic protein gene family in bone formation and repair. *Clin Orthop Relat Res*. 1998;346:26–37.
7. Rifas L. T-cell cytokine induction of BMP-2 regulates human mesenchymal stromal cell

differentiation and mineralization. *J Cell Biochem*. 2006;98:706–714.
8. Medici D, Olsen BR. The role of endothelial-mesenchymal transition in heterotopic ossification. *J Bone Miner Res*. 2012;27:1619–1622.
9. Dayoub S, Devlin H, Sloan P. Evidence for the formation of metaplastic bone from pericytes in calcifying fibroblastic granuloma. *J Oral Path Med*. 2003;32:232–236.
10. Huso DL, Edie S, Levine MA, Schindinger W, Wang Y, Harald J, Germain-Lee EL. Heterotopic Ossifications in a mouse model of Albright hereditary osteodystrophy. *Plos One*. 2011:6:e21755.
11. Fernandez-Conde M, Serrano S, Alcover J, Aaron JE. Bone metaplasia of urothelial mucosa: an unusual biological phenomenon causing kidney stones. *Bone*. 1996;18:289–291.
12. Percy DH, Barthold SW. *Pathology of Laboratory Rodents and Rabbits*. 3rd ed. Ames, IA: Iowa State Press; 2007:94-95, 219.
13. Ernst H, Dungworth DL, Kamino K, Rittinghausen S, Mohr U. Nonneoplastic lesions in the lungs. In: Mohr U, Dungworth DL, Capen CC, Carlton WW, Sundberg JP, Ward JM, eds. *Pathobiology of the Aging Mouse*. Washington, DC: ILSI Press; 1996:298.

WEDNESDAY SLIDE CONFERENCE 2013-2014

Conference 24

30 April 2014

CASE I: R08-185 (JPC 3165077).

Signalment: Adult castrated male horse, (*Equus caballus*).

History: During quarantine, five horses imported from New Zealand to Taiwan exhibited depression, anorexia and dyspnea with elevated body temperature (40.2-40.5°C) on day one after arrival. They were treated with antibiotics and supportive therapy; however, one was found dead three days later.

Gross Pathology: The horse shows poor body condition with moderate dehydration. The thoracic cavity is filled with turbid, serosanguineous and fibrinous pleural effusion, with marked thickened attachments between the

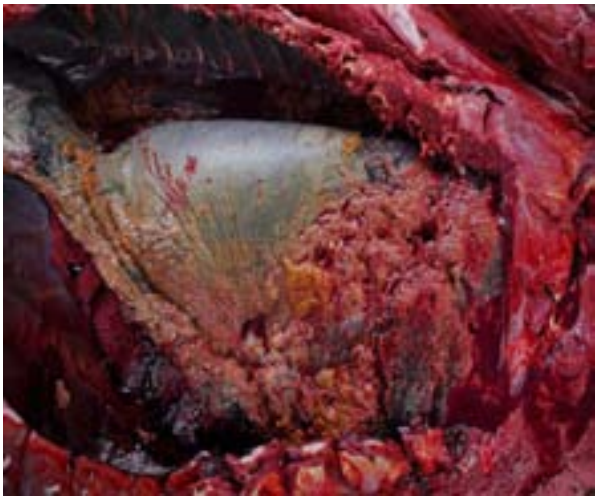

1-1. Lung, horse: Grossly, the pleural surface was covered by dense mats of fibrin and suppurative inflammation with numerous adhesions between the visceral and parietal pleura. (Photo courtesy of: Division of Animal Medicine, Animal Technology Institute Taiwan, http://www.atit.org.tw/ATIT/)

1-2. Lung, horse: The thoracic cavity is full of purulent exudate with flocculent fibrin clumps. (Photo courtesy of: Division of Animal Medicine, Animal Technology Institute Taiwan, http://www.atit.org.tw/ATIT/)

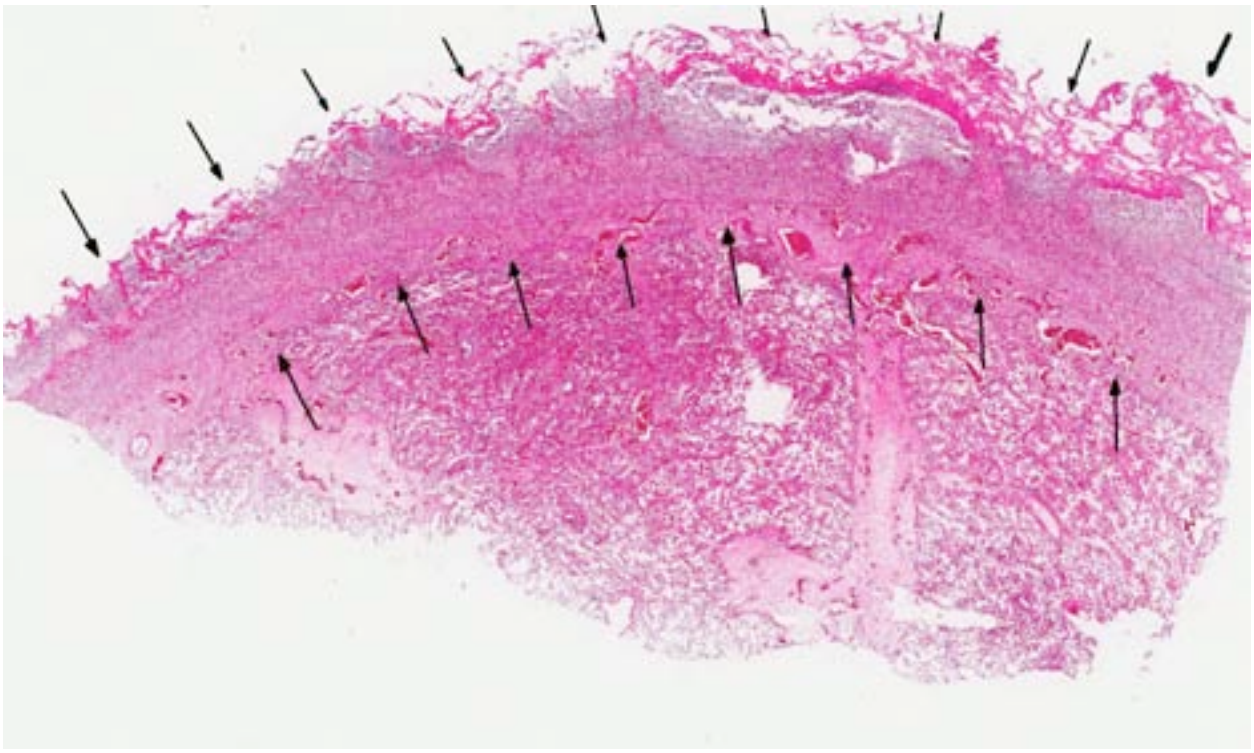

1-3. Lung, horse: The pleura is markedly expanded (arrows). (HE 0.63X)

parietal and visceral pleura. Many yellowish nodules, 0.3 to 10 cm in diameter, are scattered around the parenchyma of the lung. The tracheobronchial lymph nodes and spleen are moderately enlarged.

Laboratory Results: *Streptococcus equi* subsp. *zooepidemicus* was identified from thoracic fluid, lung and spleen.

Histopathologic Description: A dense band of degenerate neutrophils admixed with bacterial colonies and fibrinous exudates covers the visceral pleura. The subpleura contains many well-vascularized, congested vessels and organized loose fibrous connective tissue underlain by inflammatory cells. The subpleural areas are filled with viable and degenerate plasma cells, epithelioid macrophages, fewer multinuclear giant cells and lymphocytes. There is diffuse intra-alveolar and interlobular edema and congestion. Alveolar septa are congested. Some sections of lung contain large areas of abscessation (not provided). These foci contain sheets of degenerate neutrophils admixed with fewer macrophages, necrotic debris, and colonies of cocci.

Contributor's Morphologic Diagnosis:

1. Lung: Pleuritis, fibrinopurulent, diffuse, severe, subacute to chronic, with intralesional cocci colonies.
2. Lung: Abscesses, multifocal, moderate, subacute, with intralesional cocci.

Contributor's Comment: *Streptococcus equi* subsp. *zooepidemicus* is a beta-hemolytic gram-positive cocci that belongs to the Lancefield group C of streptococci and causes disease in a variety of mammals.[1,2,6] It consists of 3 subspecies, *S. equi* subsp. *equi*, *S. equi* subsp. *zooepidemicus*, and *S. equi* subsp. *ruminatorum*.

Transmission is mainly via aerosol, wound contamination, oral or contagious route.[2] Aerosol transmission is the most likely route in this case. *S. equi* subsp. *zooepidemicus* is considered to be an opportunistic pathogen in horses and alpaca; it is commonly found in the nasopharynx of clinically normal horses.[1,6] There are reports of sporadic or outbreaks in many species, including humans. *S. equi* subsp. *zooepidemicus* has been associated with mastitis,[12] abscesses, meningitis, endocarditis, reproductive system disease, orchitis, arthritis, septicemia and respiratory and uterine infections.[1,3,7] Human infections caused

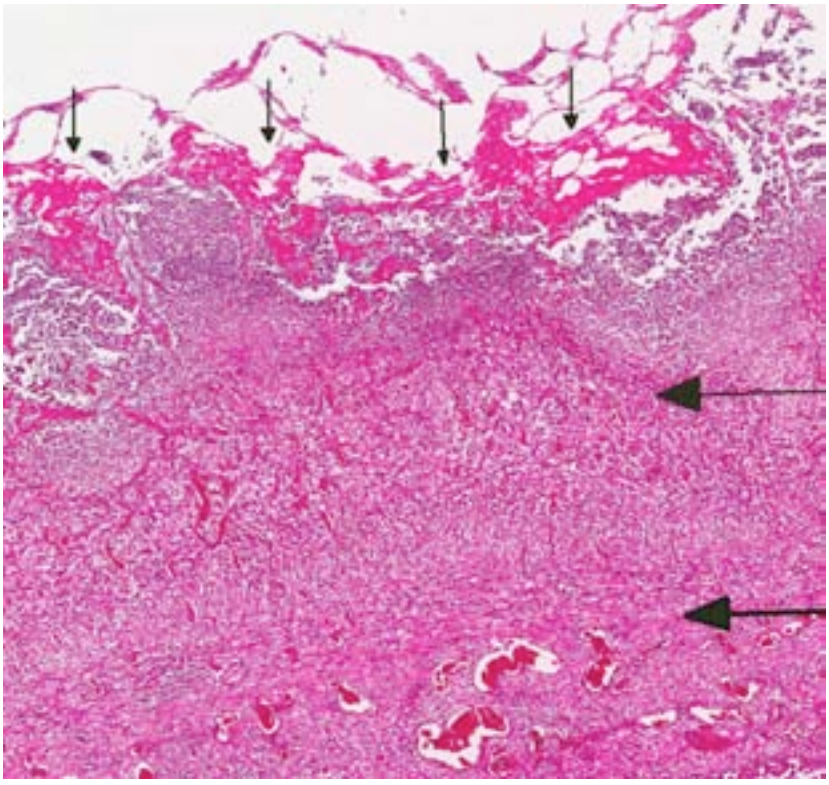

1-4. Lung, horse: Higher magnification demonstrates a thick superficial mat of fibrin and suppurative exudate (small arrows), covering a thick layer of granulation tissue (large arrows). (HE 24X)

by *S. equi* subsp. *zooepidemicus* include outbreaks of foodborne illness, meningitis, septicemia, arthritis, pneumonia, glomerulonephritis, and streptococcal toxic shock syndrome, in both immunocompromised and immunocompetent patients.[3] Severe *S. equi* subsp. *zooepidemicus* induced pleuropneumonia has been observed in horses. In Peru, infection can cause a mortality rate of 50-100% of affected alpacas (known as alpaca fever).[4,6] In China, *S. equi* subsp. *zooepidemicus* is the most commonly isolated secondary pathogen in swine since 1975. Humans may be infected via contact with sick animals, unpasteurized milk or other dairy products;[12] therefore, this bacterium poses a zoonotic health risk to animals and humans.

Since 2004, this pathogen has been isolated from three batches of horses imported (from the United States and New Zealand) to Taiwan. The source of infection in the present cases is presumably associated with transport stress. There have been no reports of *S. equi* subsp. *zooepidemicus* infection in livestock, zoo/wild animals or pets in Taiwan prior to this report.

JPC Diagnosis: Lung: Pleuritis, fibrinosuppurative, chronic, diffuse, severe, with granulation tissue, mild fibrinous interstitial pneumonia and rare colonies of cocci.

Conference Comment: Conference participants are urged to review WSC 2013-2014, conference 5, case 1 for a detailed review of various *Streptococcus* species important in veterinary medicine. *S. equi* subsp. *equi* is the causative agent of strangles, a contagious infection of the equine upper respiratory tract and local lymph nodes with occasional hematogenous dissemination to internal organs (bastard strangles). Bronchopneumonia (due to aspiration of nasopharyngeal exudate), guttural pouch empyema, laryngeal hemiplegia ("roaring" due to recurrent laryngeal nerve compression from retropharyngeal lymphadenopathy) and facial paralysis/Horner syndrome (secondary to compression of adjacent sympathetic nerves) are common sequelae to strangles. *S. equi* has also been linked with immune-mediated vasculitis and purpura hemorrhagica in horses. *S. equi*, unlike *S. equi* subs. *zooepidemicus,* is not part of the

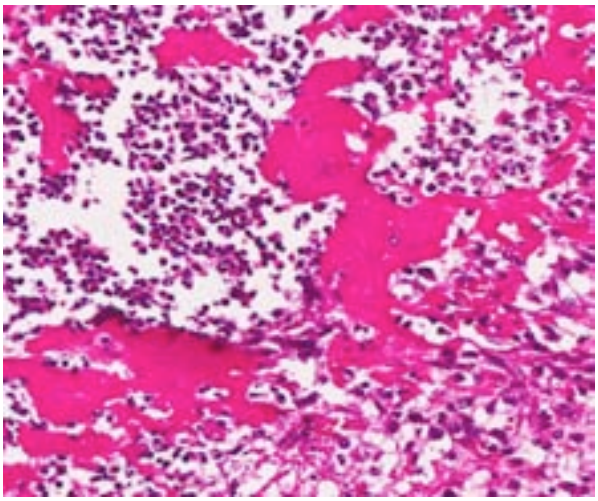

1-5. Lung, horse: Higher magnification of the most superficial layers of pleura, with dense polymerized fibrin and numerous viable and degenerate neutrophils. (HE 128X)

normal nasal flora.[8,9,13] *S. zooepidemicus* is associated with reproductive disease and bursitis (or fistulous withers) in horses,[12] as well as cervical lymphadenitis (or "lumps") in guinea pigs.[10] It was also implicated in an outbreak of acute hemorrhagic pneumonia in more than 1,000 shelter dogs in California[11] and has been associated with increased severity of clinical signs in dogs affected by the canine infectious respiratory disease complex, which likely involves challenge with both bacterial (*Bordetella bronchiseptica, Pasturella* spp., *Mycoplasma* spp., *S. zooepidemicus*) and viral (canine parainfluenzavirus and canine adenovirus) agents.[3] *S. equi* subsp. *ruminatorum* has been associated with mastitis in domestic sheep and goats, as well as abscesses (similar to strangles) with subsequent pneumonia in spotted hyenas and zebras.[5]

Contributing Institution: Division of Animal Medicine
Animal Technology Institute Taiwan
http://www.atit.org.tw/ATIT/

References:

1. Abbott Y, Khan S, Muldoon EG, Markey BK, Pinilla M, Leonard FC, et al. Zoonotic transmission of *Streptococcus equi* subsp. *zooepidemicus* from a dog to a handler. *J Med Microbiol*. 2010;59:120-123.
2. Brack M, Günther E, Gilhaus H, Salzert W, Meuthen J. An outbreak of *Streptococcus equi* subsp. *zooepidemicus* infection of probable human origin in Wanderoos (*Macaca silenus*)--case report. *Zentralbl Bakteriol*. 1997;286:441-446.
3. Chalker VJ, Brooks HW, Brownlie J. The association of *Streptococcus equi* subsp. *zooepidemicus* with canine infectious respiratory disease. *Vet Microbiol*. 2003;95:149-156.
4. Hewson J, Cebra CK. Peritonitis in a llama caused by *Streptococcus equi* subsp. *zooepidemicus*. *Can Vet J*. 2001;42:465-467.
5. Honer OP, Wachter B, Speck S, et al. Severe *Streptococcus* infection in spotted hyenas in the Ngorongoro Crater, Tanzania. *Vet Microbiol*. 2006;115:223-228.
6. Jones M, Miesner M, Grondin T. Outbreak of *Streptococcus equi* ssp. *zooepidemicus* polyserositis in an alpaca herd. *J Vet Intern Med*. 2009;23: 220-223.
7. Lamm CG, Ferguson AC, Lehenbauer TW, Love BC. Streptococcal infection in dogs: A retrospective study of 393 cases. *Vet Pathol*. 2010;47:387-95.
8. Lopez A. Respiratory system, mediastinum and pleurae. In: McGavin MD, Zachary JF, eds. *Pathologic Basis of Veterinary Disease*. 5th ed. St. Louis, MO: Mosby Elsevier; 2012:470.
9. Maxie MG, Youssef S. Nervous system. In: Maxie MG, ed. *Jubb, Kennedy, and Palmer's Pathology of Domestic Animals*. 5th ed. Vol. 1. Philadelphia, PA: Elsevier; 2007:173, 257, 358.
10. Percy DH, Barthold SW. *Pathology of Laboratory Rodents and Rabbits*. Ames, IA: Blackwell Publishing; 2007:229-232.
11. Pesavento PA, Hurley KF, Bannasch MJ, Artiushin S, Timoney JF. A clonal outbreak of acute fatal hemorrhagic pneumonia in intensively housed (shelter) dogs caused by *Streptococcus equi* subsp. *zooepidemicus*. *Vet Pathol*. 2008;45(1):51-53.
12. Pisoni G, Zadoks RN, Vimercati C, Locatelli C, Zanoni MG, Moroni P. Epidemiological investigation of *Streptococcus equi* subspecies *zooepidemicus* involved in clinical mastitis in dairy goats. *J Dairy Sci*. 2009;92:943-951.
13. Timoney, JF. The pathogenic equine streptococci. *Vet Res*. 2004;35(4):397-409.

CASE II: H13-3451 (JPC 4037901).

Signalment: 7-year-old female breed unspecified ox, (*Bos taurus*).

History: This 7-year-old cow calved 4-5 months previously, and had been at pasture since. Found dead without premonitory signs.

Gross Pathology: Carcass preservation is poor, but the animal is in good body condition. Gross lesions are confined to urinary tract, mammary gland and supramammary lymph nodes: bilateral, chronic, fibrinopurulent and severe pyelonephritis; chronic, necrosuppurative, severe cystitis; urolithiasis due to multiple sand-like calculi; and induration of the left-fore mammary gland quarter. No milk could be expressed. On cut surface, the gland parenchyma was markedly fibrosed with multifocal 2-3 mm areas of suppuration. The left supramammary lymph node was enlarged with a 1 cm diameter focus of suppuration.

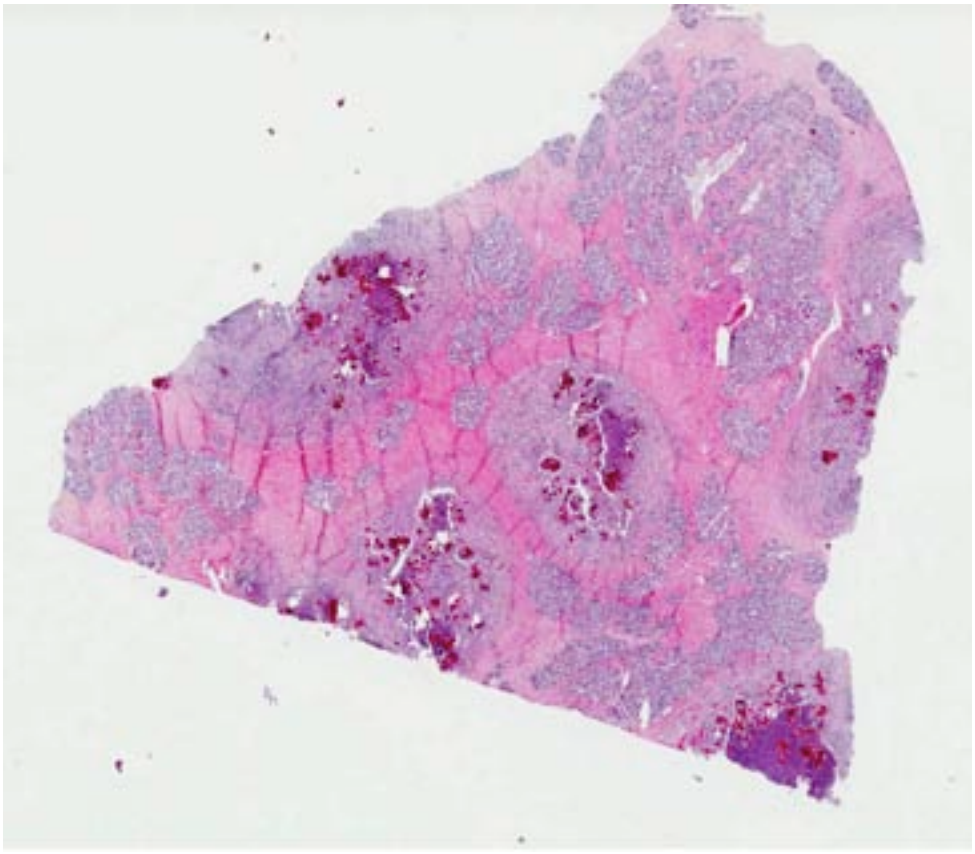

2-1. Mammary gland, ox: Glandular tissue is expanded by multiple non-confluent abscesses. (HE 0.63X)

Laboratory Results: Beta-haemolytic, coagulase-positive *Staphylococcus aureus* was isolated from the supramammary lymph node. *Corynebacterium renale* was isolated from the kidney.

Histopathologic Description: Mammary gland. Separating lobules of atrophic acini are extensive bands of mature fibrous tissue which contain multifocal to coalescing pyogranulomas up to 10 mm in diameter. Pyogranulomas are centered on colonies of gram-positive cocci (gram-stained section not submitted) within up to 100 µm long radiating columns of hyaline eosinophilic material (Splendore-Hoeppli material). These in turn are surrounded by variably sized zones of viable and degenerate neutrophils, occasionally within a large area of necrosis, bounded by large numbers of macrophages and varying numbers of multinucleated giant cells mixed with lymphocytes, plasma cells and small numbers of neutrophils, bounded by concentric bands of fibrous tissue. Mammary acini are devoid of secretory product and are lined by cuboidal to low columnar epithelium which is multifocally vacuolated or necrotic and sloughing. Multifocally there is exocytosis of low numbers of neutrophils and lymphocytes into acinar epithelium and multifocally acini contain small amounts of eosinophilic fibrillar material (fibrin) and small numbers of neutrophils and/or macrophages. Within the interstitium of the secretory tissue there is vascular congestion and a diffuse mild infiltration of lymphocytes, plasma cells and fewer macrophages and a diffuse mild fibroplasia.

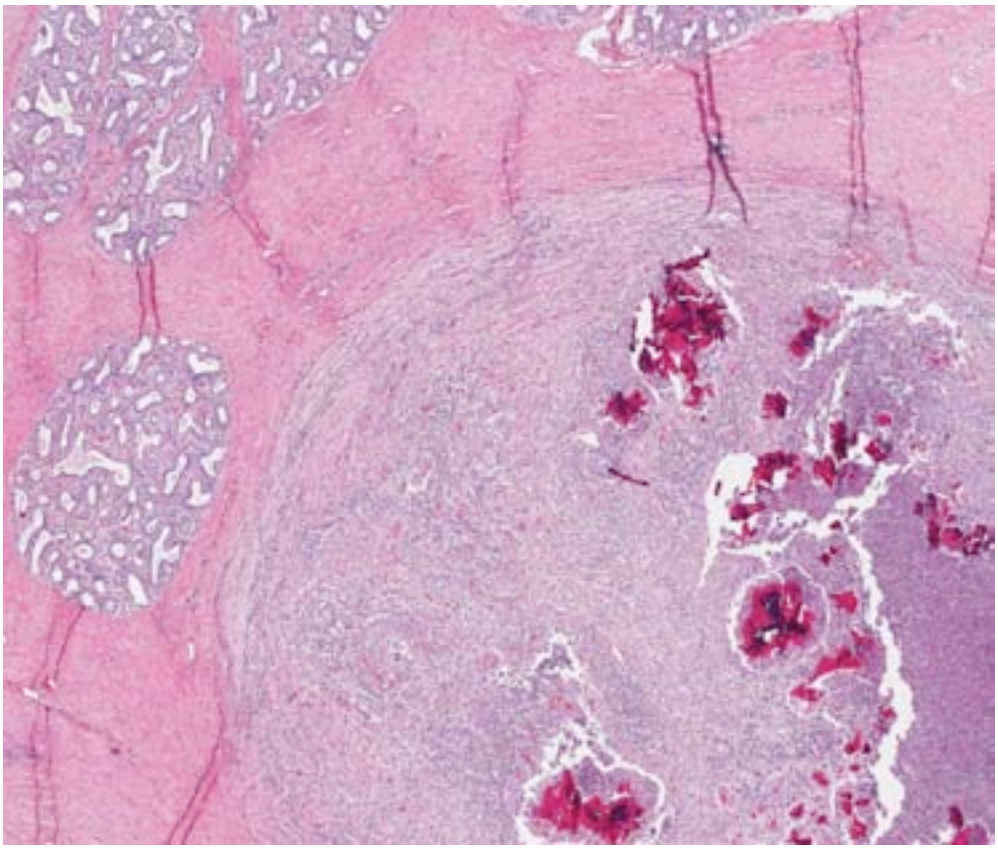

2-2. Mammary gland, ox: Higher magnification of one of the abscesses, which is centered on numerous bacterial colonies encased in brightly eosinophilic Splendore-Hoeppli material, and surrounded by a dense fibrous capsule. (HE 25X)

Contributor's Morphologic Diagnosis: Mammary gland: pyogranulomatous mastitis, chronic with intra-lesional bacteria.

Contributor's Comment: The cause of death in this case was renal failure due to pyelonephritis. The chronic mastitis was judged to be incidental with respect to the presentation of sudden, unexpected death. *Staphylococcus aureus* was isolated from the supramammary lymph node. Although culture was not performed on the mammary gland, gram positive nature of the intralesional cocci would be consistent with *Staphylococcus* spp.

S. aureus is one of the most common causes of bovine mastitis. Clinically, staphylococcal mastitis may be peracute and fulminating or milder and more chronic. The acute forms of disease generally occur shortly after parturition and tend to produce gangrene of the affected quarters with high mortality.[9] The chronic or subclinical forms are more common and thus associated with the most important economic losses. The clinical presentation may be related to the strain of *S. aureus*; strains differ in their ability to spread within herds, and to cause somatic cell count elevation, clinical mastitis, or persistent infections or loss in milk production. *In vitro*, strains differ in their ability to withstand killing by neutrophils or invade mammary epithelial cells.[1]

The main reservoirs of infection are infected quarters and lesions on the skin of the udder and teat. Once *S. aureus* contaminates the teat orifice, it can persist and multiply before entering the teat canal and sinus and disseminating within the mammary gland. Colonization of the distal part of the mammary gland may be achieved by adhesion to specific receptors on the surface of epithelial cells. The adhesion varies from very low to extremely high numbers of bacteria per cell. *In vitro* adhesion depends on multiple factors including strain and origin of mammary epithelial cells.[5] The host response to the penetration includes degeneration and necrosis of epithelial cells and exudation of neutrophils into the interlobular tissue and secretory acini. If the exudation is massive and the organisms highly toxigenic, the acute and gangrenous forms of the disease occur. *S. aureus* can also invade more deeply into the inter-acinar tissue and establish persistent foci of infection that provoke botryomycotic granulomatous reactions associated with marked fibroplasia.[9] Acinar atrophy may be due to pressure from this fibrosis and also from occlusion of small ducts by exudate or granulation tissue causing obstruction of milk flow from unaffected lobules.[9]

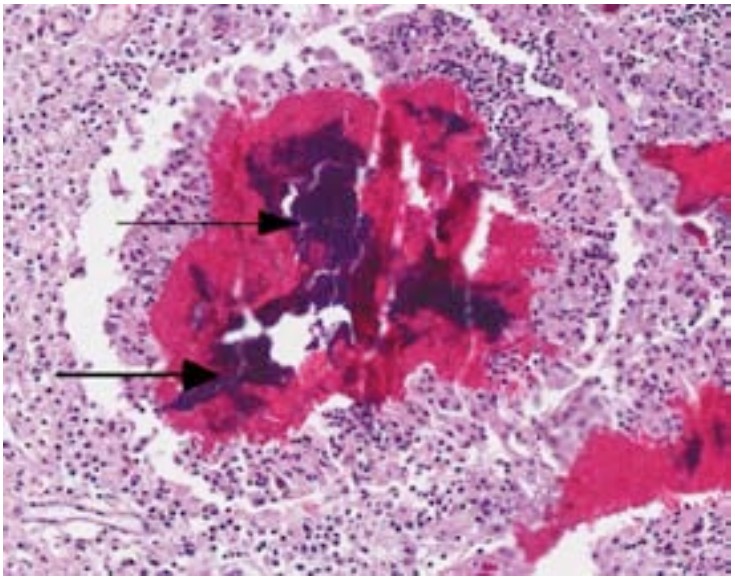

2-3. Mammary gland, ox: Dense aggregates of Splendore-Hoeppli material surround large colonies of staphylococci (arrows). (HE 225X)

JPC Diagnosis: Mammary gland: Mastitis, pyogranulomatous, multifocal, severe, with numerous cocci and Splendore-Hoeppli material.

Conference Comment: The tissue sections examined in this case are composed primarily of lobules of mammary ducts; mammary glands/ acini are largely atrophied or lost, likely due to pressure necrosis secondary to abundant inflammation. Mastitis is the single most common disease syndrome of adult dairy cows. Routes of infection vary from ascending infection of the teat canal (most common) to hematogenous or percutaneous. The most commonly bacterial isolates are *Streptococcus* spp., *Staphylococcus* spp., and gram-negative coliforms, especially *Escherichia coli* (also *Enterobacter aerogenes, Klebsiella pneumoniae, Citrobacter* spp., *Pasteurella multocida, Pseudomonas aeruginosa*, *Serratia* spp., and *Proteus* spp.). The mammary gland is the principal site of persistence or reservoir for certain bacterial species, including *Streptococcus agalactiae, Staphylococcus aureus* and *Mycoplasma bovis*, while infection with coliforms is typically acquired via teat contamination from the external environment (e.g., fecal contaminated bedding, soil or water). *Streptococcus uberis* and *S. dysagalactiae* can persist in either location. Other pathogens associated with bovine mastitis include *Trueperella pyogenes, Prototheca zopfii, Nocardia asteroides*, *Mycobacterium* spp., and less commonly, *Brucella abortus*, *Mannheimia haemolytica*, *Salmonella* spp., *Cryptococcus neoformans*, and *Candida* spp.[4,7,9]

Staphylococcus aureus is the most commonly reported etiology of mastitis. *S. aureus* isolates range from nonpathogenic to highly pathogenic; catalase and hemolysin production are the best indicators of bacterial pathogenicity.[4,9] Factors in normal milk which inhibit bacterial growth are listed in table one.[7,9] *S. aureus* has developed multiple virulence factors to overcome these defense mechanisms, which are listed in table two.[2-5,7]

Although most problematic in cattle, mastitis also affects many other domestic animal species. The major agents recovered from sheep and goats with necrotizing or gangrenous mastitis are *S. aureus* and *Mannheimia haemolytica*. For mycoplasmal mastitis, the typical causative agents are *Mycoplasma agalactiae* or *M. mycoides*. Additionally, goats and sheep infected with the small ruminant lentiviruses, caprine arthritis and encephalitis virus and maedi-visna virus, respectively, develop "hard udders" with agalactia. Equine mastitis is sporadic, and *Streptococcus zooepidemicus* is the typical cause.[4,7,9] In swine, mastitis usually occurs in lactating or recently weaned sows. Gram-negative coliforms are the most commonly isolated etiologic agents; gram-positive bacteria such as *Streptcoccus, Staphylococcus* and *Aerococcus* spp. are reported less frequently.[6] In dogs and cats mastitis is uncommon; dogs are more likely to present with mammary neoplasia, while fibroadenomatous hyperplasia (mammary hyptertrophy) is the most prevalent mammary lesion in cats. When present in dogs or cats, mastitis tends to occur in early lactation, due to *Staphylococcus* spp., *Streptococcus* spp. or *E. coli* entering lactiferous ducts via fissures in nipples.[4] *E. coli, Klebsiella pneumoniae* and *Streptococcus zooepidemicus* are commonly encountered in guinea pig mastitis, while *S. aureus* (type C) and *Pasturella multocida* tend to affect rabbits. Mastitis is also reported in rats (typically due to *Pasteurella pneumotropica, S. aureus, Corynebacterium* spp., or *Pseudomonas* spp.), and hamsters (beta-hemolytic *Streptococcus* spp., *P. pneumotropica, E. coli*).[8]

Table 1. Antibacterial factors in milk.[7,9]

Antibacterial Factor	
Phagocytic cells	Phagocytosis is less efficient in milk than in serum
Lactoferrin	Iron-binding protein that inhibits bacterial multiplication
Lysozyme	Lyses bacterial cell wall peptidoglycan
Lactoperoxidase	May inhibit *S. aureus* and streptococci
Hydrogen peroxide	A weak oxidizing agent that is a byproduct of bacterial fermentation of milk carbohydrates
Immunoglobulins	Primarily IgG, which promotes opsonization; less IgA, which may reduce bacterial adherence at epithelial surfaces

Table 2. Select virulence factors of *S. aureus*.[2-5,7]

Virulence Factor	
Leucocidin	Cytolytic to bovine leukocytes
Alpha-toxin	Binds cell membranes forming hexameric pores; not produced by all *S. aureus* isolates
Beta-toxin	A phospholipase C or sphingomyelinase
Protein A	Antiphagocytic factor that binds to the F_c fragment of IgG
Extracellular enzymes	Coagulase, hyaluronidase, phosphatase, nuclease, lipase, catalase, staphylokinase (fibrinolysin), superantigens and proteases
Bacterial capsule	Interferes with opsonization, phagocytosis, and complement activity; not present in all strains of *S. aureus*
Penicillinase	Splits beta-lactam ring of penicillin

Contributing Institution: Room 012, Veterinary Sciences Centre
School of Veterinary Medicine, University College Dublin
Belfield, Dublin 2, Ireland
http://www.ucd.ie/vetmed/

References:

1. Barkema, HW, Schukken YH, Zadoks RN. Invited review: The role of cow, pathogen, and treatment regimen in the therapeutic success of bovine *Staphylococcus aureus* mastitis. *J Dairy Sci.* 2006;89:1877-1895.

2. Biberstein EL, Hirsh DC. Staphylococci. In: Hirsh DC, Zee YC, eds. *Veterinary Microbiology*. Malden, MA: 1999:115-119.

3. DeDent AC, McAdow M, Schneewind O. Distribution of protein A on the surface of *Staphylococcus aureus*. *J Bacter*. 2007;189(12): 4473-4484.

4. Foster RA. Female reproductive system and mammary gland. In: McGavin MD, Zachary JF, eds. *Pathologic Basis of Veterinary Disease*. 5th ed. St. Louis, MO: Mosby Elsevier; 2012:198, 1121-1124.

5. Kerro Dego O, van Dijk JE, Nederbragt H. Factors involved in the early pathogenesis of bovine *Staphylococcus aureus* mastitis with emphasis on bacterial adhesion and invasion. A review. *Vet Quart.* 2002;24:181-198.

6. Martineau GP, Farmer C, Peltoniemi O. Mammary System. In: Zimmerman JJ, Karriker LA, Ramirez A, Schwartz KJ, Stevenson GW, eds. *Diseases of Swine*. 10th ed. Ames, IA: Wiley-Blackwell; 2012:282-285.

7. Morin DE. Mammary gland health and disorders. In: Smith BP, ed. *Large Animal Internal Medicine*. 4th ed. St. Louis, MO: Mosby Elsevier; 2008:1112-1143.

8. Percy DH, Barthold SW. *Pathology of Laboratory Rodents and Rabbits*. Ames, IA: Blackwell Publishing; 2007:192, 231-232, 281, 283.

9. Schlafer DH, Miller RB. Female genital system. *In:* Maxie MG, ed. *Jubb, Kennedy, and Palmer's Pathology of Domestic Animals*. 5th ed. Vol. 3. Philadelphia, PA: Saunders Elsevier; 2007:550-564.

CASE III: 12-503 (JPC 4017811).

Signalment: 15-year-old male castrated Maine Coon cat, (*Felis catus*).

History: 1-week history of lethargy and anorexia. The cat presented recumbent and minimally responsive; it went into respiratory arrest the next morning and was euthanized.

Gross Pathology: The liver and spleen contain numerous 0.5 mm white nodules. Most lymph nodes are enlarged and mottled red and white.

Laboratory Results:

Hematocrit: decreased (21)
ALT: increased
Albumin: decreased

Histopathologic Description: Lymph nodes and spleen have multifocal coalescing areas of necrosis containing macrophages and a few neutrophils. The spleen also has numerous aggregates of mast cells.

Contributor's Morphologic Diagnosis: Lymphadenitis and splenitis, necrotizing, granulomatous, multifocal, severe.

Contributor's Comment: This is a case of tularemia caused by *Francisella tularensis*. The organism was not cultured from the tissues but its presence was confirmed by PCR. *Francisella tularensis* is a potential agent of bioterrorism and is a reportable disease.

Francisella tularensis is a gram-negative bacterial rod and a facultative intracellular pathogen of macrophages. The organism is difficult to grow in artificial media and the diagnosis is best confirmed by PCR.

Francisella tularensis is the cause of the disease tularemia. Tularemia has a worldwide distribution and affects a variety of mammals, birds, amphibians and fish. The organism is maintained in the environment by various terrestrial and aquatic mammals, primarily rabbits and rodents, and is transmitted by a variety of arthropods including ticks, mites, blackflies, fleas, mosquitoes and lice.[2] The organism may also be transmitted by contact with infected vertebrates,

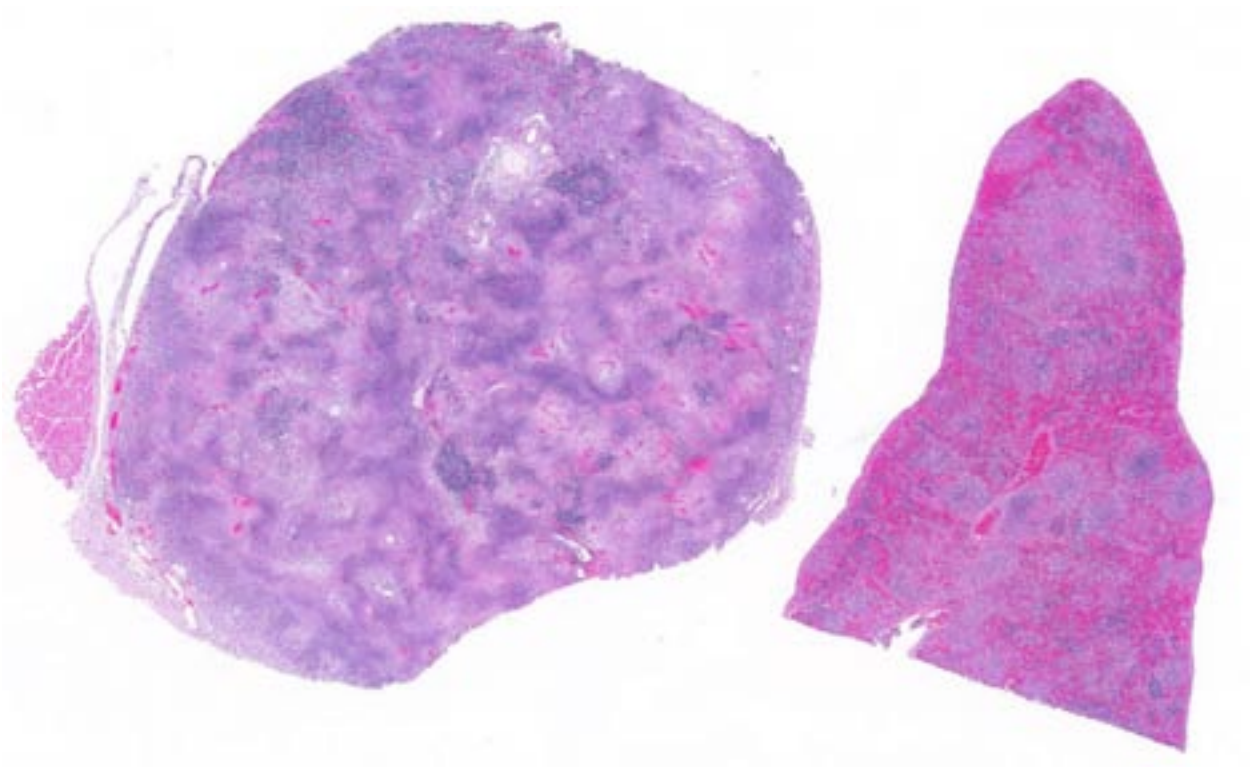

3-1. Lymph node and spleen, cat: The lymph node, and to a lesser extent, splenic architecture is effaced by confluent areas of lytic necrosis. (HE 0.63X)

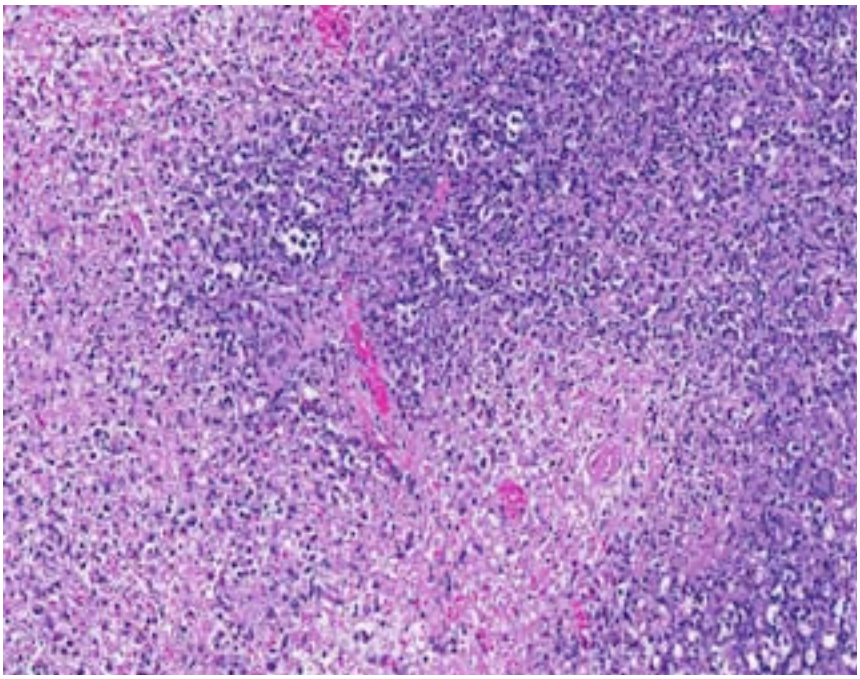

3-2. Lymph node, cat: The lymph node show almost total effacement of architecture by lytic necrosis and almost total lymphorrhexis. (HE 208X)

by inhalation of feces-contaminated dust, or ingestion of insufficiently cooked infected carcasses. Human infections usually result from skinning or dressing rabbits, and rabbits are the source of infection in 90% of human cases.[4]

Gross lesions of tularemia are multifocal white spots in liver, spleen and lymph node varying in size from pinpoint to several millimeters. Microscopic lesions are multifocal to confluent areas of necrosis with a mild influx of macrophages and neutrophils.

JPC Diagnosis: 1. Spleen: Splenitis, necrotizing, multifocal to coalescing, severe.
2. Lymph nodes: Lymphadenitis, necrotizing, multifocal to coalescing, severe.

Conference Comment: Tularemia, a zoonotic disease also known as rabbit fever or deer-fly fever, has a worldwide distribution, is currently listed as a category A select bioterrorism agent and is thus a reportable disease in the U.S.[5] Two main biovars have been described. The more virulent biotype A (*F. tularensis* subsp. *tularensis*) ferments glycerol and spreads (predominantly in North America) via ticks and hemophagous insects (mosquitoes and biting flies). The primary tick vectors described in the U.S. include the wood tick (*Dermacentor andersoni*), the American dog tick (*Dermacentor variabilis*), the Pacific coast tick (*Dermacentor occidentalis*) and the lone star tick (*Amblyomma americanum*). The less virulent biotype B (*F. tularensis* subsp. *holarctica*) does not ferment glycerol, exhibits a complex aquatic epidemiology and is more common in Eurasia, where infection usually occurs due to ingestion of infected prey or water contaminated by rodents. Type A strains are typically responsible for clinical disease in rabbits, cats and humans.[1,3] *F. tularensis* has an extensive host range, and infections in more than 200 animal species (primarily mammals, but also birds, fish, amphibians, and reptiles) have been reported. Infection rates appear to demonstrate seasonal variability; cases are reported most frequently from May to August, likely due to the activity of arthropod vectors.[5]

F. tularensis can pass transovarially within tick vectors, which are infected for life.[3] Additionally, the bacterium can survive for weeks to months in water, soil, and decaying animal carcasses.[5] Bacteria are typically inoculated into the host during tick feeding/defecation or following

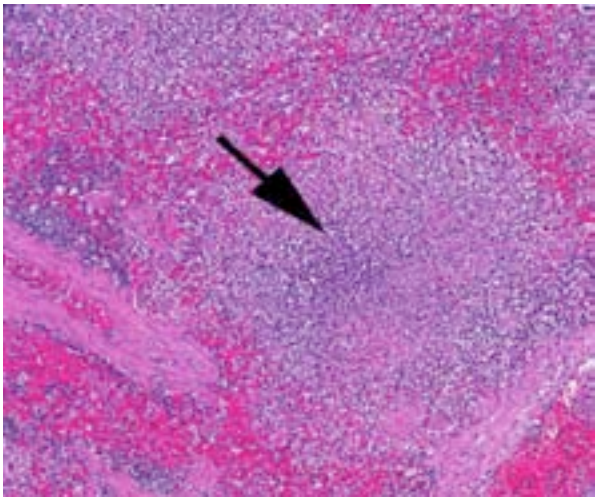

3-3. Spleen, cat: Multifocal areas of lytic necrosis are present throughout the section of spleen, primarily affecting white pulp. (HE 125X)

ingestion of infected rabbits or rodents. Dogs appear to be fairly resistant while cats and rabbits are susceptible. The infectious dose can be quite low; inhalation or parenteral inoculation of 10 to 50 colony-forming units can induce clinical disease, while 10^8 colony-forming units are required for oral infection. *F. tularensis* persists within macrophages where it inhibits phagosome-lysosome fusion; the bacterial capsule is thought to be important in intracellular survival.[1,3] Necrosis generally centers upon lymphoid tissue within the spleen and lymph nodes, although lesions within the liver and lungs (especially if bacteria are inhaled) are also commonly described.[3,5] The gross lesions associated with *F. tularensis* (foci of splenic, lymph node and hepatic necrosis and/or pyogranulomatous inflammation) are indistinguishable from lesions associated with yersiniosis. Histologically, *Yersinia* spp. often form large colonies, while *F. tularensis* coccobacilli are typically found within macrophages,[6] although individual bacterial were not readily apparent in this case.

Contributing Institution: College of Veterinary Medicine
Virginia Tech
Blacksburg, VA 24061
www.vetmed.vt.edu

References:

1. Biberstein EL, Hirsh DC. *Francisella tularensis*. In: Hirsh DC, Zee YC, eds. *Veterinary Microbiology*. Malden, MA: 1999:285-286.
2. Ellis J, Oyston CF, Green M, Titball RW. Tularemia. *Clinical Microbiology Reviews*. 2002;15:631-646.
3. Greene CE. *Francisella* and *Coxiella* infections. In: Greene CE, ed. *Infectious Diseases of the Dog and Cat*. 4th ed. St. Louis, MO: Elsevier Saunders; 2012:476-482.
4. Lamps LW, Havens JM, Anders S, Page DL, Scott MA. Histologic and molecular diagnosis of tularemia: a potential bioterrorism agent endemic to North America. *Modern Pathology*. 2004;17:489-495.
5. Spagnoli ST, Kuroki K, Schommer SK, Reilly TJ, Fales WH. Pathology in practice. *Francisella tularensis*. *J Am Vet Med Assoc*. 2011;238(10): 1271-1273.
6. Valli VEO. Hematopoietic system. In: Maxie MG, ed. *Jubb, Kennedy, and Palmer's Pathology of Domestic Animals*. Vol 3. 5th ed. Philadelphia, PA: Saunders Elsevier; 2007:297-299.

CASE IV: O20/09 (JPC 3167509).

Signalment: 5-year-old female Swedish riding pony, (*Equus caballus*).

History: The horse was euthanized, and presented for necropsy after traumatic injury to the left hock, with suspected septic bursitis of the left calcaneal bursa and possible bone involvement.

Gross Pathology: There is diffuse thickening of the dermis and focal ulceration (approximately 2x2 cm) on the dorsal aspect of the left hock, exposing dry granulation tissue. The calcaneal bursa contains fibrinopurulent and hemorrhagic material and there is hypertrophy and ecchymotic hemorrhages of the synovial membrane.

Within the cranial mesenteric artery, there is a focal area with thickening of the arterial wall and vegetative thrombotic masses attached to the vascular intima with presence of several slender nematode parasites, less than 20 mm in length.

Histopathologic Description: Large muscular artery and surrounding soft tissues: There is a marked inflammatory reaction involving tunica intima, media, and adventitia with multifocal to coalescing infiltrates of a mixed population of inflammatory cells, which in all arterial layers consist of large numbers of plasma cells and lymphocytes, and moderate to large numbers of eosinophils and histiocytes. There is extensive multifocal to coalescing necrosis, predominantly involving the tunica media and intima. Continuous with and disrupting/destructing the endothelial lining of the tunica intima, are extensive depositions of deeply eosinophilic homogenous to finely granular fibrinous masses (thrombi) containing moderate amounts of cellular debris, multifocal accumulations of erythrocytes, neutrophils, and multifocal sheets of large numbers of lymphocytes, plasma cells, and moderate numbers of eosinophils (with focal areas of mineralization present in some sections). The tunica intima also shows thickening, fibrosis and multifocal small hemorrhages.
On the luminal side of the intima and partially embedded within the thrombotic masses, are

4-1. Mesenteric artery, horse: The lumen of this opened section of artery is compromised by the presence of a large adherent thrombus. (HE 0.63X)

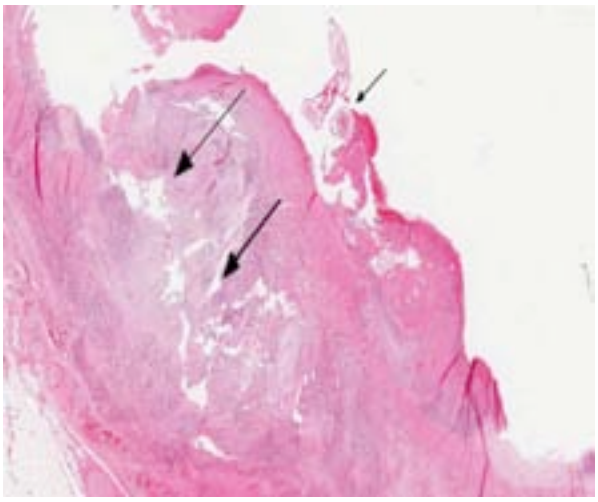

4-2. Mesenteric artery, horse: Cross sections of adult nematodes (small arrows) are present at the luminal surface of the fragmented and inflamed thrombus (large arrows). (HE 90X)

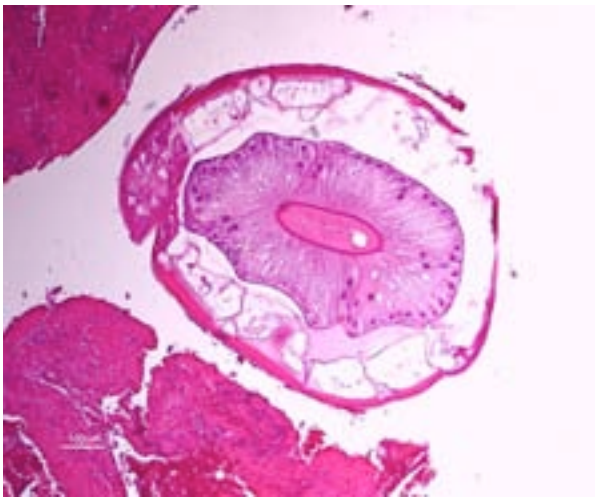

4-3. Mesenteric artery, horse: A cross-section through the adult strongyle demonstrates a smooth eosinophilic cuticle, prominent coelomyarian-polymyarian musculature, one visible lateral chord and an intestine lined by multinucleated cells with a prominent brush border. (HE 150X) (Photo courtesy of: Department of BVF, Division of Pathology, Pharmacology & Toxicology, SLU (Swedish University of Agricultural Sciences), Box 7028, SE-750 07 Uppsala, Sweden http://www.bvf.slu.se/)

several metazoan parasites (measuring approximately between 0.6 and 1.2 mm), covered by a smooth cuticle, and showing a thin hypodermis, platymyarian musculature, and a large intestine with few multinucleated cells and a prominent brush border (strongyle larvae).

In the tunica media, the heavy infiltration of inflammatory cells and areas of necrosis disrupt myocyte alignment and the borders between the tunica media and adventitia and intima. In the tunica adventitia and surrounding soft tissue, the inflammatory infiltrates are predominantly perivascular and lymphoplasmacytic, and there is hyperemia of venules. Moderate to large numbers of slender rod-shaped bacteria are also seen (post-mortem bacterial growth).

Contributor's Morphologic Diagnosis: Cranial mesenteric artery: Arteritis, lymphoplasmacytic and eosinophilic, chronic, transmural, severe, with multifocal necrosis, thrombosis and intra-luminal/-lesional strongyle larvae.

Contributor's Comment: The location and nematode morphology suggest that the presented case represents verminous arteritis caused by *Strongylus vulgaris*. No parasites were observed in the large intestine, which may have related to the necropsy being performed during winter when intestinal numbers of *S. vulgaris* are low.[2]

Strongyle nematodes are important gastrointestinal parasites of the horse. Strongyles have a worldwide distribution, and in a recent Italian study, large strongyles (*Strongylinea*) were the most abundant and most prevalent (34%) equine large intestinal parasites.[10] The three common genera of migratory large strongyles that affect horses (*Strongylus edentatus, S. equinus,* and *S. vulgaris)* live as adults in the large intestine of the horse, but have differing migratory larval routes.[11] The adults are found in the colon and cecum, and produce eggs that are passed via the feces and that develop to infective third-stage larvae (L3) outside the host.[11] Ingested L3 of *S. vulgaris* exsheath in the small intestine, penetrate the intestinal mucosa of the small intestine, colon and cecum, and moult in the submucosa to L4.[7,11] Fourth-stage *S. vulgaris* larvae then enter small intestinal arteries and migrate to the cranial mesenteric artery and its main branches, which are predilection sites for lesions caused by the larval stages.[7,11] A marked seasonality in proportions of affected arteries and arterial worm burdens have been reported, with the highest numbers encountered during winter.[9] After further development of L4 in the mesenteric circulation, L5 larvae return via the vasculature to the intestine, where nodule formation arise around larvae trapped in the smaller vessels of the intestinal wall, before young adult nematodes are released into the intestinal lumen.[11] The prepatent period for *S. vulgaris* is 6-7 months.[11]

Histopathologic arterial wall changes from necropsies most often reveal chronic (fibrosis of intima and/or media, with or without mild accumulation of mononuclear inflammatory cells) or chronic active (neutrophils, eosinophils and necrotic foci are also present) arteritis.[8] Severity of inflammatory changes have been shown to be directly related to presence of larvae, which may be entrapped in intimal thrombi, the intima itself, and less commonly in the media or adventitia.[8] Verminous arteritis can be found in necropsies of horses with no history of colic,[7,12] such as in the presented case. However, thromboembolism in the branches of the cranial mesenteric and the ileocaecocolic arteries and ischemia or infarction, interference of gut innervation related to pressure on abdominal autonomic plexuses, and release of toxic products from dying larvae have all been discussed as causes of clinical disease.[7,12]

Pathogenic effects in the large intestine relate to adult worms feeding on mucosal material and incidental damage to blood vessel, but also to disruption of the mucosa associated with the emergence of young adults.[11] Infestation may lead to poor condition and performance, anemia, temporary lameness, intestinal stasis, colic, and rarely intestinal rupture and death.[11]

JPC Diagnosis: Mesenteric artery: Arteritis, proliferative, eosinophilic and granulomatous, transmural, diffuse, severe, with thrombosis and multiple strongyle larvae.

Conference Comment: Nematodes of the subfamily *Strongylinae* (family *Strongylidae*) are "plug feeders" or "blood suckers" commonly found in the cecum and colon of horses and tend to undergo extensive extraintestinal migration.[1] As noted by the contributor, the three major genera of the *Strongylinae* subfamily are *S. vulgaris, S. edentatus* and *S. equinus*. Conference participants briefly discussed the microscopic characteristics associated with the larvae of large strongyles (also known as true strongyles), including platymyarian-meromyarian musculature, prominent lateral cords, a pseudocoelom, and a large, central intestine lined by few multinucleated cells with a prominent brush border.[4] *S. vulgaris* larvae preferentially migrate up the cranial mesenteric artery, leading to arteritis, thrombosis and, occasionally, segmental colonic necrosis. Aberrant migration into the aorta, renal and coronary arteries is also described.[1,7] Upon ingestion, infective third stage larvae of *S. edentatus* penetrate the intestinal wall, enter the liver via the portal vein, molt to L4, and migrate through the hepatic parenchyma, causing eosinophilic, neutrophilic and mononuclear inflammation and hemorrhagic/necrotic tracts. Resultant tags of fibrous scar tissue on the hepatic capsule can often be detected as incidental findings on gross necropsy. After leaving the liver via the hepatorenal ligament, larvae travel to the retroperitoneal tissue of the flank. Here they molt to L5 prior to returning to the cecum/colon, where they form nodules and hemorrhagic plaques within the gut wall (one possible cause of hemomelasma ilei) and eventually penetrate the lumen and lay eggs.[1] Aberrant migration of *S. edentatus* is also occasionally reported as a cause of orchitis in young stallions.[3] *S. equinus* is less prevalent then either *S. vulgaris* or *S. edentatus* and infection is generally clinically insignificant. Exsheathed third stage larvae penetrate into the deep layers of the ileum, cecum and colon, where they produce subserosal nodules. Fourth stage larvae migrate throughout the liver, pancreas and peritoneum, molt to L5, and ultimately return to the cecum/colon, causing mild eosinophilic inflammation.[1]

In contrast to true strongyles, members of the subfamily *Cyathostominae* feed on intestinal contents and are essentially non-pathogenic as adults, although emergence of histotropic larval stages from the intestinal wall may cause disease. Cyathostomes, also known as small strongyles, can number in the hundreds of thousands in the equine large intestine. Larvae burrow into the submucosa to develop, where they may undergo hypobiosis; emergence of large numbers can cause rupture of the muscularis mucosae with severe inflammation and edema. Clinically, affected horses present with diarrhea, ill-thrift and hypoalbuminemia, while grossly the colonic mucosa may exhibit numerous umbilicated red-black nodules containing encysted larval nematodes.[1] Much like *S. vulgaris*, the clinical syndrome (larval cyathostomiasis) associated with these infections is typically seasonal in onset, occurring most commonly in younger animals in late winter or early spring.[2] The moderator also pointed out that these small strongyles often exhibit variable degrees of ivermectin and moxidectin resistance, which can confound attempts at control/treatment.[5,6]

Contributing Institution: SLU (Swedish University of Agricultural Sciences)
Department of BVF, Division of Pathology, Pharmacology & Toxicology
Box 7028, SE-750 07 Uppsala, Sweden
http://www.bvf.slu.se/

References:

1. Brown CC, Baker DC, Barker IK. Alimentary system. In: Maxie MG, ed. *Jubb, Kennedy, and Palmer's Pathology of Domestic Animals*. Vol 2. 5th ed. Philadelphia, PA: Saunders Elsevier; 2007:247-249.
2. Chapman MR, French DD, Klei TR. Prevalence of strongyle nematodes in naturally infected ponies of different ages and during different seasons of the year in Louisiana. *J Parasitol*. 2003;89:309-314.
3. Foster RA, Ladds PW. Male genital system. In: Maxie MG, ed. *Jubb, Kennedy, and Palmer's Pathology of Domestic Animals*. Vol 3. 5th ed. Philadelphia, PA: Saunders Elsevier; 2007:587.
4. Gardiner CH, Poynton SL. Strongyles. In: *An Atlas of Metazoan Parasites in Animal Tissues.* Washington, DC: Armed Forces Institute of Pathology; 2006:22-24.
5. Lyons ET, Tolliver SC, Ionita M, Lewellen A, Collins SS. Field studies indicating reduced activity of ivermectin on small strongyles in horses on a farm in cenral Kentucky. *Parasitol Res*. 2008;103(1):209-215.
6. Lyons ET, Tolliver SC, Kuzmina TA, Collins SS. Critical tests evaluating efficacy of moxidectin against small strongyles in horses from a herd for which reduced activity had been found in field tests in Kentucky. *Parsitol Res*. 2010;107(6):1495-1498.
7. Maxie MG, Robinson WF. Cardiovascular system. In: Maxie MG, ed. *Jubb, Kennedy, and Palmer's Pathology of Domestic Animals*. Vol 3. 5th ed. Philadelphia, PA: Saunders Elsevier; 2007:89-91.
8. Morgan SJ, Stromberg PC, Storts RW, Sowa BA, Lay JC. Histology and morphometry of *Strongylus vulgaris*-mediated equine mesenteric arteritis. *J Comp Pathol*. 1991;104:89-99.
9. Ogbourne CP. Studies on the epidemiology of *Strongylus vulgaris* infection of the horse. *Int J Parasitol*. 1975;5:423-426.
10. Stancampiano L, Gras LM, Poglayen G. Spatial niche competition among helminth parasites in horse's large intestine. *Vet Parasitol*. 2010;170:88-95.
11. Taylor MA, Coop RL, Wall RL. Parasites of horses. Endoparasites: Parasites of the digestive system. In: *Veterinary Pathology*. Oxford, UK: Blackwell Publishing Ltd; 2007: 280-284.
12. White NA. Thromboembolic colic in horses. *Compendium on Continuing Education*. 1985;7:S156-S163.

Joint Pathology Center
Veterinary Pathology Services

WEDNESDAY SLIDE CONFERENCE 2013-2014

Conference 25

7 May 2014

CASE I: 3121206023 (JPC 4035610).

Signalment: 5-week-old mixed breed piglet, (*Sus domesticus*).

History: Two piglets from the faculty farm were found dead, and another piglet was weak and ataxic and, therefore, euthanized.

Gross Pathology: The submitted piglet was in good body condition. It was icteric and had a diffusely pale liver. Additionally, petechial hemorrhages were found on the kidneys, and some fibrin was present covering the abdominal organs.

Laboratory Results: The intestine was PCR positive for porcine circovirus (>9170000).

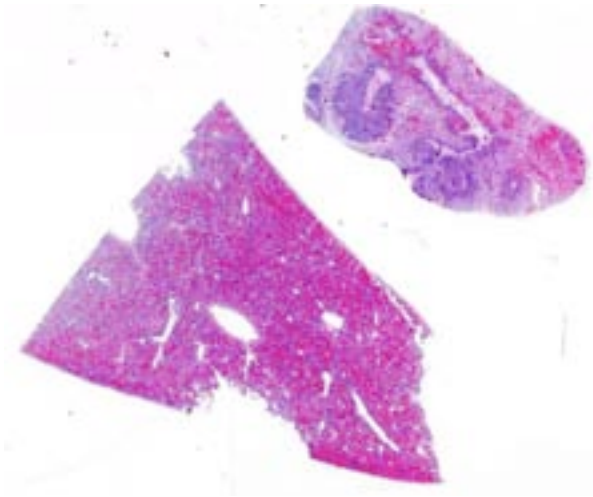

1-1. Liver and lymph node, piglet: At subgross inspection, both the liver and lymph node are diffusely hypocellular. (HE 0.63X)

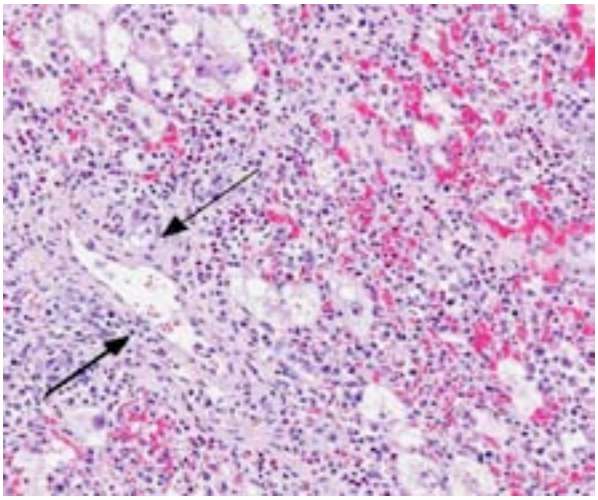

1-2. Liver, piglet: There is diffuse massive hepatocellular necrosis and stromal collapse (portal areas at right). A few massively swollen degenerating hepatocytes remain, and sinusoids. There is multifocal hemorrhage and extramedullary hematopoiesis. (HE 120X)

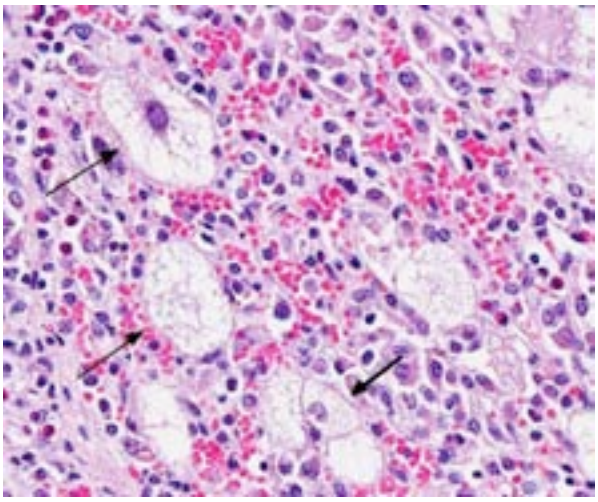

1-3. Liver, piglet: Remaining hepatocytes are degenerate as evidenced by accumulation of large numbers of discrete fat vacuoles within their cytoplasm. (HE 240X)

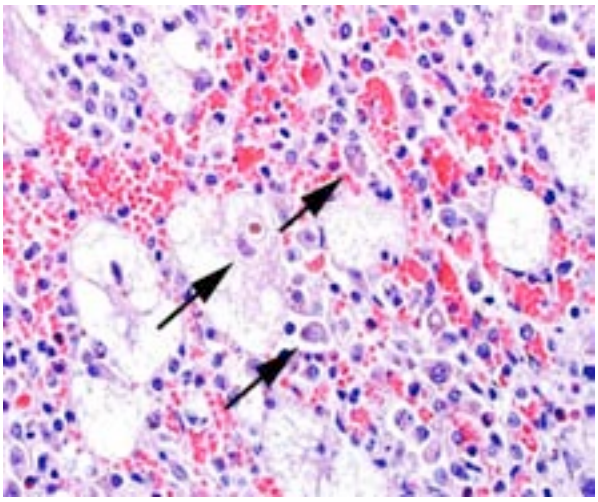

1-4. Liver, piglet: Rare hepatocytes contain intracytoplasmic botryoid viral inclusions. (HE 400X)

Histopathologic Description: Mesenteric lymph node: Diffusely, there is severe lymphoid depletion with scattered karyorrhectic debris (necrosis). Also scattered throughout the section are large numbers of macrophages and eosinophils. The macrophages often contain botryoid basophilic glassy intracytoplasmic inclusion bodies. In fewer macrophages, intranuclear basophilic inclusions can be found.

Liver: There is massive loss of hepatocytes, leaving disrupted liver lobules and dilated sinusoids engorged with erythrocytes. The remaining hepatocytes show severe swelling, with micro- and macrovesiculation of the cytoplasm and karyomegaly. Some swollen hepatocytes have basophilic intranuclear, irregular inclusions (degeneration). Throughout all parts of the liver there are scattered moderate to large numbers of macrophages (without inclusions). Within portal areas there is multifocally mild to moderate fibrosis and bile duct hyperplasia. Some bile duct epithelial cells show degeneration and necrosis, and there is infiltration of neutrophils within the lumen. The limiting plate is often obscured mainly by infiltrating macrophages and eosinophils, and fewer neutrophils, extending into the adjacent parenchyma. Scattered are small areas with extra medullary hematopoiesis.

Contributor's Morphologic Diagnosis: 1. Mesenteric lymph node: Severe lymphoid depletion with moderate diffuse chronic granulomatous lymphadenitis, with intralesional botryoid basophilic intracytoplasmic and intranuclear inclusion bodies.
2. Liver: Severe hepatic degeneration and hepatocellular loss with severe diffuse chronic granulomatous hepatitis and mild neutrophilic cholangitis.

Contributor's Comment: Porcine circovirus type 2 (PCV-2) was first isolated from pigs with postweaning multisystemic wasting disease (PWMD) in 1997. Subsequent retrospective investigations traced PCV-2 DNA antigen back to 1962, and it is likely that this virus has been present in the swine population for much longer. Besides PWMD, PCV-2 has been associated with enteric disease, respiratory disease, porcine dermatitis and nephropathy syndrome and reproductive failure. Vaccination since 2006 has proved effective in preventing PCV2–associated disease, and the prevalence of disease has been reduced. Many detection methods such as immunohistochemistry are no longer used or have been replaced by molecular methods, making the recognition of lesions even more important.

As suggested by the different syndromes associated with PCV-2 infection, clinical signs can be variable. The typical clinical picture includes enlarged lymph nodes, decreased weight gain or wasting, combined with dyspnea, diarrhea, pallor or jaundice. Other signs that have been described include coughing, fever, central nervous system signs, and sudden death.[7]

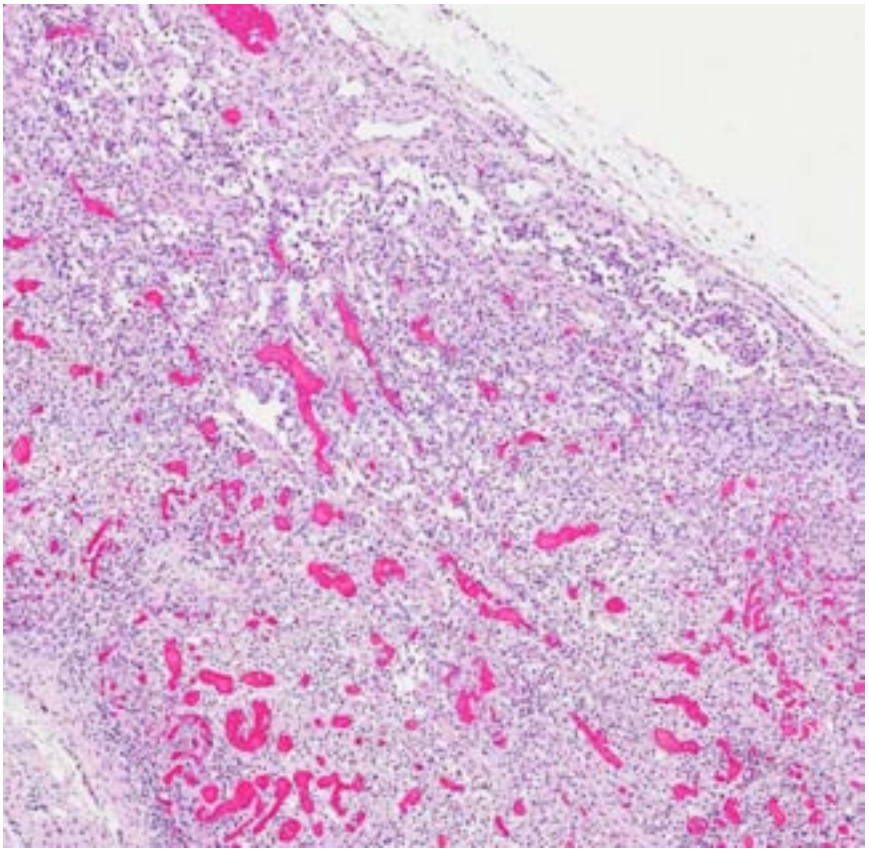

1-5. Lymph node, piglet: There is marked lymphocyte depletion within the cortex. (HE 128X)

In the case presented here, the liver lesions were the most striking feature. Although not as widely known as the respiratory, intestinal and cardiovascular lesions,[2] several reports have described lesions similar to those seen in this case. In a field study investigating 100 livers from pigs with clinical PCV2-associated disease, in 70% of the livers, the virus was associated with hepatocytes, Kupffer cells, and inflammatory infiltrates.[9] Hepatic lesions were reproduced experimentally in cesarean-derived colostrum-deprived and gnotobiotic pigs that were infected with PCV-2. Both moderate-to-severe necrotizing and granulomatous hepatitis, acute hepatitis with centrilobular necrosis of hepatocytes, and hepatic atrophy associated with nonsuppurative cholangiohepatitis were observed. In fetuses, the hepatic lesions were described as congestion with hepatocellular loss and nonsuppurative hepatitis with periacinar necrosis.[1,7]

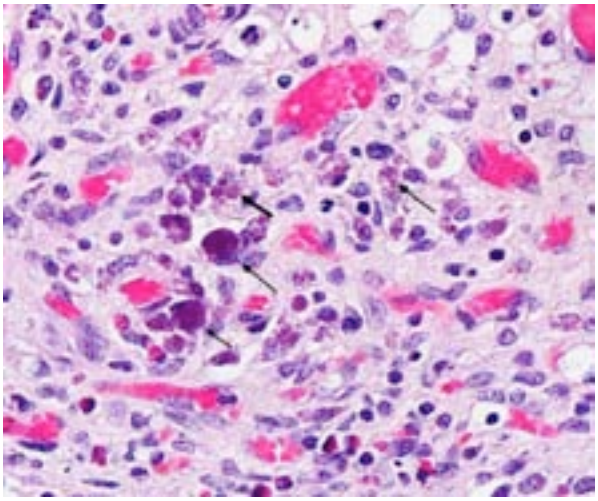

1-6. Lymph node, piglet: Multifocally, clusters of macrophages contain intracytoplasmic basophilic botryoid viral inclusions. (HE 400X)

The current case is a representation of the previously described end-stage hepatic disease[1] with extensive swelling and vacuolation of remaining hepatocytes with karyomegaly and progressive replacement of hepatocytes by histiocytic cells. Although immunohistochemistry was not available for this case, PCV-2 antigen is detectable early on in the disease process within the nuclei of hepatocytes and, as the disease progresses, within the cytoplasm of Kupffer cells and infiltrating mononuclear phagocytes.

The lymph node submitted together with the liver sample is a classical histologic presentation of the lymphadenopathy seen in the disease caused by PCV-2: severe depletion of lymphocytes and histiocytic infiltration of lymphoid tissues. It is thought that PCV-2 virus replicates within the histiocytes of lymph nodes. A study regarding the subcellular localization of PCV-2 virus found that in affected lymph nodes, viral particles were exclusively found in histiocytes. The ultrastructural changes found associated with the presence of viral particles were dilatation of the rough endoplasmic reticulum and swelling of mitochondria. With colocalization studies, a close relationship was found between the viral particles

and the mitochondria, suggesting that these organelles play a role in replication of the virus.[8]

JPC Diagnosis: 1. Liver: Hepatitis, granulomatous and eosinophilic, diffuse, severe, with portal fibrosis, biliary ductal reaction, hepatocyte karyo/cytomegaly, vacuolar degeneration, chronic-active cholangitis, and rare intracytoplasmic viral inclusion bodies.
2. Lymph node: Lymphadenitis, granulomatous and eosinophilic, diffuse, chronic, severe, with lymphoid depletion and intrahistiocytic intracytoplasmic botryoid viral inclusion bodies.

Conference Comment: Circovirus is a small, non-enveloped DNA virus with a single-stranded circular genome. In addition to porcine circovirus (PCV), members of this genus include psittacine beak and feather disease virus, columbid circovirus, goose circovirus, canary circovirus, and duck circovirus.[6] Two genotypes of PCV have been identified in swine. PCV type 1 (PCV1) does not typically induce disease in pigs, while PCV type 2 (PCV2) is virulent for pigs. Infection produces a wide array of clinical manifestations, including lymphoid depletion and, less commonly, hepatic lesions, as demonstrated in this case. Examples of disease syndromes attributed (at least in part) to PCV2 include post-weaning multisystemic wasting syndrome (PMWS, now known as PCV2-associated diseases or PCVAD), porcine respiratory disease complex (PRDC), porcine dermatopathy and nephropathy syndrome (PDNS), exudative epidermitis, and reproductive failure.[1,7,10]

PCVAD (formerly PMWS) involves multiple organ systems with a highly variable spectrum of gross lesions, the most common of which are emaciation, lymphadenopathy and mild interstitial pneumonia. Activation of the immune system followed by circovirus infection is required for the development of PMWS. Severely affected pigs may develop immunosuppression, which increases susceptibility to opportunistic infections and may result in a poor immune response to vaccines. Reported clinical signs include wasting, dyspnea, coughing, diarrhea, pallor, fever, central nervous signs, and sudden death. Although its name implies that clinical disease develops exclusively in recently-weaned pigs, PMWS can also affect mature pigs.[4,7,10]

PRDC is a multifactorial condition involving several coexisting etiologic agents, especially swine influenza, porcine respiratory and reproductive syndrome (PRRS) virus, PCV2, and porcine respiratory coronavirus. In addition to causing direct damage to the airway and lungs, these viruses predispose swine to secondary infection with pathogens such as *Mycoplasma hyopneumoniae*, *Pneumocystis carinii, Pasteurella multocida, Streptococcus suis, Bordetella bronchiseptica* and *Haemophilus parasuis*.[4] Typically, affected pigs are around 12 to 24 weeks of age and present with fever and varying degrees of sneezing, coughing, nasal discharge, and respiratory distress as well as reduced weight gain.[2,4,7]

PDNS is characterized by a systemic necrotizing vasculitis with tropism for kidney and skin, likely secondary to immune complex deposition. Although the development of PDNS has been attributed to PCV2, this condition has also been reproduced with pathogens other than PCV2, including PRRSV, Torque teno virus (arterivirus), *Staphylococcus hyicus*, *Pasteurella multocida* and *Streptococcus suis*. Grossly, affected swine exhibit irregular red to purple, often crusted papules over hindquarters, perineal area, and ears, in combination with bilaterally enlarged, pale kidneys with petechial hemorrhages.[3,5,7] PCV2 is not a primary cause of skin lesions but, in addition to the vasculitis and necrotizing skin lesions described in connection with PDNS, the virus has been demonstrated in combination with *Staphylococcus hyicus* in several cases of severe exudative epidermitis.[7]

Reproductive failure due to PCV2 is characterized by stillbirths, mummification, embryonic death, and infertility (SMEDI). Reproductive failure is probably the least important manifestation of PCV2, as it is usually only seen in individual dams and is thus not of great economic importance.[7]

Regardless of the tissue or organ affected, PCV2 tends to produce similar histological lesions. Specifically, intracytoplasmic botryoid viral inclusions, granulomatous inflammation and necrotizing vasculitis are common microscopic findings associated with PCV2. Interestingly, there are typically no PCV2-induced microscopic lesions in the musculoskeletal, endocrine and

reproductive (although as noted above, sporadic abortions are reported) systems.[2,4,7]

Although the specific mechanisms of PCV2 infection are not completely understood, recent studies have clarified several aspects of its pathogenesis. Viral antigen and/or nucleic acid may be found in multiple cell types; however, histiocytes are the main site of virus localization. Viral attachment to host cell surface receptors is mediated by heparan sulfate and chondroitin sulfate B on the viral surface.[6] Subsequently, histiocytic internalization of PCV2 occurs via clathrin-mediated endocytosis. Recent studies suggest that PCV2 replication also occurs within lymph node histiocytes and that the mitochondria likely play an important role.[8] Once internalized, PCV2 can transiently induce the PI3K/Akt pathway which inhibits apoptosis, thus promoting cell survival and viral replication. PI3K activates its downstream effector, the serine/threonine kinase Akt (also known as PKB), which phosphorylates various substrates, such as caspase-9, BAD, glycogen synthase kinase 3, and FKHR. Overall, this series of reactions leads to induction of NF-κβ and, ultimately, cell survival and growth, as well as the prevention of apoptosis via activation of antiapoptotic factors and inactivation of proapoptotic factors. Akt also results in activation of mTORC1 (which controls cell growth) and mTORC2 (which regulates the actin cytoskeleton), as well as JNK and p38 (which are involved in PCV2-induced apoptosis).[10]

Contributing Institution: Utrecht University
Faculty of Veterinary Medicine, Department of Pathobiology
Yalelaan 1, 3584 CL Utrecht, The Netherlands
www.uu.nl/faculty/veterinarymedicine/EN/labs_services/vpdc

References:

1. Allan GM, Ellis JA. Porcine circovirus: a review. *J Vet Diagn Invest*. 2000;12:3-14.
2. Caswell JL, Williams KJ. Porcine circovirus and postweaning multisystemic wasting syndrome. In: Maxie MG, ed. *Jubb, Kennedy, and Palmer's Pathology of Domestic Animals*. Vol. 2. 5th ed. Philadelphia, PA: Elsevier Saunders; 2007:583-858.
3. Langohr IM, Stevenson GW, Nelson EA, et al. Vascular lesions in pigs experimentally infected with porcine circovirus type 2 serogroup B. *Vet Pathol*. 2010;47(1):140-147.
4. Lopez A. Respiratory system, mediastinum and pleurae. In: Zachary JF, McGavin MD, eds. *Pathologic Basis of Veterinary Disease*. 5th ed. St. Louis, MO: Elsevier; 2012:519-524.
5. Maxie MG, Newman SJ. Urinary system. In: Maxie MG, ed. *Jubb, Kennedy and Palmer's Pathology of Domestic Animals*. Vol. 2. 5th ed. Philadelphia, PA: Saunders Elsevier; 2007:461-462.
6. Misinzo G, Delputte PL, Meerts P, Lefebvre DJ, Nauwynck HJ. Porcine circovirus 2 uses heparan sulfate and chondroitin sulfate B glycosaminoglycans as receptors for its attachment to host cells. *J Virol*. 2006;80(7): 3487-3494.
7. Opriessnig T, Langohr I. Current state of knowledge on porcine circovirus type 2-associated lesions. *Vet Pathol*. 2013;50(1):23-38.
8. Rodriguez-Carino C, Sanchez-Chardi A, Segales J. Subcellular immunolocalization of Porcine Circovirus type 2 (PCV2) in lymph nodes from pigs with post-weaning multisystemic wasting syndrome (PMWS). *J Comp Path*. 2010;142:291-299.
9. Rosell C, Segales J, Domingo M. Hepatitis and staging of hepatic damage in pigs naturally infected with Porcine Circovirus type 2. *Vet Pathol*. 2000;37:687-692.
10. Wei L, Zhu S, Wang J, Liu J. Activation of the phosphatidylinositol 3-Kinase/Akts signaling pathway during porcine circovirus type 2 infection facilitates cell survival and viral replication. *J Virol*. 2012;86(24):13589-13597.

CASE II: 12 0132-42 (JPC 4019843).

Signalment: 1-year-old neutered male domestic shorthair cat, (*Felis silvestris catus*).

History: A 1-year-old neutered male domestic shorthair cat was presented to our institution for a 7-day history of weakness, anorexia and intermittent dyspnea that evolved over the last hours to persistent lateral recumbency and tremor. Clinical examination revealed a right anterior uveitis with fibrin deposition cranioventrally to the lens. Neurologic examination revealed a non-ambulatory tetraparesis with proprioceptive defect; a C1-C5 myelopathy or brainstem injury was suspected. The cat died two days after its admission and the owner requested a necropsy examination.

Gross Pathology: Apart from the aforementioned right fibrinous uveitis, gross findings included: discrete icterus; a 2-mL serohemorrhagic pleural effusion (consistent with modified transudate); numerous variable-sized and coalescing yellow foci and nodules on the renal capsule and renal cortices (consistent with pyogranulomas), some of which appeared to follow venous tracts (consistent with pyogranulomatous vasculitis (phlebitis)); diffuse, moderate, fibrinous perihepatitis; severe yellow thickening of the meninges, particularly in the ventral brainstem region (consistent with severe pyogranulomatous meningitis). Discrete yellow thickening of the spinal cord meninges was also detected. These findings led to a presumptive diagnosis of feline infectious peritonitis with nervous, ocular, renal and hepatic involvement.

Laboratory Results: Cerebrospinal fluid (CSF) aspiration and examination were performed:

	Present case	Reference values
Red blood cell count (/mm^3)	160	0
Nucleated cell count (/mm^3)	720	2-8
Protein concentration (g/L)	10.6	0-0.3

2-1. Kidney, cat: Numerous raised, white granulomas are present within the renal capsule (where they appear to be tracking the renal vasculature), and within the renal cortex. (Photo courtesy of: Department of Embryology, Histology and Pathology, Ecole Nationale Vétérinaire d'Alfort,7, avenue du Général de Gaulle, 94704 MAISONS-ALFORT CEDEX, http://www.vet-alfort.fr/)

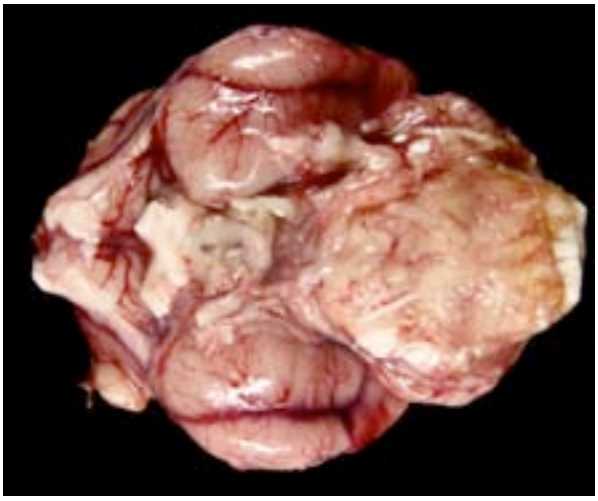

2-2. Brainstem, cat: The meninges are markedly thickened by pyogranulomatous inflammation. (Photo courtesy of: Department of Embryology, Histology and Pathology, Ecole Nationale Vétérinaire d'Alfort,7, avenue du Général de Gaulle, 94704 MAISONS-ALFORT CEDEX, http://www.vet-alfort.fr/)

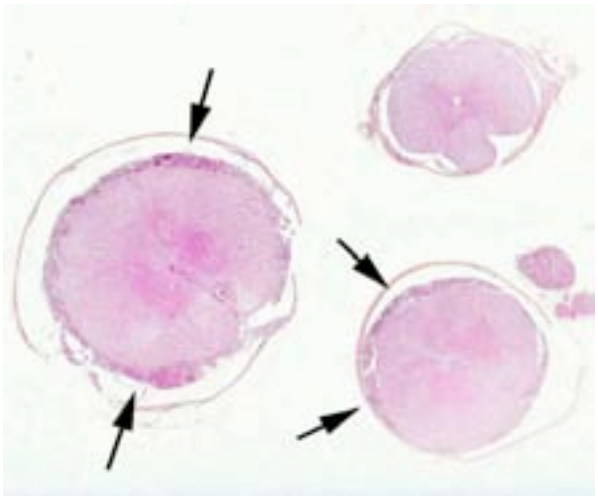

2-3. Spinal cord, cat: Upon subgross inspection, the meninges are thickened by a dense cellular infiltrate. (HE 0.63X)

On microscopic examination of the CSF, there was a marked neutrophilic pleocytosis (90%). Some neutrophils were degenerated. Few large and small mononuclear cells were also present (10%). No infectious agents or neoplastic cells were observed.

RT-PCR (reverse transcriptase polymerase chain reaction) analyses for Feline infectious peritonitis Virus (FIPV) were performed on the cerebrospinal fluid and aqueous humor and were strongly positive. RT-PCR analyses on blood and feces were negative.

Histopathologic Description: Spinal cord with meninges: Meninges (particularly leptomeninges) are severely thickened due to massive infiltration by degenerated neutrophils admixed with macrophages and few lymphocytes and plasma cells (pyogranulomatous meningitis). Infiltration is centered on vessels, particularly veins, and is associated with prominent fibrinoid necrosis and fibrin exudation (pyogranulomatous vasculitis/ phlebitis).

Inflammation extends along and inside nerves (neuritis). In nerves, secondary changes include myelin sheath destruction and axonal dilation.

In the spinal cord, there are multiple foci of myelin sheath distension and severe axonal dilation (spheroids), particularly in the ventral and/or lateral funiculi of some sections. Occasionally, inflammation from meninges extends into Virchow-Robin spaces.

Contributor's Morphologic Diagnosis: 1. Meninges: Vasculitis (mainly phlebitis), pyogranulomatous, chronic, diffuse, severe with fibrinoid necrosis and secondary meningitis (due to extension).
2. Spinal cord: Degenerative myelopathy, multifocal, chronic, moderate, with spheroids and dilation of myelin sheaths.
3. Peripheral nerves: Neuritis, pyogranulomatous, chronic, multifocal, severe.

Name of the disease: Feline infectious peritonitis (FIP)
Etiology: Feline infectious peritonitis virus

Contributor's Comment: This case is an example of Feline infectious peritonitis (FIP) with nervous and ocular involvement.

FIP is a fatal immune-mediated disease of cats caused by a member of feline coronaviruses (FCoV), the feline infectious peritonitis Virus (FIPV). Two major forms of FIP have been described: the effusive (wet) form and the non-effusive (dry) form. The distinction between these forms is sometimes arbitrary and they should be regarded as the two extremes of a continuum. Although both forms have been associated with neurological signs, the non-effusive form appears to more commonly produce nervous system lesions.[3,4]

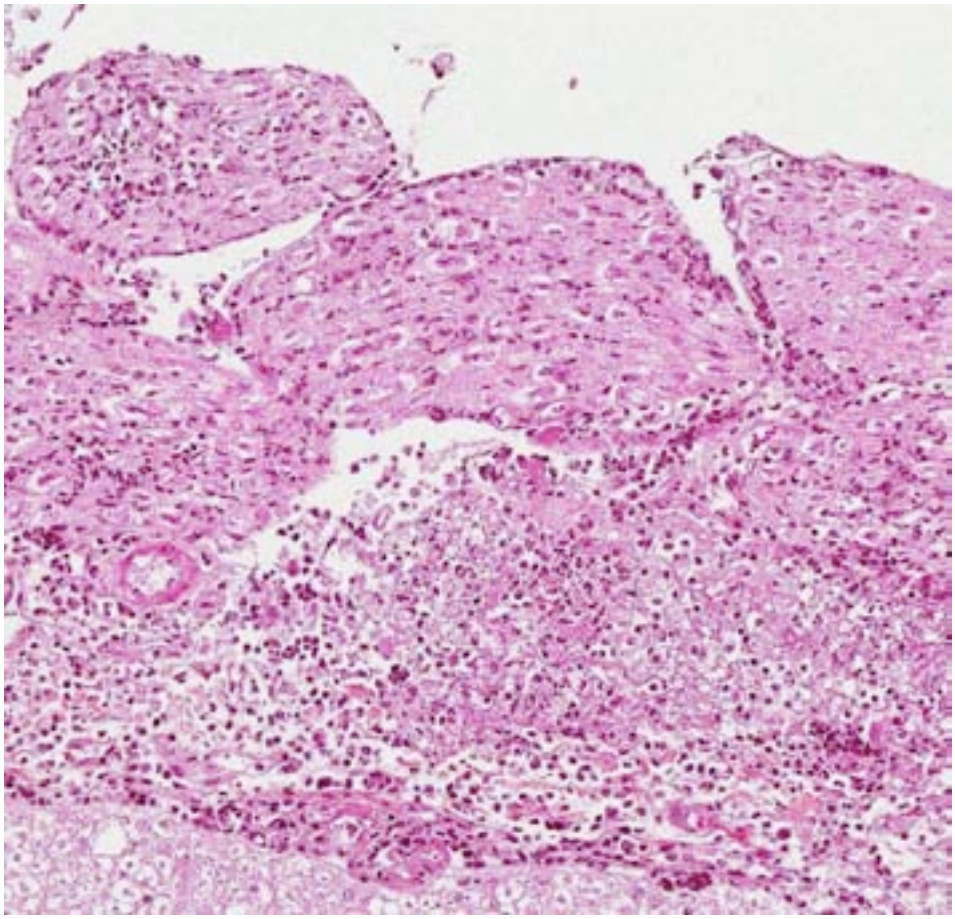

2-4. Spinal cord, cat: The meninges are expanded by a dense infiltrate of neutrophils and fewer macrophages which surround and infiltrate spinal nerves. (HE 100X)

The most widely accepted pathogenesis of FIP considers infection and replication of the virus within macrophages as a key feature. Macrophages can subsequently disseminate the virus through the body (e.g., to liver, visceral peritoneum or pleura, uvea, meninges and ependyma of the brain and spinal cord). In tissues, further replication of the virus results in attraction of neutrophils and macrophages leading to pyogranulomatous inflammation.[10] Both type III and type IV hypersensitivity reactions are believed to occur. The form of FIP is likely determined by the type of immune reaction of the host. Cats that respond with predominantly humoral immunity develop the wet form, whereas those with stronger cell-mediated immunity develop the dry form.[3,13]

The origin of FIPV is still subject to many debates. The most widely accepted hypothesis is that FIPV could be a mutant strain of the feline enteric coronavirus (FECV), another member of the FCoV that causes enteric infection. This mutant strain would be able to infect monocytes and macrophages, causing FIP. FECV is antigenically and morphologically indistinguishable from FIPV. Whether or not FIP develops would also depend on host factors (immune response, cytokine response) in conjunction with viral factors.[5,13]

Feline neurological disease accounts for approximately 10% of total referrals in some feline medicine clinics.[2,8] A specific clinical diagnosis is made in only 30-40% of cases and 30-45% of cases are believed to be infectious in origin. The most common infectious causes of encephalitis in cats are FIP and toxoplasmosis.[8]

Because FIP is a fatal transmissible disease without effective treatment, it is essential for clinicians to make a rapid diagnosis. Histopathology remains the only conclusive means of diagnosis of FIP, particularly in cases of atypical presentation. Surprisingly, FIP has been diagnosed histopathologically in the brains of cats without neurological clinical signs.[4] Occasionally, histopathology can be inconclusive and immunohistochemistry can be useful to confirm or exclude the disease.[7]

In practice, diagnosis is often based on the combination of signalment, history and clinical signs.[8] Although the nervous form of FIP can affect cats at any age, it is considered to be the most common cause of neurological disease in cats less than 4 years of age. Purebred cats are at

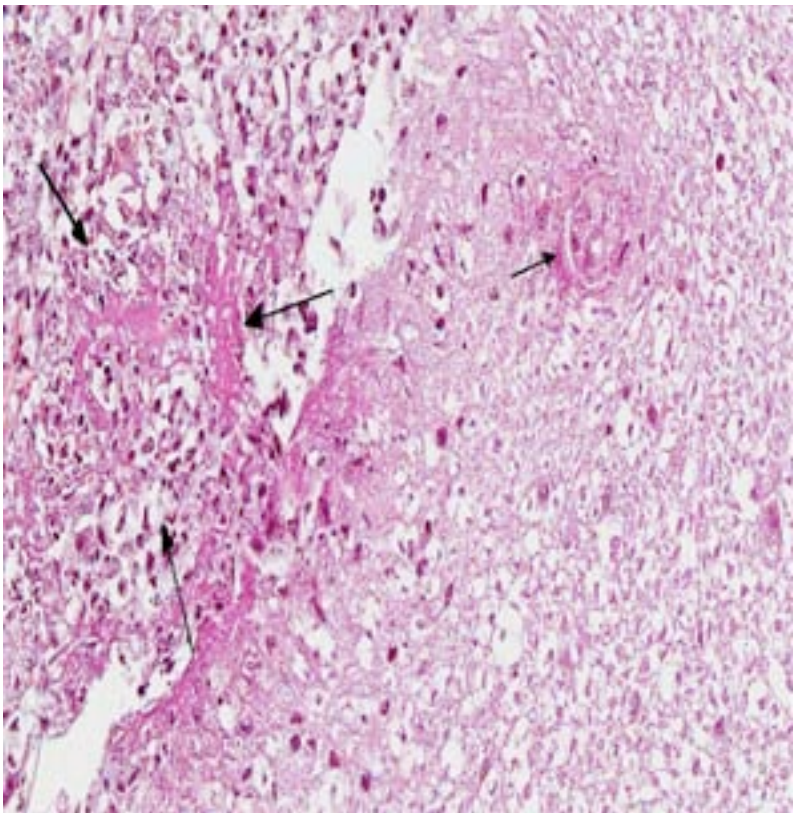

2-5. Spinal cord, cat: Multifocally, vessels are necrotic (small arrows) and effaced (large arrows) by pyogranulomatous inflammation, resulting in focal polymerization of fibrin. (HE 3200X)

JPC Diagnosis: Spinal cord: Phlebitis, meningomyelitis and polyradiculoneuritis, pyogranulomatous, multifocal, moderate, with axonal degeneration, vascular fibrinoid change and thrombosis.

Conference Comment: The viral order *Nidovirales* is composed of the families *Coronaviridae*, *Arteriviridae* and *Roniviridae*. *Coronaviridae* contains two genera: *Coronavirus* and *Torovirus*. Coronaviruses are enveloped, ssRNA viruses that are important in a wide variety of animal diseases (see table 1).[12,18] Feline coronavirus (FCoV) is a group 1 coronavirus with two serologically and morphologically indistinguishable subtypes: feline infectious peritonitis virus (FIPV) and feline enteric coronavirus (FECV). FECV (i.e., non-mutated FCoV) replicates within enterocytes of affected cats, which may shed virus but are typically asymptomatic or exhibit mild diarrhea. The development of virulent FCoV (i.e., FIPV) appears to be due to a spontaneous viral genetic mutation that occurs during replication in the infected host, although the specific nature and location of this mutation has yet to be determined. FECV carriers are thought to play an important role in the epidemiology of FIP.[11] Transmission is typically oronasal via feces, saliva/mutual grooming, and fomites (e.g. food bowls or grooming tools); transplacental transmission is reported although it is fairly uncommon.[1,3,11]

increased risk and male cats are more frequently affected than females.[4]

Abnormal laboratory findings frequently observed in FIP are hyperproteinemia with a low albumin/globulin ratio (<0.7), anemia, elevated hepatic enzyme levels and hyperbilirubinemia.[17]

CSF analysis is useful in the diagnosis of cats with FIP. Marked elevation of protein concentration (greater than 2 g/L), severe pleocytosis (> 100 cells/µL) with neutrophils (more than 70%) and systemic signs increase the index of suspicion for FIP.[14,16]

Infection by FIPV can be demonstrated by serology and by RT-PCR. Currently available serological tests have low specificity and sensitivity for detection of active infection and cross-react with FECV.[15] RT-PCR is rapid and sensitive but results must be interpreted in the context of clinical findings. RT-PCR on CSF detected only 31% of cats with neurologic FIP. This low sensitivity could be explained by the low CSF cellularity on most cats and the paucity of virus detected immunohistochemically.[6]

At present, three key features have been identified as prerequisites for the development of FIP lesions: 1) systemic infection with mutated, virulent FCoV (FIPV), 2) effective and sustainable FIPV replication in monocytes, and 3) activation of FIPV-infected monocytes, although the trigger remains unknown. Activated monocytes/macrophages upregulate their expression of adhesion molecules (e.g. CD18), and produce cytokines (such as TNF-α, IL-1b, IL6, G-CSF and GM-CSF), matrix metalloproteinases (e.g., MMP-9), and vascular

endothelial growth factor (VEGF). IL-6 stimulates hepatocytes to produce acute phase proteins (such as alpha-1 acid glycoprotein) and drives differentiation of B-lymphocytes into plasma cells. TNF-α, G-CSF and GM-CSF are neutrophil survival factors. IL-1 is a pyrogenic cytokine that activates both B- and T-lymphocytes. MMP-9 is an endopeptidase that breaks down extracellular matrix proteins. VEGF facilitates interaction with activated endothelial cells; it has been proposed that the limited distribution of vascular lesions (only veins in select organs are affected) is a consequence of selective responsiveness of the endothelium.[1,11]

As noted by the contributor, mutated FCoV-infected circulating monocytes are thought to be responsible for viral dissemination, while the nature of the adaptive immune response determines the clinical manifestations of FIP. Cats with a strong cell-mediated immune (CMI) response do not develop FIP, while a weak to nonexistent CMI and strong humoral response results in effusive, or "wet," FIP, characterized by vasculitis, peritonitis and intracavitary effusions. In contrast, noneffusive, or "dry" FIP with widespread pyrogranulomatous inflammation predominates in cats with a moderate CMI response. As the contributor noted, the "wet" and "dry" forms of FIP represent a continuum, rather than two specific disease processes; mixed effusive and noneffusive forms are not uncommon.[1,11] Additionally, antibody-dependent enhancement (ADE) can affect the severity of clinical disease. ADE is a phenomenon in which cats with preexisting antibodies (e.g. those that were vaccinated with some trial vaccines or received blood from FCoV positive donors), develop disease more quickly, and perhaps more severely than seronegative cats; however, ADE does not appear to affect seropositive cats infected naturally, who are relatively resistant to reinfection.[1]

FIP has historically been regarded as an immune complex-mediated type III hypersensitivity disease (see WSC 2013-2014, conference 22, case 4), based upon 1) the presence of cell-free fibrinogen, C3, viral antigen, IgG, and complement within leukocytes in vascular and focal granulomatous to necrotizing lesions, 2) FCoV-specific immune complexes in blood and glomeruli and 3) elevated serum γ-globulin and C3 levels. Nonetheless, circulating FCoV-specific immune complexes can also be detected in clinically healthy seropositive cats, and most cases of FIP do not exhibit typical features of immune complex vasculitis, such as the involvement of arteries and the prevalence of neutrophils. So, while type III hypersensitivity may contribute to FIP, it has not yet been confirmed as a crucial pathogenic mechanism. Other authors have proposed that type IV hypersensitivity reactions serve as a driving force behind the granulomatous and necrotizing lesions associated with FIP. As discussed above, activation of viral infected macrophages results in the release of various cytokines and growth factors, specifically VEGF, which is a potent mediator of vascular permeability that may produce vascular leakage and acute phlebitis via alterations in endothelial junctional complexes.[11]

The clinical pathology findings associated with FIP can be somewhat variable and non-specific. When present, effusions are usually classified as a modified transudate, with a high protein content (>3.5 g/dL) and a low nucleated cell count (<5,000 nucleated cells/mL), which parallels a serum hypergammaglobulinemia and decreased albumin:globulin ratio. Serum protein electrophoresis often reveals a polyclonal gammopathy (due to immunoglobulins). Normocytic, normochromic, non-regenerative anemia (or anemia of chronic disease) may also be observed.[1] The release of inflammatory mediators (such as IL-1, IL-6 and TNF-α) results in hepatic production of the acute phase protein hepcidin. Hepcidin induces the degradation of the iron export protein ferroportin, effectively sequestering iron within macrophages and enterocytes and ultimately resulting in decreased iron availability with subsequent anemia.[9] As noted by the contributor, CSF evaluation can also be useful in reaching a diagnosis of FIP; however, obtaining a specimen is often quite difficult due to the high viscosity of fluid from increased protein levels.[1] Serum levels of the acute phase protein, α1-acid glycoprotein (AGP) are often significantly elevated (>3 mg/ml), but this is not specific for FIP and may occur with other inflammatory conditions, neoplastic diseases (lymphoma) or in asymptomatic FCoV carriers, especially from households with endemic infection.[11]

Table 1. Select coronaviruses of veterinary importance.[12,18]

Group 1a		**Disease/Symptoms**
	• Feline enteric coronavirus • Mutated feline enteric coronavirus (FIP)	• None/mild gastroenteritis • Peritonitis, vasculitis, granulomatous inflammation
	Canine coronavirus	Mild gastroenteritis
	Transmissible gastroenteritis virus of swine (TGE)	Gastroenteritis, watery diarrhea, dehydration
	Porcine respiratory coronavirus (PRCV)	Mild respiratory disease/ interstitial pneumonia
	Ferret (FRECV) & mink enteric coronaviruses	Epizootic catarrhal enteritis
	Ferret systemic coronavirus (FRSCV)	FIP-like (dry/ granulomatous form) systemic dz
Group 1b		
	Porcine epidemic diarrhea virus	Gastroenteritis, watery diarrhea, dehydration
Group 2a		
	Porcine hemagglutinating encephalomyelitis virus	Encephalomyelitis, wasting, muscle tremors
	Mouse hepatitis virus	Hepatitis, enteritis, nephritis, demyelinating encephalomyelitis
	Sialodacryoadenitis virus of rats	Salivary/lacrimal gland necrosis/inflammation, chromodacryorrhea
	Bovine coronavirus	Gastroenteritis (winter dysentery), respiratory disease
Group 2b		
	Severe acute respiratory syndrome (SARS) coronavirus	Humans
	SARS coronavirus	Civets, cats, bats; subclinical
Group 3		
	Avian infectious bronchitis virus	Tracheobronchitis, nephritis, rales
	Turkey coronavirus/ Bluecomb virus	Enteritis, cyanosis

Contributing Institution: Department of Embryology, Histology and Pathology
Ecole Nationale Vétérinaire d'Alfort
7, avenue du Général de Gaulle
94704 MAISONS-ALFORT CEDEX
http://www.vet-alfort.fr/

References:

1. Addie DD, Jarrett O. Feline coronavirus infections. In: Greene CE, ed. *Infectious Diseases of the Dog and Cat*. 3rd ed. St. Louis, MO: Saunders; 2006:91-100.
2. Bradshaw JM, Pearson GR, Gruffydd-Jones TJ. A retrospective study of 286 cases of neurological disorders of the cat. *J Comp Path.* 2004;131:112–120.
3. Brown CC, Baker DC, Barker IK. Alimentary system. In: Maxie MG, ed. *Jubb, Kennedy, and Palmer's Pathology of Domestic Animals*. Vol. 2. 5th ed. London, UK: Saunders Elsevier; 2007:290-293.
4. Diaz JV, Poma R. Diagnosis and clinical signs of feline infectious peritonitis in the central nervous system. *Can Vet J.* 2009;50(10):1091–1093.
5. Foley JE, Leutenegger C. A review of coronavirus infection in the central nervous system of cats and mice. *J Vet Intern Med.* 2001;15(5):438–444.
6. Foley JE, Lapointe JM, Koblik P, Poland A, Pedersen NC. Diagnostic features of clinical neurologic feline infectious peritonitis. *J Vet Intern Med.* 1998;12(6):415–423.
7. Giori L, Giordano A, Giudice C, Grieco V, Paltrinieri S. Performances of different diagnostic tests for feline infectious peritonitis in challenging clinical cases. *J Small Anim Pract*. 2011;52:152-157.
8. Gunn-Moore DA, Reed N. CNS disease in the cat: current knowledge of infectious causes. *J Fel Med Surg.* 2011;13(11):824–836.
9. Keel SB, Abkowitz JL. The microcytic red cell and the anemia of inflammation. *N Engl J Med*; 2009;361(19):1904-1906.
10. Kent M. The cat with neurological manifestations of systemic disease. Key conditions impacting on the CNS. *J Fel Med Surg.* 2009;11(5):395–407.
11. Kipar A, Meli ML. Review Feline infectious peritonitis: Still an Enigma? *Vet Pathol*. 2014:51(2):505-526.
12. MacLachlan NJ, Dubovi EJ. *Fenner's Veterinary Virology*. 4th ed. London, UK: Academic Press; 2011:393-412.
13. Myrrha LW, Miquelitto Figueira Silva F, Fernandes de Oliveira Peternelli E, Silva Junior A, Resende M, Rogéria de Almeida M. The paradox of Feline Coronavirus pathogenesis: a review. *Adv Virol*. 2011;2011:1-8.
14. Rand JS, Parent J, Percy D, Jacobs R. Clinical, cerebrospinal fluid, and histological data

from twenty-seven cats with primary inflammatory disease of the central nervous system. *Can Vet J*. 1994;35(2):103–110.
15. Sharif S, Suri Arshad S, Hair-Bejo M, Rahman Omar A, Allaudin Zeenathul N, Alazawy A. Diagnostic methods for Feline Coronavirus: a review. *Vet Med Int*. 2010;2010:1-7.
16. Singh M, Foster DJ, Child G, Lamb WA. Inflammatory cerebrospinal fluid analysis in cats: clinical diagnosis and outcome. *J Fel Med Surg*. 2005;7(2):77–93.
17. Tsai HY, Ling-Ling C, Chao-Nan L, Bi-Ling S. Clinicopathological findings and disease staging of feline infectious peritonitis: 51 cases from 2003 to 2009 in Taiwan. *J Feline Med Surg*. 2010;13:74-80.
18. Wise AG, Kiupel M, Maes RK. Molecular characterization of a novel coronavirus associated with epizootic catarrhal enteritis (ECE) in ferrets. *Virology*. 2006;349:164–174.

CASE III: PV118/13 (JPC 4035592).

Signalment: 10-12-week-old Lohmann Brown laying hens from a breeder in Nigeria, (*Gallus gallus domesticus*).

History: The chickens were vaccinated for pox, with what was discovered later on as the wrong dosage. They started to show crusts in the eyelids, which slowly involved mucocutaneous junctions. The animals became anorectic. There was gradual spread into a large portion of the flock until revaccination was recommended.

Gross Pathology: Not available. Only eyes, including eyelids were submitted in formalin.

Histopathologic Description: Part of a sagittal section from an eye including feathered skin from eyelids.

There is locally extensive, marked epithelial and epidermal hyperplasia of the conjunctiva and feathered skin. The epithelium is up to 8-10 times its normal thickness and has extensive serocellular crusting. There are foci of heterophilic infiltration and hemorrhage. Many keratinocytes have marked cytoplasmic vacuolation (ballooning degeneration) and many are expanded by 10-30 µm eosinophilic/red intracytoplasmic inclusions (Bollinger bodies). The dermis is moderately infiltrated by lymphocytes, macrophages and heterophils.

Contributor's Morphologic Diagnosis: Feathered skin: Lymphohistiocytic and heterophilic dermatitis with epidermitis, epidermal hyperplasia and intracytoplasmic inclusions, findings typical of fowl pox.

Contributor's Comment: The submitted samples reflect a classic histological picture of fowl pox.

Avian or fowl pox are diseases caused by a variety or viruses of the genus *Avipoxvirus*, a member of the poxviridae. This DNA virus group has very large viral particles (250 to 300 nm). *Avipoxvirus* induces intracytoplasmic, lipophilic inclusion bodies, Bollinger bodies, in the epithelium of the integument. Their appearance is pathognomonic.[3,9,10] The virus is recognized in more than 232 species of wild birds representing 23 orders, however, it is likely that many more bird species are susceptible to *Avipoxvirus*.[1]

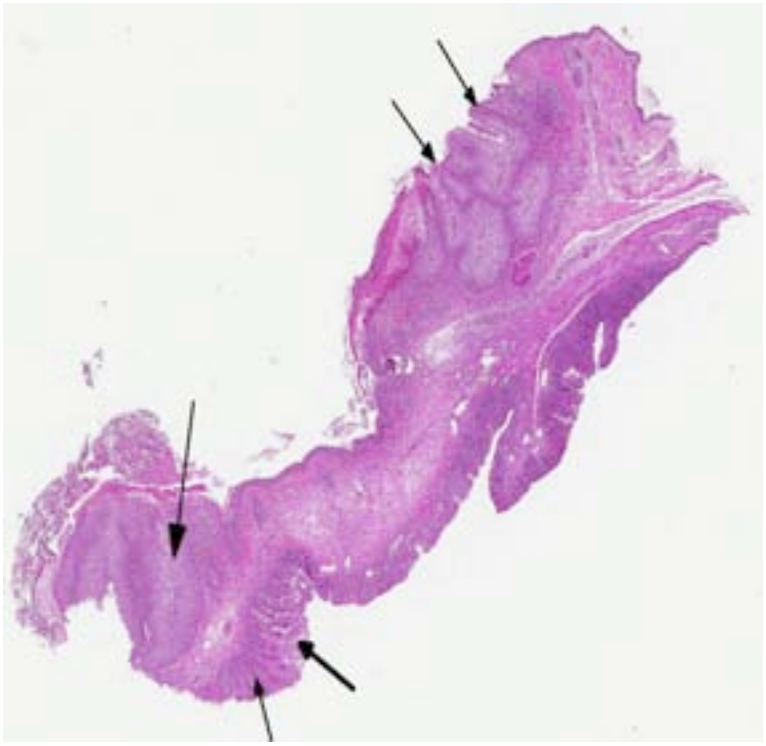

3-1. Eyelid, chicken: Multifocally, within the feathered skin, there are areas of marked epidermal hyperplasia and hypertrophy (arrows). (HE 0.63X)

Fowl pox is a slow spreading disease which may present in two forms: 1) the cutaneous form is characterized by the development of discrete nodular proliferative skin lesions on the non-feathered parts of the body, and 2) the diphtheritic form with fibrinonecrotic and proliferative lesions in the mucous membranes of the upper respiratory tract, mouth and esophagus. Flock mortality is usually low if the cutaneous form prevails, but it may be high with generalized infection, with the diphtheritic form, or when the disease is complicated by other infectious or poor environmental conditions.[1,3,9] In canaries and other finches, mortality can reach 80 to 100%.[1,3,9]

Avian pox is not of public health significance and it doesn't generally affect mammals.[9]

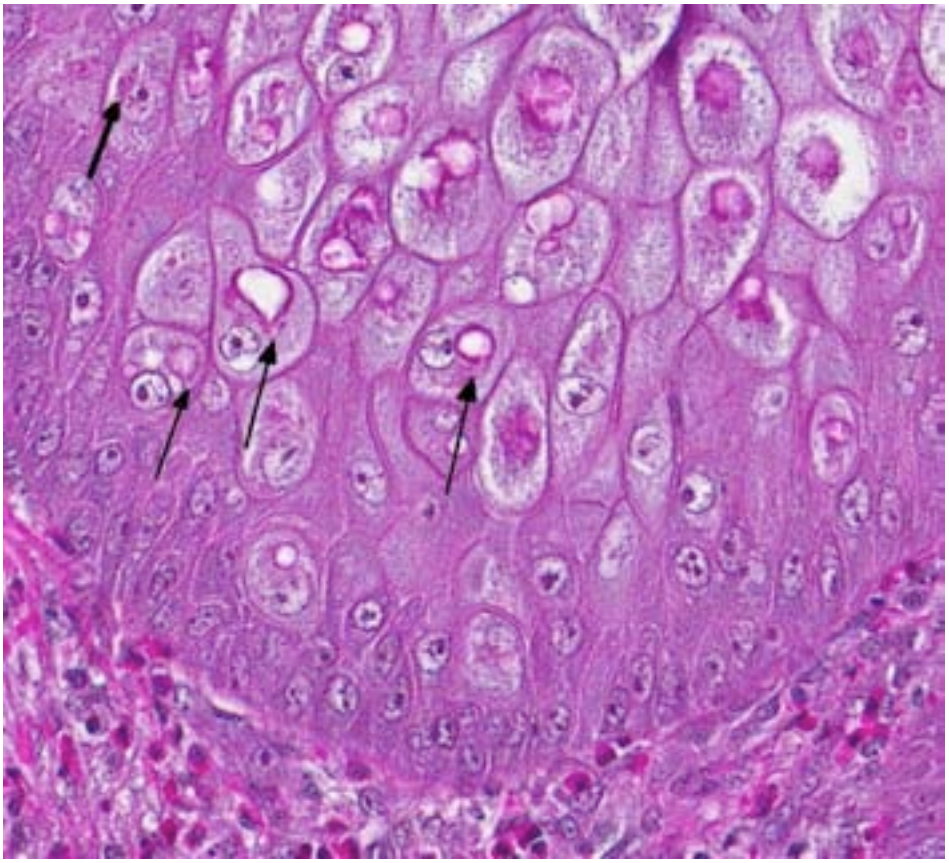

3-2. Eyelid, chicken: Keratinocytes of the stratum spinosum contain large eosinophilic cytoplasmic viral inclusions (Bollinger bodies) (arrows). (HE 260X)

The mode of transmission is through virus carriers and contaminated environment. Mosquitoes and mites are the main vectors. Aerosols generated from infected birds, or the ingestion of contaminated food or water have also been implicated as a source of transmission.[10] The disease may have a seasonal incidence, occurring during late summer and autumn, which in some countries coincides with the peak of the mosquito season. The virus can survive in the vector's salivary glands for 2 to 8 weeks. Spread of the virus within a given bird population is triggered by close contact between birds and the formation of small traumatic lesions due to pecking on one another. During latent infection or after recovery from clinical disease, the virus is intermittently shed via the feces or the skin and feather quills.[3,9]

The clinical signs seen in the cutaneous form of pox are very characteristic, with formation of nodules that first appear as small white foci and then rapidly increase in size and become yellow. Initially there is formation of papules followed by vesicles and thickened areas. Adjacent lesions may coalesce and crust, acquiring a gray, or dark brown color. Later on, there is development of inflammation with hemorrhage and formation of a scab that sloughs off and leaves a pink scar.[3]

In the diphtheritic form, slightly elevated, white, opaque nodules develop in the mucous membranes. Nodules rapidly increase in size and often coalesce, becoming a yellow, cheesy, necrotic, pseudo-diphtheritic or diphtheritic membrane. The inflammation process may extend into the sinuses and also in the esophagus, pharynx and larynx resulting in respiratory disturbances.[9]

Histopathology usually reveals epithelial hyperplasia (in both diphtheritic and cutaneous forms), with cell swelling, associated inflammatory changes, and typical large, solid or ring-like, eosinophilic intracytoplasmic inclusions known as Bollinger bodies.[3,9,10] Transmission electron microscopy (TEM) may also reveal definite proof of *Avipoxvirus* infection, demonstrating the typical particles within inclusion bodies. Avipoxvirus identification may also be carried out by negative staining electron microscopy with 2% phosphotungstic acid (PTA) on infected cells.[10]

JPC Diagnosis: Feathered skin and mucocutaneous junction: Conjunctivitis and dermatitis, proliferative and necrotizing, multifocal, marked, with epithelial intracytoplasmic viral inclusion bodies (Bollinger bodies).

Conference Comment: The family *Poxviridae* is composed of epitheliotropic DNA viruses that

Table 1: Select genera of the family *Poxviridae*.[4,6]

Genus	Virus/Disease	Major Hosts
Orthopoxvirus	Vaccinia virus Buffalopox/Rabbitpox virus*	Numerous: cattle, buffalo, swine, rabbits
	Cowpox*	Rodents (reservoir), cattle, cats, elephants, rhinos,
	Camelpox	Camels
	Ectromelia (Mousepox)	Mice, voles
	Monkeypox*	NHPs, squirrels, anteaters
Capripoxvirus	Goatpox	Goats, sheep
	Sheeppox	Sheep, goats
	Lumpy skin disease virus	Cattle, cape buffalo
Suispoxvirus	Swinepox virus	Swine (vector= *Hematopinus suis*)
Leporipoxvirus	Myxoma virus	Rabbits (*Oryctolagus* & *Sylvilagus* spp.)
	Rabbit fibroma virus, Hare fibroma virus	Rabbits
	Squirrel fibroma virus	Grey and red squirrels
Avipoxvirus	Fowlpox, canarypox, quailpox, etc	Chickens, turkeys, peacocks, etc.
Parapoxvirus	Caprine parapoxvirus (Orf; contagious ecthyma)*	Sheep, goats
	Bovine parapox (bovine papular stomatitis virus)*	Cattle
	Pseudocowpox*	Cattle
	Sealpox*	Seals
	Parapoxvirus of red deer	Red deer
Molluscipox-virus	Molluscum contagiosum virus*	NHPs, birds, dogs, kangaroos, equids
Yatapoxvirus	Yabapox virus & tanapoxvirus*	NHPs
Unclassified	Squirrel poxvirus, fish (carp edema), horsepox	

* zoonotic

cause cutaneous or systemic disease in many species of animals, including wild and domestic mammals, birds, and humans (see table 1).[4,6] This case provides an excellent example of the cutaneous ("dry") form of avian pox, which is summarized comprehensively by the contributor. Readers are also encouraged to review WSC 2012-2013, conference 3, case 4 for an example its diphtheritic ("wet") manifestation in a wild turkey.

Conference participants briefly discussed the differential diagnosis for gross findings associated with the diptheritic form of avian pox, including Gallid herpesvirus-1 (infectious laryngotracheitis), *Capillaria annulata* or *C. contorta*, *Trichomonas gallinae*, *Candida albicans*, *Aspergillus* spp., and vitamin A deficiency. Rule outs for the cutaneous form include dermatophytosis (*Trichophyton megninii* or *T. simii*), papillomavirus and the mite *Knemidokoptes gallinae*.[3,4] These conditions can generally be differentiated microscopically; histochemical staining with giemsa highlights the prominent intracytoplasmic Bollinger bodies associated with avipoxvirus, while herpesviral infection results in intranuclear viral inclusions. Identification of yeast, hyphae or pseudohyphae (in cases of candidiasis or aspergillosis), arthrospores (dermatophytosis), trichomonads, nematode adults, larvae or eggs (capillariasis), arthropod segments (knemidokoptosis), or squamous metaplasia of glandular epithelia (vitamin A deficiency) is suggestive of one of the alternative etiologies enumerated above.[2,5,7-9,11]

Contributing Institution: The Weizmann Institute of Science
Department of Veterinary Resources
http://www.weizmann.ac.il/vet/

References:

1. Bolte AL, et al. Avian host spectrum of avipoxviruses. *Avian Pathology*. 1999;28:415-432.
2. Charlton BR, Chin RP, Barnes HJ. Fungal infections. In: Saif YM, ed. *Diseases of poultry*. 12th ed. Ames, IA: Iowa State University Press; 2008:1001-1003.
3. Gerlach H. Viral diseases. In: *Harrison and Harrison's Clinical avian medicine and surgery*. Philadelphia, PA: WB Saunders Co; 1986:409-414.

4. Ginn PE, Mansell JEKL, Rakich PM. Skin and appendages. In: Maxie MG, ed. *Jubb, Kennedy and Palmer's Pathology of Domestic Animals*. 5th ed. New York, NY: Saunders Elsevier; 2007:664-673.
5. Guy JS, Garcia M. Laryngotracheitis. In: Saif YM, ed. *Diseases of poultry*. 12th ed. Ames, IA: Iowa State University Press; 2008:137-147.
6. Hargis AM, Ginn PE. The integument. In: Zachary JF, McGavin MD, eds. *Pathologic Basis of Veterinary Disease*. 5th ed. St. Louis, MO: Elsevier; 2012:1020-1024.
7. Hinkle NC, Hickle L. External parasites and poultry pests. In: Saif YM, ed. *Diseases of poultry*. 12th ed. Ames, IA: Iowa State University Press; 2008:1015-1018.
8. McDougald LR. Histomoniasis (blackhead) and other protozoan diseases of the intestinal tract. In: Saif YM, ed. *Diseases of poultry*. 12th ed. Ames, IA: Iowa State University Press; 2008:1100-1103.
9. Tripathy DN, Reed WM. Pox. In: Saif YM, ed. *Diseases of poultry*. 12th ed. Ames, IA: Iowa State University Press; 2008:291-303.
10. Weli SC, Tryland M. Avipoxviruse: infection biology and their use as vaccine vectors. *Virology Journal*. 2011;8:49-63.
11. Yazwinski TA, Tucker CA. Nematodes and acanthocephalans. In: Saif YM, ed. *Diseases of poultry*. 12th ed. Ames, IA: Iowa State University Press; 2008:1028-1029.

CASE IV: 11-1195 (JPC 4033515).

Signalment: Age-unspecified female Yorkshire pig, (*Sus scrofa*).

History: This Yorkshire pig was one of several animals belonging to a hemorrhagic shock study. This pig (animal number 30962), age unknown, was hemorrhaged over a 15-minute period until 55% of its estimated blood volume (EBV) was lost via the femoral artery catheter. At time 15 minutes, the pig received initial resuscitation therapy. Oxycyte (5 mL/kg) was given as a continuous infusion over 10 minutes via the external jugular vein. There was no reported history of clinical illness.

Gross Pathology: There were no reported gross findings at necropsy.

Laboratory Results:

- *Mycoplasma hyopneumoniae PCR: NEGATIVE*
- *Mycoplasma hyopneumoniae* IHC: NEGATIVE

Histopathologic Description: Lung: Diffusely, filling bronchi and bronchioles is an exudate composed of moderate numbers of viable and non-viable neutrophils, macrophages, fewer lymphocytes and plasma cells, admixed with edema, and rare fibrin. Multifocally, both bronchial and bronchiolar epithelium are mildly hyperplastic. A similar infiltrate extends into interlobular septa, expands and obscures alveolar septa, and fills alveolar spaces. Rarely, there is mild type II pneumocyte hyperplasia. Multifocally surrounding bronchi, bronchioles, and blood vessels (often lined by hyperplastic endothelium) are variably sized lymphoid follicles with vague germinal centers (BALT hyperplasia), with mild lymphocytolysis. Multifocally, the pleura is separated from the subjacent lung parenchyma by clear space (suspected artifact).

Contributor's Morphologic Diagnosis: Lung: Pneumonia, bronchointerstitial, suppurative and histiocytic, chronic, diffuse, severe, with lymphoid (BALT) hyperplasia, mild lymphocytolysis, type II pneumocyte hyperplasia, bronchiolar and bronchial epithelial hyperplasia, and edema, Yorkshire pig, porcine.

Contributor's Comment: This is a case of suspected *Mycoplasma hyopneumoniae*, which is a common cause of non-fatal pneumonia in young pigs. The disease is prevalent in grower-finisher pigs; however, animals as young as 5-weeks may be affected.[1] Also known as porcine enzootic pneumonia, disease progression is often insidious

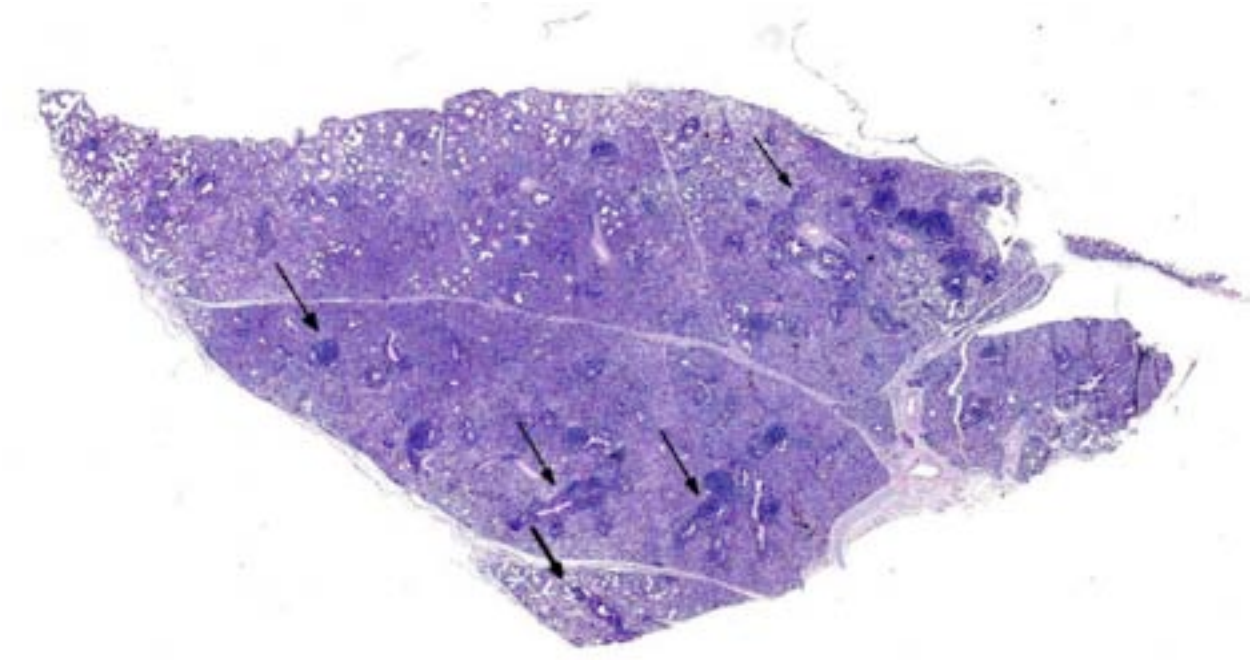

4-1. Lung, pig: The section of lung is diffusely consolidated and the airways are surrounded by dense cuffs of lymphocytes and plasma cells. (HE 0.63X)

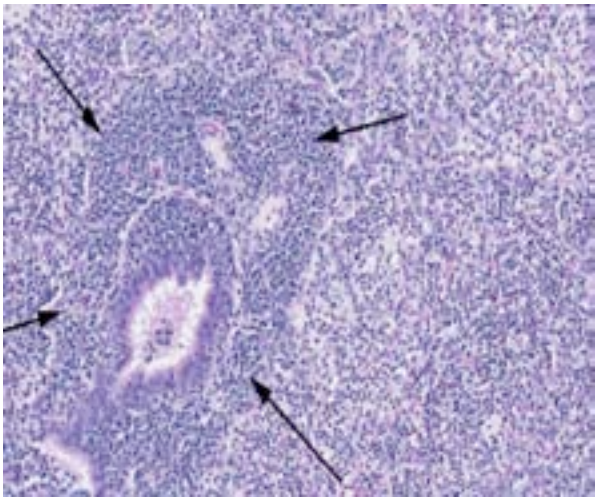

4-2. Lung, pig: Higher magnification of an affected airway demonstrating the bronchocentric distribution of lymphocytes and plasma cells (arrows), and filling of adjacent alveoli with numerous neutrophils and macrophages. (HE 150X)

in endemic areas where subclinical carriers serve as key sources of infection for naïve herds.[1]

Gross lesions associated with mycoplasmal pneumonia are discolored, collapsed, firm lungs affecting the cranioventral lung lobes.[1] Acute histologic lesions are characterized by alveoli containing macrophages and neutrophils along with edema.[1] Chronic infections in swine are similar to other species (e.g., rats, mice) where peribronchial/peribronchiolar (BALT), and perivascular lymphoid hyperplasia is a dominant histologic feature.

Although the exact pathogenesis is not completely understood, *Mycoplasma hyopneumoniae* firmly adheres to the cilia of the respiratory tree resulting in ciliostasis. Attachment to the respiratory epithelium invokes the following:

(1) Influx of neutrophils into the tracheobronchial mucosa
(2) Extensive loss of cilia (deciliation)
(3) Broncho-alveolar lymphoid tissue (BALT) hyperplasia
(4) Influx of mononuclear cells into the peribronchiolar, bronchiolar, and alveolar interstitium[3]

Diagnosis of *Mycoplasma hyopneumoniae* infection in the porcine lung is based on results of three methods: isolation of the organism by culture, immunofluorescence (IF) testing, or immunohistochemistry using polyclonal antibodies.[3]

Despite our inability to definitively diagnose *Mycoplasma hyopneumoniae* as a causative agent for the lung lesions in this case, the histologic lesions are highly suggestive of this entity.

JPC Diagnosis: Lung: Bronchopneumonia, pyogranulomatous, diffuse, chronic, severe, with BALT hyperplasia.

Conference Comment: In conference, the moderator led a brief review of the morphologic patterns of pneumonia. Bronchopneumonia is the most common type of pnuemonia in domestic animals. It is characterized by inflammatory lesions arising primarily within the airways (with occasional spread into the surrounding interstitium), and there is usually cranioventral consolidation of the lungs. Bronchopneumonias are typically caused by many types of inhaled bacteria, including *Mycoplasma* spp. Fibrinous bronchopneumonia in particular has a propensity for depositing on pleural surfaces, thus some pathologists refer to it as pleuropneumonia. In contrast, inflammatory lesions develop within alveolar walls and the bronchiolar interstitium in cases of interstitial pneumonia. The portal of entry can by hematogenous or aerogenous. Interstitial pneumonia tends to be diffuse and is generally associated with viruses, toxins, sepsis, or protozoa such as *Toxoplasma* spp. The term bronchointerstitial pneumonia describes pulmonary lesions with features of both interstitial and bronchopneumonia and is specifically associated with viruses that cause necrosis in both bronchiolar and alveolar epithelial cells (e.g. small ruminant respiratory syncytial virus, canine distemper and porcine/ equine influenza). With embolic pneumonia, sterile or septic (e.g. from vegetative valvular endocarditis), thromboemboli are delivered hematogenously to the lung; inflammation is random and multifocal and it centers upon pulmonary arterioles and alveolar capillaries. Verminous pneumonia typically exhibits a caudodorsal distribution.[3] Based on this broad classification scheme, the microscopic lesions in this case are most consistent with bronchopneumonia secondary to *Mycoplasma hyopneumoniae*.

The contributor provides an excellent summary of *M. hyopneumoniae*. See WSC 2013-2014, conference 7, case 1 for further discussion of

Mycoplasma spp., and table 1 for an abbreviated list of *Mycoplasma* species important in veterinary medicine.

Table 1. Select *Mycoplasma* species of veterinary importance.[4]

***Mycoplasma* species**	**Hosts**	**Disease**
M. mycoides subsp. *mycoides* (small colony type)	Bovine	Contagious bovine pleuropneumonia
M. bovis	Bovine	Mastitis, pneumonia, arthritis, otitis
M. agalactiae	Ovine, Caprine	Contagious agalactia (mastitis)
M. capricolum subsp. *capripneumoniae*	Caprine	Contagious caprine pleuropneumonia
M. capricolum subsp. *capricolum*	Ovine, Caprine	Septicemia, mastitis, polyarthritis, pneumonia
M. mycoides subsp. *capri* (includes strains previously classified as *M. mycoides mycoides* large colony type)	Ovine, Caprine	Septicemia, pleuropneumonia, mastitis, arthritis
M. ovipneumoniae	Ovine, Caprine	Pneumonia
M. pulmonis	Rodents--rat and mouse	Colonize nasopharynx and middle ear; affect respiratory and reproductive tracts and joints
M. hyopneumoniae	Swine	Enzootic pneumonia
M. hyosynoviae	Swine (10-30 weeks of age)	Polyarthritis
M. hyorhinis	Swine (3-10 weeks of age)	Polyserositis
M. suis	Swine	Mild anemia, poor growth rates
M. ovipneumoniae		mild pneumonia
M. haemofelis	Feline	Feline infectious anemia
M. cynos	Canine	Implicated in kennel cough complex
M. haemocanis	Canine	Mild or subclinical anemia; more severe signs in splenectomized animals
M. gallisepticum	Turkeys and Chickens	Chronic respiratory disease; infectious sinusitis
M. synoviae	Turkeys and Chickens	Infectious synovitis
M. meleagridis	Feline, Equine	Conjunctivitis in cats, pleuritis in horses
M. equigenitalium	Equine	Abortion

Contributing Institution: Walter Reed Army Institute of Research
http://wrair-www.army.mil

References:

1. Caswell JL, Williams KJ. Respiratory system. In: Maxie MG, ed. *Jubb, Kennedy, and Palmer's Pathology of Domestic Animals.* Vol 2. 5th ed. Vol. 2. Philadelphia, PA: Elsevier Saunders; 2007;591-592.
2. Kwon D, Chae C. Detection and localization of *Mycoplasma hyopneumoniae* DNA in lungs from naturally infected pigs by in situ hybridization using a digoxigenin-labeled probe. *Vet Pathol*. 1999;36:308-313.
3. Lopez A. Respiratory system, mediastinum, and pleurae. In: Zachary JF, McGavin MD, eds. *Pathologic Basis of Veterinary Disease.* 5th ed. St. Louis, MO: Elsevier Mosby; 2012:494-504, 520-521.
4. Quinn PJ, Markey BK, Leonard FC, FitzPatrick ES, Fanning S, Hartigan PJ. Mycoplasmas. In: *Veterinary Microbiology and Microbial Disease.* 2nd ed. Ames, Iowa: Wiley-Blackwell; 2011; Kindle edition.